ICONS 2013

The Eighth International Conference on Systems

ISBN: 978-1-61208-246-2

January 27 - February 1, 2013

Seville, Spain

ICONS 2013 Editors

Raimund Ege, Northern Illinois University, USA

Leszek Koszalka, Wroclaw University of Technology, Poland

ICONS 2013

Foreword

The Eighth International Conference on Systems [ICONS 2013], held between January 27th- February 1st, 2013 in Seville, Spain, continued a series of events covering a broad spectrum of topics. The conference covered fundamentals on designing, implementing, testing, validating and maintaining various kinds of software and hardware systems. Several tracks were proposed to treat the topics from theory to practice, in terms of methodologies, design, implementation, testing, use cases, tools, and lessons learnt.

In the past years, new system concepts have been promoted and partially embedded in new deployments. Anticipative systems, autonomic and autonomous systems, self-adapting systems, or on-demand systems are systems exposing advanced features. These features demand special requirements specification mechanisms, advanced behavioral design patterns, special interaction protocols, and flexible implementation platforms. Additionally, they require new monitoring and management paradigms, as self-protection, self-diagnosing, self-maintenance become core design features.

The design of application-oriented systems is driven by application-specific requirements that have a very large spectrum. Despite the adoption of uniform frameworks and system design methodologies supported by appropriate models and system specification languages, the deployment of application-oriented systems raises critical problems. Specific requirements in terms of scalability, real-time, security, performance, accuracy, distribution, and user interaction drive the design decisions and implementations. This leads to the need for gathering application-specific knowledge and develop particular design and implementation skills that can be reused in developing similar systems.

Validation and verification of safety requirements for complex systems containing hardware, software and human subsystems must be considered from early design phases. There is a need for rigorous analysis on the role of people and process causing hazards within safety-related systems; however, these claims are often made without a rigorous analysis of the human factors involved. Accurate identification and implementation of safety requirements for all elements of a system, including people and procedures become crucial in complex and critical systems, especially in safety-related projects from the civil aviation, defense health, and transport sectors.

Fundamentals on safety-related systems concern both positive (desired properties) and negative (undesired properties) aspects. Safety requirements are expressed at the individual equipment level and at the operational-environment level. However, ambiguity in safety requirements may lead to reliable unsafe systems. Additionally, the distribution of safety requirements between people and machines makes difficult automated proofs of system safety. This is somehow obscured by the difficulty of applying formal techniques (usually used for equipment-related safety requirements) to derivation and satisfaction of human-related safety requirements (usually, human factors techniques are used).

We take here the opportunity to warmly thank all the members of the ICONS 2013 Technical Program Committee, as well as the numerous reviewers. The creation of such a high

quality conference program would not have been possible without their involvement. We also kindly thank all the authors who dedicated much of their time and efforts to contribute to ICONS 2013. We truly believe that, thanks to all these efforts, the final conference program consisted of top quality contributions.

Also, this event could not have been a reality without the support of many individuals, organizations, and sponsors. We are grateful to the members of the ICONS 2013 organizing committee for their help in handling the logistics and for their work to make this professional meeting a success.

We hope that ICONS 2013 was a successful international forum for the exchange of ideas and results between academia and industry and for the promotion of progress in the field of systems.

We are convinced that the participants found the event useful and communications very open. We also hope the attendees enjoyed the charm of Seville, Spain.

ICONS Chairs:

Raimund Ege, Northern Illinois University, USA
Hermann Kaindl, Vienna University of Technology, Austria
Leszek Koszalka, Wroclaw University of Technology, Poland
Daniela Dragomirescu, LAAS-CNRS / University of Toulouse, France
Marko Jäntti, University of Eastern Finland, Finland

ICONS 2013

Committee

ICONS Advisory Committee

Raimund Ege, Northern Illinois University, USA
Hermann Kaindl, Vienna University of Technology, Austria
Leszek Koszalka, Wroclaw University of Technology, Poland
Daniela Dragomirescu, LAAS-CNRS / University of Toulouse, France
Marko Jäntti, University of Eastern Finland, Finland

ICONS 2013 Technical Program Committee

Marco Aiello, University of Groningen, The Netherlands
Mehmet Aksit (Akşit), University of Twente - Enschede, The Netherlands
Giner Alor Hernández, Instituto Tecnológico de Orizaba - Veracruz, México
César Andrés, Universidad Complutense de Madrid, España
Luis Anido-Rifon, University of Vigo, Spain
Rafic Bachnak, Texas A&M International University - Laredo, USA
Javier Bajo Pérez, Universidad Pontificia de Salamanca, Spain
Lubomir Bakule, Institute of Information Theory and Automation of the ASCR, Czech Republic
Zbigniew Banaszak, Warsaw University of Technology | Koszalin University of Technology, Poland
Jacob Barhen, Oak Ridge National Laboratory, USA
Nicolas Belanger, Eurocopter Group, France
Ateet Bhalla, Oriental Institute of Science & Technology, Bhopal, India
Jun Bi, Tsinghua University - Beijing, China
Freimut Bodendorf, University of Erlangen-Nuremberg, Germany
Mietek Brdys, University of Birmingham, UK
Mario Cannataro, University "Magna Græcia" of Catanzaro - Germaneto, Italy
Chi-Hua Chen, National Chiao Tung University, Taiwan , R.O.C.
Albert M. K. Cheng, University of Houston, USA
Ding-Yuan Cheng, National Chiao Tung University, Taiwan , R.O.C.
Lawrence Chung, University of Texas at Dallas, USA
Nicolas Damiani, Eurocopter Group, France
Peter De Bruyn, Universiteit Antwerpen, Belgium
Jianguo Ding, University of Luxembourg, Luxembourg
António Dourado, University of Coimbra, Portugal
Daniela Dragomirescu, LAAS-CNRS / University of Toulouse, France
Raimund Ege, Northern Illinois University, USA
Yezyd Enrique Donoso Meisel, Universidad de los Andes - Bogotá, Colombia
Andras Farago, The University of Texas at Dallas, USA
Miguel Franklin de Castro, Federal University of Ceará, Brazil
Laurent George, University of Paris-Est Creteil Val de Marne, France
Eva Gescheidtová, Brno University of Technology, Czech Republic

Luis Gomes, Universidade Nova de Lisboa, Portugal
Dongbing Gu, University of Essex - Colchester, UK
Aseem Gupta, Freescale Semiconductor - Austin, USA
Mohanad Halaweh, University of Dubai, UAE
Yo-Ping Huang, National Taipei University of Technology - Taipei, Taiwan
Wen-Jyi Hwang, National Taiwan Normal University - Taipei, Taiwan
Marko Jäntti, University of Eastern Finland, Finland
Jiri Jaros, Australian National University, Australia
Jaroslav Kadlec, Brno University of Technology, Czech Republic
Hermann Kaindl, Vienna University of Technology, Austria
Andrzej Kasprzak, Wroclaw University of Technology, Poland
Abdelmajid Khelil, TU Darmstadt, Germany
Leszek Koszalka, Wroclaw University of Technology, Poland
Eiji Kawai, National Institute of Information and Communications Technology, Japan
Radek Kuchta, Brno University of Technology, Czech Republic
Frédéric Le Mouël, INRIA/INSA Lyon, France
David Lizcano Casas, Universidad Politécnica de Madrid (UPM), Spain
Jaime Lloret Mauri, Polytechnic University of Valencia, Spain
Andrei Lobov, Tampere University of Technology, Finland
Jia-Ning Luo (羅嘉寧) Ming Chuan University, Taiwan
Zoubir Mammeri, IRIT - Paul Sabatier University - Toulouse, France
D. Manivannan, University of. Kentucky, UK
Patrick Meumeu Yomsi, Université Libre de Bruxelles (ULB), Belgium
Fabrice Mourlin, Paris 12 University - Créteil, France
Antonio Muñoz, Universidad de Málaga, Spain
Kazumi Nakamatsu, University of Hyogo, Japan
John T. O'Donnell, University of Glasgow, UK
Timothy W. O'Neil, The University of Akron, USA
Sigeru Omatu, Osaka Institute of Technology, Japan
Jochen Palmer, IT-Designers GmbH, Germany
Namje Park, Jeju National University, Korea
Aljosa Pasic, AtoS, Spain
Przemyslaw Pawluk, York University - Toronto, Canada
Marek Penhaker, VŠB - Technical University of Ostrava, Czech Republic
George Perry, University of Texas at San Antonio, USA
Pawel Podsiadlo, The University of Western Australia - Crawley, Australia
Chantana Pongphensri, Silpakorn University, Thailand
Iwona Pozniak-Koszalka, Wroclaw University of Technology, Poland
Zhihong Qian, Jilin University, P.R.China
Roland Rieke, Fraunhofer Institute for Secure Information Technology SIT, Darmstadt, Germany
Diletta Romana Cacciagrano, University of Camerino, Italy
Juha Röning, University of Oulu, Finland
Jarogniew Rykowski, Poznan University of Economics, Poland
Rainer Schönbein, Fraunhofer IOSB, Germany
Zary Segall, University of Maryland Baltimore County, USA
Florian Segor, Fraunhofer-Institut für Optronik - Karlsruhe, Germany
Pavel Šteffan, Brno University of Technology, Czech Republic
Miroslav Sveda, Brno University of Technology, Czech Republic

Copyright Information

For your reference, this is the text governing the copyright release for material published by IARIA.

The copyright release is a transfer of publication rights, which allows IARIA and its partners to drive the dissemination of the published material. This allows IARIA to give articles increased visibility via distribution, inclusion in libraries, and arrangements for submission to indexes.

I, the undersigned, declare that the article is original, and that I represent the authors of this article in the copyright release matters. If this work has been done as work-for-hire, I have obtained all necessary clearances to execute a copyright release. I hereby irrevocably transfer exclusive copyright for this material to IARIA. I give IARIA permission or reproduce the work in any media format such as, but not limited to, print, digital, or electronic. I give IARIA permission to distribute the materials without restriction to any institutions or individuals. I give IARIA permission to submit the work for inclusion in article repositories as IARIA sees fit.

I, the undersigned, declare that to the best of my knowledge, the article is does not contain libelous or otherwise unlawful contents or invading the right of privacy or infringing on a proprietary right.

Following the copyright release, any circulated version of the article must bear the copyright notice and any header and footer information that IARIA applies to the published article.

IARIA grants royalty-free permission to the authors to disseminate the work, under the above provisions, for any academic, commercial, or industrial use. IARIA grants royalty-free permission to any individuals or institutions to make the article available electronically, online, or in print.

IARIA acknowledges that rights to any algorithm, process, procedure, apparatus, or articles of manufacture remain with the authors and their employers.

I, the undersigned, understand that IARIA will not be liable, in contract, tort (including, without limitation, negligence), pre-contract or other representations (other than fraudulent misrepresentations) or otherwise in connection with the publication of my work.

Exception to the above is made for work-for-hire performed while employed by the government. In that case, copyright to the material remains with the said government. The rightful owners (authors and government entity) grant unlimited and unrestricted permission to IARIA, IARIA's contractors, and IARIA's partners to further distribute the work.

Table of Contents

A Codified Procedure to Assess Resilience in Irrigation Systems Based on Loop Polarity Analysis

Newton Paulo Bueno
Department of Economics
Federal University of Viçosa
Viçosa/Brazil
e-mail: npbueno@ufv.br

Abstract— **Agricultural systems are complex systems, whose study requires approaches capable of recognizing the inherent feedbacks between people`s behavior, incentives, and environmental outcomes. Although several studies deal with agricultural systems from that perspective, there are comparatively few that study irrigation schemes based on the feedback effects that may threaten their sustainability. This paper uses feedback loop polarity analysis to build an algorithm to predict irrigation systems` resilience tipping points. It concludes by suggesting that the basic ideas presented might be useful to build operational early warning signals for critical transitions in irrigation systems and in a wider range of systems where tipping points are suspected to exist.**

Keywords-irrigation systems; sustainability; resilience; system dynamics; loop polarity analysis.

I. INTRODUCTION

As defined by Holling [6], ecological resilience refers to the ability to absorb change and disturbance and still maintain the same relationships that control a system's behavior. Nonetheless, the literature is still unclear on how to measure resilience in different systems and therefore on how well that concept translates in practice to analyzing the vulnerability of social systems more broadly [2]. As we cannot hope to manage what we do not even measure, the issue of measurement seems critical for the progress of the research on the field. This paper aims at contributing to bridge that gap by proposing a codified procedure, based on loop polarity analysis [1], for identifying in advance irrigation systems` resilience thresholds.

There are comparatively few works focusing on factors that can threaten the sustainability of irrigation systems [4]. Most of them show that irrigation projects can cause catchment degradation but are also (more often than not) their victims [8]. The most obvious consequence of catchment deterioration by irrigation is erosion, leading to siltation of canals and of reservoirs. This makes poor operation and maintenance (O&M) the bigger problem for the sustainability of irrigation projects mainly in less developed countries where many of those projects are managed for incompetent bureaucracies combined with weak irrigator associations. Causality above can also manifest in reverse, because farmers may simply be unable to carry out maintenance expenses, for being caught in feedback reinforcing loops of inadequate maintenance. Elinor Ostrom [10: p.89] puts the question as follows.

"Unless farmers pay the fees used to hire O&M staff or they perform these O&M activities themselves, many irrigation agencies will not be able to do anything more than operate systems in a minimal fashion. Little investment can be made in routine or emergency maintenance. The initial lack of maintenance triggers a vicious circle that has been characteristic of many large systems constructed in recent years. Without adequate maintenance, system reliability begins to deteriorate. As reliability diminishes, farmers are less willing to make investments in expensive seeds and fertilizers that are of little benefit without a reliable water supply. Without these input investments, the net return from irrigated agriculture declines. As returns fall, farmers become still more resistant to contributing to the system`s sustainability."

This paper indicates how to identify in advance the critical points beyond which, due to the action of vicious feedback loops, irrigation systems lose resilience when hit by even tiny, and so hard to notice, environmental shocks. The remainder of the paper is organized as follows. Section II presents a hypothetical system dynamics model that underpins the above conclusion and summarizes the essence of the loop polarity analysis approach. Section III presents a codified procedure for computing resilience tipping points of irrigation systems. Sections IV and V, respectively, present and discuss the main results of simulation, suggesting how to identify leverage intervention points in collapsing irrigation systems. Section VI concludes by suggesting that the basic ideas presented might be useful to build operational early warning signals for critical transitions not only in irrigation systems, but in a wider range of systems, where tipping points are suspected to exist.

II. THE MODEL

Professor Ostrom`s ideas on the sustainability of irrigation systems outlined in the introductory section were later formalized in a system dynamics model by herself and colleagues at Indiana University [13], which we synthesize in Figure 1.

 ISBN: 978-1-61208-246-2

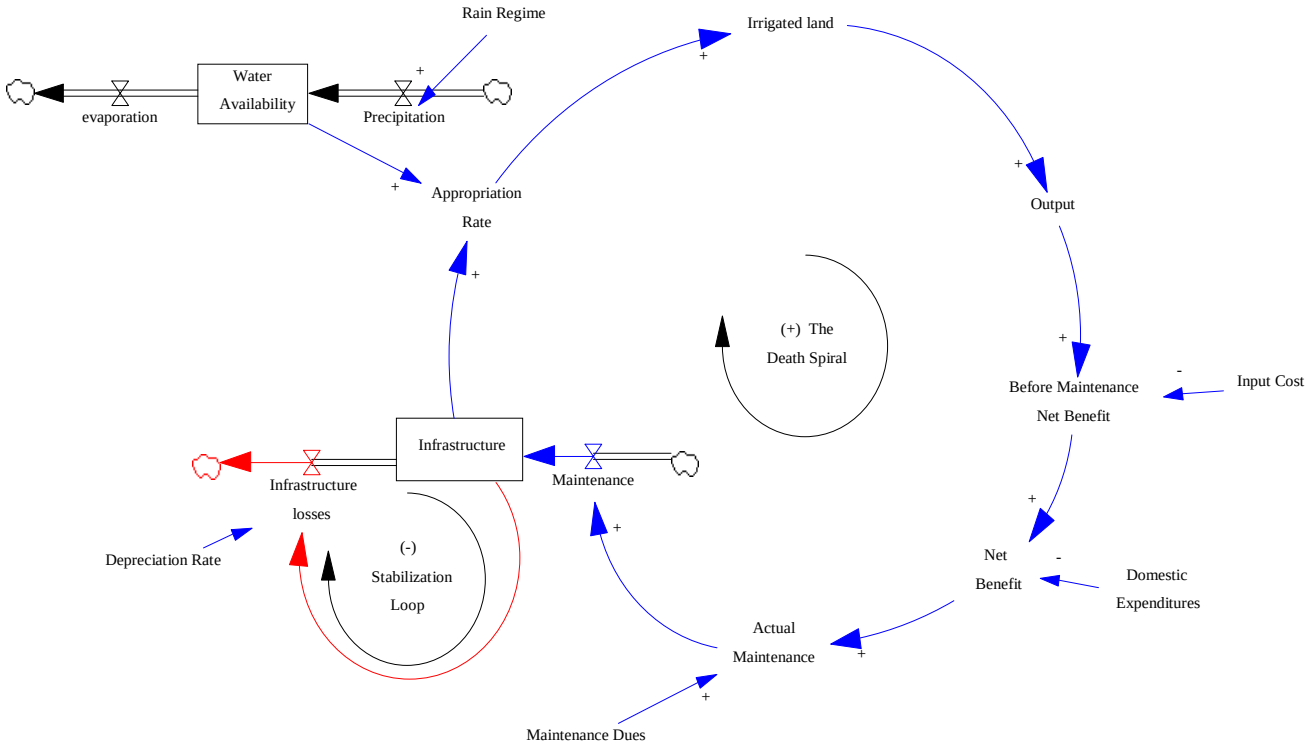

Figure 1. Loop polarity in irrigation projects.

The fully documented original Stella version model is presented in the referred paper and the present VENSIM version is available upon request. In the basic stock-flow structure of the simplified model, there are just two loops. In the self-reinforcing loop labeled as "the death spiral", the deterioration of the irrigation infrastructure due to inadequate maintenance leads to falling output, benefits and infrastructure maintenance, which further decreases the infrastructure reliability. In the stabilization loop, decreases in the depreciation flow due to the reduction in the state. The time path of the value of the infrastructure is then given by the following differential equation:

dInfrastructure/dt = Maintenance – Infrastructure Losses (1)

where:

Maintenance = min (Maintenance Dues, net Benefit) (2)

Net Benefit = Before Maintenance Net Benefit – Domestic Expenditures (3)

and

Infrastructure Losses = Infrastructure * Depreciation Rate (4)

Disturbances like changes in rain regime are modeled as follows.

Rain Regime = Mean Precipitation Level - PULSE(y, t)* R (5)

where R is the change in the precipitation level starting in year y and lasting for t years.

The degree of resilience of the above system can be assessed as follows: what level of disturbance, droughts for

 ISBN: 978-1-61208-246-2

instance, can the system withstand before the agents stop investing the total amount needed for the integral maintenance of the infrastructure?

It is easy to see that as far as irrigators are able to pay maintenance fees the infrastructure is maintained in appropriated use conditions. But if they are forced to spend less than that value, the maintenance rate will be lower than infrastructure losses and the infrastructure will decrease in size. Hence, in the next period, the amount appropriated of water, output and profits will decrease and so do maintenance spending. Once the irrigators are forced to pay less than the right maintenance dues, the system can enter into a snow-ball trajectory we have labeled "the death spiral", because the final outcome of the process is the complete deterioration of the existing infrastructure. Figure 2 presents the argument graphically. In the following sections, we indicate how to calculate resilience tipping points of irrigation systems.

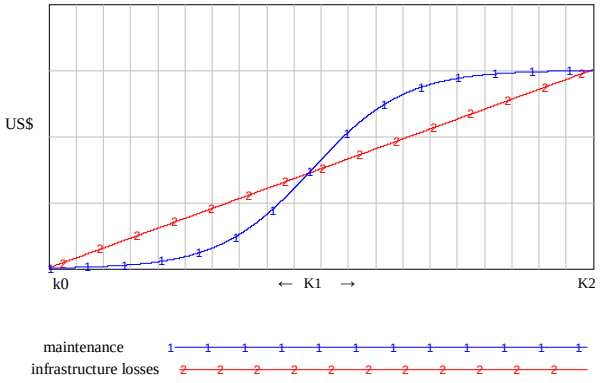

Figure 2. Maintenance and infrastructure losses: k is the value of the infrastucture at time t and k1, its resilience tipping point. Below that point, the death spiral dominates (maintenance<infrastructure losses) and the system collapses to k0, while above it the stabilization loop dominates the system`s dynamics and it will recover its former operation conditions (k2).

III. METHODOLOGY

A more rigorous analysis for how important dynamic patterns arise in social ecological from feedback structures can be found in the classical Richardson's [11] paper on loop dominance, on which this paper is based.

According to Richardson, the polarity of a single feedback loop involving a single level x and an inflow rate $\dot{x}$ = dx/dt is defined by sign $\left(\frac{d\dot{x}}{dx}\right)$, which is consistent with a more intuitive characterization as follows. The denominator of the fraction – dx – can be thought of as a small change in x, for instance a small change in fish caught in a particular fishery, which is traced around the loop until it results in a small change - $d\dot{x}$ — in the inflow rate, say in the regeneration rate of the system, $\dot{x} = \frac{dx}{dt}$. If the change in the rate, $d\dot{x}$, is in the same direction as the change in the level, dx, then they have the same sign. As $\dot{x}$ is an inflow rate and thus is added to the level, the loop is a positive one and hence reinforces the initial change In such case sign $\left(\frac{d\dot{x}}{dx}\right)$ is positive and will be negative if the polarity of the loop is negative, that is if the resulting change in the inflow rate is in the oposite direction to the change dx. If $\dot{x}$ is an outflow rate, all we have to do to extend the above definition for loop polarity is to attach a negative sign to the expression for $\dot{x}$, since variation in the same direction in the outflow, e.g in the death rate, and in the level, e.g. in the fish population means that the loop polarity is negative.

In order to identify irrigation systems' resilience tipping points, that is the points where systems dynamics shift from an equilibrium behavior pattern to an exponential decay one, we propose a codified procedure to Richardson's ideas based on a generalization of the simple stability test proposed by Ford [5: 54-55], and developed by Bueno [1].

The idea is to introduce a change in the system and watch how it reacts. The level variable is any stock in the model we wish to test. If the stock returns to the original value after the system is hit by an exogenous shock, the equilibrium is stable. On the contrary, if the stock moves farther and farther away from the equilibrium, the equilibrium is unstable. In the first case, we can say that the loop polarity of the feedback structure is negative while in the second case it is positive. Our conjecture is that the loss of resilience of irrigation systems can be seen as a bifurcation point where loop polarity changes from negative to positive sign .

The procedure is as follows:

1) Choose a variable of interest (x) that represents the resource users want to preserve and whose state they are able to assess.
2) Compute the ratio $\frac{d\dot{x}}{dx}$ for the observed conditions of the system and over a chosen reference time interval, attaching a negative sign to $\dot{x}$ if $\frac{dx}{dt}$ is an outflow rate
3) Choose a parameter that can vary $\frac{d\dot{x}}{dx}$. Use the parameter to vary that ratio until $\frac{d\dot{x}}{dx}$ changes sign in the reference time interval.

 ISBN: 978-1-61208-246-2

4) Compute the value of the variable of interest at the point where $\frac{d\dot{x}}{dx}$ changes sign and compare this value to the equilibrium value obtained in the last run before $\frac{d\dot{x}}{dx}$ shifts sign to identify the tipping point of the variable of interest which is inside this interval. The critical value of the variable of the interest assessed from the parameter chosen is the last equilibrium value before the sign shifts.

5) Repeat steps 2-4 for other parameters.

6) Select the largest of the critical value of the variable of interest obtained by steps 2-4 as the critical resilience level of the system and compare this to the actual observed level (or the simulated level at the actual observed conditions of the fishery); resilience degree is computed as:

$$\frac{observed\ level - critical\ resilience\ level}{critical\ resilience\ level} \times 100$$

IV. RESULTS

Assuming the variable of the interest is the irrigation infrastructure and performing calculations only for the parameter rain regime, Figure 3a shows that an irrigation system can lose sustainability due to small variations in environmental conditions. A reduction of 0.1% in the annual precipitation from year 20 to year 24 (35.2% drought → 35.3% drought) is enough to put the system on the collapse mode if it is operating close to its tipping point. In that mode, irrigators are unable to pay maintenance dues and, hence, maintenance falls below depreciation and the variable of interest – infrastructure – enter into a downward endogenous trajectory (Figure 3c).

It is noticed that between, say, years 25-45, unsustainable systems present a slowing down pattern before an abrupt change. This result – which indicates the tension among stabilizing (e.g., the stabilization loop) and amplifying (e.g., the death spiral) feedback loops working in tandem upon the system's dynamics near tipping points - has been identified as a universal property of systems approaching that threshold, and hence may be seen as an early warning signal of sustainability loss [14].

When the system is operating in collapse mode as in Figure 3e), the ratio $\frac{d\dot{x}}{dx}$ shifts from negative to positive in year 49, which allows to compute its resilience tipping point as indicated in step 6 above. This indicates infrastructure has started to deteriorate at an increasing rate, progressively moving away from its equilibrium value. When the system is operating in the equilibrium mode (Fig. 3d), on the other hand, the system's loop polarity shifts from positive to negative, indicating that the system will approach an equilibrium path afterwards.

As indicated in the Section I, the explanation of why the system displays an explosive behavior is that it becomes dominated by amplifying loops, as the death spiral in our basic model.

V. DISCUSSION

Simulations performed in Section III suggest that a major reason for the loss of sustainability of an irrigation system is the inability of farmers to perform O & M properly. At the system`s tipping point, i.e. at year 49, the infrastructure reaches the critical value in which profits equal household expenses: US$ 150,000. At this point, system´s resilience degree is zero, according the indicator calculated in step 6. Environmental shocks like droughts, henceforth, can lead irrigation systems to collapse by reducing the incomes of the irrigators below the level consistent with both maintenance dues and the payment of household expenses necessary for the survival of farmers and their families.

Now, imagine that after realizing that the system is on a collapse trajectory government decides to intervene, financing the total annual spending on maintenance costs in a particular year. It is easy to infer that if government acts timely by complementing private maintenance before the tipping point, say at year 47, the system will be able to recover relatively easily (Figure 4). But, if it postpones intervention even just for one or two years, the system will collapse, because it may already be dominated by the death spiral loop.

 ISBN: 978-1-61208-246-2

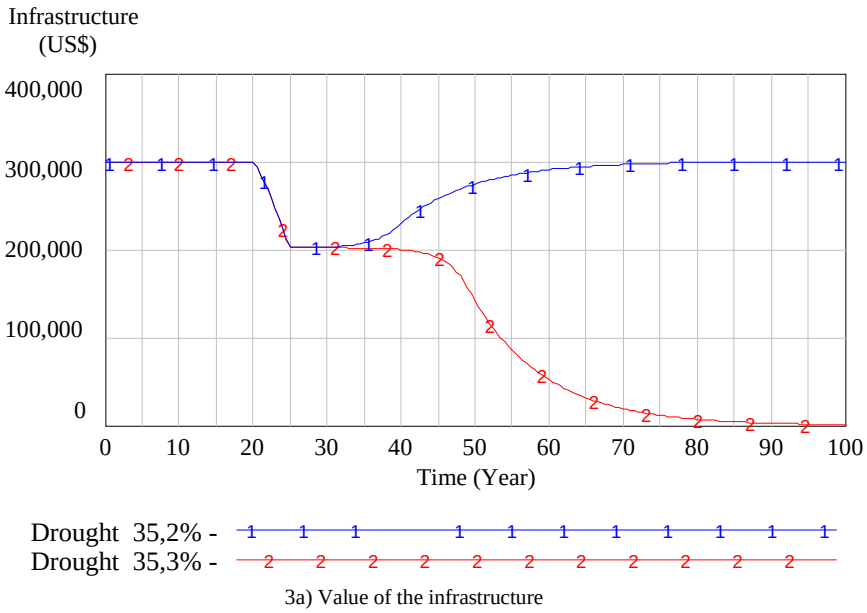

3a) Value of the infrastructure

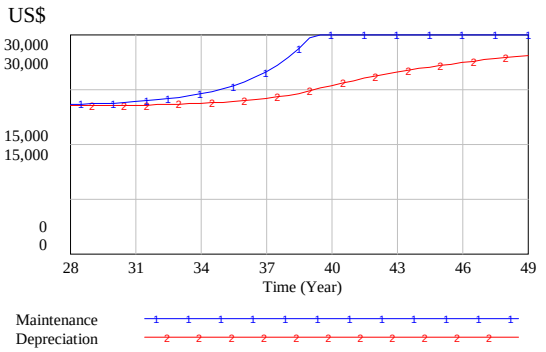

3b) Drought 35,2%-.

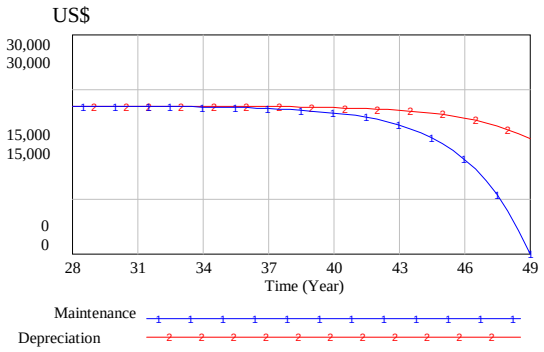

3c) Drought 35,3%-.

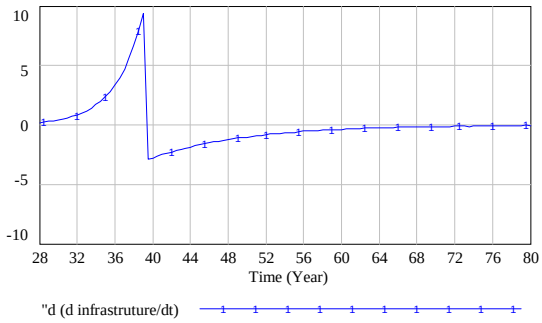

3d) Drought 35,2%-.

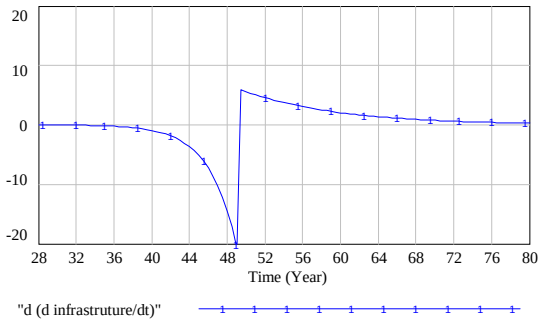

3e) Drought 35,3%-.

Figure 3. Sustainable and unsustainable irrigation systems.

 ISBN: 978-1-61208-246-2

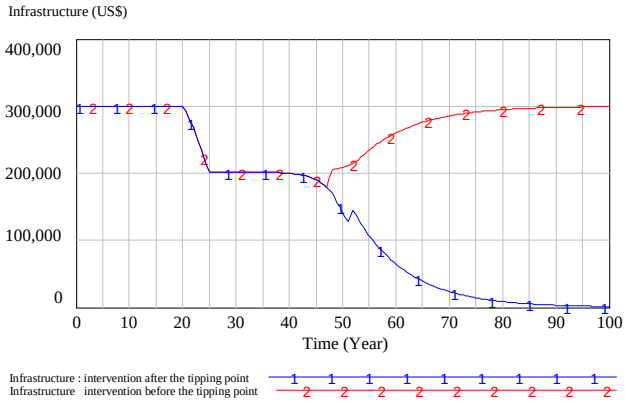

Figure 4. Leverage intervention points.

VI. CONCLUSION AND FUTURE WORK

Mostly because measurement or predictions of thresholds in socio-ecological systems (SESs) have low precision, the precise meaning of resilience and its identification still remain a subject of debate. This work has attempted to bridge that gap by providing a relatively simple procedure to assess resilience in a particular type of SESs - irrigation systems - based on loop dominance analysis. The proposed procedure uses changes in loop polarity from negative to positive as a signal of resilience loss. Specifically, it is shown that irrigation systems lose resilience when stabilizing (negative) feedback loops stop dominating dynamics forcing farmers´ income in a downward endogenous trajectory that impairs the ability of producers to carry out the necessary maintenance expenses. Hence, problems of maintenance of irrigation systems operating near tipping points can many times be explained by the inability of users to pay for maintenance of infrastructure and not by their refusal to pay the costs to maintain systems integrity. But can this approach (complemented by other techniques) help identify early signs of loss of resilience in order to enable government agencies to act timely to prevent the collapse of fragile irrigation systems?

Recent developments in the field of dynamical systems have suggested so. A number of generic symptoms may occur in a wide class of systems as they approach tipping points. One of those symptoms, which can indeed be considered as a universal property of systems approaching tipping points, is a phenomenon known in dynamical systems theory as critical slowing down [3]. Systems' dynamics in such case is dominated by a damped, driven effect created when positive and negative feedbacks operate in tandem. This implies that systems operating near tipping points become increasingly slow in recovering from small perturbations, due to the fact that amplifying (positive) feedbacks loops, such as the "death spiral", begin to offset the stabilizing effect of negative feedback loops as the stabilization loop in model presented in Figure 1, that is becoming less resilient in terms of this work [9]. Figure 4 depicts this characteristic slowing down process in action as an irrigation system approaches its tipping point: the later the system recovers original characteristics, the longer the return time to a sustainable exploitation path. Applied literature has tested a number of techniques to check whether the theoretically predicted critical slowing down may indeed be identified in actual complex systems, such as sensitivity and time series analyses. For instance, a way to test whether a system is slowing down is to interpret fluctuations in the state of the system as it responds to natural perturbations. Slowing down then should be reflected as a decrease in the rates of changing of the system near systems' tipping point (calculated by the approach proposed in this work), which may be measured by an increase in the short term correlation in key variables time series [7], such as farmer's income.

Unfortunately, there are signals that process is already taking place in several regions of the world. Growth in irrigation, mainly in arid countries in the Middle and Near East, has dramatically slowed over the last decades to a rate that is inadequate to keep up with the expanding food requirements. Besides, extensive areas of land in a number of countries have been degraded by waterlogging and salinization resulting of poor agricultural management and maintenance, which has resulted in major environmental disturbances and raised doubts about its very sustainability in many places in the world [12]. As a consequence of these problems, there will be probably fewer investments in new and existing irrigation projects in the future that have been made in the last decades, unless major improvements in the operation and maintenance of existing irrigation systems can bring those systems back to sustainable patterns of use, particularly in the world's poorest regions.

ACKNOWLEDGMENT

CNPQ AND FAPEMIG are gratefully acknowledged for their financial support.

REFERENCES

[1] N. Bueno "Assessing resilience of small socio-ecological systems based on the dominant polarity of their feedback structure". System Dynamics Review, 2012, vol. 28, 4, pp. 351-360.

[2] S. Carpenter, B. Walker, J. Anderies, and N. Abel "From Metaphor to Measurement: Resilience of What to What?", Ecosystems, 2001, vol. 4, 8, pp. 765-781.

[3] V. Dakos, M. Scheffer, E. Van Ness, V. Brovkin, V. Petoukhov, and H. Held , "Slowing down as an early signal for abrupt climate change", PNAS, 105, September 23, pp. 14308-14312.

[4] J. Férnandez and M. Selma, "The dynamics of water scarcity on irrigated ladscapes: Mazarrón and Aguilas in south-eastern Spain", System Dynamics Review, 2004, vol. 20, 2, pp. 117-137.

 ISBN: 978-1-61208-246-2

[5] A. Ford, Modeling the environment – an introduction to system dynamics models of environmental systems. Washington: Island Press, 1999.

[6] C. Holling, “Resilience and stability of ecological systems”, Annual Review of Ecological Systems, 1973, vol. 4, pp. 1-23.

[7] A. Ives, Measuring resilience in stochastic-systems. Ecological Monograph, 1995, 65, pp. 217-233.

[8] W. Jones, The World Bank and irrigation. Washington, DC.: The World Bank, 1995.

[9] S. Martin, G. Deffuant, and J. Calabrese “Defining resilience mathematically: from attractors to viability”. In: G, Deffuan and N. Gilbert (editors) Viability and resilience of complex systems – concepts, methods and case studies from ecology and society. London, New York: Springer, 2011, pp. 15-36 .

[10] E. Ostrom, Crafting institutions for self-governing irrigation systems. San Francisco, California: Institute for Contemporary Studies, 1992.

[11] G. Richardson, “Loop polarity, loop dominance, and the concept of dominant polarity”, System Dynamics Review, vol. 11, 1, Spring 1995, pp. 67-87.

[12] JD. Rhoades, “Sustainability of Irrigation: an overview of salinity problems and control strategies”, In: CRWA 1997 Annual Conference “Footprints of Humanity: Reflections of fifty years of water resource development. Lethbridge, Alberta, June 3-6, 1997.

[13] N. Sengupta, S. Swati, and E. Ostrom “Sustainability, equity, and efficiency of irrigation infrastructure”. In: R, Constanza (ed.), Institutions, ecosystems, and sustainability. Boca Raton: Lewis Publishers, 2001.

[14] M. Scheffer, J. Bascompte, W. Brock, V. Brovkin, S. Carpenter, V. Dakos, H, Held, E. Van Nes, M. Rietkerk, and G. Sugihara, “ Early-warning signal for critical transitions”. Nature, vol. 461/3, September, 2009, pp. 53-59.

 ISBN: 978-1-61208-246-2

Multi-Agent Systems: A new paradigm for Systems of Systems

Eduardo Alonso
Department of Computer Science
City University London
London, United Kingdom
e-mail: E.Alonso@city.ac.uk

Nicos Karcanias
Systems & Control Engineering Centre
City University London
London, United Kingdom
e-mail: N.Karcanias@city.ac.uk

Ali G. Hessami
Vega Systems Ltd.
London, United Kingdom
e-mail: hessami@vegaglobalsystems.com

Abstract **–We present the notion of Systems of Systems, its drivers, and the challenges we face in conceptualizing, designing, implementing and validating them. In this work in progress we propose Multi-Agent Systems as a new paradigm, taken from Artificial Intelligence, which seems to fit the purpose.**

Keywords-multi-agent systems; system of systems; autonomous agents; dynamic adaptive systems

I. SYSTEMS OF SYSTEMS

Systems of Systems (SoS) have been defined as systems that describe the large-scale integration of many independent self-contained systems to satisfy global needs or multi-system requests. The main drivers behind the notion of SoS are various yet inter-related, namely,

- The increasing number of interacting systems with strong connectivity in society and in industry –which underlies the so-called "embedded world meets the Internet world" view.
- Emergent behavior with the need to balance cooperation and autonomy.
- Growing overall complexity of systems.

Such drivers are shown in the dimensions that define SoS, typically, the geographic distribution of the overall system, their operational and managerial independence, and their evolutionary development –a SoS evolves over time as the constituent systems are changed, added or removed— and emergent behavior –a SoS is not restricted to the capabilities of the constituent systems.

Such dimensions can be recognized in several types of large systems as identified in Table 1:

TABLE 1. TYPES OF SoS

Type	System	System of Systems
ICT powered	Car, road	Integrated Traffic Network
	Wind turbine, fossil	Smart Grid
	Computer, routers	Distributed IT System
Biological	Animal, plant	Herd, forest
Sociological	Family, school, church	Town, education, religion
Environmental	Weather, river	Eco-system
Organizational	Company	SCM, stock market, economy
Political	Town council	Parliament, EU, UN

Other examples include water management, emergency response, smart grid, railways, satellites, distributed control systems, supply chain management, and inter-court law relationships –to name a few.

One fundamental aspect in the analysis of SoS is to distinguish them from Composite Systems (CoS). [1][2][3][4] identified the following commonalities and differences:

a) Both CoS and SoS are compositions of simpler objects, or systems.

b) Both CoS and SoS are embedded in the environment of a larger system.

c) The objects, or sub-systems in CoS do not have their independent goal, they are not autonomous and their behavior is subject to the rules of the interconnection topology.

d) The interconnection rule in CoS is expressed as a graph topology.

e) The subsystems in SoS may have their own goals and some of them may be autonomous, semi-autonomous, or organized as autonomous groupings of composite systems

f) There may be a connection rule expressed as a graph topology for the information structures of the subsystems in a SoS.

g) The SoS has associated with it a *global game* where every subsystem enters as an agent with their individual Operational Set, Goals.

The comparison between SoS and traditional CoS illustrates the need for a paradigm shift in studying increasingly complex systems, and that such paradigm must focus on two main requirements

1. Rather than controlling systems the aim is to find means of influencing systems towards agreed common goals.
2. Develop approaches with incomplete models and dynamically evolving/changing requirements.

It is worth noting that in a similar manner to composite systems, SoS can be the outcome of natural evolution or entirely man made or a hybrid of these. In this context, agreed common goals may be more related to the total emergent properties arising from the constituents and natural ecology as opposed to deterministic requirements imposed on the system. This is particularly relevant when dealing with SoS that need to show context/situational awareness and that must be dependable to guarantee security and safety.

Table 2 summarizes the change of paradigm from old-classic approaches in systems theory to new-SoS according to various characteristics.

 ISBN: 978-1-61208-246-2

TABLE 2. PARADIGM SHIFT

Characteristics	Old-classic	New-SoS
Scope of system	Fixed (known)	Not known
Specification	Fixed	Changing
Control	Central	Distributed
Evolution	Version controlled	Uncoordinated
Testing	Test phases	Continuous
Faults	Exceptional	Normal
Technology	Given and fixed	Uncertain
Emergence	Controller	Accidental
System development	Process model	Undefined

Apart from economic, societal and educational factors, in this transition the following technological challenges have been highlighted:

- Multidisciplinary approach (common language).
- System modeling, simulation (and verification).
- Emergent behavior.
- Methods, architectures, platforms and theory.
- Standards and requirements.

Our contention is that Multi-Agent Systems (MAS), a computing paradigm for developing intelligent systems, can be a credible instrument in addressing some of these challenges. In the rest of the paper we describe the main characteristics of software agents and of MAS and rationalize why MAS technology can be used to develop SoS. It must be noticed that the multi-agent approach we propose is understood as a means of realizing the notions of intelligent object and of system play, deviations from standard notions of system composition introduced in [1][2].

II. SOFTWARE AGENTS

Artificial Intelligence (AI) has evolved from the ideal of perfect automatic reasoning, typically in the form of axiomatic systems, which from a set of premises prove theorems by applying deductive rules, to building systems that display acceptable behavior.

From Aristotle's syllogisms, through Leibniz's universal language, Babbage's difference engine and Boole's "laws of thought" to Turing's notion of computability, an important effort has been invested in formalizing "intelligence" and in building (abstract and physical) machines to mechanize it. Early AI inherited the goal and the methods from this trend of research, and thus was devoted to develop theorem provers for mathematical reasoning.

It became soon clear however that if we were to implement systems that exhibited intelligence in real-life situations a shift of paradigm was needed. Logical systems typically assume perfect knowledge of an unchanging set of truths. As a consequence, notwithstanding the success of some expert systems, the original AI promise –to develop systems that showed general intelligence– was not fulfilled, resulting in the so-called AI Winter. Partly as a response to this situation, attention swung to "weak" AI. This new theory pivoted around the idea of "embeddedness". Intelligence was not considered as thinking logically in closed domains, rather it was an emergent property of systems situated in open environments, environments that imposed constraints on the system. The concept of intelligence moved from thinking to acting, from perfect rationality to bounded rationally, from heavy-weight logical systems to networks of light-weight reactive systems.

This alternative didn't survive either. However interesting their results may be (for instance, in the simulation of swarm intelligence) relying exclusively on the emergent behavior of loosely coupled simple systems poses serious methodological problems.

For the last couple of decades researchers have experienced the advent of new technologies such as the Internet. These demand personal, continuously running systems for which older notions of action –those resulting from either cumbersome symbolic reasoning or ever-adaptive reflexes– may be insufficient. Indeed, many researchers believe that in the XXI century for AI systems to perform "intelligently" they must be able to behave in an *autonomous*, *flexible* manner in unpredictable, dynamic, typically *social* domains. In other words, they believe that the "new" AI should develop *agents* [5] [6].

The concept of agent serves to represent the idea of a autonomous system that perceives the environment and acts on it. The agent has an internal state that represents their knowledge and their goal –typically, the maximization of their own utility function. Decisions on which actions to execute depend on the agent's internal state and on the characteristics of the environment in which they are embedded. In the next section we explore the three main characteristics of agency.

A. Autonomy

By autonomy we mean the ability of the system to make their own decisions and execute tasks on the designer's behalf. The idea of delegating some responsibility to the system is essential in scenarios where it is difficult to control directly the behavior of our systems. For example, space missions increasingly depend on their unmanned spaceships and robots to make decisions on their own.

It is precisely their autonomy the characteristic that uniquely defines agents. Traditionally, software systems execute actions (so-called methods) automatically: imagine that the Web application in your computer, the user or client, requests to access the contents of a webpage that is stored in another software system elsewhere, the server or host. The server cannot deny access to the content of the webpage; it must execute the "send" method whenever it is requested to do so. On the contrary, agents decide by themselves whether to execute their methods according to their own goals. Paraphrasing [7], "what traditional software systems do for free, agents do for money".

B. Adaptive behavior

Secondly, agents must be flexible. When designing agent systems, it is impossible to foresee all the potential situations they may encounter and specify their behavior optimally in advance. For example, the components of interaction in the Internet (agents, protocols, languages) are not known *a priori*. Agents therefore have to learn from and adapt to their environment. This task is even

 ISBN: 978-1-61208-246-2

more complex when Nature is not the only source of uncertainty, when the agent is situated in a multi-agent system (MAS) that contains other agents with potentially different capabilities, goals, and beliefs.

In addition, an agent must have the competence to display an action repertoire general enough to preserve its autonomy in dynamic environments. Certainly, an agent can hardly be called intelligent if it is not able to perform well when situated in an environment different from (yet in some way similar to) the one it was originally designed for.

Indeed, there is no need to learn anything in static, deterministic, fully observable domains where agents have perfect knowledge of state-action transitions. Nonetheless, intelligence and learning are tightly tied in environments where systems must make decisions with partial or uncertain information, that is, in domains where they must learn without supervision and without the luxury of having a complete model of the world –when facing the so-called *reinforcement learning problem* [8], in which the learner must discover which actions yield the most reward by exploiting and exploring their relationship with the environment.

C. MAS co-ordination

Agents also show social attitudes. In an environment populated by heterogeneous entities, agents would need the ability to recognize their opponents, and to form alliances when it is profitable to do so. It is not a coincidence that most agent-based platforms incorporate multi-agent tools [9]. Indeed, it is claimed that agent-oriented software engineering needs to be developed precisely because there is no notion of organizational structure in traditional software systems.

Generally speaking, the design and implementation of MAS is an attractive platform for the convergence of various AI technologies. That is the underlying philosophy of competitions such as RoboCup (http://www.robocup.org/) where teams of soccer agents must display their individual and collective skills in real-time. More importantly, multi-agent systems play several roles in IT and telecoms: for clients, they provide personalized, user-friendly interfaces; as middleware, they have been used extensively to implement electronic markets and electronic auctions.

The reasons for this happy marriage between MAS and new technologies are various. When the domain involves a number of distinct software systems that are physically or logically distributed (in terms of their data, expertise or resources), a multi-agent approach can often provide an effective solution. Relatedly, when the domain is large, sophisticated, or unpredictable, the overall problem can indeed be partitioned into a number of smaller and simpler components, which are easier to develop and maintain, and which are specialized at solving the constituent problems. That is, in most real-life applications (single) agents can grow "too big" to work well, and a *divide and conquer* strategy, where qualified agents work in parallel, seems more sensible. Examples include the geographical distribution of cameras in a traffic network or the integrated approach required to solve complex tasks, for instance collaboration between experts (surgeons, anesthetists, nurses) in an operating room.

To sum it up, it is widely accepted within the AI community that the "new" AI is about designing and implementing MAS capable of acting and learning in a quick and efficient manner. This affects MAS co-ordination and MAS learning.

Approaches to multi-agent behavior differ mainly in regards to the degree of control that the designer should have over individual agents and over the social environment, *i.e.*, over the interaction mechanisms [10]. In Distributed Problem Solving systems (DPS) a single designer is able to control (or even explicitly design) each individual agent in the domain –the task of solving a problem is distributed among different agents, hence the name. In MAS on the other hand, there are multiple designers and each is able to design only its agent and has no control over the internal design of other agents [11][12].

The design of interaction protocols is also tightly coupled to the issue of agents' incentives. When agents are centrally designed they are assumed to have a common general goal. As long as agents have to co-exist and cooperate in a single system, there is some notion of global utility that each agent is trying to maximize. Agents form teams that jointly contribute towards the overall goal. By contrast, in MAS each agent will be individually motivated to achieve its own goal and to maximize its own utility. As a result, no assumptions can be made about agents working together cooperatively. On the contrary, agents will collaborate only when they can benefit from that cooperation.

Research in DPS considers how work involved in solving a problem can be divided among several nodes so as to enhance the system's performance, that is, the aim is to make independent nodes solve a global problem by working together coherently, while maintaining low levels of communication. MAS researchers are also concerned with the coherence of interaction, but must build agents without knowing how their opponents have been designed. The central research issue in MAS is how to have these autonomous agents identify common ground for cooperation, and choose and perform coherent actions.

In MAS systems, agents typically make pair-wise agreements through negotiation about how they will co-ordinate, and there is no global control nor consistent knowledge nor shared goals or success criteria. So, the main purpose of this *incentive contracting* mechanism is to "convince" agents to reach reasonable agreements and do something in exchange for something else. In this case, AI researchers have followed the studies on bargaining with incomplete information developed in economics and game theory.

Using such approach agents are considered players that execute moves following a strategy. At the end of the game each agent receives a pay-off or return. The strategies the agents follow are typically modulated by their attitude towards risk, that is, whether they are risk-

 ISBN: 978-1-61208-246-2

averse (in which case following a minimax strategy where the agent tries to minimize the other's profit may work) or they tolerate risk. The strategies also vary according to the nature of the interaction (one-shot or continuous; simultaneous or sequential) and to the type of game itself, for instance, if the agents engage in a zero-sum game (where what one gains the other loses) or in a cooperative game (where there may exist win-win solutions). In any case, the interaction takes the form of a negotiation protocol. Negotiation is defined as a process through which in each temporal point one agent proposes an agreement from the negotiation set and the other agent either accepts the offer or does not. If the offer is accepted, then the negotiation ends with the implementation of the agreement. Otherwise, the second agent has to make a counteroffer, or reject its opponent's offer and abandon the process. So, the protocol specifies when and how to exchange offers (*i.e.*, which actions the agents will execute or abstain from executing and when) – for example, an Offer(x, y, δ_i, t_1) means that the negotiation process will start at time t_1 with agent x offering agent y a deal δ_i from the set of potential deals ($\delta_i \in \Delta$), typically of the from "I will do action 1 in exchange for action 2" or {Do(x, a_1), Do(y, a_2)}; then, in the next negotiation step, agent y will counteroffer with Accept(y, δ_i, t_2), in which case the negotiation episode ends with the implementation of the agreement, δ_i; or with Reject(y, δ_i, t_2), so that negotiation fails; or, alternatively, agent y can send a counteroffer, Offer(y, x, δ_j, t_2), with say δ_j = {Do(x, a_3), Do(y, a_2)}, "I would prefer you to execute action a_3 rather than a_1", so that negotiation progresses to the next stage in which the same routine applies.

As discussed above, intelligence implies a certain degree of autonomy in decision-making that in turn requires the ability to learn to make independent decisions in dynamic, unpredictable domains such as those in which agents co-exist.

The simplest way to extend single-agent learning algorithms to multi-agent problems is just to make each agent learn independently. Agents learn "as if they were alone". Communication or explicit co-ordination is not an issue therefore –co-operation and competition are not tasks to be solved but properties of the environment. Likewise, agents do not have models of other agents' mental states or try to build models of other agents' behaviors. However simple this approach to multi-agent learning may be, the assumption that agents can learn efficient policies in a MAS setting independently of the actions selected by other agents is implausible. Intuitively, the most appealing alternative is to have the agents learn Nash-equilibrium strategies [13][14][15].

IV. MAS TECHNOLOGY FOR SoS

We can conclude from the conceptual analysis presented above that the paradigm shift demanded by SoS requirements fits new trends in engineering computing systems. In particular, the drivers and characteristics of SoS as specified in section I are consistent with the notions of autonomous agents and of multi-agent systems as opposed to traditional objects and classes. Although MAS development still relies on object-oriented tools and techniques, it is a fact that agent-oriented engineering is the way forward in the era of large, complex, loosely connected software systems, that is, in the era of the Internet –indeed, the Open Systems Interconnection (OSI) protocol itself can be understood as a SoS. More specifically, it can be argued that the difference between CoS and SoS lies in the fact that the former are collections of objects that coordinate their behavior via DPS, whereas the latter are collections of agents that interact through incentive mechanisms such as negotiation and argumentation. In Table 3 we enumerate ontologies, architectures, methodologies, languages, platforms, infrastructures and validation tools that SoS can borrow from MAS.

TABLE 3. AGENT-ORIENTED SOFTWARE ENGINEERING (AOSE)

AOSE	**Standards, techniques and tools**
Ontologies	RDF Schema, OIL, DAML, OWL, SHOE
Architectures	BDI, InteRRAP, Touring Machines
Methodologies	Tropos, MAS-CommonKADS, PASSI, Prometheus, Gaia, ADELFE, MESSAGE
Design languages	Agent UML
Programming languages	AOP: AGENT0, PLACA, Agent-K, MetaM, April, MAIL, VIVA, GO!
	BDI: AgentSpeak, Jason, AF-APL, JACK, JADEX, 3APL
	GOAL, Golog, FLUX, CLAIM
Communication languages	KQML, FIPA, ARCOL, KIF, COOL
Coordination mechanisms	MAP, Negotiation, Argumentation, Auctions, Institutions
Tools and platforms	ZEUS, JADE, agentTool, RETSINA, JATLite, MADKIT, JAFMAS, Cougaar
Infrastructures	Jini, Ontolingua ReTAX++, OilEd
Validation	Deductive verification, model checking

In particular, perhaps the most defining characteristic of MAS is the fact that communication is understood and formalized in terms of the internal states of the agents involved. In fact, communication is understood as (speech) acts, as actions that agents execute in order to achieve their goals not as mere message passing. In addition, since the agent at the other end is also autonomous, the sender needs to consider the receiver's internal state (not just its "position" in a mailing queue) and its own intentions. For instance, unlike in object-oriented approaches, when sending a request, the sender x holds the goal of a receiver y achieving a particular proposition P, that is, of making P true. Moreover, as ix wants the receiver to really try to achieve P the preconditions also require that y intends along a run that P be eventually true. Finally, the rational effect to be achieved is that there is a run in which P eventually holds. Formally,

[x, request(y, P)]
FP: G(x, (I(y, FP)))
RE: FP

Typically, Agent Communication Languages (ACLs) come with a complete set of speech acts, including

"inform", "confirm" "agree", "promise", "disconfirm", "refuse", "declare", and of course, "request".

Of course, agents and MAS are a particular type of SoS. Agents and MAS are *software* SoS. A general theory of SoS must be more comprehensive and accommodate the characteristics of other types of systems, characteristics that cannot be reduced to conglomerates of computing devices and the way they inter-operate. Our contention is nevertheless that MAS can play the same role in developing SoS as objects and classes played in conceptualizing, formalizing and implementing CoS. In addition, and more importantly, the individual systems MASs consist of are autonomous and adaptive –the two defining properties of the systems in a SoS. In fact, MAS emerge recursively and hierarchically as a result of the free interaction of such systems and multi-agent systems – as SoS do.

REFERENCES

[1] N. Karcanias and A.G. Hessami, 2010. Complexity and the notion of Systems of Systems: Part (I) General Systems and Complexity. Proc. of the 2010 World Automation Congress International Symposium on Intelligent Automation and Control (ISIAC) 19-23 September 2010, Kobe Japan.

[2] N. Karcanias and A.G. Hessami, 2010. Complexity and the notion of Systems of Systems: Part (II) Defining the notion of Systems of Systems. Proc. of the 2010 World Automation Congress International Symposium on Intelligent Automation and Control (ISIAC) 19-23 September 2010, Kobe Japan.

[3] N. Karcanias and A.G. Hessami, 2011. System of Systems Emergence: Part (I) Principles and Framework. Proc. of the ICETET 2011, 4th Internationa Cnference on Emerging Trends in Engineering and Technology, SV129, November 18-20, Port Louis, Mauritius.

[4] N. Karcanias and A.G. Hessami, 2011. System of Systems Emergence: Part (II) Synergetics Effects and Emergence. Proc. of the ICETET 2011, 4th Internationa Cnference on Emerging Trends in Engineering and Technology, SV129, November 18-20, Port Louis, Mauritius.

[5] E. Alonso, 2002. AI and Agents: State of the Art, AI Magazine, 23 (3), 529–551.

[6] E. Alonso, 2012. Actions and Agents. In K. Frankish and W. Ramsey (Eds.), The Cambridge Handbook of Artificial Intelligence, Chapter 5. Cambridge, England: Cambridge University Press.

[7] N. Jennings and M. Wooldridge, (eds.), 1998. Agent Technology: Foundations, Applications, and Markets. Berlin: Springer-Verlag.

[8] E. Alonso, M. d'Inverno, D. Kudenko, M. Luck and J. Noble, 2001. Learning in Multi-Agent Systems, Knowledge Engineering Review 16 (3), 277-284.

[9] M. Luck, P. McBurney, O. Shehory and S. Willmott (eds.), 2005. Agent Technology: Computing as Interaction (A Roadmap for Agent Based Computing). AgentLink III.

[10] M. Wooldridge, 2009. An Introduction to MultiAgent Systems, 2nd edition. Chichester, England: John Wiley & Sons.

[11] A. H. Bond and L. Gasser, Less (eds.), 1988. Readings in Distributed Artificial Intelligence. San Mateo, CA: Morgan Kaufmann Publishers.

[12] E. H. Durfee, 1988. Coordination for Distributed Problem Solvers. Boston: MA: Kluwer Academic.

[13] L. P. Kaelbling, M. Littman and A. Moore, 1996. Reinforcement Learning: A Survey, Journal of Artificial Intelligence Research 4: 237-285.

[14] G. Weiss, (ed.), 1999. Multiagent Systems: A Modern Approach to Distributed Artificial Intelligence. Cambridge, MA: The MIT Press.

[15] G. Weiss and P. Dillenbourg, 1999. What is 'multi' in multiagent learning?, in Pierre Dillenbourg (ed.), Collaborative learning. Cognitive and computational approaches (pp. 64–80), Oxford: Pergamon Press.

 ISBN: 978-1-61208-246-2

Decentralized State-Space Control Involving Subsystem Interactions

Dušan Krokavec and Anna Filasová
Department of Cybernetics and Artificial Intelligence
Technical University of Košice, Faculty of Electrical Engineering and Informatics
Košice, Slovakia
dusan.krokavec@tuke.sk, anna.filasova@tuke.sk

***Abstract*—The paper presents new points of view to the problems concerning the robust stability of a class of large-scale systems with subsystems interactions. The asymptotic stability conditions are formulated in terms of LMI while the impact of interconnection uncertainties is minimized using H_∞ approach. As results, a sufficient condition for the existence of solutions to this constrained stabilization problem is provided and a non-iterative algorithm for the control design solution is given.**

Keywords-Decentralized control; stabilizing conditions; linear matrix inequalities; control of power systems.

I. INTRODUCTION

The control of large-scale linear systems has been studied by many researchers. If the linear model of a large dynamic system is partitioned into interconnected subsystems, the interactions of the subsystem play significant role in global system stability and, if interactions contain uncertainties, expected performances cannot be attained if the control is designed only for the nominal models. The success of these methods can be improved if the system state are grouped so that subsystem interaction is minimized and the decentralized controllers are optimized with respect to interaction uncertainties. The first results for the existence of robust decentralized controllers mostly involve the conditions under which the interconnection matrix in the considered system satisfies the prescribed matching condition [14].

Recently, a number of efforts have been made to extend the application of robust control techniques using convex optimization, involving linear matrix inequalities (LMI). It is well known that LMI-based approaches [3] are powerful for a centralized control design, but, in the decentralized case, the control design task may not be reducible to a feasibility problem because of control law structural constraints.

To meet modern system requirements, controllers have to quarantine robustness over a wide range of system operating conditions and this further highlights the fact that robustness to interconnections and interaction uncertainties is one of the major issues. Applying for power systems control, the most important terms are robustness and a decentralized control structure [10]. The robustness issue arises to deal with uncertainties which mainly come from the varying network topology and the dynamic variation of the load. On the other hand, since a real-time information transfer among subsystems is unfeasible, decentralized controllers must be used. To achieve less-conservative control gains design conditions, norm-bounded unknown uncertainties in subsystem interactions, or nonlinear bounds of interconnections, are included in terms of design [6].

This paper is sequenced in eight sections and one appendix. Following the introduction in Section I, the second section places the results obtained within the context of existing requests. Section III briefly describes the problems concerning with control of the large-scale dynamical systems with subsystem interactions. The preliminaries, mainly focused on the H_∞ design approach and the bounded real lemma, are presented in Section III. Section IV provides the quadratic stability analysis of the controlled system by use of LMIs, and states the newly proposed conditions for the state controller design. Section V illustrates the controller design task by the numerical solution and the system stability analysis and Section VI draws some concluding remarks. Appendix is devoted to a model of the multi-area power systems, used in the illustrative example.

II. THE STATE OF THE ART

During the past two decades, there has been significant but scattered activity in control of the systems with interactions. A necessary and sufficient condition for solvability, for the case of fixed interconnections, has been found, e.g., in [4], [5], [15], where a homotopic method was used to reduce the control design to a feasibility problem of a bilinear matrix inequality (BMI). Moreover, if the LMI method is adopted by using a single Lyapunov function [1], [13], it leads to very conservative results.

The paper reflects the problems concerning with the system robust stability for one class of disturbed large-scale systems, in the presence of interconnection uncertainties among subsystems. The used approach is concentrated on

 ISBN: 978-1-61208-246-2

performance improvement of control systems and is a continuation of the earlier work started in [9], [12], especially motivated by the techniques presented in [2]. Comparing with the above mentioned articles, the merit of the results proposed in this paper relies on the conservatism reducing, the disturbance transfer function norm minimization, the system dynamics improvement and the decentralized control design simplification. This represents issues which lead to a newly formulated set of LMIs, giving the sufficient conditions for design of the decentralized controllers. Results are illustrated using the load frequency control model of the multi-area power systems.

III. Problem Formulation

To formulate the control design task, it is assumed that the subsystems are given adequately to (A.10), (A.11), i.e. for $i = 1, 2, ..., p$ it is

$$\dot{\boldsymbol{q}}_i(t) = \boldsymbol{A}_i \boldsymbol{q}_i(t) + \boldsymbol{b}_i u_i(t) + \sum_{l=1}^{p} \boldsymbol{G}_{il} \boldsymbol{q}_l(t) + \boldsymbol{f}_i d_i(t) \quad (1)$$

$$y_i(t) = \boldsymbol{c}_i^T \boldsymbol{q}_i(t) \quad (2)$$

where $\boldsymbol{q}_i(t) \in I\!R^{n_i}$ is the vector of the state variables of the i-th subsystem, $u_i(t), y_i(t) \in I\!R$ are input and output variables of the i-th subsystem, respectively, $\boldsymbol{A}_i, \boldsymbol{G}_{il} \in I\!R^{n_i \times n_i}$ are real matrices, $\boldsymbol{b}_i, \boldsymbol{c}_i, \boldsymbol{f}_i \in I\!R^{n_i}$ are real column vectors.

It is supposed that all states variables of a subsystem are observed or measured, pairs $(\boldsymbol{A}_i, \boldsymbol{b}_i)$ for all i are controllable, and the i-th subsystem is controlled by the local control law

$$u_i(t) = \boldsymbol{k}_i^T \boldsymbol{q}_i(t) \quad (3)$$

where $\boldsymbol{k}_i \in I\!R^{n_i}$ is a constant vector.

Writing, in general, the subsystem interconnections as

$$\boldsymbol{G}_i \boldsymbol{h}_i(\boldsymbol{q}(t)) = \sum_{l=1}^{p} \boldsymbol{G}_{il} \boldsymbol{q}_l(t) \quad (4)$$

where $\boldsymbol{h}_i(\boldsymbol{q}(t)) \in I\!R^{n_i}$ is a vector function, it is supposed that

$$\boldsymbol{h}_i^T(\boldsymbol{q}(t)) \boldsymbol{h}_i(\boldsymbol{q}(t)) \leq \varepsilon_i^{-1} \boldsymbol{q}^T(t) \boldsymbol{w}_i^T \boldsymbol{w}_i \boldsymbol{q}(t) \quad (5)$$

where $\varepsilon_i^{-1} > 0$, $\varepsilon_i \in I\!R$ is a scalar parameter, related to interconnection uncertainties in the system, and $\boldsymbol{w}_i$ are constant vectors of appropriate dimensions, as well as that

$$\boldsymbol{q}^T(t) = \begin{bmatrix} \boldsymbol{q}_1^T(t) & \boldsymbol{q}_2^T(t) & \cdots & \boldsymbol{q}_p^T(t) \end{bmatrix} \quad (6)$$

Using the above defined overall system state variable vector $\boldsymbol{q}(t)$, (5) can be written as

$$\sum_{l=1}^{p} \boldsymbol{h}_l^T(\boldsymbol{q}(t)) \boldsymbol{h}_l(\boldsymbol{q}(t)) = \boldsymbol{h}^T(\boldsymbol{q}(t)) \boldsymbol{h}(\boldsymbol{q}(t)) \leq \leq \boldsymbol{q}^T(t) \left[\sum_{l=1}^{p} \varepsilon_l^{-1} \boldsymbol{w}_l^T \boldsymbol{w}_l \right] \boldsymbol{q}(t) \quad (7)$$

The global system model with the subsystem interactions takes the form

$$\dot{\boldsymbol{q}}(t) = \boldsymbol{A}\boldsymbol{q}(t) + \boldsymbol{B}\boldsymbol{u}(t) + \boldsymbol{G}\boldsymbol{h}(\boldsymbol{q}(t)) + \boldsymbol{F}\boldsymbol{d}(t) \quad (8)$$

$$\boldsymbol{y}(t) = \boldsymbol{C}\boldsymbol{q}(t) \quad (9)$$

where

$$\boldsymbol{u}^T(t) = \begin{bmatrix} u_1(t) & u_2(t) & \cdots & u_p(t) \end{bmatrix} \quad (10)$$

$$\boldsymbol{y}^T(t) = \begin{bmatrix} y_1(t) & y_2(t) & \cdots & y_p(t) \end{bmatrix} \quad (11)$$

$$\boldsymbol{d}^T(t) = \begin{bmatrix} d_1(t) & d_2(t) & \cdots & \boldsymbol{d}_p(t) \end{bmatrix} \quad (12)$$

$$\boldsymbol{A} = \text{diag} \begin{bmatrix} \boldsymbol{A}_1 & \cdots & \boldsymbol{A}_p \end{bmatrix}, \ \boldsymbol{B} = \text{diag} \begin{bmatrix} \boldsymbol{b}_1 & \cdots & \boldsymbol{b}_p \end{bmatrix} \quad (13)$$

$$\boldsymbol{C} = \text{diag} \begin{bmatrix} \boldsymbol{c}_1^T & \cdots & \boldsymbol{c}_p^T \end{bmatrix}, \ \boldsymbol{F} = \text{diag} \begin{bmatrix} \boldsymbol{f}_1 & \cdots & \boldsymbol{f}_p \end{bmatrix} \quad (14)$$

$$\boldsymbol{G} = \text{diag} \begin{bmatrix} \boldsymbol{G}_1 & \cdots & \boldsymbol{G}_p \end{bmatrix} \quad (15)$$

where $\sum_{i=1}^{p} n_i = n$, $\boldsymbol{q}(t) \in I\!R^n$, $\boldsymbol{u}(t), \boldsymbol{y}(t) \in I\!R^r$, $\boldsymbol{A}, \boldsymbol{G} \in I\!R^{n \times n}$, $\boldsymbol{B}, \boldsymbol{F} \in I\!R^{n \times r}$ and $\boldsymbol{C} \in I\!R^{r \times n}$.

The goal is the designing the parameters of the control law

$$\boldsymbol{u}(t) = \boldsymbol{K}\boldsymbol{q}(t) = \text{diag} \begin{bmatrix} \boldsymbol{k}_1^T & \boldsymbol{k}_2^T & \cdots & \boldsymbol{k}_p^T \end{bmatrix} \boldsymbol{q}(t) \quad (16)$$

$\boldsymbol{K} \in I\!R^{r \times n}$, which rises up the stable large-scale system.

IV. Preliminary Results

Definition 1: Let the state-space model of the linear MIMO system is described by the vector differential equation

$$\dot{\boldsymbol{q}}(t) = \boldsymbol{A}\boldsymbol{q}(t) + \boldsymbol{B}\boldsymbol{u}(t) \quad (17)$$

and by the output relation

$$\boldsymbol{y}(t) = \boldsymbol{C}\boldsymbol{q}(t) + \boldsymbol{D}\boldsymbol{u}(t) \quad (18)$$

where $\boldsymbol{q}(t) \in I\!R^n$, $\boldsymbol{u}(t) \in I\!R^r$, and $\boldsymbol{y}(t) \in I\!R^m$ are vectors of the state, input and output variables, respectively, and $\boldsymbol{A} \in I\!R^{n \times n}$, $\boldsymbol{B} \in I\!R^{n \times r}$, $\boldsymbol{C} \in I\!R^{m \times n}$ and $\boldsymbol{D} \in I\!R^{m \times r}$ are real matrices.

The transfer function matrix $\boldsymbol{G}(s)$ of the system (17), with the output relation (18), is given as

$$\boldsymbol{G}(s) = \boldsymbol{C}(s\boldsymbol{I} - \boldsymbol{A})^{-1}\boldsymbol{B} + \boldsymbol{D} \quad (19)$$

Note, this definition is used only in the Section IV.

Proposition 1: If $\boldsymbol{M}$, $\boldsymbol{N}$ are matrices of appropriate dimension, and $\boldsymbol{X}$ is a symmetric positive definite matrix, then

$$\boldsymbol{M}^T\boldsymbol{N} + \boldsymbol{N}^T\boldsymbol{M} \leq \boldsymbol{N}^T\boldsymbol{X}\boldsymbol{N} + \boldsymbol{M}^T\boldsymbol{X}^{-1}\boldsymbol{M} \quad (20)$$

Proof: [11] Since $\boldsymbol{X} = \boldsymbol{X}^T > 0$, then

$$\left(\boldsymbol{X}^{-\frac{1}{2}}\boldsymbol{M} - \boldsymbol{X}^{\frac{1}{2}}\boldsymbol{N}\right)^T \left(\boldsymbol{X}^{-\frac{1}{2}}\boldsymbol{M} - \boldsymbol{X}^{\frac{1}{2}}\boldsymbol{N}\right) \geq 0 \quad (21)$$

$$\boldsymbol{M}^T\boldsymbol{X}^{-1}\boldsymbol{M} + \boldsymbol{N}^T\boldsymbol{X}\boldsymbol{N} - \boldsymbol{M}^T\boldsymbol{N} - \boldsymbol{N}^T\boldsymbol{M} \geq 0 \quad (22)$$

It is evident that (22) implies (20). ■

Proposition 2: (Quadratic performance) If a stable system is described by the stable transfer function matrix of the form (19) of the dimension $m \times r$, there exists such $\gamma > 0$, $\gamma \in I\!R$ that

$$\int_0^\infty (\boldsymbol{y}^T(v)\boldsymbol{y}(v) - \gamma \boldsymbol{u}^T(v)\boldsymbol{u}(v))\mathrm{d}v > 0 \qquad (23)$$

where $\boldsymbol{y}(t) \in I\!R^m$ is the vector of the system output variables, $\boldsymbol{u}(t) \in I\!R^r$ is the vector of the system input variables and γ is square of the H_∞ norm of the transfer function matrix of the system.

Proof: [8] It is evident from (19) that

$$\widetilde{\boldsymbol{y}}(s) = \boldsymbol{G}(s)\widetilde{\boldsymbol{u}}(s) \qquad (24)$$

where $\widetilde{\boldsymbol{y}}(s)$, $\widetilde{\boldsymbol{u}}(s)$ stands for the Laplace transform of m dimensional output vector and r dimensional input vector, respectively. Then (24) implies

$$\|\widetilde{\boldsymbol{y}}(s)\| \le \|\boldsymbol{G}(s)\|\|\widetilde{\boldsymbol{u}}(s)\| \qquad (25)$$

where $\|\boldsymbol{G}(s)\|$ is the H_2 norm of the system transfer function matrix $\boldsymbol{G}(s)$. Since H_∞ norm property states

$$\frac{1}{\sqrt{m}}\|\boldsymbol{G}(s)\|_\infty \le \|\boldsymbol{G}(s)\| \le \sqrt{r}\|\boldsymbol{G}(s)\|_\infty \qquad (26)$$

where $\|\boldsymbol{G}(s)\|_\infty$ is the H_∞ norm of the system transfer function matrix $\boldsymbol{G}(s)$, using notation $\|\boldsymbol{G}(s)\|_\infty = \sqrt{\gamma}$, the inequality (26) can be rewritten as

$$0 < \frac{1}{\sqrt{m}} \le \frac{\|\widetilde{\boldsymbol{y}}(s)\|}{\sqrt{\gamma}\|\widetilde{\boldsymbol{u}}(s)\|} \le \frac{\|\boldsymbol{G}(s)\|}{\sqrt{\gamma}} \le \sqrt{r} \qquad (27)$$

Thus, based on Parceval's theorem, (27) gives for $m \ge 1$

$$1 < \frac{\|\widetilde{\boldsymbol{y}}(s)\|}{\sqrt{\gamma}\|\widetilde{\boldsymbol{u}}(s)\|} = \frac{\Big(\int\limits_0^\infty \boldsymbol{y}^T(v)\boldsymbol{y}(v)\mathrm{d}v\Big)^{\frac{1}{2}}}{\sqrt{\gamma}\Big(\int\limits_0^\infty \boldsymbol{u}^T(v)\boldsymbol{u}(v)\mathrm{d}v\Big)^{\frac{1}{2}}} \qquad (28)$$

and subsequently

$$\int_0^\infty \boldsymbol{y}^T(v)\boldsymbol{y}(v)\mathrm{d}v - \gamma\int_0^\infty \boldsymbol{u}^T(v)\boldsymbol{u}(v)\mathrm{d}v > 0 \qquad (29)$$

It is evident that (29) implies (23). ■

Proposition 3: (Bounded real lemma) System described by (17), (18) is asymptotically stable with the quadratic performance $\|\boldsymbol{C}(s\boldsymbol{I}-\boldsymbol{A})^{-1}\boldsymbol{B}+\boldsymbol{D}\|_\infty \le \sqrt{\gamma}$, if there exist a symmetric positive definite matrix $\boldsymbol{P} \in I\!R^{n\times n}$ and a positive scalar $\gamma \in I\!R$ such that

$$\boldsymbol{P} = \boldsymbol{P}^T > 0, \qquad \gamma > 0 \qquad (30)$$

$$\begin{bmatrix} \boldsymbol{A}^T\boldsymbol{P}+\boldsymbol{P}\boldsymbol{A} & \boldsymbol{P}\boldsymbol{B} & \boldsymbol{C}^T \\ * & -\gamma^2\boldsymbol{I}_r & \boldsymbol{D}^T \\ * & * & -\boldsymbol{I}_m \end{bmatrix} < 0 \qquad (31)$$

where $\boldsymbol{I}_r \in I\!R^{r\times r}$, $\boldsymbol{I}_m \in I\!R^{m\times m}$ are identity matrices, respectively.

Here, and hereafter, $*$ denotes the symmetric item in a symmetric matrix.

Proof: (see. e.g. [3], [11]) Defining the Lyapunov function

$$\begin{aligned} v(\boldsymbol{q}(t)) &= \boldsymbol{q}^T(t)\boldsymbol{P}\boldsymbol{q}(t)+ \\ &+\int_0^t (\boldsymbol{y}^T(v)\boldsymbol{y}(v) - \gamma\boldsymbol{r}^T(v)\boldsymbol{u}(v))\mathrm{d}v > 0 \end{aligned} \qquad (32)$$

where $\boldsymbol{P} = \boldsymbol{P}^T > 0$, $\boldsymbol{P} \in I\!R^{n\times n}$, $\gamma > 0$, $\gamma \in I\!R$, and evaluating the derivative of $v(\boldsymbol{q}(t))$ with respect to t along the system trajectories, it yields

$$\begin{aligned} \dot{v}(\boldsymbol{q}(t)) &= \dot{\boldsymbol{q}}^T(t)\boldsymbol{P}\boldsymbol{q}(t) + \boldsymbol{q}^T(t)\boldsymbol{P}\dot{\boldsymbol{q}}(t)+ \\ &+\boldsymbol{y}^T(t)\boldsymbol{y}(t) - \gamma^2\boldsymbol{u}^T(t)\boldsymbol{u}(t) < 0 \end{aligned} \qquad (33)$$

Thus, substituting (3), (4) into (33) gives

$$\begin{aligned} \dot{v}(\boldsymbol{q}(t)) &= (\boldsymbol{A}\boldsymbol{q}(t) + \boldsymbol{B}\boldsymbol{u}(t))^T\boldsymbol{P}\boldsymbol{q}(t)+ \\ &+\boldsymbol{q}^T(t)\boldsymbol{P}(\boldsymbol{A}\boldsymbol{q}(t)+\boldsymbol{B}\boldsymbol{u}(t)) - \gamma\boldsymbol{u}^T(t)\boldsymbol{u}(t)+ \\ &+(\boldsymbol{C}\boldsymbol{q}(t) + \boldsymbol{D}\boldsymbol{u}(t))^T(\boldsymbol{C}\boldsymbol{q}(t) + \boldsymbol{D}\boldsymbol{u}(t)) < 0 \end{aligned} \qquad (34)$$

and with the notation

$$\boldsymbol{q}_c^T(t) = \begin{bmatrix} \boldsymbol{q}^T(t) & \boldsymbol{u}^T(t) \end{bmatrix} \qquad (35)$$

it is obtained

$$\dot{v}(\boldsymbol{q}(t)) = \boldsymbol{q}_c^T(t)\boldsymbol{P}_c\,\boldsymbol{q}_c(t) < 0 \qquad (36)$$

where

$$\boldsymbol{P}_c = \begin{bmatrix} \boldsymbol{A}^T\boldsymbol{P}+\boldsymbol{P}\boldsymbol{A} & \boldsymbol{P}\boldsymbol{B} \\ * & -\gamma\boldsymbol{I}_r \end{bmatrix} + \begin{bmatrix} \boldsymbol{C}^T\boldsymbol{C} & \boldsymbol{C}^T\boldsymbol{D} \\ * & \boldsymbol{D}^T\boldsymbol{D} \end{bmatrix} < 0 \qquad (37)$$

Since

$$\begin{bmatrix} \boldsymbol{C}^T\boldsymbol{C} & \boldsymbol{C}^T\boldsymbol{D} \\ * & \boldsymbol{D}^T\boldsymbol{D} \end{bmatrix} = \begin{bmatrix} \boldsymbol{C}^T \\ \boldsymbol{D}^T \end{bmatrix}\begin{bmatrix} \boldsymbol{C} & \boldsymbol{D} \end{bmatrix} \ge 0 \qquad (38)$$

applying Schur complement property to (38), (37) implies (31). ■

V. State Control Design

Theorem 1: The autonomous system from (8) is asymptotically stable with bounded quadratic performance if there exist symmetric positive definite matrices $\boldsymbol{P}_i \in I\!R^{n_i\times n_i}$ and positive scalars $\gamma_i, \lambda_i, \varepsilon_i \in I\!R$ such that

$$\boldsymbol{P}_i = \boldsymbol{P}_i > 0,\ \gamma_i > 0,\ \lambda_i > 0,\ \varepsilon_i > 0 \qquad (39)$$

$$\begin{bmatrix} \boldsymbol{\Phi} & \boldsymbol{P}\boldsymbol{B} & \boldsymbol{P}\boldsymbol{F} & \boldsymbol{C}^T & \boldsymbol{P}\boldsymbol{G} & \boldsymbol{w}_1 & \cdots & \boldsymbol{w}_p \\ * & -\boldsymbol{\Gamma}_u & \boldsymbol{0} & \boldsymbol{0} & \boldsymbol{0} & \boldsymbol{0} & \cdots & \boldsymbol{0} \\ * & * & -\boldsymbol{\Gamma}_d & \boldsymbol{0} & \boldsymbol{0} & \boldsymbol{0} & \cdots & \boldsymbol{0} \\ * & * & * & -\boldsymbol{I}_r & \boldsymbol{0} & \boldsymbol{0} & \cdots & \boldsymbol{0} \\ * & * & * & * & -\boldsymbol{I}_r & \boldsymbol{0} & \cdots & \boldsymbol{0} \\ * & * & * & * & * & -\varepsilon_1 & & \boldsymbol{0} \\ \vdots & \vdots & \vdots & \vdots & \vdots & & \ddots & \\ * & * & * & * & * & * & & -\varepsilon_p \end{bmatrix} < 0 \qquad (40)$$

for $i = 1, 2, \ldots, p$, where

$$\boldsymbol{\Phi} = \boldsymbol{A}^T\boldsymbol{P} + \boldsymbol{P}\boldsymbol{A} \qquad (41)$$

The matrices

$$\boldsymbol{P} = \text{diag}\left[\begin{array}{cccc} \boldsymbol{P}_1 & \boldsymbol{P}_2 & \cdots \boldsymbol{P}_p \end{array}\right] \tag{42}$$

$$\boldsymbol{\Gamma}_u = \text{diag}\left[\gamma_1 \ \cdots \ \gamma_p\right],\ \boldsymbol{\Gamma}_d = \text{diag}\left[\lambda_1 \ \cdots \ \lambda_p\right] \tag{43}$$

are structured matrix variables, and all system matrix parameter structures are given in (13)-(15).

Proof: Defining Lyapunov function as follows

$$v(\boldsymbol{q}(t)) = \boldsymbol{q}^T(t)\boldsymbol{P}\boldsymbol{q}(t)+ \\ +\int_0^t \big(\boldsymbol{y}^T(v)\boldsymbol{y}(v)-\sum_{h=1}^{p}\left(\gamma_h \boldsymbol{u}_h^T(v)\boldsymbol{u}_h(v)+\lambda_h \boldsymbol{d}_h^T(v)\boldsymbol{d}_h(v)\right)\big)\mathrm{d}v \tag{44}$$

where $v(\boldsymbol{q}(t)) > 0$, $\boldsymbol{P} = \boldsymbol{P}^T > 0$ is given in (42), and $\gamma_h > 0$, $\lambda_h > 0$, $h = 1, 2, \ldots p$, are introduced in (43). Evaluating the derivative of $v(\boldsymbol{q}(t))$ with respect to t along the autonomous system trajectories, it yields

$$\dot{v}(\boldsymbol{q}(t)) = \dot{\boldsymbol{q}}^T(t)\boldsymbol{P}\boldsymbol{q}(t) + \boldsymbol{q}^{\boldsymbol{T}}(t)\boldsymbol{P}\dot{\boldsymbol{q}}(t)+ \\ +\boldsymbol{y}^T(t)\boldsymbol{y}(t) - \left[\begin{array}{cc} \boldsymbol{u}^T(t) & \boldsymbol{d}^T(t) \end{array}\right]\boldsymbol{\Gamma}\left[\begin{array}{c} \boldsymbol{u}(t) \\ \boldsymbol{d}(t) \end{array}\right] < 0 \tag{45}$$

where with (43)

$$\boldsymbol{\Gamma} = \text{diag}\left[\begin{array}{cc} \boldsymbol{\Gamma}_u & \boldsymbol{\Gamma}_d \end{array}\right] \tag{46}$$

Thus, substituting (8), (9) into (45) gives

$$\dot{v}(\boldsymbol{q}(t)) = \boldsymbol{q}^T(t)\boldsymbol{C}^T\boldsymbol{C}\boldsymbol{q}(t)+ \\ +\big(\boldsymbol{A}\boldsymbol{q}(t)+\boldsymbol{B}\boldsymbol{u}(t)+\boldsymbol{G}\boldsymbol{h}(\boldsymbol{q}(t))+\boldsymbol{D}\boldsymbol{d}(t)\big)^T\boldsymbol{P}\boldsymbol{q}(t)+ \\ +\boldsymbol{q}^T(t)\boldsymbol{P}\big(\boldsymbol{A}\boldsymbol{q}(t)+\boldsymbol{B}\boldsymbol{u}(t)+\boldsymbol{G}\boldsymbol{h}(\boldsymbol{q}(t))+\boldsymbol{D}\boldsymbol{d}(t)\big)- \\ -\left[\begin{array}{cc} \boldsymbol{u}^T(t) & \boldsymbol{d}^T(t) \end{array}\right]\left[\begin{array}{cc} \boldsymbol{\Gamma}_u & \\ & \boldsymbol{\Gamma}_d \end{array}\right]\left[\begin{array}{c} \boldsymbol{u}(t) \\ \boldsymbol{d}(t) \end{array}\right] < 0 \tag{47}$$

Subsequently, using (20) with $\boldsymbol{X} = \boldsymbol{I}$, it can be written

$$\boldsymbol{h}^T(\boldsymbol{q}(t))\boldsymbol{G}^T\boldsymbol{P}\boldsymbol{q}(t)+\boldsymbol{q}^T(t)\boldsymbol{P}\boldsymbol{G}\boldsymbol{h}(\boldsymbol{q}(t)) \leq \\ \leq \boldsymbol{q}^T(t)\boldsymbol{P}\boldsymbol{G}\boldsymbol{G}^T\boldsymbol{P}\boldsymbol{q}(t)+\boldsymbol{h}^T(\boldsymbol{q}(t))\boldsymbol{h}(\boldsymbol{q}(t)) \tag{48}$$

and using (5), (48) gives

$$\boldsymbol{h}^T(\boldsymbol{q}(t))\boldsymbol{G}^T\boldsymbol{P}\boldsymbol{q}(t)+\boldsymbol{q}^T(t)\boldsymbol{P}\boldsymbol{G}\boldsymbol{h}(\boldsymbol{q}(t)) \leq \\ \leq \boldsymbol{q}^T(t)\boldsymbol{P}\boldsymbol{G}\boldsymbol{G}^T\boldsymbol{P}\boldsymbol{q}(t)+\boldsymbol{q}^T(t)\sum_{h=1}^{p}\varepsilon_h^{-1}\boldsymbol{w}_h^T\boldsymbol{w}_h\boldsymbol{q}(t) \tag{49}$$

Thus, with the notation

$$\boldsymbol{q}_c^{\bullet T}(t) = \left[\begin{array}{ccc} \boldsymbol{q}^T(t) & \boldsymbol{u}^T(t) & \boldsymbol{d}^T(t) \end{array}\right] \tag{50}$$

(47) can be rewritten as

$$\dot{v}(\boldsymbol{q}(t)) \leq \boldsymbol{q}_c^{\bullet T}(t)\boldsymbol{P}_c^{\bullet}\boldsymbol{q}_c^{\bullet}(t) < 0 \tag{51}$$

where

$$\boldsymbol{P}_c^{\bullet} = \left[\begin{array}{ccc} \boldsymbol{A}^T\boldsymbol{P}+\boldsymbol{P}\boldsymbol{A} & \boldsymbol{P}\boldsymbol{B} & \boldsymbol{P}\boldsymbol{F} \\ * & -\boldsymbol{\Gamma}_u & \boldsymbol{0} \\ * & * & -\boldsymbol{\Gamma}_d \end{array}\right] + \\ +\left[\begin{array}{ccc} \boldsymbol{C}^T\boldsymbol{C}+\boldsymbol{P}\boldsymbol{G}\boldsymbol{G}^T\boldsymbol{P} & \boldsymbol{0} & \boldsymbol{0} \\ * & \boldsymbol{0} & \boldsymbol{0} \\ * & * & \boldsymbol{0} \end{array}\right] + \\ +\sum_{h=1}^{p}\left[\begin{array}{ccc} \boldsymbol{w}_h^T\varepsilon_h^{-1}\boldsymbol{w}_h & \boldsymbol{0} & \boldsymbol{0} \\ * & \boldsymbol{0} & \boldsymbol{0} \\ * & * & \boldsymbol{0} \end{array}\right] < 0 \tag{52}$$

Since it yields

$$\left[\begin{array}{ccc} \boldsymbol{C}^T\boldsymbol{C} & \boldsymbol{0} & \boldsymbol{0} \\ * & \boldsymbol{0} & \boldsymbol{0} \\ * & * & \boldsymbol{0} \end{array}\right] = \left[\begin{array}{c} \boldsymbol{C}^T \\ \boldsymbol{0} \\ \boldsymbol{0} \end{array}\right]\left[\begin{array}{ccc} \boldsymbol{C} & \boldsymbol{0} & \boldsymbol{0} \end{array}\right] \geq 0 \tag{53}$$

$$\left[\begin{array}{ccc} \boldsymbol{P}\boldsymbol{G}\boldsymbol{G}^T\boldsymbol{P} & \boldsymbol{0} & \boldsymbol{0} \\ * & \boldsymbol{0} & \boldsymbol{0} \\ * & * & \boldsymbol{0} \end{array}\right] = \left[\begin{array}{c} \boldsymbol{P}\boldsymbol{G} \\ \boldsymbol{0} \\ \boldsymbol{0} \end{array}\right]\left[\begin{array}{ccc} \boldsymbol{G}^T\boldsymbol{P} & \boldsymbol{0} & \boldsymbol{0} \end{array}\right] \geq 0 \tag{54}$$

$$\left[\begin{array}{ccc} \boldsymbol{w}_h\varepsilon_h^{-1}\boldsymbol{w}_h^T & \boldsymbol{0} & \boldsymbol{0} \\ * & \boldsymbol{0} & \boldsymbol{0} \\ * & * & \boldsymbol{0} \end{array}\right] = \left[\begin{array}{c} \boldsymbol{w}_h \\ \boldsymbol{0} \\ \boldsymbol{0} \end{array}\right]\varepsilon_h^{-1}\left[\begin{array}{ccc} \boldsymbol{w}_h^T & \boldsymbol{0} & \boldsymbol{0} \end{array}\right] \geq 0 \tag{55}$$

then, applying Schur complement property to (53)-(55), (52) implies (40). ■

Theorem 2: The system (8), with output given by the relation (9), is stabilized with bounded quadratic performance via the controller (16) if there exist symmetric positive definite matrices $\boldsymbol{X}_i \in I\!R^{n_i \times n_i}$ and positive scalars $\gamma_i, \lambda_i, \varepsilon_i \in I\!R$ such that

$$\boldsymbol{X}_i = \boldsymbol{X}_i > 0,\ \gamma_i > 0,\ \lambda_i > 0,\ \varepsilon_i > 0 \tag{56}$$

$$\left[\begin{array}{cccccccc} \widetilde{\boldsymbol{\Phi}} & \boldsymbol{B} & \boldsymbol{F} & \boldsymbol{X}\boldsymbol{C}^T & \boldsymbol{G} & \boldsymbol{X}\boldsymbol{w}_1 & \cdots & \boldsymbol{X}\boldsymbol{w}_p \\ * & -\boldsymbol{\Gamma}_u & \boldsymbol{0} & \boldsymbol{0} & \boldsymbol{0} & \boldsymbol{0} & \cdots & \boldsymbol{0} \\ * & * & -\boldsymbol{\Gamma}_d & \boldsymbol{0} & \boldsymbol{0} & \boldsymbol{0} & \cdots & \boldsymbol{0} \\ * & * & * & -\boldsymbol{I}_r & \boldsymbol{0} & \boldsymbol{0} & \cdots & \boldsymbol{0} \\ * & * & * & * & -\boldsymbol{I}_r & \boldsymbol{0} & \cdots & \boldsymbol{0} \\ * & * & * & * & * & -\varepsilon_1 & & \boldsymbol{0} \\ \vdots & \vdots & \vdots & \vdots & \vdots & & \ddots & \\ * & * & * & * & * & * & & -\varepsilon_p \end{array}\right] < 0 \tag{57}$$

for all $i = 1, 2, \ldots, p$, where

$$\widetilde{\boldsymbol{\Phi}} = \boldsymbol{X}\boldsymbol{A}^T + \boldsymbol{A}\boldsymbol{X} - \boldsymbol{Y}^T\boldsymbol{B}^T - \boldsymbol{B}\boldsymbol{Y} \tag{58}$$

The matrices

$$\boldsymbol{X} = \text{diag}\left[\begin{array}{cccc} \boldsymbol{X}_1 & \boldsymbol{X}_2 & \cdots & \boldsymbol{X}_p \end{array}\right] \tag{59}$$

$$\boldsymbol{\Gamma}_u = \text{diag}\left[\gamma_1 \ \cdots \ \gamma_p\right],\ \boldsymbol{\Gamma}_d = \text{diag}\left[\lambda_1 \ \cdots \ \lambda_p\right] \tag{60}$$

are structured matrix variables, and all system matrix parameter structures are given in (13)-(15).

If the above conditions hold, the set of control gain matrices is given by

$$\boldsymbol{K} = \boldsymbol{Y}\boldsymbol{X}^{-1} = \left[\begin{array}{cccc} \boldsymbol{k}_1^T & \boldsymbol{k}_2^T & \cdots & \boldsymbol{k}_p^T \end{array}\right] \tag{61}$$

 ISBN: 978-1-61208-246-2

Proof: Inserting the global closed-loop system matrix $\boldsymbol{A}_c = = \boldsymbol{A} - \boldsymbol{BK}$ in (41) gives

$$\boldsymbol{\Phi} = \boldsymbol{A}^T\boldsymbol{P} - \boldsymbol{K}^T\boldsymbol{B}^T\boldsymbol{P} + \boldsymbol{PA} - \boldsymbol{PBK} \tag{62}$$

Defining the congruence transform matrix

$$\boldsymbol{T} = \text{diag}\left[\, \boldsymbol{P}^{-1} \;\; \boldsymbol{I}_r \;\; \boldsymbol{I}_r \;\; \boldsymbol{I}_r \;\; \boldsymbol{I}_r \;\; 1 \;\; \cdots \;\; 1 \,\right] \tag{63}$$

and pre-multiplying both side of the (40) by (63), the next LMIs are obtained

$$\begin{bmatrix} \widetilde{\boldsymbol{\Phi}} & \boldsymbol{B} & \boldsymbol{F} & \boldsymbol{P}^{-1}\boldsymbol{C}^T & \boldsymbol{G} & \boldsymbol{P}^{-1}\boldsymbol{w}_1 & \cdots & \boldsymbol{P}^{-1}\boldsymbol{w}_p \\ * & -\boldsymbol{\Gamma}_u & \boldsymbol{0} & \boldsymbol{0} & \boldsymbol{0} & \boldsymbol{0} & \cdots & \boldsymbol{0} \\ * & * & -\boldsymbol{\Gamma}_d & \boldsymbol{0} & \boldsymbol{0} & \boldsymbol{0} & \cdots & \boldsymbol{0} \\ * & * & * & -\boldsymbol{I}_r & \boldsymbol{0} & \boldsymbol{0} & \cdots & \boldsymbol{0} \\ * & * & * & * & -\boldsymbol{I}_r & \boldsymbol{0} & \cdots & \boldsymbol{0} \\ * & * & * & * & * & -\varepsilon_1 & & \boldsymbol{0} \\ \vdots & \vdots & \vdots & \vdots & \vdots & & \ddots & \\ * & * & * & * & * & * & & -\varepsilon_p \end{bmatrix} < 0 \tag{64}$$

$$\widetilde{\boldsymbol{\Phi}} = \boldsymbol{P}^{-1}\boldsymbol{A}^T - \boldsymbol{P}^{-1}\boldsymbol{K}^T\boldsymbol{B}^T + \boldsymbol{A}\boldsymbol{P}^{-1} - \boldsymbol{B}\boldsymbol{K}\boldsymbol{P}^{-1} \tag{65}$$

respectively. Introducing the LMI variables

$$\boldsymbol{P}^{-1} = \boldsymbol{X}, \quad \boldsymbol{K}\boldsymbol{P}^{-1} = \boldsymbol{Y} \tag{66}$$

then (66) implies (61), and (64), (65) implies (57), (58). ■

VI. Illustrative Example

To demonstrate the algorithm properties, the next subsystem parameters for $i = 1, 2, 3$ are used

$$\boldsymbol{A}_i = \begin{bmatrix} -12.50 & 0.00 & -5.21 & 0.00 \\ 3.33 & -3.33 & 0.00 & 0.00 \\ 0.00 & 6.00 & -0.05 & -6.00 \\ 0.00 & 0.00 & 1.10 & 0.00 \end{bmatrix}, \; \boldsymbol{b}_i = \begin{bmatrix} 12.5 \\ 0.0 \\ 0.0 \\ 0.0 \end{bmatrix}$$

$$\boldsymbol{c}_i^T = \begin{bmatrix} 0 & 0 & 1 & 0 \end{bmatrix}, \quad \boldsymbol{f}_i^T = \begin{bmatrix} 0 & 0 & -6 & 0 \end{bmatrix}$$

and

$$\boldsymbol{G}_{ih} = \begin{bmatrix} 0 & 0 & 0 & 0 \\ 0 & 0 & 0 & 0 \\ 0 & 0 & 0 & 0 \\ 0 & 0 & -0.55 & 0 \end{bmatrix}, \; \boldsymbol{g}_x = \begin{bmatrix} 0 \\ 0 \\ 0 \\ -0.55 \end{bmatrix}$$

$$\boldsymbol{G} = \text{diag}\left[\, \boldsymbol{g}_x \;\; \boldsymbol{g}_x \;\; \boldsymbol{g}_x \,\right]$$

$$\boldsymbol{w}_1^T = \begin{bmatrix} 0 & 0 & 0 & 0 & 0 & 0 & 1 & 0 & 0 & 0 & 1 & 0 \end{bmatrix}$$

$$\boldsymbol{w}_2^T = \begin{bmatrix} 0 & 0 & 1 & 0 & 0 & 0 & 0 & 0 & 0 & 0 & 1 & 0 \end{bmatrix}$$

$$\boldsymbol{w}_3^T = \begin{bmatrix} 0 & 0 & 1 & 0 & 0 & 0 & 1 & 0 & 0 & 0 & 0 & 0 \end{bmatrix}$$

Thus, solving (56), (56) with respect to the LMI matrix variables $\boldsymbol{X}$, $\boldsymbol{Y}_i$, $\gamma_i, \lambda_i, \varepsilon_i$, $i = 1, 2, 3$ using SeDuMi package for Matlab, the feedback gain matrix design problem was feasible with the results

$$\boldsymbol{Y}_i^T = \begin{bmatrix} -12.9516 & 1.4183 & 0.1961 & -3.4268 \end{bmatrix}$$

$$\boldsymbol{X}_i = \begin{bmatrix} 14.7389 & 2.7960 & -1.9062 & 3.6230 \\ * & 5.0205 & -1.7327 & 3.4803 \\ * & * & 2.2244 & -0.6127 \\ * & * & * & 3.6596 \end{bmatrix}$$

$$\gamma_i = 16.9863, \; \lambda_i = 15.5306, \; \varepsilon_i = 11.5833$$

giving the control law gain vectors

$$\boldsymbol{k}_i^T = \begin{bmatrix} -0.4870 & 3.5065 & 1.4243 & -3.5505 \end{bmatrix}$$

The decentralized closed-loop eigenvalues spectrum is

$$\rho(\boldsymbol{A}_{ch}) = \{-0.2646 \;\; -3.2126 \;\; -3.1578 \pm 11.9004\text{i}\}$$

and rises up the stable global system.

VII. Concluding Remarks

A new characterization for interaction bounds is presented and sufficient condition for stabilizing decentralized robust control design are formulated in the sense of the bounded real lemma. The optimization, involving structured matrix variables in the linear matrix inequalities, take into account the strong interactions among subsystems, as well as the interaction uncertainties. An illustration example is presented to show that such a procedure can simplify the decentralized control design.

Acknowledgement

The work presented in this paper was supported by VEGA, the Grant Agency of the Ministry of Education and the Academy of Science of Slovak Republic under Grant No. 1/0256/11. This support is very gratefully acknowledged.

References

[1] L. Bakule, "Decentralized control. An overview", *Annual Reviews in Control*, vol. 32, no. 1, pp. 87-98, 2008.

[2] G.K. Bekefadu and I. Erlich, "Robust decentralized controller design for power systems using convex optimization involving LMIs", in *Prepr. 16th IFAC Word Congress*, Prag, Czech Republic, pp. 1743-1743, 2005.

[3] B. Boyd, L. El Ghaoui, E. Peron, and V. Balakrishnan, *Linear Matrix Inequalities in System and Control Theory*, Philadelphia: SIAM, PE, USA, 1994.

[4] N. Chen, M. Ikeda, and W. Gu, *Int. J. Control, Automation, and Systems*, vol. 3, no. 2, pp. 143-151, 2005.

[5] C. Cheng, B. Tang, Y. Cao, and Y. Sun, "Decentralized robust H_∞ control of uncertain large-scale systems with state-delays. LMIs approach", *Proc. American Control Conference*, Philadelphia, PE, USA, pp. 3111-3115, 1998.

[6] C. Dou, J. Yang, X. Li, T. Gui, and Y. Bi, "Decentralized coordinated control for large power system based on transient stability assessment", *Int. J. Electrical Power & Energy Systems*, vol. 46, no. 1, pp. 153-162, 2013.

[7] O.I. Elgert and C.E. Fosha, "Optimum megawatt-frequency control of multiarea electric energy system", *IEEE Trans. Power Apparatus and Systems*, vol. 89, no. 4, pp. 556-563, 1970.

[8] A, Filasová and D. Krokavec, "Pairwise control principle in large-scale systems", *Archives of Control Sciences*, vol. 21, no. 3, pp. 227-242, 2011.

 ISBN: 978-1-61208-246-2

[9] A, Filasová and D. Krokavec, "Partially decentralized design principle in large-scale system control", in *Recent Advances in Robust Control. Novel Approaches and Design Methods*, A. Mueller Ed., Rijeca: InTech, Croatia, pp. 361-388, 2011.

[10] Y. Guo, D.J. Hill and Y. Wang, "Nonlinear decentralized control of large-scale power systems", *Automatica*, vol. 36, no. 9, pp. 1275-1289, 2000.

[11] D. Krokavec and A. Filasová, *Discrete-Time Systems*, Košice: Elfa, Slovakia, 2008. (in Slovak)

[12] D. Krokavec and A. Filasová, "Load frequency control involving subsystem interaction", in *Proc. 9th Int. Conf. Control of Power Systems CPS 2010*, Tatranske Matliare, Slovakia, pp. 1-8, 2010.

[13] J. Lunze, *Feedback Control of Large-Scale Systems*, Englewood Cliffs: Prentice Hall, NJ, USA, 1992.

[14] D.D. Siljak, D.M. Stipanovic, and A.I. Zecevic, "Robust decentralized turbine/governor control using linear matrix inequalities. *IEEE Trans. Power Systems*, vol. 19, no. 3, pp, 1096-1103, 2004.

[15] G. Zhai, M. Ikeda and Y. Fujisaki, "Decentralized H_∞ controller design. A matrix inequality approach using a homotopy method", *Automatica*, vol. 37, no. 4, pp. 565-572, 2001.

APPENDIX

The next analysis is based on the assumption that the electrical interconnections within each area of multi-area power system are so strong, at least in relation to ties with the neighboring areas that the whole area can be characterized only by a single frequency (see, e.g., [12] and the references therein). Therefore, it is supposed that the power equilibrium applied to the area i can be written as

$$T_{Pi}\frac{\mathrm{d}\Delta f_i(t)}{\mathrm{d}t} + \Delta f_i(t) + K_{Pk}\Delta P_{Tk}(t) = \\ = K_{Pi}\Delta P_{Gi}(t) - K_{Pi}\Delta P_{Di}(t) \tag{A.1}$$

where T_{Pi} is the area model time constant (s), $\Delta f_i(t)$ is the area incremental frequency deviation (Hz), K_{Pi} is the area gain (Hz/pu MW), $\Delta P_{Ti}(t)$ is the incremental change of total real power exported from area (Hz/pu MW), $\Delta P_{Gi}(t)$ is the incremental change in generator output (Hz/pu MW), and $\Delta P_{Di}(t)$ is the unknown load disturbance (Hz/pu MW).

If the line losses are neglected, the individual line powers can be written in the form

$$P_{Ti}(t) = \frac{|V_i||V_\upsilon|}{X_{\upsilon i}P_{\upsilon i}}\sin(\delta_i(t) - \delta_\upsilon(t)) = \\ = P_{Ti\upsilon\max}\sin(\delta_i(t) - \delta_\upsilon(t)) \tag{A.2}$$

$$V_i(t) = |V_i|\exp(j\delta_i(t)),\ V_\upsilon(t) = |V_\upsilon|\exp(j\delta_\upsilon(t)) \tag{A.3}$$

is the terminal bus voltage of the line, and $X_{\nu i}$ is its reactance.

If the phase angles deviate from their nominal values by amounts $\Delta\delta_i$, $\Delta\delta_\nu$, respectively, it can be obtained

$$\Delta P_{Ti}(t) = \\ = \frac{V_i||V_\upsilon|}{X_{\upsilon i}P_{\upsilon i}}\cos(\delta_{in}(t) - \delta_{\upsilon n}(t))(\Delta\delta_i(t) - \Delta\delta_\upsilon(t)) \tag{A.4}$$

$$\Delta P_{Ti}(t) = \\ = 2\pi\frac{|V_i||V_\upsilon|}{X_{\upsilon i}P_{\upsilon i}}\cos(\delta_{in}(t) - \delta_{\upsilon n}(t))\begin{Bmatrix}\int_0^t \Delta f_i(r)\mathrm{d}r - \\ -\int_0^t \Delta f_\upsilon(r)\mathrm{d}r\end{Bmatrix} \tag{A.5}$$

respectively. Related to the area frequency changes, the derivative of the individual line powers with respect to time is

$$\frac{\mathrm{d}\Delta P_{Tiv}(t)}{\mathrm{d}t} = S_{iv}(\Delta f_i(t) - \Delta f_v(t)) \tag{A.6}$$

$$\frac{\mathrm{d}\Delta P_{Ti}(t)}{\mathrm{d}t} = \sum_{i\neq l} S_{il}(\Delta f_i(t) - \Delta f_l(t)) \tag{A.7}$$

respectively, where S_{il} is the synchronizing coefficient (electrical stiffness of the tie line).

The incremental generated power of the area i for small signals around the nominal settings can be represented by the equations

$$T_{Ti}\frac{\mathrm{d}\Delta P_{Gi}(t)}{\mathrm{d}t} + \Delta P_{Gi}(t) = \Delta x_{Hi}(t) \tag{A.8}$$

$$T_{Hi}\frac{\mathrm{d}\Delta x_{Hi}(t)}{\mathrm{d}t} + \Delta x_{Hi}(t) = \Delta P_{Ci}(t) - \frac{1}{R_i}\Delta f_i(t) \tag{A.9}$$

where T_{Ti} is the turbine time constant (s), T_{Hi} is the governor time constant (s) (generator response is instantaneous), R_i is a measure of static speed droop (Hz/pu MW), $\Delta P_{Ci}(t)$ is the incremental change of command signal to the speed changer (control input), and $\Delta x_{Hi}(t)$ is the incremental change in the governor value position (pu MW), all with respect to the area i.

The compact form of (A.1), (A.7), (A.8), and (A.9) is [12]

$$\dot{\boldsymbol{q}}_i(t) = \boldsymbol{A}_i\boldsymbol{q}_i(t) + \boldsymbol{b}_i u_i(t) + \sum_{l=1}^{p}\boldsymbol{G}_{li}\boldsymbol{q}_i(t) + \boldsymbol{f}_i d_i(t) \tag{A.10}$$

$$y_i(t) = \boldsymbol{c}_i^T\boldsymbol{q}_i(t) \tag{A.11}$$

where

$$\boldsymbol{q}_i(t) = \left[\ \Delta x_{Hi}(t)\ \ \Delta P_{Gi}(t)\ \ \Delta f_i(t)\ \ \Delta P_{Ti}(t)\ \right]^T \tag{A.12}$$

$$u_i(t) = \Delta P_{Ci}(t) \qquad d_i(t) = \Delta P_{Di}(t) \tag{A.13}$$

$$\boldsymbol{A}_i = \begin{bmatrix} -\frac{1}{T_{Hi}} & 0 & -\frac{1}{R_i T_{Hi}} & 0 \\ \frac{1}{T_{Ti}} & -\frac{1}{T_{Ti}} & 0 & 0 \\ 0 & \frac{K_{Pi}}{T_{Pi}} & -\frac{1}{T_{Pi}} & -\frac{K_{Pi}}{T_{Pi}} \\ 0 & 0 & \sum\limits_{l\neq i} S_{il} & 0 \end{bmatrix} \tag{A.14}$$

$$\boldsymbol{G}_{li} = \begin{bmatrix} 0 & 0 & 0 & 0 \\ 0 & 0 & 0 & 0 \\ 0 & 0 & 0 & 0 \\ 0 & 0 & -S_{li} & 0 \end{bmatrix},\ \boldsymbol{b}_i = \begin{bmatrix} 0 \\ 0 \\ 0 \\ \frac{1}{T_{Hi}} \end{bmatrix} \tag{A.15}$$

$$\boldsymbol{f}_i = \begin{bmatrix} 0 \\ 0 \\ -\frac{K_{Pi}}{T_{Pi}} \\ 0 \end{bmatrix},\quad \boldsymbol{c}_i = \begin{bmatrix} 0 \\ 0 \\ 1 \\ 0 \end{bmatrix} \tag{A.16}$$

Under above given model parameters, the stability of the overall system can be studied by the stability properties of all subsystems, and by global features of all subsystem interactions.

Adaptivity of Business Process

Charif Mahmoudi
Laboratory of Algorithms, Complexity and Logics,
Paris 12th University
Créteil, France
charif.mahmoudi@u-pec.fr

Fabrice Mourlin
Laboratory of Algorithms, Complexity and Logics,
Paris 12th University
Creteil, France
fabrice.mourlin@u-pec.fr

***Abstract*— Enterprise service bus is a software architecture middleware used for implementing the interaction between software applications in a Service Oriented Architecture. We have developed a strategy to dynamically manage business processes. Administrators of service bus need to reconfigure sites where the business processes are placed. This evolution has to be done during execution of service through the bus. We ensure the availability of process definition. Moreover, business process can also be autonomous. This means a process which is able to move from one site to another one, where the business process engine is installed. This provides another approach to design business process. With our "mobile process migration" template, we separate two concerns, on one side architectural features and on the other side business features. The business process can become mobile between two service busses and we improve the availability of business processes.**

Keywords-business process; BPEL; orchestration; middleware; message exchange pattern; code migration.

I. INTRODUCTION

Today, companies have tools to model and automate business processes. This type of tools allows formalizing the company's business rules to automate decision-making, that is to say, the branch of the workflow to choose from, depending on the context. The objective of this initiative is to achieve a better overall view of all enterprise business processes and their interactions in order to be able to optimize and, wherever possible, to automate up with business applications.

The lifecycle of a business process can be roughly broken down as follows: design, modeling, implementation, execution, control, and optimization. An approach of Business Process Management (BPM) is based on tools such as a tool for process modeling, tools support the implementation, a runtime loaded to instantiate processes, management tools and reporting. These reports show accurate and relevant indicators on the current deployment of business process definitions. Our first remark is on the lack of scalability of this deployment. Thus, the load of messages that flow through the middleware clearly shows an unbalance that affects the entire information system. So the first point is: how to adapt the workflow running.

A second remark is about the number of messages exchanged increases as a function of the initial placement of business process definition. Thus, a business process using local services is less costly in a number of messages than a business process using remote services. Blockings are also less numerous, and, therefore, the execution of a business process is more efficient.

This remark highlights the dependencies between two concepts, the location of business processes and its own definition. The designer should not consider his work in the placement constraints. In addition, the administrator cannot take into account all the dependencies of a process definition to find a better placement. Also, our second point is: how separate the two. These conclusions led us to consider an initial configuration of business processes is not satisfactory. This placement must be scalable over time to adapt to client needs. The implementation of this idea is described in this paper through a technical framework described subsequently. It allows the validation of the concepts presented here and provides a sample application.

The content of the paper is structured as follows. First, the following section discusses work related to our topic. In Section 3, we provide the definitions on which our work is based. Next, we describe the technical framework of our work. Finally, we provide a simple case study to validate our approach. We end with a point on the goals achieved and those that remain to be addressed.

II. RELATED WORK

The construction of information systems is usually performed by the department, each business building a subsystem adapted to its own needs and supported by heterogeneous technologies, rarely interoperable. To quickly meet the growing computerization of procedures, systems integration issues has emerged, and with them two questions:

- How to trigger in response to an event in a given subsystem, a treatment in another subsystem that is foreign?
- How to ensure consistency and spread data across multiple subsystems?

A number of technical solutions have been found to answer these questions. The implementation of these integration solutions is most often done on an opportunistic basis, to meet the immediate goals of a particular application. As these ad hoc solutions have been implemented, the problems of localization or global management have emerged:

 ISBN: 978-1-61208-246-2

- Flows have increased, sometimes redundant, and the chains binding techniques;
- Increasing the coupling systems brought its share of problems, synthesized by the concept of spaghetti effect;
- Organizations have to solve new organizational challenges. If chains of responsibility were clear for each business subsystem, what about the relations between these business systems?

Two broad categories of solutions have emerged: the ETL (Extract Transform Load) tools, to synchronize data from multiple systems, and middleware solutions, to ensure communication "real time" between heterogeneous systems.

A. ETL middleware

ETL tools provide synchronization, consolidation and spread of data between disparate subsystems. Schematically, they extract data from the master system to update subsystem, after a suitable transformation. Although they can operate continuously, ETL tools are rather intended to treat plarge data set in deferred time, they appeared initially to ensure the loading of data warehouses [1].

Their relative simplicity of implementation is their greatest strength. They also allow a first level of structure of system information, pointing to the owners for master data. Coupled to pivot formats, ETL tools allow avoiding the pitfalls of point-to-point and functional coupling between systems too narrow.

Unfortunately, the ETL approach is focused exclusively on the data, and provides only elementary business semantics. It therefore fails to solve the integration process, and more to meet the challenges of service-oriented architectures. Service orchestration is useless with that kind of tool. R. Kimball explains [1] that the notion of business process does not appear with this family of tools.

B. Network centric middleware

Middleware solutions provide a technical infrastructure mediating between two or more systems. Their historical role is to transport a message from one subsystem to another, with a level of coupling more or less important. Appeared in the early 80s, MOM (Message Oriented Middleware) has an asynchronous semantics: the client constructs a message and sends it to the middleware, which handles the routing to one or more target systems. Communication is split into two, avoiding the coupling technique of participants. The guarantee of message delivery is entrusted to the MOM.

For many years, MOM remained largely proprietary solutions, forcing each part to find out how to interface with the broker, and limiting the ability of integration environments and languages supported by the publisher of the solution. JMS, the standard messaging of Java, has partially lifted this constraint, and CosNotification, the CORBA notification Service has remained confidential [2].

The MOM also offers routing capabilities often limited, requiring efforts to important configuration, each route must be explicitly defined, making their implementation difficult on a large scale. E. Curry investigates the use of POSA (Pattern-Oriented Software Architecture) interceptor pattern [2]. This facilitates dynamic changes to the behavior of the deployed platform but its scope is limited to a local domain.

Despite their respective qualities, MOMs and ORBs (Object Request Broker) [3] remain highly technical solutions. They allow both the spread and integration of data processing, but the semantics of trade remains basically point-to-point. The client must know the format of the message he sent to third party systems, this functional coupling systems is rapidly becoming a nightmare for maintenance and operation, especially if extended to all of the information system.

C. Enterprise Application Integration (EAI)

A new class of middleware has emerged: the EAI, a hub and spoke architecture, as opposed to network-centric architecture of MOMs and ORBs, in which a central component mediates between the client and physical target. This central component takes over all low-level technical issues (location, availability, cache, communication, and transformation, interoperability through specialized connectors, audit, track, security or transactions) [4]. Like ETL, they are further able to provide data transformation in order to limit the functional coupling between systems, and apply sophisticated routing policies.

In this role of super-connector and mediator, the EAIs have more than a conductor: the EAI can host high-level business processes, aggregating treatments performed in several subsystems. R. Abate explains that Service–Based Architectures (SBA) transform traditional EAI efforts to the new level.

Despite their obvious qualities, EAI solutions suffer from their own nature:

- The protocol used for exchange and transport of messages in an EAI, is specific.
- The technology inside the EAI is specific also. Thus, application access is done through connectors still largely peculiar to each vendor despite attempts at standardization as JCA in the Java world (these connectors still often are very expensive).
- The data formats and data used in EAI is specific.

The EAIs became a too complex brick covering too many responsibilities in information systems.

D. Enterprise Service Bus (ESB)

ESBs come directly from EAI. Just check the list of major publishers of ESB to be convinced: Bea [5], Tibco [5], Oracle [6], IBM [7], Apache [8] are precisely those involved in the EAI. Embodying the architectural features of EAI solutions, ESBs focus on the functions of interconnect and mediation, and base this on a set of standards including [9]:

- The Web Services to manage synchronous communications.
- XML to define message formats
- JMS to send an asynchronous communication with MOM.
- JCA to connect to software packages and exotic systems (ERP, CRM, Main-frames, etc.).

Today, the ESBs are technology integration and intermediate application for implementing a service-oriented

 ISBN: 978-1-61208-246-2

architecture. But, they remain an elegant and sophisticated technical solution attached to the questions of inter-application integration. Their use does not guarantee success or even the reality of the implementation of an SOA. Their administration is also quite complex. When an administrator moves the definition of a service, the consequences can be unexpected. Thus, a high-level change cannot be directly applied because the runtime context can be considered with attention. M.T. Schmidt highlights that service orchestration is a key concept for the management of business unit into a whole distributed system.

E. Mobile Agent Platform

Mobile agent platforms have been proposed as a useful support for building distributed applications. They present interesting advantages, such as autonomy, flexibility, and effective usage of network bandwidth. Due to these features, they have also been considered as an enabling technology for mobile, wireless and adaptable computing. Nowadays, mobile agents are still an important focus of interest.

Mobility can be used as a way to move the code instead of moving data. This is essential when the data is very large or when safety prohibits any transportation. In our work environment, mobility is seen as a means of administration between sites. Code management in distributed systems needs this ability to be responsive to change. Using mobile agents, tasks requiring a lot of processing must be custom built to distribute the load between computers [10].

Ilarri, et al. [10] explain how code mobility can be used to manage computing resources across a network of computers. When a resource is not available, an adaptation is to move to another site where the computation can continue. Because the problem occurs at a precise location, its management is locally taken into account and a migration of context is done. We consider that this concept is translatable into another domain like software bus.

III. WORKING CONTEXT

The context of our work focuses on the management of SOA. These architectures are currently the subject of interest for many software engineering teams. These architectures are particularly interesting because they use open standards. They offer more possibility of applying new software standards and rules and to have new assembly. As part of our work, we use business services that we assemble to build orchestrations of services. As part of a distributed system, these orchestrations use services on remote sites. This brings new problems of availability of services [11].

A. Orchestration of business services

Web services are defined in two contracts: the data contract (XML schema for the operation signature [12]), and the service contract (WSDL description [13]). Our approach to building services is a classic one; it is based on the construction of a contract as the first step of the software Lifecycle (Contract First). This is a pragmatic and business driven approach, because it stresses what is expected of the service and not how it will be implemented [14]. We follow three steps for building a contract first Web service:

- The definition of service contract
- The writing of service endpoint
- The configuration of the endpoint

We adopt a similar approach to construct the definition of service composition. In other words, the coarse grain services are based on those of finer grains. We chose WS-BPEL [15] as orchestration language because it is well famous for defining business processes describing Web services interactions. Thus, we build a service oriented solution utilizing Web services with WS-BPEL, and we apply two phases:

- Build Web services as previously and then publish them to be utilized within a business process
- Compose the Web services into orchestration flows with WS-BPEL.

A first important difference between these levels is on the service status. If a service is said to be stateless, it is not the same for a composition of services regardless of the state. Thus the interpretation of a service composition requires consideration of a specific execution context. We use an orchestration engine to manage WS-BPEL scripts.

When we define an assembly of services, we depict the coordination by the logical algorithm into a WS-BPEL business process. Into a context of academic library, an orchestration is defined for the registration of a new member. The business algorithm schedules a sequence of steps: record the civility, record the profile, print member card, notifies by email the validation of registration. Each step is considered as its WSDL description.

So, we can create an orchestration to be used as a service within another, larger orchestration.

B. Use of business process with a bus

The orchestration of composite services in existing techniques is usually centralized. This is due to the features of participating services which are distributed and autonomous. A centralized orchestration model has several drawbacks with respect to scalability and availability [16]. Because of Web service characteristics are highly dynamic, autonomous and distributed, we believe that orchestration of services can be interpreted in a more dynamic way.

To make a more dynamic interpretation, it is essential to have several BPEL engines. These engines are distributed over network, for instance at least one per service bus. Thus, we define a start and arrival point. In addition, we need a way to communicate between these two points. In our context, the notion of message is known. Each operation on a BPEL description can be seen as a particular message transmitted between one or more engines. As an example, interpretation is a consequence of an input message, migration also. We consider that an intelligent routing of these messages is able to provide the dynamic interpretation. This is done by a software bus.

We decided to use an ESB because it is the technical frame where all parts of our work can be gathered: several BPEL engines, binding components and service engines (Figure 1). But monitoring tools can be added and other ESBs which can be connected into a larger distributed system. First, we started by designing a move operation of

 ISBN: 978-1-61208-246-2

business processes from one site (called Group1) to another one.

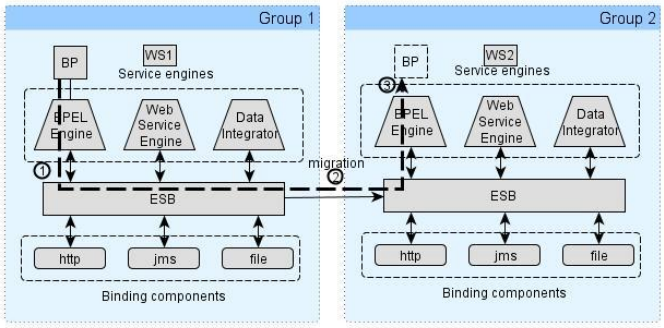

Figure 1. Relation between two ESBs

This technical operation can be considered as a kind of management operation into a large distributed system. Our nominal scenario is triggered by an event which highlights (1) that a business process called BP needs to be moved from Group 1 ESB to Group 2 ESB. Because both ends of the exchange are known, a route can be built (dashed line) and BPEL script can be downloaded (2) from a local repository to Group2 ESB. Then, this script is activated through the local BPEL engine (3). Finally an interpretation can be done by another engine.

This approach has drawbacks. In terms of safety, it is necessary that the issuer of travel demand (on a BSE Group) has a role as it has the permission to publish a definition of business processes on BSE Group 2. These non-functional constraints are taken into account in a real context.

To manage dependencies, it is important to check that the definition of business processes that is moved contains no dependence on the BPEL engine that used it originally. If this were the case would cause a shift in an execution failure in the Group 2 sites.

C. Administration of services into an ESB

The description of this management operation highlights the steps of routing. We thought a good way to automate this process is the definition of a dedicated BPEL script. Thus, we define a set of operations on the business process definitions. They focused on adding, moving, copying, deleting BPEL definition (Figure 2). The design of these operations requires an understanding of the functioning of an ESB to make the most of the modules already active. If the administrator is considered the trigger of management actions, it is the purpose of simplification, because other actors may be able to: an event configuration of ESB, a demand from the business process itself, etc.

Compared to the various modules that make up an ESB, the steps for interpreting a functionality such as "moving a business process', requires the use of the routing module, the XML transformation module, the message queue manager and the BPEL interpreter. In the scope of this document, we only interact with BPEL script, which are not under execution. If it is, such operations like “move” are postponed until the end of the execution.

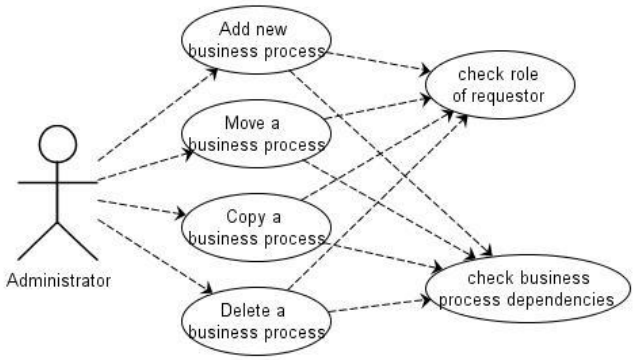

Figure 2. Use case diagram of BP management

Figure 3 describes the activity diagram of the move operation. After selecting a business process definition into the repository of a BPEL engine, its definition is parsed to detect conflicts. This operation is realized by applying technical rules onto the BPEL script. Then, the route builder is invoked to define a new route between source engine and target engine. This route is engaged and can be used for the migration of business process. Because controls have been done successfully, the BPEL can be downloaded from the intern repository into the working directory of the new BPEL engine. By the end of this action, the process has to be activated.

Then, the route is used to transfer input messages from source site to the target site. This step can be optional if we consider the operation as a clone operation to divide the traffic by two. Finally, the business process definition can be instantiated by the target engine. This instance can accept input messages previously sent to another site. The state of this instance is managed by a new BPEL engine. It may be suspended, in which case it is counted as suspended and not active. If an error occurs that does not cause the process to complete, but requires attention, the process is counted in error instead of active. If a process is terminated with the exit activity, it counts as terminated. As shown in Figure 3, only the migration of the definition is described and not the treatment of the input messages which is the normal process of a BPEL engine.

The activity diagrams of other management operations follow the same schedule even if the core actions are totally distinct. Preconditions of all operations are quite similar and there is no invariant about their applications. This set of operations is the basis of our approach of adaptability of business process. Our analysis is completed by requirements about no functional properties which are essential in a large distributed system. They specify global constraints on how the software operates: no blocking, authentication with role names, asynchronous message exchange, etc. These constraints are guidelines for our realization. No functional properties have a global nature, in opposite to local effects of functional requirements. In that case, the modification of a single bundle of the distributed system may affect the integrity of the entire application with respect to a particular

 ISBN: 978-1-61208-246-2

no functional feature, such as asynchronous communication. In next section, we focus our choices with technical aspects.

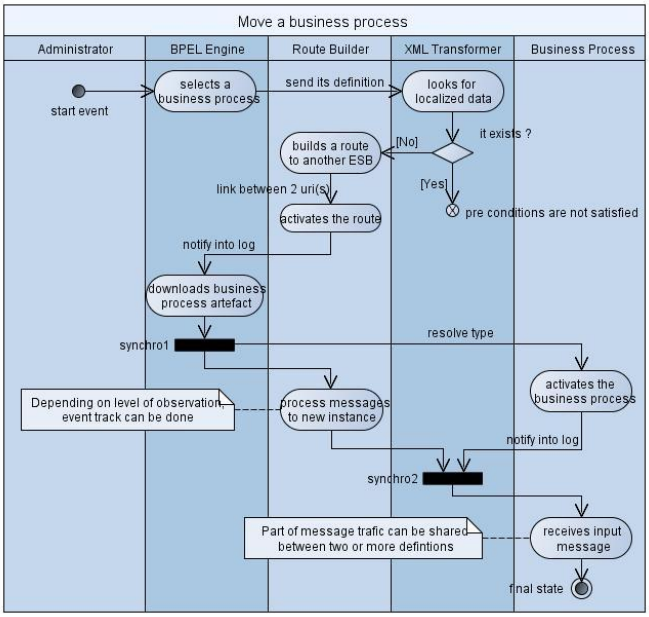

Figure 3. Activity diagram of "move business process"

IV. TECHNICAL APPROACH

Our past experience in distributed systems is based on pragmatic approach. Also, we build a prototype, because it is a true validation of our ideas. In the context of this document we use an ESB called Apache ServiceMix because it is a reference in the world of open source solution [17] and also because we participate to the evolution of this Apache project.

A. Description of technical context

Our chosen ESB allows building ESBs clustering and also linking several ESB through message queues. Several software architectures are possible and we used a cluster for the case study. The container can provide failover strategy and a configuration can be set at load time. The deployment of service units and binding components is dynamic and the Lifecycle of business objects can be managed through a programmatic API.

ServiceMix is often coupled with Apache ActiveMQ for message queues management, Apache Camel for the route management, Apache CXF, as a web service engine and Apache Ode as BPEL engine. Because all these modules are written in Java, a JMX console is used to display attributes and operations of managed Beans. These are the main modules of this bus but they rely on OSGi server called Apache Karaf which is the kernel of the ESB (Figure 4).

Thus, our project is composed of five elements which will be exploited by ServiceMix bundles.

1. The context description is an XML file which used to create all objects of the scenario. It also injects code to setup and to configure them.

2. Because, all communications are asynchronous, each part of our solution is equipped with an input message and an output message queue. These message containers are defined by a URI (Unique Resource Identifier). A URI can be an end of a route.

3. A set of routes which contains at least one route from a source business process to a target which is the business process after its migration. Both are identified by a URI.

4. A BPEL script which defines the migration procedure. It can be duplicated onto all BPEL engines of the distributed system. Another solution is to define a migration procedure per BPEL engine. This can be useful whether business processes have preconditions before moving.

5. A set of externalized rules which checks whether a business process can be moved from one engine to another one. Because a BPEL definition is first of all an XML stream, a rule is written with XSL-T language. This allows changing dynamically the rules even if the bus is running. The goal of these rules is to express if a BPEL definition depends on local resources, such as low level API or specific codes.

All the modules are assembled into an artifact which is deployed into the input folder of the ESB (ServiceMix). A first observation of the log console allows the administrator to understand if the XML descriptors of the artifact are valid. Next, we explain the deployment step and the role of message exchange.

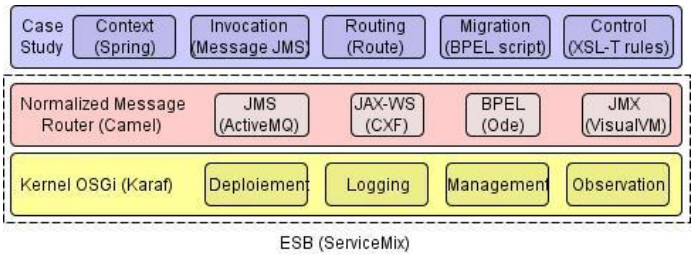

Figure 4. Layer description of our project

B. Role of normalized message

The normalized message router (NMR) is responsible for mediating messages between all the modules which are deployed into the ESB. The deployed modules do not exchange messages directly between each other. Instead, they pass messages to the normalized message router. The role of the router is to deliver the messages to the right endpoints. All functionalities are declared through its endpoint. Endpoints provides clients with access to business process. It is possible to define one or more endpoints for a service by using a combination of relative and absolute endpoint addresses.

Also, when a client sends a request to a business process, it is first received by a binding component. In our context, a client could be a traditional application, a tool like SOAP-UI or another module deployed into the ESB. The binding components are used to provide transport level bindings for the deployed processes. The normalized message model

 ISBN: 978-1-61208-246-2

decouples the service client from the service providers. The message format is defined using WSDL, which describe the called operations.

A normalized message is a generalized format used to represent all of message data passed through the NMR. It consists of three parts: meta-data and properties, payload, attachments. The binding components are responsible for normalizing all of the messages placed into the NMR. Binding components normalize messages received from external clients before passing them to the NMR. Messages sent across the NMR are not persisted anywhere but we can modify the process to write these to a database using the Data Base binding component or otherwise.

Then the message is delivered to a service unit like a BPEL engine or another module deployed into ServiceMix. Service units can be grouped into an aggregate deployment file called a service assembly. This file includes a deployment descriptor that indicates the target component for each service unit.

C. Functional requirements

The BPEL engine treats requests and instantiates process as needed except if there is rules which need management operations. In our scenario, the called process is used to register conference inscription. We added a rule that limits the number of instances. The value of this limit is one, because this triggers easily a move operation of business processes. So, this triggers our BPEL process called MAH process, this is the main line of the management operation. As mentioned in Figure 3, first a web service applies a sequence of rules to build a diagnostic. In this example, the answer is affirmative.

The first part of the MAH business script as shown in (figure 5) the dependencies of the definition with two partner links which are mentioned previously. Because all these partner links are valid, the evaluation can be done by the BPEL engine.

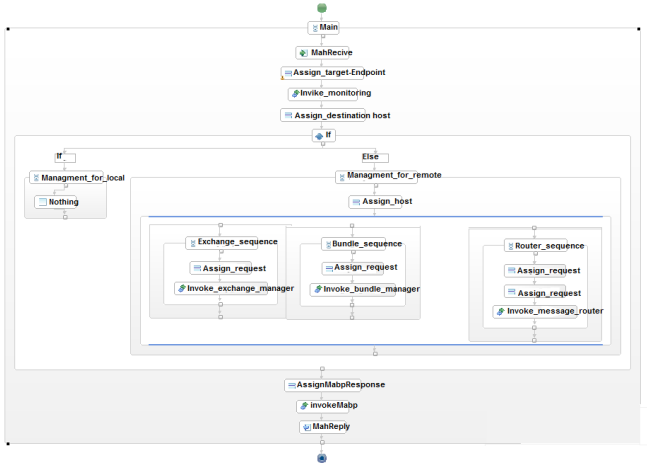

Figure 5. Design of the migration business process

V. CASE STUDY AND RESULTS

Our case study focuses on the migration of a process making two calls to web services by "localhost" because it is assumed that for security constraints, the server only accepts local connections. The process will make an initial local call to retrieve the result of the invocation of the first web service. The process will then migrate to the host which exposes the second web services in order to invoke this web service locally. The core of the definition of BPEL processes MAH is the red line of the script: each sub-process manages a step towards translating the script from one node to another. Thus the interpretation of the orchestration is not monopolized by the BPEL engine since the MAH manages the mobility aspect.

A. Evaluation of our test case

The evaluation of the sequence of actions starts with a message about a business message to move.

```
<receive name="mahReceive"
    createInstance="yes"
    operation="MAH"
    partnerLink="MAHPartnerLink"
    portType="mah:MAHPortType"
    variable="mahRequest"/>
```

Figure 6. Test BPEL request

This request identifies the process to move and also to check the technical rules such as the initiation of remote communication with the MAH as a prerequisite. Multiple Web services are used to prepare the management operation; they are exposed by the MAH: they can transport the process to enable message routing normalized and manage ongoing exchanges with the process.

Since the first invocation does not require migration, the role of the MAH will be transparent. The second invocation will require the execution of various technical tasks mentioned in the previous paragraph since the target web services is identified as external to the host.

B. Observation of the migration process

Tracking the evolution of the migration is essential to decide whether controls are applied at the right time. Moreover, it allows also summing up when administrator wishes it to know the path of a business process during a period of time:

```
  <bpel:invoke name="Invoke_monitoring"
operation="GETINFO"
    inputVariable="MonitoringRequest"
outputVariable="MonitoringResponse"
    partnerLink="MonitoringPartnerLink"
portType="mo:MonitoringPortType" />
```

Figure 7. Service invocation

 ISBN: 978-1-61208-246-2

Each step of the migration process is monitored by observation services which write into log files what happens during the migration process.

C. Impact on the other management operations

When the migration business process is evaluated by BPEL engine, a set of tools is deployed as mentioned previously. The ESB's console (Figure 8) show all the elements which are built to achieve the move of a business process.

The following figure displays a route module, several web services (these elements are outlined in red color), binding component also.

Of course, this figure shows a snapshot about what it is currently deployed by the end of the migration process. Some elements could be reused for another migration but it is not the case in this case study.

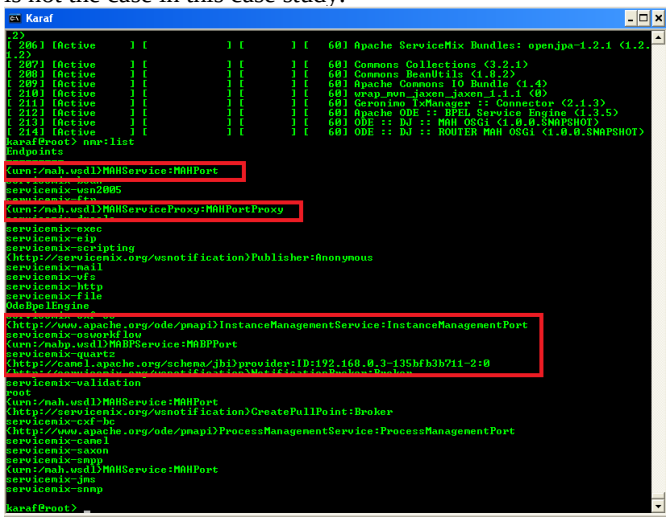

Figure 8. Console of ServiceMix ESB

VI. CONCLUSION AND FUTURE WORK

To sum up, we have described the life cycle of our approach of business process management. First, we have shown how it is possible to move a description from one server to another one into a cluster of servers. Then we have detailed how we have prototyped it as a specific BPEL process which is a conductor of a reconfiguration of the client business.

Next, we gave results about our experiments. Because this work uses dynamicity, it is not easy to highlight mobile feature, but we wanted to stress that all steps of our approach are taken into account. This validate that our approach is useful and also that ESB are servers which can exploit mobility as an ability to do an adaptation during execution.

We have realized other management operations but all these operations operate on business process definition and not on process instantiations. Also, we are working now on the mobility of instances of business processes and how to move an execution context without perturbation. We will focus on extending our approach to other orchestration languages like CAMEL DSL [18]. Our first goal is to enrich Java DSL's routing for managing dynamic mobile processes. Camel is based on the separation between aspects "definition" and "execution" of business processes. Camel business processes are based on a sequence of EAI, it allows us to add a new pattern "Migrate" which may be declared in Camel DSL and will be provided at runtime by a mechanism of self-transfer of business processes to the target host. Our second goal is to construct a formal specification in "pi-calculus" [19] of Camel's engine using the approach based on business specification [20] to highlight the mobility aspect added. Thus, the result demonstrated that the reduction leads to a transparent migration from an external point of view.

REFERENCES

[1] J. Caserta and R. Kimball, "Data Warehouse ETL Toolkit: Practical Techniques for Extracting, Cleaning, Conforming, and Delivering Data", 2004 , ISBN-10: 0764567578

[2] E. Curry, D. Chambers, and G. Lyons, "Extending Message-Oriented Middleware using Interception", presented at Third International Workshop on Distributed Event-Based Systems (DEBS '04), ICSE '04, Edinburgh, Scotland, UK, 2004.

[3] D. C. Schmidt, D. L. Levine, and S. Mungee, "The Design and Performance of Real-Time Object Request Brokers," *Computer Communications*, vol. 21, pp. 294–324, Apr. 1998.

[4] R. Abate, J. P. Burke and P. Aiken "Eai with Service-Based Architectures", 480 pages, John Wiley & Sons (Oct 2002), ISBN: 0471415154

[5] I. Charlesworth and T. Jones, "The EAI and Web Services Report", EAI Journal, 2003, pp. 11-18.

[6] J. LEE, K. SIAU and S. HONG (2003) Enterprise Integration with ERP and EAI. Communications of the ACM 46(2), pp 54–60.

[7] L. Gavin, G. Diederichs, P. Golec, H. Greyvenstein, K. Palmer, S. Rajagopalan, and A. Viswanathan, An EAI Solution using WebSphere Business Integration (V4.1), ISBN: 0738426547, 2003

[8] P. Kolb. Realization of EAI patterns in Apache Camel. Student research project, University of Stuttgart, 2008.

[9] M.T. Schmidt, B. Hutchison, P. Lambros, and R. Phippen. "The enterprise service bus: Making service-oriented architecture real". IBM Systems Journal, 44 (4): pp 781–797, 2005.

[10] S. Ilarri, R. Trillo, and E. Mena, "SPRINGS: A scalable platform for highly mobile agents in distributed computing environments," in Fourth International WoWMoM 2006 Workshop on Mobile Distributed Computing (MDC'06), Niagara Falls/Buffalo, New York, USA. IEEE Computer Society, June 2006.

[11] J. Waldo, A. Wollrath, and S. Kendall. "A Note on Distributed Computing". Springer Verlag. 1994.

[12] E. Christensen, F. Curbera, G. Meredith, S. Weerawarana: Web Services Description Language (WSDL) 1.1,15 March 2001. http://www.w3.org/TR/wsdl, retrieved: December, 2012.

[13] J. Farrell, H. Lausen "Semantic Annotations for WSDL and XML Schema", W3C Rec., Aug. 2007.

[14] S. Loughran and E. Smith. "Rethinking the Java SOAP Stack". May 17, 2005. Copyright © 2005 IEEE Telephone Laboratories, Inc..

[15] Web Service Business Process Execution Language Version 2.0, Working Draf, July 2005, OASIS Technical Committee, available via http://www.oasis-open.org/committees/wsbpel, retrieved: December, 2012.

[16] Q. Chen and M. Hsu. "Inter-Enterprise Collaborative Business Process Management". In Proc. of 17th International Conference on Data Engineering (ICDE'01), IEEE Computer Society, April 2001, pp 253-260.

 ISBN: 978-1-61208-246-2

[17] B. A, Christudas, "Service Oriented Java Business Integration" (1st ed.), Packet publishers, (August 13, 2008), pp. 436, ISBN 1847194400.

[18] C. Ibsen and J. Anstey. “Camel in Action”. Manning, 2010, pp. 113–122.

[19] R. Milner, J. Parrow, and D. Walker. A Calculus of Mobile Processes, Parts I and II. Volume 100 of Journal of Information and Computation, 1992, pp 1-77.

[20] C. Mahmoudi and F. Mourlin. International Conference on Software Engineering Advances, thinkmind , Lisboa 2012, pp 197-204.

 ISBN: 978-1-61208-246-2

Experimentation System for Evaluation of Heuristic Algorithms to Solving Transportation Problem

Kacper Rychard, Wojciech Kmiecik, Leszek Koszalka, and Andrzej Kasprzak
Department of Systems and Computer Networks
Wroclaw University of Technology
Wroclaw, Poland
e-mail: 170866@student.pwr.wroc.pl, {wojciech.kmiecik, leszek.koszalka, andrzej.kasprzak}@pwr.wroc.pl

***Abstract*—In this paper, we focus on transportation problem and different approaches to solving it. The main goal of the research was to determine accuracy and efficiency of the most popular algorithm solving the transportation problems and to test two heuristic algorithms. The additional objective was to test the optimization algorithm depending on the solution given as an input – comparison of optimizing the simple solution and the heuristic outputs. Our studies show that the processing time needed by the optimization algorithm depends on the input solution and its accuracy mostly. The experiments resulted with a complete comparison of the algorithms and a possibility to evaluate the advantages of using each one of them.**

Keywords-transportation problem; heuristic algorithms; cost reduction; experimentation system

I. INTRODUCTION

The transportation problem is a well-known issue that almost every company faces. Basically the main problem is how to move goods from group of *m* locations (for the purposes of this paper called 'factories') to *n* places ('warehouses') in a way that minimizes the total cost of transportation [1]. Main assumptions of the problem are that the cost of transportation between given factory and warehouse depends on the quantity of goods transported (all the unit costs are known) and the acceptable solution is the one that satisfies supplies of all factories and demands of all warehouses without the negative values of allocations [2].

An example graph illustrating the problem is shown in Fig. 1.

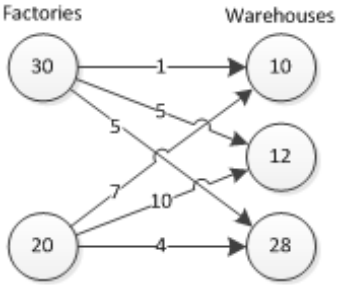

Figure 1. Example graph illustrating the transportation problem.

The factories and warehouses are represented by circles and the numbers they contain respectively stand for the factories' supplies and warehouses' demands. The arrows are meant to represent the shipping links and the numbers placed on them are the unit costs [3].Usually the matrix of costs is used to completely describe the problem. It comes with two vectors representing the supplies of the factories and the demands of the warehouses.

The problem can be defined [4] by a set of formulas:

- $C(X) = \sum_{i=1}^{m} \sum_{j=1}^{n} c_{ij} x_{ij} \rightarrow \min$, (1)
- $\sum_{j=1}^{n} x_{ij} = s_i$, (2)
- $\sum_{i=1}^{m} x_{ij} = d_j$, (3)
- $x_{ij} \geq 0 \quad i = 1,2,...,m \quad j = 1,2,...,n$. (4)

The above expressions state as following:

(1) The total cost of the problem should be minimal, where *C(X)* is the total cost, c_{ij} are the unit costs and x_{ij} represent allocations,
(2) The total amount of goods sent form each factory should be equal to its supply where s_i are the factories' supplies,
(3) The total amount of goods sent to each warehouse should be equal to its demand where d_j is the warehouses' demands,
(4) All allocations should be non-negative.

The current papers treating the problem focus, inter alia, on the advanced modifications of the problem such as:

- Bi-criterion Transportation Problem [5],
- Fuzzy Transportation Problem [6],
- New methods of solving transportation problems [7].

Our work concerns the methods of solving the original problem and profitability of the heuristic approach used.

The rest of paper is organized as follows. Section II presents the most popular algorithms for solving the transportation problem and a short description of how they work with the most important pros and cons of using them. One authorial algorithm is described as well. Section III is a short brief about the environment of the experiments and a close-up look at the created testing tool. Section IV consists of the design of the experiments and their results with comments. This section presents the way of how the tool can be used and what information it can be used to gather. The Section V concludes the work. It also contains the plans for

 ISBN: 978-1-61208-246-2

the future work and the development process of the application.

II. ALGORITHMS FOR SOLIVING TRANSPORTATION PROBLEM

The algorithms tested in the paper as well as the additional objective are shown in the Table 1.

A. North-West Corner rule (NWC)

The most basic way of finding the solution of the problem is setting the maximum possible amount transport in each shipment link given. The maximum is calculated as the smaller number from the supply of the factory and demand of the warehouse linked. The links are considered in a sequence as they appear in the matrix of a problem. This method is supposed to provide a fast way of achieving a possible but not necessarily efficient solution [8].

B. Cheap Means More (CMM)

The idea of the first heuristic algorithm is to sort the connections by the unit cost and use the cheapest ones first, setting the amount of transportation as a maximum possible [9]. However, it is not likely to use this method to provide the final solution. The idea of using *CMM* as a heuristic algorithm is novel. Main advantages of this approach are the simplicity, quickness and way better solution than the *NWC*. Whilst *NWC* is not deterministic, *CMM* algorithm is (assuming that all unit costs of transportations are different, which means there is only one possible output of the sorting). The solution returned by this algorithm meets all the main requirements (satisfying all supplies and demands without negative amount of transportation) and is supposed to be close the optimal one. The flowchart of the *CMM* algorithm is shown in Fig. 2.

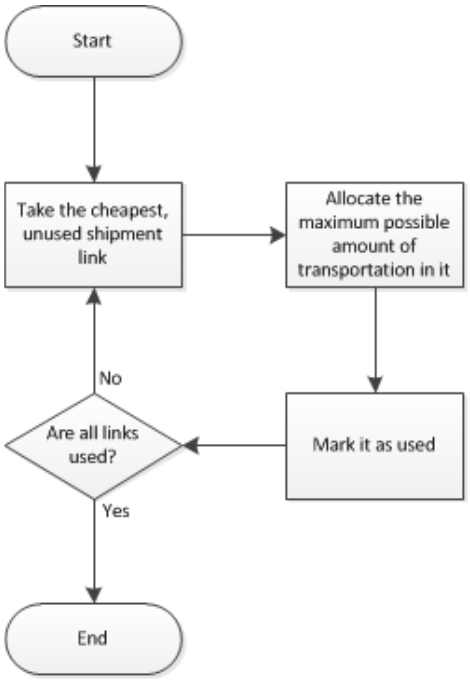

Figure 2. Flowchart of *CMM* algorithm.

TABLE I. ALGORITHMS TO TEST

Algorithm	NW corner rule	Cheap means more	Expensive means less
Optimization	✓	?	?

C. Expensive means less (EML)

The second heuristic algorithm is in theory similar to the previous one. The essential difference is that this one considers the most expensive shipment links first and sets the amount of transportation in them as little as possible. This minimum is calculated based on the rule best described as: 'How small amount of good can I send / receive here to still have enough other warehouses / factories to satisfy my supply / demand? The main problem in this approach is that it postpones achieving the solution. The *CMM* algorithm was going to satisfy all of supplies and demands as quickly as possible. On each step the current situation was known and while making the decision about each allocation no assumptions were made. In this approach each decision about transporting X units of goods has additional information: '...assuming that I can still send / receive Y units of goods elsewhere'. After a few steps of the algorithm it may be that the assumptions made in calculating the minimum are not valid anymore and given factory / warehouse cannot satisfy its supply / demand.

It was the serious issue making the *EML* almost completely different algorithm than *CMM*. After consideration and tests of a few possible ways to solve this problem it was decided to use recursive approach to this algorithm with increasing the allocations instead of setting them. This was possible thanks to the observation that increasing any allocation by a number other than 0 means that given factory / warehouse makes an assumption of sending / receiving goods through all other links available for them at their maximums. This causes satisfying the whole supply / demands of the given factory / warehouse once the amount of transportation other than 0 is added to any allocation. Then the algorithm repeats with some values already calculated (some amounts of transportation set and some supplies / demands accordingly decreased).

The algorithm ends when no allocation was increased in a single cycle (which means there was no recursive call). Just like in the case of *CMM* the solution returned by *EML* meets all the main requirements and is supposed to be close the optimal one. The flowchart of the *EML* is shown in Fig. 3.

D. Optimization

Optimization algorithm takes any valid solution of the problem as an input and gives the best possible solution as an output. It checks the optimality of the solution, finds the non-used connection that should be used to reduce the total cost of transportation (if the solution was not optimal) and then adds it to the solution increasing and decreasing other allocations and repeats the described steps. It stops when the solution is optimal. The number of circles done varies and depends on the input solution – mostly on its accuracy but at some level also on other factors associated with its structure [1].

 ISBN: 978-1-61208-246-2

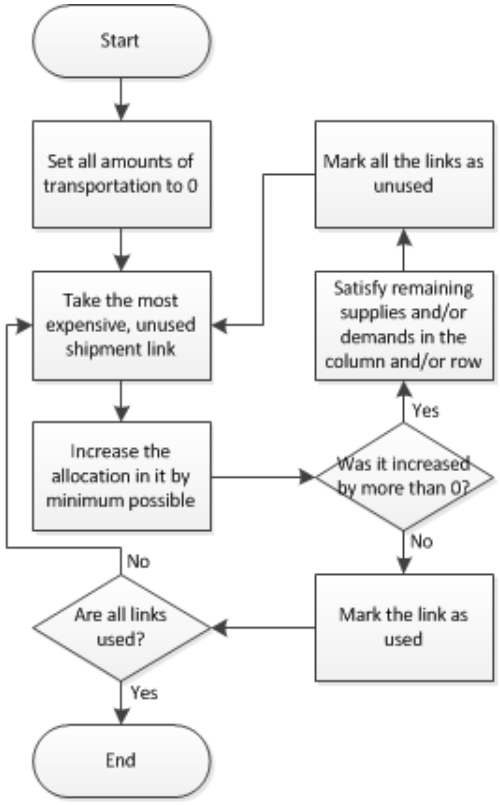

Figure 3. Flowchart of *EML* algorithm.

E. *Heuristic algorithms vs. optimization*

One of the main assumptions about the best solution for the transportation problems is that it uses no more than $(m + n - 1)$ connections where m is the number of factories and n is the number of warehouses.

Outputs of the described heuristic algorithms don't use more than the specified number of links. Unfortunately optimization algorithm can't handle the input solutions with less connections used either (degenerated solutions) [1]. This makes a necessity of marking some of the unused links as used with amount of transport equal 0. They should be chosen in a way that they don't create a closed cycle in a matrix corresponding to a problem. It is necessary for the algorithm of optimization to work properly. Creating methods of adding unused connections to degenerated solutions made the additional objectives of the project possible to complete.

III. EXPERIMENTATION SYSTEM

The testing tool was created entirely from the scratch for the purposes of the paper. I was an application implemented in C# language using Microsoft Visual Studio 2010. Class library ZedGraph was used to draw charts and present the effect of the tests in a graphical form.

The application contains two tabs which allow user to get solution for a single problem or run automatic tests of efficiency and accuracy of the algorithms.

The screenshots of the testing tool are shown in Fig. 4 and Fig. 5.

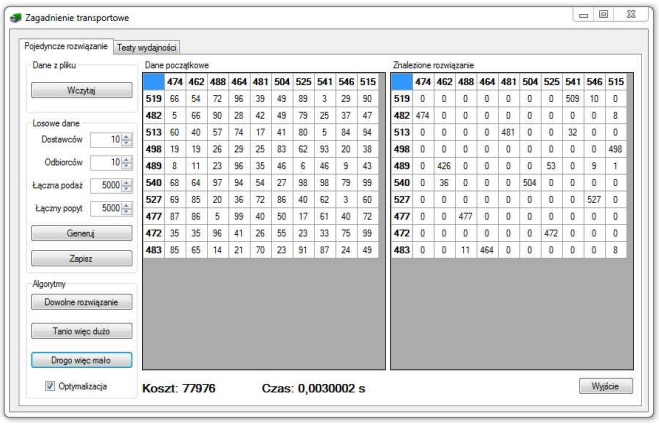

Figure 4. Single solution part of the application.

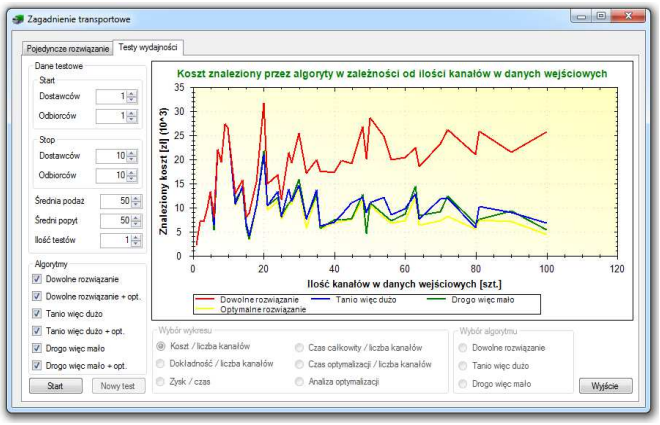

Figure 5. Automatic tests part of the application.

The application provided a complete and solid tool for testing the implemented algorithms.

IV. RESEARCH

The main part of the research was a series of experiments which were supposed to provide the data needed to determine accuracy and efficiency of the algorithms.

A. *Experiment design*

All the experiments were made using the presented tool. The main goal was to test the efficiency and accuracy of the implemented algorithms. The application allows user to select the range of the input data and the number of test from which the final answer is averaged. As for the amount of goods transported parameter, the user is allowed to input the average supply and demand. As the number of factories and warehouses varies during the test, each time the total supply and total demand is calculated and then the smaller value is rounded up to balance the other one.

The test were designed to deliver the information about the main characteristics of the implemented algorithm which are processing time and cost found. To allow the more

 ISBN: 978-1-61208-246-2

valuable analysis it is possible to get information about processing time and cost reduction with optimization algorithm enabled. Before the main part of the experiments the preliminary experiment was made to determine how the results depend on the characteristics of the input data and how to choose the input data to make the tests more reliable.

Overall, several experiments were conducted in order to investigate:

- Processing time of the algorithms depending on the size of the input.
- Cost of the solution found by algorithms without optimization in comparison to the optimal one depending on the size of the input.
- Relative error of solutions found by algorithms without optimization depending on the size of the input.
- Time needed to improve the result depending on the relative error of the input solution.
- Processing time of each algorithm and optimization of its output depending on the size of the input.

All the experiments were made on a single machine within the one instance of the application with the number of tests set to 10. As the calculations have been proceeding no other actions on the machine were made.

B. *Preliminary experiment*

The preliminary experiment was based on testing the processing time of the algorithms depending on the size of the input data. It started from the 1×1 matrix and ended at the 50×50 set of data. Measure point with the same size (for example 4×6, 6×4, 2×12 etc.) were averaged. The results showed that despite the repetitive tests and averaged results the measured values spread as showed in Fig. 6. Identifying the variance points showed that the oddest results are returned when the number of the factories and warehouses in the input differ significantly (the matrix of costs is not close to a square shape).

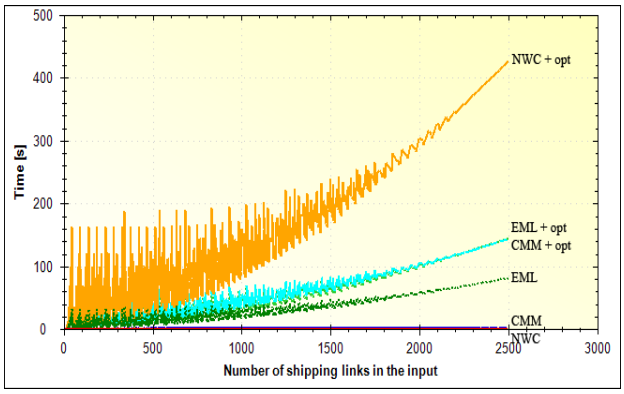

Figure 6. Preliminary experiment results.

In the further experiments it was decided to test the data with the ratio of the factories to warehouses between 0.9 and 1.1 in a range of 1×1 to 100×100.

C. *Results of Experiments*

The main experiment was made for finding the relationship between the processing time needed to return the solution and the size of the input measured by the number of shipment links. The result of the performance of the considered algorithms is shown in Fig. 7.

The result of this test is consistent with expectations. Without optimization, the first two algorithms (*NWC* and *CMM*) returned answer almost immediately. *EML* needs time to process which is probably caused by many recursive calls.

The most important observation from this part is that combining optimization with *NWC* takes much more time than calculating the best solution based on the heuristic methods. The optimization algorithm works the best with the *EML* solution as an input, but the long processing time of this algorithm causes that the quickest way of getting the optimal solution is the *CMM* plus optimization.

The second significant experiment was made for comparison of not optimized solutions found by all three algorithms with the optimum solution. The result is shown in Fig. 8. It can be easily observed that both heuristic algorithms give result that is very close to optimal. What is more, the *EML* is more accurate than the others in all cases.

The best way of evaluation of accuracy is the relative comparison of the cost of found solution and minimum cost. The relative error of the solution found by three algorithms without optimization is shown in Fig. 9. This graph shows that although the heuristic methods may seem accurate, they return the solution with cost about two times bigger than the calculated minimum. The percentage disproportion between them varies from 0 to approximately 50%.

The most important fact that this graph shows is that the bare *NWC* is unacceptable as a way of solving the transportation problem. It returns a valid solution, but it completely misses the main reason of solving the problem with a help of computer – minimizing the total cost of transportation.

The application also allows user to compare the time needed to improve the result given by the different algorithms. The result of this test is shown in Fig. 10.

This graph provides more accurate illustration of the relative error range for all three algorithms. Just as before, it is clearly visible that the heuristic algorithms return more accurate solution than the *NWC*.

Furthermore it proves that time of optimization depends not only on the relative error, but also on some other factors.

The last functionality of the created application is the analysis of two components of all algorithms joined with the optimization. The results are shown in Fig. 11, Fig. 12, and Fig. 13. These three graphs show that in case of the *NWC* and *CMM* the size of an input does not matter when it comes to the non-optimized solution. The optimizing process is the main cause of the time needed of an algorithm as a whole.

In the case of *EML* both calculating basic solution and optimizing it needs about the same amount of time. The optimization here is much faster than in the *CMM*, but the previous part takes more time so total time needed by the algorithm is bigger.

 ISBN: 978-1-61208-246-2

Based only on the three last graphs it can be said that because of the shortest optimizing time, the *EML* is supposed to return better solution than two others algorithms which is reflected in the previous graphs.

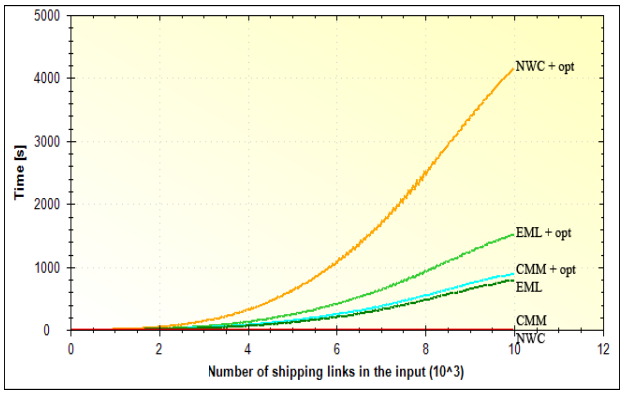

Figure 7. Processing time of the algorithms depending on the size of the input.

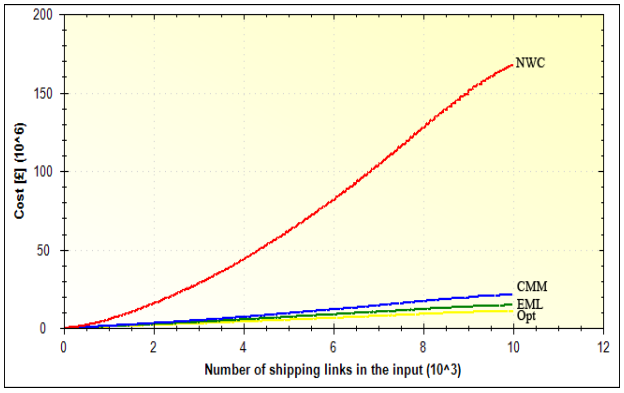

Figure 8. Cost of the solution found by algorithms without optimization depending on the size of the input.

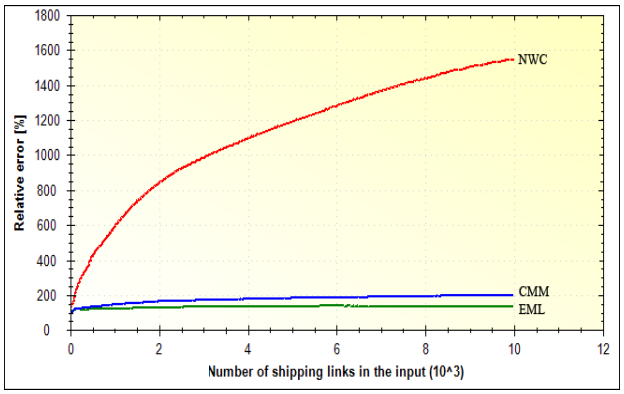

Figure 9. Relative error of solutions found by algorithms without optimization depending on the size of the input.

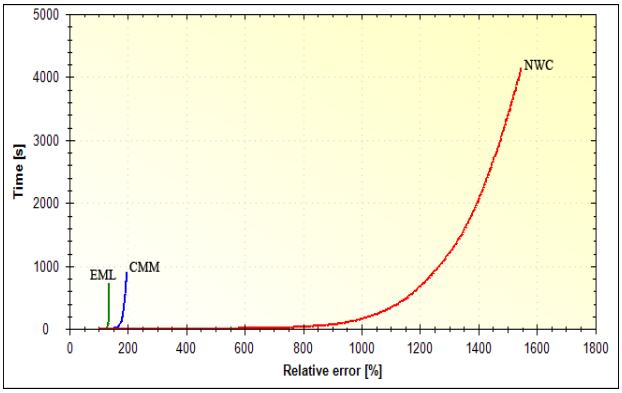

Figure 10. Time needed to improve the result depending on the relative error of the input solution.

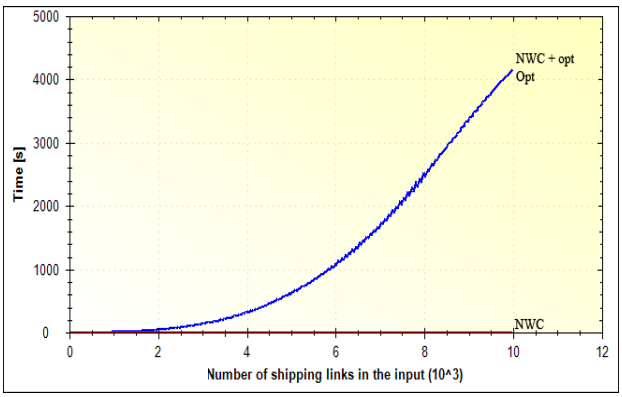

Figure 11. Time needed by the components of *NWC* with optimization algorithm depending on the size of the input.

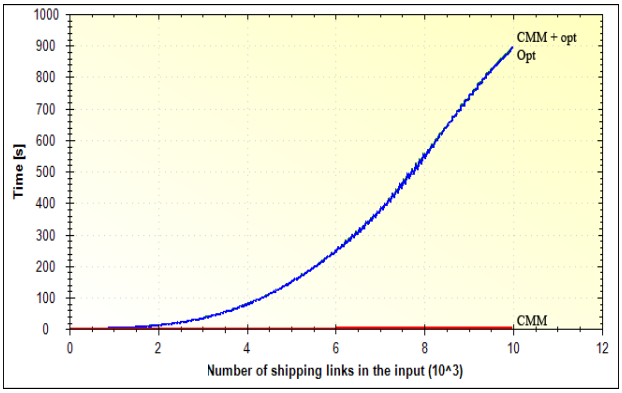

Figure 12. Time needed by the components of *CMM* with optimization algorithm depending on the size of the input.

V. CONCLUSION AND FUTURE WORK

All of the objectives of the research have been completed. The results are gathered as the graphs providing a simple, fast and clear way of evaluation main qualities of the transportation problem algorithms.

 ISBN: 978-1-61208-246-2

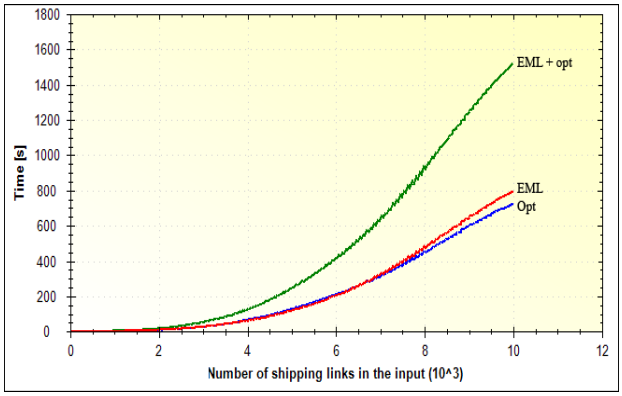

Figure 13. Time needed by the components of *EML* with optimization algorithm depending on the size of the input.

The accuracy of tested algorithms without optimization is different and should be considered while attempting to solve any given problem. On the other hand the optimized solutions take much time to be calculated.

When it comes to getting the optimal solution the *CMM* is the best algorithm to get the initial solution and optimize it. This method combined with the optimizing algorithm provides the quickest way of getting the optimal solution.

When calculating the minimum cost is remarkable time-consuming then the better solution is to choose one of two heuristic algorithms without optimization. They provide a quick way of obtaining a result much more accurate than any random solution such as the one returned by the *NWC*.

The quickest one is the *CMM* which is quite common and well known. The *EML* was an authorial idea and proved to be a great way of balancing between short time of calculations and small total cost returned. It works faster than optimized *CMM* algorithm but ends with a result nearly two times bigger.

In the future work we would like to test the influence of the 'shape' of the input data on the results and implement some additional functionality in the testing application allowing user to get solutions for more complicated versions of the problem. The most important are:

- Non-balanced problem [10],
- Costs of storage / shortage,
- Costs of production,
- Blockage of a shipment link [11],
- Partial blockage of a shipment link [12],
- Transshipment points.

All of the above can be easily transformed to a typical transportation problem. All actions needed to be taken are actions on the input matrix of costs and supplies / demands vectors. They do not make any of the algorithms work in other way and do not require any special treatment other than described preparation. This is very important from the point of view of future functionalities of the application that are planned to be implemented.

The application can be used in the real system providing a way of getting the solution to the problems in the field of transport, network traffic etc. The most profitable method of calculations can be chosen thanks to the tests results. It is significant in the cases where a lot of problems must be solved in a limited time (e.g. in computer networks flow control).

REFERENCES

[1] G. B. Dantzig, and M. N. Thapa, Linear Programming 2: Theory and Extensions, Springer, New York, 2003.

[2] A. Calczynski, J. Sochanska, and W. Szczepankiewicz, Methods of shipment rationalization in trade /in Polish/, WAE, Cracow, 1988.

[3] A. Calczynski, Optimization methods in transport services market /in Polish/, PWE, Warszawa, 1992.

[4] G. Sharma, S. H. Abbas, and V. K. Gupta, "Solving transportation problem with the various methods of linear programming problem," Asian Journal of Current Engineering and Maths, vol.1, no. 3, 2012, pp. 81-83.

[5] S. K. Kumar, I. B. Lal, and S. B. Lal, "Fixed – charge Bi-criterion Transportation Problem," International Journal of Computer Application, vol. 1, 2012.

[6] D. Dutta and A. S. Murthy, "Fuzzy transportation problem with additional restrictions," ARPN Journal of Engineering and Applied Sciences, vol. 5, no. 2, 2010.

[7] P. Pandian and G. Natarajan, "A new method for solving bottleneck-cost transportation problems," International Mathematical Forum, vol. 6, no. 10, 2011, pp.451-460.

[8] F. S. Hillier and G. J. Lieberman, Introduction to operations research, McGraw Hill, New York, 2001.

[9] G. B. Dantzig, Linear Programming and Extensions, Princeton University Press, Princeton, 1963.

[10] A. Marczuk and W. Misztal, "Agricultural produce transport optimisation in the conditions of market non-balance," /in Polish/, Journal Inzynieria Rolnicza, no 129, Cracow, 2011, pp. 221-226.

[11] K. Pienkosz, "Optimization models and methods of resource allocation" /in Polish/. Scientific Reports Series Elektronika, Warsaw University of Technology, no. 3-132. Warsaw, 2010.

[12] A. Marczuk, "A computer system for optimisation of soft fruit transportation in diffused purchasing networks," Journal Eksploatacja i Niezawodnosc, vol. 44, no. 4, Warsaw, 2009.

 ISBN: 978-1-61208-246-2

My Phone, My Car and I - And Maybe a Traffic Light Assistant

Michael Krause, Klaus Bengler
Institute of Ergonomics
Technische Universtität München
Garching, Germany
krause@tum.de, bengler@tum.de

***Abstract*—In the context of a project regarding a traffic light assistant on smart phones, a survey about ownership, usage in relation to traffic and car issues as well as acceptance of a potential traffic light assistant was carried out. The survey was conducted as a paper-based poll as well as online. 694 people took part. The user's need to browse social media while driving, as is sometimes mentioned in distraction debates, could not be found. The idea of a traffic light assistant on a smart phone (as a guide to the next green phase, or inform the driver to decelerate the car early) had different acceptance rates among males and females, and was more acceptable to men.**

Keywords-nomadic devices*; *smart phones*; *survey*; *usage*; *vehicle

I. INTRODUCTION

In the project KOLIBRI (Kooperative Lichtsignaloptimierung Bayerisches Pilotprojekt; engl: cooperative optimization of traffic signal control Bavarian pilot project) [1], an application-oriented vehicular system is prototypically developed and tested. The system, a traffic light assistant, is intended to inform the driver of a car about upcoming traffic signal states so he can adjust his driving behavior.

The project develops two different ways to deliver messages to the driver: an onboard system integrated into the instrumentation of a demonstration car and a system to inform the driver via a standard smartphone that can be installed in any car. The data is transmitted over existing 2nd and 3rd generation mobile networks (GMS, UMTS) from the traffic lights to a central server. The demonstration car or a mobile phone requests appropriate data files from the server and displays the proper speed recommendation or other messages for the next traffic light approach.

The four partners of the project are responsible for different duties. The Institute of Ergonomics at the Technische Universtität München is in charge of the human machine interface (HMI) and evaluating the system in a simulator and real field trials. The institute found the information of drivers via smart phones a promising solution and is focusing on it.

Information communication via smartphones would not involve significant extra costs for installation or purchasing. Nowadays, smart phones are widely used. Due to the use of the assistant in the car, care must be taken for suitability while driving. Ergonomic requirments, e.g. gaze durations and acceptance, led a particular human machine interface (HMI). The details are discussed in [17] and [18]. In addition to simulated and real field experiments, a parallel survey was carried out to find out more about the existing prerequisites for a traffic light assistant via smart phones. How widespread are car mounts for mobile phones? How often they are used? Would a traffic light assistant via smartphone be accepted?

The following methodology section describes the tools used for the poll and characterizes the group of test subjects. The results section shows the findings, based on the sequence of the questions in the survey. The results are grouped into subsections (Phone Type, Personal or Professional, Car Mount for Mobile Phone, Mobile Phone Usage, Car Related, Acceptance of a Traffic Light Assistant).

II. RELATED WORK

Early contribution in the field of traffic light assistance can be found in the project *Wolfsburger Welle* [2], [3]. Also Australian traffic engineers experimented in the 80's with traffic light related speed advices and identified potential benefits. [8], [9] compared an in-vehicle system to dynamic traffic signs along the road in a driving simulator experiment and found subjective preferences for the variable message signs and objective advantage for the in-car display. In [10], different HMIs for an on-board system were tested and an integration into the speedometer seems to be an adequate solution. The interface idea of the *Wolfsburger Welle* was (modified) adopted in the project TRAVOLUTION (Audi AG) [11] and the German project *aktiv* [12], [13]. *aktiv* used for the driver information a personal digital assistant (PDA) with WiFi connection to the traffic lights. The drawback of this approach is the limited connection range, to get data from a traffic light. Experimental data for the coverage and handshake times can be found in [15]. The WiFi connectivity for traffic light assistance (under different vehicle speeds) was also examined by [14]. The

 ISBN: 978-1-61208-246-2

use of already installed communication networks (GSM, UMTS) within the project KOLIBRI overcomes the limited coverage range of dedicated short range communications. Another approach, that uses the camera of a smart phone and image processing, is proposed by [16]. For this, the phone (with the camera) must be installed with view to the road. This is likely to mask the driver's field of view. Within KOLIBRI the only constraint is an acceptable GPS signal for the smart phone. On rural road this is not a restraint.

III. METHOD

The survey was carried out on paper questionnaires as well as online, using the *LimeSurvey* online system at the end of 2011 and beginning of 2012. Participants for the paper based pool were mainly acquired at the Technische Universtität München (Campus Garching). For the online survey the link to the pool was disseminated by email and through the university's Facebook page.

Twenty-five questions made up the questionnaire. It took about 10 minutes to complete.

The analysis presented here considers 373 replies to the paper-based form and 321 answers to the online survey (78 incomplete or blank forms were eliminated), for an overall total of 694 participants.

The paper based participants were 76% male and 24% female, aged between 16 and 64 with an interquartile distance from 20 to 24 (median 22).

The online survey was filled in by 87% males and 13% females, aged between 17 and 74 with an interquartile distance from 20 to 26 (median 22).

The results from both sources are reported together and are not further split up nor are analyzed independently. Thus the overall group has an average age of 23.9 years (SD 6.9) and the gender is 81 percent male and 19 percent female. The average annual mileage is 9883 km (SD 12585). Driver's licenses were obtained at an average age of 17.7 years (SD 1.4).

IV. RESULTS

A. Phone Type

As shown in Figure 1, 43% of the phones run on a proprietary operating system, 23% are based on the (proprietary) iOS, 31% are Androids and 3% of users did not answered, or have no mobile phone. The figure does not explicitly distinguish between 'smart phones' and conventional mobile phones, because definitions are evolving and there are many in-between devices. It can be concluded that all of the Android and iOS devices (i.e., iPhones) are 'smart phones', plus some of the others.

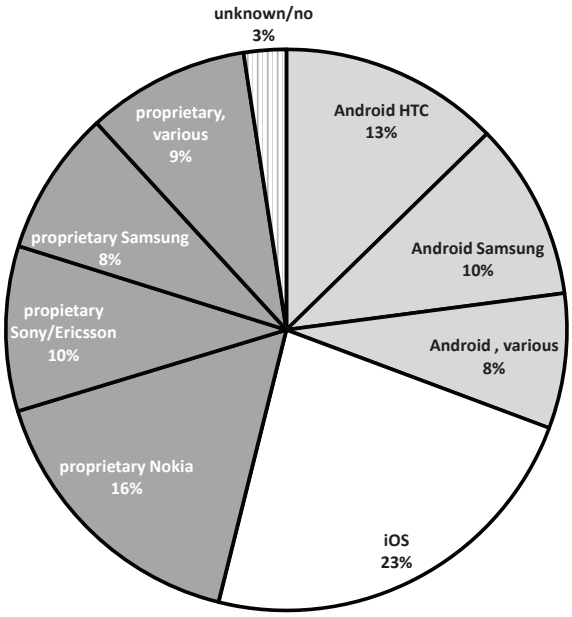

Figure 1. Phone types

B. Personal or Professional

Asked for the main reason (personal or professional) to use their mobile phone 95.7% answered *personal* and 3.5 % *professional* (0.8% undefined).

For 90%, the main reason to use a car was for *personal* use, and *professional* use for 6.5% (3.5% undefined).

52% said they used the phone in the car for *personal* reasons, while 3.5% used it for *professional* reasons and 42.4% never/seldom used it in a car (1.7% undefined).

When asked about the main type of car used, 4.9% had no car, 56.3% bought a used one, 29.2% bought a new car, 5.1% rented a vehicle and 4.3% have a company car.

C. Car Mount for Mobile Phone

For the safe use of a traffic light assistant, cradles in the cars would be a prerequisite. Asked about such a phone mount, 82.3% of the participants had no car holder for their phone. The traditional mounting method of a suction cup is used by only 11%, and 5.3% use other ways to mount the phone in the car (1.4% undefined).

Figure 2 shows the mounting locations for the phone holder. 45% of users who mount their phones use the middle area of the windshield.

When asked how frequently the phone is fixed in the holder while driving (Figure 3), one-third of the already small number of holder users mount the phone only for long distances.

 ISBN: 978-1-61208-246-2

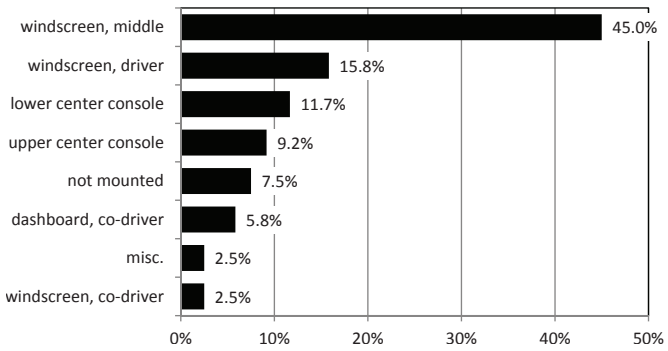

Figure 2. Location of phone holder

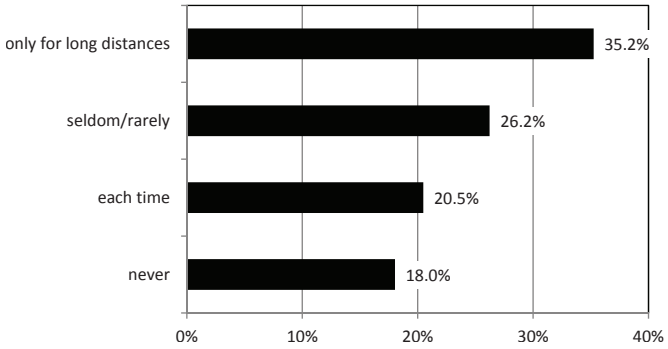

Figure 3. Frequency of holder use

The main reason most people do not have a phone mount (Figure 4) is that they do not see any need for one.

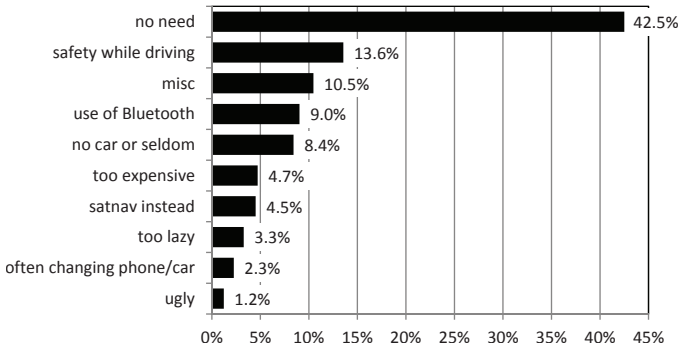

Figure 4. No Phone Holder because...

D. Mobile Phone Usage

The starting age of cell-phone usage was calculated based on how long the subject had used the mobile phone and the age of the person. Figure 5 shows that most begin at the age of 14.

The 'years per phone' (Figure 6) were calculated based on how long the subjects had been using a mobile phone and how many different phones the subject had during this time.

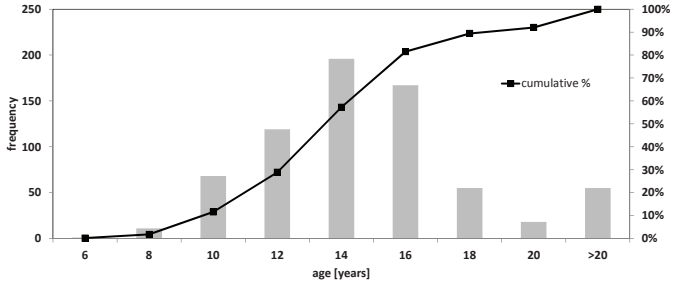

Figure 5. First use of mobile phones at age of...

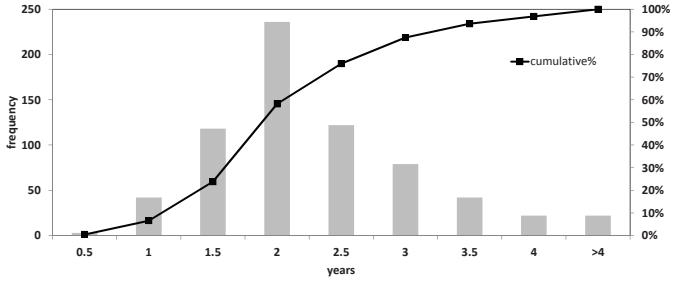

Figure 6. Service life [years per phone]

Figure 7 shows the median number of apps that Android and iOS users have downloaded to their phone (with interquartile distances). Android users have typically 10-30 apps downloaded, while iOS users loaded 20-70 apps. The mean value for Android and iOS users is 40 downloaded apps (SD 63).

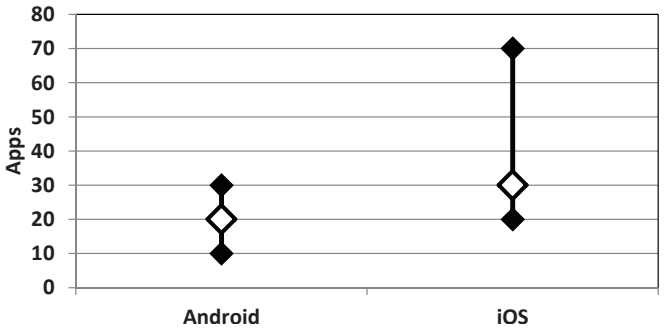

Figure 7. Typical number of apps downloaded (median and interquartile distance)

Subjects were asked to name the three apps they use most often, with the most frequently used app listed first. Figure 8 only shows an analysis of the most frequently used app. An analysis including all three named apps is shown in Figure 9 (apps equally weighted, independent of their usage priority). Some of the apps were grouped. The following provides further explanation for clusters that are not self-explanatory:

- *news* means dedicated news from newspapers, tv stations and so on.

 ISBN: 978-1-61208-246-2

- *misc information* are things like tv programs, Wikipedia, phone books, etc.
- *tools* are apps that give their users an additional value like a flashlight, alarm, calculator, etc.
- *system apps* are system-related tools like battery monitors, data counters, etc.

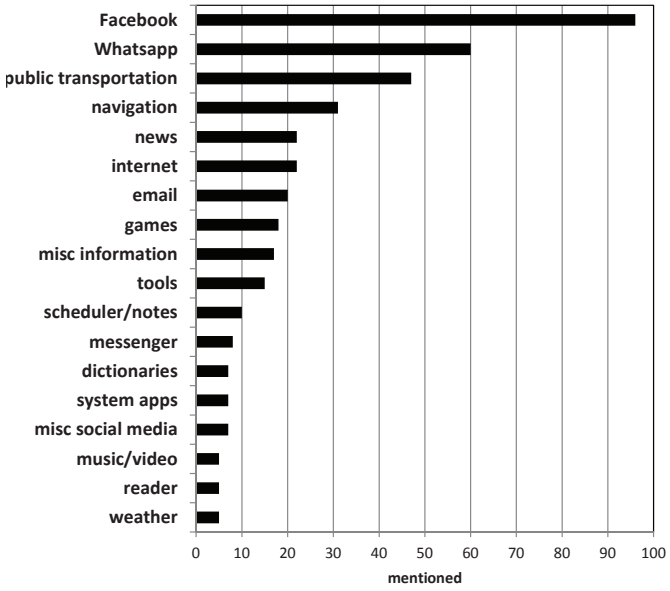

Figure 8. Question about most often used apps (first named app only)

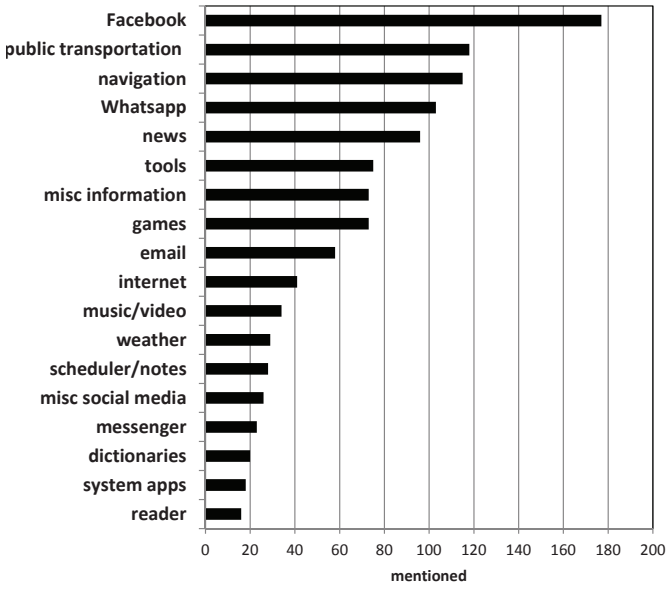

Figure 9. Question about most often used apps (up to three mentioned apps per test subject)

E. Car Related

Participants were asked which car-related apps they are using. 495 people did not use such apps. Various navigation apps were mentioned 182 times. Other named apps, with the number of occurrences in brackets: radar warnings(5), jam information(5), Drive Now(3), ADAC(1), BMW m-meter(1), Porsche gforce(1), Mini Connect(1), Dynolicious(1), OBD(1), BMW TV(1), fuel prices(1), mbservice(1), carpooling(1), parking(1).

The subjects could reveal with which devices their cars are equipped (Figure 10). The traditional CD/radio is by far the most often mentioned one, followed by external satnavs and music players.

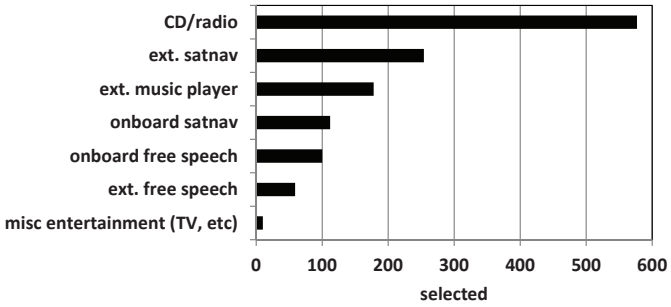

Figure 10. Car is equipped with...

Asked which phone function is the most frequent used while driving (Figure 11), the phone function is on top, followed by ‘none’, SMS and music. The option ‘named app’ is further classified in Figure 12. The app mentioned most often, by far, is navigation. Whatsapp and Facebook play only a minor role (each mentioned three times, in total by five different persons). Apps mentioned only once, and so not included in Figure 12, are: photos, flight information, music, GPS speedometer, Shazam, Siri, parking help, number plate information. It should be also noted that driving with a radar warning system is forbidden in Germany.

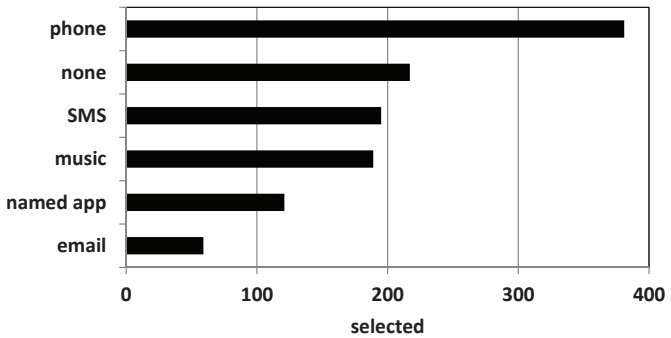

Figure 11. Functions used while driving a car

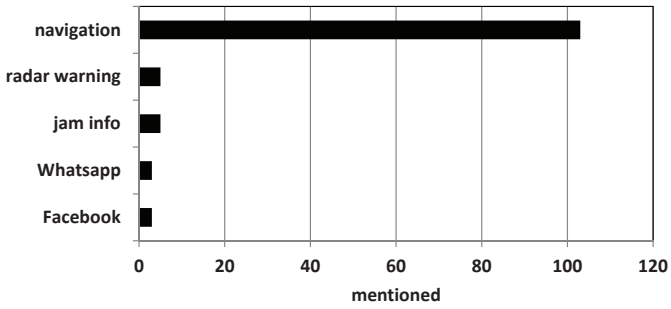

Figure 12. Apps used while driving

F. Acceptance of a Traffic Light Assistant

The test subjects were asked if they would have safety concerns if a future smartphone app could provide information about upcoming traffic signal states (traffic light assistance) and if they were to use the app themselves. Most of the males (84%) answered 'no' (no worries about safety). 62% of females share this opinion.

The question was then slightly altered: Would you have concerns about safety if other drivers were to use a traffic light assistant app? This question reduced the males' lack of concern to 66% (no worries about safety) and 57% for females.

The question as to whether a traffic light assistant app would be used by the participant was answered positively by 78% of the males and 51% of females.

The maximum price the participants would be willing to pay for a traffic light assistant app is bimodal, with peaks at zero euro and five euros (Figure 13).

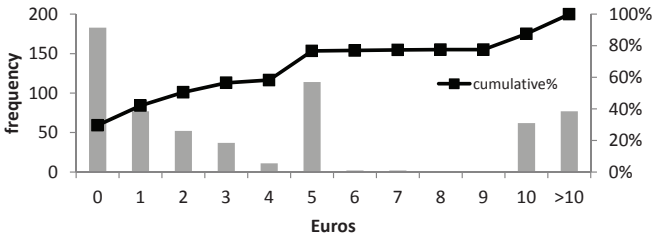

Figure 13. What people would pay for a traffic light assistant app

If a new car had an onboard traffic light assistant, the acceptable extra charge for the system is also bimodal, with peaks at zero and 100 euros (Figure 14).

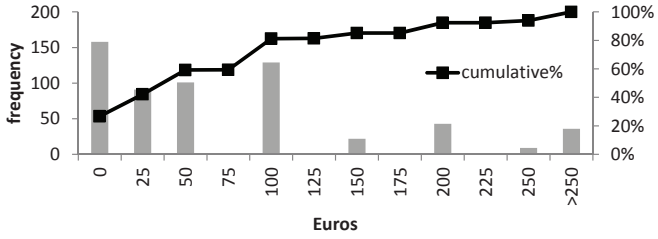

Figure 14. What would be paid for an onboard traffic light assistant system

V. Discussion

The distribution of operating systems in this study is similar to findings in other studies: [19] reported 33.6% Android and iOS 22.2% for Germany in December 2011. And [20] found 31.2% Android and 20.7% iOS for Europe. Based on the results of [21], it can be assumed that the proportion of Android smartphones is increasing. The often-used practice of implementing one app native for both systems (iOS and Android) would apply to half of the mobile phone population in this survey.

The young age, the high percentage of males and the main use of phones and cars for personal purposes in this survey is likely due to the academic, student-heavy population at the technical university.

One requirement for safely providing driver information via smartphones is having an appropriate mounting method for the phone in the car. Currently only about on in five people has a car mount for the phone and only one-fifth of these use it during each car ride. An introduction of a driver information system must also advertise good practices for mounting locations (no field-of-view occlusions and no significant deviation from the line of sight).
Most people had no phone mount because they do not see a need. Nevertheless, the high level of willingness to use a traffic light assistance system could be a chance to promote the safe integration of mobile devices into the car.

The main age for start mobile phone usage in this study seems to be 14. From data shown in [22], the actual starting age of mobile phone usage for German children seems to be somewhere between the age of 10 and 13.
Most of the time, phones are used for about two years. This could be an artifact of the contract strategy of German network providers. The contracts are generally limited to two years and are bundled with a phone.

iPhone users seem to download more apps to their phone. This is in line with [23], which found that iPhone users download 48 apps/month and Android users 35 apps/month. A higher app activity for iPhone users was also reported by [24] (37 installed apps on iPhone versus 22 apps on Android). It would be interesting to find out whether this is due to generally higher user activity, easier app installation or reasons based on the phone itself: are

 ISBN: 978-1-61208-246-2

Androids better equipped with OEM preinstalled programs? Or are the users wiser and realize that they will never use more than a couple of apps? [25] found that users installed an average of 24 apps and used 9 in the last month.

No matter how the answers for the most often used apps are analyzed, Facebook is always in first place. Facebook was also found to be the favorite app in [24]. In [20], Facebook is not the favorite app, but ranks among the top apps. The next four places in this survey change order depending on the analysis technique (Figure 8 and Figure 9), but the candidates are the same: whatsapp, public transportation information, navigation and news. Navigation was also found to be an important app in the above studies. Some differences between the previous studies and this survey: In this survey, music and weather do not play an important role; on the other hand, the information about public transportation is important here and was not mentioned in the other studies. [26] also found Whatsapp and Facebook to be top-ranking in Germany.

The most often used function of the mobile while driving is the phone, different apps play only a minor role. If an app is used while driving it is likely a navigation app. The social media referred to as driver distractions ([27], [28]) are unimportant and are used to the same degree as already forbidden radar warning systems. The vast majority of road users are responsible drivers. Another survey found that 20% of driver would use Facebook while driving if it could be controlled by speech [29].

The acceptance of a traffic light assistance system by females is surprisingly low, compared to males answers. Most men also see no safety issue. This should also be addressed if a traffic light assistant were to be introduced. The driver must be aware of his or her responsibility while driving. From the results it is likely that the early adopters will be males.
Due to the high willingness to use the system, the peaks at zero euros for an acceptable price could be a sign that people wish to use it for free. For an app this could maybe be realized through various distribution models (goverment grant, advertisement, etc). For an car onboard system it would be not feasible to get it for free. Questions about an appropriate price are also used in simulator studies and real field trials. It will be interesting to see how real-life experience with such a system influences the perceived value.

VI. Conclusion

For the traffic light assistant project it is likely that a first native app will be implemented for Android, maybe followed up by an iOS implementation. The high (male) willingness to use the system should be a chance to promote safe integration of mobile devices into the car and to raise awareness among all stakeholders about responsibility while driving. Given that a majority of participants does not have a suitable mounting option and seems to be uncritical of distraction issues, implementing this attractive app could be an opportunity to provide users with relevant information about these topics within the application.
From the small number of users found in this data the ‘social media while driving’ issue does not seem to be worth discussing at this time. This opinion is in contrast to [28].

It is important that systems are technically well designed, in terms of hard and software, and also ergonomically sound. [8] reported that usefulness of a system and the satisfaction with its use were highly anticipated by test persons. These expectations reduced after driving in a simulator with the traffic light assistance system. Another aspect is long-term use of the system in addition to motivation to use it. Through all stages of the project, human factors and ergonomics plays a major role. It is here suggested to gather subjective ratings from customers and users of systems both at an early development stage and along the way. The next step is to analyze the goals and tasks of the user, in order to gain a better perspective on the additional tasks required by the use of the system. The final step is the technical implementation of the system. Ergonomic and human factors is not a discipline for quick usability tests in a late development stage, but rather it must be involved from the beginning.

VII. Outlook

Previous studies reviewed the traffic light assistant in a driving simulator and actually prototypically tested it in real. The survey data documented in this paper will be mentioned and related to the results found in these studies. Recent experiments address the mental demands of a traffic light assistant, the gaze behavior and subjective measures.

Acknowledgment

The project is funded by Bayerische Forschungsstiftung (Bavarian Research Foundation).
The authors would like to thank Patrick Gontar und Michael Szostak (survey conduction and data input) and Markus Zimmermann (maintenance of the LimeSurvey system).

References

[1] KOLIBRI, http://www.kolibri-projekt.de checked 08/24/2012

[2] C. Voy, W. Zimdahl, W. Mainka and F. Stock, 1983, German Patent DE3126481C2

[3] G. Hoffmann, *Up to the minute informations as we drive how it can help road users and traffic management*, Transport Reviews, vol. 11, no. 1, pp. 41–61, 1991.

 ISBN: 978-1-61208-246-2

[4] A. Bell, *If you always caught the green light,* ECOS Magazine, no. Issue 40, http://www.ecosmagazine.com.au/?paper=EC40p10, 1984.

[5] J. van Leersum, *Implementation of an advisory speed algorithm in TRANSYT*, Transportation Research Part A: General, vol. 19, no. 3, pp. 207217, 1985.

[6] R.S. Trayford, B.W. Doughty, and J.W. van der Touw, *Fuel economy investigation of dynamic advisory speeds from an experiment in arterial traffic*, Transportation Research Part A: General, vol. 18, no. 5-6, pp. 415419, 1984.

[7] R.S. Trayford, B.W. Doughty, and M.J. Wooldridge, *Fuel saving and other benefits of dynamic advisory speeds on a multi-lane arterial road*, Transportation Research Part A: General, vol. 18, no. 5-6, pp. 421429, 1984.

[8] K. Duivenvoorden, *Roadside versus in-car speed support for a green wave: a driving simulator study*, Master's Thesis, University of Twente, 2007.

[9] J. Pauwelussen, M. Hoedemaeker and K. Duivenvoorden, *CVIS Cooperative Vehicle-Infrastructure Systems: DeliverableD.DEPN.4.1b Assess user acceptance by small scale driving simulator research.*

[10] S. Thoma, *Mensch-Maschine-Interaktionskonzepte fr Fahrerassistenzsysteme im Kreuzungsbereich.* Dissertation, TU Mnchen, 2010

[11] R. Braun, F. Busch, C. Kemper, R. Hildebrandt, F. Weichemeier, C. Menig, I. Paulus, and R. Prelein Lehle, *TRAVOLUTION - Netzweite Optimierung der Lichtsignalsteuerung und LSA-Fahrzeug-Kommunikation*, Straenverkehrstechnik, vol. 2009, no. 6, pp. 365374.

[12] aktiv, *Adaptive und kooperative Technologien für den intelligentenVerkehr*, German Research Initiative 2006-2010, http://www.aktivonline.org page last checked 18. Oct. 2012

[13] R. Hoyer, *Verkehrliche Potenziale des vorausschauenden Fahrens an kooperativen Lichtsignalanlagen*. 5. Tagung Fahrerassistenz M"unchen, 2012

[14] I. Iglesias, L. Isasi, M. Larburu, V. Martinez, B. Molinete, *I2V Communication Driving Assistance System: On-Board Traffic Light Assistant.* In: Vehicular Technology Conference, 2008. VTC 2008-Fall. IEEE 68th, pp. 1-5 doi: 10.1109/VETECF.2008.437
K. Katsaros, R. Kernchen, M. Dianati, D. Rieck, and C. Zinoviou, *Application of vehicular communications for improving the efficiency of traffic in urban areas*, Wireless Communications and Mobile Computing, vol. 11, no. 12, pp. 1657-1667, 2011.

[15] Thomas Otto T. Otto, *Kooperative Verkehrsbeeinflussung und Verkehrssteuerung an signalisierten Knotenpunkten*, Schriftenreihe Verkehr Heft 21 der der Universität Kassel, Dissertation, 2011

[16] E. Koukoumidis, L.-S. Peh, and M. R. Martonosi,*SignalGuru: leveraging mobile phones for collaborative traffic signal schedule advisory*, in Proceedings of the 9th international conference on Mobile systems, applications, and services, New York, NY, USA: ACM, 2011, pp. 127–140

[17] M. Krause and K. Bengler, *Traffic Light Assistant - Driven in a Simulator*, in Proceedings of the 2012 International IEEE Intelligent Vehicles Symposium Workshops, 2012.

[18] M. Krause and K. Bengler,*Traffic Light Assistant Evaluation of Information Presentation*, in Advances in Human Factors and Ergonomics 2012: Proceedings of the 4th Ahfe Conference: CRC Press, 2012, pp. 6786-6795.

[19] *Global mobile statistics 2012 Part A: Mobile subscribers; handset market share; mobile operators* http://mobithinking.com/mobile-marketing-tools/latest-mobile-stats/a checked 08/24/2012

[20] *2012 Mobile Future in Focus. Key Insights from 2011 and What They Mean for the Coming Year*, comScore http://www.comscore.com/Press_Events/Presentations_Whitepapers/2012/2012_Mobile_Future_in_Focus loaded 08/24/2012

[21] *Global market share of leading smartphone operating systems in sales from 1st quarter 2009 to 2nd quarter 2012* Statista 2012 http://www.statista.com/statistics/73662/quarterly-worldwide-smartphone-market-share-by-operating-system-since-2009/ checked 08/24/2012

[22] *Möglichkeit der Handynutzung durch Kinder und Jugendliche in Deutschland in den Jahren 2010 und 2011 nach Altersgruppen* http://de.statista.com/statistik/daten/studie/1104/umfrage/handynutzung-durch-kinder-und-jugendliche-nach-altersgruppen/ checked 08/24/2012

[23] *Smartphone Users Around the World - Statistics and Facts [Infographic] Posted on 2012-01-02* http://www.go-gulf.com/blog/smartphone checked 08/24/2012

[24] *The State of Mobile Apps. June 1, 2010* http://blog.nielsen.com/nielsenwire/online_mobile/the-state-of-mobile-apps/ checked 08/24/2012

[25] *Unser mobiler Planet: Deutschland. Der mobile Nutzer. Mai 2012* think with Google. Smartphone Study Report Germany - http://services.google.com/fh/files/blogs/our_mobile_planet_germany_de.pdf checked 08/24/2012

[26] *Mobile Monitor 2012 Presse* http://www.goldmedia.com/presse/newsroom/mobile-monitor-2012-presse.html checked 08/24/2012

[27] *Visual-Manual NHTSA Driver Distraction Guidelines for In-Vehicle Electronic Devices* Department of Transportation, Docket No. NHTSA-2010-0053 http://www.nhtsa.gov/staticfiles/rulemaking/pdf/Distraction_NPFG-02162012.pdf loaded 08/24/2012

[28] Basacik, D., Reed, N., & Robbins, R. *Smartphone use while driving: A simulator study.* TRL Report PPR592

[29] *20% of drivers would use Facebook while driving* http://media.motors.co.uk/nearly-70-of-drivers-would-use-facebook-while-driving/ checked 08/24/2012

 ISBN: 978-1-61208-246-2

An Intelligent Cloud-based Home Energy Management System Based on Machine to Machine Communications in Future Energy Environments

Jinsung Byun*, Insung Hong*, Zion Hwang**, and Sehyun Park*
*School of Electrical and Electronics Engineering, Chung-Ang University, Seoul, Korea
**College of Culture and Teacher, Hyupsung University, Hwaseong, Korea
E-mail: jinsung, axlrose11421@wm.cau.ac.kr, zhwang@uhs.ac.kr, shpark@cau.ac.kr

***Abstract*— Recent advances in machine-to-machine communication technologies facilitate location/context-aware home energy management system that can provide predefined services. Such systems can establish the context model about the structural situations and the interrelations between dynamic events and services. These systems also can reason the adaptive services according to the policy construction and user requirements. However, due to their architectural limitations, the recent systems are not so flexible with respect to system scalability and availability. The important issues, such as the enhancement of the personalized service, the energy-aware service prediction of the multi situations, and the scalability of the various service domains, have not been adequately considered in the recent researches. Therefore, this paper proposes an intelligent cloud-based home energy management system (CHEMS), considering these issues. We employ cloud computing methods to deal with problems that the existing systems have. Cloud computing technologies can help the existing HEMS to deal with a large amount of computational and storage resources required to use enormous energy management data effectively. We implemented CHEMS in the test bed and conducted an experiment to verify the efficiency of the proposed system. The results show that the proposed system reduces the service response time up to 39.4 percent.**

Keywords-cloud computing; home energy management system; machine to machine communications; pattern learning

I. INTRODUCTION

Smart grid technologies have changed the electricity infrastructure more efficiently. These technologies help both electricity provider and consumer to improve energy efficiency and to reduce greenhouse gas emissions by optimizing power generation, transmission, distribution, and management. HEMS is composed of a wireless sensor network (WSN), a smart meter, a smart distribution panel, a integrated management server, and a smart actuator. They collect a variety of information and optimize energy efficiency [1]. The conventional HEMS systems have focused on standby power reduction and pattern analysis of power consumption.

Context awareness indicates the concept that computers can sense and react based on their environment. With the increasing demand for a personal environment service (PES), context-aware systems have been implemented in various places. In recent years, these systems have been gradually applied to HEMS to improve energy efficiency. These systems can offer context-aware services to users with regard to the analysis of information about the circumstances. However, the conventional systems spend excessive resource and long-term pattern analysis time, since they have to gather and store a lot of contexts and data for reasoning.

The widespread availability of embedded sensors (e.g. smart meters or monitoring sensors) for ubiquitous computing is increasingly supporting complex HEMS applications and services. Modern embedded sensors are especially well-suited to leverage information about a user's situations because they are often integrated with the mobile devices that facilitate obtaining detailed and meaningful descriptions of a user's situation. However, large-scale usage of embedded sensors will lead to the emergence of a complex organization system which requires huge computing resources. Furthermore, an increase in the embedded sensors will lead to the great rise of machine-to-machine (M2M) communications over wired and wireless links.

To deal with these problems, we propose a novel home energy management system (HEMS), i.e. intelligent cloud based home energy management system (CHEMS). Cloud computing is an emerging technology aimed to provide computing and storage services over a network [2]. Thus, cloud computing is widely applied to various applications and systems, such as a multimedia delivery service or other novel services that require high-performance processing capability [3]. Cloud computing technologies can help the existing HEMS to deal with a large amount of computational and storage resources required to use enormous energy management data effectively. Our design goals for CHEMS are:

1. Automated deployment and management of virtual infrastructure in the cloud: CHEMS employs cloud computing concept to provide home energy management services. CHEMS takes a dynamic description of a service, which encapsulates service's requirements. Thus, according to this dynamic description of a service, CHEMS can easily deploy and manage virtual infrastructure in the cloud.

2. Pattern-based learning for optimal control: Accurate reasoning based on user's living/power consumption patterns can reduce heavy event processing since it helps to find out the period when only devices are needed to be activated with respect to user's living/power consumption pattern. While dynamically generating the policies and service patterns with respect to the energy and service states, CHEMS can minimizes the energy and system resource consumption.

3. Light-weight middleware support: We present the light-weight middleware which supports the energy-aware services. The proposed light-weight middleware is based on

 ISBN: 978-1-61208-246-2

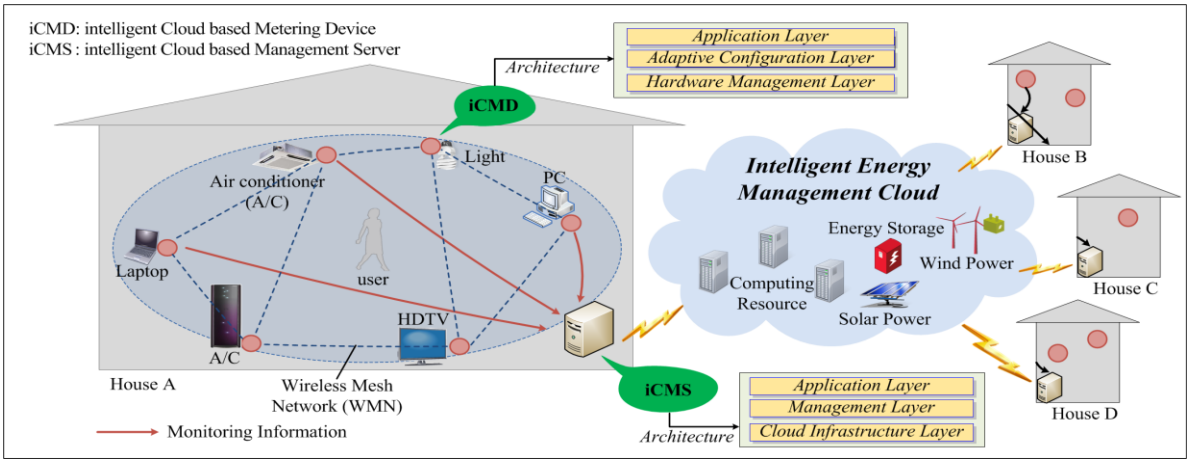

Fig. 1. Overview of intelligent Cloud-based Energy Management System (iCHEMS).

the learning mechanism which analyzes the schedule and activity of users, and also the power consumption state of devices. By grouping similar context models and pattern clustering based on user life styles, CHEMS facilitates the effective pattern learning. Then, it dynamically reconfigures the middleware on the devices that support load-balanced ubiquitous push services.

4. Extensibility and scalability: As new kinds of sensing devices, data sources, and new user activity patterns are continuously becoming available, the system is easily able to extend the service coverage to support more users. Moreover, the interface of the proposed system shouldn't be limited to a specific type of sensor connectivity. We developed a light-weight middleware and its self-configuration schemes which allow an embedded device to be reconfigured with respect to its new environment.

Furthermore, based on its pattern generation, distributed service reasoning and service prediction, it seamlessly offers the personalized and localized energy management services to residents with higher service satisfaction.

II. Related Work

A. Home Energy Management System

HEMS is an emerging technology which monitors, analyzes and controls devices such as heating, ventilating, and air conditioning (HVAC) system to reduce power consumption and CO2 emissions.

Many researchers proposed the ZigBee based HEMS systems [4]-[6]. These systems controls and monitors home appliances. In these papers, especially ZigBee (IEEE 802.15.4 standard) technology was used for implementation of HEMS, due to low-power and low-cost features of ZigBee technology. On the other hand, Son *et al* [7] presented HEMS based on power line communication (PLC). Zhao *et al* [8] presented a building energy management system (BEMS) by using a multi-agent decision-making control methodology. Nguyen *et al* [9] dealt with advanced load management strategies for BEMS. This paper suggested a real-time control using wireless sensor network. Wei *et al* [10] proposed an adaptive home/building energy management system (A-HEMS/BEMS) for managing power consumption by using the convergence of heterogeneous sensor/actuator networks. Mineno *et al* [11] proposed the system framework for building energy monitoring and analysis system based on the packet data network.

B. Electricity Smart Meter

A smart meter is an advanced metering device that can be used to measure energy consumption and can communicate this information to other devices. The smart meter is the most important component of advanced metering infrastructure (AMI) that connects HEMS and a smart grid that optimize the production, distribution, and consumption of electricity [12]. Kung *et al* [13] proposed a fuzzy-based adaptive approach to measure electric power, and also RMS (root mean square) voltage and current using a genetic algorithm (GA). Benzi *et al* [14] presented the definition of a local interface for power meters and the specific architectures for a proper consumer-oriented implementation of a smart meter network. Silva *et al* [15] proposed a data mining framework for the exploration and extraction of actionable knowledge from data generated by electric power meters. On the other hand, security is an important issue in the design of the smart meter. Kim *et al* [16] suggested a secure smart-metering protocol, considering several important aspects of security and authentication such as key management, secure transmission, and device authentication.

III. Intelligent Cloud-based Energy Management System

The current intelligent HEMS can provide smart services such as a user-centric service based on context-awareness, a power distribution service based on demand forecasting, or an autonomous energy management service based on the M2M communications. The provision of these intelligent HEMS will lead to the usage of enormous computational and storage resources as mentioned above. To deal with these problems, we propose a novel home energy management

 ISBN: 978-1-61208-246-2

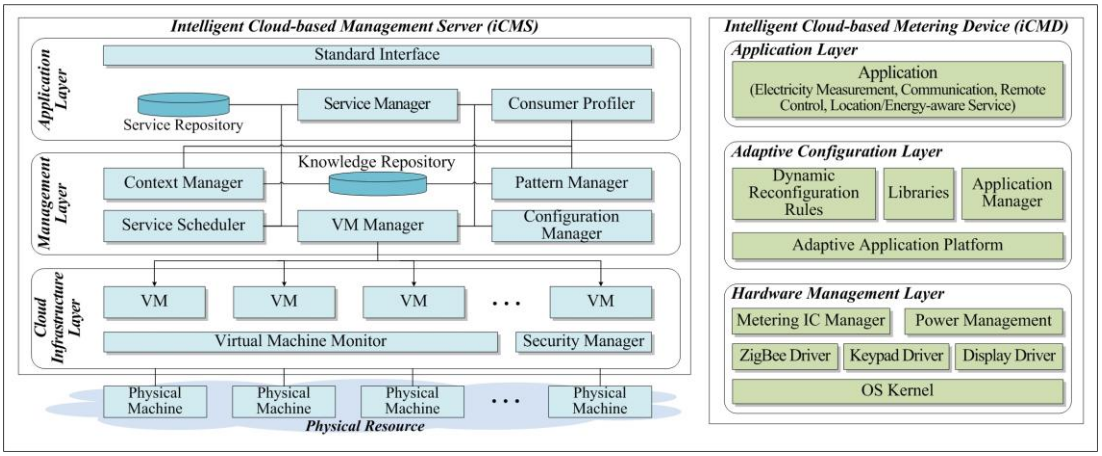

Fig. 2. Architecture of iCHEMS (iCMS and iCMD).

system i.e. CHEMS. In this section, we present the overall system architecture of CHEMS.

A. Overview of CHEMS

Fig. 1 shows an overview of CHEMS which consists of an intelligent cloud-based management server (iCMS) and an intelligent cloud-based metering device (iCMD). The main features of our system are as follows:

1) CHEMS uses cloud computing methods to process complex tasks that require enormous computational and storage resources.

2) CHEMS has the capability to manage local renewable energy.

3) CHEMS should consider energy reduction by the optimization of sensing, processing, and transmission of M2M nodes.

4) CHEMS provides users with user-friendly location- and situation-based push energy management services in order to enhance user interaction and energy efficiency.

B. Architecture

Fig. 2 illustrates the system architecture of iCMS. iCMS needs to be reconfigured to allocate additional or release unneeded resources and appropriately reorganize the deployed software, hardware, middleware components. iCMS consists of three architectural layers: application layer, management layer, and cloud infrastructure layer.

1) Application layer: This layer creates the instances of energy management service model. This layer plays a role in service analysis, service decision, service creation, service configuration, and service management. This layer includes all components related to applications which run in the cloud. This layer consists of a service manager, a consumer profiler, a service repository and a standard interface.

- Service manager analyzes requested services and interprets the service requirement of a consumer's request. When the service is requested, the service manager determines which system resources are suitable and how many system resources are needed.
- Consumer profiler gathers the information about the consumer (e.g. user or device). The information contains user's preference, location, energy consumption, etc.
- A user requests a service and the system provides a service through standard interface.

2) Management layer: This layer controls the process related to the provision of cloud and context-aware services. This layer consists of a context manager, a service scheduler, a VM manager and a configuration manager.

- Context manager gathers information about the circumstances and manages this information.
- Service scheduler determines resource entitlements for the allocated VMs. In other word, the service scheduler determines when VMs should be added or released to meet the service requirement.
- VM manager consists of an accounting manager and an energy monitor. The accounting manager checks the actual resource usage and accounts for the cost. The energy monitor analyzes energy consumption of VMs and physical resources. It enables iCMS to perform the energy-efficient resource allocation.
- Configuration manager controls all the essential parameters related to the system configuration. These parameters include the size of the virtual resources, the cloud infrastructure provider to use, or the software component.

3) Cloud infrastructure layer: This layer controls and manages the hardware/software resource in the physical level resource. This layer applies virtualization technology to hide the characteristics of the physical resources. This layer also should consider security issues caused by cloud computing. This layer consists of VMs, a virtual machine monitor, and a security manager.

- VMs dynamically run and stop on multiple physical resources.
- Security manager guarantees confidentiality, integrity and authentication. It provides strong isolation.

 ISBN: 978-1-61208-246-2

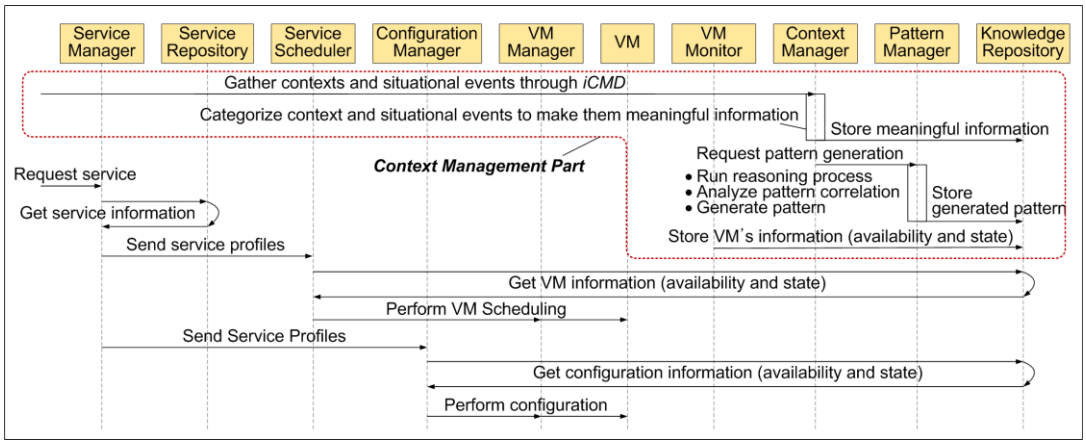

Fig. 3. Sequence diagram of provisioning cloud computing servcie.

- Virtual machine monitor observes the availability and state of VMs.

The physical resource is composed of the physical level resources such as computing, storage, power, and network resources.

On the other hand, iCMD consists of an application layer, an adaptive configuration manager, and a hardware management layer. The application layer is mainly used for service analysis, service decision, service creation, service configuration, and service management like the application layer of iCMS. The adaptive configuration manager controls and manages the rule-update process. The administrator modifies or updates the rules through the administrator mode of the iCMD. The hardware management layer has the role of managing the various hardware modules such as a metering IC, a ZigBee tranceiver, a display driver, etc.

C. Cloud Service Based on Situation-Awareness

Fig. 3 shows a sequence diagram for provisioning a cloud service according to the situational and environmental events in iCMS. The light-weight middleware operates the learning mechanism and predicts the personalized service with regard to the policy modification and the energy management. The sequence diagram divides into two independent parts that is context management part and cloud management part.

1) Context management part: The iCMS receives contexts about an environment and situations such as power consumption and a user's movement through the iCMD. The context manager then analyzes and categorizes the gathered contexts and situation event to make them meaningful information and stores them in the knowledge repository. On the other hand, the pattern manager performs reasoning task (through the inference engine), pattern correlation task (through the pattern correlator), and pattern generation task (through pattern generator). The pattern is generated based on the user's situations, the power consumption, and the service history. This pattern is used for the provision of energy management based on prediction to the local use. This generated pattern is stored on the knowledge repository.

2) Cloud management part: The cloud computing is an important property of this system. The user requests energy management service through a mobile device. The proposed platform interconnects the heterogeneous devices and networks for scalability and interoperability. When a user moves to another location, this middleware verifies the meaning events and predicts the pattern-based service. The intelligent device creates the passive events and offers active service, called push service, to user based on the interconnection. The procedure of the cloud management part is as follows.

First, the user sends requests for a service to iCMS. This request is passed to the service manager. The service manager requests the service repository to send the service profiles which include a service requirement (i.e. required virtual resources).

Second, the service manager transmits the service profiles to the service scheduler to perform the scheduling i.e. resource entitlements. The service profiles are passed to the service scheduler that employs this information to request the virtual infrastructure creation. The service scheduler requests the knowledge repository to send information about the VMs (e.g. availability and state of the VMs). When receiving this information, the service scheduler determines resource entitlements for the allocated VMs. That is, it determines when VMs should be added or released to meet the service requirement.

Third, the service manager transmits the service profiles to the configuration manager to perform the configuration according to the infrastructure's conditions. The configuration manager manages all the essential configuration parameters, such as the size of the virtual resources, the cloud infrastructure provider to use, or the software component parameters. The configuration is composed of three processes which are pre-configuration (VMs are configured before they are started), post-configuration (VMs are configured after they are started), and re-configuration (VMs are configured as a result of topological changes). To perform these configuration steps of a component, the configuration manager retrieves the

 ISBN: 978-1-61208-246-2

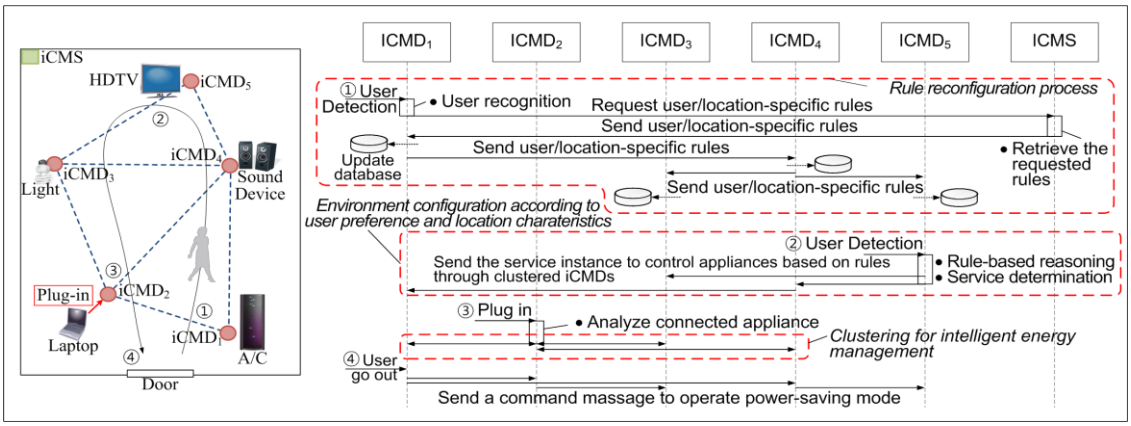

Fig. 4. Interoperation flow of a home energy management service scenario.

related configuration description from a knowledge repository, and performs the configuration.

In this section, we will show a simple service scenario to explain interoperation among both multi iCMDs and between iCMD and iCMS. Fig. 4 shows interoperation flow of a simple home energy management service scenario.

1) Rule reconfiguration: Alice enters the room. iCMD1 detects and recognizes Alice through interaction between iCMD1 and Alice's handheld ZigBee transceiver. iCMD1 then requests iCMS to transmit user/location-specific rules. When receiving the requests from iCMD1, iCMS retrieves the requested rules from the knowledge repository and sends the user/location-specific rules to iCMD1. iCMD1 then updates database and transmits these user/location-specific rules to adjacent iCMDs.

2) Environment configuration according to user preference and location characteristics: Alice walks towards HDTV in order to watch a movie and turns on the HDTV. iCMD5 performs rule-based reasoning and determines a service. It then creates a service instance.

3) Clustering for intelligent energy management: According to the location-aware clustering, iCMDs interconnects with iCMDs which are located in same location. When an iCMD detects the user movement or the energy consumption, the iCMD requests the cooperation of energy management service to clustered iCMDs.

4) operation in power-saving mode: If iCMD1 perceives that Alice goes out the room, the iCMD1 sends all the iCMDs a command message to operate in power-saving mode.

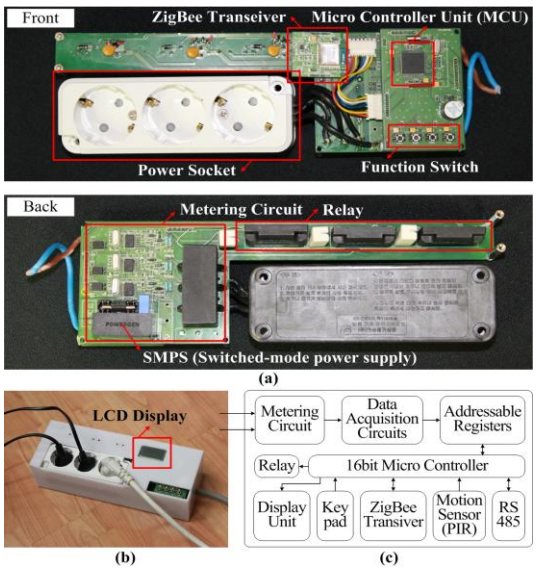

Fig. 5. Prototype of ICMD; (a) PCB layout, (b) prototype, and (c) hardware block diagram

IV. IMPLEMENTATION

Fig. 5 shows a prototype and a hardware block diagram of iCMD. Same hardware components as reference [17] are used except for the micro controller unit (MCU). In this paper, the 8-bit MCU instead of the 16-bit MCU is used as the main processor, because of the reduction of the production cost. A 250 kbps/2.4 GHz ZigBee transceiver module is used for communication. The metering circuit is used for measurement of the power consumption and monitoring the power state. The power group consists of the SMPS and power regulation circuit. A variety of information such as power, voltage, and current as well as temperature and humidity is displayed through the LCD display unit. The relay plays a role in shutting off the standby power and remote control.

V. EXPERIMENT AND RESULTS

A. *Test-bed*

We deployed CHEMS in the real home service test bed to estimate its efficiency. We analyzed the proposed mechanism according to various scenarios at real homes and enhanced the correctness of the proposed system according to user activity patterns and service scenarios. The results presented in the following were collected from 1 month dynamic experiment, where 20 iCMDs and various appliances (TVs, VCRs, humidifiers, microwave ovens, air conditioners, PCs and etc.) in our test bed. We tested three

 ISBN: 978-1-61208-246-2

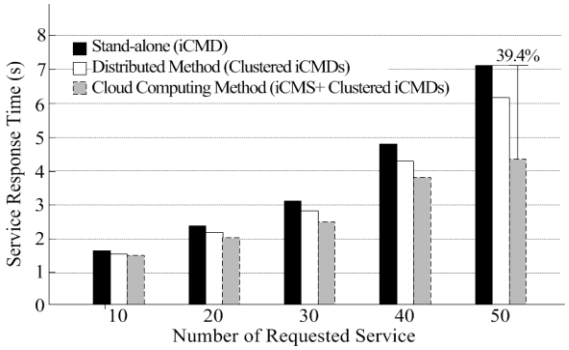

Fig. 6. Comparison of the service response time.

types of power control systems in the experiment environment.

B. Experiment and Results

Headings Fig. 6 shows the service response time by the number of requested service for home energy management. The results show that the proposed system reduces the service response time up to 39.4 percent. Even though the number of requested service increases, the proposed system maintains certain levels of delay of the home energy management due to resource allocation through iCMS. The proposed system gradually decreases the slope of the service response time according to the efficient management of metering data, and resource allocation and configuration. However, stand-alone iCMD rapidly increases the service response time due to the overhead from the increasing number of metering data and control messages.

VI. CONCLUSIONS AND FUTURE WORKS

We designed and implemented CHEMS considering new trends of HEMS which require interoperable user-centric services to the green home domains. We utilize a cloud computing concept to deal with various problems of the existing systems. We implemented and evaluated the proposed system in the real home test bed. The results show that the proposed system reduces the service response time up to 39.4 percent. We are planning to implement efficient authentication and authorization mechanisms for the reliable service domain interconnection and pattern generation.

ACKNOWLEDGMENT

This research was supported by the MKE (The Ministry of Knowledge Economy), Korea, under the ITRC (Information Technology Research Center) support program (NIPA-2012-H0301-12-4004) supervised by the NIPA (National IT Industry Promotion Agency) and by the Human Resources Development program (No.20104010100570) of the Korea Institute of Energy Technology Evaluation and Planning (KETEP) grant funded by the Korea government Ministry of Knowledge Economy.

REFERENCES

[1] D. Niyato, L. Xiao, and P. Wang, "Machine-to-machine communications for home energy management system in smart grid," *IEEE Communications Magazine*, vol. 49, no. 4, pp. 53-59, April 2011.

[2] W. Zhu, C. Luo, J. Wang, and S. Li, "Multimedia Cloud Computing," *IEEE Signal Processing Magazine*, vol. 28, no. 3, pp. 59-69, May 2011.

[3] Y. Wei and M. B. Blake, "Service-Oriented Computing and Cloud Computing: Challenges and Opportunities," *IEEE Internet Computing*, vol. 14, no. 6, pp. 72-75, Nov.-Dec. 2010.

[4] K. Gill, S.-H. Yang, F. Yao, and X. Lu, "A zigbee-based home automation system," *IEEE Trans. Consumer Electron.*, vol. 55, no. 2, pp. 422-430, May 2009.

[5] D.-M. Han and J.-H. Lim, "Design and implementation of smart home energy management systems based on zigbee," *IEEE Trans. Consumer Electron.*, vol. 56, no. 3, pp. 1417-1425, Aug. 2010.

[6] D.-M. Han and J.-H. Lim, "Smart home energy management system using IEEE 802.15.4 and zigbee," *IEEE Trans. Consumer Electron.*, vol. 56, no. 3, pp. 1403-1410, Aug. 2010.

[7] Y.-S. Son, T. Pulkkinen, K.-D. Moon and C. Kim, "Home energy management system based on power line communication," *IEEE Trans. Consumer Electron.*, vol.56, no.3, pp.1380-1386, Aug. 2010.

[8] P. Zhao, S. Suryanarayanan, and M. G. Simões,, "An Energy Management System for Building Structures Using a Multi-Agent Decision-Making Control Methodology," *IEEE Industry Applications Society Annual Meeting (IAS)*, pp. 1-8, Oct. 2010.

[9] N.-H. Nguyen, Q.-T. Tran, J.-M. Leger, and T.-P. Vuong, "A real-time control using wireless sensor network for intelligent energy management system in buildings," *IEEE Workshop on Environmental Energy and Structural Monitoring Systems (EESMS)*, pp. 87-92, Sept. 2010.

[10] C. Wei and Y. Li, "Design of energy consumption monitoring and energy-saving management system of intelligent building based on the Internet of things," *International Conference on Electronics, Communications and Control (ICECC)*, pp. 3650-3652, Sept. 2011.

[11] H. Mineno, Y. Kato, K. Obata, H. Kuriyama, K. Abe, N. Ishikawa, and T. Mizuno, "Adaptive Home/Building Energy Management System Using Heterogeneous Sensor/Actuator Networks," *IEEE Consumer Communications and Networking Conference (CCNC)*, pp. 1-5, Jan. 2010.

[12] H. S. Cho, T. Yamazaki, and M. Hahn, "Determining location of appliances from multi-hop tree structures of power strip type smart meters," *IEEE Trans. Consumer Electron.*, vol. 55, no. 4, pp. 2314-2322, Nov. 2009.

[13] C.-H. Kung, M. J. Devaney, C.-M. Huang, and C.-M. Kung, "Fuzzy-based adaptive digital power metering using a genetic algorithm," *IEEE Trans. Instrumentation and Measurement*, vol. 47, no. 1, pp. 183-188, Feb. 1998.

[14] F. Benzi, N. Anglani, E. Bassi, and L. Frosini, "Electricity Smart Meters Interfacing the Households," *IEEE Trans. Industrial Electron.*, vol. 58, no. 10, pp. 4487-4494, Oct. 2011.

[15] D. D. Silva, X. Yu, D. Alahakoon, and G. Holmes, "A Data Mining Framework for Electricity Consumption Analysis From Meter Data," *IEEE Trans. Industrial Informatics*, vol. 7, no. 3, pp. 399-407, Aug. 2011.

[16] S. Kim, E. Y. Kwon, M. Kim, J. H. Cheon, S. Ju, Y.-H. Lim, and M.-S. Choi, "A Secure Smart-Metering Protocol Over Power-Line Communication," *IEEE Trans. Power Delivery*, vol. 26, no. 4, pp. 2370-2379, Oct. 2011.

[17] J. Byun, I. Hong, and S. Park, "Intelligent Cloud Home Energy Management System Using Household Appliance Priority Based Scheduling Based on Prediction of Renewable Energy Capability," *IEEE Trans. Consumer Electorn.*, vol. 58, no. 4, Nov. 2012

 ISBN: 978-1-61208-246-2

Classification and Monitoring of Early Stage Breast Cancer using Ultra Wideband Radar

Marggie Jones, Dallan Byrne, Brian McGinley,
Fearghal Morgan , Martin Glavin, Edward Jones and Martin O'Halloran
College of Engineering and Informatics
National University of Ireland Galway
University Road, Galway, Ireland
Email: marggie.jones@gmail.com, dallan.byrne@gmail.com, brian.mcginley@gmail.com, fearghal.morgan@nuigalway.ie, martin.glavin@nuigalway.ie, edward.jones@nuigalway.ie, martin.ohalloran@nuigalway.ie

Raquel C. Conceição
Instituto de Biofísica e Engenharia Biomédica
Faculdade de Ciências
Universidade de Lisboa
Portugal
Email: raquelcruzconceicao@gmail.com

***Abstract*—This paper presents a novel Self-Organising Map for breast cancer classification and monitoring, based on Microwave/Ultra Wideband radar imaging. This approach has the potential to help clinicians to differentiate and track the development of a tumour from a benign state to different levels of malignancy based on their Radar Target Signature (RTS). Many existing studies have investigated the use of the RTS of a tumour to classify breast cancer as either benign or malignant, based on the fact that the RTS of a tumour is dependent on tumour shape, size and surface texture. In this paper, a self-organising (Kohonen) map is applied to the salient features of the tumour RTSs, developing a two-dimensional "MammoMap", where the various regions of the map correspond to the characteristics (benign or malignant) of the tumour, potentially allowing for the allowing for the classification and monitoring of tumour growth.**

***Keywords*-Microwave Imaging; Breast Cancer; Classification; radar**

I. INTRODUCTION

In the US, between 4%-34% of all breast cancers are missed by conventional X-Ray mammography [1], while 70% of all malignancies identified are found to be benign after biopsy [2]. These false positive conclusions result in unnecessary biopsies, causing considerable distress to the patient and an unnecessary financial burden on the health service [2], [3]. In the US, more than 184,000 new cases of breast cancer are diagnosed each year resulting in approximately 41,000 deaths. Early detection and intervention is one of the most significant factors in improving the survival rates and quality of life experienced by breast cancer patients [4], since this is the time when treatment is most effective.

Ultra Wideband (UWB) radar imaging is one of the most promising emerging breast imaging modalities. The physical basis of UWB radar imaging is the dielectric contrast between normal and malignant breast tissue that exists at microwave frequencies [5], [6], [7], [8], [9], [10]. This dielectric contrast is due to the increased water content present in the cancerous tissue, and this contrast suggests that when the breast is illuminated by a UWB pulse, cancerous tissue in the breast tissue will provide backscattered energy, which may be used to detect, localise, classify and track tumour development. UWB radar imaging is non-ionising, non-invasive, does not require uncomfortable breast compression, and is potentially low cost.

Several studies have also examined the use of UWB radar to classify breast cancer. This classification approach is based on the Radar Target Signature (RTS), which reflects the size, shape and surface texture of the tumour. Benign tumours typically have smooth surfaces and have spherical, oval or at least well-circumscribed contours. Conversely, malignant tumours usually present rough and complex surfaces with spicules or microlobules, and their shapes are typically irregular, ill-defined and asymmetric [11]. These tumour characteristics are generally reflected in the details of the RTS and can be used to differentiate between benign and malignant tumours, potentially negating the need for tumour biopsy.

In this paper, a Self-Organising Map (SOM) tumour classification and monitoring algorithm is considered. The map is described as "self-organising" since the learning process is completely unsupervised. In the implementation considered in this paper, the SOM produces a two-dimensional map, where the map is divided into a number of distinct regions. These regions can correspond to either tumour size (large or small) or tumour type (benign or malignant), depending

 ISBN: 978-1-61208-246-2

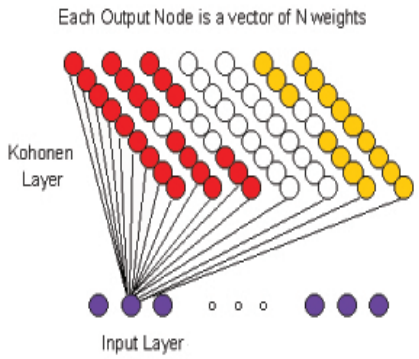

Figure 1. Kohonen SOM topology, adapted from [13]. Each output layer node is represented by an N-dimensional weights vector.

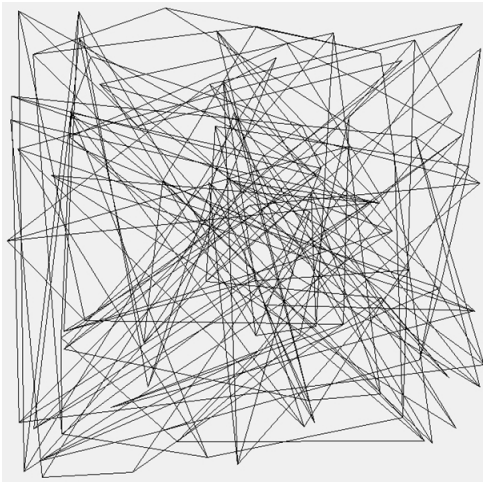

Figure 2. Plot of network weights directly after random initialization.

on the specific application. These "MammoMaps" could provide a very intuitive visual aid to clinicians for the diagnosis, monitoring and treatment of early stage breast cancer.

Self-organising maps are briefly described in the next section. This is followed by a discussion of tumour shape and electromagnetic modelling. In Section 4 details of the feature extraction method used are given. Results and discussion follow in Section 5, and finally a conclusion is drawn and future work proposed in Section 6.

II. Self-Organising Maps

Self-Organising Maps (SOMs) are a type of neural network that are trained using unsupervised learning, where the input pattern is applied and the network produces the output without being told what output should be produced [12]. Self-organising maps consist of an input and an output layer. The topology of a SOM network is shown in Figure 1. The dimension of the input layer is defined as being equal to the number of features or attributes, while the output layer is typically a two-dimensional grid (shown as red, white and yellow regions in Figure 1). In SOMs, the two layers are fully interconnected i.e., each input (ip_i) is connected to every unit or node in the output layer.

To illustrate the operation of the SOM, two-dimensional data is employed here, showing the topological mapping of the data. Although, 2-D data is used here for illustration purposes, the SOM performs very well in organising much-higher dimensional data such as that generated by the UWB feature-extraction methods used in this paper. The 2-D input data is randomly initialised and evenly distributed over the range zero to one. Weightings, wt_{j1} and wt_{j2}, initially also randomly selected from the same range, are associated with the inputs to each node j. These weights are adapted so that the network of weights, as an entirety, organises to form topological mappings of the input space. This means that the distribution of weight values in the network will reflect the distribution of input data. Details of how these network weights are adapted are given in the following section.

To more easily visualise the topological distribution of network weights, a graph is plotted with a point for each node in the output layer, the co-ordinates of each point being given by the weight values of the node (e.g. ordinate value wt_{j1} and abscissa value wt_{j2}). If nodes in the output layer are assigned indices (i, j) denoting their row and column, then joining the point for node (i, j) to the points for nodes $(i + 1, j)$ and $(i, j + 1)$ for every node in the output layer yields a plot similar to Figure 2. Figure 2 illustrates randomly selected weights chosen from the range zero to one before the Kohonen training process was applied (i.e., the plot was made directly after initializing the weight values).

A. Network Training

Having randomly initialized the weight values, the training process described by Kohonen [12] now begins. For training, the following steps are repeated for N iterations, where N is the number of training steps:

1) Randomly choose inputs to present to the SOM;
2) On the basis of a Euclidean distance metric, find the output-layer node whose weights are most similar to the input;
3) Update the weight of that node and those of its neighbours according to the following equation:

$$w_{ji}(t) = w_{ji}(t-1) + \alpha(t-1)[ip_i(t-1) - w_{ji}(t-1)] \quad (1)$$

where $w_{ji}(t)$ is the weighting between node j and input i, ip_i is the i^{th} input, and α is the gain or learning rate (an empirically chosen adjustable parameter that can be adjusted to regulate the training speed);
4) Reduce neighbourhood size and learning rate as per the following two equations:

$$D = \lceil d_0(1 - t/N) \rceil \quad (2)$$

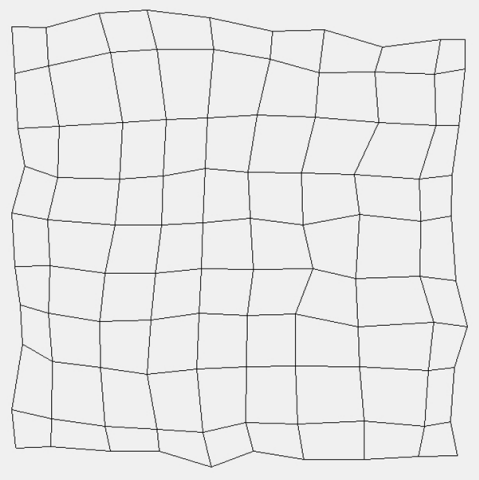

Figure 3. Network weights after training has been completed.

where d_0 is the initial neighbourhood size, t is the current updating/training iteration and N is the total number of iterations.

$$\alpha = \alpha_0(1 - t/N) \tag{3}$$

Typically the neighbourhood size begins large (e.g. one-half to one-third of the grid size). Several different forms of neighbourhood type can be used. In this paper, a simple square neighbourhood is used and neighbourhood size is restricted to integer values. After training has been completed, the weight values are once again plotted and shown in Figure 3.

B. Network Testing

Randomly chosen input patterns are applied and Euclidean distance competitions held to see which set of weights are most similar to the input patterns. Similar inputs pattern have been found to cause nodes that are adjacent in the output layer to win. This being the case, from Kohonen's definition [14], the neural network can be said to be organised: "The mapping is said to be ordered if the topological relations of the images and the patterns are similar". Using a skewed input distribution, where the second training input is chosen to be in the range [0,0.2] when the first training input is greater than 0.5, leads to the map shown in Figure 4.

This approach to testing and training, applied to the breast tumour RTS dataset, is discussed in Section V.

III. Tumour Shape and Electromagnetic Modeling

A. Tumour Shape Modelling

Shape and texture of the surface of a tumour are two of the most important characteristics used to differentiate between a benign and a malignant tumour. The tumour models used in this paper are based on the Gaussian Random Spheres (GRS) method [15], [16]. GRS can be modified mathematically to model both malignant and benign tumours of different sizes by varying the logarithmic radius and the mean radius α, respectively. The shape is determined by the radius vector, $\mathbf{r} = r(\theta, \psi)$, described in spherical coordinates (r, θ, ψ), by the logradius $s = s(\theta, \psi)$:

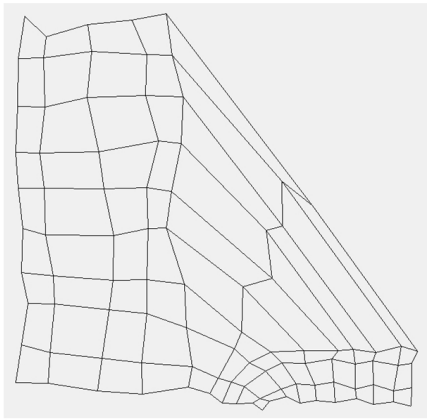

Figure 4. Plot of network weights for a skewed input distribution.

$$s(\theta, \psi) = \sum_{l=0}^{\infty} \sum_{m=-l}^{l} s_{lm} Y_{lm}(\theta, \psi) \tag{4}$$

$$r(\theta, \psi) = \alpha \exp\left[s(\theta, \psi) - \frac{1}{2}\beta^2\right] \tag{5}$$

In the equations above, β is the standard deviation of the logradius, s_{lm} are the spherical harmonic coefficients and Y_{lm} are the orthonormal spherical harmonics [15], [16]. Three different tumour models of one size are considered in this paper (macrolobulated benign, and 3 and 10-spiculed malignant tumours). Malignant tumours are represented by spiculed GRS, whereas benign tumours are modelled by macrolobulated GRS. Macrolobulated GRS are obtained by varying the correlation angle between 25 and 45 degrees and smooth GRS have a correlation angle between 50 and 90 degrees. Spiculed GRS are obtained by adding 3 or 10 spicules to smooth GRS. The average radius of all types of spheres are 2.5 mm. Ninety tumour models were developed (30 benign and 60 malignant of which 30 had three spicules and 30 had ten spicules), each having 4 recorded signals corresponding to 4 antennas.

In order to examine the effects of dielectric heterogeneity, a second set of models was created where fibroglandular tissue was introduced into the FDTD models. Fibroglandular tissue, extracted from the UWCEM Breast Phantom Repository [17], is introduced into the FDTD model (phantom ID 071904). A single piece of fibroglandular tissue is added to the FDTD models, as shown in Figure 5.

 ISBN: 978-1-61208-246-2

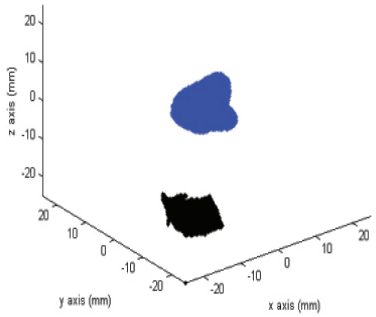

Figure 5. Example of the heterogeneous breast model. The tumour is shown in blue, while the fibroglandular tissue is shown in black.

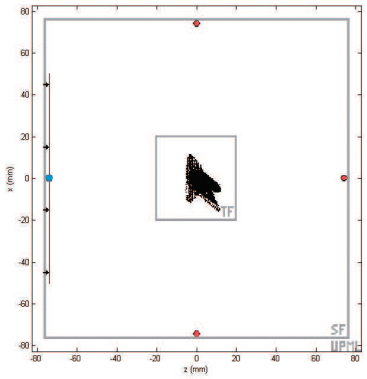

Figure 6. Cross-section of the 3D FDTD space lattice partitioned into Total Field (TF), Scattered Field (SF) and UPML regions, for a homogeneous breast model. The target, a spiculed tumour located at the centre of the TF in this example, is illuminated by a pulsed plane wave propagating in the +z direction (represented by a dark line) and backscatter is recorded at the first observer location: (0,0,-74) mm (represented by a blue circle). The remaining three antennas are represented by small red circles in the image.

B. Electromagnetic Modelling

The 90 tumours of size 2.5 mm are placed in a 3D Finite-Difference Time-Domain (FDTD) model. The FDTD model has a 0.5 mm cubic grid resolution and the backscattered signals were generated through a Total-Field/Scattered-Field (TF/SF) structure, in which the tumours and fibroglandular tissue are completely embedded in the Total Field (TF) [18], [19]. The TF/SF region has the following dimensions: the Scattered Field (SF) is a square prism with square bases measuring 153.5 mm on the side and height measuring 137.5 mm. The TF is located at the centre of the SF and is represented by a 50 mm-sided cube (the origin of the SF and the TF are at the point (0,0,0) mm). The dielectric properties of adipose, fibroglandular, and cancerous breast tissue are incorporated in the FDTD using a Debye formulation, based on the dielectric properties established by Lazebnik *et al.* [9], [10]. The TF/SF region is terminated with a 6 mm-layer Uni-axial Perfectly Matched Layer (UPML) which suppresses any boundary reflections [20].

A pulsed plane wave is transmitted towards the target from four different equidistant angles $(0°, 90°, 180°, 270°)$ and the resulting cross-polarised backscatter is recorded and analysed from antennas located at: (0,0,-74), (-74,0,0), (0,0,74) and (74,0,0) mm in (x,y,z) axes. The incident pulse is a modulated Gaussian pulse with center frequency at 6 GHz where the 1/e full temporal width of the Gaussian envelope is 160 picoseconds. For two transmitters, the pulse is linearly polarised in the x-y plane and transmitted in the z direction, and for the remaining transmitters, the pulse is polarised in the y-z plane and transmitted in the x direction. Each antenna is located in the SF at a distance of 74 mm from the center of the tumour, which is located at the centre of the TF. The acquired backscattered recorded signals are downsampled from 1200 GHz to 75GHz. Figure 6 shows a representation of the TF/SF grid, with the location of the origin of the first incident plane wave and respective observer point as well as the position of the tumour.

IV. Feature Extraction

The Discrete Wavelet Transform (DWT) is applied to the RTS and the resultant wavelet coefficients are obtained using low-pass decomposition filters. Subsequently, the low-pass band may be split again through further low-pass filters. In this paper, the chosen wavelet is *Coiflet 5* (established as the optimum wavelet by empirical analysis). The frequency band that is used for classification corresponds to the wavelet coefficients obtained from the low-pass band after a two-level decomposition, as these wavelet coefficients were found to give the best classification performance compared to other subbands, evaluated up to four levels of decomposition.

To identify the most relevant DWT coefficients for input to the SOM, a statistical analysis was performed on the dataset to identify the DWT components that exhibit the most statistically significant differences between malignant and benign tumours. A T-Test identifies the largest significant differences between the means of two independent sample groups, while taking the variances of both groups into account. The independent variable is whether the tumour is malignant or benign, while the dependent variable is the level of the DWT output. The 15 DWT components that exhibit the greatest differences between malignant and benign were identified, normalised, scaled to [-1,1] and employed for classification purposes

V. Results

Two distinct datasets were considered: data from simulations where the tumour is located in homogeneous breast tissue and a second set where fibroglandular tissue is present

 ISBN: 978-1-61208-246-2

(i.e., data from a more heterogeneous breast). Each of these datasets consisted of 360 tumour signals from models of size 2.5 mm each comprising of 15 normalised and scaled DWT values. In order to evaluate the classifier, each data-set is randomly shuffled and divided into ten combinations of 276 training and 84 testing tumours. The classification process is repeated 10 times for each of the ten files and the average performance of the classifier is calculated (note: all results presented is this paper are based on the performance of the test set).

For this particular study, weights were randomly initialized to be in the range [-1, 1] and training consisted of repeatedly applying scaled patterns of the 15 DWTs randomly chosen from the 276 tumour models in the training sample, until the network organised. The output layer consisted of a square 10x10 grid. The gain/learning rate (0.5), neighbourhood size (4) and number of training steps (5100) were empirically chosen. During training, the neural network had no input indicating whether the input pattern being presented to it belonged to a malignant or to a benign tumour model.

At the end of training, the network weights were frozen. At this point a Euclidean distance competition was held for each node in the output layer, for each of the 276 training tumour models in the training set. The tumour model pattern most similar to the weights of a node was then assigned to that node. Only at this point was the training data set examined to discover which inputs corresponded to malignant/benign tumour models.

Three-way classification is shown in the MammoMaps illustrated in Figure 7. Here, benign, 3-spiculed malignant and 10-spiculed malignant tumours are represented as green, orange and red regions, respectively.

In order to evaluate the performance of the three-way SOM classifier, the SOM is tested using a test sample of 84 tumours. Importantly, the DWT coefficients corresponding to these tumours have not previously been presented to the network. For testing, the 15 DWT values for each of the test tumour models are input to the trained network (whose weights are now frozen), a distance competition is held for each tumour model and a winning node found. The tumour is then classified based on which region it falls into on the SOM.

An average classification accuracy across 10 maps for each of the ten shuffled files was as follows:

- 99.5% for macrolobulated tumours
- 90.54% for 3 spiculed malignant tumours
- 88.28% for 10 spiculed malignant tumours

yielding an overall average accuracy of 92.77%.

The tumours fall into clear and distinct regions within the resultant SOM MammoMaps. Significantly, the region of benign tumours (shown in green) is separated in all cases from the highly malignant 10-spicule tumour region (shown in red) by the intermediate 3-spicule tumour region (shown in orange).

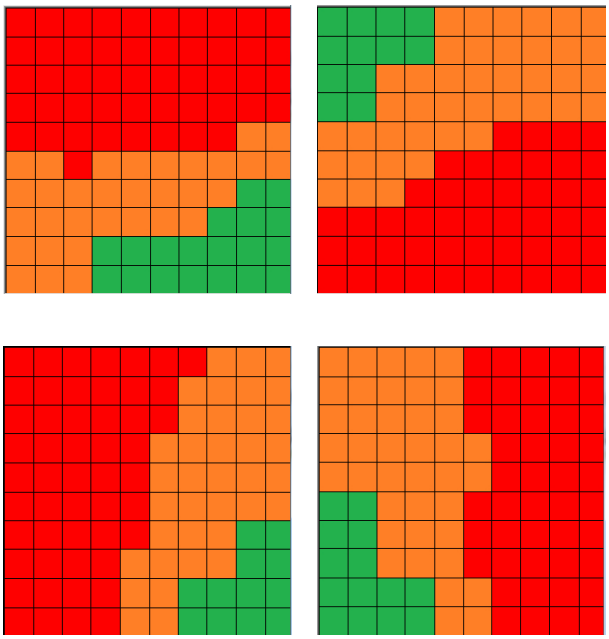

Figure 7. Four examples of three-way classification between benign macrolobulated (green), 3 spiculed malignant (orange) and 10 spiculed malignant (red) tumours using an SOM.

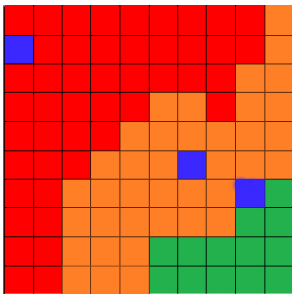

Figure 8. Tumour development tracking with an SOM. As the tumour (shown in blue) becomes increasingly malignant, it moves across the map from the green region to the red region.

Figure 8 shows a SOM being used to monitor a tumour (shown in blue) as it develops from benign macrolobulated to 3 spiculed malignant to 10 spiculed malignant. This highlights the significant potential of SOMs for tumour tracking, since SOMs preserve the input data topology.

VI. Conclusion and Future Work

In this study, "MammoMaps" have been shown to have the ability to differentiate between macrolobulated benign and two different levels of malignant tumours. Therefore, these "MammoMaps" have significant potential as a cancer classification or diagnosis tool.

 ISBN: 978-1-61208-246-2

However, more importantly they could also be used to monitor the development of a tumour due to the fact that "MammoMaps" preserve the topology of the input information. Therefore, a clinician could use these maps to determine whether a tumour is developing from benign to malignant (moving across the "MammoMap") or not (staying static on the "MammoMap"). Movement even within the benign region could indicate that the tumour is developing even before it is classified as malignant and so treatment could be offered to patients at a very early stage of their disease, when it is most effective. This potential will be further examined in future studies.

ACKNOWLEDGMENT

This research has been supported by Science Foundation Ireland (SFI) under the Starting Investigator Research Grant number 11/SIRG/12120, by Fundação para a Ciência e a Tecnologia under grant number SFRH/BPD/79735/2011 and by a Marie Curie Intra European Fellowship within the 7th European Community Framework Programme under REA grant agreement number 301269.

REFERENCES

[1] P. H. Huynh, A. M. Jarolimek, and S. Daye, "The false-negative mammogram," *RadioGraphics*, vol. 18, pp. 1137–1154, 1998.

[2] J. G. Elmore, M. B. Barton, V. M. Moceri, S. Polk, P. J. Arena, and S. W. Fletcher, "Ten-year risk of false positive screening mammograms and clinical breast examinations," *New Eng. J. Med.*, vol. 338, no. 16, pp. 1089–1096, 1998.

[3] F. M. Hall, J. M. Storella, D. Z. Silverstone, and G. Wyshak, "Non-palpaple breast-lesions, recommendations for biopsy based on suspicion of carcinoma at mammography," *Radiology*, vol. 167, no. 2, pp. 353–358, 1988.

[4] S. L. Nass, I. C. Henderson, and J. C. Lashof, *Mammography and Beyond: Developing Technologies for the early detection of breast cancer*. National Academy Press, 2001.

[5] S. S. Chaudhary, R. K. Mishra, A. Swarup, and J. M. Thomas, "Dielectric properties of normal and malignant human breast tissue at radiowave and microwave frequencies," *Indian J. Biochem. Biophys.*, vol. 21, pp. 76–79, 1984.

[6] A. J. Surowiec, S. S. Stuchly, J. R. Barr, and A. Swarup, "Dielectric properties of breast carcinoma and the surrounding tissues," *IEEE Trans. Biomed. Eng.*, vol. 35, no. 4, pp. 257–263, April, 1988.

[7] W. T. Joines, Y. Zhang, C. Li, and R. L. Jirtle, "The measured electrical properties of normal and malignant human tissues from 50 to 900 MHz," *Med. Phys*, vol. 21, no. 4, pp. 547–550, April, 1994.

[8] A. M. Campbell and D. V. Land, "Dielectric properties of female human breast tissue measured *in vitro* at 3.2 GHz," *Phys. Med. Biol.*, vol. 37, no. 1, pp. 193–210, 1992.

[9] M. Lazebnik, L. McCartney, D. Popovic, C. B. Watkins, M. J. Lindstrom, J. Harter, S. Sewall, A. Magliocco, J. H. Booske, M. Okoniewski, and S. C. Hagness, "A large-scale study of the ultrawideband microwave dielectric properties of normal breast tissue obtained from reduction surgeries," *Phys. Med. Biol.*, vol. 52, pp. 2637–2656, 2007.

[10] M. Lazebnik, D. Popovic, L. McCartney, C. B. Watkins, M. J. Lindstrom, J. Harter, S. Sewall, T. Ogilvie, A. Magliocco, T. M. Breslin, W. Temple, D. Mew, J. H. Booske, M. Okoniewski, and S. C. Hagness, "A large-scale study of the ultrawideband microwave dielectric properties of normal, benign and malignant breast tissues obtained from cancer surgeries," *Phys. Med. Biol.*, vol. 52, pp. 6093–6115, 2007.

[11] M. Nguyen and R. Rangayyan, "Shape analysis of breast masses in mammograms via the fractial dimension," in *Engineering in Medicine and Biology 27th Annual Conference*. IEEE, 2005, pp. 3210–3213.

[12] T. Kohonen, "The self-organizing map," *Proceedings of the IEEE*, vol. 78, no. 9, pp. 1464–1480, Sep. 1990.

[13] D. G. Roussinov and H. Chen, "A scalable self-organizing map algorithm for textual classification: A neural network approach to thesaurus generation," *Communication Cognition and Artificial Intelligence, Spring*, vol. 15, pp. 81–112, 1998.

[14] G. J. Deboeck and T. K. Kohonen, Eds., *Visual Explorations in Finance*, 1st ed. Secaucus, NJ, USA: Springer-Verlag New York, Inc., 1998.

[15] K. Muinonen, "Introducing the gaussian shape hypothesis for asteroids and comets," *Astronomy and Astrophysics*, vol. 332, pp. 1087–1098, 1998.

[16] ——, *Chapter 11: Light Scattering by Stochastically Shaped Particles*. Academic Press, 2000.

[17] E. Zastrow, S. K. Davis, M. Lazebnik, F. Kelcz, B. D. V. Veen, and S. C. Hagness. (2008) Database of 3d grid-based numerical breast phantoms for use in computational electromagnetics simulations. Online. Department of Electrical and Computer Engineering University of Wisconsin-Madison. [Online]. Available: http://uwcem.ece.wisc.edu/home.htm

[18] S. K. Davis, B. D. V. Veen, S. C. Hagness, and F. Kelcz, "Breast tumor characterization based on ultrawideband backscatter," *IEEE Trans. Biomed. Eng.*, vol. 55, no. 1, pp. 237–246, 2008.

[19] R. C. Conceicao, D. Byrne, M. O'Halloran, E. Jones, and M. Glavin, "Investigation of classifiers for early-stage breast cancer based on radar target signatures," *Progress in Electromagnetics Research*, vol. 105, pp. 295–311, 2010.

[20] A. Taflove and S. C. Hagness, *Computational Electrodynamics: The Finite-Difference Time-Domain Method*. Artech House Publishers, June, 2005.

 ISBN: 978-1-61208-246-2

O-MUSUBI: Ad-hoc Grouping System Enhanced by Ambient Sound – The Similarity based on Information Theoretical Features for Sound-Fields –

Sachio Teramoto, Jun Noda
Cloud System Research Laboratories
NEC Corporation
Kanagawa, Japan
Email: s-teramoto@bx.jp.nec.com, j-noda@cw.jp.nec.com

***Abstract*—The aim of this paper is to achieve ad-hoc grouping systems enhanced by ambient sounds or sound-fields. As an elemental technology of ad-hoc grouping, systems have to be equipped with a search engine with sufficient accuracy to find out users who are in similar contexts. Systems require another similarity criterion for sound-fields. Because search results from well-known similarities, such as cosine-similarity, cannot exclude false negative and cannot restrict false positives. Moreover, in order to cover a wide-variety of mobile devices including smartphones, we have the problem of the deterioration of search accuracy due to differences in microphone performances. We may also have to decrease the system-wide load. This suggests that original sound-field data should be resized as small as possible without losing valuable features to flexibly recognize different contexts. We thus propose a new similarity criterion on sound-fields for ad-hoc grouping. We also show experimental results to ensure all requirements are fulfilled.**

***Keywords*-sensor based system; ubiquitous system; ad-hoc communication; ambient-sound.**

I. INTRODUCTION

To increase the chance of grouping anytime anywhere with the growing popularity of social networking services (SNSs), constituent members for sharing pictures or communicating with each other choose to use various kinds of SNSs. Indeed, ad-hoc group communication services [1] are just beginning to be provided for smartphone users who want to temporarily set up a group consisting of ones immediate circle over a period of time.

Users who want to find constituents to add to their group automatically have usability and operability requirements. To infer constituents appropriately, it is important to guarantee high accuracy for searching for ones who have the same situation or context. We thus concentrate search accuracies on *the false negative exclusion,* and *the restriction of a false positive.* Here we consider a situation in which group constituents have been identified and the members do not want others to join in their group. A false negative is when the search could not find suitable members. A false positive is when the search finds unsuitable members. As another requirements supposed in various situations, a wide area must be covered. This cause that systems should have sensors equipped by mobile devices as their components.

There is a fundamental approach to measure proximity of user's context, such Wellman et al.'s approach [2] for acquiring and using absolute positioning of GPS that gives latitude and longitude. However, approaches based on GPS cannot be applied indoors or underground. Thus, other approaches that apply several sensors have been investigated; for example, Cricket [3] and ActiveBat [4] based on ultrasonic waves, Ekahau [5] based on wireless LAN, and LuxTrace [6] based on building illumination. However, even if these approaches were combined with GPS, it still might be difficult to apply to ad-hoc grouping systems, since we have to arrange many sensors broadly. Thus, equipment costs (deployment cost and maintenance cost) are comparatively high. Moreover, an approach may be also desired that is applicable even in places or situations in which sensors are difficult to deploy.

On the other hand, there exist approaches on positioning inferred by comparing each pair of sensor data. We refer such approaches to certification matching for descriptive purpose. Some certification might be created simply by an action occurring that can be sensed by devices: vibrating devices that enable an accelerometer [7], or clicking the same button simultaneously. The certification based on occurrence has a weakness in terms of search accuracy. The main factor for its deterioration comes from increasing probabilities of collisions occurring; users who are in different contexts doing the same action at the same time. When an ad-hoc grouping system has about 10,000 users exist, we can confirm theoretically that probabilities approach infinitely to 1, by analogies of the birthday's paradox.

In this paper, we resolve subjects mentioned above by introducing a new similarity. Specifically, the proposed similarity measures information theoretical features in ambient sound or sound-fields. The sound-fields can be sensed by a microphone equipped on many mobile devices, including smartphones. Therefore, by considering microphones equipped on many mobile devices, the requirements for covering a wide area and various scenes and equipment costs are simultaneously solvable. Moreover, utilizing sound-fields may be tractable for search-accuracy requirements related to the restriction of false positives because sound-fields have

 ISBN: 978-1-61208-246-2

many features and variations, rather than simple certifications based on occurrence of actions.

The rest of this paper is organized as follows. In Section II, we deal with related works for context proximity inference methods based on ambient sound and describe requirements for similarity between sound-fields. In Section III, we overview the architecture of ad-hoc grouping system enhanced by ambient sound and describe in detail procedures of each mobile device and the cloud server. In Section IV, we report experimental results on the accuracy of information retrieval for the proposed similarity and discuss advances fulfilling each requirement described in Section II. Finally, in Section V, we summarize the results that have been achieved and detail future works.

II. Context proximity inferences based on sound-fields

A. Related works and their problems

To infer proximity of contexts on the basis of a sound-field, Sturm et al. [8] proposed an approach for recognizing trajectories of several moving sound-sources by using microphone-arrays. However, this also requires that many microphones be deployed to cover a wide area.

As methods for no equipment costs, Tarzia et al. [9] proposed that a positioning system for single user, based on finger-prints of a sound-field. This system can allow to recognize rooms where user visited. However, it is not so easy to get a high accuracy on location retrieval. We discuss on accuracies in section IV.

Lu et al. [10] proposed a method inferring user's context, using ambient sounds. This method leverages machine learning on several features of sound-field, to classify ambient sounds into attributive categories with high accuracies. However, Lu et al. did not indicate whether their method have a capability to distinguish sound-fields in a same category.

Nakamura et al. [11] provide thorough knowledge of specific sound-fields, especially conversation-fields. They designed architectures that recognize appropriately different conversation-fields, using cosine-similarity.

However, to cover various sound-fields, cosine-similarity has a weakness in terms of search accuracies: higher *precision* or lower *false-positive.* The precision and the false-positive are defined as follows. Let R be the number of users who are constituent members by just grouping and N the number of users found out by searching. Thus, precision $p := \frac{R}{N}$; false-positive $f := \frac{N-R}{N}$. We also have a relation $p = 1 - f$. Thus we consider only the false-positive in this paper.

Here, we describe a number of disadvantages derived from measuring with cosine-similarity for sound-fields. First, search results by using cosine-similarity may contain a certain amount of false-positives. Sound-fields have mainly two discriminable sounds; *event-sounds*, which occur in an unexpected fashion, and *ambient-noise*, which are stationary background sounds. Note that a definition of ambient-noise includes sounds in which one can be observed anywhere else, such as cafeterias, offices, and also calm places though contradicting this term with noise. Comparing duration between an event-sound with a ambient-noise, ambient-noise occupy a considerable amount of sensing time, but an event-sound is rare. This implies that temporal coincidences of ambient-noise severely affect context proximity, but coincidences of event-sounds do not. This is because cosine-similarity treats ambient-noise and event-sounds evenly. Therefore, results of searching with the cosine-similarity tend to have higher false-positives rate, since results contain many false users who only are in similar ambient-noise. Therefore, similarities measuring sound-fields should give higher grades for temporal coincidence with event-sounds, but not for ambient-noise.

Second, there is a vulnerability in differences of microphone performance. Usually, according to the type of mobile devices, microphones' performances differ dramatically from each other. Differences are especially observable in sound-pressure levels. That is, cosine-similarity will misjudge users who have distinct contexts, even if both microphones sense just the same sounds. Since such unfortunate cases will be caused by cosine-similarity, inferring proximity of context will err frequently or be unable to except the false-negativeness.

Next, we consider a practical system for ad-hoc grouping enhanced by a sound-field. Then problems on system-width load emerge. Since the data size of any sound-pressure series sensed by mobile devices is not very small, data sent from each mobile device should be as small as possible. In particular, a sound-pressure series contains much more information or many more various features than required. Thus, it is inefficient from the viewpoint of both of system-wide loads and network communication costs. Specifically, receiving rather large size of data will cause high network I/O loads, as a consequence, restrict availabilities of systems. Thus, the communication cost become a bottleneck. This is a problem that users could not join a group within applicable timings. Therefore, for the sound-pressure series, a contraction method is required that has valuable features to recognize different contexts.

B. Requirements and technical idea

We describe requirements derived from problems in the previous section, and its technical idea.

i) **Higher accuracies on information retrieval**
Proposed similarity estimates temporal coincidences between singular value (derived from event-sounds) included in each sound-fields from aspects of information theoretical features. In particular, we introduce concepts of mutual information. That is, if event-sounds, which have practically lower probabilities of occurring in sound-fields, coincide, then we add higher

 ISBN: 978-1-61208-246-2

estimation to their similarity. Furthermore, we can confine contributions of ambient-noise to similarities, and then the false-positive ratio tends to decrease. Therefore, we could guarantee higher accuracy in information retrieval, and thus, could appropriately associate users with others in similar environments.

ii) **Flexible treatments for different microphones**
Performance differences are observed between equipped microphones, especially in small and large of sound-pressure values. To resolve the differences in sound-pressure values, we generate a collection of multiple *feature vectors* extracted from frequency spectrum, considering redundancy for sound-pressure values. Then, we compute information entropy, estimating coincidences between one collection and the others. This implies that proposed similarity is relatively tolerant of differences in microphones performance. Therefore, we could accept a wide variety of mobile devices, since proposed similarity may resolve flexibly.

iii) **Low communication costs**
Now we consider "large scale and real-time" ad-hoc grouping (cloud) systems enhanced by ambient sound. In such cloud systems, network communication costs may be problem for system availability, since the data size of any sound-pressure series is not very small. This also implies higher system loads. Considering an availability of a system, we also have to avoid that network I/O loads will become a bottleneck. Thus, to reduce communication costs, we apply a contraction procedure to sound-pressure series sensed originally by microphones. Note that applied contraction procedures also have to be guaranteed to meet the above two requirements simultaneously. To tackle this issue, we apply a low-pass filter like a finite impulse response (FIR). Applying a FIR filter, a sound-pressure series is shortened and consists of components only with low frequency bands. We refer any sound-pressure series applied FIR as series of beats, and show that any series of beats still holds enough features by experimental results in section IV.

III. O-MUSUBI: AD-HOC GROUPING SYSTEM ENHANCED BY AMBIENT SOUND

We show overview of proposed ad-hoc grouping system enhanced by ambient sound in Figure 1. We entitle this system O-MUSUBI, which is acronym stands for Organization scheme Measured by Universal **S**ensor data like ambient sound for UBIquitous machines. Another meaning is derived from combination of two Japanese words, "Oto" (sound in English) and "Musubi" (connection or nexus in English). cf. O-MUSUBI is Japanese traditional riceball.

Each mobile device sends sensing data consisting of a sound-pressure series to the cloud server. Then the cloud server computes similarity of each pair of given sound-pressure series.

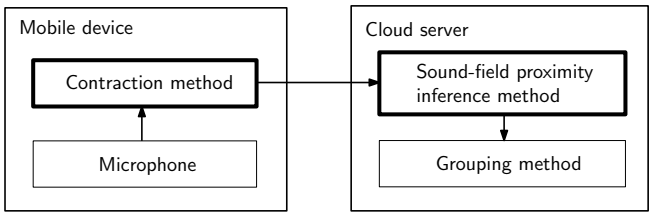

Figure 1. Overview of O-MUSUBI system.

The overview of procedures in each mobile device can be described as follows. The contraction method contracts original sound-pressure series by removing unnecessary information. Then each mobile device sends contracted data to the cloud server. We assume that sensing time is separated by a unit time (e.g. three seconds) that is determined and shared in the whole system. We also assume that the unit time is continuously resumed until a group is found or a termination message is received.

The main procedure in the cloud server is to infer each pair of users' context proximity. More specifically, sound-field proximity inference method computes similarities, or information entropies, between two of each sound-pressure series. Then, grouping method update information for groups and may notify users of new groups they should join.

A. The mobile devices side

The procedure of mobile devices mainly consists of three phases: sensing sound-pressure series, contracting the original series, and sending the contracted series to the cloud server. Here, we have known that there exist temporal gaps between any pair of sound-pressure series. Although feature vectors are created in the basis on frequency spectrum, we cannot correct the gaps by using any pair of spectrum component series. This is because spectrum component series does not have temporal information. Thus, we have to correct or synchronize at the cloud server side. This temporal synchronization procedure have been described at sub-section III-B. This is also desirable to cover various kinds of devices whose computational resources are poor.

In this section, we describe the procedure of the contraction method. To contract the original data, we borrow an idea from applying low-pass filers such as FIR. Although applying filters might loss much information contained in the originals, valuable features are still retained, such as beats. This series of beats implicitly provides occurrences of tempos of event-sounds, and coincidences of tempos with spectrum powers, or joint probability, have higher information entropies. Thus, we could ensure the accuracy of information retrieval, in spite of considerably shrinking the original sound-pressure series.

 ISBN: 978-1-61208-246-2

Algorithm 1 shows a pseudo-code of contraction method. For input, Algorithm 1 is given an array `buf` stored sound-pressure series that is sensed with a sampling frequency specified by parameter `samplingFrequency` for a given length of time specified by parameter `duration`. For output, Algorithm 1 ensures an array `contractData` stored contracted sound-pressure series whose elements are maximal ones in `buf` for each sliding time-window. Additionally, we would assume that two consecutive time-windows share overwrap each other. We specify a fraction of overwrap with `overwrapRate`, where $0 \leq$ `overwrapRate` < 1.

We note that information that should be shared by both mobile devices and the cloud server is represented by two parameters: the sensing time `duration` in mobile devices and the size of the sound-pressure series `sendDataSize`.

Algorithm 1: Contraction Procedure in Mobile Device

input : An array `buf` stored the time series-data of sound pressure values.
output: A contracted array `contractedData`

1 $w = \left\lfloor \frac{\texttt{buf}.length}{(1-\texttt{overwrapRate})\times\texttt{sendDataSize}+\texttt{overwrapRate}} \right\rfloor$;
2 $w' = w \times$ `overwrapRate`;
3 **for** $i = 1, k = 0;\ i <$ `buf`$.length;\ i{+}{+}, k{+}{+}$ **do**
4 **if** `buf`$[0] <$ `buf`$[i]$ **then**
5 `buf`$[0] =$ `buf`$[i]$;
6 **if** $k{=}{=}w$ **then**
7 `contractedData`$.push\_buck($`buf`$[0])$;
8 $k = 0; \quad i \mathrel{-}= w'$;
9 `buf`$[0] =$ `buf`$[i]$;
10 **return** contractedData;

In the case of a smartphone, the sampling frequency is configured by its specification and is sensed with at least 8 kHz. For example, when any smartphone sensing for 3 seconds, and the system configures `sendDataSize` $= 300$ and `overwrapRate` $= 0.5$, the time-window size `windowSize` becomes 162, and each element stored in output array `contractData` is a maximal among 162 values in each sliding time-window.

B. The cloud server side

In this section, we describe the procedure in the cloud server on the basis of requests from the first two requirements described in Section II-B.

In the cloud server, the sound-field proximity inference method computes a degree of similarity between any pair of sound-fields, and then, in accordance with similarities, the grouping method updates grouping information to create a new group or find a group when one user can find other users having higher similarities.

Algorithm 2 shows a pseudo-code of sound-field inference method. The procedures in the cloud server consist of two main steps: executing synchronizations in chronological order between sound-pressure series, and for each sliding time-windows, generating feature vectors and computing information entropies.

Algorithm 2: Computation of Information Entropy on Sound-Fields

input : A pair of two sound-pressure series $\{s_0, s_1\}$.
output: The similarity measured between s_0 and s_1.

1 TimeSynchronous(s_0, s_1);
2 $w = (1 -$ `FFToverwrap`$) \times$ `FFTwinSize`;
3 **for** $t = 0; t < s_1.length -$ `FFTwinSize`$; t{+}{=}w$ **do**
4 **for** $i = 0; i \leq 1; i{+}{+}$ **do**
5 $S_i =$ FFT$(s_i, t,$ `FFTwinSize`$)$;
6 $V_i =$ SpectrumQuantization(S_i);
7 CommonVectorAggregation(H, V_0, V_1);
8 **foreach** $v \in H$ **do**
9 $p_v = \frac{H[v]}{H.count}$;
10 `entropy`$+{=}\ p_v \log(p_v)$;
11 **return** $|$`entropy`$| \times H.count$;

Executing synchronization in chronological order: The procedure TimeSynchronous, Algorithm 2 (line 1), corrects small gaps for a given two sound-pressure series. Here, we describe an algorithm that corrects gaps in time-series as follows. First, we generate two arrays M_0 and M_1 consisting of maximal values for each given sound-pressure series s_0 and s_1. We define maximal as being the maximum among three for just previous and next ones, and itself, and their differences are larger than a threshold. Note that any sound-pressure series may have a number of maximal. Second, we obtain moving factors (gap size and direction.) For example, part of the procedure is as follows: for each maximal x_i in M_0, finds $y_i \in M_1$ which is the nearest to x_i; then, memorizes the minimum of $|x_i - y_i|$ and its sign of $x_i - y_i$ as the moving factor. Finally, temporal synchronization is executed on the basis of the moving factor.

Generating feature vectors and computing entropies: Here we describe the procedure of the first for-loop shown in Algorithm 2 (lines 3–7). Given two sound-pressure series s_0 and s_1 (which may be applied a synchronization), the procedure computes average information entropy and its summation for each sliding time-window whose size is specified by parameter `FFTwinSize`. We assume that `FFTwinSize` is the power of 2, since `FFTwinSize` corresponds to data size input towards fast Fourier transform (FFT). Two consecutive time-windows should share an overwrap, to prevent missing features such as event-sounds occurring at a boundary of non-overwrap consecutive time-windows. Let

 ISBN: 978-1-61208-246-2

FFToverwrap be the parameter specifying the fraction of overwrap, or overwrap ratio, for two consecutive time-windows, where $0 \leq$ FFToverwrap < 1. As described in line 2 of Algorithm 2, for example, when we configure the size of a time-window FFTwinSize with 64 and the overwrap ratio FFToverwrap with $\frac{1}{8}$, the actual size w of overwrap is equal to $56 = (1 - 0.125) \times 64$.

We generate feature vectors for each inputs s_0 and s_1 respectively, as shown in lines 3–7. The process of generating feature vectors consists of two steps as follows. First, for each s_0 and s_1, we obtain frequency spectrum S_0 and S_1, respectively, by FFT. Second, we generate a collection of multiplied feature vectors considering a redundancy by SpectrumQuantization. The domain of any feature vectors is defined by two parameters: the cut-off frequency cutOffFreq, which defines the upper bound on frequency we use, and the number of quantization levels quantLevel. For example, when cutOffFreq $= 11$ and quantLevel $= 4$, an arbitrary feature vector is defined on a finite space $[1, 10] \times [1, 4]$. Figure 2 shows a simple example.

Here, we refer to the relationship between sendDataSize of mobile devices with cutOffFreq of the cloud server. That is, cutOffFreq gives a lower bound of sendDataSize. When we generate a frequency spectrum with lower frequency than cutOffFreq by FFT, we have to hold a condition on value of parameters at least sendDataSize ≥ 2 cutOffFreq. We also note the tradeoff between the size of data sent and the strength of information entropies computed from given data. This is because the number of time-windows defined in given data increases if the size of data sent is larger.

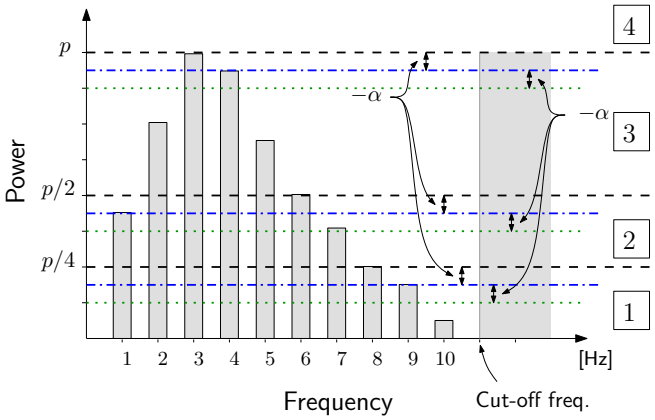

Figure 2. The characteristic-vector generation based on quantization frequency spectrum.

We describe the procedure of quantization of each frequency component in a frequency spectrum. In this description, we assume that if quantLevel $= k$, then $k - 1$ horizontal lines (quantization levels) are drawn as shown in Figure 2, and then each spectrum components are quantized into either one of $\{1..k\}$. We draw each $k - 1$ quantization level such that we settle the first or highest level with power p which has the maximum power among frequency components in frequency domain $(1, 2, ..., \text{cutOffFreq} - 1)$; then afterwards, the second or later levels with recursively are defined as $\frac{p}{2^{i-1}}$. This $k - 1$ quantization level separates the range of power in a frequency spectrum into k intervals $[0, \frac{p}{2^{k-2}}), [\frac{p}{2^{k-2}}, \frac{p}{2^{k-3}}), \ldots, [\frac{p}{2}, p), [p, \infty)$. Then we relate each interval with quantization values in increasing order from the start-point. We quantize each frequency components on the basis of power and intervals by finding an interval containing the power and then quantize with the value related. Figure 2 shows a situation with quantLevel $= 4$, and each 4 quantization levels are represented by dashed lines. As an example, a feature vector $v := (2, 3, 4, 3, 3, 3, 2, 2, 1, 1)$ is generated.

We describe how multiplied feature vectors are made redundant. To tackle frequency spectrum errors derived from the differences in microphone performances, we change each quantization level to slightly below those defined previously and then generate each multiplied feature vectors. More precisely, we introduce two parameters:numCand and jitter. The parameter numCand specifies the number of multiplied feature vectors or candidates for matching. The parameter jitter specifies tolerance from each quantization levels referenced. We could define recursively numCand $- 1$ sets of quantization levels by shifting to below with jitter from each level referenced. Figure 2 shows two different sets of quantization levels represented by dash-dotted lines and dotted lines, respectively, where numCand $=$ 3 and jitter $= \alpha$. Then in accordance with each set of quantization levels, we newly generate feature vectors $v' = (3, 3, 4, 4, 3, 3, 2, 2, 2, 1)$ and $v'' = (3, 3, 4, 4, 3, 3, 3, 2, 2, 1)$.

CommonVectorAggregation manages a table H storing joint probabilities, which are temporal coincidences of two of each feature vectors occurring. Specifically, the table H stores information on which feature vectors that occur simultaneously and how many times as a whole given sound-pressure series. The temporal coincidences of each of two collections of feature vectors are evaluated as shown in Figure 3, If after comparing or matching, there exists a feature vector contained by both sets of feature vectors, then it is the representative in the time-window. On the other hand, if several vectors coincide, then we select one unaffected from the parameter jitter as far as possible. In the case of Figure 3, the coincidence between v'_A and v_B is preferentially selected as the representative feature vector $(3, 3, 4, 4, 3, 3, 2, 2, 2, 1)$, but v''_A and v''_B.

Finally, we compute the information entropy between given two sound-fields by using the number $H.count$ of all temporal coincidences and the number $H[v]$ of occurrences of each feature vector v. The procedure described in lines 8–10 of Algorithm 2 computes the average information entropy. Thus, we return the information entropy.

 ISBN: 978-1-61208-246-2

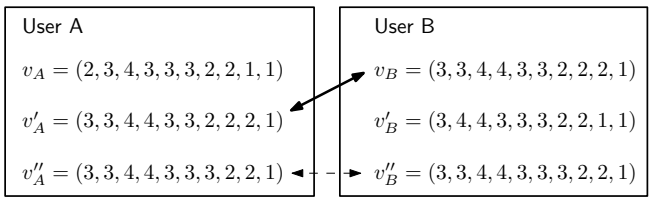

Figure 3. The matching process between characteristic vectors

IV. Empirical study for information retrieval accuracies

In this section, we present experimental results and discuss requirements described in Section II. Specifically, we observe transitions of the information entropies under each situation: sharing event-sound or not. We use two smartphones as test mobile devices, in which microphone performances differ.

Figure 4 shows an environment in which evaluation experiment we performed. We assume that there are users (A and B) who sit around a table in a cafeteria and wish to communicate in a new ad-hoc group. In this situation, we wish to observe whether proposed similarity has capabilities to distinguish conversation-fields in ambient-noise, and using microphones with different performances. For ambient-noise, we deploy a loudspeaker at the position ambient-noise source and produce crowd-noises recorded preliminarily at a cafeteria. For event-sounds, we had two people converse at positions A and B. We placed mobile device A, B, and C five meters away from ambient-noise source. Then, to make sure mobile devices A and B shared the same context, we placed them about one meter apart. On the other hand, to make sure A and C did not share the same context, we placed them about 10 meters apart.

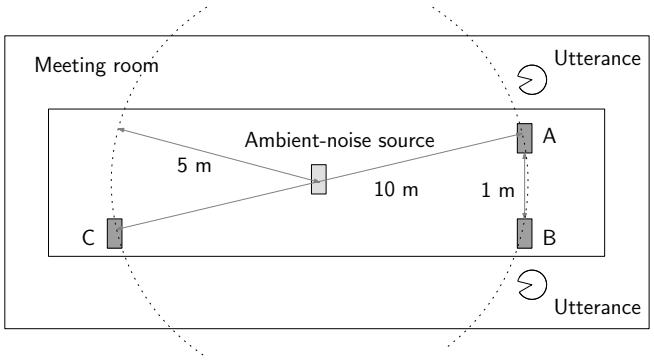

Figure 4. The overview of experimental environment

We show parameters on mobile devices and on the cloud server in Table I and Table II. Under this configuration, we performed the FFT procedures and computed information entropy 37 times for each 3-second cycle. Additionally, feature vectors are defined in the domain $[0..9]^{15}$. We generate six candidate feature vectors for each sliding time-window.

Table I
THE PARAMETER VALUES ON MOBILE DEVICES IN THE EXPERIMENT.

The sensing time	`duration`	3 sec
The frequency of sampling	`samplingFrequency`	8192 Hz
The data size after contraction	`sendDataSize`	300

Table II
THE PARAMETER VALUES IN THE SOUND-FIELD PROXIMITY INFERENCE METHOD IN THE EXPERIMENT.

The size of (FFT's) time widow	`FFTwinSize`	32
The overwrap ratio for continuous windows	`FFToverwrap`	50 %
The cut-off frequency	`cutOffFreq`	16
The number of quantization levels	`quantLevel`	10
The jitter value of each quantization level	`jitter`	0.5
The number of candidate feature vectors	`numCand`	6

Figure 5 shows increasing process for information entropy between A with B (solid line) and between A with C (dashed line). We set axis of the graph in Figure 5 such that the time progress corresponds to the horizontal axis and the entropy progress corresponds to the vertical axis. We plot each average of information entropy in a number of trials.

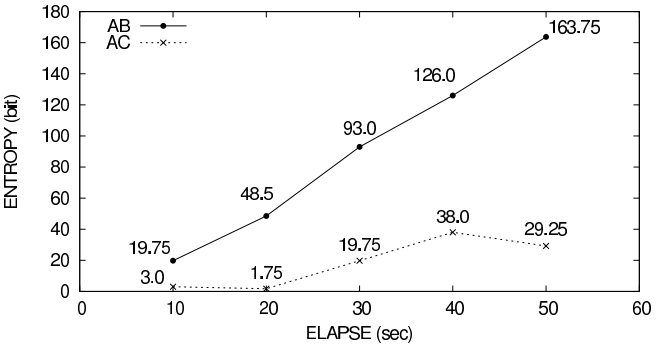

Figure 5. The increasing series on information entropy when all mobile devices are in separate positions

Discussions on accuracies of information retrievals: Here, we discuss the accuracies of information retrievals on the basis of the results shown in Figure 5. We observe from the progress of information entropies between AB(s) that the proposed similarity estimates appropriately event-sounds contained in conversation. Additionally, from results

 ISBN: 978-1-61208-246-2

of AC(s), the contributions of ambient-noise to the similarity can be more suppressed than AB(s). We note that by examining in full detail both increasing processes of entropies for each AB(s) and AC(s), we can decide suitable parameter values for the threshold used at grouping and an expired time (or terminated communications with the cloud server). In fact, breaking down with a linear regression analysis for each increasing process, the entropy of AB(s) increases at least four trials to ones of AC(s) for each cycle. Now we discuss about average values of entropies on 10 sec which are close to each other. Indeed, for AB, we have the average $\mu_{AB} = 19.75$ and the standard deviation $\sigma_{AB} = 9.42$. Similarly, for AC, we have $\mu_{AC} = 3$ and $\sigma_{AC} = 6.0$. Then, since we obtain $\mu_{AB} - \sigma_{AB} > \mu_{AC} + \sigma_{AC}$, proposed system might recognize appropriately difference contexts with high probabilities. With this knowledge from experimental results, for example, if we want searching to stop for up to 10 seconds, ad-hoc grouping systems output users who have the entropy exceeding 10 $(> \mu_{AC} + \sigma_{AC})$ as the search results. Under these conditions, we could restrict the false positive so that results AC(s) shows that we can distinguish the relative positions of A and C. Additionally, the accuracy is better than experimental results in [9]. Tarzia et al. showed localization accuracy, which measures correctness for recognizing different room where user visited, achieved 69 %, when sample time is 30 seconds. On the other hand, since there exist higher gaps between AB (93.0) and AC (19.75), proposed similarity may have higher noise-robustness than [9] at least in this case.

Finally, we discuss an essential insight for which we set the parameter information entropy thresholds with 10. We consider the probabilities of grouping with a user who attacks a system sending artificial sound-fields generated randomly. In this situation, we assume that the probabilities can be smaller than $\frac{1}{2^{10}}$.

Discussions on the differences in microphone performances: we could find out that proposed similarity evaluates appropriately on sound-fields without being dependent on the differences in microphone performance, since we can check clearly that transition of the information entropies of AB(s) increases appropriately, despite each A and B have mobile devices in different microphone performance. Therefore, it can be used as similarity between any mobile devices equipped with different microphone performances without lowering search accuracies.

Discussions on communication cost with accuracies: In the estimation experiments, under the configuration shown in Table II, each original sound-pressure series is contracted, its data size reduced to $\frac{1}{8}$, by Algorithm 1. Despite this fact, the results in Figure 5 show that search accuracies can be guaranteed sufficiently. Therefore, by deleting unnecessary features from the original sound-pressure series, we can reduce the network communication costs, or system-wide loads and network I/O loads by presented contraction algorithm.

V. Summary and future works

We proposed new similarity criteria for ambient sound based on information theoretical features of sound-fields. Experimental results verified that the similarity has sufficient search accuracy to be applied to ad-hoc grouping systems. Therefore, the proposed similarity has higher search accuracy and is more robust to differences in microphone performances. Furthermore, we proposed a contraction based on a FIR-like strategy in mobile devices. This contraction not only enables us to reduce network communication costs, but also ensures high search accuracy.

For future works for inferring context proximity in "real-time", architectures are required from the point of view of scale-out and scale-up. Supposing practical services, an ad-hoc grouping system will receive many sound-fields repeatedly for every unit time. Thus, the system has to compute in the unit time for all pairs of sound-fields received. This causes higher computation costs. Therefore, we need a technique for lightweight filtering that identifies pairs that do not need to be computed while restricting false positives.

References

[1] RingReef, http://ringreef.com/ (26.11.2012).

[2] B. Wellman, J. Boase, and W. Chen, "The networked nature of community: Online and offline," *IT & Society*, vol. 1, no. 1, pp. 151–165, 2002.

[3] N. Priyanha, A. Chakraborty, and H. Blakrishnman, "The cricket location-support system," *Proc. ACM MOBICOM 2000*, pp. 32–43, 2000.

[4] A. Harter, A. Hopper, P. Steggles, A. Ward, and P. Webster, "The anatomy of a context-aware application," *Proc. ACM MOBICOM 1999*, pp. 59–68, 1999.

[5] Ekahau, Inc., Ekahau Positioning Engine, http://www.Ekahau.com/ (26.11.2012).

[6] J. Randall, O. Amft, J. Bohn, and M. Burri, "LuxTrace: indoor positioning using building illumination," *Personal and Ubiquitous Computing*, vol. 11, No. 6, pp. 417–428, 2007.

[7] LINE, http://line.naver.jp/en/(26.11.2012).

[8] D. E. Sturm, M. S. Brandstein, and H. F. Silverman, "Tracking Multiple Talkers using Microphone-Array Measurements," *Proc ICASSP-97*, pp. 21–24, 1997.

[9] S. P. Tarzia, P. A. Dinda, R. P. Dick, and G. Memik, "Indoor localization without infrastructure using the acoustic background spectrum," *Proceedings of ACM MobiSys '11*, 2011.

[10] H. Lu, W. Pan, N. D. Lane, T. Choudhury, and T. Cambell, "Soundsense: scalable sound sensing for people-centric applications on mobile phones," *Proceedings of ACM MobiSys '09*, pp. 165–178, 2009.

[11] T. Nakamura, Y. Sumi, and T. Nishida, "Neary: Conversation Field Detection Based on Situated Sound Similarity," *IEICE Trans. INF. & SYST., Vol. E94-D*, pp. 1164–1172, 2011.

 ISBN: 978-1-61208-246-2

The Dispedia Framework: A Semantic Model for Medical Information Supply

Romy Elze
Department of Computer Science
University Leipzig
Leipzig, Germany
elze@informatik.uni-leipzig.de

Klaus-Peter Fähnrich
Institute for Applied Informatics (InfAI) e.V.
Aninsitut of the University Leipzig
Leipzig, Germany
faehnrich@infai.org

***Abstract*—The Dispedia Framework is an information system in the complex field of rare diseases. The goal of the system is to harmonize social care conditions and health care conditions with the focus on personalization and patient autonomy. The main task was to analyze the existing system of one rare disease and to structure and model the data in a tiered approach. On the basis of the Dispedia Model, we developed an information system that supports the information logistics between patients with rare diseases and other (all) players (e.g., doctors, therapists, and researchers).**

Keywords-Complex System; Ontology; Health Care; Information Model; Knowledge Mangement; Rare Disease; Patient Care Information System

I. INTRODUCTION

This work describes an approach to engineer a health information system in the context of service engineering. “Service Engineering provides methods and tools for a systematic and structured development of new information-intensive service offerings and service systems [1].” The area of service modeling as a sub-category of service science includes the formal and semi-formal description of services. Standardized and reusable methodologies and models in this area are often deficient [2]. One example of a holistic model of integrated service systems is Böttcher’s Metamodel [3]. This model includes the dimensions of service component, product model, process model, and resource model. It is particularly suitable for complex, varied services such as IT services. Considering comprehensive services which are provided collaboratively, the information model with a systemic view as a further dimension should be focused on. Only if the systems of medical services and information are understood as complex systems with highly interactive contexts and agents, the problems can be addressed through strategies that clarify the patterns and interrelationships of the system [4].

The aim of the paper is to show how patterns and interrelationships in a service system of complex disease can be found and how the information engineering can be realized. In Section 2 of the paper, the complex service system in case of rare diseases is described. In Section 3, the methods of analyzing and modeling of the system are demonstrated. Section 4 exposes the formalization of the system model. The summary in Section 5 identifies the most important facts of the paper, and in Section 6, the conclusions are drawn and fields of further work are tagged.

II. PROBLEM DESCRIPTION

The field of research about rare diseases is extremely complex because of multifaceted disease progressions, the involvement of many stakeholders from different sectors (i.e., social care, health care, therapists, and aid suppliers), and the high costs incurred from treatment and care.

The knowledge of orphan diseases is primarily limited to a few specialized institutions [5]. This restriction often leads to excessive demands on the side of the medicating agents, who lack such specific knowledge. Activities are rarely coordinated centrally. Therefore, multidisciplinary care is still insufficient [6].

Due to the unpredictability of the course of a rare disease, it is impossible to preemptively provide information or define processes across the whole course. Due to a lack of quantitative and qualitative information, the confusion is also high on the side of the patients. This lack is diametrically opposed to the goal of supporting important treatment decisions at an early stage of the disease by means of an active information policy. Complex diseases like rare diseases (see Figure 1 (B)) are characterized by non-linear processes, and information and interventions subsequently depend on more contextual influences of the recipient. [4]

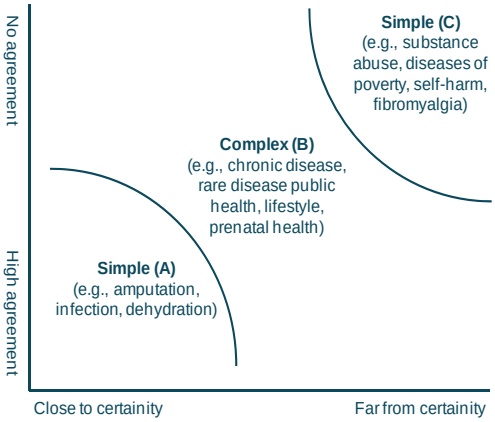

Figure 1: Complexity of diseases (according to [4])

 ISBN: 978-1-61208-246-2

Additionally, Berg constitutes that with respect to these approaches it is a vital aspect to consider the context of intervention- and information recipients [7]. These recipients can be both patients as well as other actors of the heterogeneous network. The challenge is to structure and to qualify the information for the information recipient [8],[9],[10]. Therefore a "…detailed consideration of the disease is inseparable from a detailed consideration of the whole person [11]". In the following, the methods and concepts for modeling such a complex topic are presented.

III. Analysis and Modeling of Rare Disease

To analyze problems and processes of rare diseases, we chose to use the example of Amyotrophic Lateral Sclerosis (ALS), which is a degenerative disease of the nervous system [5]. To model the knowledge and relationships in the ALS knowledge domain, a concept map was developed as a starting point. The concept map [12] and the knowledge map [13] are procedures for the graphical representation of knowledge. Modeling knowledge with these techniques supports the qualitative and quantitative knowledge acquisition. The knowledge is thereby reduced to essential concepts which are arranged in relation to one another. The concept map was formed based on the analysis of 19 medical records of patients and their families from books and web sites. After discussion with experts (e.g., Charité Campus Virchow-Clinic Neurological Clinic: http://www.als-charite.de/; German Society for Muscle Diseases e.V.: http://www.dgm.org/), the first model was consolidated. After the evaluation of an additional 41 expert interviews, the holistic Rare Disease Concept Model was completed (see Figure 2).

The demand for information is characteristic for the subject of ALS. Therefore, the model of the rare disease is designed with a focus on information. We distinguish between information for a patient, information about a patient, and information for stakeholders (see Figure 3).

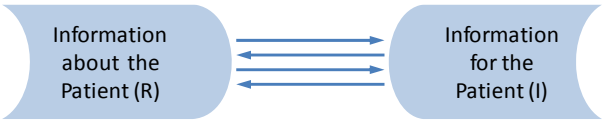

Figure 3. Information Types for Medical Information Supply

The medical field differentiates between specialized documentations of anamnesis. Especially in rare or chronic diseases and in rehabilitation, complex histories must be documented. With respect to ALS, for example, the neurologist uses the Functional Rating Scale for ALS (ALSFRS) [14]. Furthermore, therapists such as speech therapists or occupational therapists use their own anamnesis sheets. In rehabilitation, a description concerning the International Classification of Functioning, Disability

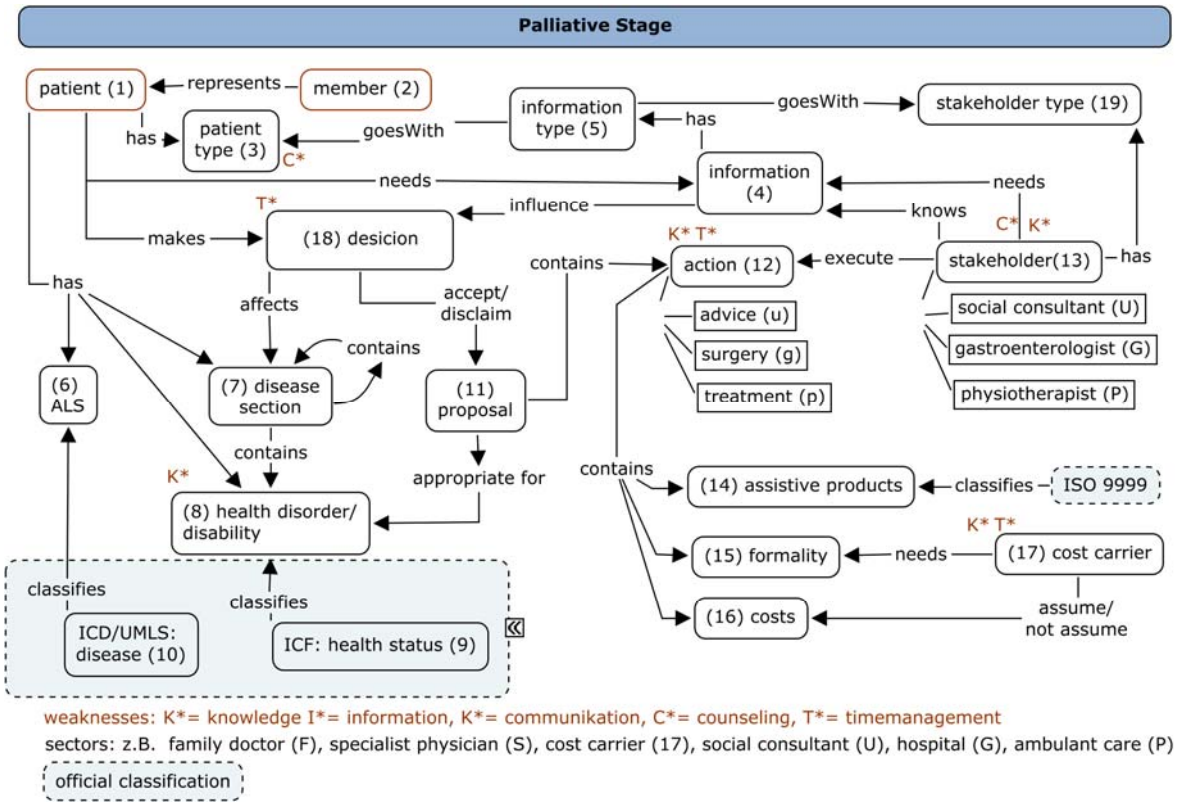

Figure 2. Concept Model of ALS Disease

and Health (ICF) is common. In the model, the utilization of all possible patient descriptions is intentional. Therefore, the idea of Linked Data [15] is pursued.

Modeled after personal consultations between professionals and patients, different information characters are represented. Patients not only have physical needs, but are also characterized by certain psychological traits. Patients and other parties involved in this process are therefore recipient types that must be categorized as specific information recipients. For instance, a very anxious and sensitive patient may be considered a special type, for example the patient type (3) ”sensitive”.

A patient who is a physician by trade would presumably hope to receive more detailed information and would be considered patient type ”skilled”. A patient who is very active and dedicated to his health may like to obtain information about treatment options to pursue by himself, for instance, anti-thrombosis injections. The information to be passed on to the patient in a counseling session would be matched exactly to the type of information recipient. For example, detailed information would be given to a skilled recipient who was listed under information type (5) ”skilled”.

As shown in Figure 2, the constructed Concept Model of ALS Disease demonstrates the relation between the concept patient (1) and the term of information (5).

IV. FORMALIZING SYSTEM MODEL

The formalization of the Disease Concept Model follows commonly used methodologies. These methodologies include the analysis as described above, coding the knowledge, reusing existing formal ontologies, evaluation, and documentation [16]. The resulting formal knowledge representation was encoded in Web Ontology Language (OWL). “OWL is intended to be used when the information contained in documents needs to be processed by applications [17]”, which allows, for instance, a modular development of complex areas and also the re-use of existing knowledge bases [18]. The employment of RDF/S [19] and OWL [17] for a representation of the Disease Model architecture has various advantages.

- The representation of information in a coherent structure without a direct connection to specific applications. This facilitates the development of applications which do not focus on the information logistics advised by this approach.
- The definite identification of the conceptual and concrete resources due to the use of dereferenceable URIs.
- The reutilization of the concepts in applied domains to generate an exchange of resources without a loss of information.
- Interlinking and reification of concrete resources.
- The application of established resources of the Linked Data Web, e.g., Dbpedia [20] and PubMed [21].

To use the formal Disease Model as a re-usable ontology, we developed the Dispedia Ontology (see Figure 4) hold under the domain www.dispedia.de. The name Dispedia is derived from the goal of the designed

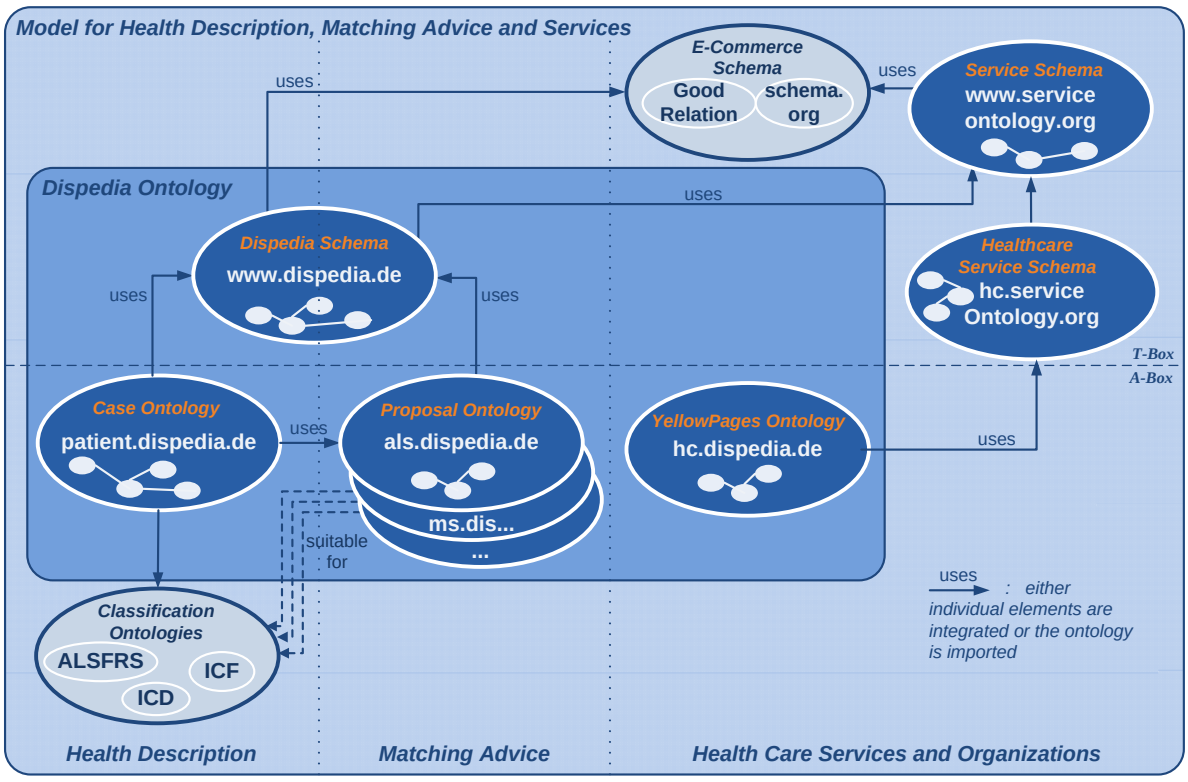

Figure 4. Dispedia Framework

knowledge base to make disease-specific information available and usable for humans and machines. The Dispedia Ontology includes the vocabulary or scheme (Core Ontology), the expert knowledge base (Proposal Ontology), the knowledge base about the patient (Case Ontology), the allocation of proposal information descriptions for patient parameters, and the concepts to interlink additional classifications (see Figure 4) as described above. The Dispedia Framework realizes the description of the whole person through subject-specific and user-dependent classifications, the modular description of disease-specific proposals, the integration of heterogeneous stakeholders, and the patient-specific allocation of information. A prototypical deployment of using the Dispedia Framework is realized on the basis of Ontowiki, a web based tool providing support for agile, distributed knowledge engineering scenarios [22].

V. SUMMARY

The semantic modeling of the medical information supply takes both the patient type and the information type into consideration. By taking advantage of the properties these types had in common, an adaptable information system could be developed. An application that uses the Dispedia Model Architecture adapted the described field of knowledge. The core ontology is the framework which includes describing classifications, domain specific knowledge, and matching. To manage information about the patient in the ALS example, the core ontology uses the classification ontologies ICF and ALSFRS. When using semantic web technologies, the modification and utilization of other classifications is feasible. At the same time, the subject of ALS information for the patient was replaced or amended with information for other recipients.

The use of the available e-commerce ontology www.schema.org furthermore allowed the information to be enriched with tangible offers and the tracking of patients, for instance, for medical aids.

VI. CONCLUSION AND FUTURE WORK

Our work focused on improving the information logistics in the existing health system regarding ALS. The actual state of our approach, which was evaluated by using select patients with ALS and the course of the disease in their specific cases, combines the following different advantages:

- The reutilization of the concepts in applied domains.
- Different information providers can operate on the same standard using the structure given by the architecture concepts and their relations.
- The ontological model of the system can be expanded by interlinking and remaining flexible with regards to accommodating new concepts.
- General aspects of the health care processes for the disease can be represented and linked to their implications for the individual stakeholder.
- Existing knowledge bases like the International Classification of Disease (ICD) [23] and the international Classification of Functioning, Disability and Health (ICF) [15] can be connected and re-used.

In the current state of development, we focus on functionalities supporting knowledge acquisition in order to allow the approach of Dispedia itself to evolve. Therefore, the integration of more usable medical classifications is targeted in a similar manner as the possibility of interlinking further proposal ontologies in addition to the actual existent ALS Ontology. We will pursue the idea of decentralizing data on the web for patients as well. After modeling the expert knowledge structure, the content of ALS hold under the domain als.dispedia.de has to be enlarged, completed and audited. In the same structure further knowledge bases about other diseases have to be developed. For the remote maintenance of patient data appropriate security concepts must be evaluated. The connectivity for cost carriers is one of the open investigation areas and so is the development of security strategies for sensitive data.

REFERENCES

[1] D. Spath, *et al.*, "Service Engineering — A Transdisciplinary Approach in Service Research," in *Services Science*, B. Stauss, *et al.*, Eds., ed: Springer Berlin Heidelberg, 2008, pp. 41-53.

[2] M. Böttcher and K.-P. Fähnrich, "Service Systems Modeling: Concepts, Formalized Meta-Model and Technical Concretion," in *The Science of Service Systems*, H. Demirkan, *et al.*, Eds., ed: Springer US, 2011, pp. 131-149.

[3] M. Böttcher, "Architektur integrierter Dienstleistungssysteme - Konzeption, Metamodell und technikraumsspezifische Konkretisierung," Dr. rer. nat., Institut für Informatik, Universität Leipzig, Leipzig, 2009.

[4] C. A. Brown, "The application of complex adaptive systems theory to clinical practice in rehabilitation," *Disability and rehabilitation*, vol. 28, pp. 587-93, 2006.

[5] J. D. Mitchell and G. D. Borasio, "Amyotrophic lateral sclerosis," *The Lancet*, vol. 369, pp. 2031-2041, 2007.

[6] L. K. Ng, Fary and S. Mathers, "Multidisciplinary care for adults with amyotrophic lateral sclerosis or motor neuron disease," in *Cochrane Database of Systematic Reviews*, ed, 2009.

[7] M. Berg, "Patient care information systems and health care work: a sociotechnical approach," *International Journal of Medical Informatics*, vol. 55, pp. 87-101, 1999.

[8] P. J. K. O. S. E. Eysenbach G, "Empirical studies assessing the quality of health information for consumers on the world wide web: A systematic review," *JAMA: The Journal of the American Medical Association*, vol. 287, pp. 2691-2700, 2002.

[9] E. M. N. M. L. S. Berland Gk and et al., "Health information on the internet: Accessibility, quality, and readability in english and spanish," *JAMA: The Journal of the American Medical Association*, vol. 285, pp. 2612-2621, 2001.

[10] H. A. Taylor, *et al.*, "Implementation of a user-centered framework in the development of a web-based health information database and call center," *J Biomed Inform*, vol. 44, pp. 897-908, Oct 2011.

[11] A. Miles, "Complexity in medicine and healthcare: people and systems, theory and practice," *J Eval Clin Pract*, vol. 15, pp. 409-10, Jun 2009.

 ISBN: 978-1-61208-246-2

[12] A. J. Cañas, *et al.*, "Concept Maps: Integrating Knowledge and Information Visualization," in *Knowledge and Information Visualization*. vol. 3426, S.-O. Tergan and T. Keller, Eds., ed: Springer Berlin / Heidelberg, 2005, pp. 205-219.

[13] A. O'Donnell, *et al.*, "Knowledge Maps as Scaffolds for Cognitive Processing," *Educational Psychology Review*, vol. 14, pp. 71-86, 2002.

[14] J. Cedarbaum, *et al.*, "The ALSFRS-R: a revised ALS functional rating scale that incorporates assessments of respiratory function," *Journal of the neurological sciences*, vol. 169, 1999.

[15] WHO, "ICF The International Classification of Functioning, Disability and Health," 2002.

[16] M. Uschold and M. Gruninger, *Ontologies: Principles, Methods and Applications* vol. 11, 1996.

[17] W3C. (2004, Februar). *OWL Web Ontology Language Overview*. Available: http://www.w3.org/TR/owl-features/

[18] R. Elze, *et al.*, "Dispedia.de – A Linked Information System for Rare Diseases," in *Information Quality in e-Health*. vol. 7058, A. Holzinger and K.-M. Simonic, Eds., ed: Springer Berlin / Heidelberg, 2011, pp. 691-701.

[19] F. E. Manola, Miller. (2004, *Rdf primer*. Available: http://www.w3.org/TR/rdfprimer/.

[20] C. Bizer, *et al.*, "Linked Data - The Story So Far," *Int. J. Semantic Web Inf. Syst.*, vol. 5, pp. 1-22, 2009.

[21] A. Névéol, *et al.*, "Semi-automatic semantic annotation of PubMed queries: A study on quality, efficiency, satisfaction," *Journal of Biomedical Informatics*, vol. 44, pp. 310-318, 2011.

[22] N. Heino, *et al.*, "Developing Semantic Web Applications with the OntoWiki Framework," in *Networked Knowledge - Networked Media*. vol. 221, T. Pellegrini, *et al.*, Eds., ed: Springer Berlin / Heidelberg, 2009, pp. 61-77.

[23] WHO, "International Classification of Diseases (ICD)," 2006.

 ISBN: 978-1-61208-246-2

A Comparison of MapReduce and Parallel Database Management Systems

Alan McClean
School of Computing
Dublin Institute of Technology
Kevin Street, Dublin, Ireland
Email: d10123501@mydit.ie

Raquel. C. Conceição
Instituto de Biofísica e Engenharia Biomédica
Faculdade de Ciências
Universidade de Lisboa
Portugal
Email: raquelcruzconceicao@gmail.com

Martin O'Halloran
Electrical and Electronic Engineering
National University of Ireland Galway
Ireland
Email: martin.ohalloran@nuigalway.ie

***Abstract*—Businesses have come to rely on their data warehouse as a key component in their Information Technology infrastructure. The costs of the architecture to support these environments are significant. Therefore, choosing the wrong architecture can be a very costly decision. However, considerable confusion exists in relation to MapReduce and Parallel Database Management Systems (DBMS). In the past, MapReduce has been presented as a replacement for the Parallel Database Management Systems, as an additional tool that works alongside the Parallel DBMS, but also as an inferior tool by others. This paper will consider the broader themes of the paradigms rather than the specific implementations of MapReduce and Parallel DBMS. It will discuss MapReduce and Parallel Database Management Systems as competing and complimentary paradigms. The aim of this paper is to provide a high-level comparison between MapReduce and Parallel DBMS, providing a selection of criteria which can be used to choose between MapReduce and Parallel DBMS for a particular enterprise application.**

***Keywords*-MapReduce; Parallel Database Management Systems**

I. INTRODUCTION

In 2008, the world's servers processed 9.57 zettabytes of information. For every worker, there is approximately three terabytes of information created every year [1]. These high volumes of data has significant potential to improve understanding, leading to scientific breakthroughs and business process improvements. Examples of these improvements include personalized genome sequencing, extracting real-time trends from business analytics and social network based recommendations. However, the amount of data collected is now outpacing improvements in data storage technology [2]. The traditional data analysis approach is to load the data into a database and the use of a query language to perform the analysis. MapReduce has been presented as an alternative method, with implementations in leading IT companies such as Google and Facebook.

MapReduce is a method for processing large volumes of distributed data, allowing the use of shared nothing clusters. In distributed architectures, a shared nothing cluster is one where the nodes of the cluster share neither a common disk space, a common CPU or common memory. The program flow of MapReduce can be subdivided into a number of stages. Firstly, the data is parsed and some computation is completed. These tasks are referred to as the "Map tasks". Next, data is repartitioned across all nodes of the cluster. Finally, a second set of tasks are executed in parallel by each node on the partition of data it receives. These tasks are called the "Reduce" tasks, taking the results of the map tasks and combining them together [3].

Conversely, Parallel DBMS can be defined as Database Management systems that run over multiple nodes. They support standard relational tables, normally partitioned over multiple nodes and the use of the Structured Query Language (SQL) [3].

Several existing studies have compared MapReduce and Parallel DBMS. Some presented MapReduce as more flexible and capable of producing better performance [4]. Others have presented the opposite opinion [5]. Finally, some suggestions that the two approaches can be used together [6]. These inconsistent opinions have resulted in considerable confusion, making it difficult to determine the most appropriate technology for a particular application.

The aim of this paper is to provide a broad comparison of the two technologies, suggesting the most appropriate solution for a particular enterprise application. The structure of the paper is as follows: Section II will introduce MapReduce; Section III will describe Parallel DBMS; Sections IV and V will examine them as competing and complementary paradigms, while the results and conclusions will be discussed in Sections VI and VII.

II. MAPREDUCE

MapReduce stems from work first completed by Google, which was introduced by Dean *et al.* in 2004 [4]. The creation of the MapReduce library came about because "people at Google implemented hundreds of special-purpose computation that process large amounts of raw data" [4]. These included crawled documents and web requests logs. The computations themselves were relatively simple, but the input data was large and out of necessity the computation was distributed across many machines. This caused a number of issues, which kept repeating across different computations. These included how to:

 ISBN: 978-1-61208-246-2

- parallelize the effort;
- distribute the data;
- handle machine or node failures.

The MapReduce library was created as an abstraction. It allowed the developer to express the simple computation while hiding the details of parallelization, fault-tolerance, data distribution and load-balancing in the library.

MapReduce tasks run on top of Distributed File Systems (DFS). These systems allow files to be spread over multiple nodes which are connected by a network. DFS can also be extended to support fault tolerance. If one of more nodes in the DFS fails, then all data is still available. MapReduce allows the user to focus on implementing the logic required to solve their particular problem.

To do this, the user must write a program which integrates with the MapReduce library. The code must support two interfaces, "Map" and "Reduce". The library runs the Map code on each node in the cluster without communication with other nodes. The results of the map tasks are stored on the DFS. The reduce tasks are then run over the resulting data, to combine the outcome of the Map Results. When performing complex MapReduce algorithms, the general approach is to add additional MapReduce cycles, rather than trying to solve all items in a single parse [3].

Google created their own version of a DFS, commonly refered to as the Google File System (GFS). The exact implementation of MapReduce is only available to Google. However, the paradigm has been implemented in a number of places. Amongst these are:

- Apache Hadoop, support by Yahoo;
- Elastic MapReduce, at Amazon;
- Neptune by Ask.com;
- Dryad by Microsoft.

Of these, Hadoop has attracted the most interest, both commercially and academically. This is partly because of the open source nature of the project and partly because of the strong support and commitment from Yahoo. Apache Hadoop has its own file system (Hadoop Distributed File System (HDFS)). HDFS is highly fault tolerant and is designed to run on low cost components. Hadoop also allows streaming access to the data. HDFS is portable form one platform to another .

The basic MapReduce approach has been extended in a number of ways, particularly to improve performance. The following are examples where the paradigm has been extended:

- Map Join Reduce: This extends the MapReduce paradigm to improve performance by adding join tasks. While chaining of MapReduce jobs can be used to produce a multiple step join, Map Join Reduce completes this in a single step. This can lead to performance enhancements [8].
- MARS Accelerating MapReduce with Graphics Processors: In his study, Fang *et al.* [9] looked at extending MapReduce in a different way. The authors propose the use Graphics Processors rather than standard processors. These processors are faster but introduce a number of issues specifically regarding synchronization;
- Hadoop DB: This uses MapReduce as communication layer. Each node in the cluster has its own DBMS instance. Hadoop DB queries are written using SQL. The queries are translated into MapReduce code using extensions of existing functionality. The main body of the work is performed by the individual database nodes [3]

MapReduce is widely used by Google. In their original paper, Dean *et al.* suggested a number of problems to which it can be deployed [4]. These included:

- Machine learning problems;
- Clustering issues for Google News;
- Extracting data to produce reports on popular queries;
- Web Page property extraction;
- Processing of satellite imagery data;
- Statistical Machine Translation;
- Large scale graph computation.

Outside of Google, the MapReduce paradigm has also been widely used. The following are some sample commercial applications:

- Hive is an open source data warehousing solution built on top of Hadoop at Facebook. It is used for ad-hoc queries and for reporting into dashboards. The system is also used in machine learning algorithms. The system is used by both novices and experts [10].
- Nokia has deployed Hadoop cluster, based on Cloudera's commercial cluster into production. This is considered the companies enterprise wide information core.
- Four Square is a social network that allows its users to check in their location. Other users can then exchange information such as restaurant reviews and travel tips. Four Square use Amazon's Elastic MapReduce to perform a wide range on analytics on their data.

In conclusion, MapReduce is a paradigm first developed by Google. Its purpose is to abstract the developer from the complexities of handling large volumes of data in the computation. It is implemented as a library, which encapsulates the handling of parallelization, fault tolerance and data distribution. The approach has been widely used, particularly the open source version Hadoop. The alternative to MapReduce, Parallel DBMS, is described in the next section.

III. PARALLEL DBMS

Parallel DBMS were developed to improve the performance of database systems. As processor performances improvements outstripped disk throughput, critics predicted that I/O bottleneck would be a major problem. Despite this

 ISBN: 978-1-61208-246-2

a number of vendors, such as Teradata and Tandem, have brought successful products to market [11].

The main reason for the success of Parallel DBMS is the success of relational DBMS systems, now the dominant type of database system. Parallel DBMS have come into existence in a number of different project simultaneously. The DIRECT DBMS project was devised by David J. DeWitt in 1979. He extended this to the Gamma project. Simultaneously, Teradata was devised from research at the California Institute of Technology (Caltech) and from the discussions of Citibank's advanced technology group [12].

Within Parallel DBMS, there is a number of different types of architectures:

- Share memory: multiple processors share memory space and access to disks;
- Share Disk: multiple processor share access the same disk space, but each has its own memory;
- Share Nothing: each node has its own memory and disk space.

The key point is that shared-nothing architectures move only questions and answers between the nodes, while the other two architectures will move data through an interconnection network. The main advantage of the shared-nothing multiple processors is that they can be scaled up to hundreds and potentially thousands of processors that do not interfere with one another.

Parallel DBMS are a stable environment. There are a number of companies which rely on their parallel DBMS as a cornerstone of their business. Due to business confidentiality reasons, it is difficult to get exact figures on the volumes of data. However, in 2008, Teradata announced that it had five "petabyte power players". These included "an online auction company with 5.0 petabytes of data in their Teradata environment; a retailer with 2.5 petabytes; two large financial service institutions with 1.5 and 1.4 petabytes respectively, and a manufacturer with a one petabyte data warehouse environment" [12].

IV. Competing Paradigms

This section will consider applications where MapReduce and Parallel DBMS technologies have competed.

A. Large Data Volumes

Both MapReduce and Parallel DBMS provide a means to process large volumes of data. As the volume of data captured continues to rise, questions have been asked as to whether the parallel DBMS paradigm can scale to meet demands. "There are no published deployments of parallel database with nodes numbering into the thousands" [3]. As more nodes are added into the parallel DBMS environment, the chance of a node failure increases. Parallel DBMS do not handle node failure. MapReduce has been designed to run on thousands of nodes and is inherently fault tolerant. It has been presented as a viable alternative to parallel DBMS. This has been disputed by parallel DBMS experts. It is therefore necessary to establish an agreed comparison mechanism.

B. Analytics

Both MapReduce and Parallel DBMS can be used to produce analytics results from big data. Parallel DBMS uses SQL as the retrieval method, while MapReduce uses programming languages. In many data mining and data clustering applications, the algorithm is complex and requires multiple passes over the data. The output from one subprocess is the input to the next. It is difficult to develop these algorithms in SQL. The aggregation in SQL is not able to process these multiple step data flows. Performing these tasks in many steps reduces the performance benefits gained from parallel DBMS. For these complex analytic algorithms, MapReduce provides a good alternative [6].

V. Complementary Paradigms

In this section, the use of parallel DBMS and MapReduce as complementary paradigms is considered. One problem associated with parallel DBMS is the time taken to load large volumes of data. If this data is repeatedly queried then the load times impact needs to be averaged over each query. MapReduce, having a simple data structure does not suffer from the same load time issue. Therefore, MapReduce can be useful for one-time queries while parallel DBMS can be useful for repeated queries. This property of MapReduce makes it ideal for transforming data prior to load into the Parallel DBMS.

Another area where parallel DMBS can struggle is complex analytics. It can be quite difficult to express some queries in SQL. MapReduce allows the user to build complex computations on the data, without the limitation of the SQL language. In conclusion, parallel DBMSs are excellent at efficient querying of large data sets. Conversely, MapReduce is much slower by comparison, but is significantly better at complex analytics and ETL tasks.

There is a number of different approaches which have been taken to integrating parallel DBMS and MapReduce. These efforts have focused on using Hadoop implementation of MapReduce. Two of these approaches will be considered here:

- Loading Hadoop data in the Parallel DBMS;
- Accessing DBMS data from Hadoop;

Each of these will be further described in the following subsections.

A. Accessing DBMS data from Hadoop

This approach was first developed by Cloudera in the form of the *DBInputFormat* class. The basic approach is for each Map node to run the same SQL statement. The statement is modified to include order by, limits and offsets on the data. This ensures that each node receives a unique set of data. The main issue with this approach is that the performance

 ISBN: 978-1-61208-246-2

is often poor, as the same SQL is essentially run for every Map node. This approach has been extended by Teradata. In their version, the SQL statement is run once, and the output stored in a temporary table. This table is partitioned by the number of MapReduce nodes. When the MapReduce node requires the data, the query provides the data based on the appropriate partition [13].

B. Accessing Hadoop data from within the Parallel DBMS

DBMS provide a mechanism to integrate to external data using User Defined Function (UDF). Once complete the workings of the UDF are transparent to the database user. This allows the database user to write SQL query calls as follows:

*INSERT INTO Tab1 SELECT * FROM TABLE(udfLoadHadoop('mydfsfile.txt')) AS T1;*

This query will load the data from the Hadoop file, called *mydfsfile.txt*, into the database table *Tab1*. The UDF function is called "udfLoadHadoop". This function will take the Hadoop file as a parameter and integrate the data using the Hadoop NameNode metadata. The NameNode identifies which nodes in the Hadoop file system contain the required data. The UDF performs calculations based on the file size and the number of parallel nodes to determine which data belongs to each node. It then requests that data using the NameNode [13]

VI. Results

This section will provide a comparison of MapReduce and parallel DBMS, across a broad range of criteria:

- Data Volume:
  - Parallel DBMS - Has been used for data volumes in the order of Petabytes;
  - MapReduce - Has been used for data volumes in the order of Petabytes;
- Cost:
  - Parallel DBMS - Enterprise level toolset. This is an expensive investment;
  - MapReduce - This is open source based solution. The investment is considered inexpensive;
- Fault Tolerance:
  - Parallel DBMS - Transaction Level, cannot survive node failure;
  - MapReduce - Fault tolerant, designed to survive multiple node failures;
- Users:
  - Parallel DBMS - Can be used by multiple user types, from Business Users using reporting tools, through SQL novices and expert users;
  - MapReduce - Requires programming skills to work with. Smaller pool of individuals capable of performing these tasks;
- Data Types:
  - Parallel DBMS - Supports structured data. Data has to be transformed into rows and columns;
  - MapReduce - Supports both structured and unstructured data. Data can be operated on in native format;
- Hardware:
  - Parallel DBMS - Homogenous, all nodes in the installation must be the same;
  - MapReduce - Heterogeneous, the nodes in the installation can be different. This allows for the use of commodity PCs;
- Maturity:
  - Parallel DBMS - Parallel DBMS have a long history of successful installation;
  - MapReduce - MapReduce is a relatively new technology. The source is continuously under development with new features being added;

VII. Conclusions and Future Work

Based on this data, for the following types of problems, the authors suggest that MapReduce is used over parallel DBMS:

- Unstructured data: If the primary data source is unstructured then the cost of transforming it and loading it into a parallel DBMS is prohibitive. Based on this, MapReduce would be a good candidate;
- Cost: If cost is the main driver for the organization, then MapReduce is the better candidate. Parallel DBMS systems are considered enterprise level tools, but this comes at a high cost;
- User skill level: If the organization has an available pool of high skilled developers then MapReduce is a good option. In addition, if the organization is one in which control of the data is important then MapReduce is also the better candidate.

Conversely, for the following types of problems, the author suggests that parallel DBMS should be chosen above MapReduce:

- Structured data: If the data is structured and will continue to be so for the foreseeable future, then parallel DBMS would be a good fit;
- Enterprise Level Support: If enterprise level support is important to the organization, then the parallel DBMS vendors would be the preferred option. Although there are companies that offer this (for example Cloudera), companies in the parallel DBMS have been providing this support for a longer time;

 ISBN: 978-1-61208-246-2

- User: If the user base is not technical, or the data is not the key focus of the business, then parallel DBMS are the better choice.

Finally, many tests have compared versions of MapReduce and parallel DBMS focus on single queries. This provides clear results for performance. However, in the author's experience, in production environments multiple queries are often run concurrently. In addition to this, queries will include different types of problems. Some will be aggregating data; some will be joining data; others will be performing complex analytics. While this data is being queried, it is common for more data to be written to the system simultaneously. To provide a thorough comparison, the author believes it is necessary to test how the systems perform under these circumstances. To do this it would be necessary to establish a set of requirements. A test bench would then be created which would allow for these requirements to be run repeatedly.

REFERENCES

[1] R. B. J.E. Short and C. Baru, "How Much Information 2010: Report on Enterprise Server Information," http://hmi.ucsd.edu/pdf/HMI_2010_EnterpriseReport_Jan_2011.pdf, Jan. 2011, [Online; accessed 27-Nov.-2012].

[2] P. Ranganathan and J. Chang, "(Re)Designing Data-Centric Data Centers," *Micro, IEEE*, vol. 32, no. 1, pp. 66 –70, Jan.-Feb. 2012.

[3] A. Abouzeid, K. Bajda-Pawlikowski, D. Abadi, A. Silberschatz, and A. Rasin, "Hadoopdb: an architectural hybrid of mapreduce and dbms technologies for analytical workloads," *Proc. VLDB Endow.*, vol. 2, no. 1, pp. 922–933, Aug. 2009, [Online; accessed 27-Nov.-2012].

[4] J. Dean and S. Ghemawat, "Mapreduce: simplified data processing on large clusters," *Commun. ACM*, vol. 51, no. 1, pp. 107–113, Jan. 2008. [Online]. Available: http://0-doi.acm.org.ditlib.dit.ie/10.1145/1327452.1327492

[5] A. Pavlo, E. Paulson, A. Rasin, D. J. Abadi, D. J. DeWitt, S. Madden, and M. Stonebraker, "A comparison of approaches to large-scale data analysis," in *Proceedings of the 35th SIGMOD international conference on Management of data*, ser. SIGMOD '09. New York, NY, USA: ACM, 2009, pp. 165–178. [Online]. Available: http://0-doi.acm.org.ditlib.dit.ie/10.1145/1559845.1559865

[6] M. Stonebraker, D. Abadi, D. J. DeWitt, S. Madden, E. Paulson, A. Pavlo, and A. Rasin, "MapReduce and parallel DBMSs: friends or foes?" *Commun. ACM*, vol. 53, no. 1, pp. 64–71, Jan. 2010. [Online]. Available: http://0-doi.acm.org.ditlib.dit.ie/10.1145/1629175.1629197

[7] Apache, "Apache HDFS," http://hadoop.apache.org/common/docs/current/hdfs_design.html, 2012, [Online; accessed 27-Nov.-2012].

[8] D. Jiang, A. Tung, and G. Chen, "Map-join-reduce: Toward scalable and efficient data analysis on large clusters," *Knowledge and Data Engineering, IEEE Transactions on*, vol. 23, no. 9, pp. 1299 –1311, Sept. 2011.

[9] W. Fang, B. He, Q. Luo, and N. Govindaraju, "Mars: Accelerating mapreduce with graphics processors," *Parallel and Distributed Systems, IEEE Transactions on*, vol. 22, no. 4, pp. 608 –620, april 2011.

[10] A. Thusoo, J. S. Sarma, N. Jain, Z. Shao, P. Chakka, S. Anthony, H. Liu, P. Wyckoff, and R. Murthy, "Hive: a warehousing solution over a map-reduce framework," *Proc. VLDB Endow.*, vol. 2, no. 2, pp. 1626–1629, Aug. 2009, [Online; accessed 27-Nov.-2012].

[11] D. DeWitt and J. Gray, "Parallel database systems: the future of high performance database systems," *Commun. ACM*, vol. 35, no. 6, pp. 85–98, Jun. 1992, [Online; accessed 27-Nov.-2012].

[12] M. O'Sullivan, "Teradata," http://www.teradata.com/newsrelease.aspx?id=7243, April 2012, [Online; accessed 27-Nov.-2012].

[13] Y. Xu, P. Kostamaa, and L. Gao, "Integrating hadoop and parallel dbms," in *Proceedings of the 2010 international conference on Management of data*, ser. SIGMOD '10. New York, NY, USA: ACM, 2010, pp. 969–974, [Online; accessed 27-Nov.-2012].

 ISBN: 978-1-61208-246-2

Fault Detection of a Linear Friction Welding Production System Using an Analytical Model

Darren T. Williams
Andrew R. Plummer
The University of Bath,
BA2 7AY, UK
E-mail: darren.williams@rolls-royce.com
a.r.plummer@bath.ac.uk

Peter Wilson
Rolls-Royce PLC. CRF,
5 Littleoak Drive, Sherwood Enterprise Park,
Annesley,Nottinghamshire,
NG15 0GP, UK
E-mail: peter.wilson3@rolls-royce.com

***Abstract*—This paper presents a fault detection and isolation (FDI) model for an industrial Linear Friction Welding (LFW) production machine in Rolls-Royce. The LFW machine is a complex 11 actuator machine which has 6 degrees of freedom. The inplane axis is the most complex axis due to the high power and high dynamic response requirements, necessitating the use of two four-stage servo valves. We adapted a previously proposed model with fault diagnosis techniques to enable fault detection and isolation for the LFW inplane welding axis. This paper will demonstrate the models ability to detect and isolate faults during production, allowing immediate detection - enabling operators or maintenance to utilize the information to effectively get the LFW machine back into production.**

Keywords-modelling; fault detection; fault isolation.

I. LFW INTRODUCTION

Linear Friction Welding (LFW) [1] has been a key technology in recent years for aircraft engine manufacture in both commercial and military market sectors. For joining Blades to Discs (Blisks) [1], LFW is the ideal process for the following reasons:

- LFW is a solid state process which gives reproducibility, and high quality bonds therefore improving performance
- More cost effective than machining Blisks from solid billets
- Blisks enable up to 30% weight saving over conventional rotors
- LFW enables hollow bladed Blisks
- Dissimilar materials can be joined for optimised blade and disc properties

The process can be divided into six phases: *contact* - initial advancement of actuators seating the blade onto the disc stub and applying a seating force, *ramp up* - blade oscillations start to occur, *conditioning* – maintaining the oscillations to enable frictional heat to build up, *burn-off* – material deforming plastically under compression, *ramp down* – blade decelerated to a static position, and *forging* – allowing the weld to complete under a constant pressure.

Fig. 1 outlines the process phases:

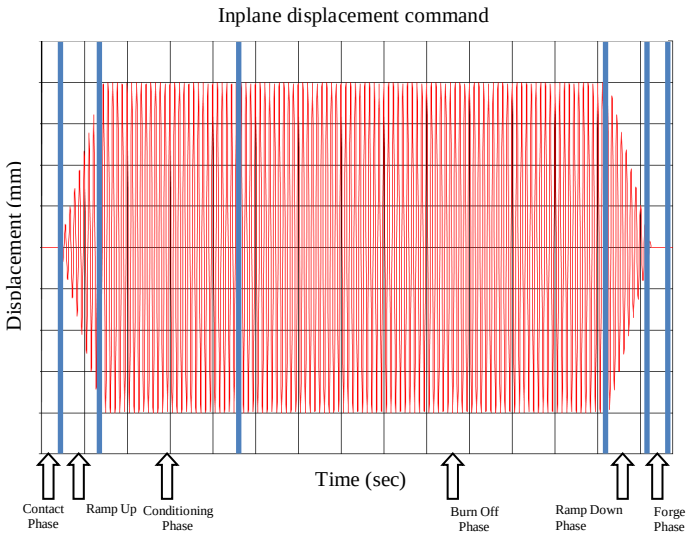

Figure 1 - LFW Process phases

Rolls-Royce's LF60 is a linear friction welding system that is designed to weld Blisks in a production environment. The system uses a combination of high performance, high accuracy servo-hydraulics to produce oscillatory motion between the components which creates frictional heating, and a forging force sufficient to produce a high strength and geometrically precise bond.

Faults occurring on the LF60 can lead to system downtime and the scrapping of components [2], both of which could lead to a monetary loss for the business. In order to reduce the likelihood of these issues a novel method of redundancy has been placed on the machine, with no additional sensors or hardware needing to be installed. Analytical redundancy in detecting faults has then been applied to the system.

Section 2 introduces the LFW machine and gives an overview of the modelled system. Section 3 reviews residual generation methods applicable to this work and section 4 outlines the chosen residual generation and evaluation methods for the FDI system. Section 5 evaluates the FDI model using two actual production fault cases. Section 6 concludes this paper.

 ISBN: 978-1-61208-246-2

II. FAULT DETECTION INTRODUCTION

Over the years different computer based diagnosis techniques have been tried and tested in a number of different domains. For the simpler and well understood systems, techniques such as decision trees, fault directories, and probability theory have been successfully applied [3, 4]. When applying these techniques with more complex systems, the accuracy of results reduces resulting in incomplete and inconsistent diagnosis. This is due to the fact that a high number of interactions could exist, therefore more complex techniques have been developed and used.
More complex techniques such as artificial intelligence have been used in the fault diagnosis area, but limitations such as incompleteness and inconsistencies in knowledge, knowledge extraction, and the dependency of the extracted knowledge exists [5]. To reduce these limitations fault diagnosis by the use of model-based techniques was approached, this involves capturing knowledge about the structure and behavior of the system, and the key system interactions. Simulating the knowledge alongside the system can then be used to predict the system behaviour, and identify when a fault could occur or diagnose it. This is done by the model generating the systems nominal behaviour, and any deviations identified.

Model-based fault detection and diagnosis/isolation (FDI) techniques have been researched widely in the literature, examples being [6-10]. This involves creating a residual signal by comparing the systems actual output signal and the estimated one from a nominal system model, once created this residual signal can be used as the indicator of abnormal system behavior. An example of residual indication can be seen in Fig. 2. As the error occurs in Fig. 2 the residual in a) appears out of its threshold, in b) there is a frequency change but the majority of the residual stays within the threshold. There is a threshold present due to system modeling uncertainties and noise. Fig. 2 identifies that faults can be detected but not simply by residuals appearing out of tolerance.

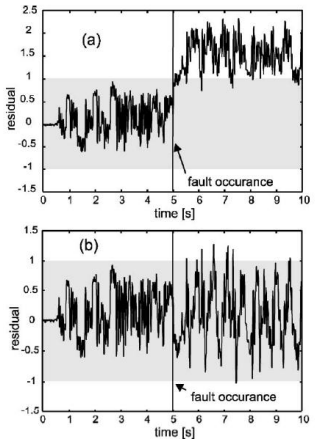

Figure 2 - (a) Detection of a sensor offset fault, (b) Detection of a sensor gain fault. [9]

FDI focuses on the use of fundamental knowledge to achieve efficient and effective diagnosis. Models of the correctly functioning system which can generate the expected system behavior are used to express the fundamental knowledge. Comparing the systems behavior with the models behavior can give the ability to derive possible faults, but the fault detection accuracy depends greatly on the existence of a good system model [11].
Other FDI techniques exist such as knowledge based methods [12] which don't involve an analytical model but are data-driven and knowledge based techniques able to estimate the system dynamics. Signal processing techniques in the time-frequency domain can also be applied to detect faults. Some examples of these are spectrogram and scalogram [13], and wavelet decomposition [14].

A fault can be defined as a departure from an acceptable range of an observed variable or a calculated parameter associated with a process [15]. The underlying cause of this abnormality is called the root cause. With increased systems complexity it is becoming difficult for human operators to continuously diagnose systems, manage system degradation, parameter drift, and component failures. This difficulty is compounded by production pressures, the amount of system variables, and incomplete or unreliable data. FDI deals with timely detection, and diagnosis of abnormal system behaviour. Once detected the human operator is able to take action accordingly.

A model of the LF60 Inplane actuation system has been developed in [16], fault detection methods have been placed onto the model to enable detection and isolation for faults which have previously occurred on the system.

III. THE LF60 LINEAR FRICTION WELDING MACHINE

Each machine axis on the LF60 is independently controlled using a combination of PID and Amplitude and Phase control (APC). The six main degrees of freedom are referred to as inplane, forge, hade, roll, pitch and yaw. The inplane actuator, which is driven by two four stage valves, oscillates the blade tangentially to the disk. Forging pressure is obtained by a combination of four PID controlled hydrostatic actuators. The six hade actuators restrain the unwanted movement in the other degrees of freedom [17].

A CAD picture of the LF60 inner cage showing the actuator attachments can be seen in Fig. 3.

 ISBN: 978-1-61208-246-2

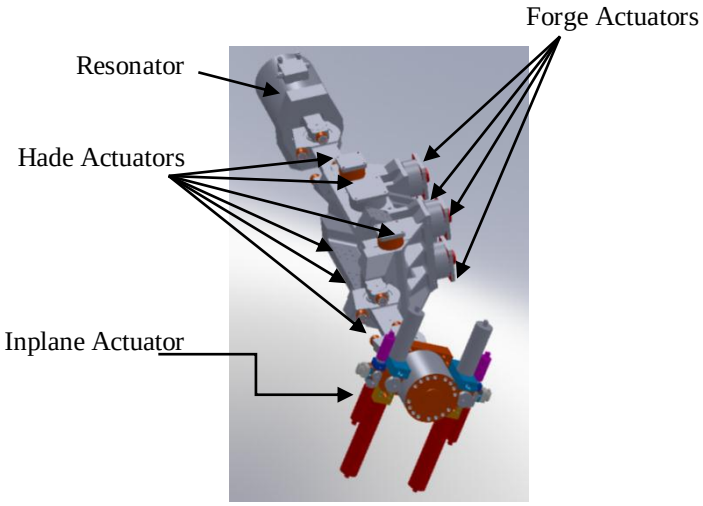

Figure 3 - Picture of the inner cage with actuators attached

The inplane actuation system provides the oscillating motion. This is the most complex system on the machine and therefore the one where the majority of faults occur [2]. It is driven by two 4 stage servo valves. Each one has a pilot two stagevalve rated at $6.31x10^{-5}m^3/s$; this drives the 3rd stage $2.52x10^{-3}$ m^3/s spool which in turn drives the 4th stage $2.52x10^{-2}$ m^3/s spool.

Fig. 4 shows a front view of the inplane servo valves.

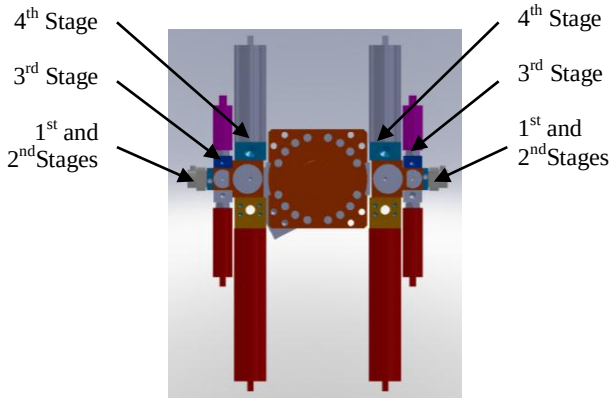

Figure 4 - LF60 4 stage inplane Valves arrangement: front view

The 4 stage servo valve works by the initial first stage torque motor controlling flow via a nozzle-flapper arrangement. The 2nd stage has a mechanically feedback spool linked to the first stage by the feedback spring. The 3rd stage spool, with electronic position feedback, acts as a flow amplifier to the 4th stage, which also has electronic closed-loop control of the spool position. The modelled system in [16] models important factors as outlined in [18] which include fluid compressibility, variable cylinder oil volumes, internal cylinder leakage, cylinder cross-port bleed, valve orifice pressure-flow characteristic, valve overlap, valve body pressure drop, manifold pressure drop and oil volume, valve spool dynamics, maximum valve opening, valve spool slew rate limit, friction, and geometric properties.

IV. RESIDUAL GENERATION

A number of fault detection approaches exist in the literature. A classification of these different approaches can be seen in Fig. 5.

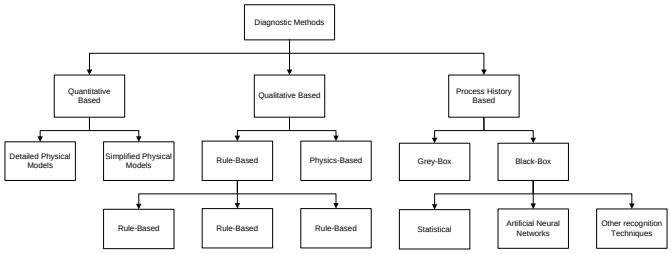

Figure 5 - Classification of the diagnostic system [19]

Quantitative based diagnosis methods involve creating analytical redundancy with the use of physical models to generate residuals that can be used for isolating process failures. These can be detailed or simplified physical models.

Qualitative based diagnosis methods can be rule based, or qualitative physics based. Rules based systems involve systems derived from expert knowledge, first principles, or limits checks.

Process history based diagnosis methods are used when a priori knowledge of the process is not known therefore input-output (black box) relationships are developed using statistical, neural network, or similar pattern recognition techniques. Grey box methods use process data to determine model parameters by using mathematical terms.

Given the availability of a system model (developed and validated in [16]) the diagnosis system used will be qualitative based, detailed physical modeling. A number of model-based fault diagnosis methods can be found in the literature [7, 8, 19]. The main two are parity equation methods and observer based approaches which are discussed in the following subsections.

A. *Parity Equation Methods*

The Parity Equation Method involves providing a proper check of the parity (consistency) of the measurements for the monitored system first proposed by [20]. Mathematical models describing the relationships between system variables are used to describe the input-output or space-state characteristics of the system, the rearrangement of these gives the parity equations [19]. Output of the parity equation in theory should be zero mean, but in reality due to model inaccuracies, measurement and process noise the output will be nonzero. Parity methods are similar to observer methods

 ISBN: 978-1-61208-246-2

but usually designed more intuitively. Fig. 6 shows two methods for parity generation, an output error method and the equation error method.

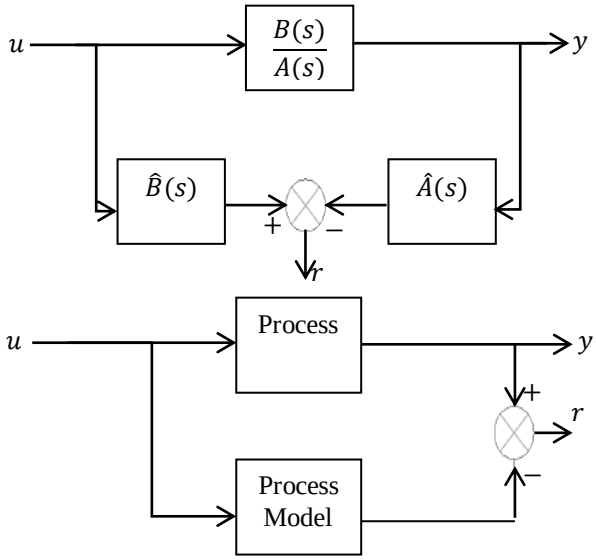

Figure 6 - Parity equations for fault detection: Equation error method (upper), Output error method (lower) [21]

B. Observer approaches

Reconstructing the outputs of a system from measurements using the estimation error with observers or Kalman filters is another commonly used approach for fault diagnosis [22]. With the observer approach the estimation error can be considered as the residual, in order to detect and isolate faults. For stochastic systems, the Kalman filtering technique can be used, which enables noise to be factored into the approach [23]. State estimation is improved with the use of Kalman filters due to the processing of all available measurements regardless of precision to estimate the current variable of interest.

For example, take the system state and measurement equations (1) and (2) respectively:

$$\dot{x} = Ax + Bu + Gw \quad (1)$$

$$y = Cx + Du + Hw + v \quad (2)$$

u is the system input, the process noise is represented by w, and the measurement white noise is represented by v with $E\,(ww^T) = Q$, and $E\,(vv^T) = R$. The state and estimation noise is uncorrelated i.e. $E\,(wv^T) = 0$. The Kalman filter equation can provide the optimal estimate of y termed $\hat{y}$:

$$\hat{x} = A\hat{x} + Bu + L(y - C\hat{x} - Du) \quad (3)$$

$$\hat{y} = C\hat{x} + Du \quad (4)$$

The weightings for Q and R are chosen by trading off fault sensitivity to the likelihood of false alarms using engineering experience. Fig. 7 shows the Kalman estimator, which uses the known inputs u and the measurement y to generate the output and state estimates $\hat{y}$ *and* $\hat{x}$. Riccati equations are solved to find the Kalman filter gain L.

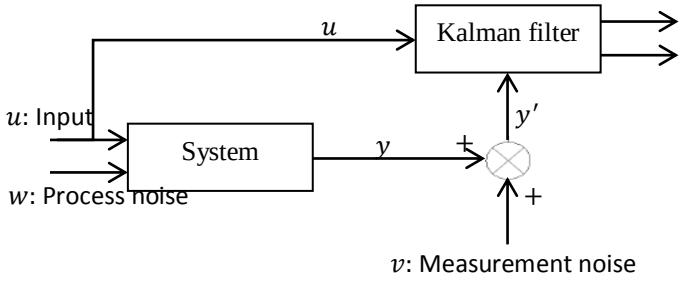

Figure 7–Kalman filter example

C. Residual Generation Summary

Each of the discussed approaches involves the creation of a residual (or series of residuals) which need to be analyzed further to provide indication and isolation of faults. Residual evaluation can be done using a constant threshold or an adaptive threshold, constant threshold residual evaluation has a number of disadvantages. Due to the inclusion of noise, or uncertainties in models false alarms can be triggered. Therefore, adaptive thresholds which take into account any modeled inaccuracies or noise can enable better fault detection, and the reduction of false alarms. Given the availability of a validated model, the preferred method of residual generation is the parity method, utilizing the model to compare outputs of the actual system to form residual signals.

V. RESIDUAL EVALUATION

The fault diagnostic method used in this paper will be of the qualitative based type with detailed physical modelling of the system used to check the consistency of the actual system. The inplane system model developed in [16] will act as an intuitively designed observer providing analytical redundancy. Residual generation will be done by comparing the measured values of the system outputs y_i, with the corresponding analytically computed values $\check{y}_i$:

$$r_i = y_i - \check{y}_i \quad (5)$$

Fig. 8 outlines a flow diagram of the fault diagnosis system, indicating residual generation, evaluation in order to detect and isolate faults.

 ISBN: 978-1-61208-246-2

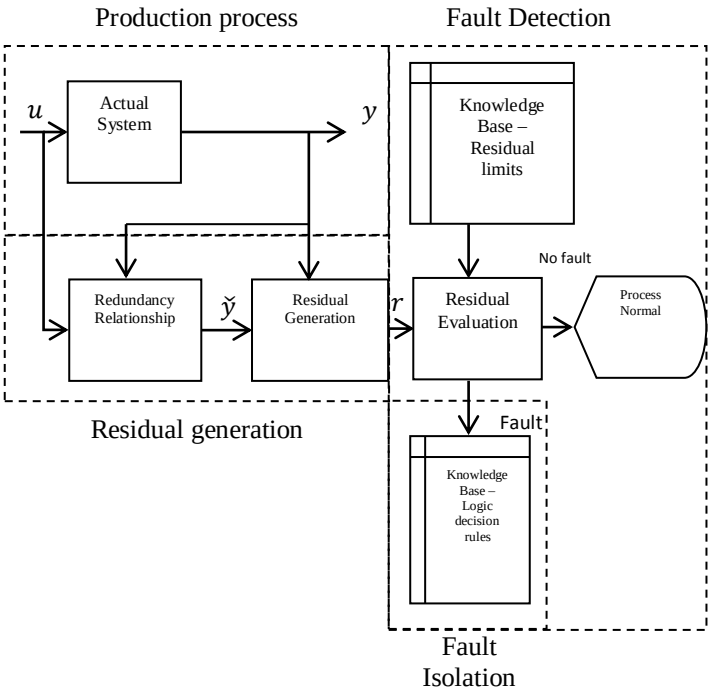

Figure 8–Fault diagnosis flow diagram

Once a residual has been generated, the residual would need to be evaluated to see if a fault is present or not. Various forms of residual evaluation exist in the literature, some of which include residual threshold setting based on the minimal detectable failure [24], posterior probabilities to process information in order to detect faulty circuits [25], the use of fuzzy logic enabling the incorporation of human operator knowledge to interoperate the residuals [26], and probabilistic methods based on likelihood ratios [27]. The residual limits in this research will be created by using previous fault free data executed through the model and used to capture the maximum residual limits for fault free conditions, therefore creating adaptive residual limits defined from previous fault free data, similar as in [28]. Due to the different components welded on the LF60 the residual limits will be component specific, therefore a number of knowledge based data files will be stored which hold residual limits for each residual and component. In the presence of a fault the residual signal will appear high i.e. $r_i = 1$ at that time signal.

The use of adaptive residual limits defined from previous fault free data will allow for any compared signals (model vs. new data) which deviate more than normal, outside of the modeling noise, disturbances, and inaccuracies to be picked up and therefore flagged by the model alerting to a fault, or a change in system performance. On the detection of a residual breach the system will decide on the type of fault, its cause, location, and possible solutions given a knowledge base of logical rules defined from previous fault occurrences. A flow diagram of the logical rules can be seen in Fig. 9. The logical rules would be triggered post residual evaluation of Fig. 8.

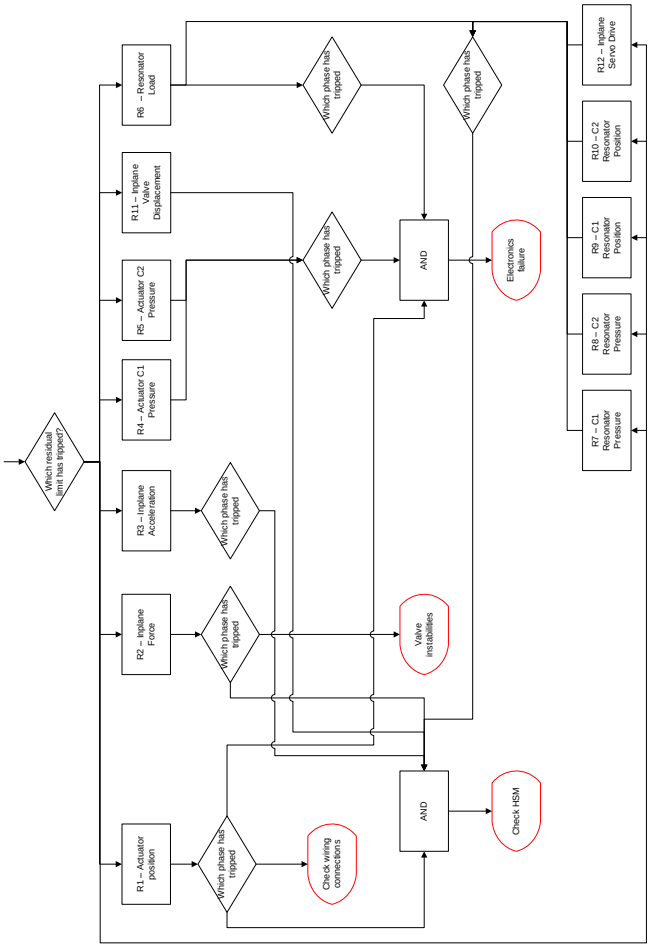

Figure 9– Flow diagram of the *Knowledge Base – Logic decision process*

The following section implements the fault detection scheme and tests it against a number of fault cases.

VI. Fault Detection And Isolation Case Studies

This section evaluates the FDI with two actual production fault cases.

A. *Fault case 1: Start-up instability*

The start-up instability shown in Fig. 10 was caused by a faulty relief valve [29], the machine alerted to this issue therefore production was immediately halted (due to Rolls-Royce confidentiality the current machine detection methods cannot be shown). The benefits of a fault detection model would not only be the ability to detect the fault, but also the isolation of the issue by the model informing the operators of its cause and possible solution.

 ISBN: 978-1-61208-246-2

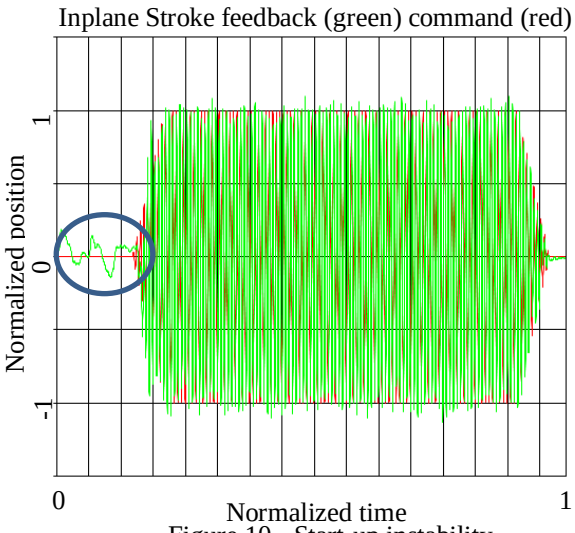

Figure 10 - Start-up instability

Simulating a non-faulty component of the same type through the FDI model yields the outputs shown in Fig. 11. The upper figure compares the actual (fault free) output with the models output, the 2nd figure shows the residual signal and adaptive limits. The 3rd figure indicates any trips of the adaptive residual limit by the residual, and the lower figure indicates detection of a fault on the signal. The fault detection signal only trips if the limit trip signal is triggered and remains triggered for a predefined persistence of 3ms, which is done to further reduce false fault detections.

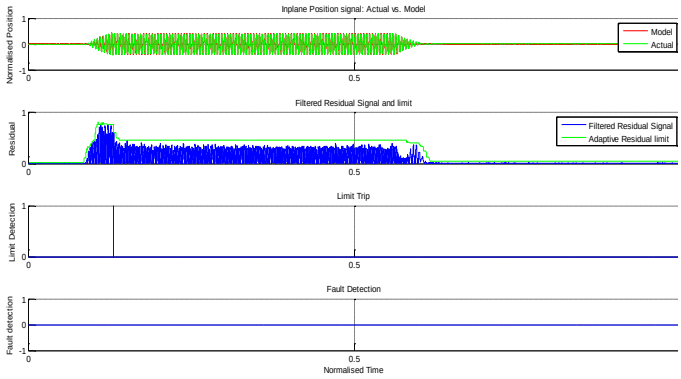

Figure 11 – Start-up Instability, Fault detection with the residual generation method (fault free)

Fig. 12 shows the FDI model simulated with the start-up instability fault. The limit trip signal is tripped immediately and a number of times throughout the simulation – therefore the fault detection signal trips also and stays high from the start of the simulation. This simulation shows an effective capture of the fault using the FDI model. Using the logic previously defined in Fig. 9, the model outputs an indication to the user to "Check HSM" after detecting the presence of the fault occurrence on the relevant signals.

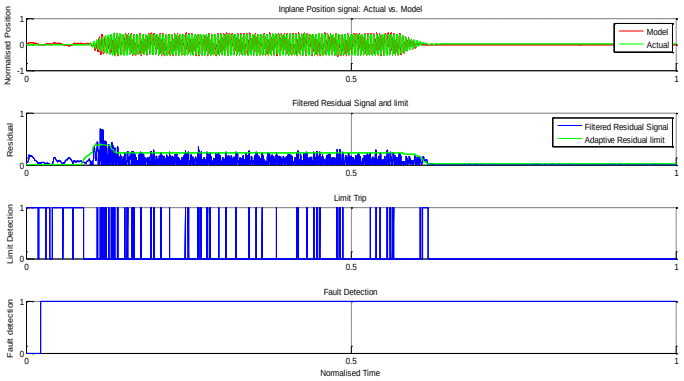

Figure 12 – Start-up instability, Fault detection with the residual generation method (fault)

B. *Fault case 2: Force holding Instability*

The Inplane force holding instability of Fig. 13 was only captured during manual review of the data post Blisk completion. Therefore the immediate detection of this type of fault would be of great benefit to potentially saving the scrapping of the Blisk and rectify the issue immediately. On simulation of the fault through the FDI model, the model and residual limits are sensitive enough to capture the instability and therefore indicate the presence of a fault, as shown in Fig. 14.

Example of the instability:

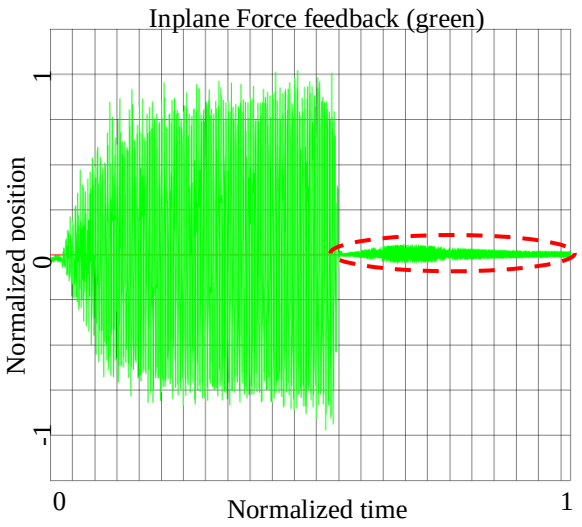

Figure 13 – Force hold Instability

FDI model output simulated with the fault in Fig. 14:

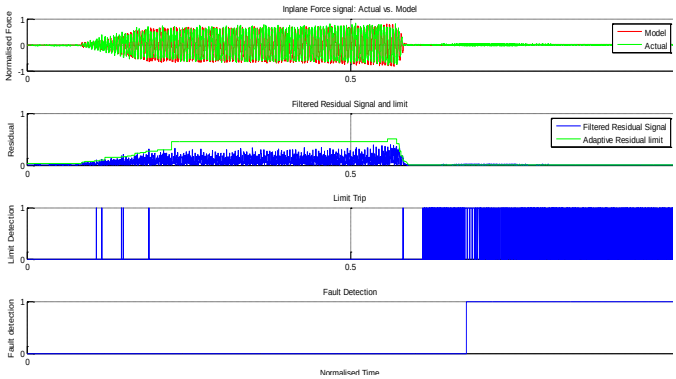

Figure 14 – Force hold instability, Fault detection with the residual generation method (fault)

FDI model simulated with fault free data:

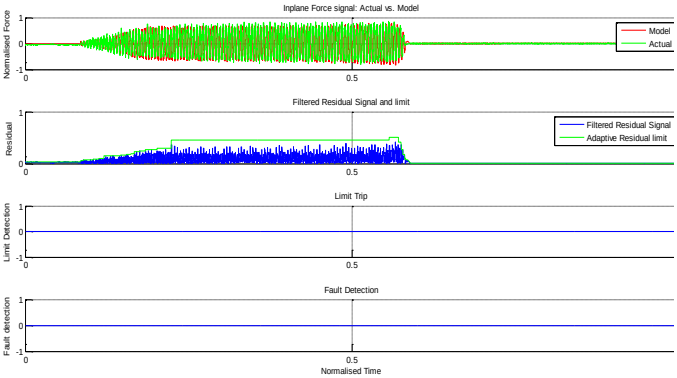

Figure 15 – Force hold Instability, Fault detection with the residual generation method (fault free)

Therefore this fault can be successfully detected and the operator/maintenance engineers notified immediately. A notification of “Valve instabilities” would be displayed post fault occurrence.

Therefore the model demonstrates effective capture of this fault at the first instance of its occurrence, enabling quick detection and isolation of the fault – reducing the potential for scrapping a component.

VII. CONCLUSION

A fault detection system has been implemented on a model previously developed in [16]. Case studies of actual production faults have been examined with the FDI model proving the model’s ability in detecting abnormal system behaviour and using a series of logic steps to isolate the fault, its cause, and possible solutions.

The FDI system will be placed alongside the LFW system in order to detect faults upon the occurrence thus providing timely detection and identification, saving the business valuable time and money. Implementing the FDI system will involve careful understanding and integration with the LFW system and its users. This will be accomplished by utilizing the latest soft systems research knowledge.

ACKNOWLEDGMENT

This work was supported by the Systems Centre and EPSRC funded Industrial Doctorate Centre in Systems (Grant EP/G037353/1) and Rolls-Royce Plc.

REFERENCES

1. Linear Friction Welding of Blisks. [online] Available at: <http://www.twi.co.uk/industries/aerospace/welding-of-aircraft-engines/linear-friction-welding-of-blisks/> [Accessed 10 September 2012].
2. G. Colin, "LFW Maintenance Issue Timeline". Rolls-Royce internal Report, 2012.
3. R.L. Flood, and R.C. Ewart, "Dealing with Complexity: An Introduction to the Theory and Application of Systems Science, Second Edition." New York: Plenum Press, 1993.
4. P.B. Checkland and L. Davies, "The use of the term "Weltanschauuug" in soft systems methodology." Jornal of Applied Systems Analysis, Vol. 13, No. 1, pp 109-115, 1986.
5. N.N. Mitev, "More then a failure? The computerized reservation systems at French railways." Information Technology & People, 9 (4), 8-19, 1996.
6. E.L. Russell, L.H. Chiang, and R.D. Braatz, "Fault Detection and Diagnosis in Industrial Systems." Springer, 2001.
7. C.H. Lo, Y.K. Wong, and A.B. Rad, "Model-based fault diagnosis in continuous dynamic systems." 2004, ISA Transactions 43 459-475.
8. R. Isermann, "Model-based fault detection and diagnosis - status and applications." 2005, Annual Reviews in Control 29 71-85.
9. M. Borner, H. Straky, T. Weispfenning, and R. Isermann, "Model based fault detection of vehicle suspension and hydraulic brake systems." 2002, Mechatronics 12 999-1010.
10. J.L. Aravena and F.N. Chowdhury, "Fault detection of flight critical systems." 2001, Proc. 20th Digital Avionics Systems Conference.
11. A. Mirijamdotter, A multi-modal systems extension to soft systems methodology. Doctoral thesis, Lulea Tekniska Universitet, 1998 (1998:06 ISSN: 1402-1544 ISRN: LTU-DT--98/06--SE).
12. S. Oblak, I. Skrjanc, and S. Blazic, "Fault detection for nonlinear systems with uncertain parameters based on the interval fuzzy model." 2007. Engineering Applications of Artificial Intelligence, Volume 20, Issue 4 pp. 503-510.
13. I. Yesilyurt, "The application of the conditional moments analysis to gearbox fault detection - a comparative study using the spectrogram and scalogram." 2003, NDT & E International Volume 37, Issue 4 pp. 309-320.
14. R. Zhou, W. Bao, N. Li, X. Huang, and D. Yu, "Mechanical equipment fault diagnosis based on redundant second generation wavelet packet transform."

 ISBN: 978-1-61208-246-2

2009, Digital Signal Processing Volume 20 Issue 1 276-288.

15. D.M. Himmelblau, "Fault detection and diagnosis in chemical and petrochemical processes." 1978, Amsterdam: Elsevier press.
16. D.T. Williams, A.R. Plummer, and P. Wilson, "Dynamic Modelling of a Linear Friction Welding Machine Actuation System." Bath/ASME Symposium on Fluid Power and Motion Control, University of Bath 12-14th September 2012.
17. MTS, LF60 Operation Manual. Internal Rolls-Royce documentation. 2000.
18. A.R. Plummer, "A Detailed Dynamic Model of a Six-Axis Shaking Table," in Centre for Power Transmission and Motion Control. 2008, University of Bath: Bath. p. Journal of Earthquake Engineering, 12:4, 631 - 662.
19. V. Venkatasubramanian, R. Rengaswamy, K. Yin, and S.N. Kavuri, "A Review of process fault detection and diagnosis Part 1: Quantitative model-based methods." 2003a, Computers and Chemical Engineering 27 (2003) 293-311.
20. E.Y. Chow, and A.S. Willsky, "Analytical redundancy and the design of robust failure detection systems." IEEE Trans. on Automatic Control, 29(7),603-614., 1984.
21. R. Isermann, "Fault Diagnosis Applications." Springer-Verlag Berlin and Heidelberg GmbH & Co. K, 2011. 04 May 2011.
22. P.M. Frank, "Fault diagnosis in dynamic systems using analytical and knowledge-based redundancy - a survey and some new results." Automatica, 26(3), 459-474., 1990.
23. R.E. Kalman, "A new approach to linear filtering and prediction problems." Transactions of the ASME-Journal of Basic Engineering,, 1960. 82(Series D):35-45,1960.
24. A. Emami-Naeini, M.M. Akhter, and S.M. Rock, "Effect of model uncertainty on failure detection: The threshold selector." IEEE Transations on Automatic Control, 1988. volume 33 no.12.
25. D. Lave, T. Larrabee, and J. Colburn, "Automatic thresholds and probabilistic Isub DDQ diagnosis." In IEEE International test conference, pages 1065-1072, 1999.
26. J.M. Koscielny, M. Syfert, and M. Bartys, "Fuzzy-logic fault diagnosis of industrial process actuators." In Journal of applied mathematics and computer science, 1999. volume 9 no. 3, pages 637-653.
27. F. Hermans and M. Zarrop, "Model Based Statistical Change Detection for Automotive Applications." IEEE International Symposium on Computer-Aided Control System Design, 1996.
28. L. Guo, Y. Zhang, and H. Wang, "Fault diagnostic filtering using stochastic distributions in nonlinear generalized H∞ setting." Fault Detection, Supervision and Safety of Technical Processes 2006, 2006. Volume 1, 2007, Pages 216-221.
29. H. Reader, Report detailing the LF60 breakdown resolution actions Rolls-Royce internal Report, 2012.

 ISBN: 978-1-61208-246-2

Universal Approaches for Overflow and Sign Detection in Residue Number System Based on $\{2^n - 1, 2^n, 2^n + 1\}$

Dina Younes, Pavel Steffan
Dept. of Microelectronics
Brno University of Technology
Brno, Czech Republic
xyoune00@stud.feec.vutbr.cz, steffan@feec.vutbr.cz

***Abstract*—This paper presents two universal efficient approaches for overflow and sign detection and correction in the addition of two numbers in unsigned and signed residue number systems (RNS). Both methods are designed to be used in systems based on the moduli set $\{2^n - 1, 2^n, 2^n + 1\}$ that provides an even dynamic range. Moreover, by applying a tiny modification, these designs can be used in any system that has (2^n) as one of its moduli (i.e. has an even dynamic range). The proposed methods depend on a simple structure that provides fast and accurate detection and correction of the sign and overflow. A comparison, which proves the efficiency of the proposed designs, in terms of time and area requirements is also presented.**

Keywords-residue number system (RNS); overflow detection; sign detection; even dynamic range; moduli set $\{2^n - 1, 2^n, 2^n + 1\}$

I. INTRODUCTION

The residue number system (RNS) is a unique, non-weighted, carry-free number system that provides parallel, high speed and fault tolerant arithmetic operations. This makes it a tough candidate for high-performance, low power, fault tolerant and secure digital signal processing (DSP) applications. This system has been intensively used in applications where addition, subtraction and multiplication are dominant, such as, digital filters, digital communications, discrete Fourier transform (DFT), image processing and video coding [1], [2].

Nevertheless, operations as division, overflow detection, sign detection and magnitude comparison are problematic and very complex in RNS. In some cases, some of these operations, such as overflow and sign detection, are essential and cannot be avoided. Moreover, they are fundamental in other operations such as division.

Sign and overflow detection are very important issues in RNS, since a wrong detection of sign or overflow ruins the whole advantage of using RNS. There is no point of using RNS in order to obtain parallel, high-speed and secure arithmetic operations if the results of these operations are wrong.

In principle, the general way to detect overflow in RNS is via comparing the result of addition with one of the addends. If $X \geq 0$ and $Y < M$ then $(X+Y) \bmod M$ causes overflow if and only if the result is less than X.

On the other hand, the general way for sign detection in RNS is via comparing the converted number from residue-to-binary with half of the dynamic range of the RNS. Thus, we can conclude, that both sign detection and overflow detection are equivalent to the magnitude comparison.

One of the most efficient ways to detect overflow in RNS is via parity checking [1], [2], [3], and [4]. It indicates whether an integer is even or odd. Suppose two integers (X, Y) have the same parity: $Z = X + Y$. An overflow occurs if Z is odd. Contrary, if (X, Y) have different parity, then an overflow occurs if Z is even. The parity checking technique is one of the best and fastest suggested methods to detect the overflow in RNS. It depends on look-up tables (LUTs) or on an extra modulo (a redundant modulo). However, this technique can only be used with moduli sets that have just odd members, i.e. odd dynamic range, which is not suitable for many moduli sets that uses 2^n as one of its moduli, especially the most famous moduli set $\{2^n - 1, 2^n, 2^n + 1\}$. RNS systems, that have even dynamic ranges, have more attractive features than those with odd dynamic ranges. Due to the reason, that using (2^n) modulo greatly simplifies and reduces the delay and complexity of the residue arithmetic operations and the residue-to-binary conversion.

Thus, it is obvious that overflow detection in RNS that has an even dynamic range is a very important issue. As aforementioned before, both sign detection and overflow detection, based on the general ways, are equivalent to the magnitude comparison. Therefore, many RNS comparators have been presented [5], [6], and [7]. They used many different techniques in order to obtain faster performance and smaller area consumption. In [6], a residue comparator based on the Chinese reminder theorem (CRT) for general modulo sets is presented. In [7], a comparator based on diagonal function, that is named SUM of Quotients Technique (SQT), is introduced. An efficient residue comparator for any odd moduli set, which is based on the parity of integers and their period, is stated in [5].

In this paper, we present two efficient techniques for sign and overflow detection and correction in RNS based on the moduli set $\{2^n - 1, 2^n, 2^n + 1\}$. Moreover, these designs can be used in any system that has 2^n as one of its moduli. Furthermore, the proposed technique can also be used in systems with odd dynamic ranges after applying a small modification on it.

The rest of this paper is organized as follows; a brief introduction to the RNS is provided in Section II. The

 ISBN: 978-1-61208-246-2

proposed methods for overflow detection and correction in unsigned and signed RNS are demonstrated in Sections III and IV, respectively. In Section V, the performances of the proposed designs are evaluated and compared with residue-to-binary converters and residue comparators that can be used for overflow and sign detection in both unsigned and signed RNS. Finally, the conclusion is drawn in Section VI.

II. RNS BACKGROUND

The RNS is defined by a set of positive pairwise relatively prime numbers $\{m_1, m_2,\ldots, m_n\}$ called moduli. In this system, each weighted number X is uniquely represented by an ordered set of residues $(x_1, x_2,\ldots, x_n)$. Each residue x_i is represented by:

$$x_i = X \bmod m_i = \langle X \rangle_{m_i} \quad ; \quad 0 \le x_i < m_i \tag{1}$$

The dynamic range of this system is defined as $M = m_1 \times m_2 \times \ldots \times m_n$. Both unsigned and signed integers can be represented in RNS. For unsigned RNS, the range of representable integers is,

$$0 \le X \le M-1 \tag{2}$$

For signed RNS, the range of representable integers is partitioned into two equal intervals,

$$\begin{aligned} &0 \le X < \lfloor M/2 \rfloor && \textit{for positive numbers} \\ &\lfloor M/2 \rfloor \le X < M && \textit{for negative numbers} \end{aligned} \tag{3}$$

In this system, the arithmetic operations (addition, subtraction and multiplication) are performed totally in parallel on those very independent residues.

$$X \circ Y = \{\langle x_1 \circ y_1 \rangle, \langle x_2 \circ y_2 \rangle, \ldots, \langle x_n \circ y_n \rangle\}; \ \circ \equiv \sim (+,-,\times) \tag{4}$$

A residue number can be converted back into its binary equivalent, by using one of the residue-to-binary conversion algorithms, such as, the Chinese Reminder Theorem (CRT), the Mixed-Radix Conversion (MRC), the new CRT-I, the new CRT-II, etc. [1], [2].

According to the CRT, a residue number $(x_1, x_2,\ldots, x_n)$ can be converted back into its binary equivalent X by,

$$X = \left\langle \sum_{i=1}^{n} \langle x_i N_i \rangle_{m_i} M_i \right\rangle_M \tag{5}$$

where, $M_i = M / m_i$ and $N_i = \langle M_i^{-1} \rangle_{m_i}$ is the multiplicative inverse of M_i modulo m_i.

III. PROPOSED METHOD FOR OVERFLOW DETECTION IN UNSIGNED RNS

As aforementioned in the introduction, the general way to detect overflow is via comparing the sum with one of the addends, i.e. If $X \ge 0$ and $Y < M$ then $(X+Y) \bmod M$ causes overflow if and only if the sum is less than X.

Our method also depends on comparison; however, we compare each of the addends with half of the RNS range (M/2).

To detect overflow during the addition of two addends X and Y in unsigned RNS based on the moduli set $\{2^n - 1, 2^n, 2^n + 1\}$, a single bit, that indicates to which half of the dynamic range M that addend belongs, is used. Based on this bit, the following three cases should be considered. The overflow will definitely occur if both of the addends are equal or greater than the half of the dynamic range M/2. No overflow will definitely occur if both of the addends are less than M/2. However, if just one of the addends is equal to or greater than M/2, then the overflow prediction becomes complex and requires further processing and evaluation of the sum (Z).

The magnitude evaluation of the addends (X and Y) is represented by a single bit (*evlt_bit*).

$$evlt\_bit_X = \begin{cases} 0 & ; \quad X < M/2 \\ 1 & ; \quad X \ge M/2 \end{cases} \tag{6}$$

The processing of the *evlt_bit* of the two addends results in the three following cases,

$$overflow = \begin{cases} 0 & ; \quad evlt\_bit_X + evlt\_bit_Y = 0 \\ 1 & ; \quad evlt\_bit_X \bullet evlt\_bit_Y = 1 \\ 'u' & ; \quad evlt\_bit_X \oplus evlt\_bit_Y = 1 \end{cases} \tag{7}$$

where, '*u*' indicates the undetermined case of overflow occurrence and $(+,\bullet,\oplus)$ refer to the logical gates (OR, AND, XOR), respectively.

In order to solve the undetermined case '*u*', the *evlt_bit* of the binary sum (Z) should be calculated by (6). Then the overflow can be indeed detected,

$$overflow = \begin{cases} 0 & ; \quad 'u' \ \ \& \ \ evlt\_bit_Z = 1 \\ 1 & ; \quad 'u' \ \ \& \ \ evlt\_bit_Z = 0 \end{cases} \tag{8}$$

Fig. 1 shows the structure of the proposed design that detects the overflow in unsigned RNS based on $\{2^n - 1, 2^n, 2^n + 1\}$.

The magnitude evaluation of the addends and their sum, based on (6), is realized by an AND gate with ($2n$) inputs and an OR gate with two inputs. The magnitude evaluation unit is shown in Fig. 1 (a).

The overflow detection unit, based on (7) and (8), is realized by a 2:1 multiplexer and a XOR gate. This unit is shown in Fig. 1 (b).

 ISBN: 978-1-61208-246-2

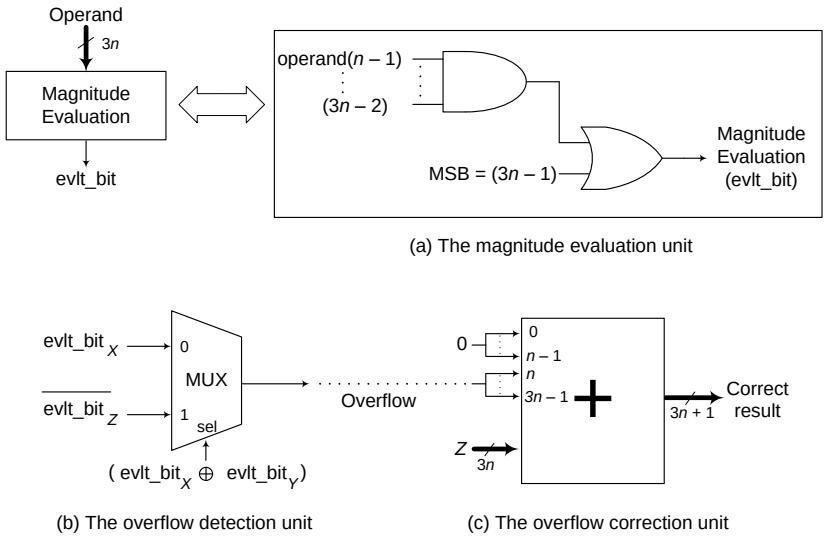

Figure 1. The internal structure of the overflow detection & correction unit for unsigned numbers : (a) Magnitude evaluation unit. (b) Overflow detection unit. (c) Overflow correction unit.

The last component of the proposed design is the overflow correction unit, which is shown in Fig. 1 (c). This unit adds back M to the sum (Z) in order to correct the overflow and obtain the final accurate result. The adder that performs the final addition can be of any type, according to the design's goal and strategy.

IV. Proposed Method for Sign and Overflow Detection in Signed RNS

In a similar manner, to detect overflow in the addition of two addends *X* and *Y* in signed RNS based on the moduli set $\{2^n - 1, 2^n, 2^n + 1\}$, a single bit, that indicates the sign of that addend, is used. As mentioned previously, in signed RNS, the positive numbers fall in the first half of the dynamic range, whereas, the negative ones fall in the second half. Thus, we have the following two cases that should be considered. No overflow will definitely occur if each of the addends has a different sign (fall in a different interval of *M*). Overflow may or may not occur if both addends have the same sign. Consequently, further processing should be done.

The sign evaluation of the addends is also represented by a single bit *evlt_bit* that is calculated by (6).

The processing of the *evlt_bit* of the two addends results in the two following cases,

$$overflow = \begin{cases} 0 & ; \quad evlt\_bit_X \oplus evlt\_bit_Y = 1 \\ 'u' & ; \quad evlt\_bit_X \oplus evlt\_bit_Y = 0 \end{cases} \quad (9)$$

where, '*u*' indicates the undetermined case of overflow occurrence and $\oplus$ refers to the logical gate XOR.

In order to solve the undetermined case '*u*', the *evlt_bit*, that determines the sign of the binary sum (*Z*) should be calculated by (6). Then the overflow can be indeed detected,

$$overflow = \begin{cases} 0 & ; \quad 'u' \quad \& \quad evlt\_bit_Z = evlt\_bit_X \\ 1 & ; \quad 'u' \quad \& \quad evlt\_bit_Z = \overline{evlt\_bit_X} \end{cases} \quad (10)$$

where, $\overline{evlt\_bit_X}$ refers to the logical negation of $evlt\_bit_X$.

Fig. 2 shows the structure of the proposed design that detects the sign and overflow in signed RNS based on $\{2^n - 1, 2^n, 2^n + 1\}$.

The sign evaluation of the addends and their sum, based on (6), is realized by an identical structure to that of the magnitude evaluation unit of the proposed design for unsigned RNS. It is shown in Fig. 2 (a).

The overflow detection unit, based on (9) and (10), is realized by a similar structure to that shown in Fig. 1 (b). It consists of a 2:1 multiplexer and two XOR gates. This unit is shown in Fig. 2 (b).

The overflow correction unit has an identical structure to that of the unsigned RNS. It is shown in Fig. 2 (c). Similarly, the adder that performs the final addition can be of any type.

V. Performance Evaluation and Comparison

Our proposed designs were compared with other two. The first one represents the general approach for overflow detection, which consists of a binary comparator based on the residue-to-binary converter presented in [8]. Whereas, the second one is an efficient residue comparator for general moduli set introduced in [6].

For the sake of fair comparison, unit gate model was used in order to estimate the time and area consumptions in the compared designs. According to the unit gate model, the delay (T) and area (A) of an inverter (NOT gate) were ignored.

 ISBN: 978-1-61208-246-2

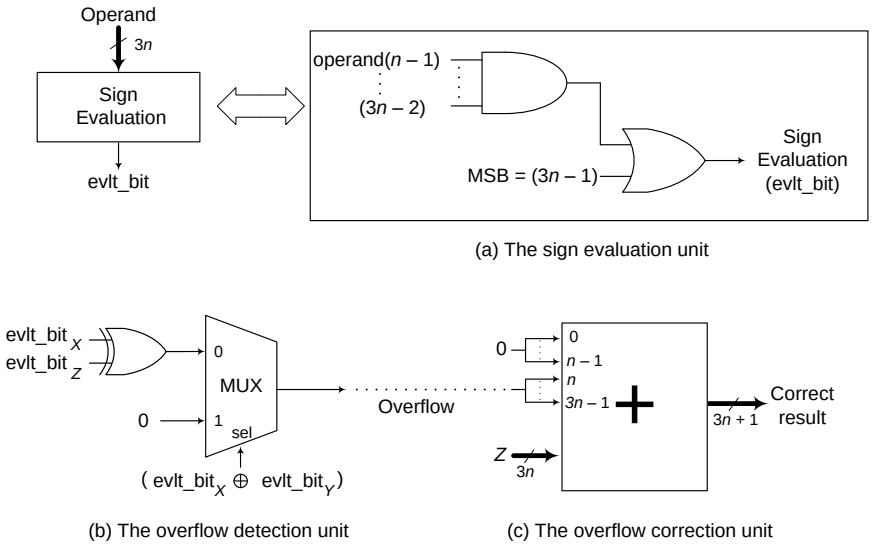

Figure 2. The internal structure of the sign and overflow detection & correction unit for signed numbers: (a) Sign evaluation unit. (b) Overflow detection unit. (c) Overflow correction unit.

Each 2-input monotonic gate (AND, NAND, OR, NOR): T = 1, A = 1. Each 2-input XOR, XNOR: T = 2, A = 2. A 2:1 multiplexer: T = 2, A = 3. Full adder: T = 4, A = 7. We have considered the 1st complement adder as a carry propagate adder with end-around carry (CPA-EAC): T= 8*n*, A = 7*n*. An *n*-bit binary comparator: T = 2*n*, A = 2*n* [9].

Table 1 summarizes the comparison and shows the delay and complexity of the proposed designs and the analogous ones.

The structures of the proposed designs are very similar; the only difference is an additional XOR gate in the overflow detection unit for signed RNS. Both of them are based on the residue-to-binary converter proposed in [8], the operand evaluation units of the addends and sum and the overflow detection unit. However, the evaluation of the addends is performed in parallel with the binary-to-residue conversion. Thus, no extra delay of these two units is presented. The *evlt_bit* of the addends are stored in two cells of RAM, each of them has a size of 1-bit. The correction unit was not included in the comparison. Thus, the critical path is composed of the residue-to-binary converter, the operand evaluation unit of the sum and the overflow detection unit.

The first analogous design is a binary comparator based on the reverse converter proposed in [8]. This method uses two binary comparators with a 2:1 multiplexer. The sizes of the binary comparators are 2*n*-bit and *n*-bit. Thus, the critical path in this design is composed of the residue-to-binary converter, the 2*n*-bit comparator and the 2:1 multiplexer.

The second analogous design presented in [6] uses a special component for generating two numbers (A_x and B_x) which are further used in the comparison. Moreover, this method uses three binary comparators and two 2:1 multiplexers. The sizes if these comparators are *n*-bit, *n*-bit and (*n*+1)-bit. Thus, the critical path of this circuit is composed of the A_x and B_x generator, the (*n*+1)-binary comparator and the two 2:1 multiplexers.

TABLE I. PERFORMANCE COMPARISON BETWEEN THE PROPOSED DESIGNS AND THE ANALOGOUS ONES

Design	Delay	Complexity
Residue comparator based on [8]	20*n* + 10	48*n* + 3
[6]	18*n* + 14	40*n* + 8
Proposed-unsigned	16*n* + log *n* + 13	37*n* + 18
Proposed-signed	16*n* + log *n* + 15	37*n* + 20

According to Table 1, both proposed designs have less delay and complexity without compromising on accuracy. Generally, lower area consumption leads to lower power consumption. However, we have not computed the estimated power consumption. Moreover, the analogous designs have not presented their power consumptions.

In case of overflow occurrence, *M* is added back to the binary sum, in order to correct the sum (*Z*) and get the final accurate result. The adder that performs this addition can be of any type, based on the design's goal and strategy. Moreover, the size of this adder is 2*n*-bit instead of 3*n*-bit, since the first *n*-bits of *M* for the moduli set $\{2^n - 1, 2^n, 2^n + 1\}$ are '0'.

$$\begin{aligned} overflow = '0' \Rightarrow \quad & final\ result = Z + "\underbrace{00\cdots00}_{2n}\underbrace{0\cdots0}_{n}" \\ overflow = '1' \Rightarrow \quad & final\ result = Z + "\underbrace{11\cdots11}_{2n}\underbrace{0\cdots0}_{n}" \end{aligned} \tag{11}$$

We have mentioned that both proposed designs can be used with any RNS that uses any moduli set that has (2^n) as one of its moduli, i.e. has an even dynamic range. This can be simply performed by applying tiny modification on the evaluation units, represented in changing the number of the inputs of the AND gate, according to the dynamic range

 ISBN: 978-1-61208-246-2

provided by the used moduli set. Moreover, in case of changing the number and the order of the AND gate's inputs, these two designs can be used with any other moduli set, even if it provides an odd dynamic range. However, for such systems, the parity checking technique will be faster and simpler than the proposed one.

VI. CONCLUSIONS AND FUTURE WORK

Overflow detection is one of the main challenges in the RNS, especially in systems based on moduli sets that provide even dynamic ranges. This paper presented two designs for overflow and sign detection and correction in unsigned and signed RNS based on the moduli set $\{2^n - 1, 2^n, 2^n + 1\}$. This set has an even dynamic range. Moreover, these designs can be considered as universal, since they can be used with any system that has an even dynamic range by applying a small modification on the evaluation unit. Both designs are faster and require less hardware components than those based on comparators. Our next step will be dedicated on designing a FIR filter based on RNS that uses the proposed sign and overflow detection and correction units in order to highlight their efficiency when embedded in a DSP application.

ACKNOWLEDGMENT

This research was supported by the Ministry of Industry and Trade of the Czech Republic under the MPO ČR č. FR-TI3/485 project and Prospective applications of new sensor technologies and circuits for processing of sensor signals, No.FEKT-S-11-16 project.

REFERENCES

[1] A. Omondi and B. Premkumar, Residue Number Systems: Theory and Implementation. Imperial College Press, UK, 2007.

[2] M. Lu, Arithmetic and Logic in Computer Systems. John Wiley & Sons, Inc., New Jersey, USA, 2004.

[3] M. Askarzadeh, M. Hosseinzadeh and K. Navi, "A new approach to overflow detection in moduli set $\{2^n - 3, 2^n - 1, 2^n + 1, 2^n + 3\}$," Second International Conference on Computer and Electrical Engineering (ICCEE'09), 28-30 December 2009, pp. 440 – 441.

[4] M. Shang, H. JianHao, Z. Lin and L. Xiang, "An efficient RNS parity checker for moduli set $\{2^n - 1, 2^n + 1, 2^{2n} + 1\}$ and its applications," Springer Journal of Science in China Series F: Information Sciences, 10 November 2008, pp. 1567 – 1570.

[5] B. Zarei, M. Askarzadeh, N. Derakhshanfard and M. Hosseinzadeh, "A high-speed residue number comparator for the 3-moduli set $\{2^n-1, 2^n+1, 2^n+3\}$," International Signals Systems and Electronics (ISSSE), 17-20 September 2010, pp. 2 – 3.

[6] S. Bi and W. J. Gross, "Efficient residue comparison algorithm for general moduli sets," 48th Midwest Symposium on Circuits and Systems, 7-10 August 2005, pp. 1602 – 1604.

[7] G. Dimauro, S. Impedovo and G. Pirlo, "A new technique for fast number comparison in the residue number system," IEEE Transactions on Computers, May 1993, pp. 608 – 611.

[8] S. J. Piestrak, "A high-speed realization of a residue to binary number system converter," IEEE Transactions on Circuits and Systems II: Analog and Digital Signal Processing, October 1995, pp. 661 – 663.

[9] F. Vahid, Digital Design with RTL Design, VHDL and Verilog, John Wiley & Sons Publishers, USA, 2011.

 ISBN: 978-1-61208-246-2

Path Planning for Rapid Aerial Mapping with Unmanned Aircraft Systems

A fast complete coverage path planning algorithm with no backtracking

Eduard Santamaria, Florian Segor, Igor Tchouchenkov, Rainer Schönbein
IAS – Interoperabilität und Assistenzsysteme
Fraunhofer IOSB
Karlsruhe, Germany
{eduard.santamaria, florian.segor, igor.tchouchenkov, rainer.schoenbein}@iosb.fraunhofer.de

***Abstract*—One focus of research at Frauhofer IOSB is the utilization of unmanned aerial vehicles for data acquisition. Past efforts have lead to the development of a hardware and software system able to rapidly generate a complete and up-to-date aerial image by combining several single high resolution pictures taken by multiple unmanned aerial vehicles. However, the path planning component of the system was not designed to support no-fly zones inside the area of interest. In this paper, we present a new complete coverage path planning algorithm that provides support for no-fly zones inside the area, and also increases efficiency by reducing the number of turns. The proposed method is suitable for complex areas that may contain known obstacles and no-fly zones, to be covered by maneuverable systems such as multirotor aircraft.**

Keywords-aerial situation image; unmanned aerial vehicles; complete coverage path planning

I. INTRODUCTION

The technical advance in the development of miniature unmanned aerial vehicles (UAVs) in the last decade has made unmanned aerial systems more capable and affordable. Hence, nowadays, a civil application is not only conceivable but already reality with some facilities of fire brigade or police. Due to the current rate of development and the varied application possibilities of miniaturized unmanned aircraft, it can be assumed that usage of these systems will rapidly increase.

At the Fraunhofer IOSB the most different applications are examined and systems are developed which should allow rescue and emergency forces to use UAVs in an easy and intuitive way [1,2].

Within the scope of this research in 2011 we presented an inspection system for generating high resolution up-to-date aerial images to support rescue forces and first responders [3]. It uses the payload capacity of one or several UAVs to scan a defined area with high-resolution image sensors to generate an image mosaic from the accumulated single frames. These mosaics can be generated with low resources and costs and their applications have been demonstrated in different realistic scenarios.

During different trials the concept proved itself to be right and the system generated useful results. However, the restriction that some zones within the inspected area could not be excluded turned out as a disadvantage. Because this feature is sometimes necessary to avoid obstacles, forbidden zones or areas of no interest, an adaptation of the original solution was required. As a part of this adaptation different alternatives were examined to further improve the efficiency of the process.

The focus of this advancement is, on this occasion, the shortening of flying time by simplifying the flight route, reducing the number of turning points, together with added support for no-fly zones inside the area of interest.

Results are compared with the raster based method previously in place. The comparison is therefore based on three metrics: total flied distance, number of turns and number of "jumps" between non-adjacent cells. While the total distance travelled by the UAV is similar in both cases, with the new method, the number of necessary turns is significantly reduced. The number of jumps is slightly incremented, but with no impact on the total travelled distance.

II. RELATED WORK

A taxonomy proposed by Choset divides coverage path planning algorithms into heuristic based algorithms and algorithms that are based on a cellular decomposition. The latter can rely on an exact, a semi-approximate or an approximate decomposition [4]. Heuristic based algorithms combine heuristics and randomness to drive the exploration process. These methods do not require expensive sensors and do not consume much computational resources. They can provide a good ratio between cost and performance; however, parts of the area of interest may remain unvisited. Therefore, complete coverage is not guaranteed. Most of complete coverage path planning algorithms implicitly or explicitly adopt cellular decomposition to achieve completeness.

An exact cellular decomposition is a set of non-intersecting regions, each termed a cell, whose union fills the target environment. Typically, the robot can cover each cell using some kind of motion pattern, e.g., back-and-forth pattern, and the path planning algorithm decides the order in which cells are visited [5, 6, 7, 8].

Semi-approximate algorithms rely on a partial discretization of space where cells are fixed in width but the top and bottom can have any shape [9, 10]. The robot moves

 ISBN: 978-1-61208-246-2

along these columns and different parts of a complex area are recursively explored in order to achieve completeness.

An approximate cellular decomposition generates a grid based representation of the area of interest. All cells have the same size and shape and their union approximates the target region. Coverage is complete when the robot visits each cell in the grid. The cell size typically depends on the footprint of the robot. This approach fits very well to our application, where the goal is to generate a complete aerial image of an area by combining aerial photos taken at different points. The size of each cell will be directly related to the sensor footprint. Many algorithms have been developed that fall into this category. Some of them are referenced in the next paragraphs.

Different authors have developed coverage path planning methods based on spanning trees [11, 12, 13]. These methods generate a continuous path around the spanning tree. In the likely situation of the UAV landing in the same zone where it took off, this is a good property. The nature of the algorithm requires that, if the cell size derived from the camera footprint is D, the area shall be decomposed into cells of size 4D. Different implementations to generate the spanning trees differ regarding computational complexity and quality of the generated results.

Zelinsky et al. proposed a complete coverage path generation method based on distance transforms [14]. With distance transforms each cell is assigned a value that represents the distance to the goal. These values can be used to find the shortest path from a starting point to the goal. Extensions to the distance transform path planning methodology can be used to generate a complete coverage path. One of the extensions proposed by Zelinsky et al. generates many unnecessary turns. An improved version creates a path that tends to follow the contour of the area. Recently, a distance transform based method has been used by Barrientos et al. to obtain optimal paths in the context of agricultural applications [15]. Their algorithm uses a costly backtracking algorithm to compute all coverage path candidates.

The method proposed by Carvalho et al. makes use of several interesting patterns to generate the path [16]. However, the scanning always takes place in the same direction, which would be a disadvantage in some circumstances, for instance, when a L-shaped area needs to be covered.

An approach developed by Choi et al. creates a path that follows a spiral pattern [17]. Such kind of pattern will not very efficient, in terms of the number of turns, when the cell grid has complex contours.

The grid that represents the area is used in the method proposed by Kang et al. to create a number of rectangular subareas by grouping cells [18]. Then, one of several patterns is applied to each subarea. We believe that this method can work well when the alignment of boundary cells tends to form rectilinear sides. A number of cells may be revisited when moving from the end of one pattern to the start of the next one.

The work presented in this paper continues previous efforts at Fraunhofer IOSB. Segor et al. describe a system that is able to use several small UAVs to efficiently obtain a complete aerial image [3]. Each UAV is allocated one subarea to scan. To cover each subarea two candidate paths are generated: one that makes progress by scanning the area column by column, and another one that does the same row by row. The one that yields better results is chosen. A drawback of such approach is that it does not adapt well to situations where a combination of different scan directions would be more beneficial. Besides, the original implementation was not designed to support no-fly zones inside the area of interest.

In this paper we present a new method for generating a path that completely covers the area. Computation is fast and the number of turns is significantly reduced when compared against the results obtained by the algorithm currently in use. Other metrics, such as travelled distance and jumps between non-adjacent cells, are also compared.

III. APPLICATION SCENARIOS

The security feeling of our society has significantly changed during the past years. Besides the risks arising from natural disasters, there are dangers in connection with criminal or terroristic activities, traffic accidents or accidents in industrial environments. Especially in the civil domain in case of big incidents there is a need for a better data basis to support the rescue forces in decision making. The search for buried people after building collapses or the clarification of fires at big factories or chemical plants are possible scenarios addressed by our system.

Many of these events have very similar characteristics. They cannot be foreseen in their temporal and local occurrence so that situational in situ security or supervision systems are not present. The data basis on which decisions can be made is rather thin and therefore the present situation is very unclear to the rescue forces at the beginning of a mission. Exactly in such situations it is extremely important to understand the context as fast as possible to initiate the suitable measures specifically and efficiently.

An up-to-date aerial image can be a valuable additional piece of information to support the briefing and decision making process of the first responders.

Figure 1 Photomosaic of Biotope at the Rhein River.

 ISBN: 978-1-61208-246-2

However, helicopters or supervision airplanes that can supply this information are very expensive or even unavailable. High-resolution pictures from an earth observation satellite could also be a good solution in many cases. But, under normal circumstances, these systems will not be available or they may not be able to deliver good pictures because of clouds or smoke. A small, transportable, fast and easily deployable system that is able to produce similar results is proposed to close this gap.

The "photo flight" tool described in this paper can provide the lacking information by creating an overview of the site of the incident in a very short time. The application can be used by first responders directly on site with relative ease. The results provide a huge enhancement to the available information.

Many other applications are also possible: support to fire-fighting work, clarification of debris and the surroundings after building collapses, search for buried or injured people, inspection of large objects, or for documentation and perpetuation purposes, as for example, of protected areas and biotopes (see Fig.1).

The AMFIS system, which the photo flight tool is part of, provides a ground control station with an intuitive and ergonomic interface, and is capable of controlling multiple aircraft simultaneously [3]. By using more than one single UAV, the same search area can be covered in less time or respectively a bigger area can be searched in the same time. The automatic path planning capabilities presented in this paper reduce the workload of the user, who only has to define the area of interest and indicate which vehicles can be used to perform the mission.

IV. PATH PLANNING ALGORITHM

The algorithm presented in this paper is applied once the grid of cells that approximates the area of interest is available. The AMFIS system already performs this step, together with a division into subareas for a multi-UAV scenario. The algorithm can then be used to compute a path to cover each subarea.

The concept of stride is central to the algorithm. We define a stride as a sequence of consecutive adjacent cells with no turns. To compute a stride of max length the following rules are used:

- The stride starts at the current cell.
- The direction of the stride is determined by its starting point and the neighbor under consideration.
- A stride contains no turns.
- A number of conditions, explained below, determine where the stride ends.

We define $L(c)$ as the number of visited neighbor cells and area limits located orthogonally to the stride direction at cell c. Being c_0 the first cell of the stride, c_l the current last cell of the stride, and c_n a potential next cell in the stride direction, addition of c_n to the stride is subject to the following conditions:

- We do not add c_n if it is already in the generated path or if it falls outside the boundaries of the area.

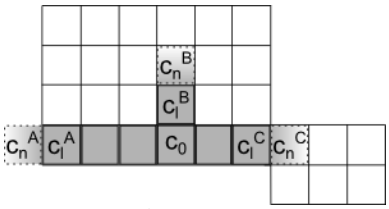

Figure 2 Stride formation starting at cell c_0.

- If the previous condition does not hold, and $L(c_l) = 2$, we always add c_n to the stride, because c_n is the only possible cell where we can go to from c_l.
- If $L(c_l) \neq 2$, any of the following conditions will prevent addition of c_n to the stride: (1) $L(c_n) = 0$; (2) $L(c_n) \neq L(c_0)$; or (3) $L(c_n) = 1$ but the limit at c_n is positioned opposite to the limit found at c_0. The purpose of condition (1) is to stop when we are not following an area limit or a "wall" formed by cells already in the path. Conditions (2) and (3) dictate that stride formation will also stop when the limits of c_n differ from the limits of c_0.

Stride formation is illustrated in Fig. 2. Starting at c_0, there are three alternative strides that can be selected. Stride A (left of c_0) ends when an area limit is reached. Stride B (up) ends because $L(c_n^B) = 0$. Finally, in stride C, both c_0 and c_n^C have an area limit located orthogonally to the stride direction. Therefore $L(c_0) = L(c_n^C) = 1$, however, since the area limits of these cells are located at opposite sides, c_n^C is not added to the stride.

The algorithm for generating the complete coverage path works as follows:

1. Set the current cell to the initial cell.
2. Find all unvisited neighbor cells of the current cell (between 0 and 4 cells are returned).
3. Generate the longest possible stride in the direction of each unvisited neighbor cell.
4. Select the longest stride.
5. Add all cells of the stride to the path and mark them as visited.
6. Set the current cell to the last cell of the stride.
7. Repeat starting at point 2 until all cells have been visited.

In the example presented in Fig. 2, stride A, with four cells, would be selected over the B and C alternatives, which respectively have two and three cells.

When all alternative strides have length two (c_0 plus a neighbor cell), some heuristics are used to perform the stride selection. These heuristics prioritize the selection of (1) the neighbors with more limits or visited cells around it, (2) the ones located in the contour of the area, and (3) the ones that lead to a longer stride. These heuristics have been chosen after extensive testing with different area shapes. Heuristics (1) and (2) promote the selection of a path that moves alongside other visited cells or the contour of the area.

Sometimes, the addition of a cell to the path partitions the area, creating two, or more, subareas of disconnected unvisited cells. When this happens, the algorithm chooses to visit the cells of the smallest sub-area first.

 ISBN: 978-1-61208-246-2

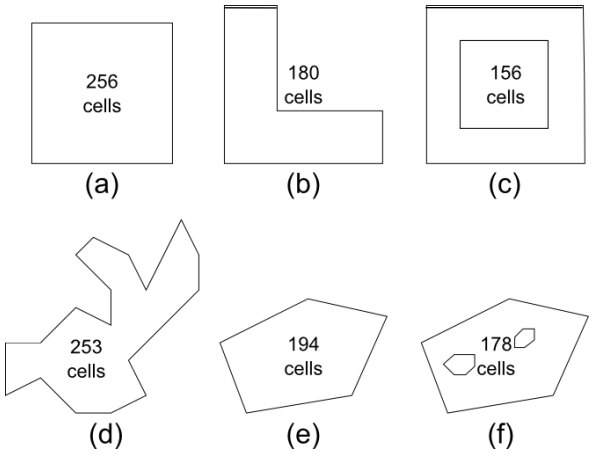

Figure 3 Contours, with their number of cells, used in tests.

Another situation that needs to be addressed happens when a dead end is reached, i.e., when there are no unvisited valid cells next to the current cell. In this case, our solution computes a path between the current cell and each one of the unvisited cells located next to cells already visited. These paths are computed using distance transform path planning as described by Zelinsky et al. in [15]. The shortest path is selected and its cells are added to the complete coverage path. This same method can be used to compute a path to the landing point.

The distance wave propagation used to compute the shortest path (see [15]), is also used to determine if the area has been partitioned.

One final step performs some clean-up on the generated path. If the path contains a sequence of revisited cells that connect two adjacent cells, the sequence of revisited cells is removed from the path. In this way, the UAV will transition directly from the first cell to the adjacent one avoiding unnecessary repeats.

V. RESULTS

The proposed algorithm has been tested with areas of different shape. In this section, the results obtained with the areas showed in Fig. 3 are presented. The new algorithm has been compared with the original algorithm of the photo flight tool. The metrics used are the number of turns, the travelled distance, and the number of jumps, which are the transitions between non-adjacent cells. Some considerations need to be taken into account to analyze the results:

- In a situation where all neighbor cells next to the current position have been visited, but coverage is not complete, the original algorithm didn't provide a safe path to fly from the current position to the next free cell. For this reason we compare the number of jumps between non-adjacent cells, instead of the number of revisited cells.
- The original algorithm was not designed to handle no-fly zones inside the area of interest. Nevertheless, if such an area is provided as input, it is able to generate a complete coverage path.

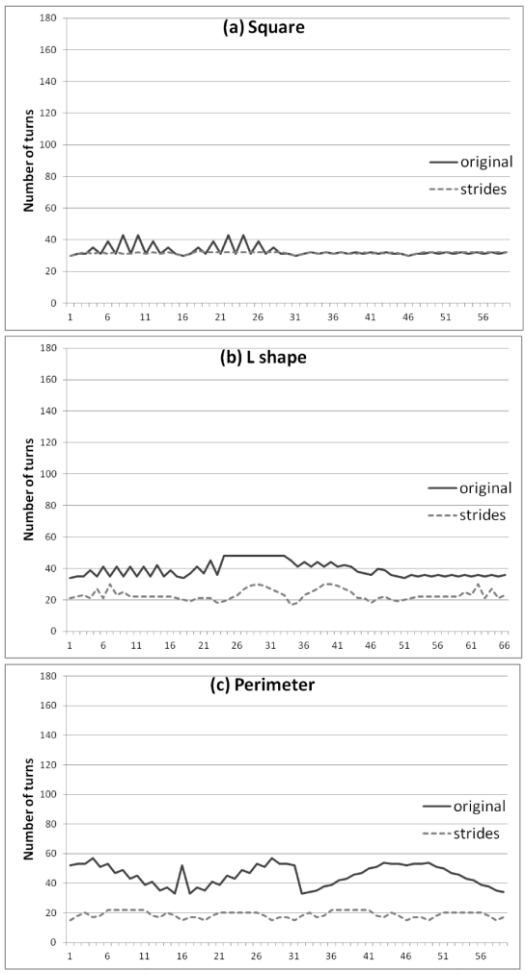

Figure 4 Number of turns starting at each contour cell of a, b and c.

- The computed distance corresponds to the path length plus the distance between the last and the first cell of the path.

In Figs. 4 and 5 the number of turns obtained running both the original and the new strides based algorithms are displayed. The algorithms have been run starting at each contour cell of the example areas in Fig. 3. As it can be observed, the new algorithm provides better results with all tested areas.

Fig. 6 displays the average travelled distance (top) and average number of jumps (bottom) obtained, with both algorithms, for each area. It can be seen that, although the number of jumps is slightly increased in some cases, this increase has almost no impact on the average travelled distance.

To understand the reasons that lead to an improvement in the number of turns, we now compare the complete paths of the areas b and e of Fig. 3. In Fig. 7a, it can be seen that one source of improvement is the ability of the new algorithm to use different scan directions in different parts of the area of interest. Another source of improvement (see Fig. 7b), comes from the fact that the new algorithm is better at getting rid of contour teeth, avoiding its propagation into the inner parts of the area (see Fig. 7b).

 ISBN: 978-1-61208-246-2

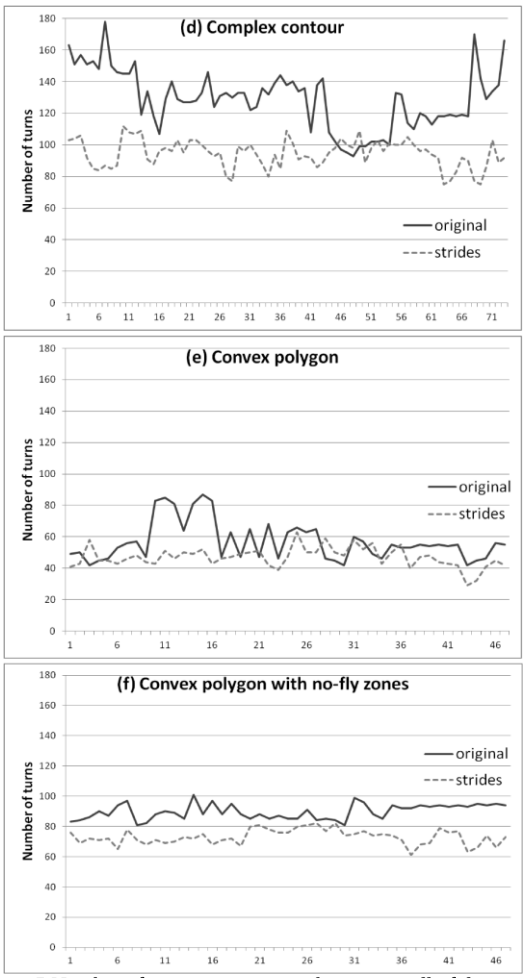

Figure 5 Number of turns starting at each contour cell of d, e, and f.

Finally, in Fig.7c (bottom), the complete path generated for a complex area with no-fly zones is shown. When there are no unvisited neighbors, a safe path to reach the next free cell is computed. Thus, the complete coverage path does not contain jumps between non-adjacent cells. The generated path can be contrasted with a path generated by the original algorithm (top), which was not really designed to cope with holes in the area, and does not provide a mechanism to generate a safe path between non-adjacent cells.

VI. CONCLUSION AND FUTURE WORK

In this paper we introduced our most recent work and advances in complete coverage path planning for generating image mosaics.

The proposed algorithm is able to compute the path in a very short time, which makes it suitable for rapid response situations. Additionally, a path computation criterion that prioritizes the selection of long straight segments results in a reduced number of turns, which can be seen as a big advantage particularly in the case of a fast moving unmanned aircrafts. Its ability to scan the area in different directions and the fact that it does not rely on pre-defined patterns allow it to efficiently generate complete coverage paths for complex contours which may contain holes.

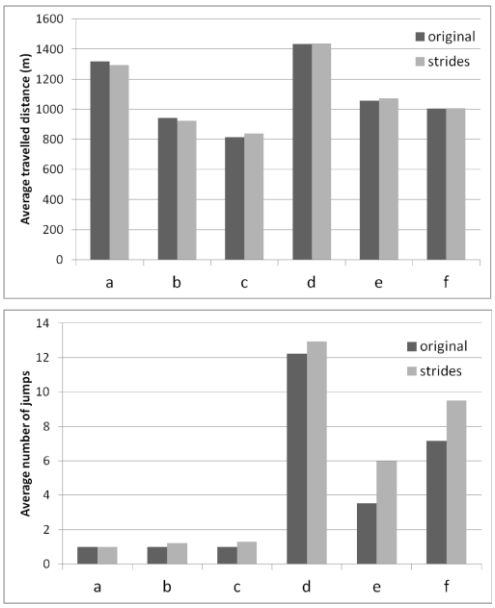

Figure 6 Average travelled distance (top) and average number of jumps (bottom).

The presented path planning method is appropriate for maneuverable systems, such as multirotor aircraft, and scenarios with known obstacles.

The photo flight tool of the AMFIS system will be updated to rely on the new algorithm for the path computation and support will be added to enable the user to specify no-fly zones. An essential aspect of the photo flight software is its support for multiple aircraft flying in parallel. In this case, the area of interest must be split among the available UAVs. In this point work is still pending as we see some potential for improvement to the system.

ACKNOWLEDGMENT

This work was carried out during the tenure of an ERCIM "Alain Bensoussan" Fellowship Programme. This Programme is supported by the Marie Curie Co-funding of Regional, National and International Programmes (COFUND) of the European Commission.

REFERENCES

[1] Bürkle, A., "Collaborating Miniature Drones for Surveillance and Reconnaissance", Proc. of SPIE Vol. 7480, 74800H, Berlin, Germany, 1-2 September (2009).

[2] Leuchter, S., Partmann, T., Berger, L., Blum, E.J. and Schönbein, R., "Karlsruhe generic agile ground station", Beyerer J. (ed.), Future Security, 2nd Security Research Conference, Fraunhofer Defense and Security Alliance, 159-162 (2007).

[3] F. Segor and A. Bürkle and M. Kollmann and R. Schönbein, "Instantaneous Autonomous Aerial Reconnaissance for Civil Applications - A UAV based approach to support security and rescue forces", 6th International Conference on Systems ICONS, 2011, pp. 72-76.

[4] H. Choset, "Coverage for robotics - A survey of recent results", Annals of Mathematics and Artificial Intelligence vol.31, 2001, pp.113-126.

[5] I. Maza and A. Ollero, "Multiple UAV cooperative searching operation using polygon area decomposition and efficient coverage algorithms", in Distributed Autonomous Robotic

 ISBN: 978-1-61208-246-2

Systems vol. 6, R. Alami and R. Chatila and H. Asama, Eds. Springer Japan, 2007, pp. 221-230.

[6] H. Choset, “Coverage of Known Spaces: The Boustrophedon Cellular Decomposition”, Autonomous Robots vol. 9, 2000, pp.247-253.

[7] R. Mannadiar and I. Rekleitis, “Optimal coverage of a known arbitrary environment”, IEEE International Conference on Robotics and Automation (ICRA), 2010, pp. 5525 -5530.

[8] W. Huang, “Optimal line-sweep-based decompositions for coverage algorithms”, IEEE International Conference on Robotics and Automation (ICRA) vol.1, 2001, pp. 27 - 32.

[9] S. Hert and S. Tiwari and V. Lumelsky, “A terrain-covering algorithm for an AUV”, Autonomous Robots vol.3, 1996, pp.91-119.

[10] V. Lumelsky and S. Mukhopadhyay and K. Sun, “Dynamic path planning in sensor-based terrain acquisition”, IEEE Transactions on Robotics and Automation 6(4), 1990, pp.462 -472.

[11] Y. Gabriely and E. Rimon, “Spanning-tree based coverage of continuous areas by a mobile robot”, Annals of Mathematics and Artificial Intelligence vol. 31, 2001, pp.77-98.

[12] P. J. Jones, “Cooperative area surveillance strategies using multiple unmanned systems”, PhD thesis, Georgia Institute of Technology, 2009.

[13] M. Weiss-Cohen and I. Sirotin and E. Rave, “Lawn Mowing System for Known Areas”, International Conference on Computational Intelligence for Modelling Control Automation, 2008, pp. 539 -544.

[14] A. Zelinsky and R. Jarvis and J. C. Byrne and S. Yuta, “Planning Paths of Complete Coverage of an Unstructured Environment by a Mobile Robot”, International Conference on Advanced Robotics, 1993, pp. 533—538

[15] A. Barrientos and J. Colorado and J. del Cerro and A. Martinez and C. Rossi and D. Sanz and J. Valente, “Aerial remote sensing in agriculture: A practical approach to area coverage and path planning for fleets of mini aerial robots”, J. Field Robot. 28(5), 2011, pp. 667--689.

[16] R. De Carvalho and H. Vidal and P. Vieira and M. Ribeiro, “Complete coverage path planning and guidance for cleaning robots”, ' IEEE International Symposium on Industrial Electronics, 1997. ISIE 97, vol. 2, pp. 677 -682.

[17] Y.-H. Choi and T.-K. Lee and S.-H. Baek and S.-Y. Oh, “Online complete coverage path planning for mobile robots based on linked spiral paths using constrained inverse distance transform”, IEEE/RSJ International Conference on Intelligent Robots and Systems, 2009. IROS 2009, pp. 5788 - 5793.

[18] J. W. Kang and and S. J. Kim and M. J. Chung and H. Myung and J.H. Park and S. W. Bang, “Path Planning for Complete and Efficient Coverage Operation of Mobile Robots”, International Conference on Mechatronics and Automation, 2007. ICMA 2007', pp. 2126 -2131.

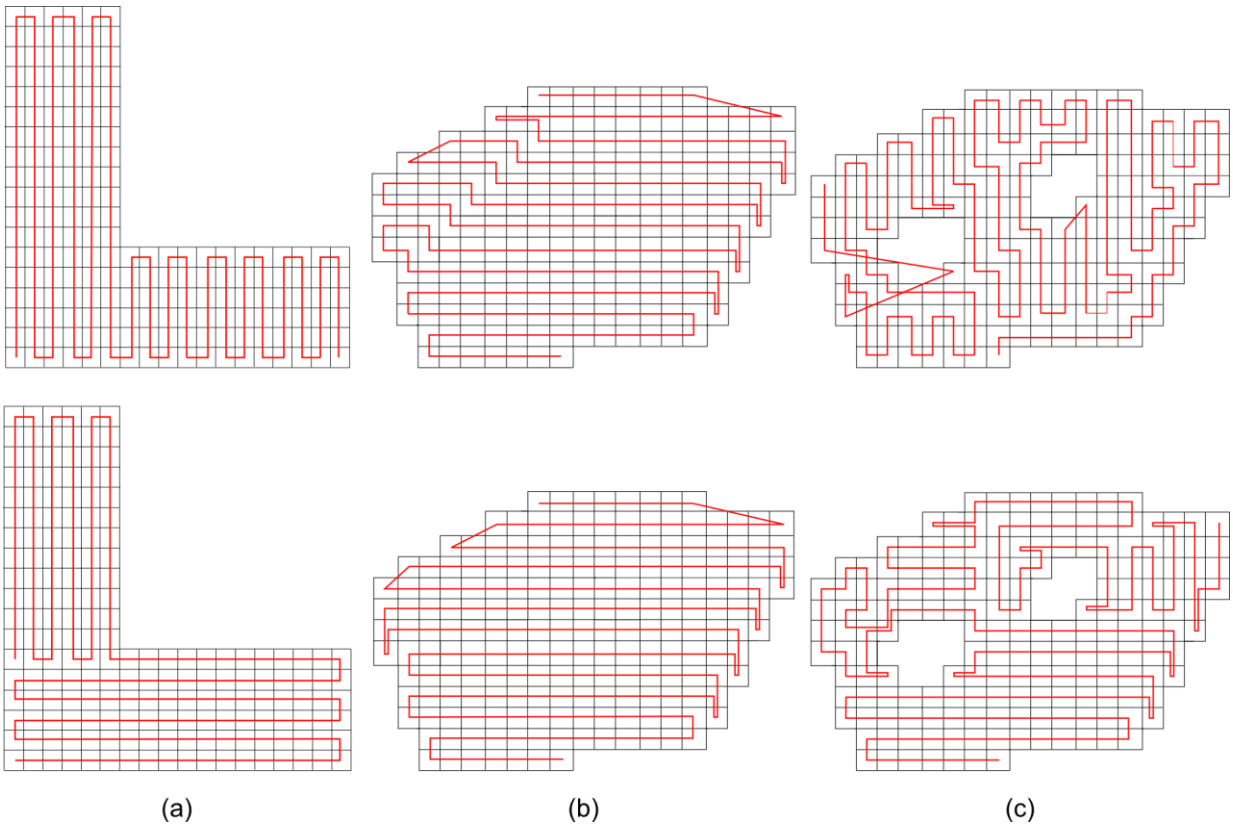

Figure 7 Complete coverage path generated for some example contours with both original (top) and strides based algorithm (bottom). In figure c the transitions between non-adjacent cells are also included.

 ISBN: 978-1-61208-246-2

Autonomous Disaster Information System for Local Residents

A Preparation to the Earthquake Disaster of the Metropolitan Area

Yuichi Takahashi
System Development Group
foreach ltd.
Tokyo, Japan
e-mail: yt@4each.biz

Sakae Yamamoto
Department of Management Science
Tokyo University of Science
Tokyo, Japan
e-mail: sakae@ms.kagu.tus.ac.jp

***Abstract*— It has been pointed out that when people lack the information needed in the event of a disaster, such as a disastrous earthquake, this could lead to social chaos, including unwanted rumors and outrages, or could disrupt rescue and relief activities. In Japan, by law in principle, self-help or mutual assistance is required immediately after a disaster, and local residents are required to make judgments for action on their own. In our prior study, we established and evaluated a service infrastructure with an autonomous wireless network, aiming at providing services to collect and deliver disaster information, which will be required by local residents. The system consists of many small sub systems. These sub systems are robust for collecting disaster information because they are small and simple. An authorized user can register information using one of the sub systems that is working correctly. Asynchronously, they search another sub system via wireless network, and then they communicate to each other in order to exchange information they have. As a result, the information will be shared within a wide area by those processes like a bucket brigade. In this study, we improved and extended the system so that it may meet more nearly actually.**

Keywords-earthquake; disaster victims; distributed autonomous system; wireless network

I. INTRODUCTION

In the event of a disaster, such as a disastrous earthquake, information provision is effective in preventing chaos at the scene. Therefore, timely and accurate information collection and delivery services are essential [3][4].

In Japan, by law in principle, self-help or mutual assistance is required immediately after a disaster, and local residents are required to make judgments for action on their own. Although disaster information systems are gradually being organized at the municipal level, actual emergency evacuation areas and essential information for local citizens are still not sufficiently ready for provision at this stage [5]. These services allow prompt rescue and relief activities and appropriate information delivery to local residents. Thus, it is urgent to establish a system to enable these services. The systems proposed so far are ones with Internet or mobile phone connections or with ad-hoc wireless LAN networks [6][7]. We call such systems communication channel dependent systems, which require communication channels or establish communication channels between clients and servers via an ad-hoc network. From the perspective of an information service, such systems that accumulate information in PDAs and send it via an ad-hoc network when a communication channel is established are also regarded as communication channel dependent systems.

There are two issues of concern regarding this system: 1) the system is not available until a communication channel is established, and 2) as users access the server to gain information, the intense access may lower server performance or cause communication channel congestion. In prior study, we would like to propose an approach to resolve these issues. As it is difficult to generalize the situations of earthquake disasters, we set the following assumptions: (a) assuming a strong earthquake of approximate magnitude 7 in a residential area, (b) all the lifelines including electricity and communication channels stopped functioning, (c) lines for land phones and mobiles are congested and not working, and (d) the proposed system (hereafter called "the system") can be preliminarily placed.

II. METHOD

In order to resolve the above issues, we placed servers, which store information, closed to users in prior study [1][2]. By doing this, the system can run without a communication channel established, and the service can be continuously provided even with a narrow bandwidth. Since disaster information system users, such as local residents, shelter authorities, rescue and relief crews, and municipal employees are diverse and geographically dispersed, multiple servers are required to meet the condition in which servers must be placed close to users. Each server must hold information and be synchronized with each other. Also, they must independently run, communicate with each other, and dynamically detect others in case some are damaged in a disaster.

The service infrastructure consists of many small sub-systems. Each of these systems independently provides information collection and delivery services. Also, these sub-systems can autonomously work together with other sub-systems to exchange information. By appropriately allocating sub-systems within a region, regional information is continuously shared, which can solve the issue of information shortages in a disaster. We adopted general

 ISBN: 978-1-61208-246-2

consumer hardware products that are supposed to work approximately 72 hours with batteries. Though each hardware product itself is not robust, they are all independent so even if some of them are damaged, they do not affect others. Also, as it is allowed to dynamically add sub-systems, damaged ones can be easily replaced to immediately recover the entire service.

The network configuration of this system is illustrated in Figure 1. The system is formed by a group of small servers (hereafter called nodes) with server abilities and dynamic communication functions. Each node can function as a web server and allows clients (e.g. PCs and PDA) to connect to register or browse information. Nodes also detect others within the communication range to synchronize information. With these functions, the system can still work as an integrated unit even when part of the hardware is damaged in a disaster. Figure 2 illustrates the hardware configuration of the nodes. We selected only devices that can function approximately 72 hours with either dry-cell or rechargeable batteries. In addition, dedicated PCs can be equipped with server functions for information entries. This means that users can initiate the registration of information even if no communication channels are established.

However, in previous studies, there were still some issues such as:

a) The synchronization of the information was often delayed,

b) The distance between nodes with a vertical interval which can be communicated is short.

This study improves the following points:

a) Improvement of the node detection logic and the information synchronizing logic,

b) Using two types (vertical no directivity and horizontal directivity, wide directivity) of anntena in order to be fit to our target area.

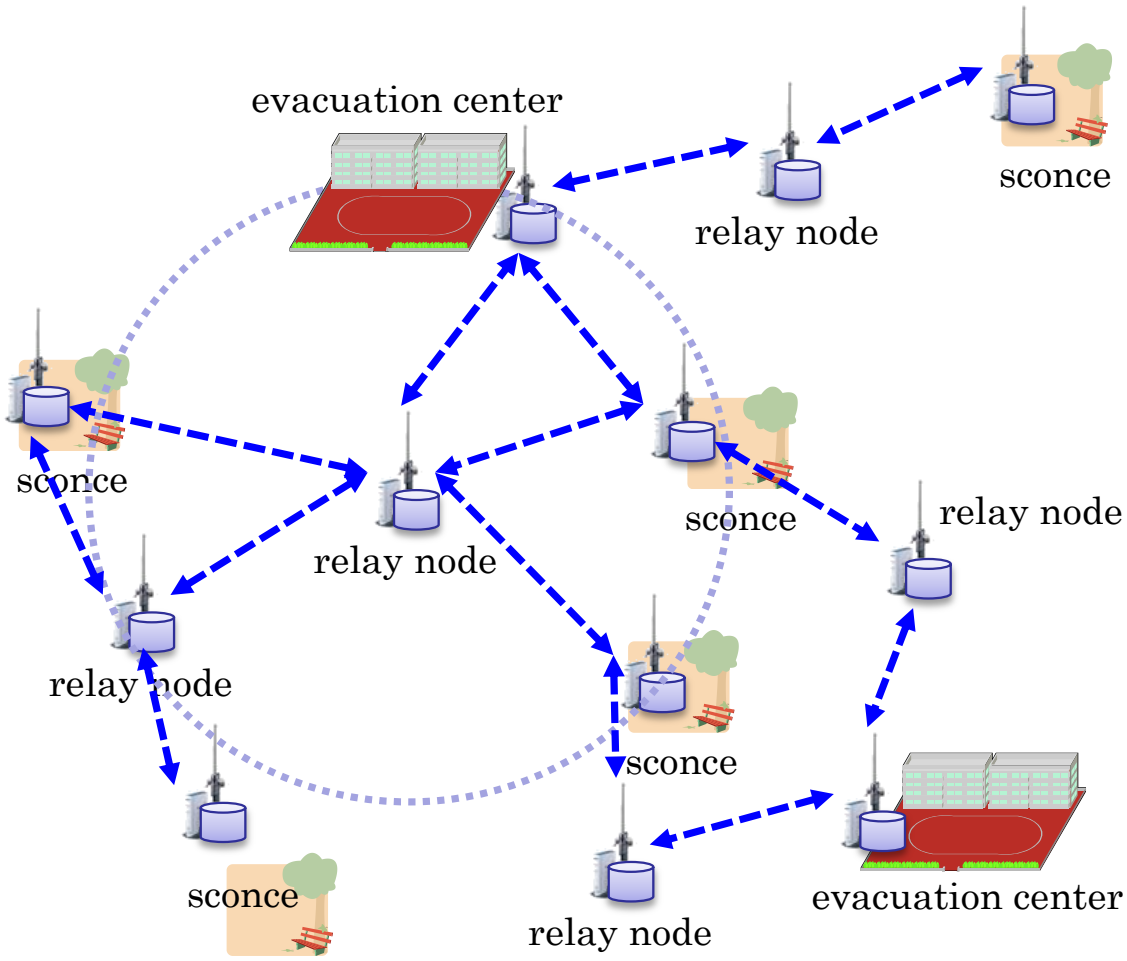

Figure 1 Whole image of the system: all nodes search another sub system, and then they communicate to each other in order to exchange information they had.

 ISBN: 978-1-61208-246-2

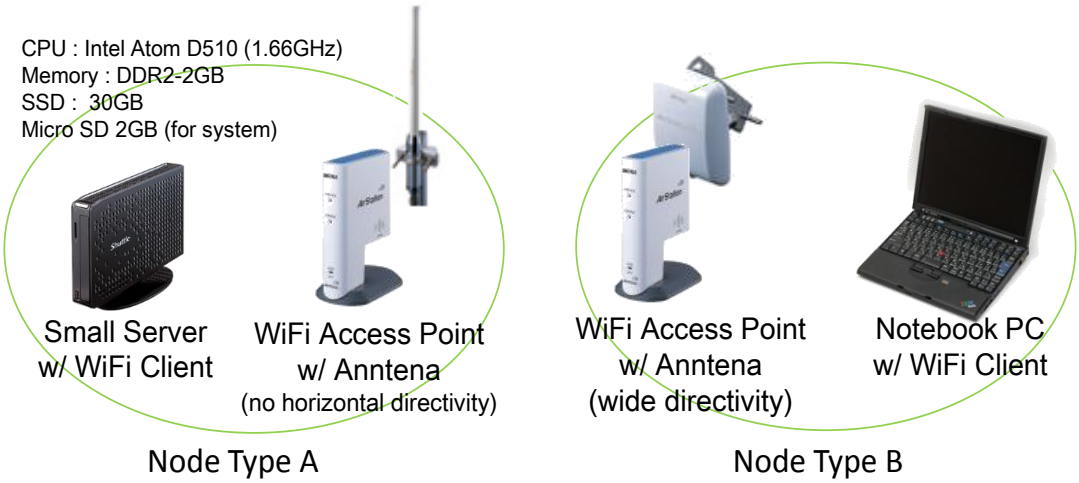

Figure 2 Elements of the nodes

III. RESULT

By the first improvement, the delay in the synchronization of the information was decreased.

A. *Node Detection Method*

Each node executes the following procedures by a timer process in every minute.

1. The node scans APs (: Access Points) in range, and makes a list of available APs. Then the node selects a suitable AP (: Access Point) using an ESSID filter pattern and the connection history list.
2. The node connects to the selected AP. Then a server connected to the AP via Ethernet, gives IP address to the Wi-Fi client of the node (Figure 3).
3. The node calculates the IP address of the server from the given address of Wi-Fi client. Then the node executes synchronization program with the server.
4. The node disconnects from the AP, after the synchronization program finished.

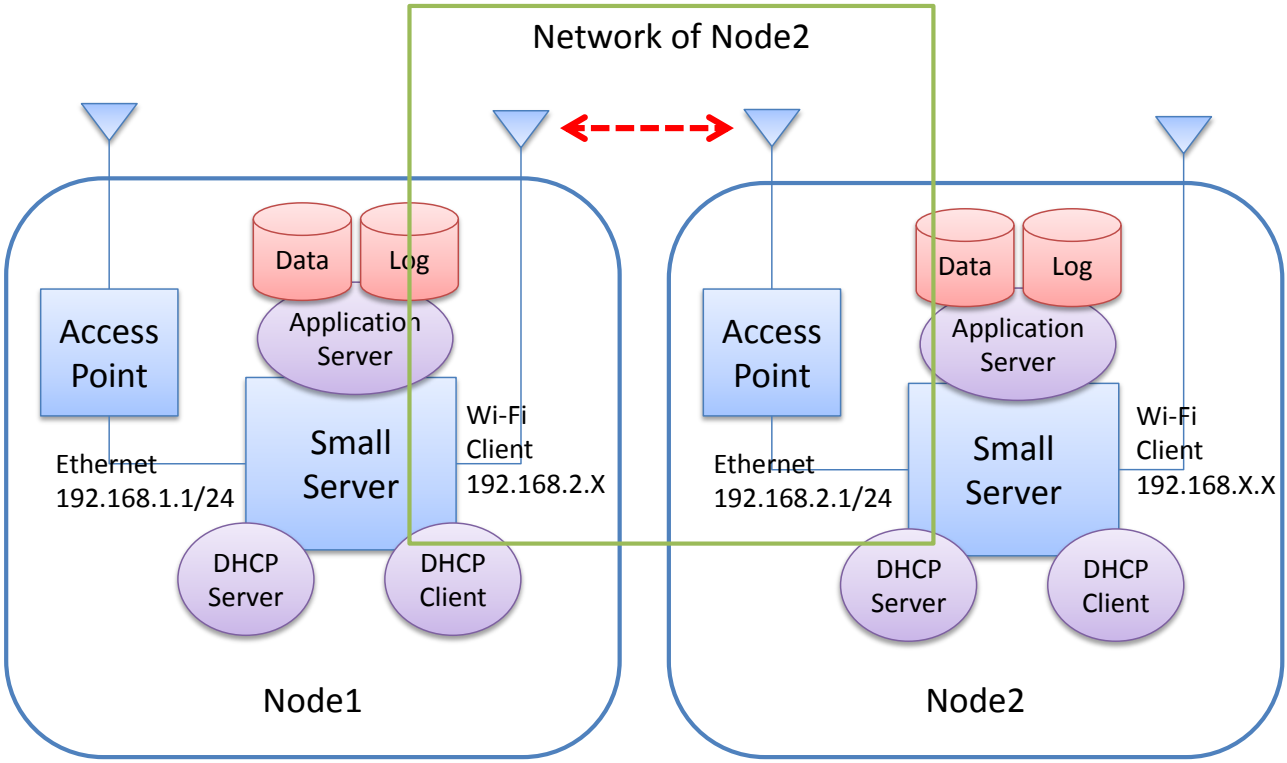

Figure 3 Network between the nodes

 ISBN: 978-1-61208-246-2

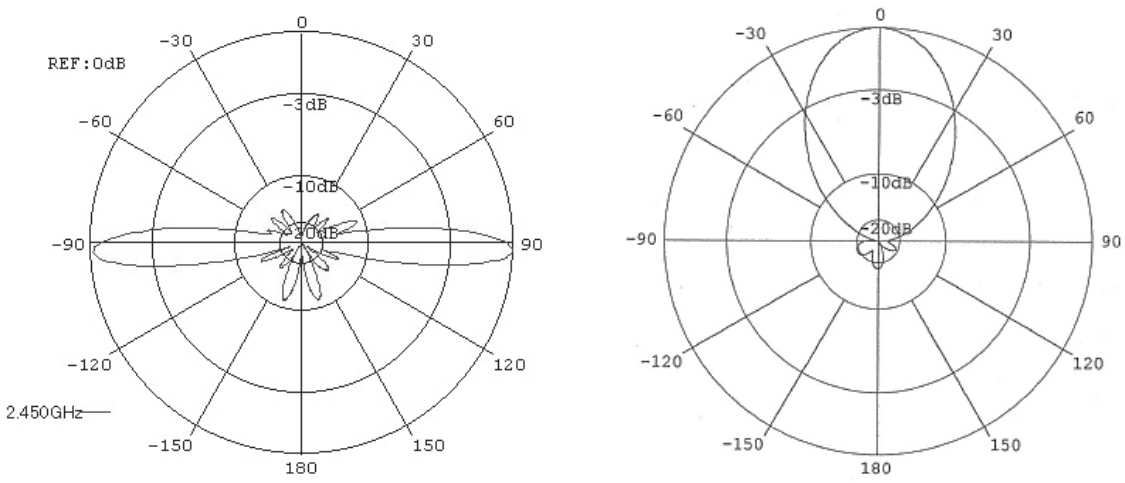

Figure 4 Vertical no directivity and horizontal directivity, wide directivity

B. Data Synchronization Method

Applications on the server such as registration of someone's safety, update the database table using special driver. The driver updates both of data and log tables. The log table contains node id, sequence number, operation type (create/update/delete), table name, update time and the data. Synchronization process is a client server model. The client makes list of the holding data as array of the range of the sequence numbers and the node name. Then the client sends the list to the server. The server finds and sends back the data that the client doesn't have. The server executes same process as the client, if the list sent by the client contains entries the server doesn't hold. While this process is executing, the client becomes a server.

By the second improvement, the system will become the form of being suitable for use in actual evacuation areas. Moreover, in a simulation, it carries out as a result for the layout planning of nodes, by using three-dimensional (instead of two-dimensional) geography data and taking the characteristic of antennas (Figure 4) into consideration.

IV. CONCLUSION

By those improvements, the system will be more practical. At present, the functions are well working in the field. However, only four nodes were evaluated at actual evacuation area. In order to deploy the system for real disaster, evaluations are needed with more nodes at wider actual evacuation area.

REFERENCES

[1] Y. Takahashi, D. Kobayashi, S. Yamamoto, "Disaster Information Collecting/Providing Service for Local Residents", In Proceedings of the 1st international conference on Human interface and the management of information: interacting with information - Volume Part II (HCII'11), Gavriel Salvendy and Michael J. Smith (Eds.), Vol. Part II. Springer-Verlag, Berlin, Heidelberg, 2011, pp.411-418.

[2] Y. Takahashi, D. Kobayashi, S. Yamamoto. "A Development of Information System for Disaster Victims with Autonomous Wireless Network". In Proceedings of the Symposium on Human Interface 2009 on Human Interface and the Management of Information. Information and Interaction. Part II: Held as part of HCI International 2009, Gavriel Salvendy and Michael J. Smith (Eds.). Springer-Verlag, Berlin, Heidelberg, 2009, pp. 855-864.

[3] O. Hiroi, et.al, Disaster information and social psychology, Hokuju Shuppan, Tokyo, 2004, p.177

[4] O. Hiroi, et al, Hanshin-Awaji (Kobe) Earthquake investigation report in 1995-1, Institute of Socio-Information and Communication Studies, the University of Tokyo, 1996

[5] S. Yamamoto, The Providing Disaster Information Services in Ubiquitous Days, Journal of the Society of Instrument and Control Engineers, vol.47, no.2, 2008, pp.125-131

[6] N. Fukuwa, H. Takai, J. Hida, Intercommunications system "AnSHIn-system" and mobile disaster information unit "AnSHIn-Kun", AIJ J. Technol. Des. No.12, 2001, pp.227-232

[7] Y. Takahashi, Y. Owada, H. Okada, and K. Mase, "A wireless mesh network testbed in rural mountain areas," The Second ACM International Workshop on Wireless Network Testbeds, Experimental Evaluation and Characterization, 2007, pp.91-92

 ISBN: 978-1-61208-246-2

Security Audit Trail Analysis Using Harmony Search Algorithm

Mourad Daoudi
Faculty of Electronics and Computer Science, Laboratory LSI, USTHB
BP 32 16111 El Alia, Bab-Ezzouar,
Algiers, Algeria
m-daoudi@usthb.dz

***Abstract*—Security Audit trail Analysis can be accomplished by searching audit trail logs of user activities for known attacks. The problem is a combinatorial optimization problem NP-Hard. Metaheuristics offer an alternative to solve this type of problems. In this paper, we propose to use Harmony Search metaheuristic as intrusion detection engine. It is a population-based evolutionary algorithm well suited for constrained optimization problems. Experimental results for simulated attacks are reported. The effectiveness of the method is evaluated by its ability to make correct predictions. Our new approach has proven effective and capable of producing a reliable method for intrusion detection.**

Keywords-metaheuristics; harmony search; evolutionary Algorithm; intrusion detection; security audit.

I. INTRODUCTION

Intrusion Detection System (IDS) is one of the primary approaches to the crucial problem of computer security in order to preserve the confidentiality, integrity and availability of data stored in computers [1], [2].The study of effective methods for intrusion detection by audit file analysis is an important part of the vast effort to improve the security of computer systems. Different methods, like Neural Networks, Immune Systems, and Genetic Algorithms have been developed. Intrusion detection by security audit trail analysis can be performed by searching audit trail logs of user activities for predefined attacks. Because the problem is a combinatorial optimization problem NP-Hard [3], heuristic methods will need to be used as data bases of events and attacks grow.

This paper presents a method to perform misuse detection using Harmony Search metaheuristic (HS) [4], under the guidelines of previous works [5]-[10].

Harmony Search algorithm is a population-based evolutionary algorithm taking inspiration from the music improvisation process, where musicians improvise their instruments' pitches searching for a perfect state of harmony. It has proven its abilities in solving various optimization problems [11], [12]. We define HS as an intrusion detection engine, and then evaluate its performances.

The rest of the paper is as follows: Section 2 outlines intrusion detection systems. A formalization of security audit trail analysis problem as a combinatorial optimization problem is given in Section 3. HS metaheuristic is presented in Section 4. Our contribution using HS for misuse detection is presented in Section 5. Experimental results are reported in Section 6. Comparisons with a biogeography inspired intrusion detection approach are performed and experimental results are presented in Section 7. Our conclusions are given in Section 8.

II. INTRUSION DETECTION SYSTEM

An intrusion is defined as a series of actions that attempt to compromise the integrity, confidentiality or availability, or to bypass the security mechanisms of a computer or network. Any operation undertaken on the computer system results in a sequence of actions performed by the system called system activities. A system activity occurring at a point of time is called event. These events are recorded chronologically in a log file.

Intrusion Detection Systems usually process log records received from the operating system for a specific period of time in order to have a complete set of user activity and then perform analysis of the current activity [13],[14]. According to Intrusion Detection Working Group of IETF [15], IDSs include three vital functional elements: information source, analysis engine and response component. Five concepts are defined for their classification: the detection method, the behavior on detection, the audit source location, the detection paradigm and the usage frequency. The detection method is one of the principal characters of classification. When the IDS uses information about the normal behavior of the system it monitors (anomaly detection or behavioral approach), we qualify it as behavior-based. When the IDS uses information about the attacks (misuse detection or scenario approach), we qualify it as knowledge-based. However, both approaches may be complementary [16].

The behavioral approach was first proposed approach, introduced by Anderson [17], and extended by Denning[18]. It is to define a profile of normal activity of a user, and consider the significant deviations of the current activity of users, compared with normal patterns of behavior, as an anomaly.The techniques developed in behavioral approach include the expert systems, statistical models [19],and artificial immune systems [20], [21]. Other techniques like Bayesian parameter estimation [22] and clustering [23]-[26], Genetic Algorithms[27], [28] are also used.

In Misuse detection, IDS processes log records from the operating system for a specific period of time in order to have a complete set of user activity [19]. Then, the IDS performs analysis of the current activity, using a rule base system, statistics, or a corresponding heuristic, in order to determine the possible occurrence of intrusion. The misuse mechanism uses a predefined matrix of intrusion patterns,

 ISBN: 978-1-61208-246-2

so the system knows in advance the appearance of the misuse and/or abuse.

An intrusion can be specified by an array of activities to check, where each entry specifies the number of activities of a specific type that should occur in order to have an intrusion. Likewise, the results of the user records gathered can be seen as an array, where each entry specifies the total number of activities of that specific type performed by a user. If an intrusion array pattern is such that each entry of it is less or equal than each entry of the user's activity, then, it is possible that intrusion H has occurred. However, looking at some possible intrusions together, it is possible that one or several can occur, but not all together, because adding each corresponding entry, some results could be greater than the corresponding entry of the user activity vector. This is called a violation of the constraint. Neural networks have been extensively used to detect both misuse and anomalous patterns [29]-[31].

We investigate in what follows Security Audit Trail Analysis Problem.We give in the next section the formulization of the problem.

III. SECURITY AUDIT TRAIL ANALYSIS PROBLEM

Formally, the Security Audit Trail Analysis Problem can be expressed by the following statement [5]:

Let:

- N_e the number of type of audit events
- N_a the number of potential known attacks
- AE an N_e x N_a attack-events matrix which gives the set events generated by each attack. $AE_{i\,j}$ is the number of events of type i generated by the attack j ($AEi\,j \geq 0$)
- R a N_a-dimensional weight vector, where R_i ($R_i > 0$) is the weight associated with the attack i (R_i is proportional to the inherent risk in attack scenario i)
- O a N_e-dimensional vector, where O_i is the number of events of type i present in the audit trail (O is the observed audit vector)
- H a N_a-dimensional hypothesis vector, where H_i = 1 if attack i is present according to the hypothesis and H_j= 0 otherwise (H describes a particular attack subset).

To explain the data contained in the audit trail (i.e. O) by the occurrence of one or more attacks, we have to find the H vector which maximizes the product RxH (it is the pessimistic approach: finding H so that the risk is the greatest), subject to the constraint $(AE.H)_i \leq O_i$, $1 \leq i \leq N_e$ (Fig. 1).

Because finding H vector is NP-Complete, the application of classical algorithm is impossible where N_a equals to several hundreds.

The heuristic approach that we have chosen to solve that NP-complete problem is the following: a hypothesis is made (e.g. among the set of possible attacks, attacks i, j and k are present in the trail), the realism of the hypothesis is evaluated and, according to this evaluation, an improved hypothesis is tried, until a solution is found.

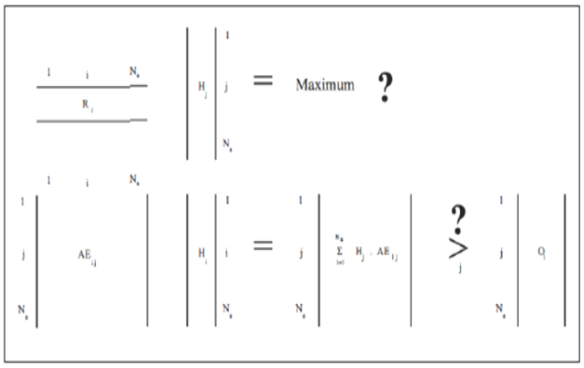

Figure 1. Security Audit Trail Analysis Problem.

In order to evaluate a hypothesis corresponding to a particular subset of present attack, we count the occurrence of events of each type generated by all the attacks of the hypothesis. If these numbers are less than or equal to the number of events recorded in the trail, then the hypothesis is realistic.

To derive a new hypothesis based on the past hypothesis,we propose to use HS algorithm we present in the next section.

IV. HARMONY SEARCH METAHEURISTIC - AN OVERVIEW

Harmony Search was devised as a new metaheuristic algorithm, taking inspiration from the music improvisation process, where musicians improvise their instruments' pitches searching for a perfect state of harmony. Analogies with optimization process are such that:

- Instrument i ↔ Decision variable x_i , i ϵ{1,2,…,n}
- Music note from instrument i ↔Value of variable x_i
- Harmony ↔ Solution vector
- Musical easthetic ↔ Fitness

The HS metaheuristic algorithm consists of the following steps [12]:

A. *Initialization of the Optimization Problem and Algorithm Parameters*

In the first step, the optimization problem is specified as follows:

Minimize (or Maximize) f(x)
subjected to $x_i \in X_i$, i= 1, 2, . . .,n.

where f(.) is a scalar objective function to be optimized; x is a solution vector composed of decision variables x_i, i= 1, 2, . . ., n; X_i is the set of possible range of valuesfor each decision variable x_i , that is, ${}_Lx_i \leq X_i \leq {}_Ux_i$, where ${}_Lx_i$ and ${}_Ux_i$ are the lower and upper bounds for each decision variable in the case of continuous decision variables and $x_i \in \{x_i(1), \ldots, x_i(k), \ldots, x_i(K)\}$, when the decision variables are discrete. N is the number of decision variables.

In addition, the control parameters of HS are also specified in this step. These parameters are the Harmony

Memory Size (HMS) i.e., the number ofsolution vectors (population members) in the HM (in each generation); the HM considering rate (HMCR); the pitch-adjusting rate (PAR) and the number ofimprovisations (NI) or stopping criterion.

B. Harmony Memory Initialization

In this step, each component of each solution vector in the parental population (HM) is randomly chosen. Then, obtained solutions are reorderedin terms of the objective function value:f $(x^1) \leq f(x^2) \ldots \leq f(x^i) \ldots \leq f(x^{HMS})$, where $x^i = (x_1^i, x_2^i, \ldots, x_n^i)$ is the ith solution vector.

Harmony Memory is represented by the following matrix:

$$HM = \begin{bmatrix} x_1^1 & x_2^1 \ldots & \ldots & x_n^1 \\ x_1^2 & x_2^2 \ldots & \ldots & x_n^2 \\ \vdots & \ldots & \ldots & \ldots \\ x_1^{HMS} & x_2^{HMS} & \ldots & x_n^{HMS} \end{bmatrix}$$

C. New Harmony Improvisation

In this step, anew harmony vector $x' = (x_1', x_2', \ldots, x_n')$ is generated based on three rules: memory consideration; pitch adjustment and random selection. Generating a new harmony is called 'improvisation'.

The memory consideration rule stipulates that the decision variable x_i, i= 1…n, takes a new value $x_i'$from HM matrix (in the set $\{x_i^1, x_i^2, \ldots, x_i^{HMS}\}$), with a probability HMCR (parameter value between 0 and 1), and takes a fresh value randomly selected from the set Xi with probability (1-HMCR). This rule can be summarized in equation (1).

$$x_i' \leftarrow \begin{cases} x_i' \in (x_i^1, x_i^2, \ldots, x_i^{HMS}) \text{with probability HMCR} \\ x_i' \in Xi \quad \text{with probability } (1 - HMCR) \end{cases} \quad (1)$$

Every component obtained in the memory consideration step is further examined to determine whether it should be pitch adjusted. This operation uses the parameter PAR (pitch adjustment rate) as follows:

- In the case of discrete variables:$x_i' = x_i(k)$

$$x_i \leftarrow \begin{cases} xi(k+m) & \text{with probability PAR} \\ x_i & \text{with probability } (1 - PAR) \end{cases} \quad (2)$$

where : m∈ {-1, 1}.

- In the case of continuous variables:

$$x_i \leftarrow \begin{cases} x_i \pm \text{rand}(0\ 1) * bw \text{ with probability PAR} \\ x_i \quad \text{with probability } (1 - PAR) \end{cases} \quad (3)$$

where bw is an arbitrary distance bandwidth (a scalar number), and rand() is a uniformly distributed random number between 0 and 1. Evidently, the new harmony improvisation strategy is responsible for generating new potential variation in the algorithm and is comparable to mutation in standard evolutionary algorithms.

D. Harmony Memory update

If the new harmony vector $x' = (x_1', x_2', \ldots, x_N')$ is better than the worst harmony in the HM, judged in terms of the objective function value, the new harmony is included in the HM, and the existing worst harmony is excluded from the HM. This is actually the selection step of the algorithm, where the objective function value is evaluated to determine if the new variation should be included in the population (HM).

E. Check Stopping Criterion

If the stopping criterion (maximum NI) is satisfied, the computation is terminated. Otherwise, steps *C* and *D* are repeated.

V. HARMONY SEARCH-BASED SECURITY AUDIT TRAIL ANALYSIS

The approach aims to determine if the events generated by a user correspond to known attacks, and to search in the audit trail file for the occurrence of attacks by using a heuristic method (HS algorithm) because this search is an NP–complete problem. The goal of the heuristic used is to find the hypothesized vector H that maximizes the product R*H, subject to the constraint $(AE.H)_i \leq O_i$,$1 \leq i \leq N_e$, whereR is a weight vector that reflects the priorities of the security manager, AE is the attack-events matrix that correlates sets of events with known attacks, and N_e the number of types of audit events.

HS method is based on a stochastic optimization process and on the musical performance process of finding the perfect harmony in a musical orchestra where each musician plays a note to find a better harmony. We are in a situation where the coding of harmonies is immediate since the solution of the problem is expressed specifically in the form of a binary sequence. A Harmony is considered as a series of N_a notes with values 0 or 1.The Harmony Memory matrix is thus a matrix of dimension HMS x N_a.Each harmony (that is a line vector in HM matrix) is a particular instance of the vector H. In other words, the note i in the harmony will be 1if the harmony is a solution in which the attack i is declared present. Otherwise, this note takes the value 0. We note that the sum of the component elements in a harmony indicates the number of attacks that are detected.

The HS method should return a binary N_a –vector H = $(H_1, \ldots, H_{Na})$, where the value H_i=1 in the ith position indicates the presence of the attack I in the audit file O and 0 its absence. As we have to solve a maximization problem, the best solution is associated with the hypothesis H of larger value of the selective function

$$F(H) = R^* H = \sum_1^{N_a} R_j * H_j \quad (4)$$

which represents the total risks incurred by the system under surveillance. In addition, as we deal with a constrained problem, any solution to the problem must verify the inequalities: $(AE \times H)_I \leq O_i$ avec $0<i<n_e$. Thus, we have to eliminate the solutions that do not comply, setting to zero the value of the corresponding objective function (that is a

 ISBN: 978-1-61208-246-2

harmony in which each note has a zero value). There combination process is repeated until a solution satisfying the constraints is generated. Recall that R_i is the weight of the attack i, that is the risk incurred to the system if the attack is not detected. For simplicity, the R_i value is taken equal to 1 for all i, i=1 … N_a. In this case, the objective function F resumes in computing the number of detected attacks.

It is now necessary to correctly represent the matrix HM. It is a ($HMS*N_a$) - matrix, where N_a is the number of predefined attacks and HMS the population size parameter. We associate to each row i of the matrix HM (a solution vector to our problem) a value of the objective function F. The different parameters HMS, HMCR, PAR and NI must be initialized. Then, HMS initial solution vectors are randomly generated and saved in the HM matrix. The fitness value F(i), corresponding to the ith solution i = 1…HMS, is evaluated. Then, the optimization process evolves. It generates a new solution $x = (x_1, ...,x_n)$ from the HM matrix, using the parameters HMCR and PAR. These parameters help the algorithm to obtain better solutions locally or globally.

VI. EXPERIMENTATION RESULTS

During the simulations, all the attacks actually present in the analyzed audit file must be known in advance. Thus, the events corresponding to one or more attacks are included in the observed audit vector O. Each of the experiments conducted is characterized by the 5-tuple (NI, HMS, HMCR, PAR, Ia), where NI is the number of generations, HMS the population size, HMCR the harmony memory consideration rate, PAR the adjustment rate and Ia the number of attacks actually present in the audit file (number of attacks injected).

Ratios TPR, FPR, Accuracy and Precision [32] are used to evaluate our approach intrusion detection quality, with:

- TPR (True positive rate): TP / (TP+FN)
- FPR (False positive rate): FP / (TN+FP)
- Accuracy: (TN+TP) / (TN+TP+FN+FP)
- Precision: TP / (TP+FP)
-

where True negatives (TN) as well as true positives (TP) correspond to correct intrusion detection: that is, events are successfully labeled as normal and attacks, respectively. False positives (FP) refer to normal events being predicted as attacks; false negatives (FN) are attack events incorrectly predicted as normal events.

To evaluate our approach, many tests were performed using Attack-Events matrices of different sizes. All results are obtained as the average of 10 executions carried out for the same better value of the 5-tuple (NI, HMS, HMCR, PAR, I_a).

We observe that after a certain number of generations, all injected attacks are detected, and no false attack (TPR= 1 and FPR =0). In addition, the number of attacks injected has no influence on these results. Best results are obtained with HMS value between 20 and 30. Further, the study of the influence of the two rates HMCR and PAR is important because they contribute significantly in the algorithm in finding the best solution. There is a strong correlation between HMCR and PAR on the Harmony Search metaheuristic optimization process [33]. To study their influence on the quality of intrusion detection, we varied the parameter PAR between 0.1 and 0.9 with a step of 0.2; HMCR is selected it in the set {0, 0.3, 0.5,0.7, 0.9,0.98}. We observe that the best results are obtained for values of HMCR and PAR, such as: 0.8≤ HMCR≤0.98 and PAR≥0.3.

Reported results concern tests performed on an attack-events matrix of size (28x24) issued from [5] and on larger data randomly generated (AE-matrices of larger size). Table I and Table II show the quality of our intrusion detection approach.

Data considered in Table I, are issued from [5], and use an attack-events matrix of size 28x24, with 24 attacks and 28 types of events. The HS parameters values are: HMS = 30,HMCR= 0.98, PAR =0.3, and 24 attacks are injected. We observe that all attacks are detected after 0.056 seconds (TPR=100% and FPR=0).

The results given in Table II concern tests performed on data with an attack-events matrix of size (100x200). The different parameters are such that: HMS = 30,HMCR= 0.98, PAR =0.3. The number of injected attacks is200.

TABLE I. INTRUSION DETECTION QUALITY (28x24)

Generation number (NI)	Execution time (sec)	TPR %	FPR %	Exactitude %	Precision %
1	0.002	66.67	0	66.67	100
5	0.003	70.83	0	70.83	100
50	0.020	83.83	0	83.83	100
100	0.037	91.67	0	91.67	100
200	**0.056**	**100**	**0**	**100**	**100**
220	0.064	100	0	100	100
250	0.077	100	0	100	100

TABLE II. INTRUSION DETECTION QUALITY (100x200)

Generation number (NI)	Execution time (sec)	TPR %	FPR %	Exactitude %	Precision %
0	0.010	57	0	78.3	100
50	0.030	66	0	83	100
100	0.043	71	0	85.5	100
200	0.075	82	0	91	100
400	0.135	94	0	97	100
500	0.165	97	0	98.5	100
600	0.196	99	0	99.5	100
700	**0.225**	**100**	**0**	**100**	**100**
750	0.238	100	0	100	100
800	0 .251	100	0	100	100

All attacks are detected after 0.225 seconds (TPR=100% and FPR=0).

The results indeed show the good performance of the proposed approach. An important result was the consistency of results, independently of the number of attacks actually present in the analyzed audit file. This means that the performance of the detection system is not deteriorated in

 ISBN: 978-1-61208-246-2

the case of multipleattacks. The execution time is very satisfying.

An intrusion detection approach based on security audit trail analysis usinga "Biogeography Based Optimization" algorithm (BBO) has been developed [9], [10]. It showed good performances. Comparisons with our new method are made.

VII. COMPARISONS WITH A BIOGEOGRAPHY INSPIRED INTRUSION DETECTION APPROACH

Biogeography-based optimization (BBO) was first presented by D. Simon in 2008 [34]. In BBO, problem solutions are represented as islands, and the sharing of features between solutions is represented as migration between islands. Islands that are well suited as habitats for biological species are said to have a high island suitability index (ISI). Features that correlate with ISI include rainfall, topographic diversity, area, temperature, etc. The variables that characterize these features are called suitability index variables (SIVs). SIVs are the independent variables of the island, and ISI is the dependent variable. Islands with a high ISI tend to have a large number of species, and those with a low ISI have a small number of species. Islands with a high ISI have many species that emigrate to nearby islands because of the accumulation of random effects on its large populations. Emigration occurs as animals ride flotsam, fly, or swim to neighboring islands. Suppose that we have some problem, and that we also have several candidate solutions. A good solution is analogous to an island with a high ISI, and a poor solution is like an island with a low ISI. High ISI solutions are more likely to share their features with other solutions, and low ISI solutions are more likely to accept shared features from other solutions. An intrusion detection approach with BBO has been developed [9]. We compare the latter with our new method. Several tests are performed on different data using the same machine.

The results reported in Table III concern:

- a (28x24) - Attack-Events matrix (noted T1) issued from [5] with NA=24 attacks injected,
- a (100x300)- Attack-Events matrix (noted T2) with NA=300 attacks injected

a (100x700) - Attack-Events matrix (noted T3) with 700 attacks injected.

ET represents the execution time in seconds.

TABLE III. HS vs. BBO-BASED APPROACH

	T1		**T2**		**T3**	
	NA	ET	NA	ET	NA	ET
BBO	24	0.109	300	9.040	700	498
HS	24	**0.056**	300	**3.773**	700	**7.125**

The different parameters involved in BBO algorithm are set to: Mutation rate = 0.005, Population size = 50 and Elitism value = 2. In our HS based method, the parameters values are: HMS = 30,HMCR= 0.98 andPAR =0.3.

In both approaches, all attacks are detected. However, we clearly observe that the intrusion detection process duration for all attacks is better using our new approach, and the difference increases as the AE matrix size grows.

VIII. CONCLUSION

Security Audit trail Analysis can be accomplished by searching audit trail logs of user activities for known attacks. The problem is a combinatorial optimization problem NP-Hard. Metaheuristics offer an alternative for solving this type of problem when the size of the database events and attacks grow. We proposed to use Harmony Search metaheuristic as detection engine.

Experimental results of simulated intrusions detection are given. The effectiveness of the approach is evaluated by its ability to make correct predictions. It proved to be effective and capable of producing a reliable method for intrusion detection. The results indeed show the good performance of the proposed approach. An important result was the consistency of results, independently of the number of attacks actually present in the analyzed audit file. This means that the performance of the detection system is not deteriorated in the case of multiple attacks. The execution time is very satisfying. All this allows us to consider that the proposed approach constitutes an efficient and reliable intrusion detection system. Comparisons with a biogeography inspired approach is made. We observe clearly that the intrusion detection duration of all attacks is significantly lower when using our new HS-based approach. However, these systems are usually developed for predefined environments and do not offer a solution to some network characteristics such as changes in behavior of users and services, the increasing complexity and evolution of the types of attacks that they may be subject, the speed of attacks that can occur simultaneously on several machines, etc.

REFERENCES

[1] E. Cole, R. K. Krutz, and J. Conley, Network security bible, Wiley Publishing, 2005.

[2] B. C. Tjaden, Fundamentals of secure computer systems. Franklin and Beedle & Associates, 2004.

[3] L. Mé, Audit de sécurité par algorithmes génétiques. Thèse de Doctorat de l'Institut de Formation Supérieure en Informatique et de Communication de Rennes, 1994.

[4] Z.W. Geem, J.H. Kim, and G.V. Loganathan, A new heuristic optimization algorithm: harmony search, Simulation, vol. 76, no. 2, pp. 60-68, 2001.

[5] L. Mé, GASSATA, A genetic algorithm as an alternative tool for security audit trails analysis. Proc. of the 1st International Workshop on the Recent Advances in Intrusion Detection (RAID 98). Louvain-la-Neuve, Belgium, pp. 14–16, 1998.

[6] P. A. Diaz-Gomez, and D. F. Hougen, Improved off-line intrusion detection using a genetic algorithm. Proc. of the seventh International Conference on Enterprise Information Systems, pp. 66-73, 2005.

 ISBN: 978-1-61208-246-2

[7] P. A. Diaz-Gomez, and D. F. Hougen, A genetic algorithm approach for doing misuse detection in audit trail files. Proc. of International Conference on Computing (CIC-2006), pp. 329-335, 2006.

[8] A. Ahmim, N. Ghoualmi, and N. Kahya, Improved off-line intrusion detection using a genetic algorithm and RMI. Proc. of the International Journal of Advanced Computer Science and Applications (IJACSA), vol. 2, no. 1, 2011.

[9] M. Daoudi, A. Boukra, and M. Ahmed-Nacer, A biogeography inspired approach for security audit trail analysis. Journal of Intelligent Computing, vol. 2, no. 4, December 2011.

[10] M. Daoudi, A. Boukra, and M. Ahmed-Nacer, Security audit trail analysis with biogeography based optimization metaheuristic. Proc. of the International Conference on Informatics Engineering & Information Science: ICIES 2011, A. Abd Manafet al. (Eds.): ICIEIS 2011, Part II, CCIS 252, pp.218–227, 2011.© Springer-Verlag Berlin Heidelberg; 2011.

[11] L. S. Coelho, and D. L. Andrade Bernert, An improved harmony search algorithm for synchronization of discrete time chaotic systems. Industrial and Systems Engineering Program, LAS/PPGEPS, Pontifical Catholic University of Parana PUCPR, Imaculada Conceição, 1155, 80215-901 Curitiba, Paraná, Brazil, 2008.

[12] S.Das, A. Mukhopadhyay, A. Roy, A. Abraham, and B. K. Panigrahi, Exploratory power of theharmony search algorithm: analysis andimprovements for global numerical optimization. IEEE. Transactions on systems, man, and cybernetics—part b: cybernetics. 1083-4419/© 2010IEEE, 2010.

[13] R. Bace, and P. Mell, NIST Special publication on intrusion detection systems, 2001.

[14] P. Roberto, and V. Luigi, Intrusion detection systems, ISBN: 978-0-387-77265-3, 2008.

[15] H. Debar, M. Dacier, and A. Wespi, A revised taxonomy for intrusion detection systems. Annales des Telecommunications, 55(7-8), 2000.

[16] E. Tombini, Amélioration du diagnostic en détection d'intrusions: etude et application d'une combinaison de méthodes comportementale et par scénarios. Thèse de Doctorat de l'Institut National des SciencesAppliquées de Rennes, 2006.

[17] J. Anderson, Computer security threat monitoring and surveillance. Technical Report 79F296400, James Anderson, Co., Fort Washington, PA, 1980.

[18] D. Denning, An intrusion detection model. In Proc.of the 1986 IEEE Symposium on Security and Privacy, pp. 118-131, 1987.

[19] R. G. Bace, Intrusion detection systems. Mac Millan Technique Publication, USA, 2000.

[20] Y. Haidong, G. Jianhua, and D. Feiqi, Collaborative RFID intrusion detection withan artificial immune system. Journal of Intelligent Information System, Vol. 36, N°1, pp. 1-26, 2010.

[21] Z. Banković, A. Álvaro, and J.M. de Goyeneche, Intrusion detection in sensor networks using clustering and immune systems. Lecture Notes in Computer Science, Vol. 5788, Intelligent Data Engineering andAutomatedLearning - IDEAL 2009, pp. 408-415.

[22] S. Cho, Web session anomaly detection based on parameter estimation. Computers & Security,vol. 23, no. 4, pp. 265-351, 2004.

[23] B. Xu, and A. Zhang, Application of support vector clustering algorithm to network intrusion detection. Proc. of the International Conference on Neural Networks and Brain, ICNN & B '05. vol. 2, pp. 1036 – 1040, 2005.

[24] O. SH, and L. WS, An anomaly intrusion detection method by clustering normal user behavior. Computers & Security, vol. 22, no. 7, pp. 596-612, 2006.

[25] E. Leon, O. Nasraoui, and J. Gomez, Anomaly detection based on unsupervised niche clustering with application to network intrusion detection. Proc. of the IEEE Conference on Evolutionary Computation (CEC),pp. 502-508, 2004.

[26] Y. Guan, A. Ghorbani, and N. Belacel, Y-MEANS: A clustering method for intrusion detection. Proc. of the Canadian Conference on Electrical and Computer Engineering, pp. 1083-1086, 2004.

[27] M. Saniee Abadeh, J. Habibi, and C. Lucas, Intrusion detection using a fuzzy genetics- based learning algorithm. Journal of Network and Computer Applications, pp. 414-428, 2007.

[28] T. Ozyer, R. Alhajj, and K. Barker, Intrusion detection by integrating boosting genetic fuzzy classifier and data mining criteria for rule prescreening. Journal of Network and Computer Applications , pp. 99–113, 2003.

[29] G. Kumar, and M. Sachdeva, The use of artificial intelligence based techniques for intrusion detection: Artificial Intelligence Review, vol. 34, no. 4, pp. 369-387, 2010.

[30] M. Castellano, G. Mastronardi, and G. Tarricone, (2009). Intrusion detection using neural networks: a grid computing based data mining approach. Lecture Notes in Computer Science, 2009, vol. 5864, Neural Information Processing, pp. 777-785, 2009.

[31] S.Mukkamala, D.Xu,and A.Sung, intrusion detection based on behavior mining and machine learning techniques. Lecture Notes inComputer Science, Vol. 4031. Advances in Applied Artificial Intelligence, pp. 619-628, 2006.

[32] S.Wu, and W. Banzhaf, The use of computational intelligence in intrusion detection systems: a review. Computer Science Department, Memorial University of Newfoundland, St John's, NL A1B3X5, Canada. 2008.

[33] W. Ling, Y. Xu,M. Yunfei, F. Minrui, Discrete harmony search algorithm. Shanghai Key. Laboratory of Power Station Automation Technology, School of Mechatronics and Automation, University of Shanghai,2007.

[34] D. Simon, Biogeography-based optimization, IEEE Transactions on Evolutionary Computation, vol. 12, pp. 702-713, (Decembre 2008), 2008.

 ISBN: 978-1-61208-246-2

Secure Trust Management for the Android Platform

Raimund K. Ege

Dept. of Computer Science
Northern Illinois University
DeKalb, IL, USA
ege@niu.edu

***Abstract*—Smartphones change the way we use the Internet. No longer are we limited to media consumption, but participation in Social Media etc. allows us all to become media producers. Moreover, with its computing power and network connectivity, the smartphone can become a peer in a peer-to-peer based content delivery network. Securing property rights to the media must be part of such sharing and propagation. This paper explores the capabilities available to the Android platform to secure such participation, and it describes an architecture for adding trust management to the exchange of media to and from a smartphone user.**

Keywords-Android; security; trust; management; peer-to-peer systems; multi-media content delivery

I. INTRODUCTION

Personal digital assistants (PDA) have grown up into Smartphones: with computing power, display and recording capabilities, and – foremost – with broadband internet connectivity. No longer is a phone user limited to making phone calls and reading email, but the user can participate in a host of social applications that are rich in multimedia exchange. The social media scene is full of sites such as Facebook, YouTube, Instagram, Vimeo, etc. Participating in such venues requires that user reveal, typically via a user registration, their identity. In addition some proof might be required to authenticate the identity. Most sites, however, are satisfied once an email address is verified. The registration serves the purpose of adding a layer of trust to the consumption but also to the submission of media to these sites.

The next step in the evolution of the smartphone is to not just consider it a client to such social media sites, but to let it become an active player in the delivery of the media. The computing power and network connectivity enable the provision of peer-to-peer (P2P) content delivery networks: rather than just down- or up-loading media to one site, media can be shared in such P2P network at a much higher throughput, i.e. no single source bottleneck, and without central control, i.e. big brother registration. The aim of our research is to allow the forming of very large P2P content sharing networks, without central control, but with provisions that instill a degree of trust into the participants.

This paper describes an architecture for adding trust management to the exchange of media to and from a smartphone user. Section 2 gives some background on access control, identity and trust management and relates out work to current research. Section 3 surveys which elements of security to ensure confidentiality, integrity and availability are available to mobile platforms, with a specific focus on what is available to Android smartphones. Section 4 elaborates on how our approach defines and gauges trust, and how such trust is maintained, secured and shared in a central-server-less P2P environment. Section 5 outlines our prototype implementation with Java peers, including peers running on Android smartphones. The paper concludes with some lessons we learned and our future perspective.

II. BACKGROUND

Much research has been conducted on access control and digital rights management. Access control is common place in many applications. A server maintains a database of user and account information. A user gains access to the system by providing a user id with additional security information, typically a password. Once authenticated, the user is "trusted", i.e. is allowed to participate in the system's mission. The information stored by the server can include the users past history of participation, which in turn can be used to augment the level of trust in the user. Other users might contribute to the trust evaluation by submitting feedback on others. The level of trust might determine the level of participation a user is allowed, e.g. users with a low level of trust might be able to consume content, while users with a high level of trust might be able to contribute media.

While central access control makes sense for central systems, systems that don't have a central point of service, typically out-source their authentication aspect to other players: OpenID [1] is an example: OpenID providers maintain identity information and allow users to choose to associate information with their OpenID that can be shared with the media sites they visit. With OpenID, a password is only given to the identity provider, and that provider then confirms the identity.

In a peer-to-peer system peers need to collaborate and obtain services within an environment that is unfamiliar or even hostile. Therefore, peers have to manage the risks

 ISBN: 978-1-61208-246-2

involved in the collaboration when prior experience and knowledge about each other are incomplete. One way to address this uncertainty is to develop and establish trust among peers. Trust can be built either via a trusted third party [2] or by community-based feedback from past experiences [3] in a self-regulating system. Other approaches reported in the literature use different access control models [4] [5] that qualify and determine authorization based on permissions defined for peers.

In such a complex and collaborative world, a peer can benefit and protect itself only if it can respond to new peers and enforce access control by assigning proper privileges to new peers. Trust management can help minimize risk and ensure the network activity of benign entities in distributed systems [6].

Digital rights management has been the focus of many secure content delivery systems. Peer-to-peer and mobile schemes have been introduced. One such effort, OMA DRM [7] – undertaken by the Open Mobile Alliance, an industry consortium – provides a standard framework to secure media for mobile devices. It uses public key infrastructure (PKI [8]) style certificates and public/private key pairs to protect media. Our approach goes further in that it does not require certainty of access right, but rather allows building of graduated trust which enables graduated access control to digital media.

In our prior work [9] we started to develop an understanding on how trust can be quantified, especially when related to the potential reward garnered by a peer who participates in a peer-to-peer content delivery network. In this paper we focus on how to create and maintain trust in a distributed fashion, and how to secure it in a mobile environment.

III. ELEMENTS OF MOBILE SECURITY

Security concepts include confidentiality, integrity and availability. All three of these basic tenants of computer security are essential to our goal of securing trust information in a mobile environment. Via confidentiality we ensure that the communication among peers is only observable to authorized peers. Via integrity we ensure that communication as well as the history of communication is maintained without improper alteration. Via availability we insure that peers can readily join the content delivery network and that their trust values and histories are available in making decisions on their degree of participation.

We ensure confidentiality via encryption. Today's smartphones have enough computing power to handle encryption: asymmetric encryption, e.g. the Diffie-Hellman key exchange protocol, can be used to establish session keys that ensure the confidentiality as data, such as identity and trust information, and media streams are exchanged. Standard block cyphers, e.g. DES or AES, are used to encrypt sensitive data, and standard stream cyphers, e.g. RC4, secure media streams. We ensure integrity via digital signatures. Again, modern smartphones can handle standard algorithms such as DSA, etc. Key management is also standardized and it is quite common for a smartphone to maintain a local key store on the device itself.

Our prototype implementation is done entirely using the Java programming language. The Java platform strongly emphasizes security, including language safety, cryptography, public key infrastructure, authentication, secure communication, and access control. The Java Cryptographic Architecture [10] defines a "provider" architecture. Multiple providers are available in a typical Java development environment. We choose the "Bouncy Castle" [11] Java implementation, which is widely available, including for the Android platform. On Android we are actually using the "Spongy Castle" [12] variant that replaces the standard (but older) Bouncy Castle version for Android which is provided by Google.

In summary, all elements of a public key infrastructure (PKI) are readily accessible to any peer in a peer-to-peer content delivery network, even to a mobile ad-hoc peer via a smartphone.

IV. TRUST MODEL

Peer-to-peer is a communications model in which each party has the same capabilities and either party can initiate a communication session. Each party can become a peer. Once a peer is identified, it is a matter of trust whether and to what degree the peer is allowed to partake in the shared media content. We start by assigning each peer a numeric trust value in the range of -1 to 1, where 0 represent a neutral value, i.e. the network as a whole does not have a judgment on the trustworthiness of the peer. A positive value reflects more trust, a negative value reflects mistrust. As a peer participates in the network, i.e. is part of the "swarm", each of the peer's transactions is judged and results in an update to the trust value. At +1, a peer is considered trustworthy enough to partake in the shared trust management of the swarm. At -1, the peer is disqualified from any further participation in the swarm.

The trust value and the peer's history of relevant transactions are maintained in a container we call "trust nugget". This nugget contains detailed information on a peer's participation, such as length and quality of stream transmission, ratio of seed vs. leech behavior, judgments of other stream participants, etc. The nugget content is signed with a special master private key. It can be verified only via the special master public key. This ensures that the trust information maintains its integrity, even as it is shared with peers in the swarm that have lower trust values.

Trust information per peer is maintained by trusted peers, i.e. peers with trust values greater than 1. The sole requirement for starting a new swarm is the existence of an initial trusted peer that we call the "boot strap peer". This peer initially creates the master public/private key pair that is only shared with other trusted peers. A trusted peer maintains a database of trust nuggets for all peers in the swarm. Again, initially, only one peer, i.e. the boot strap peer, has such a

 ISBN: 978-1-61208-246-2

database, but as new peer attains trusted peer status, it receives the database, and also participates in synchronizing the database among all trusted peers.

The trust value for a peer is computed from the peer's history of transactions. The computation is done by a trusted peer whenever a peer reports on another peer. A common scenario is that a peer serves as a source of media content: it makes the content available to the peers in the swarm. Once a peer has consumed the content, the "source" peer notifies a trusted peer of the peer's behavior: good or bad. The trusted peer enters a new transaction into the peer's nugget and signs it with the master private key.

When a peer acts as a source peer, i.e. it makes new content available to the swarm; it can set a trust threshold, i.e. a minimum trust value, required for any peer to access the content. Only peers whose trust value meets the threshold can participate. The source peer also determines the weight of a peer's participation when computing a peer's new trust value.

Trusted peers are the backbone of our trust model. New peers need to register with one trusted peer which creates a trust nugget for the new peer. The new peer also creates a public/private key pair and submits its public key to the trusted peer. Other components of the model are the provider of the original source data, i.e. a "source peer", and peers that consume the multimedia content. Peers can also serve as further sources in a peer-to-peer download model.

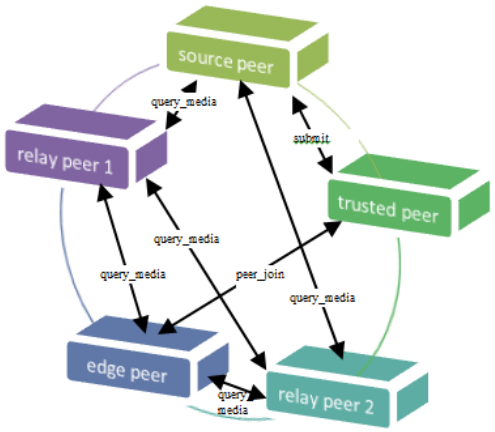

Figure 1: peer-to-peer network

Figure 1 shows an example snapshot of a content delivery network with one source peer, one trusted peer, and 3 regular peers: 2 relay peers and one edge peer. The source peer is where the content data is produced, en-coded, encrypted and made available. The source submits the stream info to a trusted peer. Peers connect to a trusted peer for authentication and to receive the download credentials. A peer that only downloads is called an "edge peer". Once the peer starts serving the stream to other peers, it becomes a "relay peer".

All peers together maintain a peer group, i.e. information on which peers are actively part of the content delivery network. The trusted peer initially informs the peers in the peer group which source peer to download from: peer 1 is fed directly from the source peer; peer 2 joined somewhat later and is now being served from the source peer and peer 1; the edge peer joined last and is being served from peer 1 and peer 2. In this example, peer 1 and 2 started out as edge peer, but became relay peers once they had enough data to start serving as intermediaries on the delivery path from original source to ultimate consumer.

V. JAVA IMPLEMENTATION

Our implementation has 4 major components:

(1) A set of trusted peers, initially just one: the boot strap peer;

(2) An application that allows a source peer to submit information about a content stream;

(3) A relay peer that consumes data, e.g. shows the video, and makes it available to other peers; and

(4) An edge peer to run on an Android mobile device. Android is implemented in Java and therefore offers a flexible and standard set of communication and security features.

A. *Trusted Peer*

The central component of our architecture is the trusted peer. It maintains a database of all peers and a tracks the collection of data streams that are made available by sources. Our trusted peer prototype presents a display of all peers and streams (see Figure 2).

When a new peer connects to a trusted peer, authentication is achieved via the peer's openID, which is validated the openID provider. If the peer is new, i.e. the trusted peer has no trust nugget for the peer, the new peer must provide its public key and a new trust nugget is created. The peer's public key is later provided to source peers who will use it to encrypt content destined for that peer. "ellie@aol.com" could have been the result of the peer leaking parts of the stream to non-authorized parties.

 ISBN: 978-1-61208-246-2

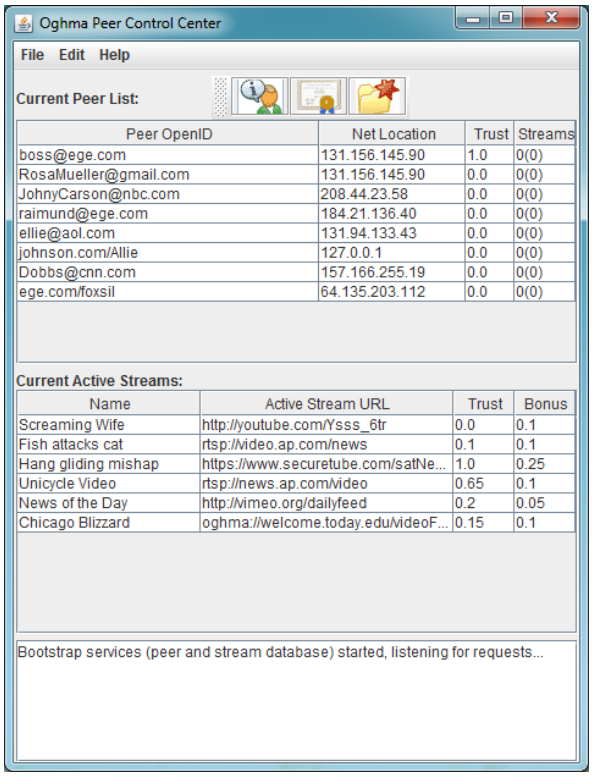

Figure 2: Trusted Peer Prototype

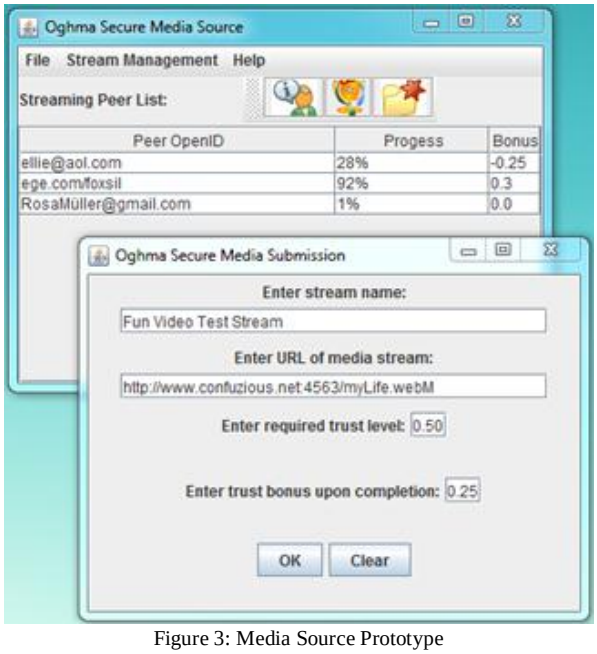

Figure 3: Media Source Prototype

B. *Relay Peer*

The relay peer application is used to allow a peer to authenticate with a trusted peer, get a listing of available streams, make a selection, display the stream and finally also make the stream available to other peers downstream. Figure 4 shows a screen capture of the Java Peer Client prototype:

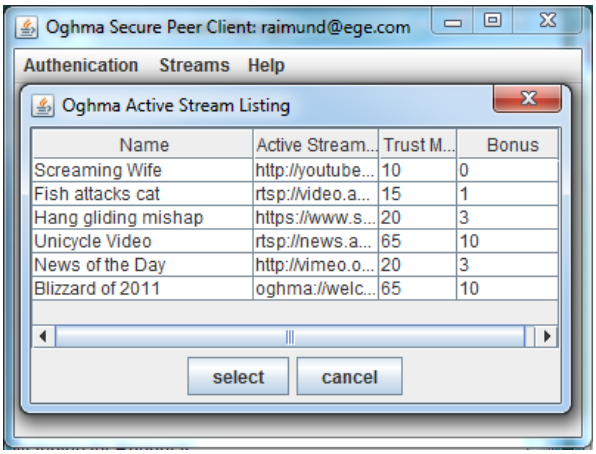

Figure 4: Relay Peer Prototype

Once the peer is authenticated with a trusted peer, it can request a list of available streams. Figure 4 shows all streams that are currently available with their name, required trust value, and potential bonus. The peer can make any selection. The reason why all stream are displayed, even the ones which require a higher trust value than what the peer currently has, is to give the peer an incentive to first participate in another stream to add the bonus to its trust value. However, only streams can actually be selected for which the peer is currently qualified.

Once the peer has selected a stream for viewing, the trusted peer will transmit the necessary information to enable the peer to start download. It will get the set of all locations at which the media stream is available. The peer then contacts the source locations at their streams' URLs and starts downloading content data, i.e. the sequential frames of the video stream.

In general, peers can do 3 things:

(1) they continuously request frames from other peers (the original source is viewed as just another peer) and store them;

(2) they may display the frames as video to the user of the peer device;

(3) and they make the stored frames available to other peers. Figure 5 shows our prototype Java implementation of our Peer Client while it displays the requested video:

 ISBN: 978-1-61208-246-2

Figure 5: Relay Peer Prototype

Peers don't need to provide all 3 services. A peer that provides only service (1) and (2) is an "edge" peer, i.e., an end user consumer. A peer that provides service (1) and (3) is a "relay" peer. Relay peers are specifically important for peers that have limited access to the public Internet, i.e., peers behind network boundaries, such as a NAT firewall. In addition, peers stay in contact with each other to continuously update the peer group and source data availability.

C. Edge Peer

The final component of our prototype framework is our proof-of-concept edge peer implementation for the Android platform. Figure 6 shows three screens: "login", "stream selection", and "stream play" of our Android prototype edge peer application.

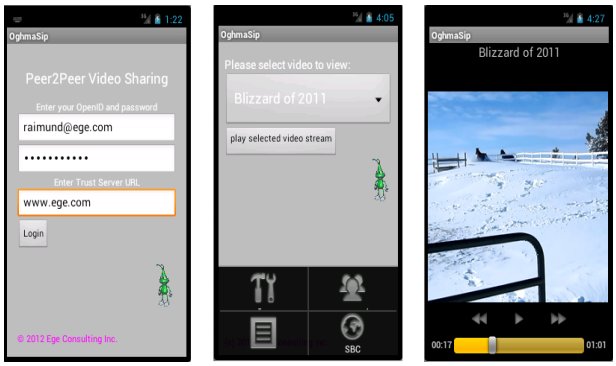

Figure 6: Android Prototype App

First, each peer is authenticated with its OpenID credentials. The user enters userid and password, plus the URL of a boot strap trusted peer. If the peer is new to the content delivery network, it will also generate a public/private pair of Diffie-Hellman keys, keep one private and submit the public one to the trusted peer. Once authentication is achieved, i.e. the OpenID provider has sent the authorization token, the user is shown which streams are currently available on the next screen. Once the "play selected video stream" button is pressed, and a sufficient read-ahead buffer has been accumulated, the video stream starts playing on the Android device.

CONCLUSION

In this article, we described an architecture for peer-to-peer based content delivery networks that empowers participating peers. Peers joining peer groups and establish trust among each other. Benevolent participation, i.e., consuming, producing, sharing and propagating media content, increases the understanding of shared trust. The trust information, i.e., the history of p2p transactions, is maintained in secure manner, signed with the private key of a trusted peer. Trust can also be lost; each unsuccessful transaction lowers the peer's trust value, ultimately to the point where the peer is ejected from the peer group.

We also described a prototype implementation written in Java to boot strap a P2P network, and includes a Java-based client for the Android platform for smartphones. Our intention was to demonstrate that the security capabilities of the Java Cryptographic Architecture are sufficient, and that its provider implementations run well on Android smartphones.

Our next steps will be to orchestrate and simulate a large actual swarm, i.e. an actual network with a large number of participating peers. Our goal is to measure how robust our trust management is and how well it withstands the introduction of malevolent peers.

 ISBN: 978-1-61208-246-2

REFERENCES

[1] OpenID, http://www.openid.net. [accessed September 13, 2012]

[2] J Y. Atif. Building trust in E-commerce. IEEE Internet Computing, 6(1):18–24, 2002.

[3] P. Resnick, K. Kuwabara, R. Zeckhauser, and E. Friedman. Reputation systems. Communications of the ACM, 43(12):45–48, 2000.

[4] E. Bertino, B. Catania, E. Ferrari, and P. Perlasca. A logical framework for reasoning about access control models. In SACMAT '01: Proceedings of the sixth ACM symposium on Access control models and technologies, pages 41–52, New York, NY, USA, 2001.

[5] S. Jajodia, P. Samarati, M. L. Sapino, and V. S. Subrahmanian. Flexible support for multiple access control policies. ACM Transaction Database System, 26(2):214–260, 2001.

[6] H. Li and M. Singhal. Trust Management in Distributed Systems. Computer, vol. 40, no. 2, pp. 45-53, Feb. 2007.

[7] OMA Digital Rights Management V2.0, http://www.openmobilealliance.org/technical/release_program/drm_v2_0.aspx. [accessed September 20, 2012]

[8] [10] C. Adams and S. Lloyd. Understanding PKI: concepts, standards, and deployment considerations. Addison-Wesley Professional. ISBN 978-0-672-32391-1. 2003.

[9] Raimund K. Ege. OghmaSip: Peer-to-Peer Multimedia for Mobile Devices. The First International Conference on Mobile Services, Resources, and Users (MOBILITY 2011), pages 1-6, Barcelona, Spain, October 2011.

[10] Java Cryptography Architecture (JCA) Reference Guide. http://docs.oracle.com/javase/6/docs/technotes/guides/security/crypto/CryptoSpec.html. [accessed September 20, 2012]

[11] The Legion of the Bouncy Castle. http://www.bouncycastle.org/java.html. [accessed September 20, 2012]

[12] Spongy Castle. http://rtyley.github.com/spongycastle. [accessed September 20, 2012]

 ISBN: 978-1-61208-246-2

Implementation of Improved DES Algorithm in Securing Smart Card Data

Ariel M. Sison
School of Computer Studies
Emilio Aguinaldo College
Manila, Philippines
ariel@eac.edu.ph

Bartolome T. Tanguilig III
College of Information Technology Education
Technological Institute of the Philippines
Quezon City, Philippines
bttanguilig_3@yahoo.com

Bobby D. Gerardo
Institute of Information and Communications Technology
West Visayas State University
Lapaz, Iloilo City, Philippines
bgerardo@wvsu.edu.ph

Yung-Cheol Byun
Faculty of Telecommunications and Computer Engineering, Cheju National University
Jeju City, Korea
ycb@jejunu.ac.kr

***Abstract*— Although smart cards have already provided secure portable storage device, security is still a major concern to electronic data systems against accidental or unlawful destruction or alteration during transmission or while in storage. One way of ensuring security is through encryption so that only the intended parties are able to read and access the confidential information. The software simulation result proved that the inclusion of the Odd-Even substitution to DES has provided additional confusion technique to DES and was essential in providing adequate security whilst having the stability and speed of handling encryption and decryption processes.**

Keywords-DES; AES; Triple DES; Blowfish; Confusion; Brute Force Attack; Linear Cryptanalysis; Differential Cryptanalysis; Smart Card; Card Skimming.

I. INTRODUCTION

Smart cards have been used in security-sensitive applications from identification and access control to payment systems. Smart cards store confidential information and can deliver secure and accurate identity verification much more difficult to counterfeit than ordinary magnetic stripe cards [2]. These cards can be utilized to provide secure and strong authentication and have been designed to provide greater performance, portability, efficiency, and interoperability. Smart cards enable business establishments to automatically identify, track, and capture information electronically [3].

However, confidential information is vulnerable to potential intruders who may intercept and extract or alter the contents of information during transmission or while in storage [4], [14], [37]. Anyone can interpose a computer in all communication paths and thus can alter or copy parts of messages, replay messages, or emit false material [7]. Secure communication channel is difficult to achieve or there is minimal reliance of network-wide services [8]. As data crosses over an unsecured channel, it is already susceptible to eavesdropping, illegal retrieval, and intended modification [5]. A problem confronting security in an open network includes how to identify the individual making the transaction, whether the transaction has been altered during transmission, or how to safeguard the transaction from being redirected or read to some other destination [6]. Criminals use this opportunity to steal identities and commit fraud [2]. Confidential information can be the subject of manipulation and misuse.

Security measures are needed to safeguard data. According to Zibideh and Matalgah [37], encryption is a vital process to assure security. Encryption is necessary before any data is passed between physical vulnerable networks and decrypted back to plaintext when it is read back from the storage. Encryption is any form of coding, ciphering, or secret writing [17], and a practical means to achieve information secrecy [19].

According to Grabbe [8], Data Encryption Standard (DES) is one of the most widely used symmetric encryption algorithm and its design idea is still used in numerous block ciphers. A symmetric encryption uses series of numbers and letters and some shifting of characters (bits) to alter the message. Over the last three decades, DES has played major role in securing data [9] since it was adopted as Federal Information Processing Standard (FIPS) in November 1977 [10]. It has been endorsed by the United States of America as the standard of encryptions [23], [24].

However, all encryption techniques are subject to attacks. Just like any other encryption techniques (e.g., IDEA, RC5, RC6), DES is no exception. Intruders have exploited its weaknesses to bypass secure encryption to steal sensitive information since it has been publicly known as a standard of encryptions. One major concern surrounding DES security is the key length (56 bits). Intruders have devised attacks that can work against it. Attacks known to have successfully broken DES security are Brute Force (exhaustion attack), Differential Cryptanalysis [18], [19], [20], [36], and Linear Cryptanalysis [21], [22], [36].

 ISBN: 978-1-61208-246-2

While smart card is a secure portable storage device used for several applications, there is a need to look into the security aspects of the device as it has introduced an array of security and privacy issues. Information inside the card could potentially be exploited by an undetected modification or unauthorized disclosure caused by poor design or implementation. Data can be stolen without leaving the users wallet or bag through an illegal activity called *card skimming*. Card skimming involves the intruder hiding a device inside a bag close to a victim's card proximity to steal the data without the victim's knowledge [33].

Since smart cards are becoming prevalent for payment mechanisms (e.g., pay TV access control, transport, supermarket, banks, and cashless vending machines), sending personal information (e.g., health cards, government ID cards), and for security access (e.g., authentication and controlled access to resources); therefore, appropriate measures to protect and secure data during transmission or while in storage must be implemented.

II. REVIEW OF RELATED LITERATURE

A. Evolutions of DES

DES has gone through many enhancements and served as basis for later techniques in the field of encryption. One of its successors is the Triple DES (3DES or TDEA). According to Dhanraj et al. [25], 3DES uses 48 rounds to encrypt the data. Using this technique gives the data three levels of security making it highly resistant to differential cryptanalysis and boosting the security. However, since 3DES involves going through DES three times, its performance also takes three times as long to encrypt and decrypt [26]. The 3DES works by forward and inverse encryptions. DES encrypts with K_1, K_2 and K_3. To decrypt data it starts with K_3, then with K_2 and with K_1 [29].

Ammar et al. [27] proposed an extended DES called Random Data Encryption Algorithm (RDEA). New features added to the DES include pseudo randomized cipher key for encryption and protocols for sending cipher key embedded in the ciphertext. Random generator sequence length and its memory capacity have hampered the RDEA's overall efficiency this along with its weakness to linear attacks to the S-Box and its key scheduling.

Fan Jing et al. [25] proposed the idea of TKE (Two Key), which is versatile in the sense that it can perform faster and works easily with hardware. Aside from these advantages, it also has high-level security like the DES. However, TKE requires two keys and its data block has different length. This gives the process a heavier load slowing the encryption.

Blowfish encryption encrypts a 64-bit block of data using a key with lengths ranging from 32 to 448 bits. The encryption itself is a sixteen round encryption revolving around utilizing S-Boxes and complex key schedules [30]. The strength of the Blowfish lies in the fact that in its full round form cryptanalysis techniques have no effect on it. However, anything less than four rounds are susceptible to cryptanalysis and the algorithm is not immune to brute force attacks [31].

DES has also been used in conjunction with other encryption techniques. Hamami et al. [28] proposed fusion of DES and Blowfish encryption. The proposed fusion aimed to strengthen the key generation of the DES. It encrypts a 64-bit data block using two keys by initial permutation followed by sixteen rounds of crossover iterations using two keys and going through a final inversed permutation. Its weaknesses are the same with regular Blowfish although it offers more resistance to Brute Force attacks but the two keys added to the encryption slowed the process.

AES (Advanced Encryption Standard) is the successor to the DES as a standard for encryptions [32]. AES encrypts data blocks of 128 bits using keys of 128, 192, 256 bits. AES works through phases. First, round keys derived from the main key through key schedules are expanded. In the next rounds or iterations, the plain text is subjected to left shifts as well as column mixing using the derived round keys and S-Boxes. This phase repeats for a final round with the exemption of the column mixing. Although AES has tighter security compared to DES or 3DES, it also has the longest encryption time and load due to all the variables needed to process encryption. AES key schedule has also come under scrutiny since its key schedule is too simple and can be exploited by cryptographers through newer cryptanalysis techniques [34].

B. Known Attacks on DES

Among known attacks on DES, the common techniques used were Brute Force and cryptanalysis techniques. Brute Force is the most basic and effective form of attack on any encryption system to date [35]. It attacks the encryption head on by trying every possible key in a turn. Although Brute Force is proven to work successfully, the machine used and time consumed by the method proved non feasible [23]. Differential Cryptanalysis works by presuming the attacker has a piece of the original plaintext using this knowledge. The attacker diminishes the security of the encryption until he deciphers the key. To break the full 16 rounds, differential cryptanalysis requires 2^{47} chosen plaintexts. Linear Cryptanalysis works like differential cryptanalysis although it only needs 2^{43} known plaintexts due to its linear nature. The number of rounds used by the DES defines these types of attacks. The shorter the rounds give higher probabilities of success for such techniques. Analysts gain knowledge on the security margins needed by DES through these attacks.

Both cryptanalysis attacks require the attacker to gain a part of the plaintext, which gives the method tricky prerequisites.

 ISBN: 978-1-61208-246-2

III. DESIGN ARCHITECTURE OF THE MODIFIED DES

A. Key Encryption Process

In Figure 1, the encryption process starts by converting a 64-bit key into a binary value. The result is reduced to 56-bit and went through the Odd-Even substitution. The Odd-Even substitution process substitutes 1 for every even position and 0 for every odd position in the 56-bit block. Afterwards, the 56-bit block is divided into two 28-bit halves (C_0 and D_0). Each half contains 28-bits and performs the left shift. After shifting is applied, the two halves are combined and reduced to 48 bits. The pipes (||) demonstrate the combination of the two halves. The 48-bit produced is now the first key. The 56 bits (C_1 and D_1) are used to generate the remaining keys and undergo the same steps in generating the first key. This will be performed for 16 rounds. The graphical illustration of key generation process presented in Figure 1 is simulated in Table I. After 16 rounds of iterative operation, the 16 keys produced are shown in Table II.

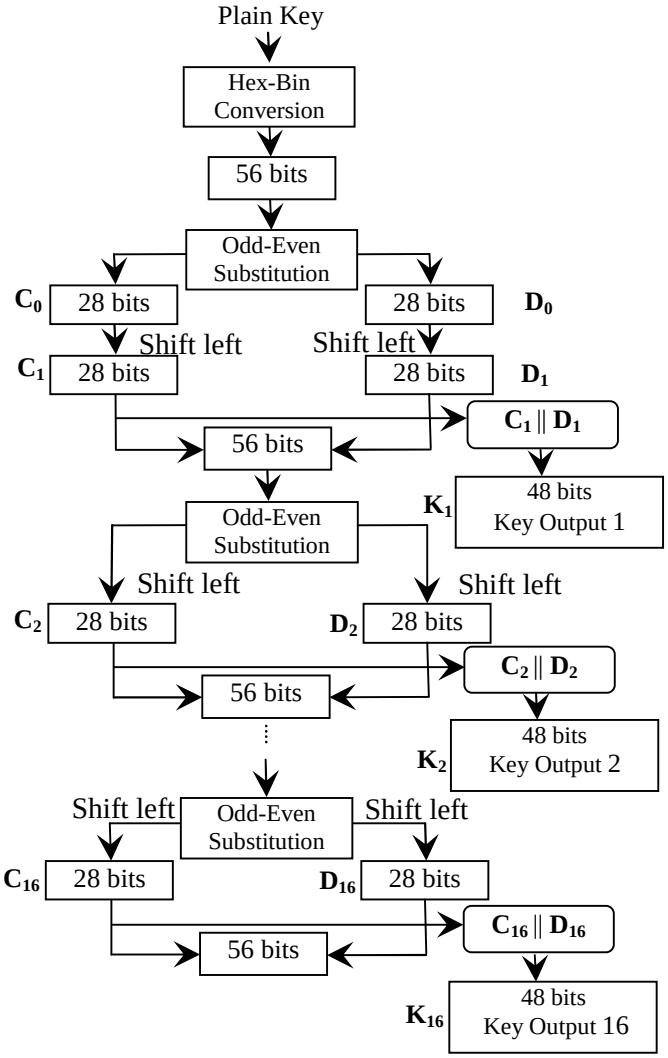

Figure 1. Modified DES algorithm key generation process.

The *Odd-Even* substitution process provided additional confusion to DES. Confusion is one of the two basic techniques of cryptography [35] that is achieved through the XOR operations making the relationship between the ciphertext and the key complex as possible. The enhancement was simple that it does not slow down the whole process of encryption.

TABLE I. ILLUSTRATION OF THE MODIFIED KEY GENERATION PROCESS

Step	Process	Result	
1	Convert the key *p@SSWoRD123 45TiP* from hexadecimal to binary value	01110000010000000101001101010011010111011011101101001000100000110001001100100011001100110001101000011010101010001101001010100000	
2	Reduce the result to 56 bits using the permuted choice 1.	00000000111111110010000101010111110010110000001000001101	
3	Apply Odd-Even substitution to the result.	01010101010101010101010101010101010101010101010101	
4	Divide the result into two halves.	C_0 01010101010101010101010101	D_0 01010101010101010101010101
5	Shift left both C_0 and D_0.	10101010101010101010101010	10101010101010101010101010
6	Assign C_0 to C_1 and D_0 to D_1.	C_1 10101010101010101010101010	D_1 10101010101010101010101010
7	Combine C_1 and D_1 to produce the 56-bits then apply permuted choice 2 to produce the 48-bit key output.	01101110101011000001101010111100111001100100000010 (6eac1abce642)	
8	Combine C_1 and D_1 in Step 6 to generate the next keys (C_2 and D_2, C_3 and D_3 ... C_{16} and D_{16}) and repeat Step 3 to Step 7. Perform this for 16 rounds.		

TABLE II. KEY GENERATION RESULT

Key	Value
1	6eac1abce642
2	6eac1abce642
3	9153e54319bd
4	9153e54319bd
5	9153e54319bd
6	9153e54319bd
7	9153e54319bd
8	9153e54319bd
9	6eac1abce642
10	9153e54319bd
11	9153e54319bd
12	9153e54319bd
13	9153e54319bd
14	9153e54319bd
15	9153e54319bd
16	6eac1abce642

 ISBN: 978-1-61208-246-2

B. *Plaintext Encryption Process*

In the plaintext encryption, the input is of any length. This is a significant contribution to DES since any size or length of plaintext could already be encrypted. The plaintext is then subsequently divided into 64-bit block plaintext. This is shown in Figure 2. For example, if the given plaintext is *I will meet you at 7:00am today at the park*, this will be grouped into 8 characters per block where each character is 8 bits. The result is shown in Table III. Take note that at Block 6, the length of the remaining characters is *3*, which is less than 8 characters. The system automatically padded 5 spaces to make it 8 characters. Each block is encrypted using the 16 keys generated in Table II.

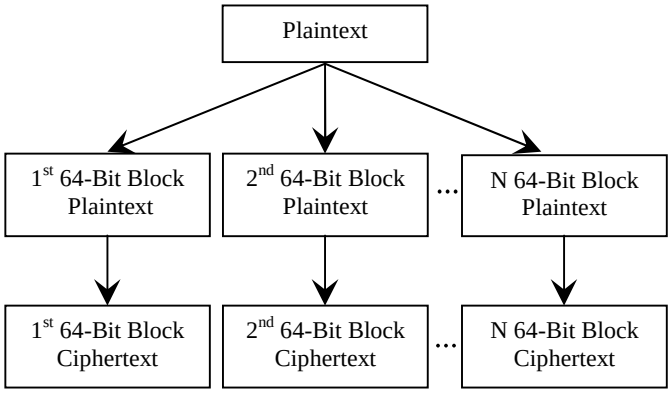

Figure 2. Division of the plaintext into 64-bit block.

TABLE III. 64-BIT BLOCK PLAINTEXT

Block	Plaintext
1	I will m
2	eet you
3	at 7:00a
4	m today
5	at the p
6	ark

In Figure 3, the plaintext is converted to 64 bits and is divided into two 32-bit halves (L_0 and R_0). The value of R_0 is first assigned to L_1 ($L_1 = R_0$) before undergoing E-Bit selection process to produce the 48 bits needed. The result will be XORed (⊕) to the first key in Table 2. The XOR result will then be grouped to 8 blocks. Each block consists of 6 bits. Afterwards, the S-Box $_{(1..8)}$ substitution will be applied. Each S-Box $_{(1..8)}$ has 4 rows and 16 columns with a corresponding value. For example, if the first block is 101000, get the first and the last bits. So $10_2 = 2$ denotes row 2. The remaining middle 4 bits $0100_2 = 4$ denotes column 4. S-Box$_1$ [2][4] will return the value of *13* or *D* in hexadecimal value. Repeat this for the other remaining 7 blocks. Permutation function is then applied to the result to produce 32 bits. Next is to XOR L_0 with the permutation value. The result is then assigned to R_1. $L_{n+1} = R_n$ are swapped to proceed to the next round. This means that $L_2 = R_1$, $L_3 = R_2$, so on and so forth. Iteratively perform this for 16 rounds. Table IV simulates the graphical illustration of Figure 3.

Table IV discussed the encryption process of the plaintext in the first block of Table III.

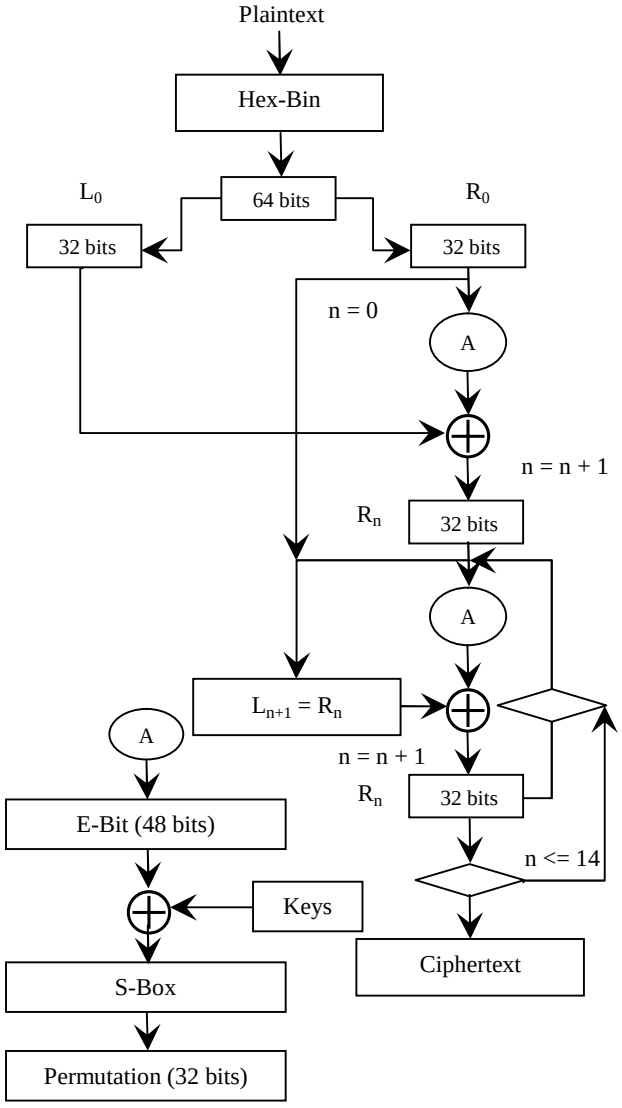

Figure 3. Plaintext encryption process.

TABLE IV. ILLUSTRATION OF THE ENCRYPTION PROCESS OF THE PLAINTEXT PER 64-BIT BLOCK

Step	Process	Result	
1	Convert the text *I will m* from hexadecimal to binary value.	01001001001000000111011101101001011011000110111000001000001101101	
2	Apply initial permutation to the result then convert to hexadecimal value.	bd04b48d00feb904	
3	Divide the result into two halves to form the Left and Right values.	L_0	R_0
		bd04b48d	00feb904

4	Apply E-bit selection table to the result of R_0.	0017fd5f2808
5	Using the first key in Table II, perform XOR with R_0.	6ebbe7e3ce4a
6	Apply S-Boxes substitution to the result.	5f766bef
7	Apply permutation function to the result.	5c7ffcb7
8	Perform XOR with L_0 and the result.	e17b483a
9	Assign the value of R_0 to L_1.	L_1
		00feb904
10	Assign the result of Step 8 to R_1.	R_1
		e17b483a
11	Repeat Steps 3 to 10 having L_1 and R_1 as input to the next round. Perform this for 16 rounds using the remaining keys in Table II. This will produce 16 round output block as shown in Table VI for decryption.	
12	Concatenate the value of R_{16} *(1ba732b1)* and L_{16} *(69bbb462)* from Table VI. Apply inverse on initial permutation (IP^{-1}) to the result. This is now the encrypted value of *I will m*.	Encryption Value: f17618e06dbf8239
13	Read the next plaintext in Table III then perform Steps 1-12 to have the next encrypted value.	

After performing the steps in Table IV, the complete encrypted values of Table III are shown in Table V.

TABLE V. ENCRYPTION RESULT OF THE PLAINTEXT PER 64-BIT BLOCK

Plaintext (64-bit block)	Ciphertext
I will m	f17618e06dbf8239
eet you	a0032d56e3fda715
at 7:00a	2460491262022a41
m today	228db1b8c8102503
at the p	7846ab84750c1e3b
ark	f2d0e39d5784b196

C. Decryption Simulation Process

Although encryption and decryption use the same algorithm, the key processing is performed in reverse order during the decryption process and the input is the ciphertext. Development of the decryption process is necessary to make sure that the modified DES algorithm can decrypt the ciphertext back to its original form.

After finishing the encryption process illustrated in Table IV, the 16 round output block is also generated for each ciphertext block and is shown in Table VI. The decryption starts by applying E-Bit selection table to L_1 *(00feb904)* and K_1 *(6eac1abce642)* getting the result of *6ebbe7e3ce4a*. S-Boxes substitution is then applied to the XOR result to have *5f766bef* followed by permutation function to obtain *5c7ffcb7*. XOR *5c7ffcb7* and R_1 *(e17b483a)* to get the new value for R_1 = *bd04b48d*. This process is shown in Figure 4.

Finally, by concatenating R_1 || L_1 yields to *bd04b48d00feb904*. Thus, $X = IP^{-1} = (L_1 \,||\, R_1) =$ *492077696c6c206d*. Subsequently convert this hexadecimal to ASCII value. Hence, the plaintext *I will m* is recovered.

TABLE VI. ENCRYPTION BLOCK OF THE FIRST CIPHERTEXT

Index	L	R
1	00feb904	e17b483a
2	e17b483a	f6960904
3	f6960904	cd843f3f
4	cd843f3f	75853adf
5	75853adf	b62ff04d
6	b62ff04d	727534d3
7	727534d3	48c03366
8	48c03366	4b5a3d7d
9	4b5a3d7d	8542aa8b
10	8542aa8b	512adb84
11	512adb84	3bbf9555
12	3bbf9555	0d816157
13	0d816157	2bde0e6e
14	2bde0e6e	bd378359
15	bd378359	69bbb462
16	69bbb462	1ba732b1

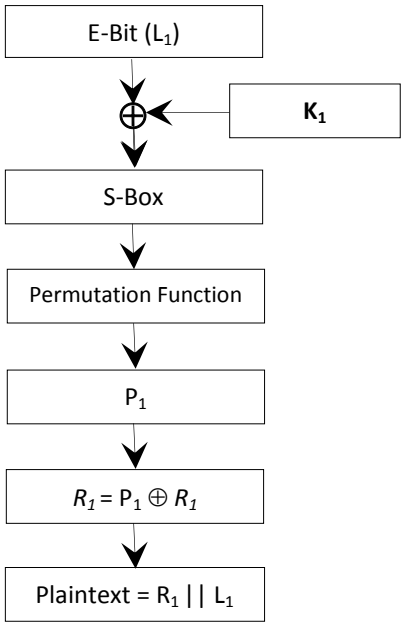

Figure 4. Ciphertext decryption process.

D. Implementation

The smart card device used in the study was ACR122U type. The unit is a contactless reader/writer with an effective proximity of 5 mm. The software was written in Java and

developed using the Eclipse Integrated Development Environment. The average running time of the five attempts with the modified DES was 365.2 milliseconds while 355.8 milliseconds with the typical DES. There is a relatively slight difference in the utilization of the CPU's memory using the typical and the modified DES. This is presented in Table VII. The Average CPU usage is the average of the five attempts in executing both algorithms.

Although there is no performance comparison on how fast the data was written in the card, the encrypted data was successfully written in and read from the card without any problem.

TABLE VII. CPU UTILIZATION COMPARISON

CPU Processor (Intel Core i3 2.67 GHz, 2GB RAM)	Minimum CPU Usage	Maximum CPU Usage	Average CPU Usage
Typical DES	10%	18%	14%
Modified DES	18%	25%	21.2%

IV. CONCLUSION AND FUTURE WORK

Smart card is like an *electronic wallet* replacing all of the things we carry around in our wallets, including credit cards, licenses, cash, and even family photographs and is like carrying digital credentials [4]. There is no doubt that smart cards will be the next generation of the highest level of security card technology that will soon replace magnetic stripes, bar code, and some proximity technologies. It will soon play significant role in personal identity verification.

According to Gong-bin et al. [36], improvement and perfection to DES are still very important. Encrypting information ensures that only the intended parties are able to read and access the confidential information inside the smart card. The inclusion of the Odd-Even substitution to DES ensures that even the data is intercepted by other networks or is redirected to other destinations; its integrity and confidentiality will not be compromised. More so, the Odd-Even substitution has provided additional confusion to the complexity of security capable of resisting cryptanalysis whilst having the stability and speed of handling encryption and decryption processes. Aside that this enhancement can be easily implemented to smart card, it can encrypt or decrypt any length of plaintext and does not require intensive processing, memory, and time compare to AES or 3DES.

Future plans for the study include separate keys for each 64-bit block. Hopefully, additional keys will provide the algorithm more resistance to all known attacks of DES.

REFERENCES

[1] C. Chang and K. Hwang, "Some forgery attacks on a remote user authentication scheme using Smart Cards", Informatica, 2003, Vol. 14, No. 3, pp. 289-294.

[2] W. Wang, Y. Yuan, and N. Archer, "A contextual framework for combating identity theft", IEEE Security & Privacy, Vol. 4, Issue 2, pp. 30-38, 2006.

[3] A. Reid, "Is society smart enough to deal with smart cards?", Computer Law & Security Report, Vol. 23, Issue 1, pp. 53-61, 2007.

[4] B. Lewis, "Making Smart Cards work in the enterprise", SANS Institute InfoSec Reading Room, SANS Institute 2002, http://www.sans.org/reading_room/whitepapers/authentication/making-smart-cards-work-enterprise_138 [retrieved: April, 2011].

[5] P. Rakers, L. Connell, T. Collins, and D. Russel, "Secure contactless smartcard ASIC with DPA protection", IEEE Journal of Solid-State Circuits, Vol. 36, Issue 3, pp. 559-565, 2001.

[6] J. McAndrews, "E-money and payment system risks", Contemporary Economic Policy, Vol. 17, Issue 3, pp. 348-357, July 1999.

[7] R. Needham and M. Schroeder, "Using encryption for authentication in large networks of computers", Communications of the ACM, Vol. 21, No. 12, pp. 993-999, December 1978.

[8] O. Grabbe, "The DES algorithm illustrated", Laissez Faire City Times, Vol. 2, No. 28. (http://www.doc88.com/p-281792313650.html) [retrieved: April, 2011].

[9] K. Rabah, "Theory and implementation of data encryption standard: a review", Information Technology Journal, Vol. 4, pp. 307-325, Asian Network for Scientific Information, 2005.

[10] Data Encryption Standard, Federal Information Processing Standards Publication (FIPS Pub) 46, National Bureau of Standards, Washington, DC, 1977.

[11] M. Hwang and L. Li, "A new remote user authentication scheme using smart cards", IEEE. Transactions Consumer Electron, Vol. 46, No. 1, pp. 28-30, 2000.

[12] A. Awasthi and S. Lal, "An enhanced remote user authentication A. scheme using smart cards", IEEE Transactions on Consumer Electronics, Vol. 50, No. 2, pp. 583-586, May 2004.

[13] X. Zhao and F. Zhang, "A new type of id-based encryption system and its application to pay-tv systems", International Journal of Network Security, Vol. 13, No. 3, pp. 161-166, November 2011.

[14] T. Diament, H. Lee, A. Keromytis, and M. Yung," The efficient dual receiver cryptosystem and its application", International Journal of Network Security, Vol. 13, pp. 135-151, November 2010.

[15] M. Peyravian and N. Zunic, "Methods for protecting password transmission", Computers & Security, Vol. 19, No. 5, pp. 466-469, 2000.

[16] R. Needham and M. Schroeder, "Using encryption for authentication in large networks of computers", Communications of the ACM, Vol.21, Issue 12, pp. 993-999, December 1978.

[17] L. Gilman, "Encryption of data", Encyclopedia of Espionage, Intelligence, and Security. (http://www.faqs.org/espionage/Ec-Ep/Encrption -of-Data.html) [retrieved: April, 2011].

[18] E. Biham and A. Shamir, "Differential Cryptanalysis of DES-like Cryptosystems", Journal of Cryptology, Vol. 4, pp. 3-72, IACR, 1991.

[19] D. Coppersmith, "The data encryption standard (DES) and its strength against attacks", IBM Journal of Research and Development, Vol. 38, Issue. 3, pp. 243-250, May 1994.

[20] N. Courtois, "The best differential characteristics and subtleties of the Biham-Shamir attacks on DES", IACR Cryptology ePrint Archive, Vol. 2005, pp. 202, 2005, (http://eprint.iacr.org/2005/202).

[21] P. Junod, "Linear cryptanalysis of DES", http://citeseerx.ist.psu.edu/viewdoc/summary?doi=10.1.1.12.9652 [retrieved: June, 2012].

[22] C. Harpes, G. Kramer, and J. Massey, "A generalization of linear cryptanalysis and the applicability of Matsui's piling up lemma", Theory and Application of Cryptographic Techniques - EUROCRYPT, Vol. 921, pp. 24-38, 1995.

[23] M. Smid and D. Branstad, "The Data Encryption Standard Past and Future", Proceedings of the IEEE, Vol .76, Issue 5, pp. 550-559, May 1988, in press.

[24] United States Department of Commerce/National Institute of Standards and Technology, FIPS PUB 46-3 Reaffirmed October 1999.

 ISBN: 978-1-61208-246-2

[25] American National Standard for Financial Institution Message Authentication (wholesale), ANSI x9.9-1986 (revised), American Bankers Association, X9 Secretariat, American Bankers Association, 1986.

[26] Dharaj, C. Nandini, and M. Tajuddin, “An enhanced approach for secret key algorithm based on data encryption standard”, International Journal of Research and Reviews in Computer Science (IJRRCS) Vol. 2, No. 4, pp. 943-947, ISSN: 2079-2557, Science Academy Publisher, United Kingdom, August 2011.

[27] America National Standard for Personal Identification Number (PIN) Management and Security, ANSI x9.8-1982, American Bankers Association, Washington, D.C., 1982.

[28] A. Al-Hamami, M. Al-Hamami, and S. Hashem, “A proposed modified data encryption standard algorithm by using fusing data technique”, World of Computer Science and Information Technology Journal, Vol. 1, No. 3, pp. 88-91, 2011.

[29] W. Barker, “Recommendation for the triple data encryption algorithm (TDEA) block cipher”, U.S. Dept. of Commerce, Technology Administration, National Institute of Standards and Technology, Gaithersburg, MD, United States, 2004.

[30] B. Schneier, ”Description of a new variable-length key, 64-bit block cipher (blowfish)”, Fast Software Encryption, Cambridge Security Workshop, pp. 191-204, Springer-Verlag London, UK, 1994.

[31] S. Vaudenay, “On the weak keys of blowfish”, Fast Software Encryption, Cambridge, United Kingdom, Lecture Notes in Computer Science No. 1039, pp. 27-32, Springer-Verlag , 1996.

[32] H. Alanazi, B. Zaidan, A. Zaidan, H. Jalab, M. Shabbir, and Y. Al-Nabhani, "New comparative study between DES, 3DES and AES within nine factors“, Journal of Computing, Vol. 2, Issue 3, pp. 152-157, March 2010.

[33] Consumer Reports Magazine: June 2011, ”Newer cards can be hijacked, too”, http://www.consumerreports.org/cro/magazine-archive/2011/june/june-2011-toc.htm [retrieved: June, 2012].

[34] A. Bogdanov, D. Khovratovich, and C. Rechberger, ”Biclique cryptanalysis of the full AES”, ASIACRYPT'11 Proceedings of the 17th international conference on The Theory and Application of Cryptology and Information Security, pp. 344-371, Springer-Verlag Berlin, Heidelberg, 2011, in press.

[35] C. Shannon, "Communication theory of secrecy systems", Bell System Technical Journal, Vol. 28, pp. 656-715, 1949.

[36] Q. Gong-bin, J. Qing-feng, and Q. Shui-sheng “A new image encryption scheme based on DES algorithm and Chua’s circuit”, IEEE International Workshop on Imaging Systems and Techniques, pp. 168-172, Shenzhen, China, May 2009, in press.

[37] W. Zibideh and M. Matalgah, “Modified-DES encryption algorithm with improved BER performance in wireless communication”, 2011 IEEE Radio and Wireless Symposium (RWS), pp. 219-224, Phoenix, AZ, January 2011, in press.

 ISBN: 978-1-61208-246-2

On the Estimation of Missing Data in Incomplete Databases: Autoregressive Bayesian Networks

Pablo H. Ibargüengoytia, Uriel A. García
Electric Research Institute
Reforma 113, Palmira,
Cuernavaca, Mor., 62490, México
{pibar,uriel.garcia}@iie.org.mx

Javier Herrera-Vega, Pablo Hernández-Leal,
Eduardo F. Morales, L. Enrique Sucar, Felipe Orihuela-Espina
National Institute for Astrophysics, Optics and Electronics
Luis Enrique Erro 1,
Tonantzintla, Puebla, México
{vega,pablohl,emorales,esucar,f.orihuela-espina}@ccc.inaoep.mx

***Abstract*—Missing data can be estimated by means of interpolation, time series modelling, or exploiting statistically dependent information. The limits of when one approach is preferable to the alternatives have not been explored, but are likely to be a compromise between a signal autoregressive information, availability of future observations, stationary behaviour and the strength of the dependence with concomitant information. This paper takes a first step towards clarifying dataset characteristics delimiting the realm of application for each technique. In addition, this paper introduces autoregressive Bayesian networks (AR-BN), a variant of Dynamic Bayesian Networks for completing databases which exploits latent variable relations while still benefitting from autoregressive information of the variable being filled. Using AR-BN, new estimated values are calculated using inference in the dynamic model. Our results unveil how the interplay between the variable autoregressive information and the variable relationship to others in the dataset is critical to selecting the optimal data estimation technique. AR-BN appears as a good candidate ensuring a consistent performance across scenarios, datasets and error metrics.**

***Keywords*-dynamic probabilistic graphical models; incomplete data series; value estimation; knowledge discovery; autoregressive models.**

I. INTRODUCTION

Instrumentation failure, human error or interferences during data storing give rise to a number of disagreements between the real data and the repository. A wealth of literature is available on data validation methods for addressing any of the more common issues; outliers [1], [2], [3], [4], [5], [6], [7], sudden changes [8], [9], [4], [5], [6], [7], rogue values [10] and missing data [11], [12], [13]. Moreover, full data validation suites can be envisaged [14], [15], [16]. This paper concentrates in estimation of missing data.

Missing data can be estimated by means of interpolation, time series modelling, or exploiting statistically dependent information. Arguably the most widely applied methods are the various interpolation techniques [17] together with classical time series modelling [18] such as ARMA or ARIMA. Interpolation and time series modelling are appropriate for isolated time series. In isolated time series missing data is reconstructed exploiting within-variable information. The simplest method will replace missing data with the distribution average [12]. However, in complex databases, statistical dependencies among variables can be further exploited to fill information gaps. Hence a number of techniques have been developed to make the most out of this dependent information. Vagin and Fomina [12] proposed a method based on nearest neighbour. This consists in the definition of a metric that relates the similarity between different variables in a database. Lamrini et al [11] applied self organizing maps for reconstructing data from monitoring a water treatment process with a complex sensor configuration. In another example, a virtual sensor estimates the value of the fuel oil viscosity using related variables of a combustion process in power plants [19]. It can be argued, that these later approaches exploit information present in adjacent variables at the cost of ignoring any signal own information. It is yet unknown when the dataset characteristics will favour application of one technique over another. Moreover, it can be hypothesized that a method that utilizes both sources of information, the signal internal information and the related information present in the repository, will achieve data reconstruction with high accuracy.

This paper aims at demarcating the dataset characteristics advocating for the application of a particular approach for estimating missing data in incomplete dataset. Towards better exploiting the presence of both aforementioned sources of information, we further introduce the autoregressive Bayesian networks (AR-BN), a variant of Dynamic Bayesian Networks (DBN) for incomplete data estimation based upon dynamic probabilistic modelling. AR-BN exploits statistical dependencies among related variables as well as the variables' autoregressive information. The main contribution of this work is twofold. First, a preliminary exploration of dataset features hypothesized to guide the decision on missing data estimation process, as well as a comparative in missing data error reconstruction from a range of techniques. Second, the enrichment of a static probabilistic model with previous and posterior values of the variable set to afford an autoregressive probabilistic model. The reconstruction capabilities of the technique are demonstrated in two datasets from different domains.

II. METHODS

A beautiful mathematical formulation of the problem of incomplete data can be found in [13].

 ISBN: 978-1-61208-246-2

A. Autoregressive models

Autoregressive models are linear systems for predicting future values of a time series based on previous observations. The general autoregressive model of order n -denoted AR(n)- is defined as:

$$X_t = c + \sum_{i=1}^{n} \alpha_i X_{t-i} + \epsilon_t \quad (1)$$

where $\alpha_{i|i=1...n}$ are the model parameters, c is a constant and ϵ_t is noise. In an off-line repository, future data may also be available and can be easily incorporated:

$$X_t = c + \sum_{i=1}^{n} \alpha_i X_{t-i} + \sum_{j=1}^{m} \beta_j X_{t+j} + \epsilon_t \quad (2)$$

where $\alpha_{i|i=1...n}$ and $\beta_{j|j=1...m}$ are the AR(n,m) model parameters.

B. Probabilistic modelling

A Bayesian network is a directed acyclic graph (DAG) representing the joint probability distribution of all variables in a domain [20]. The topology of the network conveys direct information about the dependency between the variables. In particular, it represents which variables are conditionally independent given another variable.

Given the knowledge represented as a Bayesian network, it can be used to reason about the consequences of specific input data, by what is called probabilistic reasoning. This consists of assigning a value to the input variables, and propagating their effect through the network to update the probability of the hypothesis variables. The updating of the certainty measures is consistent with probability theory, based on the application of Bayesian calculus and the dependencies represented in the network. Several algorithms have been proposed for this probability propagation [20]. Bayesian networks can use historical data to acquire knowledge but may additionally assimilate domain experts' input.

Dynamic Bayesian Networks (DBN) are an attempt to add temporal dimension into the BN model [21], [22]. Often a DBN incorporates two models; an initial net B_0 learned using information at time 0, and the transition net $B_{\rightarrow}$ learned with the rest of the data. Together B_0 and $B_{\rightarrow}$ conform the DBN [23]. An important assumption is made for DBNs; the process is Markovian, this is, the future is conditionally independent of the past given the present. This assumption allows the DBN to use only the previous time stage information in order to obtain the next stage. DBN can be unfolded over as many stages as necessary and the horizontal structure can change from stage to stage. The resulting network is highly expressive but often unnecessarily complicated. Alternatives have been proposed to reduce this complexity [24]. In datasets arising from physical processes, statistical dependencies among variables can be expected to be stable across time. That is, if two variables X and Y are statistically dependent at time t_i they will likely be also statistically dependent at time t_{i+j} for any arbitrary samples i and j, and similar reasoning can be made for independencies. This can be exploited to simplify the network topology.

C. Autoregressive Bayesian Networks

Autoregressive Bayesian Networks are a simplified variant of DBNs. They incorporate the temporal dimension by observing time-shifted versions of the variables, whether past or future, therefore the Markovian assumption is not needed. Conceptually they can be regarded as bringing an autoregressive model AR(n,m) to the BN domain.

Suppose a time series dataset. Figure 1 illustrates the proposed probabilistic model. Variable X represents the variable to be estimated, variables Y and Z represent pieces of Bayesian network corresponding to all the related variables to X. X_post represents the value of variable X at the time $t+1$, and X_ant represents the value of variable X at the time $t-1$.

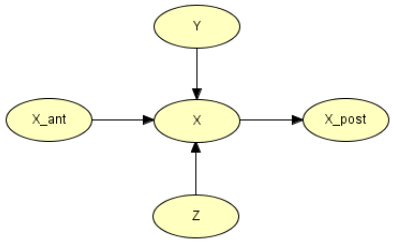

Fig. 1. Dynamic probabilistic model proposed for data estimation.

This proposed model represents a dynamic model which provides accurate information for estimating the variable in two senses. First, using related information identified by automatic learning algorithms or experts in the domain, or both. Second, using information of the previous and incoming values. This information includes the change rate of the variable according to the history of the signal.

In this approach the horizontal (inter-stage) topology of the network is fixed. The persistency arcs among a variable and its shifted versions are enforced, whereas those between different variables at different stages are forbidden.

D. Estimating missing data from incomplete databases using AR-BN

Summarizing, the proposed procedure for estimating missing data from incomplete databases is in Algorithm 1. The first 4 steps build the model, the last 3 propagate knowledge to estimate data holes.

III. Experiments and Results

Simulations were carried out to reconstruct missing data from 2 different industrial datasets of different nature (variables have been enumerated for confidentiality). The first dataset comprises 10 variables. It corresponds to a manufacturing process. The second dataset comprises 3 variables. It corresponds to an energy domain. Intrinsic dimensionality of the datasets as found by Principal Component Analysis is 7 and 1 respectively (99% of variance included). For the

 ISBN: 978-1-61208-246-2

Algorithm 1 Estimation of missing data

1: Obtain a complete data set that includes information from the widest operational conditions of the target process.
2: Clean the outliers and discretize the data set.
3: Utilize a learning algorithm that produces the static Bayesian network relating all the variables in the process. During the learning process a complete train set with data from all variables is needed as indicated in step 1.
4: Modify the static model to include previous and posterior values of every variable.
5: For all registers in an incomplete database, if one value is missing, instantiate the rest of the nodes in the model.
6: Propagate to obtain a posterior probability distribution of the missing value given the available evidence.
7: Return the estimated value with the value of the highest probability interval, or calculate the expected value of the probability distribution.

dataset 2, the scale of one of the variables is 5 orders of magnitude larger than the remaining 2 variables. Hence, the global intrinsic dimensionality is perceived to be 1 by PCA, but local dimensionality of the dataset remains 3, which can be determined by the Fukunaga and Olsen's algorithm [25]. The pairwise Pearson correlations among variables for the datasets in Fig. 2 hint about the dependencies among variables. Variables autoregressive order n was estimated using the Akaike Information Criterion [26] providing an indication of the signal own predictability. The autoregressive orders found with this criterion are summarised in Table I. Stationarity of the time series was estimated using the Kwiatkowski-Phillips-Schmidt-Shin (KPSS) test for stationarity and is summarised in Table II.

TABLE I
AUTOREGRESSIVE ORDERS AS CALCULATED WITH THE AKAIKE INFORMATION CRITERION.

Var.#	1	2	3	4	5	6	7	8	9	10
Dataset 1	2	2	1	2	2	9	7	9	9	9
Dataset 2	25	1	25							

TABLE II
KWIATKOWSKI-PHILLIPS-SCHMIDT-SHIN (KPSS) STATIONARITY TESTS. ** INDICATES A HIGHLY SIGNIFICANT VALUE ($p < 0.01$). * INDICATES A SIGNIFICANT VALUE ($p < 0.05$).

Var.#	**Dataset 1**	**Dataset 2**
1	$p < 0.01$**	$p = 0.01$*
2	$p < 0.01$**	$p = 0.014$*
3	$p < 0.01$**	$p = 0.01$*
4	$p < 0.01$**	
5	$p < 0.01$**	
6	$p < 0.01$**	
7	$p = 0.04061$*	
8	$p = 0.05843$	
9	$p = 0.04314$*	
10	$p = 0.02301$*	

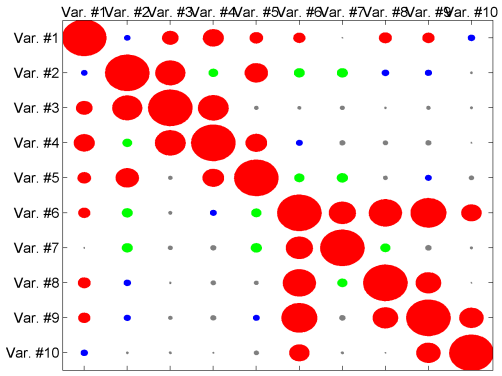

(a) Dataset 1

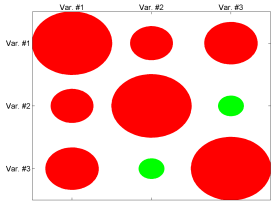

(b) Dataset 2

Fig. 2. Pairwise Pearson correlations among variables for the datasets. Circle size is proportional to correlation coefficient r. Circle color indicates significance: gray, non significant; blue, $p < 0.05$; green, $p < 0.001$; red, $p < 0.0001$;

From the datasets, specific samples were hidden to simulate missing values in three different fashions:

- Random Missing Data (**RMD**): Ghosted samples were chosen at random. Ghosted data accounts for 10% of each variable.
- Random Missing Blocks (**RMB**): Ghosted samples were chosen in blocks to have consecutive subseries of missing data. Ghosted data accounts for 10% of each variable. However, the location of the ghosted block and the number of blocks is random.
- All Missing Data (**AMD**): One full variable was ghosted at a time. Reconstruction can only occur from related information.

For each fashion, 10 train/test pairs were prepared for a 10-fold cross-validation. Note that the AMD has d test for each train case where d correspond to the number of variables in the dataset. After preparation of the ghosted test datasets, reconstruction was attempted by means of the following techniques:

- Static Bayesian Network (BN). Discretization was set to 5 equidistant intervals. Structure was learned using the PC algorithm [27].
- Autoregressive Bayesian Network (AR-BN). Autoregression order was fix to $< p, q >=< 1, 1 >$. Vertical (intra-stage) structure was learned using the PC algorithm. Equidistant intervals were used at all times, with the number of intervals being either 4 or 5 as bounded by memory limitations. The exemplary network for the Dataset 2 is illustrated in Fig. 3

 ISBN: 978-1-61208-246-2

- Linear interpolation (LI).
- Cubic spline interpolation (CSI).
- Autoregressive Models (AR(1))
- Autoregressive Models (AR(n)). Order n was chosen according to Table I. Notwithstanding, during the preparation of the train/test sets, some of the test sets did contain a number of samples lower than the autoregressive order i.e. AR order 25 for Dataset 1 variables 1 and 3. In those cases, the highest possible order was chosen based on the number of available samples.

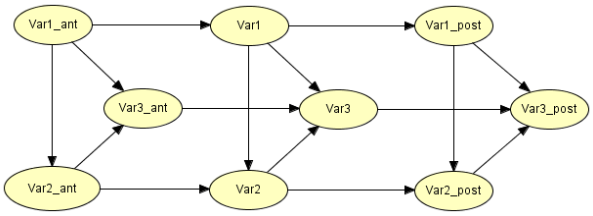

Fig. 3. Autoregressive Bayesian network proposed for data estimation for the Dataset 2.

In order to establish the accuracy of the estimation of the missing value the following error metrics were computed [28]:

Let E_i be the relative deviation of an estimated value x_i^{est} from an experimental value x_i^{obs}:

$$E_i = \left[\frac{x_i^{obs} - x_i^{est}}{x_i^{obs}}\right] \times 100 \qquad i = 1, 2, \ldots, n \qquad (3)$$

with n being the number of missing data.

- **Root Mean Square Error**:

$$e_{rms} = \left[\frac{1}{n}\sum_{i=1}^{n} E_i^2\right]^{1/2} \qquad (4)$$

- **Average Percent Relative Error**:

$$e_r = \frac{1}{n}\sum_{i=1}^{n} E_i \qquad (5)$$

- **Average Absolute Percent Relative Error**:

$$e_a = \frac{1}{n}\sum_{i=1}^{n} |E_i| \qquad (6)$$

- **Minimum and Maximum Absolute Percent Relative Error**:

$$e_{min} = min_{i=1}^{n}|E_i| \qquad (7)$$
$$e_{max} = max_{i=1}^{n}|E_i| \qquad (8)$$

As indicated above, for each reconstruction technique and ghosting fashion, a 10-fold validation was made. Since AMD scenario can only be reconstructed from related information, this scenario cannot be resolved by interpolation or autoregressive models. In total, 280 simulations were executed using MATLAB and Hugin [29]. For 3 simulations mistakes in pipeline from training to test were detected and their results not included for further analysis. Statistical analysis was carried out in R. R is a language and environment for statistical computing and graphics. See http://www.r-project.org/.

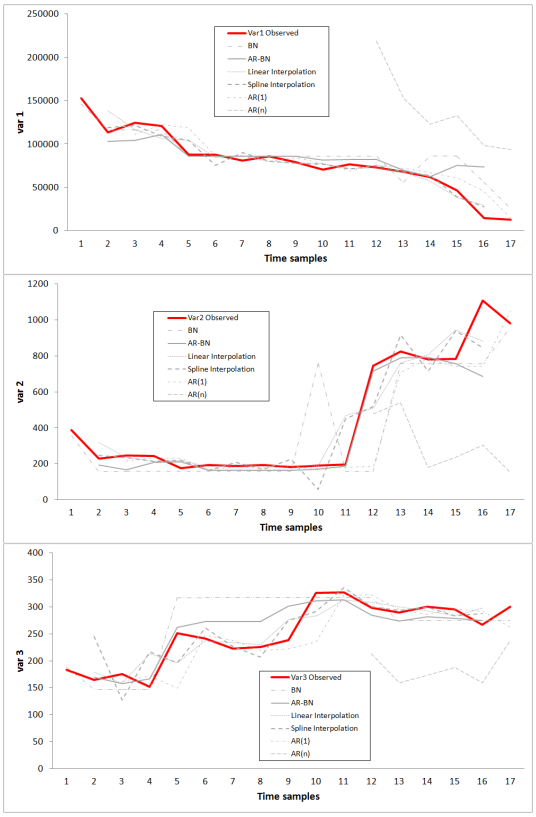

Fig. 4. Example of the missing data estimation using the different techniques. The example corresponds to the 3 different variables of Dataset 2 respectively for an RMD scenario. For this example, each sample of the time series is hidden one at a time, and the missing sample is estimated using the rest of the series as necessary by the different estimation techniques.

A. AR-BN performance

An example of the reconstruction with the different techniques is illustrated in Fig. 4. Fig. 5 summarizes the errors incurred by each technique, and Fig. 6 provides a more detailed view by dataset and error metric. From this detailed view, it can be appreciated that the proposed AR-BN achieves a good compromise in the reconstruction across different scenarios, datasets and error metrics. Unexpectedly, linear interpolation achieves better overall reconstruction than the more advanced spline interpolation. Classical autoregressive models achieve a reasonable performance but are highly unstable in their predictions as demonstrated by the large standard deviations coupled with disparate differences between e_{min} and e_{max}.

B. Limits of missing data estimation approaches

Fig. 7 relates the variable feature space given by the variable autoregressive order and its average relation to all other variables in its dataset (avg_r) against the dominant technique. The dominant technique is that which affords the lowest error in a particular region of the variable feature space. Regions are

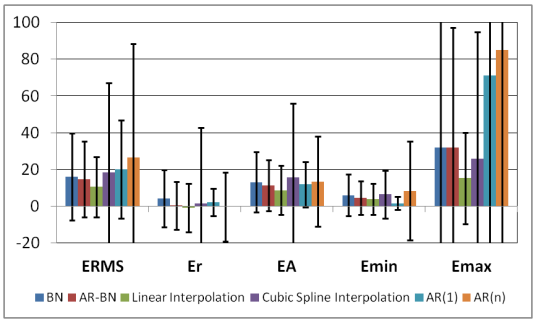

Fig. 5. Reconstruction errors incurred by each technique across datasets, scenarios, folds and variables. Bars and error lines correspond to average values and standard deviation respectively.

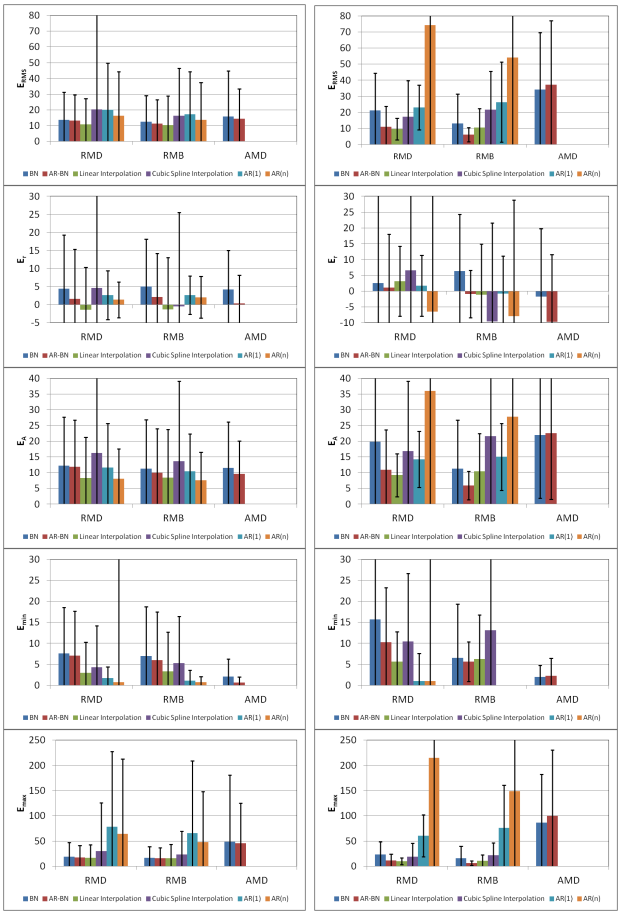

Fig. 6. Reconstruction errors incurred by each technique across folds and variables. Columns correspond to dataset; Left: Dataset 1; Right: Dataset 2; Rows correspond to different error metric: From top to bottom: e_{rms}, e_r, e_a, e_{min} and e_{max}. Bars and error lines correspond to average values and standard deviation respectively.

calculated using the Voronoi partition. It can be appreciated how the use of one technique over the other is subjected to the characteristics of the variable in terms of its autoregressive information as well as the amount of dependency that the variable share with fellow variables in the dataset as hypothesized. In particular, linear interpolation performs particularly well in these examples when the estimated autoregressive orders of the variables are low. When a full variable needs to be reconstructed from related information, it is obvious that the AR-BN dominance of the variable feature space grows as the autoregressive information does so.

IV. Conclusions and Future Work

We have explored the relation between a variable feature space represented by its autoregressive order and its relation to other variables in its dataset against different reconstruction techniques. Our results suggest that the interplay between the variables characteristics in the dataset dictates the most beneficial reconstruction option.

Unfortunately, the two datasets used in these simulations are not large enough to allow us exploring the variable feature space in detail. Yet some patterns start to be discernible. In particular, we have shown that the proposed AR-BN achieves a particularly competitive reconstruction regardless of the scenario, dataset and error metric used. Although we have reported signals stationarity for reproducibility, it has not further been considered for this paper. We believe signal stationarity will also be a critical element in the variable feature space supporting the decision over which estimation technique to use. Consequently, we plan to explore its effect.

The AR-BN model can be trivially extended to any level auto-regression and can be easily adapted for non-numerical data. In this sense, different autoregressive stages whether past or future must be added "in parallel" rather than "in series" so that these observations can be appreciated through the Markov blanket. We believe the proposed AR-BN profits from both within-variable information and statistical dependencies across variables, thus representing a valuable tool for the estimation of missing data in incomplete databases.

Acknowledgments

This research work is supported by the grant 146515 from CONACYT-SENER Sectorial Found.

References

[1] K. Hoo, K. Tvarlapati, M. Piovoso, and R. Hajare, "A method of robust multivariate outlier replacement," *Computers and Chemical Engineering*, vol. 26, pp. 17–39, 2002.

[2] B. Walczak, "Outlier detection in multivariate calibration," *Chemometrics and Intelligent Laboratory Systems*, vol. 28, pp. 259–272, 1995.

[3] J. Peng, S. Peng, and Y. Hu, "Partial least squares and random sample consensus in outlier detection," *Analytica Chimica Acta*, vol. 719, pp. 24–29, 2012.

[4] C. Muirhead, "Distinguishing outlier types in time series," *Journal of the Royal Statistical Society. Series B (Methodological)*, vol. 48, no. 1, pp. 39–47, 1986. [Online]. Available: http://www.jstor.org/stable/2345636

[5] R. S. Tsay, "Outliers, level shifts, and variance changes in time series," *Journal of Forecasting*, vol. 7, pp. 1–20, 1988.

[6] N. S. Balke, "Detecting level shifts in time series," *Journal of Business & Economic Statistics*, vol. 11, no. 1, pp. 81–92, 1993. [Online]. Available: http://www.jstor.org/stable/1391308

[7] B. Abraham and G. E. P. Box, "Bayesian analysis of some outlier problems in time series," *Biometrika*, vol. 66, no. 2, pp. 229–236, AUG 1979. [Online]. Available: http://www.jstor.org/stable/2335653

[8] D. Marr and E. Hildreth, "Theory of edge detection," *Proceedings of the Royal Society London B*, vol. 207, pp. 187–217, 1980.

 ISBN: 978-1-61208-246-2

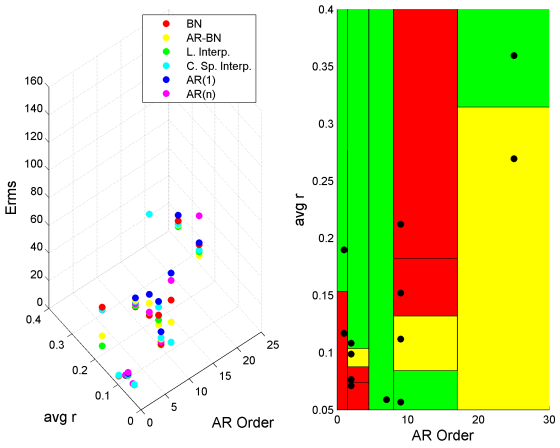

(a) RMD

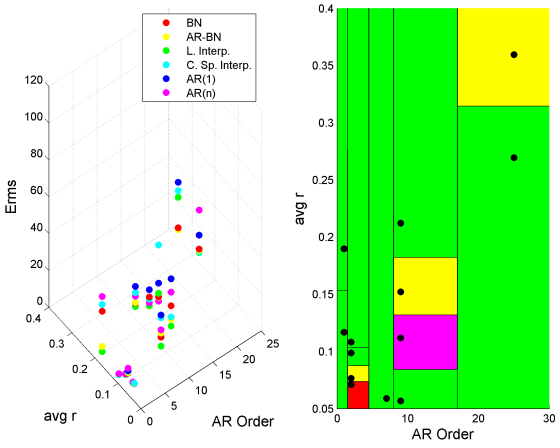

(b) RMB

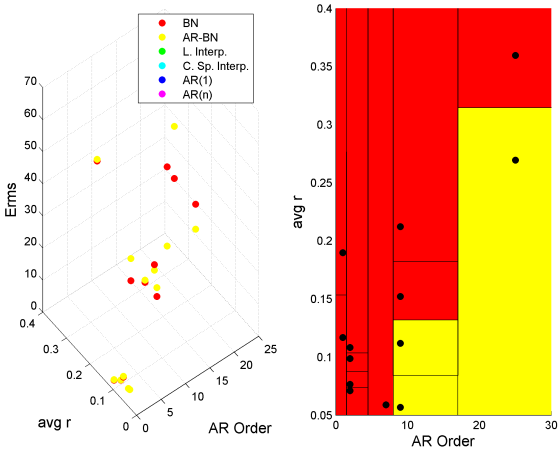

(c) AMD

Fig. 7. Relation between the variable feature space and the techniques for the three different scenarios. Left: Scatter plots of the variable feature space versus the error for each variable reconstructed through different techniques. The technique that achieves the lowest error is considered to dominate the region of the variable feature space. In order to determine the region of the variable feature space the different feature vectors for each of the variables for both datasets are used as seed vector quantizers for establishing a Voronoi partition. Each region of the Voronoi parcellation is then coloured according to the dominant technique.

[9] H. Sato, N. Tanaka, M. Uchida, Y. Hirabayashi, M. Kanai, T. Ashida, I. Konishi, and A. Maki, "Wavelet analysis for detecting body movement artifacts in optical topography signals," *NeuroImage*, vol. 33, pp. 580–587, 2006.

[10] J. Herrera-Vega, F. Orihuela-Espina, P. H. Ibargüengoytia, E. F. Morales, and L. E. Sucar, "On the use of probabilistic graphical models for data validation and selected application in the steel industry," *International Journal of Approximate Reasoning, In revision.*, 2012.

[11] B. Lamrini, E.-K. Lakhal, M.-V. Le Lann, and L. Wehenkel, "Data validation and missing data reconstruction using self-organizing map for water treatment," *Neural Computing and Applications*, vol. 20, pp. 575–588, 2011.

[12] V. Vagin and M. Fomina, "Problem of knowledge discovery in noisy databases," *International Journal Machine Learning & Cyber*, vol. 2, pp. 135–145, 2011.

[13] A. P. Dempster, N. M. Laird, and D. B. Rubin, "Maximum likelihood from incomplete data via the em algorithm," *Journal of the Royal Statistical Society. Series B (Methodological)*, vol. 39, no. 1, pp. 1–38, 1977.

[14] J. Herrera-Vega, F. Orihuela-Espina, E. Morales, and L. Sucar, "Validation data system based on a bayes network approach," in *Research Meeting on Dynamic Probabilistic Graphical Models and Applications*. Puebla, Mexico: FONCICYT, 3-4 JUN 2011.

[15] J. Herrera Vega, F. Orihuela-Espina, E. F. Morales, and L. E. Sucar, "A framework for oil well production data validation," in *Workshop on Operations Research and Data Mining (ORADM'2012)*, L. Villa-Vargas, L. Sheremetov, and H.-D. Haasis, Eds., Cancún, Mexico, 12-14 MAR 2012, pp. 226–235.

[16] P. H. Ibargüengoytia, S. Vadera, and L. Sucar, "A probabilistic model for information and sensor validation," *The Computer Journal*, vol. 49, no. 1, pp. 113–126, January 2006.

[17] P. Lancaster and K. Salkauskas, *Curve and surface fitting: an introduction*. Academic Press, 1986.

[18] C. Chatfield, *The analysis of time series: An introduction*. Boca Ratn: Chapman & Hall/CRC, 2004.

[19] P. H. Ibargüengoytia and M. A. Delgadillo, "On-line viscosity virtual sensor for optimizing the combustion in power plants," in *Advances in Artificial Intelligence - IBERAMIA 2010, LNAI 6433*, A.Kuri-Morales and G.Simari, Eds. Berlin Heidelberg: Springer-Verlag, 2010, pp. 463–472.

[20] J. Pearl, *Probabilistic reasoning in intelligent systems: networks of plausible inference*. Morgan Kaufmann, San Francisco, CA., 1988.

[21] D. T. and K. K., "A model for reasoning about persistence and causation." *Computational Intelligence*, vol. 5, no. 3, pp. 142–150, 1989.

[22] V. Mihajlovic and M. Petkovic, "Dynamic bayesian networks: A state of the art," University of Twente. Dept. of Electrical Engineering, Mathematics and Computer Science (EEMCS), CTIT technical report series TR-CTI 36632, 2001. [Online]. Available: http://doc.utwente.nl/36632/

[23] D. Koller and N. Friedman, *Probabilistic graphical models: principles and techniques*. MIT press, 2009.

[24] P. Hernández-Leal, L. E. Sucar, and J. A. González, "Learning temporal nodes bayesian networks," in *Twenty-Fourth International Florida Artificial Intelligence Research Society Conference (FLAIRS'2011)*. Florida, USA: Association for the Advancement of Artificial Intelligence, 18-20 MAY 2011, pp. 608–613.

[25] K. Fukunaga and D. R. Olsen, "An algorithm for finding intrinsic dimensionality of data," *IEEE Transactions on Computers*, vol. 20, no. 2, pp. 176–183, 1971.

[26] L. Ljung, *System Identification: Theory for the User*. Upper Saddle River, NJ, USA: Prentice Hall, 1999.

[27] P. Spirtes, C. Glymour, and R. Sheines, *Causation, Prediction and Search*. Cambridge, Massachusetts. U.S.A.: MIT Press, 2000.

[28] E. A. Osman, O. A. Abdel-Wahhab, and M. A. Al-Marhoun, "Prediction of oil pvt properties using neural networks," in *SPE Middle East Oil Show*. Bahrain: Society of Petroleum Engineers (SPE), 17-20 MAR 2001, p. 14 pp.

[29] S. K. Andersen, K. G. Olesen, F. V. Jensen, and F. Jensen, "Hugin: a shell for building bayesian belief universes for expert systems," in *Proc. Eleventh Joint Conference on Artificial Intelligence, IJCAI*, Detroit, Michigan, U.S.A., 20-25 August 1989, pp. 1080–1085.

 ISBN: 978-1-61208-246-2

Development of an Accelerator Safety System Using IEC 61508 and Design Pattern

Hao Zhang, Elder Matias

Canadian Light Source Inc.
University of Saskatchewan
Saskatoon, Canada
hao.zhang@lightsource.ca, elder.matias@lightsource.ca

***Abstract*—For particle accelerator facilities, Access Control and Interlock Systems (ACIS) are required to protect personnel from radiation hazards associated with accelerator operations. As an early adopter of IEC 61508 standard for safety system development, the Canadian Light Source, Inc. (CLS) faced several challenges in how to design engineering processes around the standard that reflected the safety requirements as well as the domain specific environment that we were working within. This industrial report outlines some of the challenges, considerations, and decisions on the adoption of IEC 61508 into a research facility like CLS. By following these principles and methods, overall Safety Integrity Level three (SIL-3) has been achieved. One contribution the CLS made in the adoption of IEC 61508 is that, applied design pattern approaches to domain specific safety algorithms like those used in ACIS. This paper outlines the introduction of design pattern approaches in CLS. A CLS developed design pattern is given as an example.**

Keywords-IEC 61508; ACIS; Design Patterns

I. INTRODUCTION

Historically, accelerator safety systems relied on relay-based interlock systems. As safety-rated Programmable Logic Controller (PLC) equipment became available in the market, it has been widely used for industrial safety systems. However, until very recently, the use of safety rated PLC equipment in accelerator safety systems has been rare. Accelerators built over the past five years have started to adopt safety rated PLC equipment primarily intended for the process control industry. CLS was an early adopter of such equipment.

Within the accelerator research and medical therapy community, the industry consensus has been that IEC 61508 [1] forms the basis of best practice, and this has resulted in wide adoption of this standard with specific examples including:

- Synchrotrons: ALBA Synchrotron [2], and Diamond Light Source [3].
- Accelerators: Large Hadron Collider (LHC) of the European Organization for Nuclear Research (CERN) [4], Jefferson Labs' Thomas Jefferson National Accelerator Facility (TJNAF) [5], Mégajoule Laser Program [6], and ISIS spallation neutron source [7].
- Medical Accelerator Facilities: Heidelberg Ion Therapy Facility [8], and Selective Production of Exotic Species (SPES) [9].

When applying the IEC 61508 standard to the design of the Access Control and Interlock Systems (ACIS) for CLS accelerator, the special contexts of the accelerator environment need to be taken into considerations. To address these considerations, a design pattern approach is introduced into the system life cycle for the CLS ACIS system.

Conventional software engineering techniques have embraced the concept of design pattern over the past two decades. However, these approaches have seen limited use in safety critical systems design [10]. Some recent work has focused on very generic design patterns [11] [12]. Yet, we are not aware of these approaches being applied to domain specific algorithms across the entire IEC 61508 life-cycle.

The following lists some key points and considerations when adopting design pattern approaches in CLS ACIS design:

a) Unlike other systems, in the case of accelerator access control and interlock, some common safety scinarios repeat themselves from one accelerator zone to another. In this contxt, we see pattern as a valuable tool in the design of ACIS. In this design approch, the ACIS algorithm involves a series of design patterns that provide general solutions to the common recurring situations for accelerator access control and interlock.

b) Though all lockup zones operate in similar manners, there are different variations based on the number of entrieis, exits, lockup stations and search paths.The ACIS design patterns provide a set of templates or guidelines with the flexibility that the patterns can be altered to fit specific design needs for individual zones.

c) The hazard analysis, design, verification and validation procedures must be able to effectively manage and deal with both the generic issues in common safey situations and special cases and exceptions for individual zones in an effective way. Here, again, the extended concept of design pattern provides a good solution.

The motivation of this industrial report is to give an overview of major aspects of CLS ACIS with the following two emphases:

1) The application of IEC 61508 principles, methods, and processes in the design and development of the CLS

 ISBN: 978-1-61208-246-2

ACIS. Some of the challenges, considerations, and decisions on the adoption of this industrial standard into a research facility like CLS will be outlined. By following these principles and methods, overall SIL-3 rate, as defined in [1], has been achieved for the ACIS.

2) The adoption of design pattern methods in the CLS ACIS design. By using patterns in ACIS design, we are able to create reusable solutions for common accelerator safety scenarios, promote software reuse, and save time in the design and engineering stages.

In Section II, additional background is provided on aspects of regulatory context, the development process and requirements of the system, and the considerations and practices for CLS to establish system boundaries. Section III gives details of the major safety functions for the ACIS. Sections IV, V, and VI, cover the aspects of hardware, software, and interface of ACIS, respectively. A short introduction to the validation and verification procedure is given in section VII. Section VIII identifies possible future works for improvement.

II. BACKGOUND

A. Application Context

The Canadian Light Source (CLS) facility consists of two accelerators in series used to take electrons from rest to 2.9 GeV, the electronics are then deposited into a high current storage ring. Synchrotron light (covering a wide spectrum from visible to hard x-ray) is extracted from the storage ring and used to perform experiments on suite of independent beamlines covering a wide range of science from advanced materials, to environmental and life sciences.

Particle accelerators can produce hazardous levels of radiation if not appropriately shielded during operation. This is usually accomplished through the use of shielding and a safety system that ensures that staffs are not present during normal operation. Due to safety considerations, a systematic systems engineering process needs to be adopted, and tailored to provide sufficient flexibility for use in a research organization such as the CLS.

In CLS, ACIS is used in restricted areas to protect personnel from radiation hazards. The ACIS controls access to the accelerator hall and tunnels during accelerator operation to ensure staffs are not present when the accelerators are in operation. These areas are divided into lockup zones, which contain the Linear Accelerator (Linac), Linac-to-Booster Transfer Line (LTB), the Booster Ring (BR), the Booster-to-Storage Ring Transfer Line (BTS), and the Storage Ring (SR). Lockup zones are locked up independently, each having its own Emergency off Stations (EOS), Door Interlock Switches (SWDI), Lockup Stations (LUS), zone lockup lights (ZLL), and horns (HRN).

This system adopts a two-level, redundant protection mechanism, which consists of two independent chains, one is governed by a PLC system rated SIL-2 as defined by [1], and a relay based hardware logic to provide diversity for major safety functions. Overall, the ACIS requirement is for SIL-3. SIL-3 is achieved by the use of the two independent, redundant, fail-safe systems that are SIL-2 certified.

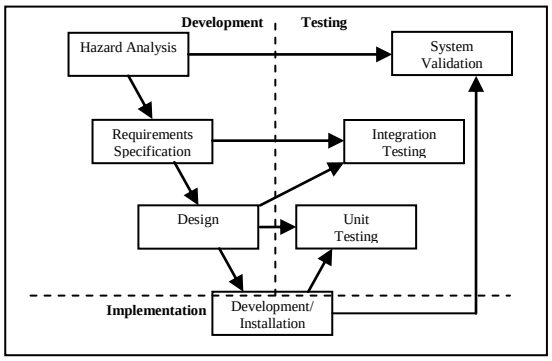

Figure 1. Safety System Development Process.

B. Regulatory Context

CLS holds a Particle Accelerator Operating Licence (Class IB) issued by the Canadian Nuclear Safety Commission (CNSC); as a result, the definition of internal process is left to the CLS to define and propose with the CNSC providing regulatory oversight.

C. Safety System Development Process

In the past, when accelerator facilitates designed safety systems, the common approach was to simply scale up the rigor used in the design of their non-safety critical systems, and try to make the system as fail safe as possible. Over the past decade and a half, there has been an increasing interest in the community in the adoption of broader industrial standards and certified equipment, more specifically IEC 61508. CLS was one of several facilities that were early adopters of IEC 61508.

The above Figure 1 shows the Safety System Develop Process. As illustrated in Figure 1, the CLS safety system development process starts with the Hazard and Risk Analysis [1]. The mitigation measurements identified by the Hazard and Risk Analysis are then allocated to different sub-systems, which includes administrative procedures, preventive measurements, and safety systems. Those allocated to the safety system become the basis of design requirements and specifications. Once detailed requirements are generated and documented, the design and implementation can be carried out. Testing and validation are performed in all development stages. Respectively, integration and unit testing verify the design meets the requirements, and the installation is done as the design.

D. System Boundaries

Establishing system boundaries is critical in this type of environment. The main control for the CLS facility has in excess of 600 control computers working with 50,000 to 100,000 data points. Clearly, generating system boundaries between safety systems, equipment protection systems, critical control functions developed by the facilities, and

 ISBN: 978-1-61208-246-2

systems modified by outside researches and users to meet their specific experimental needs are important.

A strong emphasis is placed on high system cohesion and minimizing inter-system coupling within the design. After ten years of evolution of these systems, we have found it necessary to periodically revisit the boundaries and adjust the allocation of requirements based on evolving system requirements.

The primary accelerator control system is implemented using a distributed control system platform called Experimental Physics and Industrial Control System (EPICS) [16]. EPICS was originally developed at Los Alamos for the control of particle accelerator and has gain wide acceptance within the accelerator and nuclear physics community. However, it is not suitable for implementation of the safety functions directly. Care is taken to ensure that the system boundaries between the ACIS system and the rest of the control system are failsafe.

E. Hazard Analysis

The ACIS development process starts with the Hazard and Risk Analysis to identify the hazards and their causes, and to list appropriate mitigations needed to achieve a tolerable risk level. The document issued was used as input to the following development stage.

IEC 61509 [1] defines several alternative risk analysis tools/techniques. On most CLS safety projects the As-Low-As-Reasonably-Practical (ALARP) technique is used [1]. Using a qualitative as opposed to quantitative process appears to be the best practice for CLS, especially given the unique nature of some of the limit custom designed components that are used in some of the systems. Special care has been needed in doing the Hazard and Risk Analysis to try to identify anticipated changes in ensuring that the design does not preclude potential future experimental programs.

This process involves conceptual design review to determine if there are hazards intrinsic to the design, human factors task analysis to understand how operators and users interact with the systems., simulation and desktop walk-throughs to examine any potential failures at each stage using hazard guide words, in the forms of one-one interviews with stakeholders or a structured meeting/workshop driven by keywords.

For some common hazards found in the accelerator operation context, basic design pattern concept is also applied in the Hazard and Risk Analysis process. We express each of such hazards in a generic way when analyzing the hazards posed by a generic hazardous situation; this allows us to subsequently examine special cases that may exist in specific applications of the pattern.

Within the hazard analysis the mitigation is identified for each hazard to bring the residual risk to an acceptable level.

F. Design Requirements

The mitigations identified in the Hazard and Risk Analysis are then allocated to the sub-systems and refined to generate design requirements for the ACIS. Other internal or external guidelines, such as human factor guideline [13] and Canadian Electrical Code were also incorporated as requirements in this stage. A design manual is generated to document all requirements. Lockup zone layout drawings are generated to capture detailed requirements and design information. The drawings show zone configurations, lockup paths, and all safety components, which were all identified and numbered. The ACIS layout drawings make an IO count possible and will be used as the input documents for generation of engineering details in the following design phases.

III. SAFETY FUNCTIONS

The ACIS provides four major functions: *secure*, *lockup*, *annunciation*, and *interlocking*. As described in earlier sections, the system consists of two separate chains, each having their own inputs and outputs. The PLC chain provides all four functions; the relay chain provides redundant functions in safety critical aspects of secure and interlocking.

A. Secure

A lockup zone is secured only when all the doors are closed and none of the EOSs is pressed. The secure function is implemented independently in both chains.

Limit switches are used to monitor door position. Each door has two physically independent switches for signalling the two separate chains.

An EOS consists of an emergency off button, a reset button, and three mechanically interlocked and latching contacts - two normally close contacts for signaling the two chains and one normally open contact for activating a local red LED when the EOS is pressed. If the emergency off button is pressed, all contacts remain latched and the red LED remains on until the reset button is pressed.

The accelerator is interlocked if any of the zones are not secured. The redundant design ensures even component in one chain fails, the other still functions to interlock the accelerator.

B. Lockup

A zone is considered locked up only when the lockup sequence, designed by the CLS Health Safety and Environment (HSE) department specifically for each individual zone, has been performed successfully in this particular zone. Two inspectors are required to perform the sequence, which involves walking through a prescribed path within certain time limit to ensure every part of the zone is inspected in a timely manner.

LUSs are installed in selected locations to ensure the path is followed and the process is timed. Each LUS has a lockup button for signalling the PLC chain, and a green LED to provide visual indication to the inspectors.

As an administrative procedure, the lockup sequence is performed by inspectors and redundantly verified by the PLC. As the complexity of a system increases, so does the potential to introduce errors and possibly hazards. Implementing the multiple sequences in hardware is more likely to introduce error and potential hazards than it is to

 ISBN: 978-1-61208-246-2

provide extra protection. Therefore, lockup function is implemented only in the PLC chain.

C. Annunciation

Horns and flashing lights are positioned in the zones and control room to provide audible and visual annunciations to personnel in those areas.

D. Interlocking

The accelerator is interlocked from both chains through multiple permissive channels to avoid single failure point. When the accelerator is interlocked the radiation source is removed and the system falls to the safe state.

Figure 2 shows the implementation of safety functions of Secure, Lockup, and Interlocking.

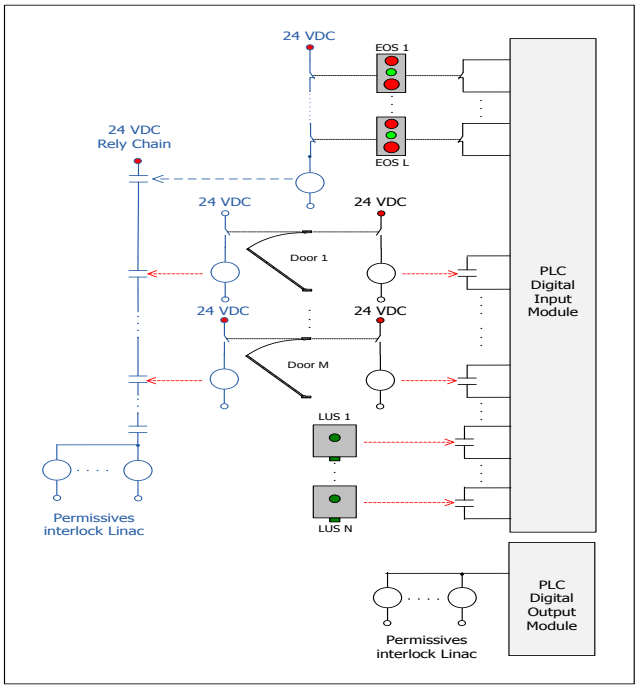

Figure 2. Implemetation of Secure, Lockup, and Interlocking

IV. ACIS HARDWARE

A. PLC Configuration

Siemens AS414-4H processor was selected for the CPU. With the fault-tolerant run-time license installed on the processor, the built-in fail-safe run-time logic is activated. Password protection is also activated to protect the processor from re-programming.

SIL-3 certified modules with internal diagnostics and redundant circuitry are used for field Inputs/Outputs (I/O). These modules are installed in remote I/O stations communicating with the CPU over Profibus using the PROFISAFE protocol. Fibre-optic cable is used for data link. This configuration is based on accepted practice for SIL-3 applications. The protocol is deterministic and failsafe when used with failsafe hardware. The use of distributed I/O via fibre-optic cable provides electrical decoupling of the system, thus avoiding problems associated with running signals over long distances. Given potential problems with ground loops, Electromagnetic Interference (EMI) noise and signal degradation using conventional means, this architecture is more reliable and safe.

B. Field Wiring

Some of the field wirings are located in the basement Linear Accelerator (Linac) hall, where leaking underground water at certain locations can cause problem. For this reason, National Electrical Manufacturers Association (NEMA) Type 4 rated enclosures were carefully chosen for PLC panels, junction boxes, EOSs, and LUSs to achieve water protection. For the same reason, field instrumentations are wired using water-proof multi-conductor armoured instrumentation cables, which run in dedicated conduit with distinct color and not shared with other systems or equipment. All field components are Canadian Standard Association (CSA) approved.

Extended design pattern concept is also adopted for the wiring design. Standard patterns associated with common sensor types and their common combinations are identified, and optimized wiring templates are developed. These patterns repeat themselves over and over for each common sensor type and combination and are generated using automated scripts in AutoCAD.

C. Operator Interface

The principle operator interface is based on the use of hard-wired operator panels. Some discrete I/O points are provided from the safety system to the EPICS based control system.

V. ACIS SOFTWARE

The PLC programming toolset is Siemens SIMATIC Manager, using Continuous Function Chart (CFC), a graphical language involving interconnecting elementary Function Blocks (FB) to implement control logics.

A. Design Pattern Based Program Sturcture

The concept of design pattern was first introduced in the field of architecture [14] and later has been adopted in other disciplines, especially software domain [15]. A design pattern involves three major elements: context, problem and solution [14]. Generally speaking, a design pattern is a solution to a commonly reoccurring problem in a given context.

In CLS ACIS design, several design patterns have been developed. These design patterns include the Zone Lockup design patter, the Major-Fault design pattern, and the All-Clear design pattern, each provides solution to a common ACIS problem. In this section, the Zone Lockup design pattern is used as an example to illustrate how design pattern approaches are used in CLS ACIS design.

For CLS lockup zones, although each of them are different in layout and geographical size, and contains different numbers of ACIS components, with different

 ISBN: 978-1-61208-246-2

lockup paths designed individually; the types of ACIS components in each zone are limited to a common set including Emergency Off Stations (EOSs), Lockup Stations (LUSs), Door Interlock Switches (SWDIs), Zone Lockup Lights (ZLLs), and Horns (HRNs), and the lockup sequence and interlock logic for all zones follow the same principles. Locking up an individual zone, and interlocking the accelerator based on zone lockup status, is a recurring problem in the context of CLS accelerator operations. A well-designed, optimized, and thoroughly tested set of best practices should be standardized to provide reusable solution to this problem. This formed the basis for design pattern based program structure.

The Plant View function under the Siemens SIMATIC Manager provide an ideal tool to support design pattern based program structure. In Plant View, the software is structured hierarchically following the actual lockup zone layout. A folder is assigned to each zone, and each zone folder has three CFC charts, known as the standard zone charts. The names of the standard zone charts comply with conventions as follow:

- ZONE<ID>_EOS
- ZONE<ID>_DOORS
- ZONE<ID>_LOCKUP

In the above naming convention, <ID> is a generic descriptor, when assigned to a specific zone, the real zone ID number should be used instead.

The ZONE<ID>_EOS chart contains codes to monitor EOS inputs of this zone and provide EOS status output to the ZONE<ID>_LOCKUP chart. The ZONE<ID>_DOORS chart monitors SWDI inputs of all doors and gates in this zone and provide shielding status output to the ZONE<ID>_LOCKUP chart. The ZONE<ID>_LOCKUP chart monitors inputs from zone LUSs and incorporated these inputs with the inputs from the other two charts to perform lockup sequence and provide outputs to annunciation and interlock modules.

In each of the standard zone charts, standard ACIS FBs are used to handle functions associated with generic components and process. All these ACIS FBs are developed in CLS, and have been thoroughly tested. The implementation details of FBs can be hidden from programmers who are new to ACIS design. For a programmer to use these FBs, all he or she needs to do is, choosing the right types and numbers of ACIS FBs based on the actual zone situation, and making interconnections between the inputs/outputs of component and process FBs .

The zone folder, standard charts, and standard ACIS FBs, as a whole, defines the structure of the Zone Lockup design pattern. As a template and a set of guidelines for the zone lock up problem, the design pattern is generic in nature, however, when instantiated, can accommodate differences and variations from zone to zone.

In a sense, the Zone Lockup design pattern encapsulates the initial ACIS designers' time and expertise to a reusable standard solution for the zone lock up problem. Therefore, the future designers need not to reinvent the wheel, and thus helps to lower cost and save time for future ACIS development. And reuse of well tested pattern also increases the reliability and continuity of the system as a whole.

B. Failsafe Code

Safety critical codes are developed using TÜV-certified function blocks from S7 Fail-Safe Systems Library to ensure fail-safe feature. All failsafe codes are assigned to Organizational Block (OB) 35 by default and are executed cyclically every 100ms in runtime.

Siemens allows developers to create their own standard or failsafe FBs. In CLS, FBs for typical ACIS functions were developed in earlier projects and a CLS ACIS block library are created to save them. As mentioned in earlier section, those ACIS FBs play an important role in the implementation of design pattern based program structure.

C. Simulation

The ACIS program had been tested thoroughly using Siemens software simulator, PLCSIM, before it was downloaded to the CPU for on-line testing. Since the system involves only On/Off variables, software simulation is sufficient to test the control logic.

D. Real-time Requirements

Based on the PLC cycle time, and execution time for the logic blocks, a spreadsheet is used to calculate the algorithm executive time and verify that the real time performance of the system can be achieved.

E. Version Control

For safety system software, it is critical to ensure correct version is loaded onto the processor. Siemens S7 F system provides safety program signature to uniquely identify a particular state of the safety program. Generally speaking, a 32-bit number known as the signature is generated across all the fail-safe blocks of the safety program at the end of the compilation phase.

In CLS, a commercial version control software called MKS Source Integrity [18] is used for version control. Versions of the ACIS program at different development and maintenance stages are saved in the MKS repository. With the signatures as identifiers, the correct version can be easily located for download.

VI. EPICS INTERFACE

Currently, a limited number of discrete digital I/O channels are used to provide an interface between the ACIS and the EPICS system, with the EPICS based control system not performing a direct safety function.

The EPICS software is implemented in C/C++ running on either Real-Time Executive for Multiprocessor Systems (RTEMS) [17] or Linux based computers. The process variables from acquired by EPICS can be displayed to the operator as well as being feed into a central alarm management system for the entire facility.

An expected future enhancement is to feed both the ACIS and other high speed control interlocks into a custom sequence of events record to provide more accurate first fault indicator information.

 ISBN: 978-1-61208-246-2

VII. VALIDATION AND VERIFICATION

Validation and Verification (V&V) procedures are developed to examine if the operation of the ACIS within specifications as outlines in requirements and design documents. The overriding approach to the testing methodology is a meticulous and exhaustive series of tests to ensure that the system operates as required. The V&V document was developed by staffs who were not involved in the design process to assure independence. The V&V procedure is executed by HSE department, which was independent of the responsibilities for the design of the system. Any modifications to the system after the V&V will cause the V&V procedure being updated and the V&V has to be performed again.

VIII. CONCLUSION AND FUTURE WORK

As an early adopter of IEC 61508, we faced several challenges in how to design engineering processes around the standard that reflected the safety requirements as well as the domain specific environment that we were working within. The use of design patterns played an important role through the entire process in being able to effectively and efficiently design these systems.

Tighter integration between the ACIS and EPICS is required to more effectively provide operational staff with the ability to accurately understand the sequence of events on an accelerator machine trip. There is currently a simplified sequence of events recorder in use for the Storage Ring (SR); however, this needs to be expanded. It is expected that such as system will require the use of high speed electronics.

Work is also underway in developing methods to streamline the verification and validation process, where testing is targeted separately at both the generic pattern that is reused as well as those aspects of the pattern that have the potential to be incorrectly implemented.

ACKNOWLEDGMENT

Research described in this paper was performed at the Canadian Light Source, which is supported by the Canadian Foundation for Innovation, Natural Sciences and Engineering Research Council of Canada, the National Research Council Canada, the Canadian Institutes of Health Research, the Province of Saskatchewan, Western Economic Diversification Canada, and the University of Saskatchewan.

REFERENCES

[1] International Electrotechnical Commission, IEC 61508, “Functional Safety of Elecronic/Programmable Electronic Safety-Ralated Systems" International Electrotechnical Commission, Geneva, 1998

[2] D. Fernandez-Carreiras et al., "ALBA, the PLC based protection system," in Proc. ICALEPCS 2009, pp. 397-399, Kobe, Japan, 2009.

[3] M. C. Wilson and A. G. Price, "Development of the Diamond Light Source PSS in conformance with 61508," in Proc. of ICALEPSC2011, pp. 1289-1292, Grenoble, France, 2011.

[4] P. Nanin, "IEC 61508 experience for the development of the LHC Functional Safety Systems and future perspectives," in Proc. of ICALEPCS 2009, pp. 400-402. , Kobe, Japan, 2009.

[5] K. Mahoney and H. Robertson, "Jefferson Lab IEC 61508/61511 safety PLC based safety systems," in . Proc. ICALEPCS 2009, pp. 394-396., Kobe, Japan, 2009.

[6] J. C. Chapuis, J. P. Arnoul, A. Hurs, and M. Manson, "The Laser Megajoule Facility personal safety system," in Proc. of ICALEPCS 2011, pp. 1070-1072, Grenoble, France, 2011.

[7] D. J. S. Findlay et al., "ISIS upgrade – a status report.," in Proc. HB2006, pp. 20-23, Tsukuba, Japan, 2006.

[8] S. Scheloske, S. Hanke, and J. Mosthaf, "Overview of the personal protection System at the Heidelberg Ion Therapy Facility," in Proc. of PCaPAC08, Ljubljan, Slovenia, pp. 88-90, 2008.

[9] G. Bassato et al.,"Safety requirements in SPES control system: preliminary design," in Proc. of ICALEPCS09, pp. 585-587, Kobe, Japan, 2009.

[10] A Armoush., E. Beckschulze, and S. Kowalewski. “Safety assessment of Design Patterns for safety-critical embedded systems” in Proc. 35th Euromicro Conference on Software Engineering and Advanced Applications pp. 523-527. DOI 10.1109/SEAA.2009.12, Paras, Greece, 2009

[11] S. P Kumar, P. S. Ramaiah, and V. Khanaa, “Architectural patterns to design software safety based safety-critical systems.” in Proc. ICCCS11, pp. 620-623, Odisha, India

[12] J. Rauhamäki1, T. Vepsäläinen1, and S. Kuikka1 “Functional safety system patterns.” in Proc. VikingPLoP 2012, pp. 47-68, Saariselkä, Finland

[13] M. McKibben, “CLS human factors workscope”, 0.1.1.1, Rev 1, 2008, unpublished

[14] C. Alexander, “A pattern languge : twons, buildings, construction.” Oxford University Press, New York, 1977

[15] E. Gamma, R. Helm, R. Johnson, and J. Vlissides. “Design Patterns: element of resusable object-oriented software.” Addison-Wesley, Boston, MA, USA, 1997

[16] http://www.aps.anl.gov/epics/ [retrieved: December, 2012]

[17] http://www.rtems.org/ [retrieved: December, 2012]

[18] http://www.mks.com/ [retrieved: December, 2012]

 ISBN: 978-1-61208-246-2

A New Laboratory Equipment for Characterization of Smart Concrete Materials

Ladislav Machan, Pavel Steffan
Department of microelectronics
BUT, FEEC
Brno, Czech Republic
machan@feec.vutbr.cz, steffan@feec.vutbr.cz

***Abstract*—"Smart Concrete" materials are concrete composites prepared according to the final application to achieve high electrical conductivity or strain gauge characteristics. Large electrical conductivity is used for heating control (protection sidewalks and roads from freezing). Strain properties can be used to measure the deformation of concrete structures (bridges, beams, pillars) or for weighing-in-motion of road vehicles.**

Keywords—smart concrete; impedance measurement; heating controll

I. INTRODUCTION

"Smart materials" are drawing more and more attention these days. One of the most common structural materials used in engineering construction is cement and its mixtures (concrete and mortar). Cement is slightly conducting material, but its electrical conductance, EMI shielding effectiveness and wave absorbing property are very poor. In order to increase the ability of cement materials to conduct and shield EMI, additional conductive or absorbent fillings and loadings have to be introduced to admixture to provide higher EMI preventing effectiveness [1]. "Smart concrete" (SC) and its derivatives could be consider as a material of the future. Due to its attractive features, SC can be used as a strain-sensing element, as a resistive heating or as an EMI shielding.

II. MEASUREMENT OF STRAIN PROPERTIES

Strain properties of the composite can be evaluated by impedance changing. The impedance changing sensitivity regarding the deformation can be widely affected by a proper choice of concrete admixtures [2]. Generally, in all types of admixtures, the real component is not much affected by the deformation, on the other hand, the imaginary component is, and can be used to detect the changes [3]. For impedance measuring, an excitation frequency of 1 KHz, and an excitation voltage of 1 V (peak-peak) were experimentally set [4]. During the measurements of experimental samples, a necessity to a simple, relatively inexpensive and portable device has been raised.

A. Construction of "Z-meter"

This battery-powered device facilitates its usage in the experimental field. According to the aforementioned requirements, a block diagram of the instrument has been suggested. The diagram is shown in Fig. 1. The device function is based on 16-bit MSP430F5438 microcontroller, which uses RISC architecture. This microcontroller can be "in circuit" programmed via JTAG interface. Interface also allows real-time debugging of firmware, which ensures all device functions. A 16-level yellow Organic Light Emitting Diode (OLED) graphical display that has 256 x 64 pixel resolution is used for visualizing the measured values and navigating during measurement parameters setting. The communication with OLED display is done via Serial Peripheral Interface (SPI). The function of those pushbuttons is determined during the navigation and shown on the bottom part of the display. The device is equipped with a buzzer that warns the user of important states of the device. This feature is built for convenient usage of the device. An integrated 4 Mb memory and SD card, which can be inserted into a side slot, are enclosed for saving the measured data. Both memories communicate with the microcontroller via SPI interface. A special circuit designed by FTDI Company enables USB interface connection for transferring the measured data into the PC. This circuit communicates with the microcontroller via UART.

Moreover, the aforementioned USB is used for device supplying and internal Li-Pol accumulator charging. This feature helps to supply the device in case of necessity to perform outdoor measurements. The supply voltage supervising is maintained by a group of supply blocks located at the bottom part of the diagram, shown in Fig. 1. The charge control circuit, designed by Microchip Company, controls the accumulator changing, and stops it when the maximum voltage is reached. A buck-boost converter provides 3.3V for supplying the digital circuits. On the other hand, analog blocks are supplied by 5 V and 3 V. The 5 V supplying circuit is realized by charge pump. The 3 V supplying circuit is realized by the reference voltage source with minimal noise, designed by Analog Devices. The reference voltage 3 V is used for supplying the AD5933 impedance converter [5].

 ISBN: 978-1-61208-246-2

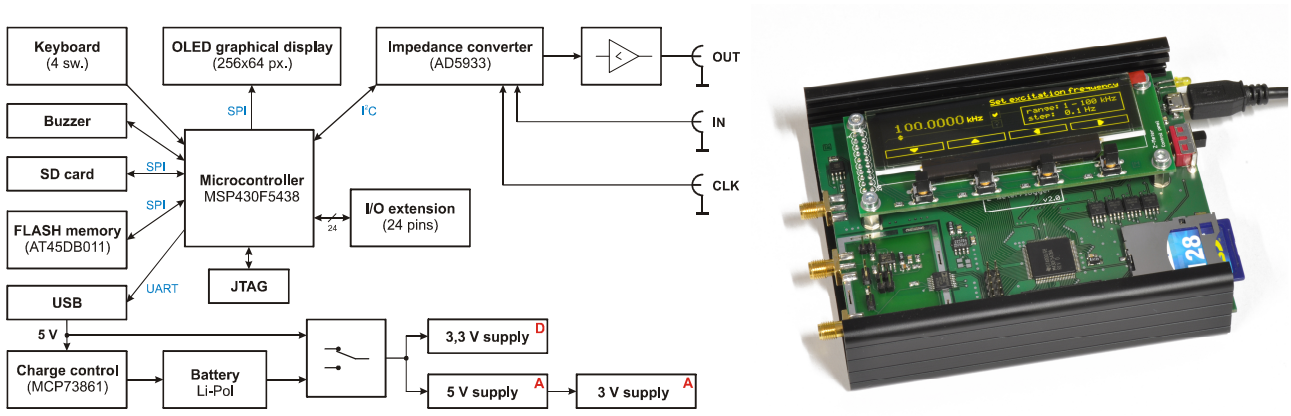

Figure 1. The block diagram and physical appearance of proposed Z-meter

The 24 unused I/O pins of the microcontroller are attached to an expansion connector for universal use. The mechanical design of the proposed device is realized according to the following requirements: portability and durability. The printed-circuit boards along with the supplying accumulator are enclosed in the aluminum case.

B. Impedance converter AD5933

The impedance measuring depends on the AD5933 integrated circuit, which permits setting the required value of the excitation voltage and frequency. The excitation frequency can be set between 1 and 100 kHz in steps of 0.1 Hz. The impedance measuring range is 100 Ω to 10 MΩ with a 12-bit resolution. The communication with the circuit is done via the serial I^2C bus.

C. Measurement automation and data processing

The device is equipped with a galvanic isolated external input that triggers the start of the measurement and synchronizes it with other measuring devices. Some measuring devices don't have that external trigger. The proposed device handles that synchronization according to a time sequence. The measured data can either be stored in the device internal memory (FLASH, SD card) or transferred via USB interface to the PC.

III. HEATING CONTROL AND MONITORING

The aim when designing the control electronics for the new panel has been tempered to direct regulation of cement composite with carbon nanoparticles based on processes inside the composite material tempered. The system is controlled by a set of sensors located inside and outside the composite (tempered) panel. Sensors implemented inside the composite material provide immediate information on the status of the material, external sensors will evaluate the state of environment and to effectively regulate the entire system.

Using SC as a resistance heating is a complementary method that needs to be investigated. The resistivity of concrete can be diminished by using an electrically conductive admixture, such as discontinuous carbon nanofibers, discontinuous steel fibers, steel shaving and graphite particles [6], [7]. Combining and changing an admixture ratio leads to different value of resistivity. A control device had to be designed to test and evaluation of the samples and to find the ideal admixture ratio and heating element pattern.

A. Construction of temperature control unit - "RCT"

The control unit can be divided into two parts, namely the power and control. Power section contains only a toroid transformer 230 V / 2 x 24 V (500 W), which provides ample power for heating elements and tempered serves to control the power that is supplied from the converter with high efficiency 3.3 V. Unit can independently control Load up to 3 (3 tempered components) with power consumption up to 6 A for each channel. The maximum allowable current is monitored as the sensor current and fuse.

The control part consists of parts, which includes the control part with the microcontroller, high-contrast alphanumeric LCD display, backlit, a system of sensors to measure temperature, humidity and electrical power, power section with a converter with high efficiency, switching thyristors excited by optotriacs, Bluetooth Module Class 1 terminal server (XPort) for communication over Ethernet. The overall block diagram and physical appearance is shown in Figure 2. Data is automatically saved on the SD / MMC card or via Ethernet to a remote server or over Bluetooth to other mobile devices. Choice of connection depends only on the user.

The control section provides all system functions RCT. MCU processes the data from sensors, switches different circuits, stores data on SD / MMC card, controls the communication with the environment and writes the current data on the LCD display. For sufficient computing power was voted an 8-bit Microcontroller Atmel ATmega128 with the type designation.

 ISBN: 978-1-61208-246-2

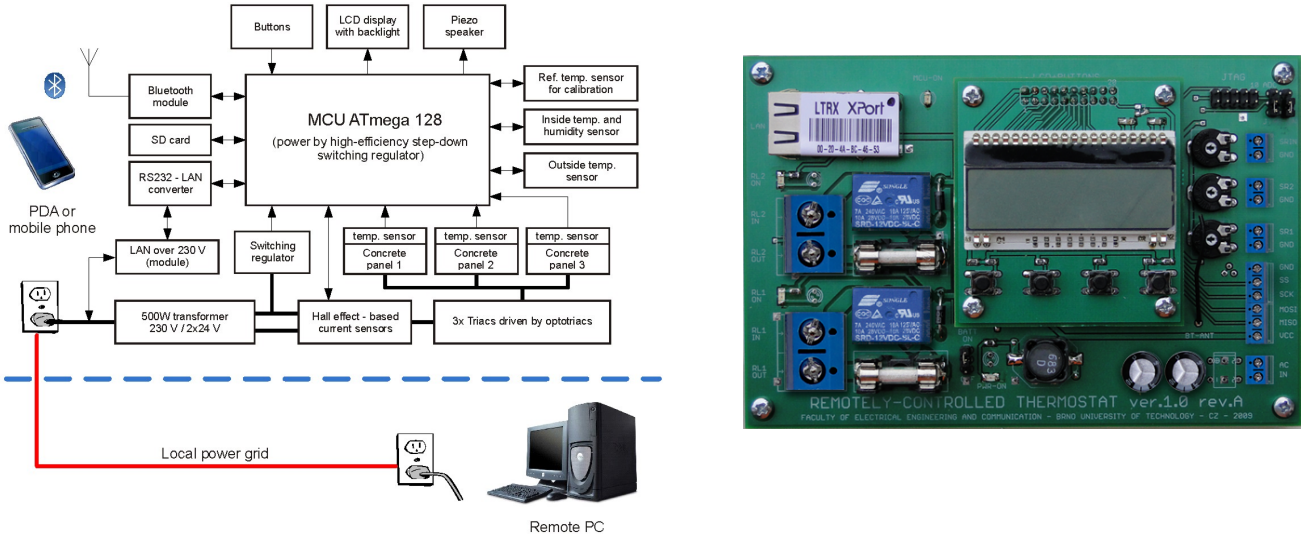

Figure 2. The block diagram and physical appearance of proposed RCT device

RCT contains several types of sensors. To measure temperature of composite materials there are used three PTC thermistors connected to the MCU. Analog inputs for sensing outdoor temperature are used for accurate 12-bit digital sensor. Indoor temperature and humidity devices RCT captures digital sensor SHT11. Electric current flowing through each sample is scanned 20 A hall sensor.

B. Communication

RCT is equipped with a Bluetooth module WT11 that offers a range of up to 100 m. Any Bluetooth-enabled devices (PDAs, mobile phones) can be used to control RCT. Another way to check RCT is Ethernet (TCP / IP). Terminal server - Xport - converts data from the UART directly to Ethernet. XPort supports 10/100 Ethernet, built-in web server provides a complete set of network protocol, security, speed and other parameters. The output of the XPort is brought to Ethernet Bridge module. This allows control over RCT grid 230 V without pulling the LAN cable.

C. Data storage

For storing data can be used for standard SD / MMC cards. The presence of the card is detected during system initialization. RCT also supports high-capacity SDHC cards. Data can be written in a different format of settings and needs. The default format is a CSV file. Output data can be readily evaluated using standard PC software.

D. Working modes

Workload management components can be tempered to use four different modes:

- The first mode “STANDARD” allows you to control each channel separately. The system controls the temperature of each channel and switches individually tempered connected component, if the temperature drops below the set limit. In this mode, does not reflect the ambient temperature.
- The second mode is called “COMMON”. In this mode, all channels driven simultaneously and critical temperature of the ambient temperature. If the temperature drops below the set level, all channels are closed.
- The third mode is the “ECO” mode. This is the last COMMON mode, which is also supplemented by the upper and lower limits. Thus, if the outside temperature drops below the preset extreme (e.g., -15 ° C), the concrete panels would no longer be able to effectively drowning, therefore they will shut down and power saving. You can also set the upper limits (e.g. 5 ° C), in which parts are no longer needed further tempered.
- The fourth mode is called “SWITCH” mode, because there is a periodic switching (distributing) of energy between different parts of tempered parts. It can thus make better use of the overall device performance, or you can use a transformer with one secondary and acclimatized to force him more sections. Time can be set from 1 to 60 seconds.

In the heating / tempering carried out production of several types of heated parts. In their design had to take into account the reciprocal interaction of composite heating insert and the concrete member itself, and I address this issue in analyzing the processes that occur inside components. The heating panel was implemented copper electrodes, used to bring the necessary capabilities, and temperature sensors that allow evaluating the process inside the composite material. An integral part of the analysis of thermal images was a composite panel that

 ISBN: 978-1-61208-246-2

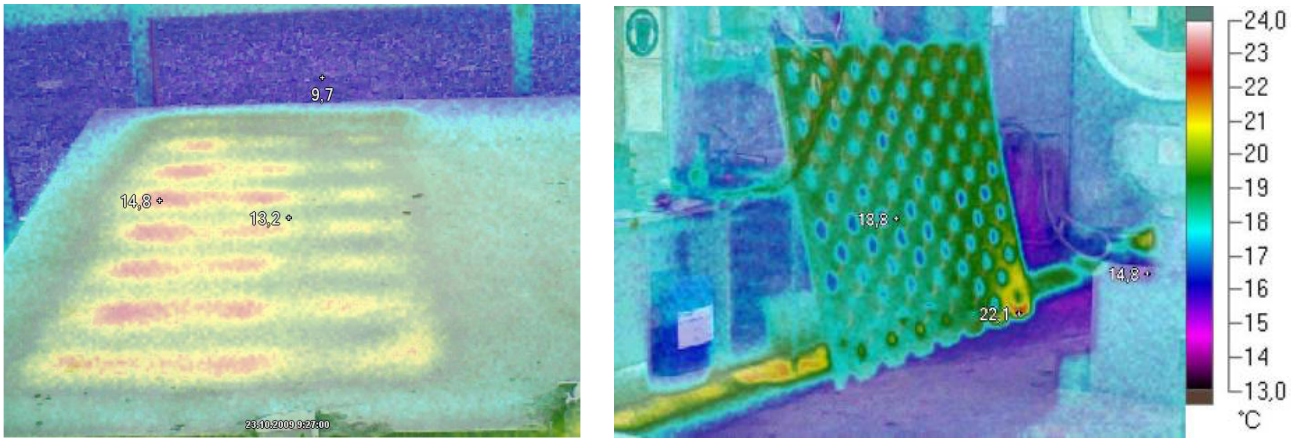

Figure 3. Infrared photos of heated concrete panel with admixture of conductive fillings

make it possible to precisely define the current load of locations composite liners. Subsequently, this area developed control unit. It is a three-channel digital thermostat with data recording (data logger) that is equipped with advanced features and allows remote control via Ethernet or Bluetooth, and data storage on an SD card.

The facility has implemented a number of heating modes. Among the most elaborate one "ECO" mode is based on evaluation of environmental conditions regulates the heating of composite material so as to avoid unnecessary heating of components in a time when the power system is not sufficient to prove the part is tempered heat up.

Both concrete samples include a temperature sensor integrated in the middle of the concrete block to provide precise internal temperature. Currents that flow through concrete samples are measured by Hall effect-based current sensors and controlled by 10 A relays. Together with the outside temperature sensor, RCT can effectively control dissipation power of the resistive heating and hold set temperatures.

As an example, two concrete blocks were tested (Fig. 3). Resistance varies from 4 Ω to 6 Ω that gives output power up to 114 W when using 24 V voltage source.

CONCLUSION

A development of new laboratory instruments was presented in this paper, the suggested block diagram, realization and design of the PCBs and overall structure of the design. These instruments are currently used for laboratory measurements and characterization of smart concrete panels at department of microelectronics.

ACKNOWLEDGMENT

This research was supported by the Ministry of Industry and Trade of the Czech Republic under the MPO ČR č. FR-TI3/485 project, Prospective applications of new sensor technologies and circuits for processing of sensor signals, No.FEKT-S-11-16 project and MEDTECH CZ.1.07/2.4.00/31.0016 from European Social Fundand project.

REFERENCES

[1] Drinovsky J., Kejik Z.: *Electromagnetic Shielding Efficinecy Measurement of Composite Materials* Measurement Science Review, 2009, vol. 9, No. 4, pp. 109-112.

[2] Chung D.D.L.: Composite Materials - Second Edition, Springer, London, 2010, p. 349 ISBN 978-1-84882-830-8.

[3] Chung D.D.L.: Functional Materials – Vol.2 Electrical, Dielectric, Electromagnetic, Optical and Magnetic Applications (With Companion Solution Manual), World Scientific Publisher, 2010, p345 ISBN 978-981-4287-15-9.

[4] Steffan, P.; Barath, P.; Stehlik, J.; Vrba, R.: The Multifunction Conducting Materials Base on Cement Concrete with Carbon Fibers. Electronics, 2008, č. b4, p. 82-86. ISSN: 1313- 1842.

[5] Analog Devices [online]. 2012 [cit. 2012-01-05]. Product Information AD5933. Available from: < http://www.analog.com/static/imported-files/data_sheets/AD5933.pdf>.

[6] Junek J., Cechmanek R., Steffan P., Barath P. *Vliv uhlikovych primesi na elektricke vlastnosti anorganickych kompozitu* XIIIth international conference Ecology and new building materials and products, 2009, Telc, 978-80-254-4447-4

[7] Shoukai Wang, Sihai Wen and D.D.L. Chung, "Resistance Heating Using Electrically Conductive Cements", Adv. Cem. Res. 16(4), 161-166 (2004).

 ISBN: 978-1-61208-246-2

Safety Critical Multiprocessor Real-Time Scheduling with Exact Preemption Cost

Falou Ndoye
INRIA Paris-Rocquencourt
Domaine de Voluceau BP 105
78153 Le Chesnay Cedex - France
falou.ndoye@inria.fr

Yves Sorel
INRIA Paris-Rocquencourt
Domaine de Voluceau BP 105
78153 Le Chesnay Cedex - France
yves.sorel@inria.fr

***Abstract*—In this paper, we address for safety critical applications the problem of multiprocessor real-time scheduling while taking into account the exact preemption cost. In the framework of multiprocessor real-time partitioned scheduling, we propose a greedy heuristic which balances the load of the tasks on all the processors and minimizes the response time of the applications. That heuristic uses a schedulability condition which is based on the $\oplus$ operation. That operation performs a schedulability analysis while taking into account the exact preemption cost. A performance analysis is achieved which compares the proposed heuristic to the branch and bound exact algorithm and to the worst-fit and best-fit heuristics.**

Keywords-multiprocessor real-time scheduling; partitioned scheduling; exact preemption cost; load balancing.

I. Introduction

For computation power and modularity issues, multiprocessor architectures are necessary to tackle complex applications found in domains such as avionics, automotives, mobile robotics, etc. Some of these applications are safety critical, leading to hard real-time task systems whose number of resources are fixed and constraints must be necessarily satisfied in order to avoid catastrophic consequences. Although fixed priority preemptive real-time scheduling allows a better success ratio than non-preemptive real-time scheduling, preemption has a cost. That cost is usually approximated in the WCET (Worst Case Execution Time) as assumed, explicitly, by Liu and Layland in their pioneering article [1]. However, such approximation is dangerous in a safety critical context since an application could miss some deadlines during its real-time execution even though schedulability conditions have been satisfied. This is why it is necessary to be aware of the exact preemption cost. In this paper, we address the problem of multiprocessor real-time scheduling while taking into account the exact preemption cost in safety critical applications. In the framework of multiprocessor real-time partitioned scheduling, we propose a greedy heuristic [2] using all the processors and which balances the load of the tasks on all the processors. That heuristic tends to minimize the response time (makespan) of the tasks. The schedulability condition is based on the algebraic $\oplus$ operation which performs a schedulability analysis taking into account the exact preemption cost.

The remainder of the paper is organized as follows: Section II presents related work about preemption cost and multiprocessor real-time scheduling. Section III describes the model and the schedulability analysis we propose. Section IV presents the proposed multiprocessor scheduling heuristic as well as its complexity, and Section V presents a performance analysis for that heuristic by comparing it with the Branch and Bound (B&B) exact algorithm, the Worst-Fit (WF) and Best-Fit (BF) heuristics. Finally, Section VI concludes and gives some directions for future work.

II. Related work

A. Exact preemption cost in real-time scheduling

There have been very few studies addressing the exact number of preemptions. Among them, the most relevant are the following. A. Burns, K. Tindell and A. Wellings in [3] presented an analysis that enables the global cost due to preemptions to be factored into the standard equations for calculating the worst case response time of any task, but they achieved that by considering the maximum number of preemptions rather than the exact number. Juan Echagüe, I. Ripoll and A. Crespo also tried to solve the problem of the exact number of preemptions in [4] by computing the schedule using idle times and counting the number of preemptions. However, they did not really determine the execution overhead incurred by the system due to these preemptions. Indeed, they did not take into account the cost of each preemption during the analysis. Hence, this amounts to considering only the minimum number of preemptions because some preemptions are not considered: those due to the increase in the execution time of the task because of the cost of preemptions themselves.

In order to reduce the preemption cost and improve the schedulability of tasks, a lot of work has focused on limited-preemption policies; among these we can cite fixed priority scheduling with deferred preemption (FPSDP) also called cooperative scheduling [5] and fixed priority scheduling with a preemption threshold (FPSPT) [6], [7]. According to FPSDP, each job of a task is a sequence of sub-jobs, where sub-jobs are not preemptive. When a job is being executed, it can only be preempted between two consecutive sub-jobs. For FPSPT, each task is assigned a nominal and a threshold

 ISBN: 978-1-61208-246-2

priority. A preemption will take place only if the preempting task has a nominal priority greater than the preemption threshold of the executing task. None of the previous works considers the exact number of preemptions. Nonetheless, that can affect the correct behavior of the system at run-time, or in any case leads to resources being wasted in terms of time and memory. It is typical and not difficult to determine the constant cost of every preemption which includes the context switch necessary to make the preemption possible together with the choice of the task with the highest priority. However, the exact number of preemptions is difficult to determine since it may vary according to every instance of a task. To our best knowledge there are only few studies that take into account the exact preemption cost in the schedulability conditions, except those presented in [8], [9]. The authors proposed a scheduling operation named $\oplus$ that performs a schedulability analysis while computing the exact number of preemptions. The principle of this operation is presented in Section III-B.

B. Multiprocessor real-time scheduling

The scheduling of real-time tasks on multiprocessor architectures can be achieved according to three main approaches: partitioned scheduling, global scheduling, and semi-partitioned scheduling.

In the partitioned scheduling approach [10], [11] the system of tasks is divided into a number of disjoint subsystems less than or equal to the number of processors in the multiprocessor architecture, and each of these subsystems is allocated to one processor. All the instances, or jobs, of a task are executed on the same processor and no migration is permitted. In this approach, it is necessary to choose a scheduling algorithm for every processor, possibly the same algorithm, and also an allocation algorithm. On the other hand, the allocation problem has been demonstrated to be NP-Hard [12]. This complexity is the main drawback of the partitioned scheduling approach.

Heuristics are considered to be the best suited solutions when the execution time is crucial as in the rapid prototyping phase of the design process. In the case of fixed priority scheduling and independent tasks, Davari and Dhall were the first to propose in [13] two preemptive scheduling algorithms RM-FF (Rate Monotonic First Fit) and RM-NF (Rate Monotonic Next Fit) to solve the multiprocessor real-time scheduling problem. In the proposed algorithms, the uniprocessor RM algorithm [1] is used to verify if a task is schedulable on a processor with respectively First-Fit (FF) and Next-Fit (NF) to solve the allocation problem. Another heuristic, RM-BF (Rate Monotonic Best Fit) was proposed in [14]. It makes it possible to minimize the remaining processor load $(1-U_{p_j})$, called the unutilized capacity of the processor p_j [15], where U_{p_j} is the load of the tasks on p_j. In contrast to RM-BF, RM-WF [14] (Rate Monotonic Worst Fit) maximizes the remaining processor load. All these approaches uses the classical Liu and Layland [1] model of tasks that assumes the preemption cost is approximated in the WCET. In order to tackle this problem [16] presents a first solution to take into account the exact preemption cost in multiprocessor real-time scheduling.

In the global scheduling approach [10], [11], a unique scheduling algorithm is applied globally for every processor of the multiprocessor architecture. All the ready tasks are in a unique queue shared by all the processors. In this queue, the m tasks with the highest priorities are selected to be executed on the m available processors. Besides preemptions, task migrations are permitted. The advantage of the global scheduling approach, is that it allows a better use of the processors. The main drawback of the global scheduling approach, is that each migration nowadays has a prohibitive cost.

In the semi-partitioned scheduling approach [17], [18], derived from the partitioned scheduling approach, each task is allocated to a specific processor as long as the total utilization of the processor does not exceed its schedulable bound. In this approach, some tasks can be portioned for their executions among multiple processors. During run-time scheduling, a portioned task is permitted to migrate among the allocated processors, while the partitioned tasks are executed on specific processors without any migration. The semi-partitioned scheduling approach allows a reduction of the number in migrations. But again, it is necessary to be aware that every migration has a cost.

C. Our choices

The cost of migrations in the global and semi-partitioned scheduling approaches leads us to choose the partitioned scheduling approach. In addition, since the partitioned scheduling approach amounts to transform the multiprocessor scheduling problem into several uniprocessor scheduling problems, we can take advantage of the numerous research results obtained for the uniprocessor scheduling problem. In order to achieve rapid prototyping, we propose an allocation heuristic rather than a metaheuristic [19] or an exact algorithm [20], and a schedulability condition to verify if a task is schedulable on a specific processor. Next-fit (NF) and first-fit (FF) heuristics can not optimize the load of the tasks on the processors, their choice is only based on the first processor which satisfies the schedulability condition. The BF heuristic using the load as a cost function, tries to fill a processor as much as possible before using another one. This technique does not induce load balancing. The only heuristic among the bin-packing heuristics which permits load balancing is WF. But, as with all the other bin-packing heuristics, WF tries to reduce the number of processors and that limits the balancing while multiprocessor architectures used in industrial applications, which we are interested in, have a fixed number of processors. That is why we propose a greedy heuristic similar to the WF heuristic, but which uses all the

 ISBN: 978-1-61208-246-2

available processors. This heuristic aims at minimizing the load on each processor. That induces to balance the load on all the processors. This proposed heuristic will be compared to the WF and BF heuristics and to the B&B exact algorithm.

Although preemptive scheduling algorithms are able to successfully schedule some task systems that cannot be scheduled by non-preemptive scheduling algorithms, the preemption has a cost. Indeed, Liu and Layland [1] assume that the preemption cost is approximated in the WCET. Thus, there are two possible cases: the approximation in time and memory space is high enough and thus will probably lead to wasting resources, or the approximation is low and thus a task system declared schedulable by, let us say RM, may miss some deadlines during its real-time execution. Consequently, we propose using the $\oplus$ operation [8], [9]. This is an algebraic operation that two tasks are schedulable, or not, while taking into account the exact preemption cost.

III. Model and Schedulability analysis

A. Model

Let $\Gamma_n = \{\tau_1, \tau_2, \cdots, \tau_n\}$ be a system of n preemptive, independent and periodic real-time tasks. Every task is denoted by $\tau_i = (r_i^1, C_i, D_i, T_i)$ where r_i^1, C_i, D_i and T_i are the characteristics of the task. r_i^1 is the first activation date, C_i is the EET (Exact Execution Time) without any approximation of the preemption cost, D_i is the relative deadline, and T_i the period of the task τ_i. We assume that $C_i \leq D_i \leq T_i$. Here we use the EET rather than the WCET because we assume that the code associated to a task is purely sequential, i.e. there are no conditional branches. Our hypothesis to consider the EET may seem unrealistic, but since we are considering safety critical applications it is mandatory to known the EET. Of course, when dealing with uncritical applications the WCET can be used. Also, we assume that Γ_n is scheduled according to the rate monotonic (RM) fixed-priority scheduling policy [1] on m identical processors (all the processors have the same computation power). Eventually, we assume that the processors have neither cache nor pipeline, or complex internal architecture. Both preview assumptions are usually made in safety critical applications where determinism is a key issue.

B. Schedulability analysis based on the $\oplus$ operation

Our schedulability analysis is based on the $\oplus$ scheduling operation [9] . This operation is applied to a pair of tasks (τ_i, τ_j), such that τ_i has the highest priority. It gives as a result a task $\mathcal{R}$, that is $\mathcal{R} = \tau_i \oplus \tau_j$. The $\oplus$ takes into account the exact preemption cost incurred by the task τ_j. The schedulability interval, i.e. the interval in which we study the schedulability of the tasks, comes from the theorem 1 below which was introduced by the J. Gossens [21].

Theorem 1: For a system $\Gamma_n = \{\tau_1, \tau_2, \cdots, \tau_n\}$ of n periodic tasks arranged by decreasing priorities with respect to a fixed-priority scheduling policy, let $(s_i^{'})_{i \in \mathbb{N}^*}$ be the sequence defined by:

$$\begin{cases} s_1^{'} = r_1^1 \\ \\ s_i^{'} = r_i^1 + \left\lceil \dfrac{(s_{i-1} - r_i^1)^+}{T_i} \right\rceil \cdot T_i, \quad 2 \leq i \leq n \end{cases} \tag{1}$$

If there exists a valid schedule of Γ_n until the time $s_n^{'} + H_n$ where $H_n = lcm\{T_i \mid i = 1, \cdots, n\}$, and $x^+ = max(x, 0)$, then this schedule is valid and periodic of period H_n from $s_n^{'}$.

Proof: The proof of this theorem is similar to that performed by *J. Goossens* in his Ph.D. thesis [21]. ■

A direct consequence of the previous theorem is that in the case of a valid schedule, the result of the schedule of the i first tasks is periodic of period $H_i = lcm\{T_j \mid j = 1, \cdots, i\}$ from $s_i^{'}$. Thus, the interval which precedes $s_i^{'}$ necessarily contains the *transient phase*, corresponding to the initial part of the schedule and the interval starting at time $s_i^{'}$ with length H_i is isomorphic to the *permanent phase* of the schedule of the i first tasks which repeats identically from the instant $s_i^{'}$.

In order to compute $\mathcal{R} = \tau_i \oplus \tau_j$ with $j = i + 1$, we set $\epsilon = min(r_i^1, r_j^1)$. Since ϵ always exists, the interval $[\epsilon, s_j^{'}]$ defines the transient phase and the interval $[s_j^{'}, s_j^{'} + H_j]$ defines the permanent phase, s_j and H_j are given by the theorem 1. The schedulability study of the tasks is performed in the interval $[\epsilon, s_j^{'} + H_j]$. In this interval, the number of instances of a task τ_j is given by $n_j = \frac{(s_j^{'} + H_j) - r_j^1}{T_j}$.

1) Principle of the $\oplus$ operation: The principle of $\oplus$ applied to a pair of tasks (τ_i, τ_j) consists in replacing the available time units of the highest priority task τ_i with the time units of the lowest priority task τ_j. In order to do that, both tasks are initially referenced to the same time origin ϵ. Then, task τ_i is rewritten according to the number of instances of task τ_j in the interval $[r_j^1, s_j^{'} + H_j]$ of both task periods. This operation allows not only the identification of the available time units in task τ_i, but also the verification that task τ_j does not miss any deadlines.

When the task τ_j is preempted by the task τ_i the exact number of preemptions must be computed for each instance of τ_j by considering all its time units. When τ_j is preempted, we increment its number of preemptions and we add the cost associated with one preemption in the remaining execution of τ_j, i.e. the number of time units that τ_j must execute in order to complete its execution. That scheme is repeated to take into account a preemption generated by a previous preemption, and so on. In contrast to other works presented in the literature, this principle makes it possible to have the exact number of preemptions. The cost associated to that

 ISBN: 978-1-61208-246-2

exact number of preemptions is added to the EET of τ_j to obtain its PET (Preemption Execution Time).

Figure 1 illustrates the PET. In this figure, the PET of task τ_i in the instance $k+1$ is given by $C_i^{k+1} = C_i + 2\alpha$ due to two preemptions, with α being the cost of one preemption. If the amount of PET unit of times fits in the available time

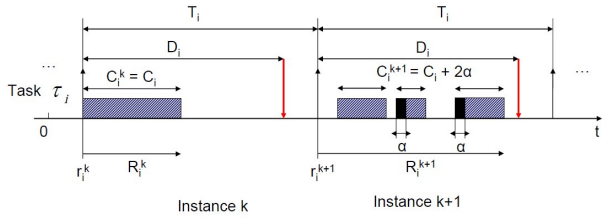

Figure 1. PET of a task

units of task τ_i, the task τ_j is schedulable, giving as a result task $\mathcal{R}$, otherwise it is not schedulable. $\oplus$ is an internal operation, i.e. the result given by $\oplus$ is also a task, that result may be in turn used as the highest priority task in another $\oplus$ operation. Thanks to this property it is possible to consider more than two tasks.

In order to perform the schedulability analysis of the task system $\Gamma_n = \{\tau_1, \tau_2, \cdots, \tau_n\}$, ordered according to the decreasing priorities of the tasks, the $\oplus$ operation is applied from the task with the highest priority to the task with the lowest priority. Consequently, if $\mathcal{R}_n$ is the scheduling task result of Γ_n, then $\mathcal{R}_n$ is obtained by successive iterations:

$$\begin{cases} \mathcal{R}_1 = \tau_1 \\ \mathcal{R}_{i+1} = \mathcal{R}_i \oplus \tau_{i+1}, \quad 1 \leq i < n \end{cases}$$

As such we have $\mathcal{R}_n = ((\tau_1 \oplus \tau_2) \oplus \cdots \oplus \tau_{n-1}) \oplus \tau_n$. The system Γ_n will be said schedulable if and only if all the tasks are schedulable. If this is not the case, then the system Γ_n is said to be not schedulable.

The complexity of $\oplus$ applied to a pair of tasks τ_i and τ_j is $O(l)$ with l is the LCM between the period of τ_i and the period of τ_j.

We denote by $H_j = lcm\{T_l : \tau_l \in hp(\tau_j)\}$ where T_l represents the period of task τ_l and $hp(\tau_j)$ denotes the subsystem of tasks with a priority higher than the priority of τ_j. The number of instances of task τ_i in the permanent phase is given by:

$$\sigma_{perm_j} = \frac{H_j}{T_j} = \frac{lcm\{T_l : \tau_l \in hp(\tau_j)\}}{T_j} \qquad (2)$$

The exact permanent load of a task τ_j, i.e. the load of the task τ_j, while taking into account the exact preemption cost, is given by:

$$U_j^* = \frac{C_j^*}{T_j} \text{ with } C_j^* = \frac{1}{\sigma_{perm_j}} \sum_{l=1}^{\sigma_{perm_j}} C_j^l \qquad (3)$$

In equation 3, C_j^l corresponds to the PET of the l^{th} instance in the permanent phase. As such, the exact permanent load of the system Γ_n composed of n periodic tasks scheduled on a processor p_i is given by:

$$U_{p_i}^* = \sum_{j=1}^{n} U_j^* \qquad (4)$$

2) Example: We apply the $\oplus$ operation to a system of periodic preemptive real-time tasks while taking into account the exact preemption cost. Let us consider such a system $\Gamma_3 = \{\tau_1, \tau_2, \tau_3\}$ of 3 tasks where τ_1 is the task with the highest priority, and τ_3 is the task with the lowest priority. We consider the cost of one preemption to be one time unit for all tasks. The characteristics of the tasks are summarized in table I.

Table I
TASKS' CHARACTERISTICS

Tasks	r_i^1	C_i	D_i	T_i
τ_1	0	3	7	15
τ_2	5	2	6	6
τ_3	3	4	10	10

The $\oplus$ operation is applied to a pair of operands. The left operand called the "executed task" corresponds to the result of the tasks previously scheduled, and the right operand called the "executable task" corresponds to the task to be scheduled. We represent an instance of the executable task by a unique sequence of symbols "**e**", in bold, followed by a sequence of symbols "a". Each symbol "**e**", in bold, in the executable task represents an executable time unit, i.e. the time unit that the task to be scheduled, must execute. Each symbol "a" represents an available time unit. Actually, such representation is repeated indefinitely since the task is periodic. We represent an instance of an executed task by a sequence of symbols "e" followed by a sequence of symbols "a", possibly repeated several times. Each symbol "e" in the executed task represents one executed time unit, i.e. the time unit executed by all the tasks previously scheduled. From the end of the transient phase, given by theorem 1, such representation is repeated according to the LCM of the tasks already scheduled.

The $\oplus$ operation aims at replacing all the available time units of the executed task (left operand) by the executable time units of the executable task (right operand). In order to make both tasks comparable, first the executable task is repeated according to the number of its instances in the schedulabity interval. Second, the executed task is rewritten according to the number of instances of the executable task in the schedulability interval. Therefore, the task resulting of the $\oplus$ operation applied to a pair of tasks, is an executed task represented by a sequence of symbols "e" followed by a sequence of symbols "a", possibly repeated several times.

 ISBN: 978-1-61208-246-2

According to these definitions, each task instance of the system Γ_3 is represented as:

$$\begin{cases} \tau_1 = \{\mathbf{e}, \mathbf{e}, \mathbf{e}, a, a, a, a, a, a, a, a, a, a, a, a\} \\ \tau_2 = \{\mathbf{e}, \mathbf{e}, a, a, a, a\} \\ \tau_3 = \{\mathbf{e}, \mathbf{e}, \mathbf{e}, \mathbf{e}, a, a, a, a, a, a\} \end{cases}$$

The scheduling task result $\mathcal{R}_3$ which describes the schedule of the task system is obtained by the following successive iterations:

$$\begin{cases} \mathcal{R}_1 = \Lambda \oplus \tau_1 \\ \mathcal{R}_i = \mathcal{R}_{i-1} \oplus \tau_i, \quad i = 2, 3 \end{cases}$$

Λ represents a task only composed with symbols "a" since there are no executed time units. $\mathcal{R}_1 = \Lambda \oplus \tau_1$ is computed as follows: according to equation 1 we have $s_1^{'} = 0$ and $H_1 = T_1 = 15$. Thus, the result of $\oplus$ applied to the pair (Λ, τ_1) is periodic of period $H_1 = T_1$ and is repeated indefinitely from $s_1^{'}$. We obtain $\mathcal{R}_1$ by replacing the 3 first available time units of Λ by the 3 executable time units of τ_1. Then, we have:

$\mathcal{R}_1 = \{e, e, e, a, a, a, a, a, a, a, a, a, a, a, a\}_{[0,15]}$

First iteration: Computation of $\mathcal{R}_2 = \mathcal{R}_1 \oplus \tau_2$. Thanks to equation 1, we have:

$$\begin{cases} s_1^{'} = 0 \\ \\ s_2^{'} = 5 + \left\lceil \dfrac{(0-5)^+}{6} \right\rceil \cdot 6 = 5 \end{cases}$$

We have $H_2 = lcm(15, 6) = 30$, thus the transient phase belongs to the interval $[0, 5]$ and the permanent phase belongs to the interval $[5, 35]$. In the schedulability interval $[0, 35]$, $\mathcal{R}_1$ is rewritten as follows:

$$\mathcal{R}_1 = \{e, e, e, a, a\}_{[0,5]}\{a, a, a, a, a, a, a, a, a, a, a, a, a, a, a, e, e, e, a, a\}_{[5,35]}$$

Task τ_2 begins its execution at $t = 5$ corresponding to the beginning of the permanent phase. Its number of instances in the schedulability interval is $n_2 = \frac{(s_2^{'}+H_2)-r_2^1}{T_2} = \frac{(5+30)-5}{6} = \frac{30}{6} = 5$. According to the number of instances of τ_2 in the schedulability interval, $\mathcal{R}_1$ is rewritten as follows:

$$\begin{array}{l} \mathcal{R}_1 = \{e, e, e, a, a\}_{[0,5]}\{a, a, a, a, a, a\} \\ \{a, a, a, a, e, e, \}\{e, a, a, a, a, a\} \\ \{a, a, a, a, a, a\}\{a, e, e, e, a, a\} \end{array} \quad (5)$$

$\mathcal{R}_2 = \mathcal{R}_1 \oplus \tau_2$ is obtained by replacing in the equation 5 for each corresponding instance of τ_2 in $\mathcal{R}_1$, the available time units "a" of $\mathcal{R}_1$ with the executable time units "**e**", in bold, of τ_2. During this replacement a preemption of τ_2 by τ_1 corresponds to the transition ("a" $\rightarrow$ "*e*"). The preemption of τ_2 by τ_1 is denoted by the time unit "**p**" called preemption time unit. When τ_2 is preempted, the next available time unit of $\mathcal{R}_1$ after this preemption is replaced by a preemption time unit "**p**". After replacing all the available time units of τ_1 with the executable time units of τ_2 and after adding the preemption time unit "**p**" in $\mathcal{R}_1$, we obtain:

$$\begin{array}{l} \mathcal{R}_2 = \{e, e, e, a, a\}_{(0,5)}\{\mathbf{e}, \mathbf{e}, a, a, a, a\} \\ \{\mathbf{e}, \mathbf{e}, a, a, e, e\}\{e, \mathbf{e}, \mathbf{e}, a, a, a\} \\ \{\mathbf{e}, \mathbf{e}, a, a, a, a\}\{\mathbf{e}, e, e, e, \mathbf{p}, \mathbf{e}\} \end{array}$$

For each corresponding instance of τ_2 in $\mathcal{R}_2$, its PET is given by the sum of the number of its executable time units **e**, in bold, and the number of its preemptions time unit "**p**". In the 4 first corresponding instances of τ_2 in $\mathcal{R}_2$, the PETs are the same and equal to 2 (PET=EET) because τ_2 is not preempted in these instances, but in its 5^{th} instance, it is preempted once. That is the reason why its PET is equal to 3. In any corresponding instance of τ_2 in $\mathcal{R}_2$, the PET fits in the available time units left by $\mathcal{R}_1$ in this instance. Thus, the task τ_2 is schedulable while taking into account the exact preemption cost. Actually, we have:

$$\begin{array}{l} \mathcal{R}_2 = \{e, e, e, a, a\}_{[0,5]}\{e, e, a, a, a, a, e, e, a, a, e, e, \\ e, e, e, a, a, a, e, e, a, a, a, a, e, e, e, e, p, e\}_{[5,35]} \end{array}$$

The differences with the previous expression of $\mathcal{R}_2$ is that the executable time units "**e**", in bold, become executed time units "e", and $\mathcal{R}_2$ does not exhibit the corresponding instances of τ_2.

Second iteration: Computation of $\mathcal{R}_3 = \mathcal{R}_2 \oplus \tau_3$. Thanks to equation 1, we have:

$$\begin{cases} s_2^{'} = 5 \\ \\ s_3^{'} = 3 + \left\lceil \dfrac{(5-3)^+}{10} \right\rceil \cdot 10 = 13 \end{cases}$$

We have $H_3 = lcm(lcm(15, 6), 10) = lcm(30, 10) = 30$, thus the transient phase belongs to the interval $[0, 13]$ and the permanent phase belongs to the interval $[13, 43]$. In the schedulability interval $[0, 43]$, $\mathcal{R}_2$ is rewritten as follows:

$$\begin{array}{l} \mathcal{R}_2 = \{e, e, e, a, a, e, e, a, a, a, a, e, e\}_{[0,13]}\{a, a, e, \\ e, e, e, e, a, a, a, e, e, a, a, a, a, e, e, e, e, p, e, e, e, a, \\ a, a, a, e, e\}_{[13,43]} \end{array}$$

Task τ_3 begins its execution during the transient phase at $t = 3$. Its number of instances in the schedulability interval is $n_3 = \frac{(s_3^{'}+H_3)-r_3^1}{T_3} = \frac{(13+30)-3}{10} = \frac{40}{10} = 4$. According to the number of instances of τ_3 in the schedulability interval, $\mathcal{R}_2$ is rewritten as follows:

$$\begin{array}{l} \mathcal{R}_2 = \{e, e, e\}\{a, a, e, e, a, a, a, a, e, e\}_{[3,13]} \\ \{a, a, e, e, e, e, e, a, a, a\}\ \{e, e, a, a, a, a, e, e, \\ e, e\}\{p, e, e, e, a, a, a, a, e, e\} \end{array} \quad (6)$$

$\mathcal{R}_3 = \mathcal{R}_2 \oplus \tau_3$ is obtained by replacing in the equation 6 for each corresponding instance of τ_3 in $\mathcal{R}_2$, the available

time units "a" of $\mathcal{R}_2$ with the executable time units "**e**", in bold, of τ_3. During this replacement, a preemption of the task τ_3 by τ_1 or by τ_2 corresponds to a transition ("a" $\rightarrow$ "e"). When τ_3 is preempted, the next available time unit of $\mathcal{R}_2$ is replaced by a preemption time unit "**p**". After replacing the available time units of $\mathcal{R}_2$ with the executable time units of τ_3 and after adding the preemption time units "**p**" in $\mathcal{R}_2$, we obtain:

$$\mathcal{R}_3 = \{e, e, e\}\{\mathbf{e}, \mathbf{e}, e, e, \mathbf{p}, \mathbf{e}, \mathbf{e}, a, e, e\}_{[3,13]}$$
$$\{\mathbf{e}, \mathbf{e}, e, e, e, e, e, \mathbf{p}, \mathbf{e}, \mathbf{e}\}\{e, e, \mathbf{e}, \mathbf{e}, \mathbf{e}, \mathbf{e}, e, e, e, e\}$$
$$\{p, e, e, e, \mathbf{e}, \mathbf{e}, \mathbf{e}, \mathbf{e}, e, e\}$$

For each corresponding instance of τ_3 in $\mathcal{R}_3$, its PET is given by the sum of the number of its executable time units "**e**", in bold, and the number of its preemptions time units "**p**". In the 2 first corresponding instances of τ_3 in $\mathcal{R}_3$, the task τ_3 suffers one preemption. Its PETs in every instance are the same and equal to 5. In its other instances there is no preemption of τ_3 and the PETs of τ_3 in these instances are the same and equal to 4 (PET=EET). In any corresponding instance of τ_3 in $\mathcal{R}_3$, the PET fits in the available time units of $\mathcal{R}_2$ in this instance. Thus, the task τ_3 is schedulable while taking into account the exact preemption cost. Finally, we have:

$$\mathcal{R}_3 = \{e, e, e, e, e, e, e, p, e, e, a, e, e\}_{[0,13]}\{, e, e, e,$$
$$e, e, e, e, p, e, e, e, e, e, e, e, e, e, e, e, p, e, e, e, e, e,$$
$$e, e, e, e\}_{[13,43]}$$

The differences with the previous expression of $\mathcal{R}_3$ is that the executable time units "**e**", in bold, become executed time units "e", and $\mathcal{R}_3$ does not exhibit the corresponding instances of τ_3.

Since all the tasks are schedulable then the system $\Gamma_3 = \{\tau_1, \tau_2, \tau_3\}$ is schedulable.

Figure 2 presents the result of the schedule of Γ_3. In this figure, the permanent phase corresponds to the highlighted zone of the schedule and the transient phase corresponds to the interval preceding that zone. The disk represents only the permanent phase in a more compact form. This double representation of the schedule is obtained from the SAS software [22].

IV. Multiprocessor scheduling heuristic

The heuristic presented in *Algorithm*1 is a greedy heuristic. The solution is built step by step. In each step a decision is taken and this decision is never questioned during the following steps (no backtracking). The effectiveness of such a greedy heuristic is based on the decision taken to build a new element of the solution. In our case, the decision is taken according to a cost function which aims at minimizing the load.

A. Cost function

The cost function allows the selection of the best processor p_j to schedule a task τ_i. In our case, this cost function

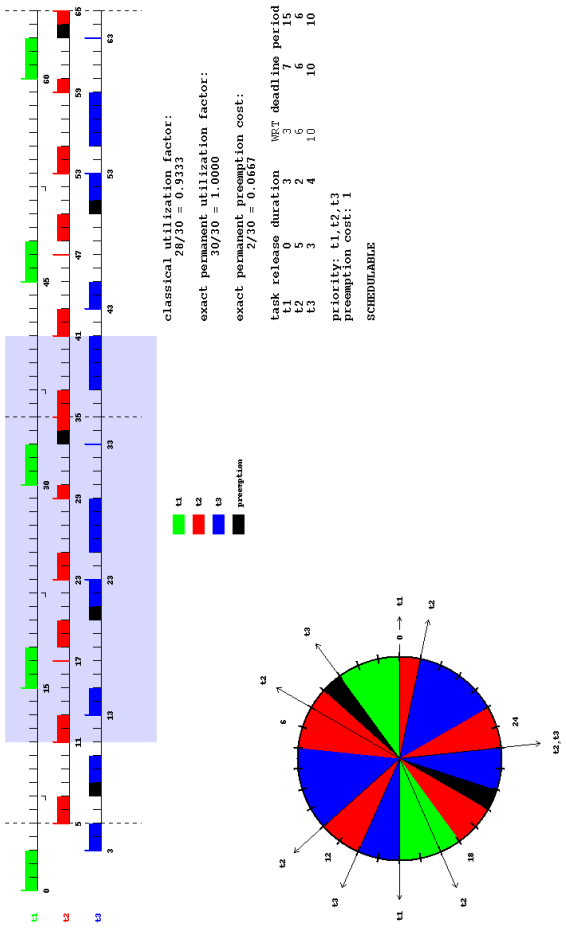

Figure 2. Result of the scheduling of Γ_3, taking into account the exact preemption cost

is the load $U^*_{p_j}$ (equation 4) of the task τ_i and all the tasks already allocated on the processor p_j. The processor which minimizes this cost function for τ_i among all the processors, is considered to be the best processor to schedule the task τ_i.

In the case of the previous example, according to equation 4, the exact permanent load of the system Γ_3 scheduled on a processor p is given by:

$$U^*_p = \frac{3}{15} + \frac{1}{6} \cdot \frac{(2+2+2+2+3)}{5} + \frac{1}{10} \cdot \frac{(5+4+4)}{3} = 1$$

B. Principle of our allocation heuristic

We use a "list heuristic" [23]. In our case, we initialize this list, called the "candidate task system", with the task system given as input. We use for that candidate task system the decreasing order of the task priorities (according to RM fixed-priority scheduling policy [1]). At each step of the heuristic, the task with the highest priority is selected among the candidate task system, and we attempt to allocate it to its best processor according to the cost function presented

 ISBN: 978-1-61208-246-2

previously. The heuristic minimizes the load $U^*_{p_j}$ of the task system on the different processors. It is similar to the WF bin-packing heuristic but all the available processors are used rather than the first processors necessary to schedule the task system.

If Γ_n is the task system with n tasks and m is the number of processors, the complexity in the worst case of our heuristic is equal to $O(n.m.l)$, with $l = lcm\{T_i : \tau_i \in \Gamma_n\}$.

Algorithm 1 Greedy heuristic

1: Initialize the candidate task system W with the task system given as input and in the decreasing order of their priorities, initialize the boolean variable $TasksSchedulable$ to $true$
2: **while** W is not empty and $TasksSchedulable = true$ **do**
3: Select in W the highest priority task τ_i
4: *% Verify on each processor p_j if task τ_i is schedulable.%*
5: **for** j=1 to m **do**
6: **if** task τ_i is schedulable on p_j with the exact preemption cost (scheduling operation $\oplus$ [9]) **then**
7: Compute the cost function of task τ_i on the processor p_j, i.e. the load of p_j using the equation 4 given in subsection III-B
8: **end if**
9: **end for**
10: *% Using the cost function again, choose the best processor for τ_i among all the processors on which τ_i is schedulable.%*
11: **if** τ_i is schedulable on one or several processors **then**
12: Schedule the task τ_i on the processor which minimizes the cost function
13: Remove the task τ_i from W.
14: $TasksSchedulable = true$
15: **else**
16: $TasksSchedulable = false$
17: **end if**
18: **end while**

V. Performance Analysis

Our heuristic is compared with the B&B exact algorithm and the WF and BF heuristics. The B&B enumerates all the possible solutions in order to find the best solution which minimizes the load of the tasks on the processors. In the B&B, WF and BF heuristics, we use the $\oplus$ operation presented in Section III-B as the schedulability condition. We compare the algorithms according to their execution time, their success ratio, the response time of the task systems, i.e. the total execution time of the tasks, and the unutilized capacity of the processors used during the allocation.

A. Execution time of the heuristics

We perform two kinds of tests to compare the execution time of the four algorithms. First, we fix the number of processors to 10 and we vary the number of tasks between 100 to 1000 tasks. Every task system is scheduled with the four algorithms and the corresponding execution times are computed. We obtained the results shown in Figure 3. In the second test, we use a single task system composed of 1000 tasks randomly generated and we vary the number of processors. We obtained the results shown in Figure 4.

In both tests, we notice that the exact algorithm explodes very quickly whereas the heuristics keep a reasonable execution time. Our heuristic up to 1000 tasks is close to the WF and BF heuristics in terms of execution time. However, for higher numbers of tasks less good results are obtained with our heuristic. In Figure 4 we also notice that when the number of processors varies, the execution times of WF and BF are constant, because these heuristics use the minimum number of processors. Another remark about Figure 4 is that the execution time of our heuristic does not increase monotonically with the number of processors, in contrast to Figure 3. Indeed, in our heuristic, increasing the number of processors leads to distributing the tasks on all the processors. That increase in terms of processors, can decrease locally the LCM of the tasks on some processors, and consequently can reduce the execution time of the $\oplus$ operation.

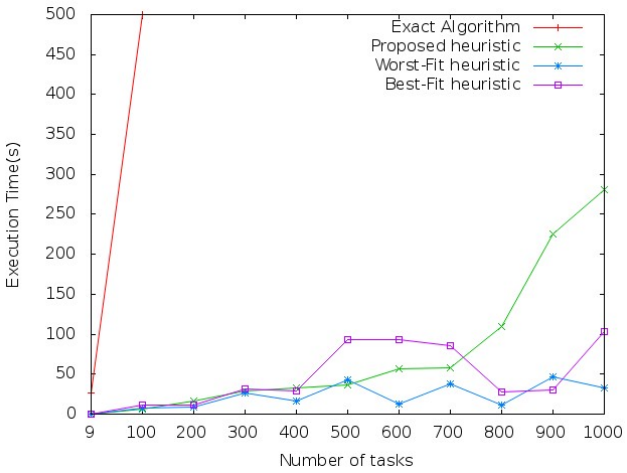

Figure 3. Execution time of the algorithms according the number of tasks

B. Success ratio

In these tests, we compare the success ratio of our heuristic with the B&B exact algorithm and the WF and BF heuristics. The success ratio of an algorithm is defined as follows:

 ISBN: 978-1-61208-246-2

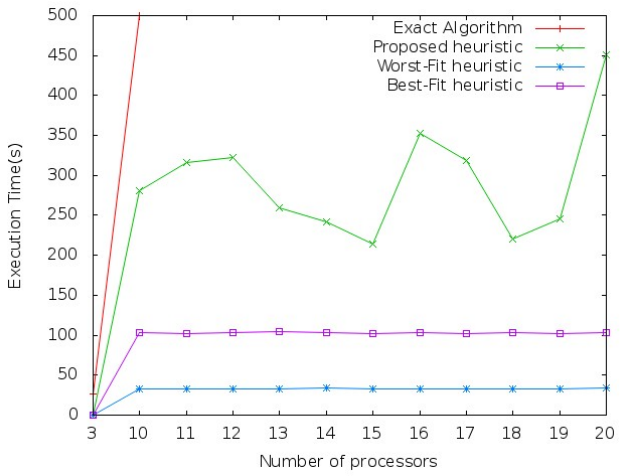

Figure 4. Execution time of the algorithms according to the number of processors

$$\frac{number\ of\ task\ systems\ schedulable}{total\ number\ of\ task\ systems}$$

Due to the complexity of the B&B and in order to compare it with the heuristics, we executed each algorithm on 6 task systems. Each task system is composed at most of 10 randomly generated tasks and is executed on 2 processors. At each execution we determine for each algorithm the number of schedulable task systems.

As shown in Figure 5, we notice that WF and BF give better results than our heuristic in terms of success ratio. This loss in terms of success ratio is largely compensated by the gain in terms of response time of the task systems and by the unutilized capacity of the processors, as described in the subsections V-C and V-D.

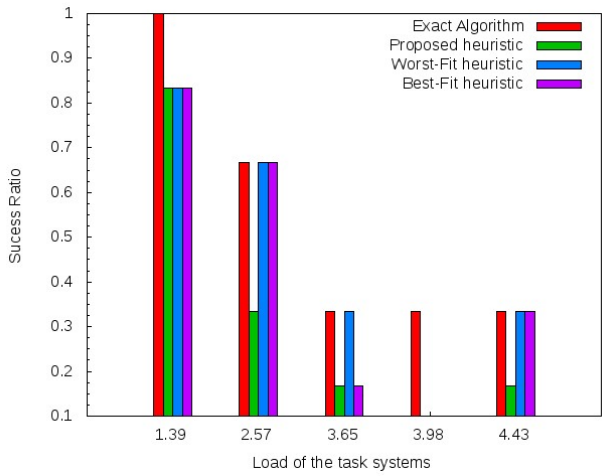

Figure 5. Sucess ratio

C. Response time of the task systems

In these tests, we consider 10 task systems. The number of tasks in the task systems varies between 100 and 1000 randomly generated tasks and each task system is executed on 10 processors. We limit the tests to the WF and BF heuristics and our proposed heuristic because of the complexity of the B&B exact algorithm and we know that the B&B already gives better results than the heuristics. For each task system, we determine the allocation found by each heuristic and for this allocation the response time of the task system, i.e., the total execution time of all the tasks, is computed. We compare the response time of the task systems between the heuristics, as shown in Figure 6.

In this figure, we notice that the allocation found by our heuristic gives a better response time than those found by WF and BF. This is due to the fact that the execution of the tasks is parallelized on all the available processors whereas WF and BF attempts to reduce the number of processors rather than parallelize the execution of the tasks.

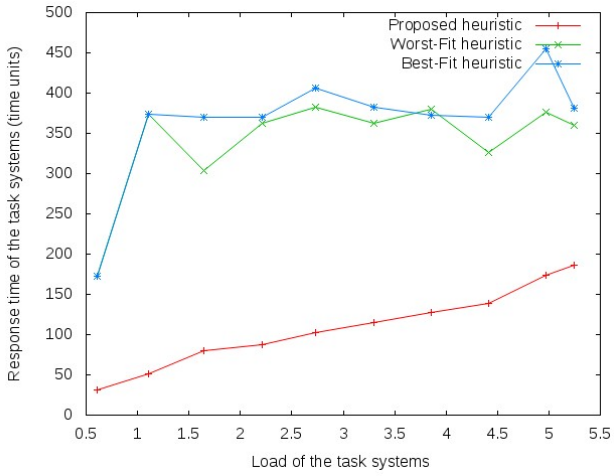

Figure 6. Execution time of the task systems

D. Average of the unutilized capacity of the processors

In these tests, we consider 10 task systems. The number of tasks in the task systems varies between 100 and 1000 randomly generated tasks and each task system is executed on 10 processors. We limit the tests to the WF and BF heuristics and our proposed heuristic because of the complexity of the B&B exact algorithm. In addition, we know that the B&B already gives better results than the heuristics. For each task system we determine the allocation found by each heuristic and for this allocation we compute the average of the remaining processor load $(1 - U_{p_j})$, called untilized capacity, on the processors p_j used in this allocation. We compare the unutilized capacity of the processors used with the heuristics as shown in Figure 7.

In this figure, we observe that the allocation found by our heursitic gives for each processor more flexibility, i.e., more unutilized capacity, than those found by WF and BF. This is due to the fact that our heuristic balances the load on all the available processors, which ensures an execution time slack, whereas the BF heuristic fills the processors as much as possible, which that increases the risk of non schedulabily of a task system at run-time. On the other hand, the WF heuristic, balances the load only on the processors already used and does not consider all the available processors.

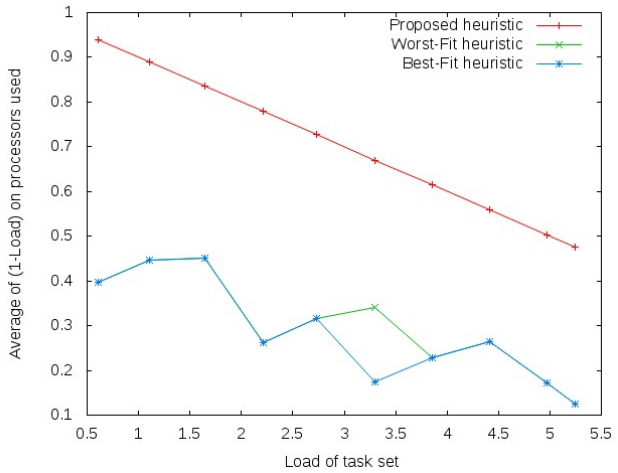

Figure 7. Average of (1-load) on the processors used

VI. Conclusion and future work

In this paper, we have presented a greedy heuristic which allocates and schedules, on a multiprocessor architecture, a system of real-time tasks while balancing the load on the processors. In addition, this heuristic takes into account the exact preemption cost that must be carefully considered in safety critical applications, which is the focus of our work.

We have carried out a performance analysis showing that, up to 1000 tasks, the proposed greedy heuristic, has results close to those of the WF and BF heuristics in terms of execution time. For higher number of tasks less good results can be obtained with our heuristic. On the other, hand the proposed heuristic is better than the WF and BF heuristic in terms of load balancing and flexibility, i.e., more not-utilized capacity, of tasks at run-time. Also the allocation found with our heuristic has better response time than those with WF and BF heuristics.

In future works, we plan to study the multiprocessor real-time scheduling of dependent tasks which leads to deal with data transfers and shared data management.

References

[1] C. L. Liu and J W. Layland. Scheduling algorithms for multiprogramming in a hard-real-time environnment. *Journal of the ACM*, vol. 20(1), January 1973.

[2] S. Martello E.G. Coffman, G. Galambos and Daniele Vigo. Bin packing approximation algorithms: Combinatorial analysis. *Handbook of combinatorial optimization*, 1998.

[3] A. Burns, K. Tindell, and A. Wellings. Effective analysis for engineering real-time fixed priority schedulers. *IEEE Trans. Softw. Eng.*, 21:475–480, May 1995.

[4] J. Echague, I. Ripoll, and A. Crespo. Hard real-time preemptively scheduling with high context switch cost. In *Proceedings of 7th Euromicro workshop on Real-Time Systems*, Los Alamitos, CA, USA, 1995. IEEE Computer Society.

[5] Alan Burns. Preemptive priority-based scheduling: An appropriate engineering approach. In *Advances in Real-Time Systems, chapter 10*, pages 225–248. Prentice Hall, 1994.

[6] Y. Wang and M. Saksena. Scheduling fixed-priority tasks with preemption threshold. In *Proceedings of the 6 International Conference on Real-Time Computing Systems and Applications*, RTCSA'99, Washington, DC, USA, 1999.

[7] M. Saksena and Y. Wang. Scalable real-time system design using preemption thresholds, November 2000.

[8] P. Meumeu Yomsi and Y. Sorel. Extending rate monotonic analysis with exact cost of preemptions for hard real-time systems. In *Proceedings of 19th Euromicro Conference on Real-Time Systems, ECRTS'07*, Pisa, Italy, July 2007.

[9] P. Meumeu Yomsi and Y. Sorel. An algebraic approach for fixed-priority scheduling of hard real-time systems with exact preemption cost. Research Report RR-7702, INRIA, August 2011.

[10] Robert I. Davis and Alan Burns. A survey of hard real-time scheduling algorithms and schedulability analysis techniques for multiprocessor systems. Technical report, University of York, Department of Computer Science, 2009.

[11] O.U.P. Zapata and P.M. Alvarez. Edf and rm multiprocessor scheduling algorithms: Survey and performance evaluation. *http://delta.cs.cinvestav.mx/ pmejiamultitechreport.pdf*, Oct 2005.

[12] Garey and Johnson. *Computers and intractability: a guide to the theory of NP-completeness*. W.H. Freeman and Company, New York, NY, USA, 1979.

[13] S.K. Dhall and C.L. Liu. On a real-time scheduling problem. *Operation Research*, vol. 26(1), 1978.

[14] Y. Oh and S.H. Son. Tight performance bounds of heuristics for a real-time scheduling problem. Technical Report CS-93-24, Univ. of Virginia. Dep. of Computer Science, Charlottesville, VA 22903, May 1993.

 ISBN: 978-1-61208-246-2

[15] L. George I. Lupu, P. Courbin and J. Goossens. Multi-criteria evaluation of partitioning schemes for real-time systems. In *The 15th IEEE International Conference on Emerging Technologies and Factory Automation, ETFA'10*, Bilbao, Spain, September 2010.

[16] F. Ndoye and Y. Sorel. Preemptive multiprocessor real-time scheduling with exact preemption cost. In *Proceedings of 5th Junior Researcher Workshop on Real-Time Computing, JRWRTC'11, in conjunction with the 18th International conference on Real-Time and Network Systems, RTNS'11*, Nantes, France, September 2011.

[17] S. Katoa and N. Yammasaki. Semi-partitioning technique for multiprocessor real-time scheduling. In *Proceedings of WIP Session of the 29th Real-Time Systems Symposium (RTSS), IEEE Computer Society*, 2008.

[18] J. H. Anderson, V. Bud, and C. U. Devi. An edf-based scheduling algorithm for multiprocessor soft real-time systems. In *Proceedings of the 17th Euromicro Conference on Real-Time Systems*, pages 199–208, Washington, DC, USA, 2005. IEEE Computer Society.

[19] E. G Talabi. *Metaheuristics*. Wiley, 2009.

[20] J. E. Mitchell. Branch-and-cut algorithms for combinatorial optimization problems. pages pp 65–67, 2002.

[21] J. Goossens. *Scheduling of Hard Real-Time Periodic Systems with Various Kinds of Deadline and Offset Constraints*. PhD thesis, Universit Libre de Bruxelles, 1999.

[22] P. Meumeu Yomsi, L. George, Y. Sorel, and D. de Rauglaudre. Improving the quality of control of periodic tasks scheduled by fp with an asynchronous approach. *International Journal on Advances in Systems and Measurements*, 2(2), 2009.

[23] K. M. Chandy L.T. Adams and J. R. Dickson. A comparison of list schedules for parallel processing systems. *Commun. ACM*, 17:685–690, December 1974.

 ISBN: 978-1-61208-246-2

Performance Evaluation of Distributed M3 Applications via ABSOLUT

Subayal Khan, Jukka Saastamoinen, Jussi Kiljander, Jyrki Huusko, Juha Korpi
VTT Technical research Center of Finland,
FI-90570, Oulu, Finland
email:{subayal.khan, jukka.saastamoinen, jussi.kiljander, jyrki.huusko, juha.korpi}@vtt.fi

Jari Nurmi
Tampere University of Technology,
Department of Computer Systems
P.O.Box 553 (Korkeakoulunkatu 1),
FIN-33101 Tampere, FINLAND
jari.nurmi@tut.fi

***Abstract*—For future smart applications running on nomadic embedded devices operating in smart environments, the information sharing without human involvement, availability of the services and the quest for better alternative services will go hand in hand to enable the best-possible experience for the end-user. These tasks are challenging since the devices operating in a smart environment are usually heterogeneous and targeted for different uses. M3 is a layered architecture which aims at providing interoperability between heterogeneous devices in a Smart Space. M3 divides the interoperability challenge into three layers, i.e., information, service and communication level. The information level ensures that the information is understood in the same way by all devices. The service level guarantees the seamless access to services and discovery of new services while the communication level provides means for data transmission among devices. The design and development of new M3 applications is challenging not only due to various application design alternatives but also due to many solutions for achieving interoperability at different M3 levels. Therefore, a brisk performance evaluation phase is required for evaluating the feasibility of new M3 applications. In other words, the methodology should not only provide the feasibility of information, service and device level solutions employed by the instantiation of M3 but also the feasibility of the M3 applications on various platforms. This article describes an approach for the design and system level performance evaluation of M3 systems via UML2.0 MARTE profile and ABSOLUT and is experimented via a case study.**

Keywords- M3; SystemC; Performance Simulation

I. INTRODUCTION

Distributed embedded systems involve collaboration among connected embedded devices for example mobile handheld devices, embedded PC's, wireless sensors, robotics systems and microcontrollers. By accessing and making use of information from other sensors and embedded devices on the same network, rich scenarios can be created in different application domains of distributed systems. The overall value of the embedded sector worldwide is about 1600 billion Euros (€) per year. The three main market segments for embedded systems are telecommunications, automotive, and aerospace. The combined value of these segments is 1,240 billion € per year and are growing at a rate of over 10 per-cent [1].

In order to realize the full potential of this market segment, the efforts of industry and research communities are focused at the development of new pervasive standards and protocols for communication and information sharing among networked devices. These technologies will enable the services and software entities hosted on the devices in a pervasive environment to collaborate efficiently for information sharing to enable a richer end-user experience.

The networks of such devices are generally called smart spaces. The smart spaces are based on the concepts which are strongly correlated with those employed in the area of pervasive computing or ambient intelligence [2][3].

The devices from different domains which are a part of smart space can share information if they can interoperate. Currently several domain and vendor specific solutions of interoperability exist such as UPnP in the entertainment domain and Apple ecosystem controlled by a single vendor. These domain and vendor specific solutions, generally, do not allow the devices from one vendor and domain to interoperate with devices from other vendors or domains. The only way a device can overcome this barrier currently is to implement several different standards, which will enable it to participate in the use inter-domain and inter-vendor use-cases. Also, the existing standards often target specific use cases rather than attempt to specify a general framework for interoperability [4].

M3 (Multi-vendor, multi-device, multi-domain) is a generic interoperability framework for smart environments. It is semantic information sharing solution for smart environments which instantiates information level on top of NoTA (Network on Terminal Architecture) or any other service level interoperability solution [4]. This layered architecture allows for the separation of concerns at each layer. The concerns at each layer can vary between M3 applications. For example, an M3 application can demand both service access (over various transport technologies) and common service discovery mechanisms. In order to achieve these two objectives, an M3 service level IOP (interoperability) solution (such as NoTA) can be used to enable seamless service access while an M3 information level IOP solution, such as RIBS (RDF (Resource Description Framework) Information Base Solution), can be used for service discovery [5].

NoTA implements the multi-transport mechanism in the form of a DIP (Device Interconnect Protocol) that abstracts away the complexity and algorithmic details involved in service access over multiple transports and provides a simple modified Socket API (application interface) to application programmer collectively called NoTA BSD-SOCKET API functions. In this article, we utilize the M3 information level for enhancing the service discovery in NoTA based M3 applications (employing NoTA as service level IOP). This is achieved by presenting semantic descriptions of the functionalities provided by NoTA services. This allows the clients to find the suitable services more efficiently.

Deployment of new M3 applications is challenging not only due to the heterogeneous parallelism in the modern mobile platforms, but also due to performance and energy constraints. For efficient development and deployment of

 ISBN: 978-1-61208-246-2

M3 applications, it is of pivotal importance that the application design phase acts as a blue print for the SLPE (system-level performance evaluation) approach. Another major requirement is that the SLPE approach must be able to identify the potential bottlenecks at all the M3 levels in the M3 instantiation employed. In other words, before the deployment of an M3 application, the performance of IOP solutions operating at each level of M3 must be evaluated. An instantiation of M3 means the deployment of a specific interoperability solution at each M3 layer.

For SLPE of M3 applications, Abstract workload based performance simulation (ABSOLUT) has been used. ABSOLUT is a Y-Chart [6] based system level performance simulation approach consisting of application workload and platform model [7]. ABSOLUT employs model-based approach for applications, platform services, middleware technologies and platform [7].

So far, ABSOLUT has not been used for the SLPE of distributed M3 systems, i.e., the systems which comprise of multiple devices operating in a smart environment. Performance evaluation of distributed M3 applications via ABSOLUT demands the design, implementation and integration of information, services and communication level M3 models into the ABSOLUT methodology.

The first novel contribution of this article is to elaborate the design of M3 applications at service and information level via UML 2.0 MARTE profile [32]. The NoTA application (operating at the M3 service level) was previously presented in the case study described in [8]. In this research article, an additional application view was provided to represent the M3 information level in the NoTA application model. Also SSAPI (Simple Sockets Application Interface) was used for sharing information among information level M3 entities like KPs (Knowledge Processor) and RIBS. In other words, modelling of M3 applications employing NoTA is achieved by defining the information level in a separate application view within the overall NoTA application model. The rest of the application views represent the service level components of the software system.

The second contribution is the design and integration of information level protocol models to the ABSOLUT framework. The extended ABSOLUT framework is applied for the SLPE of the distributed M3 application presented in the case study. The framework can be used to evaluate the performance of IOP solutions operating at each of the three levels of M3.

The rest of the paper is organized as follows: Section II first gives a brief outline of landmark performance simulation and application modelling tools and techniques. Afterwards, it provides an overview of NoTA and M3 technologies. Section III describes the way M3 based smart space applications can be modelled. The section describes different application views and the way non-functional properties are carried through application modelling phase. Section 4 describes the modelling of M3 applications via a case study. Section 5 describes the performance modelling approach. Section 6 describes the performance modelling of the application described in Section 4. Section 7 first elaborates the system level performance evaluation results of the application, i.e., the way non-functional properties of the application are validated. This section also shows the performance of components in the platforms on which the application components were mapped. Afterwards, it describes the performance of IOP solutions operating at each of the three levels of M3. Conclusions and future work are outlined in Section 8 followed by acknowledgements and list of references.

II. RELATED WORK

A detailed survey of the salient system level performance evaluation methodologies is provided in. Therefore, in the current section, we first provide a brief overview of these methodologies/tools. This is followed by a description of the M3 Framework and NoTA SOA (service-oriented architecture).

A. *Existing Application modelling Tools/Languages*

Object Management Group (OMG) defines Model Driven Application Architecture (MDA) relying on efficient use of system models to facilitate transformations between different model types. Various Architectural Description Languages (ADLs) have been proposed. MBASE provides integrated models for capturing the product success, process and properties [10]. ACME relies on a core ontology comprising of seven elements representing architectural elements [11]. MAE [12] triggers the modelling, analysis, and management of different versions of architectural artefacts supporting domain-specific extensions to capture other system properties.

B. *Existing System Level Performance Evaluation Techniques*

Performance modelling has been approached in different ways. SPADE [13] treats applications and architectures separately via a trace-driven simulation approach. Artemis [14] extends SPADE by involving virtual processors and bounded buffers. The TAPES [15] abstracts functionalities by processing latencies covering the interaction of associated sub-functions on the architecture without actually running application code. ABSOLUT [7] is system level performance evaluation for embedded systems which employs model based approach for both application and platform.

C. *M3 framework*

The aim of M3 is to provide multi-device, multi-domain and multi-vendor interoperability by combining Semantic Web technologies with publish/subscribe-based interaction. The interoperability challenge in M3 is divided into three levels: communication, service and information. The basic principle of M3 is that the information level interoperability is achieved by agreeing on common ontology models. On the communication and service levels, M3 relies on existing solutions. In this work, we utilize the NoTA technology to provide interoperability in the lower levels.

In M3, the W3C's (World Wide Web Consortium) Semantic Web specifications, such as RDF [33], RDFS (RDF Schema) [34], and OWL (Web Ontology Language) [35], provide the key technologies for the ontology-based interoperability. The RDF is a W3C standard designed to represent Web resources in a structured manner using subject, predicate and object triples. RDFS and OWL in turn provide vocabularies on top of RDF to describe any information as machine-interpretable ontologies. In M3, these technologies are exploited for representing information about the real world in order to create location-aware services to physical places.

The M3 functional architecture defines two types of entities: KP and SIB (Semantic Information Broker). KPs are software agents that provide the end-user with services

 ISBN: 978-1-61208-246-2

by interoperating with each other. SIB is a shared blackboard providing methods for KPs to share machine-interpretable data in the smart space. The publish/subscribe based SSAP (Smart Space Access Protocol) defines the rules for KP-SIB communication. The SSAP provides following operations: *join(), leave(), insert(), remove(), update(), query(), subscribe(),* and *unsubscribe()*. The Fig.1 illustrates how the SIB and KPs form M3-based smart spaces.

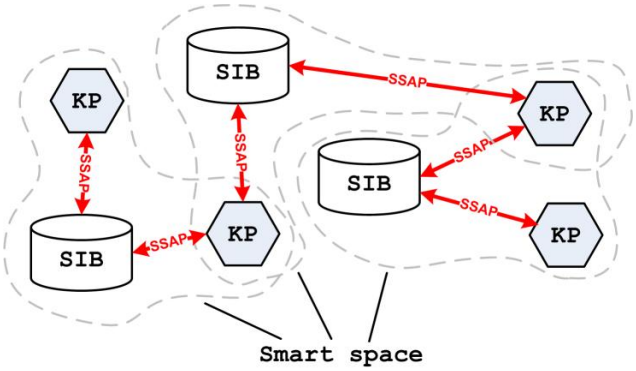

Figure 1. Composition of M3-based smart spaces.

Two versions of the M3 concept have been published: Smart-M3 and RDF Information Base Solutions (RIBS) [5]. Smart-M3 is the first official implementation of the M3 concept. It is a Linux based implementation that utilizes XML (Extensible Markup Language) serialized format of the SSAP. Smart-M3 provides both NoTA and plain TCP/IP based communication technologies and it has been also implemented as a service in OSGi (Open Services Gateway initiative) framework [16]. The Smart-M3 supports two types of query formats: simple template queries and WQL (Wilbur Query language) [17]. In template query the query string consists of separate RDF triples, which are matched against the RDF database of the SIB. The WQL query in turn consists of start node and a path to be traversed from the start node.

The RIBS is an ANSI-C implementation of M3 concept designed for portability, security, and performance. Similarly to Smart-M3, it supports both plain TCP (Transmission Control Protocol) and NoTA based transports. In contrast to Smart-M3 the RIBS uses WAX (Word Aligned XML) serialized SSAP format. The WAX serialized SSAP messages are more compact and faster to parse and therefore provide better performance and portability to low capacity devices. The query languages supported by the RIBS are also bit different from the Smart-M3.RIBS does not support WQL but provides limited support for SPARQL [5]. TLS (Transport Layer Security) and RDF-triple level access control mechanisms are used to provide security and privacy in smart spaces.

M3 concept is based in the voluntary sharing of information by objects in physical space. It is solely up to information owner to decide what and how information is published. M3 ensures the availability of information from physical world to devices and novel applications in smart environments. In this way the applications can enhance end-user experience by taking advantage of the available information in the smart space and by creating create new cross-domain use cases. In this article, we use M3 to enhance the service discovery of NoTA services available in the smart environment.

D. *Network on Terminal Architecture (NoTA)*

NoTA is a novel SOA which consists of three types of logical elements: SNs (Service Node), ANs (Application Node) and DIP (Device Interconnect Protocol). Service nodes are services that can be used by ANs and other SNs. Application nodes are the application functionalities composed of service calls and other logic. Communication between the Application and Service Nodes takes place always over the DIP.

The DIP defines both types of socket based communication, i.e., it supports both message and streaming type of data flows. NoTA DIP is divided into two main functional blocks. The first one is called H_IN, which manages service registration, discovery, access and security. The second is called L_IN, which is responsible for connecting the subsystems together.

From a software architect's perspective, the applications supported by NoTA systems are modelled as NoTA SOA [9]. In other words, a NoTA application consists of a set of Application Nodes (ANs) and Service Nodes (SNs) which collaborate via NoTA Device interconnect protocol to satisfy a use-case. For modelling a novel SOA for embedded nomadic devices (in this case NOTA SOAD), UML 2.0 MARTE profile comes as a natural choice [9].

III. MODELLING NOTA BASED M3 APPLICATIONS

In this article, we focus on the design of M3 applications which employ RIBS and NoTA at information and service level respectively.

NoTA based M3 applications are those M3 applications which use NoTA as a service level IOP. From this point onwards, we use the term "M3 applications" for these applications. It should be noted that the same modelling languages and techniques can be employed for M3 applications based on other serviced level IOP, such as ADIOS (Adaptive Input/Output System) and OSGi. In each case, the SOA concepts are used with additional view(s) representing the information level.

It should be noted that, since the M3 information level is instantiated on top of service level, therefore, each information level software entity is also represented as an entity at the service level. In case of Smart M3, the information level entities are KPs and SIB/RIBS while the service level (generally speaking) entities consist of servers and clients (called SNs and ANs in NoTA SOA).

Therefore, in case of NoTA based M3 systems, each KP is an AN at the service level and each SIB/RIBS is a SN at the service level. After M3 application design, the software components representing service and information level application components (KPs, RIBS, ANs, and SNs) and technologies are mapped to platforms to constitute the complete M3 system. In the next subsections, we elaborate the modelling of a complete M3 application (employing NoTA as service level IOP).

a. *M3 application views*

The M3 application modelling process starts by describing a set of views that are sufficient for the modelling objective. These views are instantiated by using UML2.0 MARTE profile and are illustrated in conjunction with the RM (Restaurant Multimedia) Application case study. The use case view describes the functionality of a system at a higher abstraction level by means of use cases. The structural view defines the interface between an application and the sub-systems of the execution platform.

 ISBN: 978-1-61208-246-2

The interfaces are implemented by the ANs and SNs. The syntactical view describes the syntax of the messages passed between ANs and SNs. The behavioural view reflects the behavioural aspects of an application and its encompassing services. All the views described so far describe the service level of the modelled application. The information level is described in a separate view, called the semantic view, which describes the semantic description of the information used by the information level entities called KPs and RIBS/SIB. The KPs are the ANs, which use the information contained in RIBS/SIBS which in turn are SNs at service level.

b. *Non-Functional Properties*

In case of M3 applications, the end user experience can be affected by the IOP solutions operating at device, service and information level. Therefore, the performance of IOP solution at each layer of M3, as well as the application, must be analysed to identify the potential bottlenecks.

It means that in case of NoTA based M3 systems, apart from the end-end delays of messages exchanged among devices, the processing times of NOTA DSD (Data Structure Diagram) API functions and SSAP API functions are also important. Hence we will employ ABSOLUT for analysing the following non-functional properties.

- The processing times of the targeted application functions and external libraries.
- At the M3 device level, we will analyse throughput at MAC-Level, throughput at Transport-Level, Average Frame Delays, Average Transport Delays, Frame loss rate and Packet Loss rate.
- Processing times of the NoTA API functions.
- Processing times of SSAP functions which gives a good insight into the performance of RIBS (Information level IOP).

The non-functional properties of an M3 application (from the end-user perspective) are identified and elaborated in the syntactical view. Firstly they are shown in the extended behavioural view and later on validated by the performance simulation. We focus in the sequel on one non-functional property, FrameRate, showing the way it is carried through the design process for the design of a certain NoTA SN in the distributed M3 application at service level. This is outlined in Figure 2.

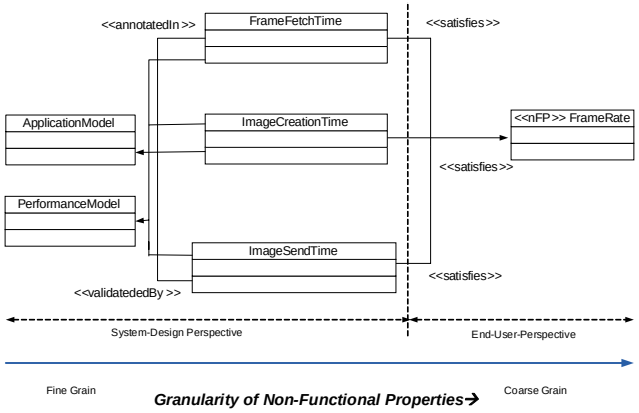

Figure 2. Carrying FrameRate through the application modelling and performance simulation process

IV. CASE STUDY: MODELLING RESTAURANT MULTIMEDIA M3 APPLICATION

We now describe the modelling of a RM M3 Application. This application allows a customer to request his preferred multimedia service and is hosted on his mobile device. At the service level, the application is like a control, which can request any of the three Application Nodes (ANs) for a specific functionality, i.e., for viewing a News Channel, a music video or a movie. Each of these ANs then requests its corresponding Service Node (SN) to access the streaming multimedia content. The nodes, and their required and provided interfaces, are elaborated in the application model.

The information level is expressed in the Semantic view which illustrates the information regarding the available services in the smart space. This information is used by the mobile devices of customers entering the restaurant to avail the desired multimedia services.

A. *Application use-case view*

The use case view shows a system level capability i.e., selection of Multimedia Service, as shown in Figure 3.

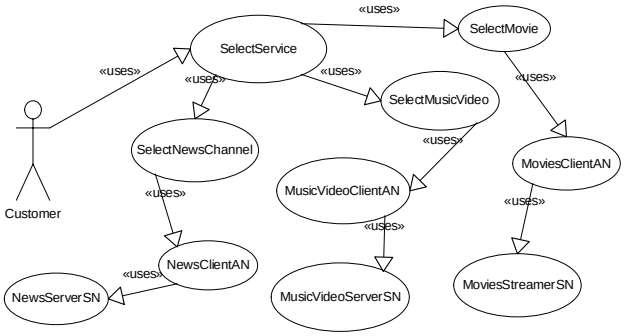

Figure 3. Restaurant Multimedia application use-case view

a. *Application syntactical view*

The syntactical view describes the syntax of messages passed between the ANs and application and also between ANs and SNs. This is shown in Figure 4.

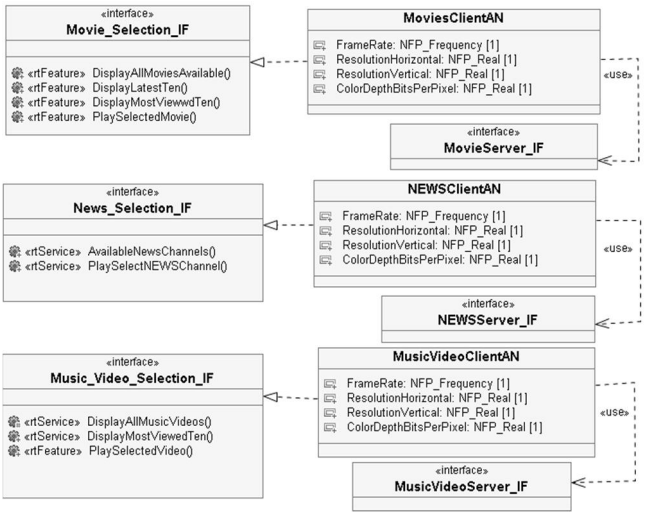

Figure 4. Diagram showing Interfaces realized and required by ANs.

The interfaces needed by ANs are provided by SNs and are shown similarly. The NFPs (non-functional properties) [18] are assigned values in respective slots of their instances and are shown in Figure 5.

 ISBN: 978-1-61208-246-2

Figure 5. The non-functional properties represented as slot values

b. Application Semantic View

The semantic view illustrates the semantic descriptions of SNs used in the discovery process. The ontology suite designed for the discovery consists of two ontologies: NSO (NoTA Service Ontology) and VSSO (Video Stream Service Ontology). Figure 6 illustrates these ontologies as an RDF graph.

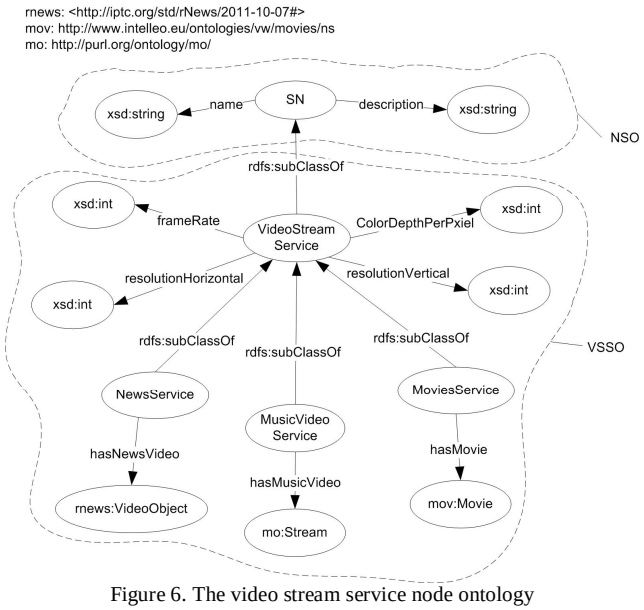

Figure 6. The video stream service node ontology

NSO is general purpose ontology for describing NoTA services. It contains just a one class (ServiceNode), which presents common information such as the name and the human readable description about the NoTA service. The idea is that when new NoTA services are designed for specific application domains, the domain specific ontologies import the NSO ontology and introduce new subclasses for the common ServiceNode class.

The purpose of the VSSO is to describe the capabilities of video stream services in a machine-interpretable format. The VideoStreamService class is the main class of the ontology. It is defined as a subclass of the ServiceNode class of the NSO ontology, but it is also possible to utilize it with different SOA technologies. The VideoStreamService class contains properties such as frameRate, resolutionHorizontal, resolutionVertical, and ColorDepthPerPixel for describing the non-functional properties of the video stream service. By querying the values for these properties form the SIB, the ANs are able to select the service that best meets their requirements. The VSSO contains also three subclasses for the VideoStreamService class: NewsService, MusicVideoService, and MovieService. These classes represent services that provide specific types of video streams and contain properties such as hasNewsVideo, hasMusicVideo, and hasMovie for representing the actual video streams provided by the service. To provide suitable ranges for these properties we have imported following ontologies: rNews [19], Music Ontology [20] and IntelLEO [21] Movies Ontology.

c. Application Behavioral View

The behavioral view shows the behavior of the application as shown in Figure 7. First of all, the end-user application becomes aware of the services available in the smart environment by communicating via RIBS using SSAP API functions. This is called the service discovery phase.

Once the end-user application knows about the available multimedia services, it allows the user to avail the desired services. The functionalities of the multimedia services are implemented by (allocated to) NoTA ANs and SNs. These ANs and SNs must satisfy the non-functional properties annotated in the syntactical view for a better end-user experience. These non-functional properties are refined to a set of non-functional properties from the implementation perspective as shown in Section 5 and are validated by the performance simulation phase as shown in Section 6.

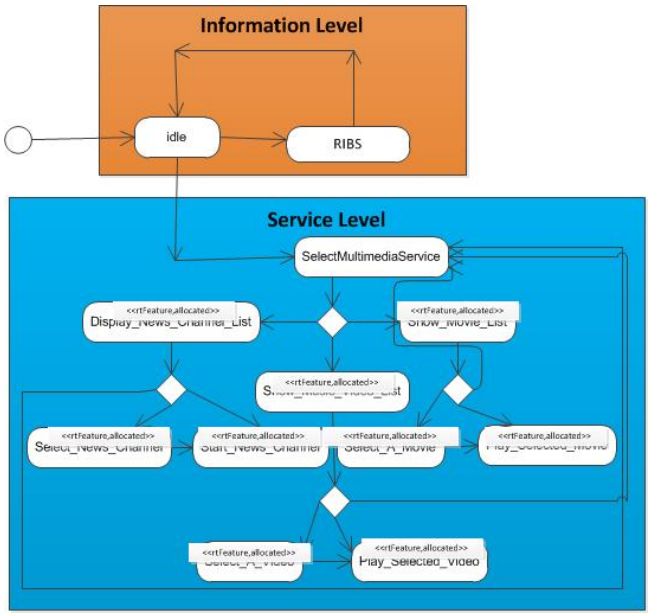

Figure 7. Behavioural view of Application.

V. PERFORMANCE MODELLING APPROACH

The performance modelling of NoTA based M3 systems requires the modelling of NoTA SOA workload models (workload models of ANs and SNs), modelling of SSAP API, KPs and RIBS at the information level, modelling of NoTA DIP operating in different modes and modelling of device level protocols/services, for example transport protocols, such as TCP/IP and UDP. We now describe the performance modelling of the aforementioned NoTA based M3 system in ABSOLUT.

A. Modelling NoTA SOA workload models

In order to integrate the NoTA SOA to ABSOLUT [22] seamlessly, the behavioural view of NoTA application model is extended to form a layered hierarchical structure of applications as described in [8]. The corresponding layers in the application workload models are identified. In this way, the application model acts as a blue print for the application workload models, reducing the time and effort in the performance evaluation phase [8].

In case of NoTA application model, the behavioural view represents a use_case as a controlled collaboration of ANs or SNs. Therefore, *USE_CASE = {C, N_1, N_2, N_3,…., N_N}*, where N_i is an *AN* or *SN* and *C* represents the control of the application. Corresponding workload model layer is *USE_CASE_MODEL= {C_{WLD}, NM_1,……,NM_N}*, where NM_i is the workload model of an AN or SN and C_{WLD} is the control. Each of these workload models is an Application-Level ABSOLUT workload model.

Each AN or SN contains a set of processes and control, i.e., N_i ={C_P,P_1,P_2,…,P_N}, where P_i is the model of a single process in an *AN* or *SN*. The corresponding workload model layer is *NMi={C_{PM},PM_1,PM_2,…..,PM_N}*,
where PM_i is the model of the *ith* process model. The processes models of a single *AN or SN* communicate via ABSOLUT IPC models as elaborated in [23] and are scheduled by the ABSOLUT operating system model [7].

The processes of an *AN* or *SN* can call library functions, system calls and functions of user-space code. For communication with other processes, they can call BSD_API functions or make use of IPC. The corresponding Process workload models call Function workload models and workload models for external library functions obtained by ABSINTH-2 [24]. The BSD API functions are modelled as Transport Services registered to the OS models [25].

The control and the functionalities of the MusicVideoServerSN (which consists of a single process) are shown in Figure 8. The non-functional property i.e. FrameRate is assigned the required value (40 Frames/sec) in the model element representing MusicVideoServerSN in Figure 5. This non-functional property is further refined to three non-functional properties from the design perspective, i.e., FrameRetrievalTimeMax, ImageCreationTimeMax and ImageSendingTimeMax. These refined non-functional properties are annotated in the behavioural view to their corresponding functionalities, i.e., Get a Frame, Create Image and Send the Image. The OPENcv [26] library functions, i.e., cvQuerryFrame and cvCreateImage and user-space function SendImage, providing these functionalities are mentioned below the name of these functionalities. Each of these non-functional requirements are analysed in the performance simulation phase to check whether the required FrameRate has been achieved. Due to the pipelined nature of the functionalities, each of them has to be performed within 1/40 seconds (to fulfil the required frame rate). The function SendImage is a wrapper around the NoTA BSD API Hsend() function [27].

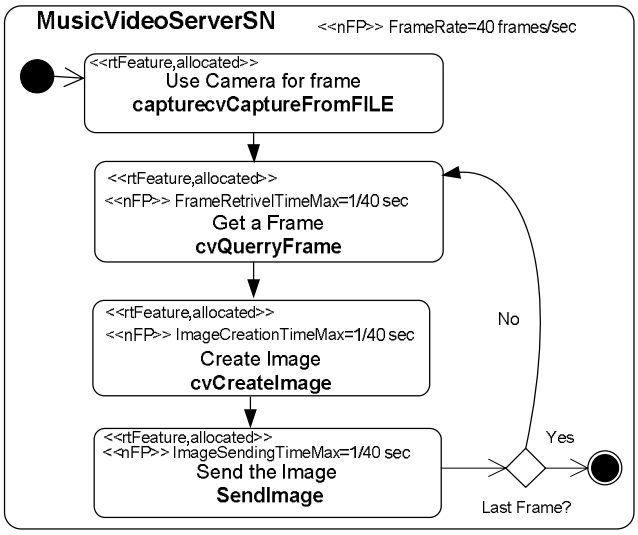

Figure 8. MusicVideoServerSN control with functionalities mentioning refined non-functional properties

Hence a single process of an AN or SN, *"P_i"*, can be represented as P_i={C_F,F_1,F_2,…,F_N, S_1, S_2,.. S_K}, where F_i is a function and S_i is a service requested from platform. The corresponding workload model layer is PM_i={C_{FM},FM_1,FM_2,…,FM_N, SM_1, SM_2,.. SM_K}, where FMi is a function workload model and SMi is a platform service workload model. The mapping between the NoTA Application model layers and the corresponding Workload model layers are shown in Table I.

TABLE I. COMPARING NOTA APPLICATION MODEL LAYERS AND ABSOLUT WORKLOAD MODEL LAYERS

Application Layers	Workload Model Layers
use_case= {C,N_1,N_2,……,N_N}	use_case_model={C_{WLD},NM_1,..,NM_N}
N_i = {C_P,P_1,P_2,…,P_N}	NMi={ C_{PM} ,PM_1,..,PM_N}
P_i={C_F,F_1,F_2,…,F_N,S_1,.. S_K}	PMi={C_{FM},FM_1,,FM_N,SM_1,..SM_K}

a. Modelling SSAP API, RIBS and KPs

At the information level, the information repository and users, i.e., RIBs and KPs communicate via SSAP API. The workload models of RIBs and KPs are easily extracted via ABSINTH-2 [24] in exactly the same way as the ANs and SNs of NoTA SOA. The reason is that RIBS and KPs are nothing but SNs and ANs in terms of SOA (at M3 service level), which implement a specific functionalities, i.e., storing and using information using a protocol called SSAP API. SSAP API is in turn a set of wrapper functions over NoTA BSD API functions in case of NoTA based M3 systems. The workload models of SSAPI can be obtained via ABSINTH-2 [24].

b. Modeling NoTA DIP workload models

NoTA DIP is available as an external library and has also been implemented as platform service implemented in LINUX Kernel [8]. When used as an external library, NoTA DIP operates in two modes i.e., Single Process (SP) mode or Daemon mode [8]. In both cases, NoTA DIP services be requested by applications as modified NoTA BSD API functions. Linking NoTA Application architecture design to ABSOLUT demands the modelling of both NoTA implementations.

The design and integration of ABSOLUT workload models corresponding to different NoTA implementations (as services or external libraries) and operating modes (SP and daemon mode) are described in detail in [8].

 ISBN: 978-1-61208-246-2

c. *Modelling Device Level Services*

Modelling of device level services, for example transport protocols, such as TCP and UDP, is described in [25]. The MAC and transport layer models were compared to the corresponding models of widely used network simulators, i.e., ns-2 and OMNeT++ [29][30]. The results were 75-85% accurate as compared to these benchmarks and were always pessimistic. In other words, if the use-case requirements are validated by the ABSOLUT MAC and transport models, the results are surely validated by ns-2 and OMNeT++ simulators. The reason is that ABSOLUT models always give higher values of MAC and transport level delays and throughput under the same network conditions for example number of nodes and channel bit rate [25].

d. *Overall M3 systems performance model*

Therefore, the overall ABSOLUT performance model of an M3 system contains the hardware services, software services, platform components, the models of device level services**,** the ABSOLUT models of different NoTA DIP implementations and modes, the workload models of ANs and SNs extracted by extended application models and the workload models of SSAP API functions. Figure 9 shows the possible components of an overall ABSOLUT performance model of a M3 system. The ABSOLUT models corresponding to different M3 levels are shown in different colours in Figure 9.

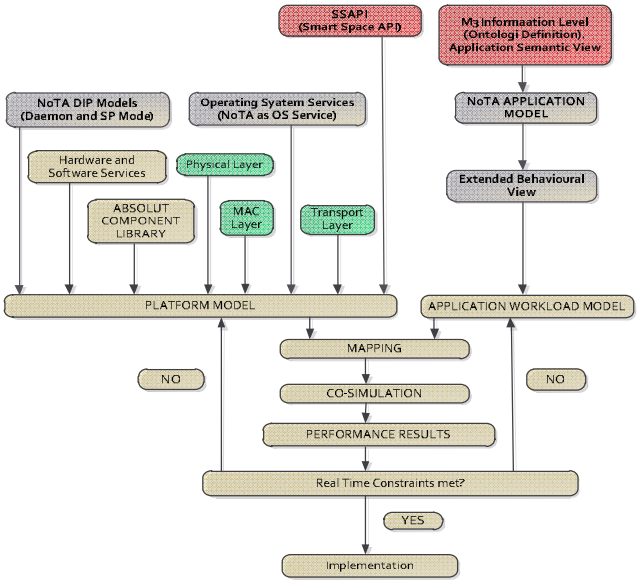

Figure 9. The modelled protocols/components of M3 in the corresponding ABSOLUT performance model

VI. PERFORMANCE MODELLING OF CASE STUDY

Each server and client (called SNs and ANs in NoTA) in real case study presented in Section 4 is modelled as a separate application-level workload model. Each Application-Level workload model of a NoTA AN or SN instantiates the process workload model mimicking its' execution in the real use-case. KPs and SIBs are also ANs and SNs, which store and share/use information about available services or contained in different devices. Hence the ABSOLUT workload models of SIBs and KPs are generated in the same way as other ANs and SNs [8]. Therefore, from this point onwards, we do not use the terms KP or SIB explicitly.

B. *Overall ABSOLUT Performance Model*

Each AN and SN presented in the application model is mapped to a separate ABSOLUT platform model to analyse the performance results and identify the potential bottlenecks at the software and hardware side. The overall performance simulation model is shown in Figure 10.

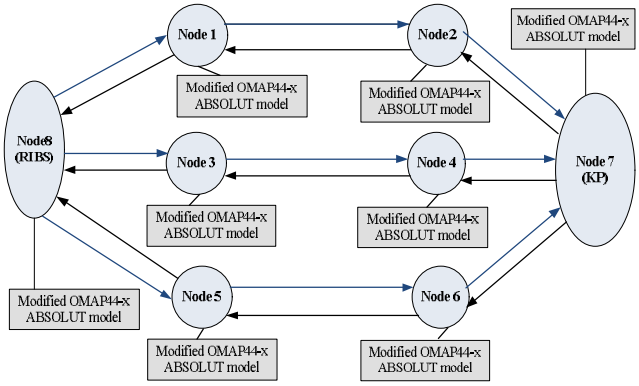

Figure 10. Performance model of the Restaurant Multimedia application

Node 1 and Node 2 represent the NewsServerSN and NewsClientAN. Node 3 and Node 4 represents the MovieStreamerSN and MovieClientAN, whereas Node 5 and Node 6 represent the MusicVideoServerSN and MusicVideoClientAN. Node 7 represents the application hosted on the mobile device of a customer entering the restaurant. The application is in the form of a control [22] and the user decides which services to use. Node 7 (the end-user application) first retrieves the information related to the available services (three multimedia services implemented by other nodes) while Node 8 represents SN implementing RIBS. Therefore, Node 7 acts as a KP. After knowing about the available services, the Node 7 contacts the related service on end-user's direction and the desired multimedia content is streamed to the customer's device.

It should be noted that the service nodes also communicate with the RIBS via SSAP to inform it about their presence. In this way, the information related to their capabilities and presence is made available to devices in the smart environment. The applications hosted by these devices can then use these services when desired by the end-user.

a. *ABSOLUT Device Platform Models*

Each ABSOLUT platform model used in the case study is a modified OMAP-44x platform model. It consists of two ARM Cortex-A9 processors consisting of four cores respectively instead of two (as in case of original TI OMAP44-x platform) along with SDRAM, a POWERVR SGX40 graphics accelerator and an Image signal processor. This is shown in Figure 11. The NoC infrastructure was abstracted out and replaced with on-chip bus as shown in Figure 11 . Each processor core (Cortex-A9 CPU model) has an L1 and L2 cache and can possibly share an L3 cache with one or more cores in the Multi-Core Processor model as described in [8].

 ISBN: 978-1-61208-246-2

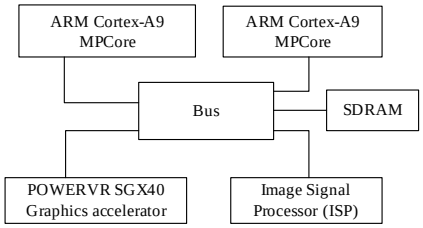

Figure 11. OMAP 44x Platform ABSOLUT model.

b. Application and M3 IOP workload Models

All the SNs (except RIBS) were programmed using OpenCV library [26]. The workloads of all ANs (including KPs), SNs (including RIBS) and IOP solutions (device, service and information level IOP solutions) operating at different levels of M3 in NoTA based M3 systems were modelled as described in Section V.

c. Simulation parameters

The simulations were carried out in WLAN environment. The simulation parameters for physical and MAC layer are adjusted by assigning them the values shown in Table II. The parameters include the IEEE 802.11 DCF configuration parameters and the value of channel bit rate.

TABLE II. EXPERIMENT PARAMETERS

Parameters	Values
SIFS	10 micro seconds
DIFS	50 micro seconds
Slot Interval	20 micro seconds
Preamble Length	144 bits
PLCP header Length	48 bits
Channel bit rate	2 Mbps
CWmin	32
CWmax	2048
CWo	32
EW	16

VII. PERFORMANCE RESULTS

At first, when a customer enters the restaurant, his mobile device application (an information level KP and a service level AN) contacts the RIBS (an information level SIB and a service level SN) to become aware of the available services in the Smart Space. The communication takes place via SSAP API at information level and over NoTA BSD API at service level. SSAP API functions are wrappers of NoTA BSD API functions which facilitate information sharing.

After knowing about the available services, the end-user application requests the music videos on the customer's direction. The video frames are streamed form the MusicVideoClient AN to the mobile device of the Personal mobile device of a customer via NoTA BSD API functions instead of SSAP API functions. The customer invokes other ANs one by one, switching between available services after 3→5 minutes each, the ANs then invoke the corresponding SNs to provide the required services to the application.

Each AN and SN workload model is mapped to its respective platforms as shown in Figure 10. The resultant performance model is run to obtain performance results of each platform (including its hosted ANs and SNs) separately. The performance results are written to a text file in the form of different sections, one for each platform. The section of each platform contains a separate subsection for the platform component performance, M3 device level, M3 service level, and M3 information level. We only present the performance results of the platform hosting the MusicVideoServerSN. The performance results of other platforms also contain the similar information.

A. Performance Results (Platform Components)

Since the MusicVideoServerSN was implemented entirely as software, the Graphics Accelerator and Image Processor Services available from the platform were not used. Therefore, only the utilization of the processor cores of platform hosting MusicVideoServer SN is shown in Figure 12. The simulation was run for streaming of 10, 100 and 1000 packets. The solid bar corresponds to 10 packets, bar with horizontal pattern shows use-case of 100 packets and diagonal pattern correspond to 1000 packets respectively.

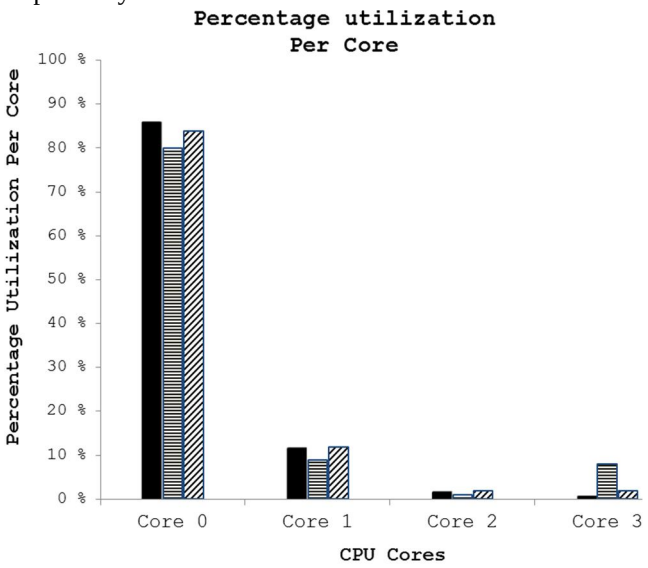

Figure 12. Utilization time of processor cores as compared to overall Utilization time of the CPU

The similar information is reported for other platform components. The cache hits, misses and accesses are also reported as described in [8] and are not shown in this case study.

B. Performance Results (M3 device level)

The performance statistics related to the M3 device level services (MAC and Transport protocols) are recorded via probes. The performance statistics of Transport (UDP) and MAC layer protocol models are shown in Table III.

TABLE III. MAC AND TRANSPORT PERFORMANCE STATISTICS

MAC/Transport Performance statistic	Values
Throughput at MAC-Level (ratio of successful Frame transmissions and total Frame transmissions)	.99
Throughput at Transport-Level (ratio of successful Packet transmissions and total Packet transmissions)	.98
Average Frame Delays	.52 millisec
Average Transport Delays	1.7 millisec
Frame loss rate(Percent)	.022%
Packet Loss rate(Percent)	.983%

The results in Table III satisfy the non-functional property (FrameRate) only if all the functions in the

 ISBN: 978-1-61208-246-2

MusicVideoServer SN, which make use of these OS Services, satisfy the non-functional properties from the design perspective. In case of MusicVideoServer SN, only the SendImage function makes use of NoTA API function (Hsend() for sending image data), which in turn uses the transport and MAC layer ABSOLUT protocols. As shown in Figure 8, this function must be executed within 25 milliseconds (1/40 seconds) in order to satisfy the required FrameRate of 40 Frames/Second. The processing time of this function along with the other application functions are presented in next subsection.

C. Performance Results (Application). Validating Non-Functional Properties

By analysing the processing times of the application source code and the percentage utilization of multi-core processor model by different external library and user-space code, we can find the potential bottlenecks in the application implementation, which will help to perform required optimizations. In other words, after identifying the functionalities which can affect a particular non-functional property, the processing times of these functionalities are analysed to find out whether the implementation of the software components satisfies this non-functional property.

We now elaborate the way non-functional property the FrameRate is analysed and validated by the performance simulation results. This non-functional property is annotated in the application syntactical view and refined to three non-functional properties in the extended behavioural view as shown in Figure 8. It is shown that due to the pipelined nature of the execution of these functionalities, each of these functionalities must be executed within 1/40 seconds (25 milliseconds) in order to achieve a frame rate of 40 frames/seconds. These functionalities and their corresponding (OpenCV library [26] functions are shown in Table IV.

TABLE IV. SHORTLISTED FUNCTIONS THAT CAN AFFECT THE FRAME RATE (A NON-FUNCTIONAL PROPERTY) OF FACETRACKERSTREAMERSERVER

Functionality	Shortlisted Function
Get a frame from Selected File	cvQuerryFrame
Create Image from Frame	cvCreateImage
Send the Image	SendImage

The processing times and the percentage processor utilization of the aforementioned functions are shown in Figure 13 and Figure 14. It is seen that all the operations are performed within 12 milliseconds. The results show that the SendImage function takes less than 6 milliseconds which is well below 25 milliseconds required to achieve the required FrameRate. In this way, the results presented in Table III are also validated. In other words, the performance of MAC and transport protocols is sufficient to satisfy the use-case.

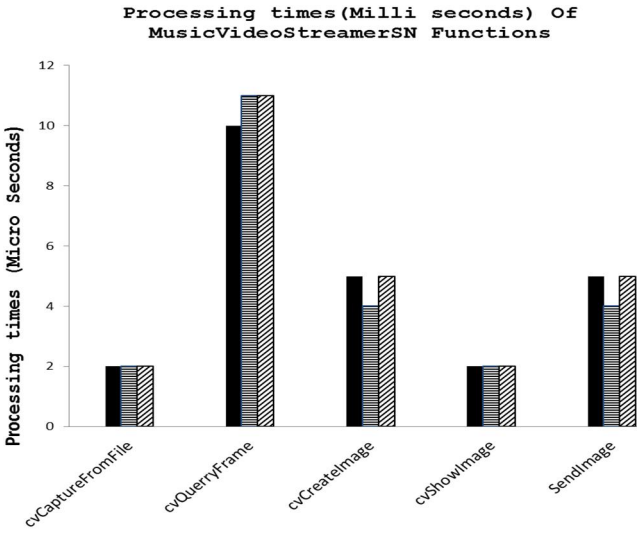

Figure 13. Execution times of functionalities attributing to Frame rate in Face Tracker Subsystem

The processor utilization graph shows that cvQuerryFrame, which fetches a frame for sending it to corresponding AN takes 54% of the overall CPU time taken by the execution of the RM application.

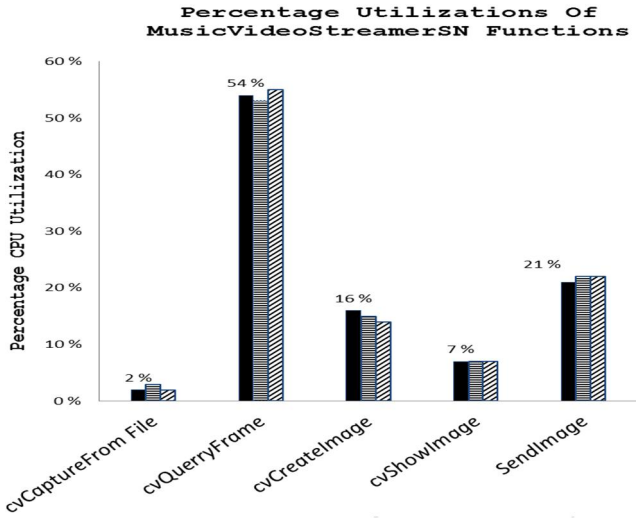

Figure 14. Execution times of functionalities attributing to Frame rate in Face Tracker Streamer Subsystem

The obtained performance results are used to perform appropriate changes in the application models by replacing the software components with more lightweight implementations or by making changes in the platform model if the performance requirements (non-functional properties) are not met. If the performance requirements are met by all the platform and software components, the architectural exploration stops and the implementation phase starts.

A. Performance results M3 Service Level

The processing times of a subset of the NoTA BSD API functions (used by the MusicVideoStreamerSN) are shown in Figure 15. The results show that the average processing times of all the NoTA API functions used by the SN are below 1 millisecond and therefore NoTA does not act as a performance bottleneck. Hence NoTA does not need to be replaced by a more optimized and lightweight Service-Level IOP such as ADIOS [31].

 ISBN: 978-1-61208-246-2

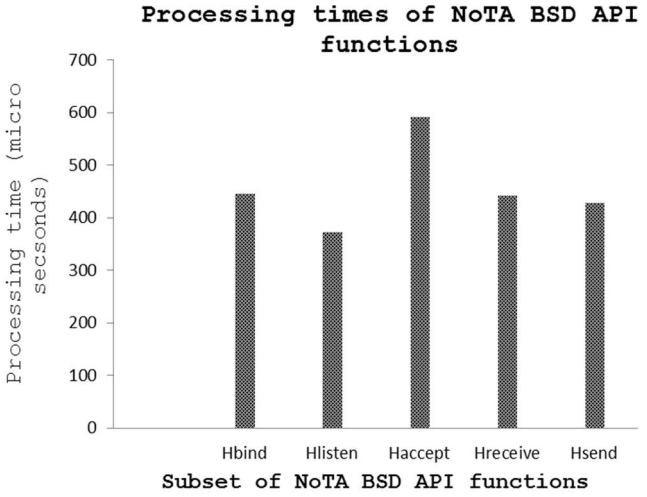

Figure 15. Processing times of M3 service level IOP (NoTA DIP).

B. *Performance results M3 information Level*

The processing times of a subset of the SSAP API functions are shown in Figure 16. The processing times were recorded inside the end-user application, which uses the SSAP API functions to communicate with RIBS for retrieving the information regarding the available services in the Smart Space. The results show that the processing times of all the SSAP API functions are below 1 millisecond and therefore RIBS and SSAPI do not act as a performance bottleneck.

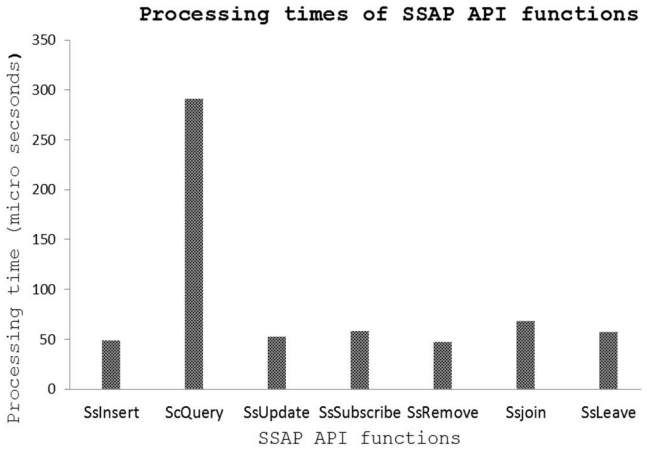

Figure 16. Processing times of SSAPI functions measured from inside user application (KP).

VIII. CONCLUSION AND FUTURE WORK

The system level performance simulation of NoTA based M3 systems was demonstrated using a Restaurant Multimedia application case study. The NoTA application previously presented in [8] was re-modelled and re-implemented at the information level of M3. The used information level entities were SSAP API, KPs and RIBS. The application design methodology describes the information level in a separate application view. UML2.0 MARTE profile and Papyrus were used as the modelling language and toolset respectively.

It was shown that the performance bottlenecks at the device, service and information level IOP solutions can be identified for performing optimizations before the development and deployment phase of M3 systems. The performance evaluation phase shows that the performance results of each M3 level, the platform components and Application can be reported and analysed separately.

The ABSOLUT methodology can be further improved by developing a GUI for easy instantiation of platform models, application workload models and selection of different protocols operating at different M3 IOP levels.

REFERENCES

[1] http://msdn.microsoft.com/en-us/library/dd129911.aspx.

[2] Aarts, E. Ambient Intelligence: a multimedia perspective. IEEE Multimedia, January-March 2004, vol. 11, 12-19.

[3] Chen, H. An Intelligent Broker Architecture for Pervasive Context-Aware Systems. Ph.D. dissertation, University of Maryland, 2004.

[4] Lappeteläinen, Antti et. al., 'Networked Systems, Services, and Information - The Ultimate Digital Convergence'. 1st International Conference on Network on Terminal Architecture, June 11, 2008, Helsinki.

[5] Kiljander, Jussi; Keinänen, Kari; Eteläperä, Matti; Takalo-Mattila, Janne; Soininen, Juha-Pekka.Autonomous file sharing for smart environments.PECCS 2011, Vilamoura, Algarve, Portugal, March 5 - 7, 2011PECCS 2011 Proceedings of the 1st International Conference on Pervasive and Embedded Computing and Communication Systems (2011), 191-196.

[6] Kienhuis, E. Deprettere, K. Vissers and P. van der Wolf. Approach for quantitative analysis of application-specific dataflow architectures. The IEEE International Conference on Application-Specific Systems, Architectures and Processors (ASAP '97), pp. 338–349, Zurich, Switzerland. July 1997.

[7] Jari Kreku, Mika Hoppari, Tuomo Kestila, Yang Qu, Juha-Pekka Soininen and Kari Tiensyrja, Combining UML2 and SystemC Application Platform Modelling for Performance Evaluation of Real-Time Systems, EURASIP Journal on Embedded Systems, volume 2008, ARTICLE ID 712329.

[8] Khan, Subayal; Saastamoinen, Jukka; Nurmi,Jari. (2011c).System-level performance evaluation of distributed multi-core NoTA systems. 2nd IEEE International Conference on Networked Embedded Systems for Enterprise Applications. NESEA 2011, Fremantle, Dec. 8-9, 2011. IEEE (2011).

[9] Tero Kangas, "Methods and Implementations for Automated System on Chip Architecture Exploration", PhD Thesis, Tampere University of Technology, Publication 616, 2006, 181 pages.

[10] USC Center for Software Engineering, Guidelines for Model-Based (System) Architecting and Software Engineering, http://sunset.usc.edu/research/MBASE, 2003.

[11] Garlan, R. T. Monroe and D. Wile. Acme: An Architecture Description Interchange Language. Proceedings of CASCON '97, November 1997.

[12] R. Roshande, B. Schmerl, N. Medvidovic and D. Garlan, D. Zhang. Understanding tradeoffs among different architectural modeling approaches. Software Architecture, 2004. WICSA 2004. Proceedings. Fourth Working IEEE/IFIP Conference on software architecture.12-15 June 2004, pp. 47 – 56.

[13] P. Lieverse, P. van der Wolf, K. Vissers, and E. Deprettere, A methodology for architecture exploration of heterogeneous signal processing systems. Kluwer Journal of VLSI Signal Processing 29 (3), 2001, pp. 197-207.

[14] Pimentel and C. Erbas. A Systematic Approach to Exploring Embedded System Architectures at Multiple Abstraction Levels. IEEE Transactions on Computers, vol. 55, no. 2, Feb. 2006, pp.99 –112.

[15] T. Wild, A. Herkersdorf and G.-Y. Lee. TAPES—Trace-based architecture performance evaluation with SystemC. Design Automation for Embedded Systems, Vol. 10, Numbers 2-3, Special Issue on SystemC-based System Modeling, Verification and Synthesis, 2006, pp 157-179.

[16] D. Manzaroli, L. Roffia, T. Salmon Cinotti, E. Ovaska, P. Azzoni, V, Nannini and S. Mattarozzi, "Smart-M3 and OSGi:

The Interoperability Platform", *In Proc. SISS 2010*, IEEE Press, 2010, pp. 1053-1058.
[17] O. Lassila, Programming Semantic Web Applications: A Synthesis of Knowledge Representation and Semi-Structured Data, doctoral dissertation, Helsinki University of Technology, Department of Computer Science and Engineering, Laboratory of Software Technology, 2007.
[18] Instantiation and feasibility evaluation of NoTA SOAD via MARTE profile and binary instrumentation. Khan, Subayal; Tiensyrjä, Kari; Nurmi, Jari. The 7th International Conference and Expo on Emerging Technologies for a Smarter World. CEWIT 2010. Incheon, 27 - 29 Sep. 2010.
[19] http://dev.iptc.org/rNews
[20] http://musicontology.com/
[21] http://www.intelleo.eu/ontologies/vw/movies/spec/
[22] Subayal Khan, Susanna Pantsar-Syväniemi, Jari Kreku, Kari Tiensyrjä and Juha-Pekka Soininen, "Linking GENESYS Application Architecture Modelling with Platform Performance Simulation", in Proceedings of the 12th Forum on Specification and Design Languages (FDL 2009), September 22-24, Sophia Antipolis, France, 2009.
[23] Multi-threading support for system-level performance simulation of multi-core architectures. ARCS 2011 - 24th International Conference on Architecture of Computing Systems.Como, Italy. 02/22/2011- 02/23/2011. Saastamoinen, Jukka; Khan, Subayal; Tiensyrjä, Kari.
[24] Application workload model generation methodologies for system-level design exploration. DASIP 2011. November 2-4 2011.Tampere, Finland. Jukka Saastamoinen, Jari Kreku.
[25] Subayal Khan, Jukka Saastamoinen, Mikko Majanen, Jyrki Huusko and Jari Nurmi. Analyzing Transport and MAC Layer in System-Level Performance Simulation, International Symposium on System-on-Chip 2011,Tampere, Finland, October 31 - November 2, 2011.
[26] http://opencv.willowgarage.com/wiki/
[27] http://projects.developer.nokia.com/NoTA
[28] Khan, Subayal; Saastamoinen, Jukka; Nurmi,Jari. (2011c).System-level performance evaluation of distributed multi-core NoTA systems. 2nd IEEE International Conference on Networked Embedded Systems for Enterprise Applications. NESEA 2011, Fremantle, Dec. 8-9, 2011. IEEE (2011).
[29] http://www.isi.edu/nsnam/ns/
[30] http://www.omnetpp.org/
[31] Eteläperä, Matti; Keinänen, Kari; Kiljander, Jussi. Feasibility Evaluation of M3 Smart Space Broker Implementations Applications and the Internet (SAINT), 2011 IEEE/IPSJ 11th International Symposium on (2011), 292-296.
[32] A UML Profile for Modeling and Analysis of Real-Time and Embedded Systems (MARTE), www.omg.org/technology/documents/profile_catalog.html
[33] Resource Description Framework, www.w3.org/RDF/
[34] RDF Semantics, www.w3.org/TR/rdf-mt/
[35] OWL 2 Web Ontology Language Reference, www.w3.org/TR/owl-ref/F

 ISBN: 978-1-61208-246-2

Towards evolvable state machines for automation systems

Dirk van der Linden, Georg Neugschwandtner
Electromechanics Research Group
Artesis University College of Antwerp
Antwerp, Belgium
{*dirk.vanderlinden, georg.neugschwandtner*}*@artesis.be*

Herwig Mannaert
Department of Management Information Systems
University of Antwerp
Antwerp, Belgium
herwig.mannaert@ua.ac.be

***Abstract*—Since several decades, the pressure on organizations to swiftly adapt to their environment has been increasing. This also applies to industry. One of the consequences is the increasing importance of evolvability in production control systems. Many such systems are modelled using finite state machines. This paper presents an explorative attempt to define design rules and constraints that should be applied to state machines to enable evolvability. Our design of an evolvable state machine is based on normalized systems theory. Without loss of generality, this design is inspired by the typical requirements of automation systems.**

***Keywords*-Normalized Systems; Evolvability; Finite State Machines; Automation Systems.**

I. INTRODUCTION

Current organizations need to be able to cope with increasing change and increasing complexity in most of their aspects and dimensions [1]. We shall call a system *evolving* when changes in terms of the system's capabilities occur. The effort or cost required for adding or changing a specific capability is a property of a system – the property of *evolvability*. Evolvability is increasingly important for organizations to allow them to swiftly adapt to an agile and complex environment. This paper focuses on the evolvability of production control and automation systems.

In general, the behaviour of any system, subsystem or process can be categorized as *static* or *dynamic*. Static behaviour means that the (sub)system does not experience any internal change during its lifetime. A system is said to have dynamic behaviour if it changes its behaviour during its existence [2]. If dynamic reconfiguration can be achieved, downtimes of production control and automation systems can be reduced: a change which can be performed without a complete shutdown is called a 'dynamic reconfiguration', while a 'static reconfiguration' requires the complete shutdown of a system [3].

Efforts to improve the flexibility and maintainability of automation systems go back decades. The first approach to implement automation control logic was based on hard-wired relay systems. In the late 1960s, GM Hydramatic issued a request for proposal for an electronic replacement. The result was a Programmable Logic Controller (PLC), built by Bedford Associates. One of the main advantages was that changes in control logic could now be made by changing the program rather than changing wiring and bypassing or adding relays. In addition, programs could be reused for another application. The technology shift from hardware to software provided more flexibility and an improvement of maintainability. While this was certainly an improvement, the characteristic of evolvability is still not totally reached. Changing or debugging a few lines of software code is easier than rewiring relay circuits, but the number of software problems and bugs does not grow proportionally with the software size. Instead, they grow out of proportion. After reaching a certain size, software becomes a problem in its own right [4].

Besides maintainability, reusability and flexibility, evolvability is a critical non-functional requirement on software. In their review of evolvability as a characteristic of software architectures, Ciraci and van den Broek [5] define it as "a system's ability to survive changes in its environment, requirements and implementation technologies." However, evolvability is hard to measure, and existing software development methodologies focus on functional requirements almost exclusively.

In order to better satisfy non-functional requirements, giving software a clear, well-defined and if possible standardized structure is essential. This includes the use of standardized programming languages. As further discussed in Section IV of this paper, PLCs are usually programmed in one of the languages of the IEC 61131-3 standard [6]. Another important technique is to employ formal models wherever possible. A prime example in this context are finite state machines. For example, the ISA-88 standard recommends specifying elementary operations in batch manufacturing processes (e.g., filling a tank) by way of state machines. In the simplest case, the state machine for a so-called "equipment phase" contains the states "Idle", "Running" and "Complete". An equipment phase specification will, among other things, describe additional states, the conditions for transitions between these states (e.g., after a specified amount of time has elapsed) and the actions to take upon such a transition (e.g., close a valve).

While state machines are a valuable tool to increase system maintainability, they do not automatically guarantee

 ISBN: 978-1-61208-246-2

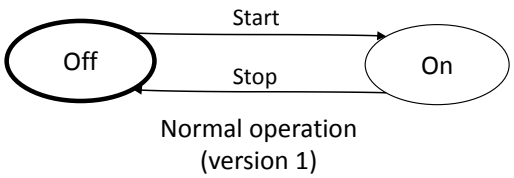

Figure 1. Motor control state machine, version 1

evolvability. The research presented in this paper focuses on the design of an evolvable state machine which can be implemented in one or more of the IEC 61131-3 languages, independent of vendor or CPU type. The design supports dynamic reconfiguration wherever possible.

The remainder of the paper is structured as follows: Section II gives an example of a state machine in an automation system going through subsequent evolution steps. Section III explains the basics of the normalized systems theory, which offers a formal guideline to system evolvability. Section IV introduces a concept for cross-vendor PLC system evolution which supports the coexistence of different versions of the same reusable, generic module. Section V proposes a set of design rules for evolvable state machines in the context of the concept presented in Section IV, derived from normalized systems theorems. In addition, implementation considerations are discussed. Section VI concludes the paper.

II. An Evolving State Machine

A finite state machine is an abstract machine that can be in one of a finite number of states. The machine is in only one state at a time; the state it is in at any given time is called the current state. The current state can change upon a triggering event or condition. This is called a transition. A particular state machine is defined by the list of its states, the possible transitions between them, and the triggering condition for each transition.

In automated production installations, the behaviour of a large portion of the control equipment (such as valves, light curtains, pumps, mixers or conveyers) can be – and is – modelled using state machines. In the following, a motor control state machine is presented as an example. As the automation system evolves in response to new requirements and hardware capabilities, new versions of the state machine are introduced.

The initial version of the state machine, shown in Figure 1, shows a very simple model. The motor has two states, 'On' and 'Off'. Two conditions affect the state of the motor: the 'Start' and the 'Stop' command.

This is a very idealized and simplistic view. In an actual industrial environment, additional conditions such as failure conditions or interlocks must be taken into account. As an example for such an additional condition, the second version of the state machine considers the condition of a fuse.

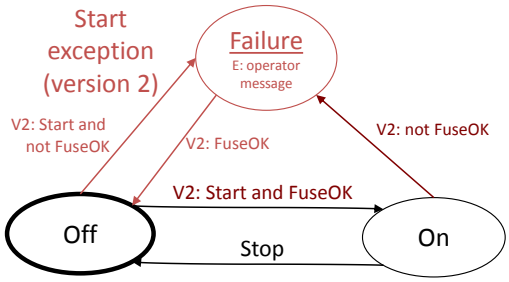

Figure 2. Motor control state machine, version 2

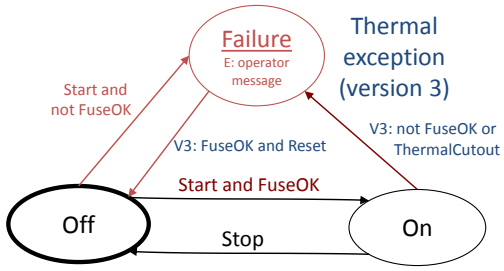

Figure 3. Motor control state machine, version 3

The start condition becomes 'Start and FuseOK' (Figure 2). The additional state 'Failure' is introduced. The condition for transitioning from the 'Off' state to the 'Failure' state is 'Start and not FuseOK'. The condition to go from the 'Failure' state to the 'Off' state is 'FuseOK'. If the fuse blows during the 'On' state, a transition to the 'Failure' state results. In addition, when entering the failure state, a notification is made to trigger an operator to solve the issue.

The third version considers the situation that the motor can stop due to a thermal cut out in the 'On' state (Figure 3). This is modeled with a new version of the transition to the 'Failure' state. In addition, the operator must push a reset button before the 'Off' state can be entered again after a failure, which is reflected by a new version of this transition as well.

III. Normalized Systems Theory

Software undergoes an aging process, as recognized by Parnas [7]. Since there are indications that this aging process is also happening with business processes [8], we must consider the possibility that this phenomenon may actually apply to all non-physical systems in general which undergo an evolution in our society and economy.

For software systems, Manny Lehman formulated the law of increasing complexity, expressing the degradation of a system's structure over time [9]:

> *"As an evolving program is continually changed, its complexity, reflecting deteriorating structure, increases unless work is done to maintain or reduce it."*

 ISBN: 978-1-61208-246-2

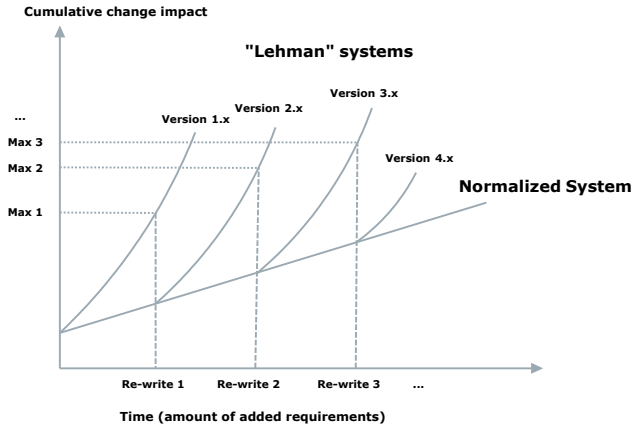

Figure 4. Improving software structure with a re-write [10]

In software development, this deterioration progresses with each update or hotfix. Over time, the deficiency of the structure renders the system unworkable. To mitigate this problem, a re-write of the whole system can help (Figure 4 [10]). The theory of normalized systems was introduced to challenge Lehman's law [11]. Other than most previous efforts to achieve maintainability of software, the contribution of the normalized systems theory goes beyond heuristics; instead of only advocating guidelines such as "low coupling and high cohesion", it provides theorems to derive yes/no answers to questions about evolvability.

In the context of normalized systems, an action entity shall be defined as a module which contains functionality, and a data entity shall be defined as a set of tags (fields). Action entities and data entities are the two main elements from which a system can be constructed. Action entities use data entities as input and output parameters. States, conditions, commands or events can be stored in a data entity. The four core theorems of normalized systems are:

1) Separation of concerns: *An action entity can only contain a single task.*

   A task is functionality which can evolve independently. If the system's developer anticipates that two or more parts of the core functionality can change independently, these parts must be separated. Therefore, normalized systems shall be constructed of action entities dedicated to one core activity.

2) Data version transparency: *Data entities that are received as input or produced as output by action entities must exhibit version transparency.*

   It must be possible to update one or more data entities which are passed between action entities and let multiple versions co-exist without affecting other versions of action entities.

3) Action version transparency: *Action entities that are called by other action entities must exhibit version transparency.*

   It must be possible to update an action entity, which is coupled with another action entity, while multiple versions of both modules can co-exist. In other words, introducing a new version of an action entity shall not require changes to any other action entity.

4) Separation of states: *The calling of an action entity by another action entity must exhibit state keeping.*

   Every action entity must keep track of its requests to other action entities. If the response to a request is not as expected, the calling action entity must not block indefinitely; rather, it shall handle the exceptional situation as appropriate for its own state.

Two additional theorems have recently been introduced as extensions of the theorems on data and action version transparency [12]. They address the challenge of managing the diversity of run-time *instances* of data and action entities in an evolving system.

5) Data instance transparency: *A data instance has to keep its own instance ID and the version ID on which it is based or constructed.*

   If the type definition (source code) of a data entity is updated to a new version, instances based on the previous version continue to exist in the system.If an action entity receives a data instance for processing, the action entity must have a way of knowing the version of this data instance to be able to handle the data instance in a version-compliant way. Therefore, every data instance must contain a version ID reflecting the version of the data entity it is an instance of. The instance ID serves to tell apart multiple instances of the same version.

6) Action instance transparency: *An action instance has to keep its own instance ID and the version ID on which it is based or constructed.*

   When run-time instances of action entities interact, they must consider the fact that the other action entity can be based on one of various versions of its type definition. A version ID is necessary to give the calling action instance information about which interactions are possible. Again, the instance ID serves to tell apart multiple instances of the same version.

Note that there is no supersedure relationship between *versions* in our context; versions may continue to exist in parallel indefinitely to reflect variants of a type of equipment.

IV. Cross-vendor programs and instance version diversity in a PLC system

When an update of a PLC project includes the introduction of a new CPU type, or even a conversion of the software to another brand, software developers often re-engineer the whole project. Also, when a motor is replaced

 ISBN: 978-1-61208-246-2

with a different one – or the update includes the introduction of a frequency drive, which requires a vendor dependent system function block –, engineers tend to re-write the module which is controlling the motor.

In the following, a concept is introduced to reduce the amount of these re-writes. A new motor should no longer require a new software module; neither should the entire project require re-engineering because of changing to a new brand or PLC family. To achieve this, we propose that programming is based on generic modules. There shall only be one module for every core function (e.g., motor control), with the variations between physical motors and their control being addressed by multiple, co-existing, versions of this module.

In this concept, the vendor independence brought about by the IEC 61131-3 standard is an important element. In the first decades after the introduction of the first PLC, these controllers were programmed in vendor-dependent languages. However, during the nineties, the need for a more generalized way to program PLCs increased. As a result, the IEC 61131-3 standard was introduced. It was definitely successful: nowadays, most common brands support at least some of the IEC 61131-3 languages. However, the standard does not include hardware configuration. Consequently, the connection to process hardware (process I/O) remains vendor-dependent. In addition, the standard allows some liberties (e.g., implementation-dependent parameters in Annex D [6]). Commercial IEC 61131-3 programming environments show some differences. Therefore, developers still often re-write a whole software project in case another brand of PLC is required.

Our approach to truly generic, vendor-independent PLC programming is shown by way of an example in Figure 5. A generic module, which strictly sticks to IEC 61131-3 code, contains the core functionality of a device, for example controlling a motor. Instances of this module represent individual motors. Before the generic module can be downloaded to a specific brand of PLC in order to control a specific motor, it undergoes an automatic vendor-mapping procedure, which converts part of the module code according to what is required by the vendor's specific environment. In addition, the vendor-mapping procedure adds an extra module to the (mapped) core module: a connection entity (CE). This connection entity is dedicated for a specific motor (instance), and includes all the details needed to connect the (mapped) core functionality with the process hardware (I/O). If necessary, this connection entity can also include vendor-specific function blocks (e.g., a scaling block for analog values, or a system block dedicated to control a specific frequency drive).

Each new version of the functionality is referred to as a class version, and each individual physical motor as an instance. Class versions correspond to the functionality *available* in the PLC (potentially in several co-existing versions), while instance versions correspond to the *instantiated* functionality for controlling a specific type of motor. Instance IDs refer to one single, specific physical motor; they tell the connection entity which hardware addresses an individual motor control module instance has to be connected to.

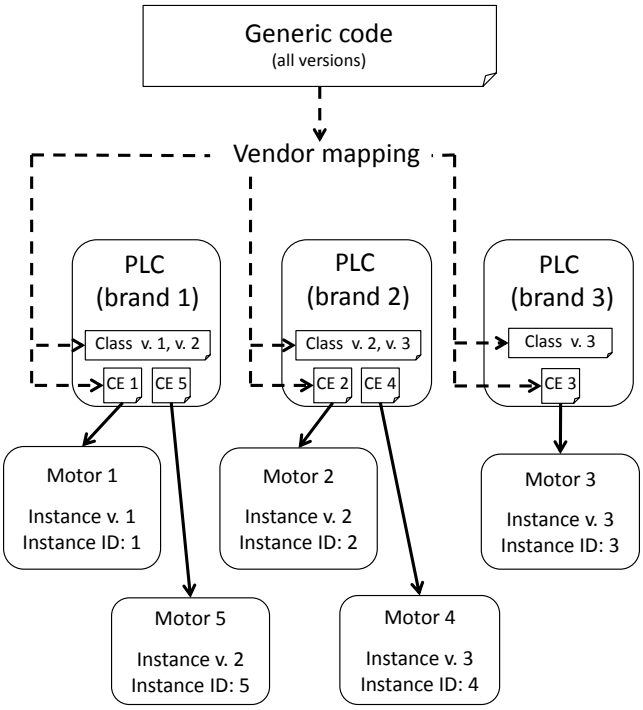

Figure 5. A generic software module with heterogeneous instances

For example, motor 1 could be controlled by an instance of version 1 of the state machine presented in Section II, since status feedback is not required for it. Motor 2 is controlled by an instance of version 2 of this state machine, since for it the fuse condition must be taken into account. Motor 5 is also controlled by an instance of version 2 of the state machine; while motor 2 and motor 5 thus share the same instance version, they have different instance IDs.

V. EVOLVABLE STATE MACHINES

The previous sections discussed the benefits of version transparency and co-existence. In the following, we propose rules – based on normalized systems theory – that shall be followed by state machines and the program code implementing them in order to achieve these properties, and, thus, evolvability.

S1. *The functionality of a state machine shall be implemented in an action entity, while the state and transition trigger information should be stored in a separate entity – a data entity.*

When the functionality of a state machine is updated, a new class version is introduced. We want to be able to

deploy instances of this new version to the system without disrupting the operation of instances of previous versions, which may still be adequate for part of the equipment. Thus, several instances of devices controlled by different versions of the state machine should be able to co-exist, and we require the logic of the state machine to change independently of these instances. Remember that if two parts of a module can change independently, they shall be separated following the separation of concerns principle (Theorem 1); from this follows the separation called for in this rule.

Every version of the data entity contains state and condition fields. In each state, a particular state of the associated process hardware is effected (e.g., letting the motor run in the 'On' state). This is done by way of a connection entity. Values for the condition fields are provided by other action entities (in particular, connection entities); when the conditions for a particular transition are fulfilled, the state machine action entity changes the current state of the instance.

S2. *The state machine data entity shall include an instance ID.*

The instance ID allows the connection entities to map this instance to the correct hardware addresses. This is necessary so that changes on hardware inputs are reflected as changes in transition fields, which in turn will cause the state machine action entity to perform the appropriate state transition. Likewise, the mapping is necessary in order for the required hardware outputs to be set to perform the action associated with a state of the state machine.

For example, in version 1 of the state machine presented in Section II (Figure 1), the output should be 'TRUE' when in the 'On' state and 'FALSE' in the 'Off' state.

S3. *The state machine action entity shall include a class version ID, and the state machine data entity shall include an instance (data type) version ID.*

To comply with the version transparency theorems, the data entity must contain its own version (the version of the state machine it is an instance of). This version ID lets action entities recognize the class version corresponding to the instance and act accordingly. The action entity should store its class version on the moment of compilation as a hard-coded constant.

Following our first rule (S1), the data and the functionality within the system should be separated. Therefore, we have a data entity to store the system's data in one or more data fields, and an action entity to perform actions based on the data in this data entity. Several versions of both data entities and action entities have to be able to co-exist. When a recent action entity instance encounters an older data entity instance, it must interpret its data fields in the way the older action entity instance would have. If necessary, default values need to be defined for fields not present in the older data entity instance. When a more recent data entity instance is processed by an older action entity instance, only old data fields are used, because the older action entity instance is not aware of the recently added data field(s). To enable proper interaction with instances of older versions, or at least prevent version conflicts, instance version IDs are required (Theorems 5 and 6).

For example, suppose we have an action entity version 2 (class version), which should process a data entity instance version 1 (data type). After reading the data entity instance's version ID, the action entity decides to never manipulate the 'FuseOK' data field, nor allows any transition to the state 'Failure'. These actions must be prevented because these fields do not exist in version 1 of the data entity; undefined behaviour would result. Instead, any information on the fuse or thermal cut out (if available) is ignored, corresponding to the (older) functionality of action entity version 1. Conversely, consider an instance of action entity version 1, which should process a younger instance of data entity version 2. This action entity instance is not even aware of the existence of fuse information nor the state failure, so it will never read nor manipulate these fields.

The potential 'ThermalCutout' transition of version 3 from the 'On' state to the 'Failure' state will simply never happen if not both the data entity instance and action entity are of version 3. In addition, the action entity must include a selection to decide whether or not a reset command from the operator is needed for the transition from the 'Failure' state to the 'Off' state (Figure 3).

S4. *States or transitions shall not be deleted between versions.*

The version transparency theorems (Theorems 1 and 2) state that multiple versions of both data entities and action entities have to be able to co-exist. If a state or a transition is deleted during an update of a state machine, the behaviour of instances of older versions of the action entity can become undefined. If following the transition logic of an old version a state should become active which does not exist any more after an update, the older version cannot co-exist with the recent one. Consequently, deletions of states or transitions are violations of the version transparency theorems.

S5. *State modifications shall apply transparent coding or version wrapping.*

Deletions of states can cause violations of the version transparency theorems, so only additions and modifications are allowed. Modifications shall adhere to the principles of transparent coding or wrapping versions [13]. Transparent coding is defined as the writing of internal code in a module which is not affecting the functionality of previous versions. When transparent coding is not possible (e.g., because of conflicting functionality of the versions, or when the combination of the functionality of different versions requires too complex code), version wrapping can be applied. Following this principle, different versions of a module co-exist in

 ISBN: 978-1-61208-246-2

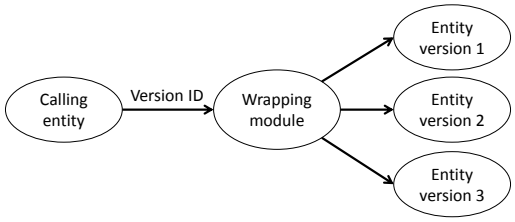

Figure 6. The concept of version wrapping

parallel, and a wrapping module selects the desired version based on the version ID (see Figure 6).

Summary

In summary, in order to attain the property of evolvability for a state machine, updates must be confined to the following set of anticipated changes:

- An additional state
- An additional transition
- A new version of a state following the principle of transparent coding
- A new version of a transition following the principle of transparent coding
- A new version of a state following the principle of version wrapping
- A new version of a transition following the principle of version wrapping

VI. Conclusion

The state machine is a valuable artefact for modelling systems. However, when systems evolve, it follows from Manny Lehman's law of increasing complexity that their further evolution is restrained when the systems' size increases over time. In a rapidly changing environment, there is a need for evolvable state machines: when production systems evolve, corresponding changes have to be made in the automation software.

This paper presented a design for evolvable state machines that can be used in automation systems software. The design is based on the normalized systems theory. Rules were derived to constrain changes to state machines in order to achieve the property of evolvability. In addition, case scenarios were discussed showing how instances of different versions of such an evolvable state machine can coexist.

The design supports dynamic reconfiguration, as called for by Kuhl and Fay, to update a system without the need for a complete system shutdown. Compiling an IEC 61131-3 project includes allocating memory to variables. A shutdown is only necessary when this memory must be remapped. Changing the value of a data field in a data instance can be done without recompilation, so no shutdown is required. When, for example, a motor is replaced by a new one, this change is reflected by a change to the instance version ID of the data entity in our design. Therefore, dynamic reconfiguration is supported for such a situation.

Regarding future work, state machine libraries and toolkits should be improved by adding constraints to follow the rules presented in this paper, increasing system evolvability by ensuring compliance with the theorems on normalized systems.

References

[1] H. Mannaert, P. De Bruyn, and J. Verelst, "Exploring entropy in software systems: Towards a precise definition and design rules," in *Proc. 7^{th} Intl. Conference on Systems (ICONS 2012)*, 2012, pp. 93–99.

[2] J.-P. Kruth, T. V. Ginderachter, P. I. Tanaya, and P. Valckenaers, "The use of finite state machines for task-based machine tool control," *Computers in Industry*, vol. 46, no. 3, pp. 247–258, 2001.

[3] I. Kuhl and A. Fay, "A middleware for software evolution of automation software," *Proc. 16^{th} IEEE Intl. Conf. on Emerging Technologies and Factory Automation (ETFA)*, 2011.

[4] O. Niggemann, "System-level design and simulation of automation systems," in *Proc. 8^{th} IEEE Intl. Workshop on Factory Communication Systems (WFCS)*, 2010, pp. 173–176.

[5] S. Ciraci and P. van den Broek, "Evolvability as a quality attribute of software architectures," in *Proc. 2^{nd} Intl. ERCIM Workshop on Software Evolution*, 2006, pp. 29–31.

[6] IEC 61131-3, *Programmable controllers – Part 3: Programming languages*. International Electrotechnical Commission, 2003.

[7] D. L. Parnas, "Software aging," in *Proc. 16^{th} Intl. Conf. on Software Engineering (ICSE)*, May 1994, pp. 279–287.

[8] D. Van Nuffel, "Towards Designing Modular and Evolvable Business Processes," Ph.D. dissertation, University of Antwerp, 2011.

[9] M. Lehman, "Programs, life cycles, and laws of software evolution," *Proceedings of the IEEE*, vol. 68, pp. 1060–1076, 1980.

[10] D. van der Linden, G. Neugschwandtner, and H. Mannaert, "Industrial automation software: Using the Web as a design guide," in *Proc. 7^{th} Intl. Conf. on Internet and Web Applications and Services (ICIW)*, 2012.

[11] H. Mannaert, J. Verelst, and K. Ven, "The transformation of requirements into software primitives: Studying evolvability based on systems theoretic stability," *Science of Computer Programming*, vol. 76, no. 12, pp. 1210–1222, 2011.

[12] D. van der Linden and H. Mannaert, "In search of rules for evolvable and stateful run-time deployment of controllers in industrial automation systems," in *Proc. 7^{th} Intl. Conf. on Systems (ICONS)*, 2012, pp. 67–72.

[13] D. van der Linden, H. Mannaert, W. Kastner, and H. Peremans, "Towards normalized connection elements in industrial automation," *International Journal On Advances in Internet Technology*, vol. 4, no. 3&4, pp. 133–146, 2011.

 ISBN: 978-1-61208-246-2

Odor Classification by Neural Networks

Sigeru Omatu Mitsuaki Yano
Department of Electronics, Information, and Communication Engineering
Osaka Institute of Technology
Osaka, 535-8585, Japan
omatu@rsh.oit.ac.jp yano@elc.oit.ac.jp

***Abstract*—It is important to detect an odor in the human living space and artificial electronic noses have been developed. This paper considers an array sensing system of odors and adopts a layered neural network for classification. We use all measurement data obtained from fourteen metal oxide semiconductor gas (MOG) sensors. Some sensors are not sensitive while others are sensitive. In order to classify odors, we use data from all fourteen sensors even if some of them are not sensitive so much. We will propose three methods to use the data by insensitive sensors to find the features of odors. Then, applying those features to a layered neural network, we will compare the classification results.**

***Keywords*-odor classification; odor sensors; neural networks; layered neural network; features of odor.**

I. INTRODUCTION

Recently, much research has been done about the recognition and classification of odors [1],[2],[3],[4]. It is important for human beings to obtain high quality information on odor, since it is one of our five senses. We have used these five senses to enjoy comfortable human life with communication and mutual understanding. Artificial odor sensing and classification systems through electronic technology are called an electronic nose and they have been developed according to various odor sensing systems and several classification methods [1],[2].

We have developed electronic nose systems to classify the various odors under different densities based on a layered neural network and a competitive neural network of the learning vector quantization method [5], [6],[7],[8].

From our experience, it is difficult to achieve the perfect classification even if we use many MOG sensors [9] since some of them are insensitive for some odors. This means that some sensors are actively sensitive and effective for classification. But insensitive sensors may become sensitive for other odors and we cannot take away those sensors even if they are insensitive for an odor since they could be useful for the classification of other odors.

To solve the dilemma, we use all sensors regardless of sensitive or insensitive sensors. We extract the features of odors by processing all sensors by reforming the data such that insensitive data become useful. In this paper, we propose three methods to extract the feature vectors by processing the insensitive data.

After brief survey of the electronic nose and its measurement and classification methods, we propose three methods to reform the data. The first method (Method 1) is to reverse the data belonging to an insensible group with respect to horisontal axis and enlarge the negative data. The second method (Method 2) is to rank the negative data of the method 1 and according to the ranking we assign some weights. The third one (Method 3) is to add more information about the transient property of odor data in addition to a maximum value. Finally, simulation results for odor data are discussed to see the effectiveness of the proposed methods.

II. HUMAN OLFACTORY PROCESSES

Although the human olfactory system is not fully understood by physicians, the main components of the anatomy of human olfactory system are the olfactory epithelium, the olfactory bulb, the olfactory cortex, and the higher brain or cerebral cortex as shown in Fig. 1. The process of the human olfactory system is shown in Fig. 2.

The first process of human olfactory system is to breathe or to sniff the odor into the nose as shown in Step 1 of Fig. 2. The difference between the normal breath and the sniffing is the quantity of odorous molecules that flows into the upper part of the nose. In case of sniffing, most air is flown through the nose to the lung and about 20% of air is flown to the upper part of the nose and detected by the olfactory receptors.

In case of sniffing, the most air flow directly to the upper part of the nose interacts with the olfactory receptors. The odorous molecules are dissolved at a mucous layer before interacting with olfactory receptors in the olfactory epithelium as shown in Step 2 of Fig. 2.

The concentration of odorous molecules must be over the recognition threshold. After that, the chemical reaction in each olfactory receptor produces an electrical stimulus. The electrical signals from all olfactory receptors are transported to olfactory bulb as shown in Step 3 of Fig. 2.

The input data from olfactory bulbs are transformed to be the olfactory information to the olfactory cortex as shown in Step 4 of Fig. 2. Then the olfactory cortex distributes the information to other parts of the brain and human can recognize odors precisely as shown in Step 5 of Fig. 2. The other parts of the brain that link to the olfactory cortex will control the reaction of the other organ against the reaction of that odor. When humans detect bad odors, they will suddenly expel those odors from the nose and try to avoid breathing them directly without any protection. This is a part of the reaction from the higher brain.

 ISBN: 978-1-61208-246-2

Finally, the cleaning process of the nose is to breathe fresh air in order to dilute the odorous molecules until those concentrations are lower than the detecting threshold as shown in Step 6 of Fig. 2. The time to dilute the odor depends on the persistence qualification of the tested odor.

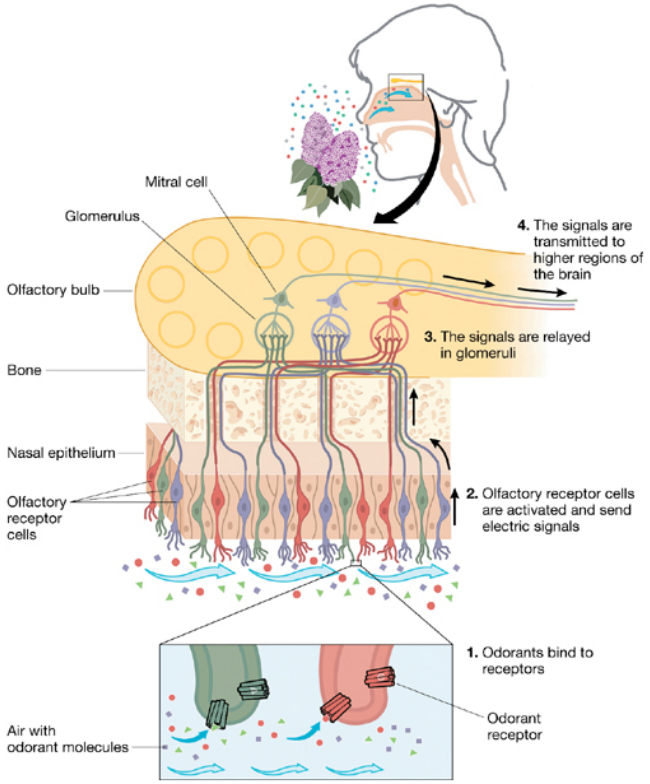

Fig. 1. Olfactory system:EMBO reports (2007).

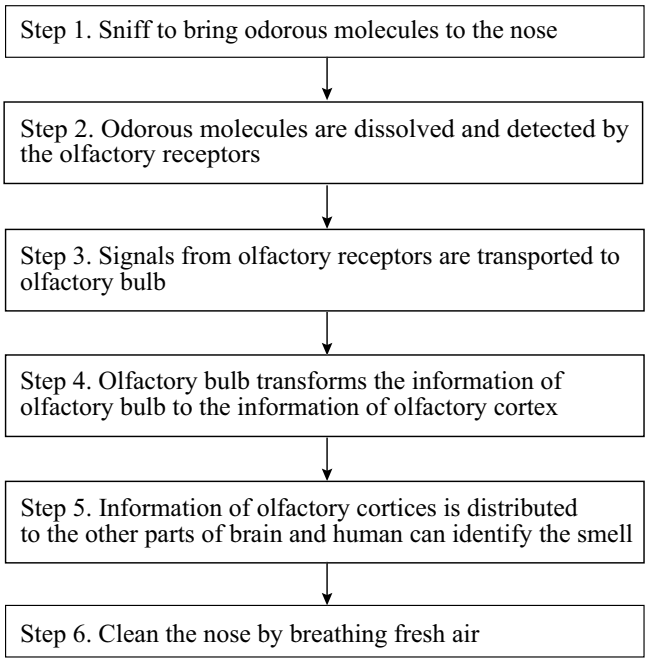

Fig. 2. Process of olfactory system.

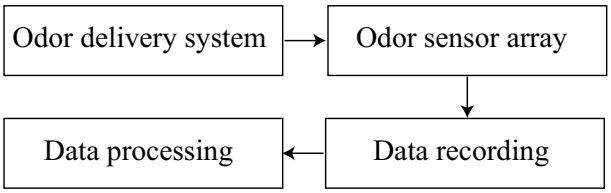

Fig. 3. Main parts of electronic nose systems.

III. Electronic Nose System

The electronic nose system is an alternative method to analyze odor by imitating the human olfactory system. In this section, the concept of an electronic nose is explained. Then various sensors for odors applied as the olfactory receptors are explained. Finally, the mechanism of a simple electronic nose that will be developed in this paper is described in detail by comparing the function of each part with the human olfactory process.

The mechanism of electronic nose systems can be divided into four main parts as shown in Fig. 3.

A. Odor delivery system

The first process of the human olfactory system is to sniff the odorous molecule into the nose. Thus, the first part of the electronic nose system is the mechanism to bring the odorous molecules into the electronic nose system. There are three main methods to deliver the odor to the electronic nose unit, sample flow, static system, and pre-concentration system.

The sample flow system is the most popular method to deliver odorous molecule to the electronic nose unit. Some carrier gas such as air, oxygen, nitrogen, and so on, is provided as a carrier gas at the inlet port to flow the vapor of the tested odor through the electronic nose unit via the outlet port. The mechanism to control the air flow of an electronic nose may contain various different parts such as a mass flow controller to control the pressure of the carrier gas, a solenoid valve to control the flow of inlet and outlet ports, a pump to suck the tested odor from the sampling bag in case that the tested odor is provided from outside, a mechanism to control humidity, and so on. Most commercial electronic noses contain complicated odor delivering systems and this makes the price of the electronic noses become expensive.

The static system is the easiest way to deliver odorous molecules to the electronic nose unit. The electronic nose unit is put into a closed loop container. Then an odor sample is injected directly to the container by a syringe. It is also possible to design an automatic injection system. However, the rate to inject the test odors must be controlled to obtain accurate results. Normally, this method is applied for the calibration process of the electronic nose. But, in this case, the quantity of the odor may not be enough to make the sensor reach the saturation stage, that is, the stage that sensor adsorbs

 ISBN: 978-1-61208-246-2

the odor fully.

The pre-concentration system is used in case of the tested odor that has a low concentration and it is necessary to accumulate the vapor of the tested odor before being delivered to the electronic nose unit. The pre-concentrator must contain some adsorbent material such as silica and the tested odor is continuously accumulated into the pre-concentrator for specific time units. Then the pre-concentrator is heated to desorb the odorous molecule from the adsorbent material. The carrier gas is flown through the pre-concentrator to bring the desorbed odorous molecules to the electronic nose unit. By using this method, some weak odors can be detected by the sensor array in the electronic nose unit.

B. Odor sensor array

The second process of the human olfactory system is to measure various odors corresponding to various receptors in the human olfactory system. In order to realize many receptors artificially, we adopted two types of sensors. One is MOG type and the other is QCM type. The idea of the present paper is to use many sensors which are allocated in an array structure for each type of MOG and QCM types. This structure is adopted based on the human olfactory system. As we will explain in what follows, the odor sensors are not so small and a rather wide space is required to measure odors.

C. Data recording

The data recording is corresponding to temporal memory for the human olfactory system. In the latter case, after learning odors we could identify an odor suddenly, we store sensing data of odors in a computer. To read and write the data, we design an efficient data base structure.

D. Data processing

Using the data base of odors, we must apply an intelligent signal processing technique to recognize odors correctly. We pre-process the odor data for noise reduction, normalization, feature extraction, and so on. Then we use layered neural networks and competitive networks for odor classification since learning ability and robustness are important in odor classification. The most difficult and important process in the odor classification is to find excellent features which are robust for environment like temperature, humidity, and density levels of odors.

IV. Principle of Odor Sensing

Nowadays, there are many kinds of sensors that can measure odorous molecules. However, only a few kinds of them have been successfully applied as artificial olfactory receptors in commercial electronic noses. Among them, we use MOG sensors which will be explained in what follows.

A. Principle of MOG sensors

MOG sensors are the most widely used sensors for making an array of artificial olfactory receptors in electronic nose systems. These sensors are commercially available as the chemical sensor for detecting some specific odors. Generally, a MOG sensor is applied in many kinds of electrical appliances such as a microwave oven to detect the food burning, an alcohol breathe checker to check the drunkenness, an air purifier to check the air quality, and so on.

Generally, it is designed to detect some specific odor in electrical appliances such as an air purifier, a breath alcohol checker, and so on. Each type of MOG sensors has its own characteristics in the response to different gases. When combining many MOG sensors together, the ability to detect a odor is increased.

TABLE I
List of MOG sensors from the FIS Inc. used in this experiment

Sensor No.	Model number	Main Detecting Gas
1	TGS2600	Tobacco, Cooking odor
2	TGS2602	Hydrogen sulfide, VOC, Ammonia
3	TGS2610	Liquefied petroleum gas, Butane
4	TGS2611	Methane
5	TGS2620	Alcohol, Organic solvent
6,7	TGS826	Ammonia, Amine compound
8,9	TGS816	Methane, Liquefied petroleum gas, Butane
10	TGS821	Hydrogen
11	TGS832	Freon gas
12	TGS825	Hydrogen sulfide
13	TGS80	Freon gas
14	TGS822	Alcohol, Organic solvent

In order to classify the odors we adopt a three-layered neural network based on the error back-propagation method.

V. Experimental Data

We have carried out two experiments, Experiment I and Experiment II, as shown in Table II where variation means fluctuation level for each species. In Experiment I, we have measured the odors for the same kind of coffees produced in the different countries such as Colombia, Guatemala, and Ethiopia and the odors of two kinds of blend coffees such as blend coffee 1 and blend coffee 2. In Experiment I, six times of odors measurements have been repeated for each coffee. Thus, the total number of features of odors are thirty for five kinds of coffees. In Experiment II, we have measured odors of three kinds of teas, coffee, and cocoa as shown in Table II. In Experiment II, we have measured six times for each species as done in Experiment II. Thus, total number of the features in Experiemnt II is also thirty as in Experiment I. The experimental conditions for both Experinet I and II are summarized in Table III.

TABLE II
Experiment Iand II

No.	Variation	Species
I	large	Three districts cofee (Colombia, Guatemala, Ethiopia), Two blend coffees
II	small	Tea, Green Tea, Oolong tea, Coffee, Cocoa

The neural network is a layered type based on the error back-propagation method. The number of neurons for this experiment are fourteen in the input layer, thirty in the hidden layer, and three in the output layer, that is, 14-30-3 structure.

 ISBN: 978-1-61208-246-2

TABLE III
ENVIRONMENTAL DATA FOR EXPERIMENT IAND II

Subject	Units
Gas flow	1[l/min]
Temperature of gas	35[°C]
Odor measurement time	12[min]
Dry air flow time	7[min]

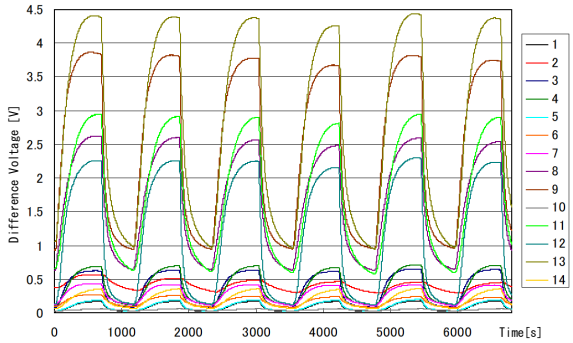

Fig. 4. Sample path of blend coffee 2 of Experiment I.

The reason why three neurons in the output layer is that three bits can represent eight neumerals where in Experimet I and Experiment II, we use five pattern for classification.

We have separated the six measurement data for each odor into three training data and three test data. The combination of the data is ${}_6C_3$=20 for each odor and total number of the test data becomes 32×10^5. Among them we have selected six thousand data for the evaluation. In Fig. 4 and Fig 5, we show the sample paths of blend coffee 2 of Experiment I and Tea of Experiment II, respectively.

We select the maximum value of each sample path as a feature of an odor for a sensor. The reason to use the maximum value is that the odor will be accumulated in the sensor for a while in the beginning and then, the molecule will be oxidized, which means that the resistance of the sensor becomes lowest. Thus, the maximum value reflects steady state of the odor. In the experiments, we have used fourteen sensors. Thus, for each odor, we have a vector of fourteen dimensions. In Fig. 6 we show the feature vectors for three coffees of Colombia, Guatemala, and blend 2 in Experinet I.

The classification results using the data measured by using fourteen sensors for Experinets I and Experiment 2 are given by Table IV and Table V, respectively.

We notice that these experimental results are not so good. Paticularly, in Experiment I it is necessary to improve the classification results. In this case, from Fig. 6 we can see that there are two groups for the feature vectors. One is sensitive for odors and the other is insensitive among fourteen sensors. Thus, if we could use the data of insensitive sensors, we could expect to improve the classification results since there exist differences of features between odors even if the fluctuation levels are not large.

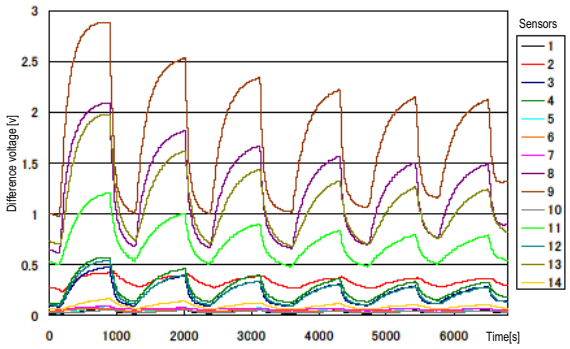

Fig. 5. Sample path of tea of Experiment II.

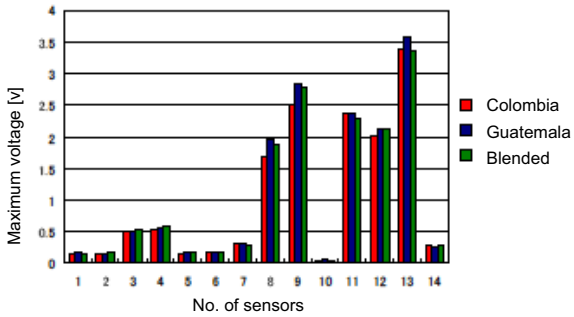

Fig. 6. Feature vectors for coffees in Experiment I.

VI. THREE METHODS FOR IMPROVING THE CLASSIFICATION RESULTS

In what follows, we will propose three methods to use the data in order to improve the classification rate.

A. Method 1

Neurons become sensitive near thresholds since the derivative of the sigmoid function becomes maximum at the threshold value. In other words, the outputs of the neurons become insensitive when the absolute value of the net input becomes very large. Thus, it is preferable to move the net input to become some regions such as [-5,5]. Thus, we propose Method 1 stated as follows. First, we make two groups for the feature vectors such that one is sensitive and the other is insensitive. In Experiment I, lower ranking group (G1) is sensors 1, 2, 5, 6, 7, and 14 and higher ranking group (G2) is sensors 3, 4, 8, 9, 11, 12, 13.

Then, reverse the sign of values in G1 (cf. Fig 7) and scale the values with negative sign such that the maximum among G2 is equal to the absolute value of the smallest value of G1 by linearly interpolation (cf. Fig 8) .

B. Method 2

This method is a ranking of the measurement data. First, separate the data into two groups, G1 and G2 as Method 1 and reverse the sign of values in G1. Then, arrange in decreasing order of absolute value and assign the value 1.4 for the first

 ISBN: 978-1-61208-246-2

TABLE IV
CLASSIFICATION RESULTS FOR EXPERIMENT I. HERE, A IS COLOMBIA COFFEE, B IS GUATEMALA COFFEE, C IS ETHIOPIA COFFEE, D IS BLENDED COFFEE 1, AND E IS BLENDED COFFEE 2.

Odor data	Classification results(60.4%)						
	A	B	C	D	E	Total	Correct
A	4686	0	0	0	1314	6000	78.1%
B	1022	121	0	0	4857	6000	2.0%
C	1387	0	4067	546	0	6000	67.8%
D	956	499	2	3765	1678	6000	62.8%
E	522	0	0	0	5478	6000	91.3%

TABLE V
CLASSIFICATION RESULTS FOR EXPERIMENT II. HERE, A IS TEA, B IS GREEN TEAS, C IS OOLONG TEA, D IS COFFEE, AND E IS COCOA.

Odor data	Classification results(74.3%)						
	A	B	C	D	E	Total	Correct
A	4525	100	513	0	862	6000	75.4%
B	101	3967	0	0	1932	6000	66.1%
C	983	423	3959	635	0	6000	65.8%
D	0	283	0	5717	0	6000	95.3 %
E	629	1234	2	0	4135	6000	68.9 %

sensor, 1.3 for the second sensor, etc. in order of decreasing absolute vale. After that, scale the value in G2 in the same way by assigning values from 1.7, 1.4, 1.3, 1.1, 0.9, 0.3, 0.3. The scaled values were determined by trial and error according to the rule that G2 is more important than G1 values (cs. Fig 9

C. Method 3

This method uses additional information about the transient property. In addition to the maximum value we use the slop of the transient slope (cf. Fig. 4). In this case, we must change the number of neurons in the input layer and the neural network becomes 28-30-2.

Using those methods, we have simulated Experiment I and Experiment II. The simulation results for Experiment I by three methods are shown in Table VI, Table VII, and Table VIII, respectively. From these results, we can see Method 1 could improve the classification results by 31% compared with the result of Table IV.

Among three proposed methods, Method 1 is the best, Method 2 is medium, and Method 3 is the worst for Experiment I. This means that the slope information is not so much efficient to improve the classification results for Experiment I. The reason is that from Fig. 4 it is so sensitive to calculate the slopes from the data and rough estimated values of the slope results in worse classification results. As for Method 2, by trial and error the classification results may be improved more. But such trial is not so welcome in computation.

The simulation results for Experiment II by three methods are shown in Table IX, Table X, and Table XI, respectively. From these results, we can see Method 1 could improve the classification results by 11% compared with the result of Table V.

Among three proposed methods, Method 1 is the best, Method 3 is medium, and Method 2 is the worst for Experiment II. This means that Method 2 is sensitive to the method

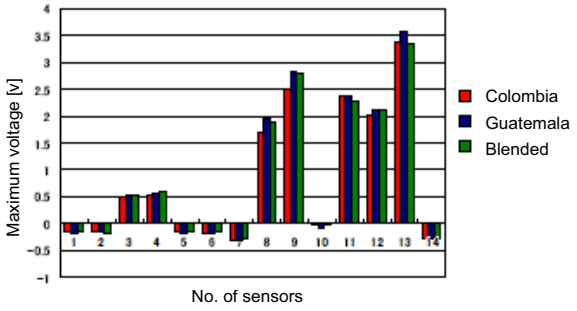

Fig. 7. Feature vectors of the sign reversed version of Experiment I.

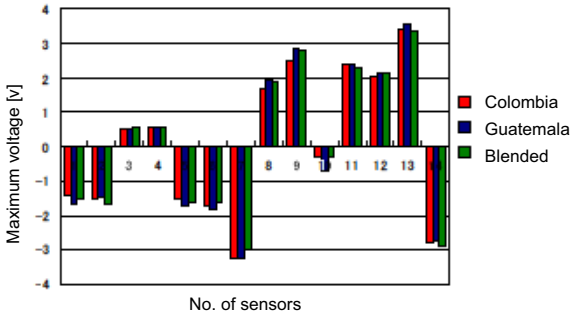

Fig. 8. Feature vectors of linearly interporated version of Experiment I.

by trial and error. Method 3 is rather stable and the result is not so bad. Therefore, Method 1 is most preferable to improve the classification results.

TABLE VI
CLASSIFICATION RESULTS BY METHOD 1 FOR EXPERIMENT I.

Odor data	Classification results (91.0%)						
	A	B	C	D	E	Total	Correct
A	5952	23	4	1	20	6000	99.2%
B	51	4793	0	214	942	6000	79.9%
C	4	0	5996	0	0	6000	99.9%
D	0	440	2	4555	1003	6000	75.9%
E	0	0	0	0	6000	6000	100%

TABLE VII
CLASSIFICATION RESULTS BY METHOD 2 FOR EXPERIMENT I.

Odor data	Classification results (87.9%)						
	A	B	C	D	E	Total	Correct
A	5949	51	0	0	0	6000	99.2%
B	1255	4445	4	296	0	6000	74.1%
C	494	0	4353	1153	0	6000	72.6%
D	0	390	0	5610	0	6000	93.5%
E	0	0	0	0	6000	6000	100%

VII. CONCLUSIONS

In this paper, a new approach to odor classification has been presented and discussed by using MOG sensors. After surveying the odor sensing and classification methods, we have examined two examples, Experiment I and Experiment II to

 ISBN: 978-1-61208-246-2

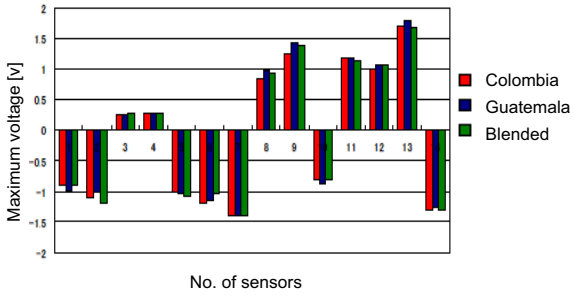

Fig. 9. Feature vectors of ranked version of Experiment I.

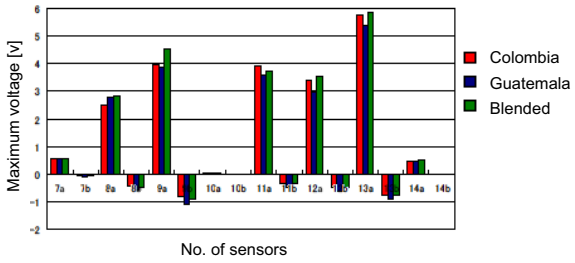

Fig. 10. Feature vectors of the scaled version of Experiment I. Here, holisontal axis simbols are sensor number+slope(a)+vertical intercept(b).

increase the classification accuracy. Basically, we have proposed three methods by using the data measured by insensitive sensors. From these results, using those data is efficient to improve the classification accuracy so much. We will search new features of odor information for classification in the future.

ACKNOWLEDGMENT

This work was supported by JSPS KAKENHI Grant-in-Aid for Scientific Research(B)(23360175). The authors would like to thank JSPS to support this research work.

TABLE VIII
CLASSIFICATION RESULTS BY METHOD 3 FOR EXPERIMENT I.

Odor data	Classification results (78.1%)						
	A	B	C	D	E	Total	Correct
A	4182	1	0	0	1817	6000	69.7%
B	2	5337	1	642	18	6000	89.0%
C	404	308	4344	944	0	6000	72.4%
D	23	1146	190	4457	184	6000	74.3%
E	881	0	0	0	5119	6000	85.3%

TABLE IX
CLASSIFICATION RESULTS BY METHOD 1 FOR EXPERIMENT II.

Odor data	Classification results (85.6%)						
	A	B	C	D	E	Total	Correct
A	4902	0	1098	0	9	6000	81.7%
B	81	5768	0	9	142	6000	96.1%
C	324	5	5421	248	2	6000	90.4%
D	0	0	450	5550	0	6000	92.5%
E	1031	94	588	260	4027	6000	67.1%

TABLE X
CLASSIFICATION RESULTS BY METHOD 2 FOR EXPERIMENT II.

Odor data	Classification results (59.7%)						
	A	B	C	D	E	Total	Correct
A	5178	754	9	0	59	6000	86.3%
B	952	3253	0	0	1795	6000	54.2%
C	504	1166	556	532	3242	6000	9.3%
D	0	347	469	5184	0	6000	86.4%
E	601	1644	0	9	3746	6000	62.4%

TABLE XI
CLASSIFICATION RESULTS BY METHOD 3 FOR EXPERIMENT II.

Odor data	Classification results (75.9%)						
	A	B	C	D	E	Total	Correct
A	4559	0	1276	93	72	6000	76.0%
B	1101	4198	0	597	104	6000	70.0%
C	743	0	3686	1571	0	6000	61.4%
D	0	15	242	5743	0	6000	95.7%
E	71	644	15	706	4564	6000	76.1%

REFERENCES

[1] Milke J. A. (1995), "Application of Neural Networks for discriminating Fire Detectors", *International Conference on Automatic Fire Detection*, AUBE'95, 10th, Duisburg, Germany, pp. 213–222

[2] Bicego M. (2005), "Odor classification Using similarity-Based Representation", *Sensors and Actuators B*, Vol. 110, pp. 225–230.

[3] Distante C., Ancona N., Siciliano P., and Burl M. (2003), "Support Vector Machines for Olfactory Signal Recognition", *Sensors and Actuators B*, Vol. 88, pp. 30–39.

[4] Gardner J. and Bartlet P. (1998), "Electronic Noses: Principles and Applications", *Oxford University Press*, Pennsylvania, USA, pp. 1–30.

[5] S. Omatu and M. Yano (2011), "Intelligent Electronic Nose System Independent on Odor Concentration", *International Symposium on Distributed Computing and Artificial Intelligence, Salamanca, Spain*, pp. 1–9.

[6] s. Omatu, H. Araki, T. Fujinaka, and M. Yano (2012), "Intelligent Classification of Odor Data Using Neural Networks",*ADVCOMP 2012, Barcelona, Spain*, pp. 1–7.

[7] S. Omatu (2012), "Pattern Analysis for Odor Sensing System", *IGI Global*, pp. 20–34.

[8] T. Fujinak, M. Yoshioka, S. Omatu, and T. Kosaka (2008), "Intelligent Electronic Nose Systems for Fire Detection Systems Based on Neural Networks", *The second International Conference on Advanced Engineering Computing and Applications in Sciences, Valencia, Spain*, pp. 73–76.

[9] General Information for TGS sensors, *Figaro Engineering*, available at www.figarosensor.com/products/general.pdf (2012).

 ISBN: 978-1-61208-246-2

A Practical Approach to Quality Requirements Handling in Software Systems Development

Yuki Terawaki
Research Center for Computing and Multimedia Studies
Hosei University
Tokyo Japan
yuki.terawaki.dc@k.hosei.ac.jp

Tetsuo Tamai
Department of Advanced Sciences, Faculty of Science and Engineering
Hosei University
Tokyo Japan
tamai@hosei.ac.jp

Abstract— **Quality requirements (non-functional requirements or NFR) are vital for the success of software systems. Therefore, to define the quality requirements and to check the quality attributes carefully is necessary for bringing good-quality software and ensuring quality of the service. This paper proposes a framework that measures the quality attributes in the requirement document. The output of proposed framework shows where quality attributes are contained and how much. The framework's objectives are to assist defect detection of requirements statements with focus on quality requirements. We analyzed the requirement specification document using the framework, and confirm the efficacy of this framework.**

Keywords; Quality Requirements; Non-Functional Requirements;Text-mining Approach

I. INTRODUCTION

Many of the problems in a software development project are caused by faults in the requirements that properly the customer (or user) should determine. It is said that items of re-work due to faults in the requirements account for 30~50% of the total cost of development, resulting in cost overruns [1]. Furthermore, the expenses for correction of defects discovered in the latter half of the lifecycle of software development become more massive than the expenses for correction during the first half [2]. For these reasons, it is important to ensure quality of description content of documents that created in upper process of software development such as RFP (Request for Proposal) or SRS (Software Requirements Specification). Requirements that have to be written in these documents are functional requirements and non-functional requirements (or quality requirements) [3].

A functional requirement describes the software's behavior (what is to be executed by the software), and a non-functional requirement is a description which indicates how well the software's behavior is to be executed. It is widely recognized that in real systems, meeting the quality requirements often is more important than meeting the functional requirements in the determination of a system's perceived success or failure [4].

In IEEE830-1998 [15], the basic issues that the SRS writer(s) shall address are the following: Functionality, External interfaces, Performance, Attributes, Design constraints. Especially, IEEE830 insists on the importance of Attributes.

Software quality attributes have to be specified so that their achievement can be objectively verified because there are a number of attributes of software that can serve as requirements. Therefore, this paper proposes a framework that measures the quality attributes in the requirement document. The proposed framework supports to improve the SRS and to lighten the human workload in carrying out Inspection as well.

The paper is organized as follows. In section 2, we point out the current problem. In section 3, our approach is described. The proposed framework and the implementation of tool are described in section 4. Section 5 introduces case studies. The related works are stated briefly in section 6. In section 7 conclusion and future works are provided.

II. THE CURRENT PROBLEM

Despite a general awareness of software quality attributes, functional requirements are highly focused and the quality attributes are not necessarily sufficiently defined. [4]. Quality attributes are difficult to define [6], because customers generally don't present their quality expectations explicitly. An independent administrative institution, Information-technology Promotion Agency (IPA), Japan study shows that NFR demand has a rate of documentation lower than functional requirements.

To address the difficulty of definition of NFR, ISO/IEC25010 is available. The quality model of ISO/IEC 25010 defines the quality attributes which should be considered in software and system development. ISO/IEC25010 defines seven ways to use the quality model [9]. Here are some of uses of the quality model of ISO/IEC25010: i) identifying software and system requirements, ii) validating the comprehensiveness of requirements definition, iii) identifying acceptance criteria for a software product and/or software-intensive computer system.

We can apply a sentence of requirements to each characteristic of the software quality attributes of ISO/IEC 25010 and can check the requirements for quality. However, it is difficult to evaluate correspondence with attribute and requirements for a general reason. This is because some quality requirements overlap two or more quality attributes. Also, when identifying attributes and requirements, human judgment may change over time. Thus, it is difficult to review every quality requirements in terms of coherent thinking.

 ISBN: 978-1-61208-246-2

Though software development requires quick delivery today, it is not unusual for development documents (such as SRS or RFP) to be over several hundred pages long. As the scale of the SRS gets bigger, the structure of the SRS becomes complex. At present, despite the increasing number of documents which should be inspected, shortening of development time is desired. Additionally, almost all development documents are described in natural language. If the quality requirements needed are written to the document created to the upper process, quality can be measured at the time of the acceptance inspection. However, it is difficult to review every quality attributes in terms of time. These problems bring deterioration in the quality of development document and play a role in the failure of the project.

III. OUR APPROACH

When we manage the quality, we have to know the object of management. As mentioned in section 2, in order to improve a SRS with low quality, we focused on software quality attribute (ISO/IEC25010). If the quality attributes can be quantitatively measured, then they could potentially help the author of SRS decide if a revision is needed.

In order to solve the problem described in section 2 (in terms of coherent thinking and time), text-mining technique is effective. The Requirements Process has 4 processes. There are requirements elicitation, evaluation, specification (documentation) and quality assurance. This process is iteration on successive increments according to a spiral model [5]. In the spiral process, when requirements document will become elaborate, the error of requirements may be made.

In spiral process, the revised document (SRS) can check without spending hours as much as possible using text-mining technique. The quality attributes contained in SRS are showed quantitatively because the text mining analyzes where quality attributes are contained, and how much. The rate of documentation of quality attribute can be showed using the output of text mining. Thus, the quality requirements are checked by coherent thinking. Therefore, the workload for verification of SRS will be decreased.

IV. PROPOSED FRAMEWORK

A. Overview of Framework

We propose a framework to improve the quality of SRS through the requirements definition process. As criteria for evaluating the quality requirement, the quality model of ISO/IEC25010 is used. The proposed framework contains a text mining tool which can specify the statement related to quality attribute of ISO/IEC 25010.

The proposed framework analyzes the SRS by text mining to identify where quality characteristics are contained, and how much. The output of this framework provides the consistent evaluation criterion of quality requirements for revising the requirements specification.

The conceptual diagram of the framework is shown in Figure 1. When the document such as SRS or RFP is inputted to the proposed framework, the quality attributes in the document are identified. There are two outputs. One is goodness of fit to each quality characteristic of arbitrary sentences. The other is goodness of fit to each quality characteristic of whole document. From these results, it is shown where sentences expressing quality characteristics occur, and how well they fit the characteristics. Thus, the output shows sentences that need improvement in the SRS and the quality attribute which is not written becomes clear.

This framework can be used after the SRS is documented. However, SRS does not need to be completed. In the documentation process, if a elementary error [7] were to detect even as the author is making the SRS, the perfectibility of SRS would increase before quality assurance process. Moreover, in the quality assurance process, the inspector can reduce the inspection time and implement a more effective inspection. Inspection is a clearly defined procedure performed by a number of inspectors [8]. Before meetings by all the inspectors, each inspector has to read and understand all documents. So, it requires a great investment of time to complete the whole inspection. If this framework used in quality assurance process, it is possible to aim at improving the efficiency of review.

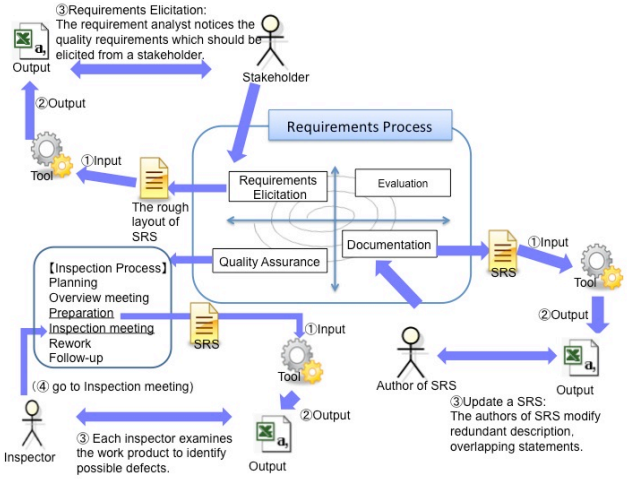

Figure 1 The Conceptual Diagram of Framework

B. Tool with Text Mining

This Tool consists of two comportments: one is the morphological analyzer (MA) and the other is the index generator (IG). MA breaks down the requirements specifications into sentences, and then each sentence is separated by morphological analysis. After that, MA tally the number of word and frequency of appearance, then makes term-document matrix.

The IG have some files. Each file includes statements that represented the quality attributes of ISO / IEC 25010. IG has eight files so that ISO / IEC 25010 consists of eight quality attributes. The sentence in each file is reviewed by the specialist. IG first performs a morphological analysis against each file and removes characteristic words. Then, IG creates the frequency file. When frequency file are created, synonyms are added by using the concept dictionary. The reasons for adding synonyms are as follows. For example

 ISBN: 978-1-61208-246-2

the word "user" is able to represent "customer" "End-user", or "consumer". Moreover, the Japanese word for "user" is "riyousya (kanji)" but "u-zer (katakana)" is also recognized as Japanese. These meanings are identical, and such synonyms need to be considered within the proposed method. After that, IG creates Word Article Matrix (WAM) file by executing mkw commands of Generic Engine for Transposable Association (GETA) [10]. Finally, this method analyzes the rate of content of the quality attributes in the requirements documents using the term-document matrix in MA and the WAM file created in IG.

C. Implementation of Tool

This method was developed as a CUI application by using Java programming language and shell scripts. The Japanese morphological analyzer Sen [11] is employed for morphological analysis in MA and IG. Synonyms are added to IG through Japanese WordNet [12], a concept dictionary, and extracted through a method that first acquires a lower level of the word group against the original words and then acquires the sum of the sets of each upper level word group. For the WAM file creation in IG and search operations in MA, a generic engine for transposable association (GETA) is employed. In IG, the mkw GETA command is used in the script. Since the search parts in GETA are provided only as the C library, GETA must create an execute format to wrap the I/O for the connection by using the Java program and standard I/O. The results will be output in CSV format, which facilitates easy use of the scores included in the search results.

V. CASE STUDY

This section describes the trial practice using the proposed method. The RS used for this trial practice was created in the university. This RS involves replacing the network infrastructure and getting software (web-based application) across the university. In 2006, this RS was already created by their system implementation committee after multiple reviews. However, the author of this RS is not an expert in Requirements Engineering (RE). In short, the author didn't know the quality requirements (or quality attributes).

In this trial, the section relating to software, particularly Learning Management System (LMS) was picked out the RS. This portion has about 4,600 characters. Initially, this portion was analyzed manually by two experts of RE. After that it was analyzed by the proposed method.

A. Result

Figure 2 shows the result of the manual analysis. Figure 3 shows the result of the analysis by the proposed framework. It is clear from the graph that the manual analysis and the analysis by the proposed framework denote the same tendency. In this RS, usability, functional suitability and security are describing most frequently requirements. Figure 4 shows that the quality attributes are distributed throughout. In figure 4, there is a sentence showing two or more quality attributes. For example, sentence of No.45 consists of Functional Suitability (FS), Performance Efficiency (PE), and Functional Requirements (FR).

B. Discussion

The results obtained by the manual analysis and by the proposed method were compared, and it was concluded that the tendencies were similar. Thus, it was concluded that the output of this framework is close to a reviewer's evaluation.

Let's take a look at Figure 4 of each sentence. For example, the sentence of No. 45 has described two requirements in one sentence. The first half of No.45 described, "being able to time on the use of the LMS (to answer a questionnaire)", and is "about security, performance and stability which can respond to concurrent access" in the second half. The first half of No.45 represents functional requirements and the second half represents performance efficiency. The sentence of No. 45 is undesirable sentence because one sentence described two requirements. So, this sentence needs modification. If the output of the proposed framework is provided to the author of the specification, it will contribute to its improvement.

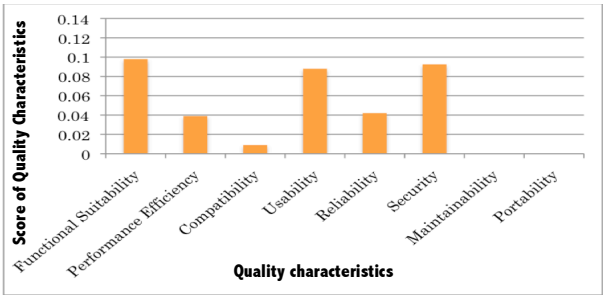

Figure 2 Result of Manual Analysis

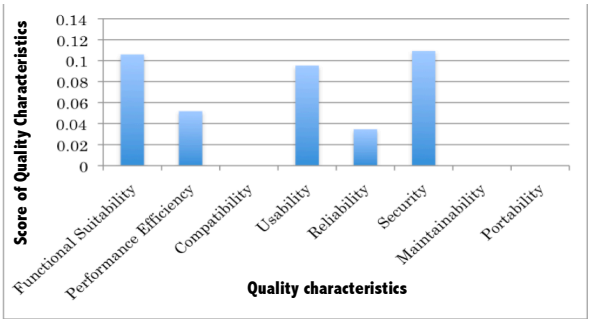

Figure 3 Result of the Analysis by the Proposed Framework

VI. RELATED WORKS

The following researches are developing the tool which detects the defect of requirements. William M. Wilson et al proposed the Automated Requirements Measurement (ARM) [13]. The Quality Analyzer for Requirements Specifications (QuARS) was proposed by A. Fantechi et al [14]. These researches aim at pointing out the inaccuracy of the requirement specification document written by natural

language. The advantage of this research over these researches is as follows. This research provides stronger the support function for quality requirements. This framework gives the evaluation criterion of quality requirements (development documents) to the author of RS. The author of RS can focus on improving the quality requirements.

VII. CONCLUSION

In this research, a framework for quantitatively evaluating the quality requirements was proposed. The proposed framework analyzes the requirements specification by text mining to identify where quality attributes are contained, and how much. The case study shows that the quality attributes are contained in the requirements specification. As reflected by our case study, the proposed method shows mostly good performance. This paper could give an initial evaluation of the extent to which the framework's objectives are met. It helps improve the requirements specification because framework can show the consistent evaluation criterion. And it helps improve the next requirements elicitation in the requirements definition of spiral process. We began to analyze several requirements specifications using the proposed framework. These RSs were used for the real system development. In future work we will explain that the proposed framework provides a consistent evaluation criterion of quality requirements for revising the requirements specification.

REFERENCES

[1] Boehm Barry W., and Philip N. Papaccio, "Understanding and Controlling Software Costs", IEEE Transactions on Software Engineering 14(10), 1998, pp. 1462-1476.

[2] Grady Robert B., "An economic Release Decision Model: Insights into Software Project Management", In Proceedings of the Applications of Software Measurement Conference, , pp. 227-239, 1999.

[3] Robert N Charette, "Applications Strategies for Risk Analysis", Mcgraw Hill Software Engineering Series, 1991.

[4] Karl E. Wiegers, "Software Requirements", Microsoft Press, 2003.

[5] Kotonya, G. and Sommerville, I., "Requirements Engineering: Processes and Techniques", John Wiley & Sons Ltd. 1997.

[6] L. Bratthall and C. Wohlin, "Understanding Some Software Quality Aspects from Architecture and Design Models", 8th IEEE International workshop on Program Comprehension, 2000.

[7] Gursimran S. Walia et al., "Requirement Error Abstraction and Classification: An Empirical Study", In proceedings of the ACM/IEEE international symposium on International symposium on empirical software engineering, pp. 336 – 345, 2006.

[8] Michael Fagan, "Design and Code Inspections to Reduce Errors in Program Development", IBM Systems Jornal 15(3), pp. 182-211, 1976.

[9] ISO/IEC, "ISO/IEC 25010 Systems and software engineering-Systems and software Quality Requirements and Evaluation (SQuaRE) -System and software quality models", 2011.

[10] GETA, http://geta.ex.nii.ac.jp/e/index.html, December 2010.

[11] Sen, "http://ultimania.org/sen/", December 2010.

[12] WordNet, " http://nlpwww.nict.go.jp/wn-ja/index.en.html ", December 2010 (In Japanese) .

[13] William M. Wilson et al., "Automated Analysis of Requirement Specifications", in Proceedings of the International Conference on Software Engineering ICSE97, pp. 161-171, 1997.

[14] A. Fantechi et al., "Application of Linguistic Techniques for Use Case Analysis", in Proceedings of the IEEE Joint International Conference on Requirements Engineering, pp. 157-164, 2002.

[15] IEEE, "IEEE Recommended Practice for Software Requirement Specifications IEEE Std 830-1998", 1998.

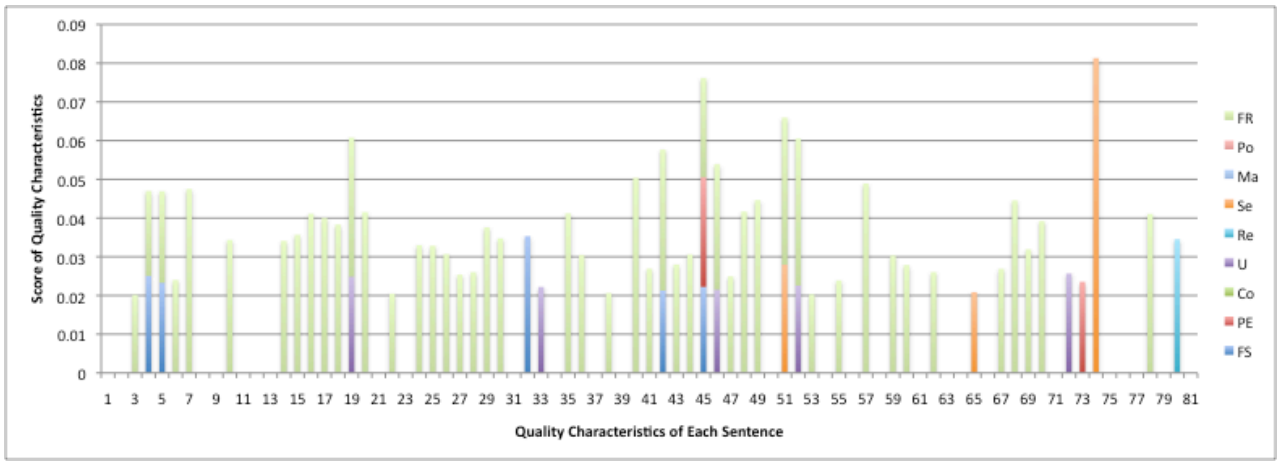

Figure 4 Quality Attributes of Each Sentence

XCOMP: A Multidimensional Approach for Composing Specific Domains

Asmaa Baya, Bouchra EL Asri, Mahmoud Nassar
IMS Team, SIME Laboratory. ENSIAS
ENSIAS
Rabat, Morocco
bayaasmaa@gmail.com, {elasri, nassar}@ensias.ma

***Abstract*—Despite the interest of DSM (Domain Specific Modeling), the definition of new specific domains is still expensive and difficult to achieve. To overcome this problem, several research works propose the composition of existing domains in order to get the maximum benefit from domains that have already been developed and tested. In this context, this article proposes a new approach for composing specific domains models. First, we analyze some related works. On the basis of the key findings and conclusions drawn from the analysis, we propose a multidimensional approach based on the composition of crosscutting concerns contained in the source domain models.**

Keywords-Composition; DSM; separation of concerns; modularization; abstraction

I. INTRODUCTION

The main interest of DSM (Domain Specific Modeling) is to capitalize on the concepts of a given domain and to promote the reuse of domain artifacts. In fact, DSLs (Domain Specific Languages) [15][16] help to reduce the complexity introduced by the specification of general-purpose modeling languages such as UML, since their concepts are aligned with the problem domain [10][11].

Although the importance of DSM is obvious, the development of new specific domain is still expensive; because it is time-consuming as it requires experience and expertise in the new field. To solve this problem, the research community focuses on finding alternative orientations such as Configurable Domain-Specific Development Environment (CDSDE) [1] and domain composition [7][8]. In this paper, we are interested in domain composition as a practical solution to get the maximum benefit from domains that have been already developed and tested.

Developing domains by composition is intensified through a wide range of research to extend the use of specific domains [7][8][9][12][13]. Indeed, the trend is to build libraries of subdomains metamodels that are reusable. These basic domains (like interconnection of modules, specialization, finite state machines, Petri networks, etc.) are used in the construction of most domains. Thus, modeler can construct new domains just by extending and defining rules of composition between these basic subdomains. On this basis arises the need to define a new domain composition approach which provides clear and practical mechanisms to extend and compose domains.

In this paper, we treat domain composition issues. The paper is structured as follows: The first section presents some composition approaches and their comparative study. The second section presents our approach to compose specific domain. We begin this section by explaining the context of the work and then present the different phases of this approach.

II. COMPOSITION APPROACHES FOR SPECIFIC DOMAINS: THE STATE OF ART

In this section, we analyze some current composition approaches for specific domains, as we draw up a summary of the criteria that guide our contribution.

A. Current domain composition approaches

Several research studies focused on the problem of composition for specific domains. This contributed to the emergence of several orientations. In what follows, each paragraph presents a specific orientation.

Conceptual composition: The approach of Vega [7] proposes to compose domains at the conceptual level rather than components infrastructure, an additional level is inserted between the two levels in order to ensure their synchronization. The first step of this approach is to materialize the concepts of the composite domain by classes of metamodel. The metamodel of the composite domain become an extension of the source domain metamodels.

Transformation to pivot language: "Multi-modeling views" approach offers a solution to the composition of heterogeneous models (called high-level models) by transforming both high-level models into low level models that conform to the same existing metamodel, or conform to an extension of it [8]. A correspondence model ($CM_{high\text{-}level}$) is used to align high-level models by describing the relationships of correspondence between the composing elements. Then high-level models specified in different domain specific languages submit a sequence of transformation steps in order to translate them into a common low level language. A $CM_{high\text{-}level}$ needs also to be propagated through the complete transformation chains in order to automatically derive $CM_{low\text{-}level}$ (correspondence model of low level models). Finally, this approach proposes

 ISBN: 978-1-61208-246-2

to make a homogeneous model composition like "Package merge" [14].

Composition by adopting Template: "Template instantiation" is a metamodel composition approach [9]. This approach is based on the reuse of common metamodeling patterns in a single composite metamodel. Those patterns are saved as abstract metamodel templates and will be instantiated in domain-specific metamodels. This approach of composition does not bring any changes to the source metamodels; however, it automatically creates new relationships between the pre-existing entity types in a target metamodel to make them play roles in a common metamodeling pattern.

Extending languages: Many approaches propose to extend language in order to support domain composition [17] [12]. For example the approach of Ledeczi proposes to extend UML with new operators in order to combine source metamodels [12]. Another approach proposes to extend the UML metamodel with behavior describing symmetric, signature-based composition of UML model elements [17].

Coordination: the composition by coordination was adopted in [13]. This approach proposes architecture of coordination where every participant preserves its autonomy, and the coordinator organizes the collaboration of all participants. Another work proposes to compose an inter domain specific languages coordination [18]. This work introduces an inter-model traceability and navigation environment based on the complementary use of megamodeling and model weaving.

Graphical composition: Some works solve the problem of composition at the graphical level. In [19], researchers define a layer for graphical syntax composition. This work provides formally defined operators to specify what happens to graphical mappings when their respective metamodels are composed.

B. Review of domain composition approaches

The proposed approaches are non-exhaustive; Model Driven Engineering (MDE) contains a lot more approaches. However, we chose these methods because each one illustrates a particular orientation. The approaches above have several advantages and disadvantages that we present in what follows.

In Vega's approach, the conceptual stage before the composition of metamodels aims at conceptualizing the concepts of composite domain. Thus, the composition is expressed at a high level abstraction. The disadvantage is that the approach remains complex as long as this high level abstraction is not supported by simple and practical methods.

The approach "Multi-modeling views composition" is based on a simple principle which is the transformation of a high-level language to a low-level language. However, it follows a long process and goes through several transformations and intermediate models before getting the final model. This increases the complexity of this approach and its margin of error.

"Template instantiation" approach ensures a high-level abstraction through the use of abstract metamodel templates. However, these templates have several limitations such as validity, adaptation and instantiation, which greatly minimize their context of use.

Extending languages maximizes reuse and makes profit of existing languages. However, this orientation is not generative because of its limitation to specific languages.

The composition by coordination presents a lot of advantages like the independence of source domains and a high level of abstraction. However, it proposes usually many languages and techniques which are not easy to use by domain experts.

A graphical composition is a limited orientation, because it solves the problem of composition at the syntactical level only.

Based on these results, we can conclude that high-level abstraction approaches often provide a high level reuse and a good operating range. However, this advantage is often accompanied by a high level of complexity. Thus, the challenge to overcome is to ensure a high level of abstraction while avoiding both introduction of complex mechanisms and limitation of the context of use.

III. MULTIDIMENSIONAL COMPOSITION APPROACH

Looking through the approaches of domain composition presented in section II, we can conclude that every approach is designed for a specific context or language. In addition, approaches are not enough flexible to support modifications in domain models structure. For these reasons, we propose a generative approach applicable in all contexts and languages. This approach pays particular attention to the composition of concerns contained in the domain models. So, it allows the composition of domain models or just a composition of domain models and concerns (security, persistence, etc.). This approach allows also the remodularization on demand; because every designer organizes the source models according to his point of view so the result of composition changes.

In this section, we describe the context of this work, as we present our approach.

A. Work context

In this work, we will focus on developing large-scale systems. This context presents additional challenges to overcome, namely, working simultaneously on several specific domains or extensive domains, heterogeneity of models and languages, integration of new non-functional concerns throughout the system life cycle.

To meet these requirements, this work will be based on three strategic axes (see Figure 1):

- Functional: Deals with the Composition of the business part of domains. Indeed, the composite domain must capitalize all the concepts contained in the source domains.

 ISBN: 978-1-61208-246-2

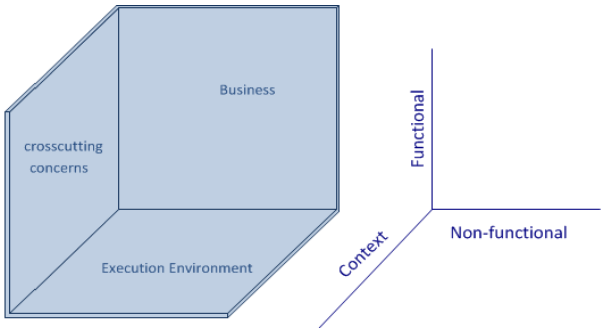

Figure 1. Axes of work.

- Non-functional: The crosscutting concerns contained in each source domain must remain valid in composite domain
- Context: Additional concerns may appear in the composite domain to meet the changing context.

B. *XCOMP: A multidimensional composition approach*

In this context, particular attention to crosscutting concerns is required. For this, we thought to divide the domains to compose into dimensions. This notion of dimensions was introduced in the multidimensional separation of concerns, which is a general and very ambitious approach: It provides scalability and modularity [1][2].

Multidimensional separation of concerns suggests introducing as many arbitrary dimensions as needed. Separation of concerns will be carried out according to defined dimensions. This allows great flexibility because each actor can define its own dimensions depending on his own vision, as it can add dimensions (not provided a priori) throughout the system life cycle. In principle, concerns are considered as independent and orthogonal, but it is not fully applicable in practice. That is why we will have to define integration rules in order to specify inter-concerns interactions and overlaps in a later step.

The basic principle of our approach is to organize the domain models to compose in independent dimensions, where each dimension is represented by a part of the model. Then compose these dimensions in order to have a composite domain model. In what follows we will detail the steps of our approach.

➢ Step 1:

The first step is to define the dimensions contained in each source domain, where each dimension contains a set of concerns. The choice of dimensions is not governed by rules; however, care should be taken to minimize the inter dimensions relations in order to obtain orthogonal dimensions. Then, decompose the source domain models following these dimensions. Each dimension must be represented by a part of the model (called block). To keep the consistency of the model, we must trace the relationships between the blocks.

Thus, each source domain model is represented by the following triple **M = < D, B, R >**

where:

- $D = \{D_1, D_2 ..., D_n\}$ is the set of dimensions ,and D_i are defined dimensions
- $B = \{B_1, B_2, ..., B_n\}$ is the set of blocks corresponding to the dimensions
- $R = \{R_{1,1}, R_{1,2}, ..., R_{n,n}\}$ is the set of relations which rely the different blocks of domain model. $R_{i,j}$ is the relation that rely the block i to the block j.

The new architecture of the domain model will be presented in a matrix as shown in Figure 2.

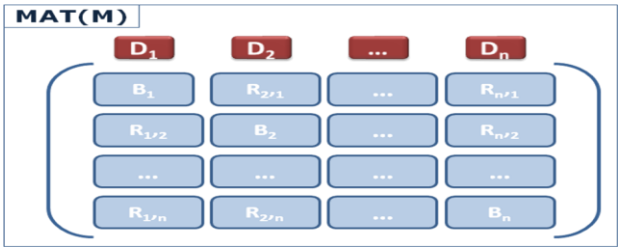

Figure 2. Matrix of domain model.

➢ Step 2:

Once we have defined the source model matrices, we

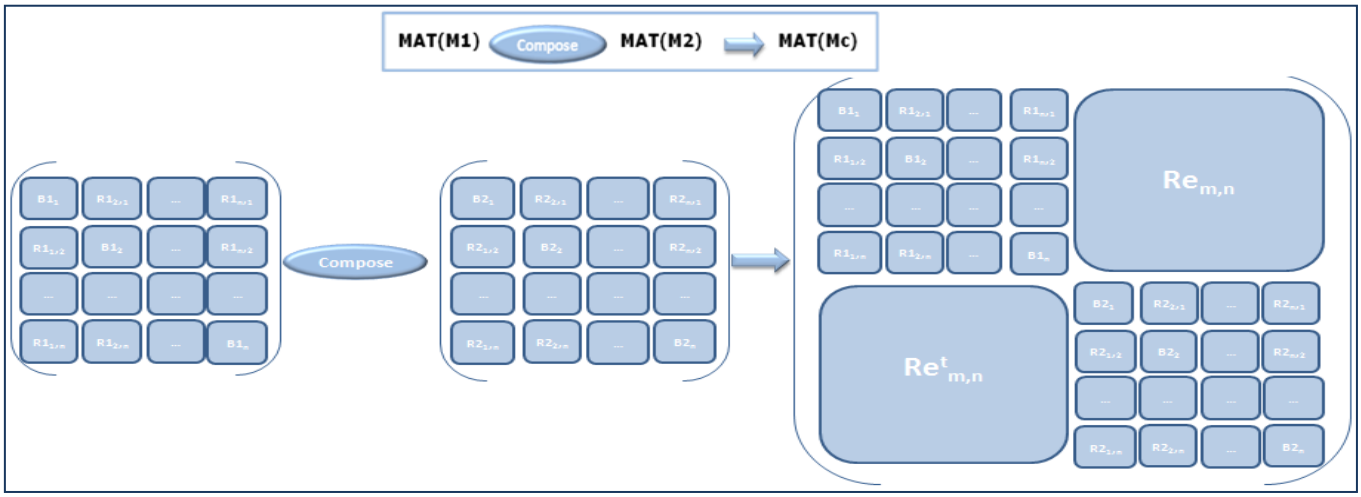

Figure 3. Composition of domain model matrices.

must eliminate repeated dimensions in the models so that they appear only once in the entire source models. Then compose source matrices (MAT (M1) and MAT (M2)) in order to obtain the composite matrix (MAT (Mc)), using the relation in Figure 3.

The diagonal of MAT (Mc) contains blocks which represent the dimensions of source models. The $R_{i,j}$ represent the relationships between blocks from the same models. To ensure coordination between blocks from different models, we will define new relationships that will meet the composite domain requirements. These emergent relationships are represented by $Re_{m,n}$ in MAT (Mc).

$Re_{m,n}$ is a matrix which organize relationships between blocks of the first domain model and blocks of the second domain model. Relations can be expressed in one of the domain specific languages used in source domain models.

The matrix of the composite domain contains all dimensions contained in the source models. At this level, new concerns can be inserted into composite domain in order to adapt it to specific context.

- Step 3:

At this stage, we obtain a matrix of composite domain model. This matrix is represented by a set of blocks and relationships. However, the orthogonality of dimensions is not necessarily assured because of the introduction of new relationships ($Re_{m,n}$). In this step, we will make transformations to MAT (Mc) in order to have a domain with independent dimensions.

To achieve this, we propose to represent all relations $Re_{m,n}$ in a new dimension instead of dispersing them throughout the model. The new dimension must make reference to all dimensions and its sub-elements that are members of relations, as it must contain the detailed specification of relationships. To model this new dimension, we can use one of the source domain specific languages or another language that meets requirements of inter-blocks relations.

The resulting model is constituted by a set of blocks from different models, so they are described in various domain specific languages. Our approach stops at this level, since all proposals to homogenize blocks must specify the target language (DSL or a GPL generative programming language). However, our goal is to propose a generative approach applicable to any type of language. Indeed, to adapt the composite domain model, there are other alternatives such as keeping models heterogeneous and proceeding directly to the code generation, or applying one of the transformation methods from DSLs to DSL or from DSLs to GPL to unify the language used in the model [3][4].

IV. USE CASE

To illustrate what we explain above, we present a simple example of composition of data domain and workflow domain. Figure 4 shows the model of data domain and Figure 5 shows the model of workflow domain.

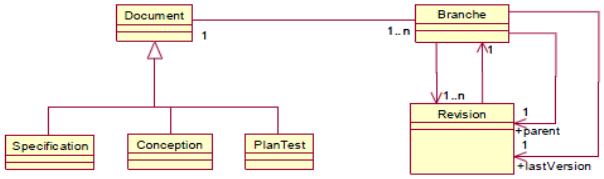

Figure 4. Model of data domain

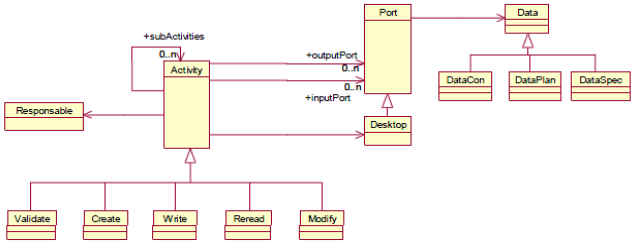

Figure 5. Model of workflow domain

The first step is to identify dimensions, blocks, and relations of domain models. The model of data domain can be organized in two dimensions of concerns: Data and organization. Each dimension is represented by a block. Figure 6 shows the blocks and relations contained in the model of data domain.

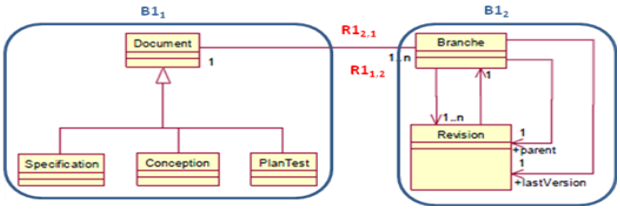

Figure 6. XCOMP applied to model of data domain

The model of workflow domain can be organized in three dimensions: Data, control, resource. Blocks and relations of this model domain are shown in Figure 7.

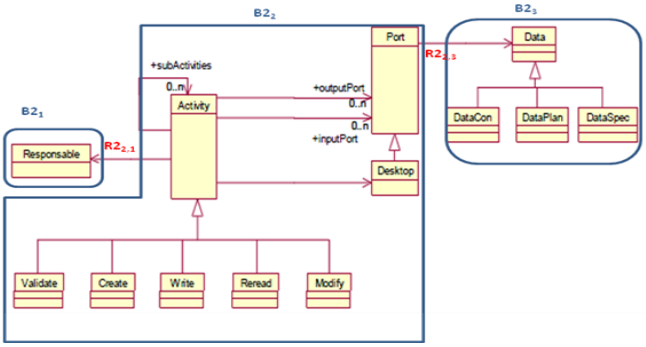

Figure 7. XCOMP applied to model of workflow domain

As we can see through the models; the dimension data appear in two models, so we must eliminate it from one model (for example from workflow domain model). The relation between this dimension and the rest of the model will appear in the matrix ($Re_{m,n}$). To simplify, we suppose that we have no emergent relationships.

 ISBN: 978-1-61208-246-2

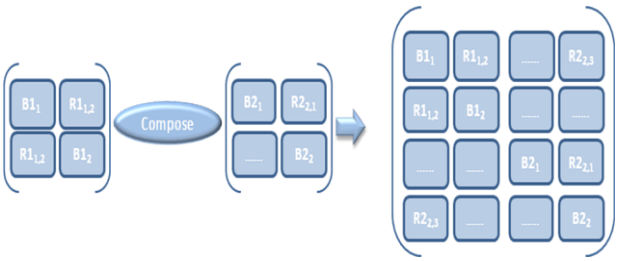

Figure 8. Composition of data model domain matrix and workflow model domain matrix

The Figure 8 presents the source model matrices as it presents the result of composition.

V. CONCLUSION AND FUTURE WORK

This paper presented a generative approach to compose domains. The main motivation behind this proposal is to promote the composition of crosscutting concerns, and to allow the insertion of new concerns throughout the domains life cycle. However, this approach uses several theoretical basis that must be implemented in order to have a practical approach. Our future work will focus mainly on proposing practical methods to decompose domains on orthogonal dimensions. We consider this point as a prerequisite in our approach, but it is not often easy to achieve it. So the approach must be supplied with additional mechanisms to facilitate decomposition of models on orthogonal and independent dimensions.

The last step of the approach should also be extended. In fact, the new dimension representing the relationships between the blocks can be defined in any language. Whether we choose a generative language or one of the source specific languages to model this dimension, we recognize that they are not suitable for all purposes, especially when they do not provide enough abstraction to reference dimensions, blocks, and describe the relationships. So, we propose to define a new specific language dedicated to the description of inter-dimensions relations. This DSL will be used also to formally define the matrix $Re_{m,n}$.

To build this approach, we used the basic principle of the multidimensional separation of concerns. This type of separation has several advantages: The separation is done according to multiple concerns, which deal with the problem of the dominant decomposition according to only one kind of concern at a time. In addition, it allows on-demand remodularization. Indeed, it is possible to add or omit concerns throughout the life cycle without having to change the entire model.

This domain composition approach begins first with a multidimensional decomposition of concerns and then, composes all dimensions to obtain a composite domain. Finally, it proposes to insert a new dimension which includes the relationships between dimensions.

REFERENCES

[1] P. L. Tarr, H. Ossher, W. Harrison, and S. Sutton, "N degrees of separation: multi-dimension separation of concerns," In Proceedings of the ICSE 99, International Conference on Software Engineering, Los Angeles, CA, USA, pp. 107-119, May 1999

[2] H. Ossher and P. Tarr, "Multi-dimensional Separation of Concerns in hyperspace," ECOOP'99 workshop on Aspect-Oriented Programming, Lisbon, June 1999.

[3] M. Brambilla, P. Fraternali, and M. Tisi, "A transformation framework to bridge domain specific languages to MDA," Models in Software Engineering: Workshops and Symposia at MODELS 2008, Toulouse, France, pp.167-180, Sept. 2008.

[4] J. Bezivin, G. Hillairet, F. Jouault, I. Kurtev, and W. Piers, "Bridging the ms/dsl tools and the eclipse modeling framework," International Workshop on Software Factories at OOPSLA, 2005

[5] M. Wimmer, A. Schauerhuber, M. Strommer, W. Schwinger, and G. Kappel, "A semi-automatic approach for bridging DSLs with UML," 7th Workshop on Domain- Specific Modeling at OOPSLA, Montreal, Oct. 2007

[6] A. Hovsepyan, S. V. Baelen, Y. Berbers, and W. Joosen, "Specifying and composing concerns expressed in domain specific modeling languages. Objects, components, models and patterns," 47th International Conference, TOOLS EUROPE 2009, Zurich, June 2009.

[7] G. Vega, "Développement d'applications à grande echelle par composition de méta-modèles, " Ph.D. thesis, University Joseph Fourier, December 2005.

[8] A. Yie, R. Casallas, D. Deridder, and D. Wagelaar, "A practical approach to multi-modeling views composition," Proceedings of the 3rd International Workshop on Multi-Paradigm Modeling, Denver, Colorado, USA, jan. 2009

[9] M. Emerson and J. Sztipanovits, "Techniques for metamodel composition" OOPSLA – 6th Workshop on Domain Specific Modeling, pp. 123-139, October, 2006

[10] M. Harsu, "A survey on domain engineering" Report 31, Institute of Software Systems, Tampere University of Technology, pp. 26, Dec. 2002.

[11] DSM Forum, Why DSM, http://www.dsmforum.org/

[12] A. Ledeczi, G. Nordstrom, G. Karsai, P. Volgyesi, and M. Maroti, "On metamodel composition," Proceedings of the 2001 IEEE International Conference, Mexico, pp. 756-760, Sept. 2001.

[13] T. Le-Anh, "Fédération: une architecture logicielle pour la construction d'applications dirigée par les modèles," Ph.D. thesis, University Joseph Fourier, january 2004.

[14] J. Dingel, Z. Diskin, and A. Zito, "Understanding and improving UML package merge," Software and Systems Modeling, Vol. 7, pp. 443-467, Oct. 2008.

[15] J. L. Bentley, "Programming pearls: little languages," Communications of the ACM, Vol. 29, N. 8, pp. 711–721, August 1986.

[16] A. V. Deursen, P. Klint, and J. Visser, "Domain-specific languages: an annotated bibliography," ACM SIGPLAN Notices,Vol. 35, N . 6, pp. 26–36, june 2000

[17] F. Fleurey, R. Reddy, B. Baudry, and S. Ghosh, "Providing support for model composition in metamodels," Proceedings of EDOC 2007, Annapolis, MD, USA, October 2007

[18] F. Jouault, B. Vanhooff, H. Bruneliere, G. Doux, Y. Berbers, and J. Bezivin, "Inter-dsl Coordination support by combining megamodeling and model weaving," In: Proceedings of the 2010 ACM Symposium on Applied Computing, Suisse Sierre, pp. 2011-2018, Mar 2010.

[19] L. Pedro, M. Risoldi, D. Buchs, B. Barroca, and V. Amaral, "Composing visual syntax for domain specific languages," 13th International Conference, HCI International 2009, San Diego, CA, USA, pp. 889-898, July 2009.

 ISBN: 978-1-61208-246-2

Towards System Level Performance Evaluation of Distributed Embedded Systems

Jukka Saastamoinen, Subayal Khan, Jyrki Huusko,
Juha Korpi, Kari Tiensyrjä
VTT Technical Research Center of Finland,
FI-90570, Oulu, Finland
email: {jukka.saastamoinen, subayal.khan,
jyrki.huusko, juha.korpi, kari.tiensyrja}@vtt.fi

Jari Nurmi
Tampere University of Finland,
Department of Computer Systems
P.O. Box 553 (Korkeakoulunkatu 1),
lFIN-33101 Tampere, Finland
jari.nurmi@tut.fi

***Abstract*— In order to manage the increasing complexity and heterogeneity of the distributed embedded systems, the system level performance evaluation must be performed at an early design phase using abstract models of the platforms and applications. Thus, the system level performance simulation techniques for embedded systems play a key role in the architectural exploration phase. The salient performance evaluation methodologies are developed around some key concepts and employ a variety of modelling styles, models of computation and programming languages for performance modelling of embedded systems. The aspects of a performance evaluation methodology might limit it to certain domain(s) of embedded systems and therefore must be investigated. In order to span different domains of distributed systems, a methodology must provide the models for technologies, such as communication protocols and middleware technologies, which are employed in different domains of distributed embedded systems. Once achieved, the methodology will be able to provide an estimate of the contribution of these technologies in the non-functional properties of the distributed system. The goal of this survey is to shortlist the performance modeling methodologies feasible for the performance evaluation of different domains of distributed systems. The abstraction level used to model these protocols is investigated since the accuracy of the related performance numbers depend on the used abstraction level. After comparing the salient methodologies on the basis of modeling style, tools and languages, targeted domain etc., we shortlisted the feasible contributions for performance evaluation of different domains of distributed systems. Afterwards, we describe the models and tools needed by the shortlisted methodologies in order to span the different domain of distributed systems. The article acts as a reference for researchers and industries involved in developing methods and tools for system level performance simulation.**

***Keywords*-Performance Model; Application Model; Platform Mode;, Kahn Process Networks; Y-Char; UML; SystemC**

I. INTRODUCTION

Distributed systems are used in diverse market segments including consumer electronics, medical devices, environment monitoring, industrial control, automotive and office automation. The complexity of these systems has increased enormously in all these industrial domains. Therefore, these systems are accompanied with various design challenges [1].

Firstly, the design space is huge not only due to many alternatives for datalink, transport and middleware technologies (for example, specialized MAC (media access control) protocols in WSN (wireless sensor networks) and multitude of middleware technologies in multimedia applications domain) but also in terms of available platforms and various application implementation alternatives. Secondly, due to computational complexity of many distributed applications and the strict design constraints (non-functional properties), the designer has to make critical design decisions at an early stage in order to compare a particular system design with other possible alternatives before the actual implementation and integration of the system proceeds [1].

Moreover, both the functional and non-functional properties of the overall distributed system not only depends on the computations performed within the network nodes but also on the interaction of the various data streams on the common communication media [1].

Therefore, in order to span different domains of distributed systems, a methodology must provide models of MAC, Transport protocols and middleware technologies. This is important because in case of distributed applications, MAC, Transport and Middleware technologies also contribute to the non-functional properties of the system. These non-functional properties include for example end-to-end packet delays and packet loss rate. Also, the increasing complexity of distributed applications demands that the application design phase shall act as a starting point for the application workload modelling phase to reduce the time and effort in the performance simulation and architectural exploration phase [1].

The main contribution of this article is to provide a literature review of the existing performance simulation methodologies in order to evaluate their feasibility for the performance evaluation of multiple domains of distributed systems. The survey first defines important features which must be investigated in order to evaluate the feasibility of performance evaluation methodologies in various domains of distributed embedded systems. Afterwards, the availability of the models and tools which provide these features are highlighted in salient performance evaluation approaches. Based on this information, the methodologies which fulfil these requirements are shortlisted.

 ISBN: 978-1-61208-246-2

The rest of the paper is organized as follows: in Section 2, a comparison of the salient system level performance evaluation (SLPE) methodologies is provided in order to investigate their feasibility for the performance evaluation of (different domains of) distributed systems. In Section 3, the requirements for the SLPE methodology to span different domains of distributed embedded systems are listed. In Section 4, the methodologies which fulfil these requirements are shortlisted on the basis of the information provided in Section 2. Section 5 evaluates the feasibility of ABSOLUT for the performance evaluation of distributed systems in different domains. The conclusions drawn by the survey are presented in Section 6. This is followed by acknowledgements and list of references.

II. COMPARISON OF METHODS AND TOOLS

The main concepts employed by different SLPE methodologies have been described in detail in [2] and [3] and are therefore not presented in this article. The objective of this case study is to investigate the methods and models employed by the salient performance evaluation methodologies to assess their feasibility for performance evaluation of different domains of distributed systems.

Therefore, in this section, we first classify the SLPE methodologies on the bases of four salient features. These features include the modelling style, used languages and frameworks, non-functional properties validation and targeted system and application domains. In Section 3, we use this information to identify the SLPE methodologies which can span different domains of distributed systems.

A. Modelling style

Different design space exploration methodologies employ either static (analytical) or dynamic (simulation) estimation methods. Usually, the static estimation methods shrink the vast design space briskly but the models employed are very coarse. The models used by dynamic estimation methods are more accurate and detailed but are slow at pruning the vast design space. In other words, the static estimation favour speed instead of accuracy for design space exploration while the dynamic exploration methods favour accuracy instead of speed. Some methods utilize a combination of static and dynamic simulation for exploiting the advantages of both methods. Static methods employ analytical or highly abstract models of applications and usually ignore the dynamic behaviour of the application which depends on the input data. As a result, the static methods do not offer the level of accuracy for exploration and communication scheduling as the dynamic simulation methods. Most of the salient performance simulation approaches utilize the dynamic estimation approach while ARTEMIS, MESH and KOSKI use both static and dynamic estimation methods as shown in Table I. It was observed that different methodologies model the applications and platforms at various levels of abstraction and refinement. ABSOLUT employs layered application and platform models. The platform models operate at the transaction level while the lowest layer of application models comprise of abstract instructions. Detailed description of ABSOLUT modelling methodology is provided in [4].

Some methodologies, for example SPADE, TAPES, ARTEMIS and KOSKI, model applications as KPN (Kahn Process Network) MOC (Model of Computation) [5]. Platform models in SPADE are instantiated via a library of generic building blocks which model different resources in the platform. The processing elements in the platform are modelled as TDEUs (trace driven execution unit). Each process of the modelled application is mapped to a TDEU in the platform [6]. TAPES abstracts the processing of tasks by their execution latencies on the corresponding resources in the platform [7]. Further details of platform modelling in TAPES are mentioned in [7].

The architecture models in ARTEMIS operate at transaction level, which simulate the computation and communication events that are generated by the application model [8]. An architecture model is made from a library of generic building blocks which contains templates of performance models for different platform elements [8]. KOSKI employs UML (unified modeling language) for modelling platform which is later on transformed to an abstract model via UML interfaces [9].

ARTS employs static data flow graphs (SDFG) MOC to model the applications while the architecture models operate at transaction level and simulate the performance consequences of the computation and communication events generated by the platform [10][11].

Baghdadi et al. (2000) [12] describes the system-level specifications in SDL (specification and description language) which results in heterogeneous multi-processor architectures consisting of both hardware and software components. SDL can model a variety of embedded software applications (both real time and non-real time).

Fornaciari et al., (2001,2002) [13], [14] uses software execution profiler for the cycle accurate simulation of the application while the data and address bus streams are generated via a dynamic tracer.

Jabber et al., (2009) [15] model applications via DIPLODOCUS tool. A DIPLODOCUS application comprises of a network of tasks which communicate via communication semantics defined by the methodology. The architecture comprises of a network of physical resources which are abstracted by one of three types of architecture nodes, .i.e., the computation nodes (for example CPUs, DSPs, and hardware accelerators etc.), the communication nodes (for example busses, routers and switches etc.) and the storage nodes (for example memories) [15].

Lahiri et al., [16], [17] uses highly abstract application models and only targets the domain of custom communication architectures for on chip communication architectures.

Mesh models applications as dynamic threads made on top of physical threads [18] which model the platform. MILAN [19] uses HiPerE rapid performance estimation

 ISBN: 978-1-61208-246-2

tools for estimating the performance of designs (SoC architectures) at the system level. Applications are modelled as trace files in HiPerE which contain an ordered list of communication and computation tasks. HiPerE uses a generic model (GenM) for modelling SoC architectures [19].

Posadas [24] et al., aims at system level estimation of execution time from a system level performance description written in SystemC. It uses a C++ library for this purpose and therefore does not require any change to the source code of the description. The way different methodologies model the application and platforms are summarised in Table I.

Furthermore, some methodologies are capable of exploiting third party tools for different modelling and refining purposes, for example ABSOLUT's workload generation tool called ABSINTH-2 and SAKE [20] use Valgrind [32] for workload extraction of external libraries. KOSKI employs existing compilers and code generators in order to refine the application to the final processing elements [21]. ARTEMIS [25] uses Laura tool-set for the generation of synthesizable VHDL code from the KPN application description. Furthermore, it was found that all the landmark contributions considered in Table I employ simulation for computing performance numbers.

B. Languaged, standards and frameworks

The landmark performance evaluation methodologies described in Table I use a variety of widely used modelling, scripting and Programming languages such as C, C++, Perl, UML and XML for various modelling purposes.

Some methodologies use specification languages such as SDL or LOTOS OSI specification language for system-level specifications. Some methodologies such as MILAN use other tools such as HiPerE and DESERT for modelling and simulation purposes [19]. Lahiri et al. [16] [22] uses POLIS and PTOLEMY frameworks for designing communication architectures of SOCs.

It was observed that some methodologies use modelling languages and simulation frameworks such as SystemC which is widely used for the system-level modelling, architectural exploration, performance modelling etc., of electronic systems. The programing and modelling languages used by the landmark methodologies are shown in Table I.

C. Non-functional properties validation

The distributed embedded systems support applications which consist of many components running on different networked devices. In such cases, the application components communicate via transport, data link and (possibly) middleware technologies. These distributed applications are generally message based or streaming applications which satisfy the end-user requests by (in turn) requesting one or more services provided by different devices which implement these services. Therefore, the end-user experience is not merely a consequence of the application implementation since the transport protocols, data link protocols as well as physical layer plays a key role in the end-user experience since the end-end delays and packet/frame errors at these layers can deteriorate the end-user experience. Therefore, for a methodology to be able to estimate reliable performance numbers for distributed applications, it must model these OSI model layers with sufficient level of detail. These models must preserve the functionality to a level that the estimated delays show a close correlation with delays estimated by network simulators such as OMNeT++ and ns-2.

It has been noticed that some methodologies are totally focused on one particular domain of applications and systems. The methodologies such as ARTEMIS, KOSKI, SPADE and TAPES which model applications via KPN MOC are limited to the performance estimation of streaming applications since KPN models only model streaming applications very well. Therefore a wide variety of message based distributed applications cannot be modelled via these methodologies. Some methodologies such as Lahiri et al. and ARTS use other models of computations such as CAG (communication analysis graph) and SDFG (static data flow graph) for modelling applications. It was also observed that some methodologies use their own model of computation for describing applications while the others such as ABSOLUT employ a layered application model [4].

In all the methodologies which employ a model of computation to describe the applications, we observe that the functionality of the transport and datalink layer has been abstracted by the communication paradigm employed by the MOC. This means that the non-functional properties of a distributed application (such as end-end delays and packet/frame loss rate) cannot be reliably estimated since the functionality of transport and datalink layers have been swapped by that of the communication means defined by the employed MOC. All the MOCs use simple channels for communication among processes for example KPN MOC use simple FIFO (first-in first-out) channels for passing synchronization tokens among processes. On the other hand in networked devices, datalink layer MAC protocols resolve the contentions for occupancy of the common channel (wired or wireless). The level of abstraction used to model channels should be comparable to the abstraction level employed by network simulators such as OMNeT++ and ns-2 [23]. The MOCs, targeted application domain and the availability of models for transport, datalink and Middleware technologies models are highlighted in Table I for the landmark performance simulation methodologies. In short, the emphasis is on the model of computation employed by the methodologies, since it can potentially restrict an approach to a specific domain of applications. Also, the models of transport and MAC protocols employed by different approaches are investigated since they play an important role in determining the non-functional properties such as end-end message delays in distributed applications.

 ISBN: 978-1-61208-246-2

These non-functional properties can play an important role in end-user experience and must be estimated with reasonable accuracy.

D. Targeted system and application domains

The use of multiprocessor based platforms is increasing in high-end mobile handheld devices such as smart phones and internet tablets. On the other hand, in case of wireless sensor networks very low power single processor based systems are commonly used. Hence, for the performance simulation of a wide variety of distributed embedded systems, it is important that the methodology is not restricted to a certain type of platforms (single or multiprocessor based). Also, it should not be strictly targeted at the performance evaluation of a particular subsystem or components of a platform such as performance evaluation of on-chip communication architectures. The system and application domains (of embedded systems) targeted by salient performance evaluation methodologies are listed in Table I. In Table I, we add the domain of distributed networked systems to the three domains of embedded systems elaborated in [21].

Some methodologies are totally focused at the performance evaluation of a particular domain of systems, for example TAPES and Fornaciari et al. target single processor based systems, SPADE and Baghdadi et al. only target Multi-Processor based systems while Lahiri et al. is only focused on the performance evaluation of on-chip communication architectures. The other landmark methodologies are also focused on only two out of the three performance simulation objectives, .i.e., performance evaluation of single processor based SoC, multi-processor based SoC and on-chip communication architectures [21]. Only three methodologies .i.e.; ABSOLUT, ARTEMIS and KOSKI have no such restriction.

TABLE I. ANALYSIS OF SALIENT DESIGN SPACE EXPLORATION METHODOLOGIES

Name of approach	Modelling Styles, Tool Coupling and Performance Estimation					Languages, Standards and Other Frameworks Used		Non-functional properties validation				Targeted System Domain			
	Performance estimation type	Application Model	Architecture Model	Tool Coupling	Simulation Based Approaches	Programming/Modelling Languages and Standards Spanned	Other Approaches/Frameworks Used	Model of computation	Targeted Application Domain	Transport and Data-link Model	Middleware Layer Workload Models	Non-Distributed Systems: Single Processor based systems	Non-Distributed Systems: Multi-Processor based SOC	Non-Distributed Systems: On-Chip/Intra-Platform Communication Architectures	Distributed Networked Systems
ABSOLUT	D	X^{11}	X^{12}	X^{13}		C/C++/SystemC2.2/TLM2.0/UML		TLM	A			X	X	X	
ARTEMIS	D/S	X^{21}	X^{22}	X^{23}		PEARL, SystemC, RTL	SPADE, SESAME	KPN	ST			X	X	X	
ARTS	D	X^{31}	X^{32}			SRTS Scripting Language, SystemC		SDFG	ST				X	X	
Baghdadi et al	D	X^{41}	X^{42}			C,RTL,SDL,	MUSIC, CODESIM	N	X^{42}				X		
Fornaciari et al	D	X^{51}	X^{52}			C/C++	MEX, Shade, X^{53}	N	ST			X^{54}			
Jaber et al	D	X^{61}	X^{62}			UML, SystemC, LOTOS OSI Specification Language	DIPLODO-CUS	N	X^{63}			X	X		
Koski	D/S			X^{71}		TUT UML Profile, XML	Existing Code Generators and Compilers	KPN	A			X	X	X	

Lahiri et al	D		X			Languages/Tools used by POLIS & PTOLEMY	POLIS, PTOLEMY	CAG	X[81]					X	
MESH	D/S		X			C		X[91]	A			X	X		
MILAN	D	X[101]	X			Languages/ Tools used by DESERT & HiPerE	DESERT, HiPerE, X[102]	X[103]	A						
Posadas et al	D	X[111]				C++/SystemC		X[112]	X[113]			X	X		
SPADE	D	X	X			C/C++	YAPI, TSS	KPN	ST				X		
TAPES	D		X			SytemC, XML		KPN	ST			X			

Abbreviations	
A	No restriction as per our assessment. Also no mention of a particular application domain by the authors.
ST	Streaming Applications.
D	Dynamic
S	Static
N	No MOC (Model of Computation) such as KPN, CAG, TLM and CDFG used or affectively adapted/employed by the methodology. The modelling of applications is elaborated in the corresponding reference in the second column.
TML	Transaction Level Modelling

E. Methodology specific information used in Table I

1) ABSOLUT: **(X[11])** ABSOLUT uses layered workload models consisting of application, process and Function workload layers. The function workloads consist of abstract instructions and control.

(X[12]) The platform model is layered and consists of three layers, .i.e. component, subsystem and platform architecture layer.

(X[32]) The ABSINTH-2 tool uses Valgrind for workload extraction of external libraries.

2) ARTEMIS: (**X[21]**) Applications are modelled as KPNs which are either generated by a framework called Compaan or derived manually from sequential C/C++ code.

(X[22]) Architecture models operate at the transaction level and an architecture model is made from a library of generic building blocks containing template performance models for processing cores, communication media, and various types of memory.

(X[23]) ARTEMIS uses Laura tool set for automatic generation of VHDL code from KPN based application model.

3) ARTS: **(X[31])** Applications are modelled using static dataflow task graphs.

(X[32]) Platform consists of multi-processor models, memories, communications and other platform resources.

4) Baghadi et al.: **(X[41])** Information related to application and architecture modelling and tool coupling is mentioned in Section 2 A (modelling style).

(X[42]) The system-level specifications are described in SDL. This results in heterogeneous multi-processor architectures comprising of both hardware and software. SDL does not explicitly specify any particular domain or restriction as far as its ability to model software (both real time and non-real time) is concerned.

5) Fornaciari et al: **(X[51])** The simulation framework is based on a software execution profiler for cycle-accurate instruction set simulation of the application and a dynamic tracer to generate data and address bus streams.

(X[52]) Design space exploration is focused on the processor to memory communication through the memory hierarchy and includes configurable bus and memory models, with the latter having behavioural models of on and off-chip level 1 and 2 caches and main memory. The bus and memory models use the bus traces from the software execution profiler as input.

(X[53]) The architecture exploration is done by using a tool called MEX. It simulates the execution of a program compiled for the Sparc V8 architecture with configurable memory architecture. MEX exploits the Shade [14] library to trace the memory accesses made by a SPARC V8 program and consequently simulates the target memory architecture to obtain accurate memory access statistics. The MEX tool developed by authors uses Shade tool which is based on C/C++ [14] [13].

(X[54]) Design space exploration is focused on the processor to memory communication through the memory hierarchy. The technique aims at finding the best platform configuration for the application without an exhaustive search of the parameter space. The parameters for the exploration include cache size; block size and instruction cache associativity.

6) Jaber et al.: **(X[61])** Applications are modelled via DIPLODOCUS tool. A DIPLODOCUS application consists of a network of communicating tasks which can communicate via three communication elements .i.e., the channels, events and requests. The channels exchange the

 ISBN: 978-1-61208-246-2

abstract data samples, events exchange signals and the requests ask for and thus trigger the execution of another task.

(X^{62}) The architecture is modelled as a network of physical resources, including computation, communication and storage nodes. All resources have parameters like processing capacity in millions of cycles per second or memory size in bytes.

(X^{63}) A variety of real-time and embedded applications can be modelled with sufficient accuracy by using the data and functional abstraction described by authors in [15].

7) KOSKI: **(X^{71})** KOSKI uses existing compilers and code generators for refining the application to the final processing element.

8) Lahiri et al: **(X^{81})** It is only targeted at design of custom communication architectures of systems on chip.

9) MESH: **(X^{91})** The framework is based on a layered composition of threads, with the dynamic logical threads made on the top of physical threads. The physical threads model the hardware components of a platform and represent their computational power. The application software is modelled as logical threads. The execution of a dynamic number of logical threads is scheduled (by the scheduling layer of MESH) onto a processing element (for example a processor modelled as a physical thread).

10) MILAN: (**X^{101}**) Applications are modelled as trace files by HiPerE and consist of a list of communication and computation tasks.

(X^{102}) DESERT and HiPerE are used for rapid design space exploration. DESERT shrinks the design space by shortlisting designs and HiPerE estimates the performance.

(X^{103}) The methodology proposed by [19] is only aimed at system level estimation of execution times from a system level performance description written in SystemC. No MOC is employed by this methodology.

11) Posadas et al.: **(X^{111})** This methodology aims at system level estimation of execution time from a system level performance description written in SystemC and therefore does not employ application models. It estimates the execution time of the application via a C++ library.

(X^{112}) Application is modelled as a set of Processes which can only interact with each other via predefined channels.

(X^{113}) Only C++ applications can be simulated.

12) Summary: In this section, the important aspects of salient system level performance simulation methodologies were elaborated. We observed that these methodologies employ a variety of tools and modelling languages and mostly focus on a few modelling (targeted system domain) objectives shown in Table I. Different methodologies describe the application and platform models at different levels of abstraction and employ different models of computation for describing the application models.

Also, some of the methodologies use third party tools for modelling or simulation purposes and some provide tools coupling for extending the usability of the methodology for other simulation objectives. In the next section we further investigate the feasibility of landmark performance evaluation approaches described in this section for the SLPE of distributed embedded systems.

III. TOWARDS PERFORMANCE EVALUATION OF DISTRIBUTED EMBEDDED SYSTEMS

After investigating the salient features of landmark performance evaluation approaches in Section 2, we conclude that in order to validate the non-functional properties of distributed embedded systems in different domains the methodology must fulfil the following salient requirements.

A. MOC agnostic

The methodology must not employ a specific model of computation for modelling applications since this will restrict the methodology to a particular domain of applications or systems, for example the methodologies which uses KPN MOC for application or platform are mainly targeted at performance evaluation of streaming applications.

B. Multithreaded applications modelling

In order for the methodology to evaluate the performance of multi-threaded applications, the methodology must model the multi-threading support for system level performance simulation of these applications.

C. Physical and transport layer models

Physical layer models such as channel models, coding and modulation techniques as well as the functional models of datalink and transport layer protocols must be provided for evaluating their contribution in non-functional properties [23]. Also, the methodology must be capable of evaluating the performance of protocols operating on a particular layer of the OSI model in isolation just like OMNeT++ and ns-2 [23].

D. No domain restrictions

In order to span the domain of distributed systems such as WSNs, the methodology must be capable of evaluating the percentage utilization of the platform by data link and transport Protocols. WSNs in particular employ highly efficient and specialized datalink protocols to reduce power consumption.

E. Workload modelling of user-spacecode, libraries and system calls

From an implementation perspective, all the applications processes use user-space code, external libraries, background processes and system calls. Therefore, the methodology must provide tools and methods for generating the workload

 ISBN: 978-1-61208-246-2

models of not only the user space code but also the external libraries, background processes and system calls.

F. Workload generation of middleware technologies

It must be capable of workload extraction of API functions of the various Middleware technologies such as NoTA (network on a terminal architecture) SOA (service oriented architecture). This will enable the methodology to span the domain of distributed streaming and context aware applications.

G. Detailed as well as highly abstracted workload modelling

The methodology must provide/define application workload modelling tools/techniques for generating the application workload models with varying degrees of refinement and detail. The more refined and detailed workload models result in slower simulation speed due to increased structure and control while the less detailed workload models usually result in faster simulation speed [29] [4] [30]at the expense of accuracy. Once this is achieved, the system designer can freely choose the workload models that will provide the right balance between accuracy and speed for the modelling objective.

H. Integration of application design and performance evaluation

For early phase evaluation of the distributed applications, the methodology must automate the workload extraction process by seamless integration of application design and performance simulation phase. This can be achieved if the application and workload modelling phases are linked such that application models act as a starting point for the application workload modelling. The proposed technique must be experimented with modern SOAs such as GENESYS and NoTA.

I. Non-functional properties validation

The non-functional properties must be carried through the application design phase and validated by the performance simulation approach. The non-functional properties are usually modelled and elaborated in the application model views [1][27][28].

IV. FEASIBILITY OF EXISTING SLPE APPROACHES

As shown in Table I, none of the methodologies is capable of providing reliable estimates of the non-functional properties of distributed applications. The reason is that in case of distributed embedded systems, the transport, datalink and (possibly) middleware technologies contribute to the non-functional properties such as end-end frame and packet delays. In order for a methodology to accurately estimate the effects of these protocols on non-functional properties; it must employ functional MAC and Transport Protocols.

As shown in Table I, majority of the performance modelling techniques are limited to a particular domain of embedded systems and applications due to which they cannot be employed for the performance evaluation of different domains of distributed embedded systems.

Only three out of all the approaches mentioned in Section 2, .i.e., ABSOLUT, ARTEMIS and KOSKI are not restricted to any particular domain of embedded systems. Furthermore, out of these approaches, ARTEMIS and KOSKI use KPN MOC for modelling applications which can only model streaming applications well [6]. Therefore, out of all the system level performance evaluation methodologies presented in Table I, ABSOLUT is most feasible for the performance evaluation of distributed embedded systems since it is not limited to any particular system or application domain. As explained before, this is due to the fact that it does not employ any MOC for modelling applications or platforms. In the next section, we describe the tools and models employed by ABSOLUT for fulfilling the requirements mentioned in Section 3.

V. EVALUATIN FEASIBILITY OF ABSOLUT

A. MOC agnostic

ABSOLUT uses SystemC for modelling platform components. ABSOLUT methodology does not employ any specific MOC for modelling platforms and applications. It employs a component library for instantiating platform models and ABSINTH-2 and SAKE tools for automatic application workload generation.

B. Multithreaded applications modelling

Multi-Threaded support has been modelled and integrated to ABSOLUT due to which it can be used for the performance evaluation of multithreaded applications. The approach has been described via a case study in [26].

C. Performance evaluation of protocols

ABSOLUT provides an operating system (OS) model which is hosted on the processor model in the platform. The ABSOLUT OS model consists of a scheduler and provides the possibility to model different OS Services. The scheduler schedules the application model processes. Platform services can be implemented by the system designer as described in [23]. The implementation of services closely mimics the way services are scheduled by the widely used platforms (mostly via scheduling queues). Highly accurate transport, datalink and physical layer models have been designed and integrated to ABSOLUT [23] [27].

D. No domain restriction

ABSOLUT does not model the application workload models and platform capacity models by employing a certain MOC. This property allows the system designers to employ ABSOLUT for the performance evaluation of different domains of embedded systems.

 ISBN: 978-1-61208-246-2

E. Workload modelling of user-space code, libraries and system calls

ABSOLUT can model the workload models of user-space code and external libraries. Furthermore, the automatic workload modelling of system calls for a variety of platforms is performed via CORRINA **Error! Reference source not found.**.

F. Workload modelling of middleware technologies

The workload modelling of middleware technologies is performed via ABSINTH-2. The middleware technologies can also be modelled as system calls. The workload modelling of NoTA device interconnect protocol (DIP) has been demonstrated in a case study aimed at the SLPE of distributed NoTA systems [27].

G. Detailed as well as highly abstract workload modelling

ABSOLUT provides different tools for modelling application workloads at various abstraction levels and refinement. This allows the system designer to choose the tools which provide the right compromise between speed and accuracy.

H. Integration of application design and performance evaluation

ABSOLUT application workload models can be easily modelled by extending the application model which acts as a blue print for application workload models. The seamless integration of application design and performance evaluation minimizes the time and effort involved in performance evaluation phase.

I. Non-functional properties validation

For the validation of non-functional properties, the non-functional properties must be carried through the application design phase and validated by the performance evaluation phase. The seamless integration of application design and ABSOLUT workload modelling has been demonstrated for different service oriented application architecture design methodologies such as GENESYS and NoTA [1] [27].

ABSOLUT has been successfully employed for the performance simulation of NoC based SOCs and distributed embedded systems [1] [27]. We now list the features mentioned in Section 3 which are provided by ABSOLUT and also provide the references to the research articles which demonstrate these features via case studies. This information is presented in Table II.

TABLE II. FEATURES PROVIDED BY ABSOLUT FOR THE PERFORMANCE EVALUATION OF DISTRIBUTED EMBEDDED SYSTEMS

Number	Feature	References
I	*MOC Agnostic*	[4]
II	*Multithreaded Applications Modelling*	[26]
III	*Performance Evaluation of Protocols*	[23]
IV	*No Domain Restriction*	[1][27][28]
V	*Workload Model Generation of User-Space code, External Libraries and System Calls*	[4][20][30]
VI	*Workload Generation of Middleware technologies*	[27][20]
VII	*Detailed and Highly abstract workload modelling*	[29][4][30]
VIII	*Integration of Application Design and Performance Evaluation*	[1][28][27]
IX	*Non-functional Properties Validation*	[1][28][27]

From Table II it is clear that all the features which are required by a SLPE methodology to evaluate the performance of distributed embedded systems in different domains are provided by ABSOLUT.

VI. CONCLUSION AND FUTURE WORK

We therefore conclude from the survey that many methodologies have been developed for the SLPE of distributed systems. Those methodologies which employ a MOC for modelling applications or platforms are restricted to a particular domain of embedded systems. Also, these methodologies cannot provide reliable performance numbers of certain non-functional properties of distributed systems since the MAC and Transport protocols models are absent or abstracted out. These protocols play a key role in the end-user experience by contributing to non-functional properties. These non-functional properties such as end-end packet delays, packet loss rate and frame loss rate must be taken into account for performance modelling of distributed embedded systems so as to ensure a good end-user experience after the development and deployment of the distributed system.

We found that ABSOLUT can be used for the performance evaluation of distributed systems in different domains. The reason is that it does not employ any MOC for modelling applications and platforms. Also, ABSOLUT provides the models of different protocols (for example MAC and transport) which are important for the SLPE of distributed systems. Of course, all the performance evaluation methodologies have not been covered in this

 ISBN: 978-1-61208-246-2

survey. The main contribution of this article is to describe a disciplined approach for classifying the performance evaluation methodologies which helps to determine their feasibility for the performance evaluation of distributed embedded systems. By evaluating a methodology on the basis of requirements looking at the requirements we can evaluate its potential for SLPE of distributed embedded systems. If all the requirements mentioned in Section 3 are fulfilled by a methodology, it can be used to evaluate the performance of a wide range of distributed embedded systems.

ABSOLUT fulfils these requirements and provides the tools for the workload modelling at different levels of abstraction and refinement. Also, the ABSOLUT application workload models can be obtained by extending application model. The extended layered application architecture is analysed to identify the corresponding ABSOLUT workload model layers. This reduces the time and effort in performance modelling which is important to consider due to increasing complexity of distributed applications.

In the future, a number of widely used MAC and Transport protocol models will be designed and integrated to ABSOLUT. Currently IEEE 802.11 DCF, UDP and TCP models are provided. Also, a GUI front-end will be beneficial for easy instantiation of ABSOLUT performance models. It will also help to reduce the learning curve for SLPE via ABSOLUT toolset.

ACKNOWLEDGMENT

This work was performed in the Artemis SOFIA and SMECY projecst partially funded by Tekes – The Finnish Funding Agency for Technology and Innovation and the European Union. The work was performed in cooperation with Finnish ICT SHOK research project Future Internet. Authors would like to thank all their colleagues for valuable discussions about the topic.

REFERENCES

[1] I. Lee, J.Y.T Leung, S. H. Son. Handbook of Real-Time and Embedded Systems. Publisher: Chapman and Hall/CRC (July 23, 2007) .800 pages. Language: English.ISBN-10: 1584886781. ISBN-13: 978–1584886785.

[2] S. Khan, S. Pantsar-Syväniemi, J. Kreku, K. Tiensyrjä, J.-P. Soininen, ”Linking GENESYS application architecture modelling with platform performance simulation,” Forum on Specification and Design Languages 2009 (FDL2009). Sophia Antipolis, France, September 22-24, 2009. ECSI. France (2009)

[3] S. Khan, E. Ovaska, K. Tiensyrjä, J. Nurmi, “From Y-chart to seamless integration of application design and performance simulation,” Proceedings 2010 International Symposium on System-on-Chip - SOC. Tampere, Finland, 29-30 Sept. 2010. IEEE. Piscataway, NJ, USA (2010), pp. 18-25.

[4] J. Kreku, M. Hoppari, T. Kestilä, Y. Qu, J.-P. Soininen, P. Andersson, K. Tiensyrjä, “Combining UML2 application and systemc platform modelling for performance evaluation of real-time embedded systems,” EURASIP Journal on Embedded Systems. DOI: 10.1155/2008/712329.

[5] M. Gries, “Methods for evaluating and covering the design space during early design development,” Integration, the VLSI journal, vol. 38, 2004, pp. 131–183.

[6] P. Lieverse, P. van der Wolf. E. Deprettere, “A trace transformation technique for communication refinement,” Proc. 9th International Symposium on Hardware/Software Codesign (CODES 2001), pp. 134–139.

[7] T. Wild, A. Herkersdorf, G.Y. Lee, “Tapes—trace-based architecture performance evaluation with SystemC,” Design Automation for Embedded Systems 10(2–3): Special Issue on SystemC-based System Modelling, Verification and Synthesis , pp. 157–179..

[8] A.D. Pimentel, L. Hertzberger, P. Lieverse, P. van der Wolf, E. Deprettere, “Exploring embedded systems architectures with Artemis,” IEEE Computer 34(11), Nov 2001, pp. 57–63.

[9] T. Kangas, P. Kukkala P, H. Orsila, “UML-based multiprocessor SoC design framework. ACM Transactions on Embedded Computing Systems (TECS), Vol. 5 Issue 2, May 2006, pp. 281–320.

[10] S. Mahadevan, F. Angiolini, M. Storgaard, R. Olsen, J. Sparso J, J. Madsen, “A network traffic generator model for fast network-on-chip simulation,” Proceedings of the Design, Automation and Test in Europe (DATE05), 2005, pp. 780–785.

[11] S.Mahadevan, M. Storgaard, J. Madsen, K. Virk, “Arts: a system-level framework for modeling MPSoC components and analysis of their causality,” Proceedings of the International Symposium on Modeling, Analysis, and Simulation of Computer and Telecommunication Systems, 2005, pp. 480–483.

[12] A. Baghdadi, N. Zergainoh, W. Cesario, T. Roudier T, A.A. Jerraya, “ Design space exploration for hardware/software codesign of multiprocessor systems,” Proc. 11th International Workshop on Rapid System Prototyping (RSP), 2002, pp. 8–13.

[13] W. Fornaciari, D. Sciuto, C. Silvano, V. Zaccaria, “A sensitivity-based design space exploration methodology for embedded system,” . Design Automation for Embedded Systems, 7, 2002, pp. 7-33.

[14] W. Fornaciari, D. Sciuto, C. Silvano, V. Zaccaria, “A design framework to efficiently explore energy-delay tradeoffs,”. Proc. Ninth International Symposium on Hardware/Software Codesign (CODES), 2001, pp. 260–265.

[15] C. Jaber, A. Kanstein, L. Apvrille, A. Baghdadi, P.L. Moenner, R. Pacalet, “High-level system modeling for rapid hw/sw architecture exploration,” Proc. IEEE/IFIP International Symposium on Rapid System Prototyping (RSP ’09), Paris, France, pp. 88–94.

[16] K. Lahiri, S. Dey, A. Ragunathan,”Evaluation of the traffic-performance characteristics of system-on-chip communication architectures,” Proc. Proceedings of 14th International Conference on VLSI Design, 2001, pp. 29–35.

[17] K. Lahiri K, A. Ragunathan, S. Dey, “Efficient exploration of the SoC communication architecture design space,” Proc. IEEE/ACM International Conference on Computer Aided Design (ICCAD), 2000, pp. 424–430.

[18] J. Paul, A. Bobrek, J. Nelson, J. Pieper, D. Thomas, “Schedulers as model-based design elements in programmable heterogeneous multiprocessors,” Proc. Design Autamation Conference, 2003, pp. 408-411

[19] S. Mohanty, V. Prasanna, “Rapid system-level performance evaluation and optimization for application mapping onto soc architectures,”. Proc. Proceedings of the IEEE International ASIC/SOC Conference, 2002, pp. 160–167.

[20] J. Saastamoinen, J. Kreku, ”Application workload model generation methodologies for system-level design exploration,” Proceedings of the 2011 Conference on Design and Architectures for Signal and Image Processing, DASIP 2011. Tampere, Finland, 2-4 Nov. 2011. IEEE Computer Society (2011), pp. 254-260

[21] T. Kangas, "Methods and Implementations of Automated System for a Chip Architecture Exploration", PhD Thesis, Tampere University of Technology, Publication 616, 2006, 181 pages.

[22] K. Lahiri, A. Ragunathan, S. Dey, ”System-level performance analysis for designing on-chip communication architectures,” IEEE

 ISBN: 978-1-61208-246-2

Transactions on Computer-Aided Design of Integrated Circuits and Systems 20(6), 2001, pp. 768–783.

[23] S. Khan, J. Saastamoinen, M. Majanen, J. Huusko, J. Nurmi, " Analyzing transport and MAC layer in system-level performance simulation," 2011 International Symposium on System on Chip, SoC 2011. Tampere, Finland, 31 Oct. - 2 Nov. 2011. IEEE Computer Society (2011), 8 p.

[24] H. Posadas, F. Herrera, P. Sanchez, E. Villar E, F. Blasco, "System-level performance analysis in SystemC," Proceedings of Design, Automation and Test in Europe Conference and Exhibition (DATE 2004), Paris, France, 2004, pp. 378–383.

[25] A.D. Pimentel, P. van der Wolf, E. Deprettere, L. Herzberger, "The Artemis Architecture Workbench," Proceedings of the Progress Workshop on Embedded Systems, Utrecht, Netherlands, 2000, pp. 53-62.

[26] J. Saastamoinen, S. Khan, K. Tiensyrjä, T. Taipale, "Multi-threading support for system-level performance simulation of multi-core architectures," ARCS 2011. 24th International Conference on Architecture of Computing Systems 2011, Workshop Proceedings. VDE Verlag Gmbh, 2011, pp. 169-177

[27] S. Khan, J. Saastamoinen J. Nurmi, "System-level performance evaluation of distributed multi-core NoTA systems," 2nd IEEE International Conference on Networked Embedded Systems for Enterprise Applications. NESEA 2011, Fremantle, Dec. 8-9, 2011. IEEE (2011)

[28] S. Khan, J. Saastamoinen, K. Tiensyrjä, J. Nurmi, "SLPE of distributed GENESYS applications on multi-core platforms," The 9th IEEE international symposium on Embedded Computing (EmbeddedCom 2011). Sydney, Dec 12-14, 2011

[29] J. Kreku, M. Hoppari, T. Kestilä, Y. Qu, J.-P. Soininen, K. Tiensyrjä, "Languages for Embedded Systems and their Applications" volume 36 of Lecture Notes in Electrical Engineering, chapter Application Workload and SystemC Platform Modeling for Performance Evaluation, pp. 131–148. Springer.

[30] J. Kreku, J. Penttilä, J. Kangas, J.-P. Soininen, "Workload simulation method for evaluation of application feasibility in a mobile multiprocessor platform," Proc. Proceedings of the Euromicro Symposium on Digital System Design, 2004, pp. 532–539.

[31] S. Khan, J. Saastamoinen, K. Tiensyrjä, J. Nurmi, "Application workload modelling via run-time performance statistics,". IJERTCS-2012 *(Submitted-Under Review)*

[32] N. Nethercote, J. Seward, "Valgrind: A Framework for Heavyewight Dynamic Binary Instrumentation, in Proceedings of ACM SIGPLAN 2007 Conference of Programming Language Design and Implementation (PLDI2007), San Diego, California, USA, June 2007

 ISBN: 978-1-61208-246-2

An Expert System for Design-Process Automation in a CAD Environment

Gerald Frank
V-Research GmbH – Industrial Research and Development
Technical Logistics
Stadtstr. 33, 6850 Dornbirn, Austria
Gerald.Frank@v-research.at

Abstract— **For enterprises operating in markets, where customer needs can only be fulfilled with highly individualized products (which in turn necessitate a high degree of variety of lines of products), finding ways to reduce design and manufacturing costs is a crucial issue. This paper presents an expert-system approach to help solving correspondent challenges. The main methodology applied is to separate the design process into creative and repetitive tasks: Mapping the design logic of repetitive tasks onto a knowledge base then facilitates the creation of an expert system. This system supports engineers by automating those portions of a design process, which are based on repetitive tasks. Thereby, design-task complexity is reduced und there is a significant speedup of up to 90 % within construction processes. Finally, such a system enables engineers to focus on creative, value-creating tasks.**

Keywords*— *Expert System; Knowledge-Based Engineering; CAD

I. INTRODUCTION

Companies try to fulfill customer needs. For a manufacturing company, this can result in an extensive number of assemblies and parts, in order to cover the specific needs of every customer. Since this approach is very costly regarding development and production, enterprises aim at optimizing their costs while still maintaining the possibility of satisfying their customers.

Liebherr-Werk Nenzing GmbH (LWN) [6] is a manufacturer of a wide range of products including ship-, offshore- and harbor mobile cranes as well as hydraulic duty cycle crawler cranes and lift cranes. Its mission is to fulfill customers' needs. While standardization is possible in many of its products, there are also segments which require adaption of the crane to specific market demands. This results in a partial or complete engineering of a crane. In particular, the design of ascent assemblies and boom boxes for offshore and ship cranes (see the following section "Business cases") results in substantial efforts and constitutes a major part of the overall engineering costs.

As a result of this situation, LWN intended to minimize these costs by improving the design process in close co-operation with the industrial research centre V-Research in order to analyze possibilities of optimizing the development process and of reducing design and production costs.

By investigating the design process of ascent assemblies and boom boxes, we found that the design process is mainly based on repetitive tasks. Consequently, designing those assemblies is based on a set of invariant rules that can be modeled and stored. The only exception is the structural analysis of the assemblies. The results showed that the statics of ascent assemblies can be represented by rules. However, the statics calculations of boom boxes are more complex. To verify static stability of these assemblies, dedicated structural analysis simulation algorithms have to be integrated into the design process.

Furthermore, the current building blocks of the assemblies were analyzed. By doing so, we pointed out that a high amount of part variants existed, which in turn led to high costs. To reduce the number of part variants, we proposed to develop a fixed set of standardized parts, which is sufficient to designing all required assemblies.

These prerequisites enabled the standardization and optimization of the engineering process of nearly all ascent assemblies and boom boxes by automating the design process. The result of this approach is an expert system that permits more efficient design of the described assembly types.

This paper starts out with a short overview of related work. After presenting the business cases underlying our approach, this paper continues with a detailed explanation of the concept of the developed knowledge-based engineering (KBE) application. Then, the developed interfaces of the KBE-system and the resulting software framework are detailed. The paper closes with a short case study, summary and conclusion.

II. RELATED WORK

The result of our research was that there are product configurator approaches, which solve configuration problems automatically.

In the field of Artificial Intelligence, a configuration problem is understood as "the generation of a structure with predetermined properties by means of the combination of a certain number of objects" [4]. Bourke expands this definition and describes a product configurator as "[...] software modules with logic capabilities to create, maintain, and use electronic product models that allow complete definition of all possible product options and variation combinations, with a minimum of data entries and maintenance" [2].

Sabin et al. classify product configurators according to their concept of configuration knowledge as rule-based,

 ISBN: 978-1-61208-246-2

model-based, and case-based product configurators. According to them, each approach represents the configuration knowledge and the instances of the product to be configured in a different way [9].

In [3] Brinkop presents a list of leading providers of product configurators.

The expert-system approach presented in this paper starts one step before product configuration: based on user-defined assembly functionalities and a design knowledge-base (i.e. not only a configuration one), all parts are first generated and then assembled. Furthermore, the whole design process of a specific product is supported: Apart from a 3D CAD model, production drawings, bills of material and the production costs are provided as well. That is, the whole engineering process is automated.

III. BUSINESS CASES

LWN defined two assembly types, which served as business cases for our research: ascent assemblies and boom boxes. Design efforts and production costs related to these parts were rather high.

On the left side of fig. 1, an offshore crane is illustrated. For maintenance and inspection, several strategic points on the crane have to be easily accessible. Therefore, an ascent concept has to be developed, consisting of multiple ascent assemblies (platforms, stairs, ladders or roundplatforms). In the figure, they are highlighted in red.

On the right side of the image, a ship crane is shown. For this crane, the boom has to be engineered to fulfill specific customer requirements, consisting of lifting capacity as well as of working and interference area. These requirements are derived from the ship design of the customer and allow for little variation. Therefore, the boom section highlighted in red is designed individually for each application. This type of boom consists of a pivot, a middle and a head section. The middle section, representing the second business case, consists of bottom, top and side plates as well as stiffeners and bulkheads. Their dimensions and their quantity depend on the results of the structural analysis. This complex analysis is performed based on the customers' requirements.

IV. CONCEPT OF A KBE-APPLICATION

The objective of our approach is an expert system. According to Steinbichler [10], an expert system is a system, which stores and accumulates specific knowledge of different areas and generates solutions in a user interface to given problems. Leondes [7] extends that definition by equating the terms "knowledge-based system" (KBS) and "expert system". He clarifies that a knowledge-based engineering (KBE) system is a subset of a KBS. According to Stokes [11], knowledge-based engineering can be defined as "the use of advanced software techniques to capture and re-use product and process knowledge in an integrated way." To use the KBE-approach, users' expertise has to be acquired and stored. The captured knowledge is then permanently available. Hence, the product development can be regarded as a holistic process. All relevant design know-how can be extracted and mapped onto the product model [4].

Figure 1. Ascent assemblies and boom box (red)

Concerning the approach of this paper, KBE is based on an IT application of high usability that supplies and processes knowledge and interacts with a CAD system. The result is an automatically generated solution, in accordance with a designer's input. The CAD system itself is completed with explicitly modeled knowledge in form of a programmable application. This knowledge contains all information about a product, i.e. its structure, function and behavior as well as its manufacturability and quality. This is all the data a designer has to know and to enter into a CAD system.

Based on the previously explained methodologies and requirements of LWN, we developed a concept for integrating KBE-design and structural analysis.

The concept relies on some restrictions and approaches which are explained in the following subsections.

A. *Influencing Factors*

To model a design process, it is necessary to investigate all influencing factors. Engineering of assemblies is based on a variety of restrictions, namely:

- industrial and internal standards
- statics requirements
- production costs
- implicit design restrictions (e.g., assembly erection or maintenance aspects) and
- production restrictions (e.g., disposal factors)

For example, if designing a platform, these restrictions are special assembly logics or platform entries conforming to standards.

B. *Modelling of the Design Knowledge*

To build a KBE system, the relevant engineering expertise has to be acquired. Our analysis showed that engineering processes can be differentiated into repetitive and creative processes. In contrast to creative processes, repetitive ones consist of nearly identical tasks and are therefore independent of creative decisions. This condition is necessary for modeling them as a system of rules.

In contrast to repetitive processes, creative ones occur typically only once. Because of that, modeling them as rules within reasonable time is economically not viable.

One of the goals defined by LWN was that a specific repetitive design task should always result in the same, ideal solution. Because of the limited ability of a human to re-

 ISBN: 978-1-61208-246-2

execute cognitive tasks identically, it is important to support users with a tool (i.e. a software application).

To fulfill this goal, and to capture all relevant steps for designing the focused-on assemblies, we conducted numerous interviews with engineering experts at LWN. The retrieved information served as a base for analyzing the repetitive design processes. Most of the time spent was used for detecting the restrictions defined in section IV.A.

The obtained data were prepared to be stored as rules in an IT system. These rules represent directed dependencies in a form common for expert systems, namely "IF (condition/-s) THEN (action/-s)", i.e. all conditions must be known and must be fulfilled before a rule can be applied [4].

The rule set can be used for arbitrary types of assemblies. Rules can be changed without editing the source code. In addition, if a full range of rules is acquired, nearly every form of assembly is supported. Therefore, repetitive tasks in designing new or adapting existing assemblies can be automated. This enables engineers to focus on creative, value-creating activities [12].

C. *Decision support by cost optimization*

The elaborated automation algorithm follows the explained system of rules. To evaluate all design alternatives, the resulting combinatorial programming problem is based on standardized manufacturing costs. These costs were retrieved by an analytical method which analyzes bills of material and task schedules [13].

All engineering tasks, which are not covered by this system (e.g., structural analysis of booms) are integrated in the expert system by defining an interface for data exchange with external applications.

Based on the defined customer parameters, e.g. maximum lifting capacity as well as working and interference area, the external applications calculate a weight-optimized geometry of an assembly version. However, due to the nature of the boom production processes, a weight-optimized geometry is not necessarily cost-optimized. Based on the resulting structure, the developed algorithm uses a defined set of rules to translate the calculated geometry into a cost-optimized structure, while still adhering to the boundaries of the statical calculation. The final result is an assembly that is cost-optimized and statically verified.

This algorithm guarantees an optimal design process for the considered assemblies.

V. INTERFACES OF THE KBE-APPLICATION

The above described approaches are fundamental to the developed expert system.

In the following sections, the most important components of the application are described.

A. *Man-machine interface*

The graphical user interface is an important component of the developed application. This interface is used to exchange data between a user and the algorithm. Our focus was put on minimizing user input. The goal was to allow users to define an assembly as efficiently as possible. Finally, design engineers only have to provide data which cannot be retrieved automatically. Furthermore, they are supported by interactive sketches. Inputs are immediately visualized (see fig. 2).

Every irregularity as to a defined process is highlighted by interaction dialogs. For example, if a design engineer defines inconsistent data, the application alerts the user.

In addition, a user is supported by some assisting tools. One of them is concerned with the combination of assemblies: there is a wizard that visually supports the user to form a valid combination of assemblies (e.g., a complete access solution for an entire crane) (see fig. 2).

B. *CAD-System Interface*

1) *Component Assembly*

Once an assembly is defined by the user, and, if necessary, the structural data are calculated, the respective data are then handed over to the automated design-to-cost algorithm. After calculating all necessary information for generating a 3D CAD model, the computed data is sent to a CAD software in an iterative way, using the application programming interface (API) of the CAD system.

First, each part is loaded and, if necessary, the geometry is adapted. Then, the parts are positioned in reference to an existing part to ensure that all parts refer to each other. This is important because as a result every manual change directly affects all parts. For example, if a user manually changes the length of a part, the positions of all dependent parts are adjusted automatically.

This principle has also been applied to assembly combinations.

2) *Production Drawings*

To complete the design process, production drawings have to be generated. As a consequence, the developed application also generates these documents automatically.

In order to efficiently use the space available on the drawing sheets, the positions of all required views are calculated by an algorithm based on trim optimization. To

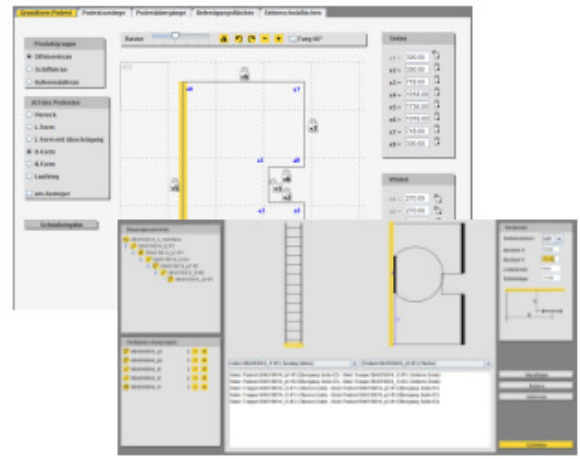

Figure 2. Example of an interactive sketch for assembly dimensions and an assistant wizard for assembly-combination definitions

 ISBN: 978-1-61208-246-2

ensure a good and fast solution, the concept of trim optimization was simplified. Each view is reduced to a rectangle or a combination of it, which is put at the most appropriate and still available position.

After all views have been positioned, all production-relevant dimensions and the according measurements are automatically added by a generic framework. This framework is implemented with the API, provided by the CAD system. It is based on a classification of dimension types. Dimensions can relate to

- an edge
- an edge to point
- a point to point or
- an angle.

For every mentioned type, a dedicated positioning function has been implemented.

Finally, the bill of materials is added to the drawing.

C. Structural-Analysis Software Integration

As each individual boom box requires a separate structural analysis, we developed a method that is based on a KBE-system which interacts with a structural analysis system (ANSYS).

1) Structural Complexity of Boom Boxes

From a statical perspective, ascent assemblies and boom boxes are designed to carry load. However, construction principles differ significantly between the two.

Ascent assemblies contain specific components, which ensure the adequacy of the design according to safety and overall requirements of the structure. Based on these parts, there is a limited set of variants with a fixed geometry. As a consequence of that, all statically relevant components can be pre-calculated by using suitable software. The resulting parameters, e.g., the maximum load per square millimeter or the maximum gap to the next structurally relevant component, can be pre-assigned and therefore stored in rules. For example, the base frame of stairs consists of stringers. However, the main static load is carried by cantilever arms. In order to guarantee the stability of each assembly version, depending on its dimension and based on the precalculated statical parameters, the number and/or dimensions of these parts may vary.

In contrast to the described ascent assemblies, all components of a boom box are structurally relevant elements. Because of the market-segment specific requirements and due to LWN's commitment to fulfill them (i.e. to provide arbitrary lengths and loads, according to customer demands as to boom boxes), their dimensions largely vary and cannot be limited to a standard set of parts.

Furthermore, different load scenarios have to be considered when designing a boom box. Because of that, a structural pre-calculation of every possible dimension of the individual components is not possible as the boom has to be considered as a complete system. Therefore, the statical logic for boom boxes cannot be mapped to simple rules regarding its components. Nevertheless, an integration of the structural analysis into an automated process is possible and has been realized in the scope of this project.

2) Interaction with the Structural-Analysis Application

In [6], the author defines structural analysis as follows: "Structural analysis is a process to analyze a structural system in order to predict the responses of the real structure under the excitation of expected loading and external environment during the service life of the structure."

A standard structural-analysis process is shown in fig. 3. This process works for boom boxes at LWN in a similar way. In a first step, the design manager of the project converts the customer requirements into load cases. A load case mainly consists of a boom position (inclination angle) and a load capacity. After taking into account additional factors, a set of load cases is generated.

Based on this input, a simplified model is generated and processed by the structural analysis software (ANSYS). In ANSYS, the model is analyzed with all the load cases. Based on multiple iterations, the defining parameters of the components (e.g., plate thickness) are optimized.

The result is an iteratively calculated optimal structure of a boom box. For each section, the material dimensions, part quantities and positions are defined. Based on these data, the CAD model of the boom can be generated.

As the existing structural analysis procedure is a very time-consuming, complex and effort-intense process, we tried to simplify and increase its efficiency. In the end, we automated nearly all manual activities and integrated them into the developed KBE-system.

To supply the structural analysis software with all relevant information, we developed a standardized data exchange format. Now, the only manual activity consists of defining the load cases based on customer requirements. The developed algorithm then transforms these data into an ANSYS-suitable configuration and hands them over to the structural-analysis simulation application. Once the simulation has started, no further user interaction is necessary. At the end of the simulation process, the structural

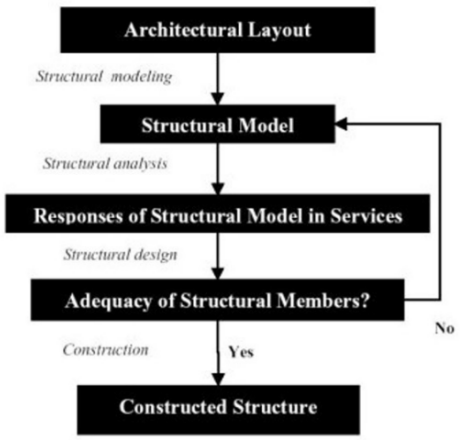

Figure 3. Structural analysis process

engineer receives all the data for double-checking.

For returning the results to the KBE-system, an additional interface format was developed.

Finally, the calculated assembly structure is statically optimized. The utilization of the material is maximized and as a result, the weight of the total structure is minimized. However, as stated before, a weight-optimized structure does not necessarily mean that it is cost-optimized. Therefore, based on a set of design rules, the KBE-system translates the data to achieve a cost-optimal solution and generates a CAD model as described in subsection B above.

By employing this approach, the development process of a structurally complex assembly becomes significantly faster and more effective. This also enables LWN to react quickly to changes in the requirements of a customer.

VI. Overview of Developed Framework

Fig. 4 visualizes all components of the here described software. For data exchange, the framework provides several interfaces. These are prepared for assembly-independent use. The brown boxes in the center of the below figure represent the developed algorithm. Since an in-depth explanation of all these modules is beyond the scope of this article, we dispense with details.

In order to prove the generic character of the developed framework, we used it for the design of the two above discussed business cases (ascent assemblies and boom boxes) as well as for houses on stilts (i.e. an illustrative case for an open-house day).

VII. The Expert System in Practice

As explained in the previous section, we used our framework for the engineering of ascent assemblies, like platforms. To illustrate design and functionality of the KBE-System, fig. 5 illustrates the process of the automated design of such a platform.

First, the user defines the geometry (e. g., length and width) and the functionalities (e. g., entry and fixing areas) of the platform to be engineered. Subsequently, all data is submitted to the KBE-System. Using the knowledge base and the part building set, the developed algorithm calculates all parameters to generate a 3D CAD model in a CAD system and establishes a connection to that system. Then, data is transferred bidirectionally. The result is an automatically generated 3D CAD model, including the corresponding production drawings, bill of materials and the resulting production costs.

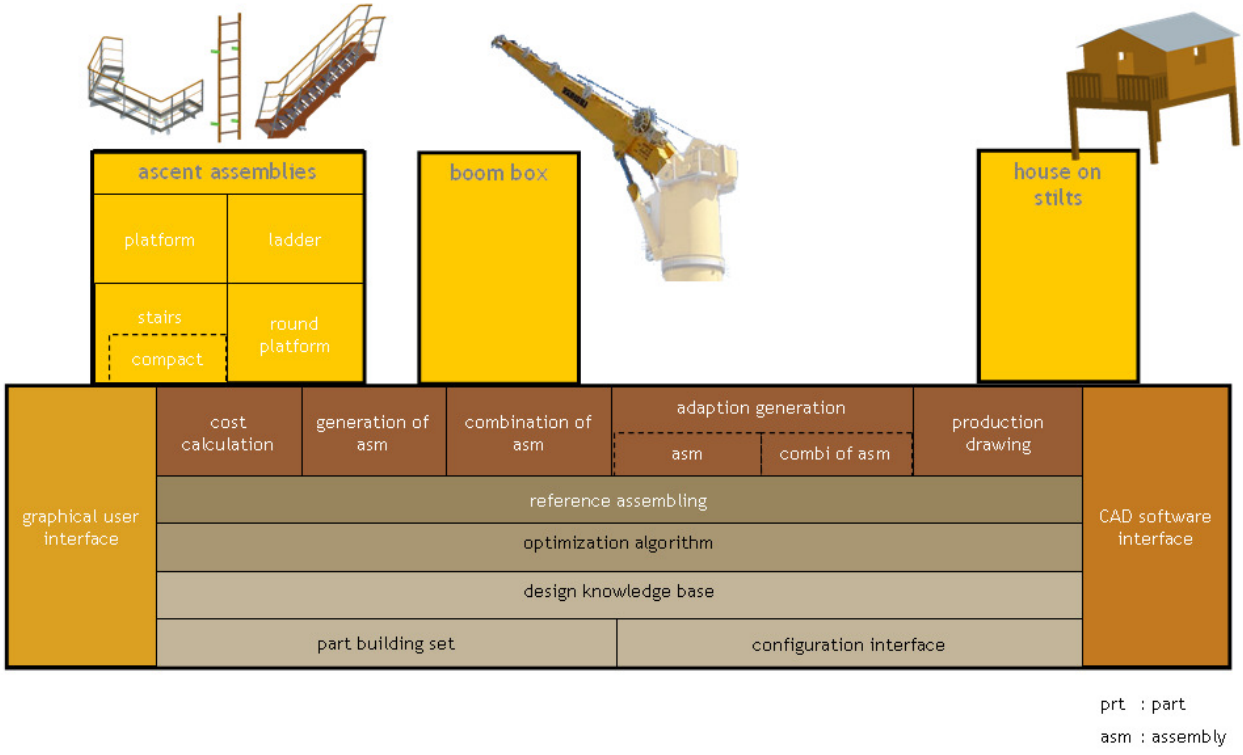

Figure 4. Overview of framework

 ISBN: 978-1-61208-246-2

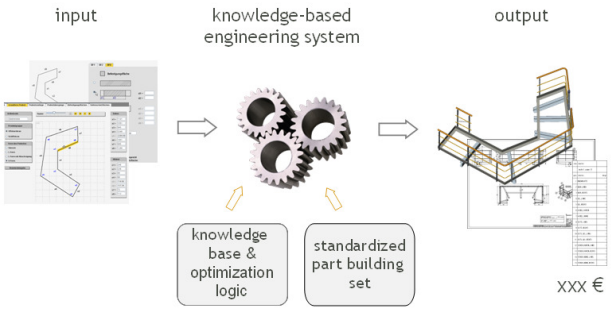

Figure 5. Automatic platform design process

VIII. SUMMARY AND CONCLUSIONS

For enterprises which operate in markets where customer needs can only be fulfilled by way of highly individualized products (in turn necessitating a high variety of products, assemblies and parts), it is crucial to find ways of reducing design and manufacturing costs. This paper presented a KBE-approach to help solving such challenges.

From the start, the described application was developed towards a generic framework. While the framework was so far mainly used for the business cases of ascent assemblies and boom boxes, it is not limited to these tasks. An adaptation and extension towards other assemblies and components is possible.

All assemblies, the design process of which is based on a repetitive logic, can be generated automatically. Also, if a part set of all necessary parts of an assembly type exists and if the design know-how is modeled in a rule system, a design from scratch is possible.

The main challenge is to identify these processes and determine as well as capture the engineering knowledge they represent. By way of operational use of the presented methodology and KBE-application in its engineering department, LWN gained valuable insight and further builds on this experience in future application areas.

By automating the creation of new assemblies and the adaption of existing ones, the complexity of design processes is well reduced and a significant speed-up is achieved. The engineering of ascent assemblies of an LWN offshore crane used to require up to 150 hours. Employing the here proposed software, these efforts can be cut down to 10 to 20 percent.

These savings in terms of cost and time were realized with the presented application through the following features:

- minimized engineering costs
- integration of structural analysis
- extensive reduction of the engineering period
- production-suitable CAD models (models, characterized by feasible dimensions, tolerances and adequate material attributes for manufacturing them [5])
- reproducibility of all created assemblies
- enabled iterative engineering
- storing the expert knowledge in a rule-base.

IX. ACKNOWLEDGEMENTS

This paper discussed results and findings of a research project within the K-Project “Integrated Decision Support Systems for Industrial Processes (ProDSS)”, financed through the Austrian funding program COMET (COMpetence centers for Excellent Technologies).

[1] E. S. Aziz, C. Chassapis, “Engineering with computers - A decision-making framework model for design and manufacturing of mechanical transmission system development” , Springer London, 2005.

[2] R. Bourke, “Product Configurators: Key Enabler for Mass Customization – An Overview”, Midrange Enterprise, 2000.

[3] A. Brinkop, „Marktführer Produktkonfiguration“, http://brinkop-consulting.com/guide/marktfuehrer.pdf, 2012

[4] A. Brinkop, "Variantenkonstruktion durch Auswertung der Abhängigkeiten zwischen den Konstruktionsbauteilen", Dissertationen zur Künstlichen Intelligenz ed. 204, Infix St.-Augustin, 1999.

[5] H. Brockmeyer, A. Lucko, F. Mantwil, „Entwicklung von wissensbasierten Assistenzen zur frühzeitigen Produktbeein¬flussung am Beispiel des Karosseriebaus“, Die digitale Produktentwicklung, G. Tecklenburg, expert verlag Renningen, 2008, p. 107 f..

[6] W. Kanok-Nukulchai, “Structural Analysis” in “Civil engineering”, K. Horikawa, EOLSS Publishers Co Ltd Oxford, 2009.

[7] C. T. Leondes, “Intelligent Knowledge-Based Systems: Business and Technology in the new Millenium”, Springer London, 2004.

[8] Liebherr-Werk Nenzing GmbH, http://www.liebherr.com/en-GB/35267.wfw.

[9] D. Sabin, R. Weigel, „Product Configuration Frameworks – A Survey“, IEEE Intelligent Systems, vol. 13, no. 4, 1998, pp. 42-49.

[10] G. Steinbichler, “Methoden und Verfahren zur Optimierung der Bauteilentwicklung für die Spritzgießfertigung“, Thesis University Erlangen-Nuremberg, 2008.

[11] M. Stokes, “Managing Engineering Knowledge: MOKA - Methodology for Knowledge Based Engineering Applications”, ASME Press, 2001.

Article in a conference proceedings:

[12] H. Adickes, J. Arnoscht, A. Bong, R. Deger, S. Hieber, R. Krappinger, M. Lenders, P. Post, M. Rauhut, M. Rother, J. Schelling, G. Schuh, J. Schulz, „Lean Innovation – Auf dem Weg zur Systematik.“, Aachner Werkzeugmaschinen Kolloquium ´08 – Aachener Perspektiven, Brecher, C., Klocke, F., Schmitt, R., Schuh, G., Apprimus Verlag Aachen, 2008, pp. 494 f..

[13] R. Krappinger, „Optimierung des Produktentwick-lungsprozesses durch automatisierte Konstruktion“, 2nd Innovation Leadership Summit, WZL RWTH Aachen, 2008

 ISBN: 978-1-61208-246-2

Ontology-Based Meta Model in Object-Oriented World Modeling for Interoperable Information Access

Achim Kuwertz
Institute for Anthropomatics (IFA)
Karlsruhe Institute of Technology (KIT)
Karlsruhe, Germany
Email: achim.kuwertz@kit.de

Gerd Schneider
Fraunhofer IOSB - Institute for Optronics,
System Technologies and Image Exploitation
Karlsruhe, Germany
Email: gerd.schneider@iosb.fraunhofer.de

***Abstract*—Many systems rely on the integration of environment observations provided by sensor systems to fulfill their tasks. The Object-Oriented World Model (OOWM) is an information fusion architecture allowing to integrate observations from heterogeneous sensing systems and to provide consolidated information to higher level processing modules in a compound system. Both, data integration and the provision of consolidated information require to exchange information in a meaningful and semantic interoperable way. To promote the semantic interoperability in the OOWM, an ontology-based meta model is presented, allowing to structure the knowledge used to represent application domains as well as interface information objects. This meta model defines an upper level ontology for world modeling, which can be extended by specific domain models and facilitates the integration of additional sensor systems. To allow semantic access to OOWM information, the use of OGC Web Feature Services and Sensor Observation Services based on the meta model is proposed.**

***Keywords*-object-oriented world modeling; knowledge representation; ontology; semantic interoperability; WFS; SOS**

I. INTRODUCTION

Information on their environment is a prerequisite to the successful operation of many systems that support decision making or even decide autonomously. Nowadays, environment information often is available in considerable quantities, provided by heterogeneous sensing systems. A major challenge for making use of this information is to manage it adequately. Such managing includes tasks like the integration, processing and consolidation of information as well as providing the means to make this information accessible for further analysis and available to stakeholders.

One approach to this task of managing environment information is the use of a world modeling system. World modeling generates a computational representation of a considered environment, both by capturing background information (i.e., general facts) on the application domain and by acquiring current information on the state of the environment based on observations and measurements. An example of such a world modeling system is the Object-Oriented World Model (*OOWM*) [1]. The OOWM is a probabilistic information fusion architecture for managing acquired sensor information. It has been successfully applied to domains like autonomous systems [2], video surveillance [3] and situation assessment [4].

The OOWM is suited for integrating and consolidating observations from heterogeneous sensing systems. It has been designed to act as a central information hub in a compound system and can supply connected modules (like higher level processing or analysis modules) with the information they need. Interoperability on a syntactic as well as on a semantic level is a key issue for such compound systems to function properly. It is needed on the one hand for integrating observations from different sensing systems, as input to the OOMW, and on the other hand, when providing access to the information within the OOWM to higher level processing modules. Currently, much configuration effort and possibly data transformations are needed for integrating additional sensing systems into the OOWM. Concerning information access, though standard-based mechanisms are defined within the OOWM, these mechanisms yet rely on proprietary data models containing only sparse semantics.

To promote semantic interoperability and information exchange to and from the OOWM, this contribution proposes an ontology-based meta model for structuring the background information used to represent an application domain as well as to formalize the information objects necessary for providing semantically enriched access interfaces.

An example of an intelligent system based on the OOWM is the ISR Analytics Architecture [5], a framework for analyzing and accessing information related to the domain of intelligence, surveillance and reconnaissance. Within this architecture, a specialized software layer is responsible for providing observation data from different sources to the OOWM, and software modules from an analytics layer access OOWM information to perform their analyses. Against the background of such compound systems, we present how the proposed ontology can be integrated into state-of-the-art service-oriented interfaces like the Web Feature Service (*WFS*) [6] or the Sensor Observation Service (*SOS*) [7] standardized by the Open Geospatial Consortium (*OGC*).

This paper is structured as follows. Section II gives an

 ISBN: 978-1-61208-246-2

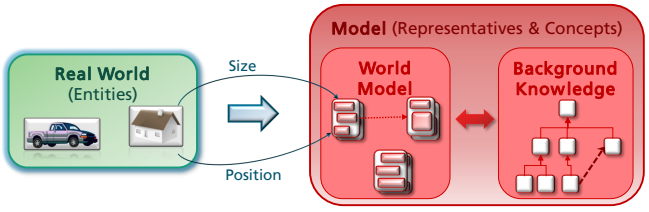

Figure 1. Overview of Object-Oriented World Modeling. Observed real-world entities are represented as objects in the World Model, based on concepts defined in Background Knowledge given as taxonomic structure.

introduction to the OOWM approach. Section III discusses semantic interoperability in world modeling. In Section IV, the proposed meta model ontology is presented in detail. Section V then introduces the web-services based access interfaces to the OOWM and discusses an approach for their model-driven implementation.

II. Object-Oriented World Modeling

The OOWM [1], [2] is a probabilistic data and information fusion framework which allows to represent the current and historic state of a considered real-world domain based on observation data. Intended as a general framework for world modeling, the OOWM is able to integrate observations delivered by heterogeneous sensing systems and can thus be employed in many different application domains. It is designed to serve as a persistent memory structure and information hub, providing higher level processing modules with integrated information.

The OOWM is based on the concept of using observations of entity features (e.g., dynamic features like position or static features like size), to model real-world entities (e.g., objects, persons or abstracta). Observed entities and relations are represented as structured objects in a dynamic World Model. The objects are based on a priori modeled Background Knowledge, which contains the concept classes representing the entities and relationships occurring in an application domain. This Background Knowledge is the basis for evaluating, classifying and completing information derived from observations as well as for querying the World Model for information about observed entities. Figure 1 summarizes the Object-Oriented World Modeling approach.

For managing and updating the information stored in the OOWM, information processing based on the Bayesian methodology is employed. Information about attribute values of observed entities and the existence of relations is represented by probability distributions, thus allowing the OOWM to explicitly treat uncertainties e.g. arising from sensor measurements. Using the Bayesian methodology, these values can be subject to probabilistic information processing, including updates and fusion with related or newly acquired information, prediction in time, aging or further processing within higher level modules. This information processing is supported by probabilistic data association algorithms like the JIPDA [8], relying on the spatial position of observations and entities for data association. The classification of observed entities based on their attribute values, i.e., the mapping of an entity representation to a concept class, can be handled within the Bayesian methodology as well.

All information processing within the OOWM is applied on the basis of a discrete model of time. For each discrete point of time, attribute values and relations get stored in a state-of-the-art database, thus allowing to access domain state information for past points of time. Such historic information is needed for traceability of information states, for example in applications where decisions are based on a certain information set available up to this point of time.

III. Semantic Interoperability in World Modeling

Interoperability is a key issue to systems like the OOWM which integrate heterogeneous observations and provide information to various higher level processing modules. For information exchange, syntactic interoperability relies on the definition of common data types and interfaces. Semantic interoperability builds up on these definitions and aims at allowing a meaningful interpretation of exchanged information by defining a semantic information model, e.g., an ontology. Within the OOWM, XML Schema definitions or lightweight concept hierarchies are employed to ensure syntactic interoperability, specifying the data structures used to represent domain entities as well as their observations. An expressive ontology supporting semantic interoperability has not yet been employed as a conceptual domain model.

Besides structuring the representation of domain knowledge, the semantics of interface information has to be defined. The OOWM up to now offers proprietary web-service interfaces which e.g. allow to query for instances or retrieve the XML-based data model. For integrating additional sensing systems, no interface semantics exist. In consequence, this integration requires manual configuration effort and the transformation of observation data.

A recent approach to the problem of integrating observations from heterogeneous sensor systems (employed e.g. by [9]) is given by the OGC Sensor Web Enablement (*SWE*) initiative [10]. In this approach, a conceptual UML data model is specified, which allows sensor systems on the one hand to publish their capabilities (e.g., which qualities can be measured) and on the other hand to present their measurements according to a standardized description [11]. The SWE approach is a significant step towards promoting interoperability. Yet, when regarded as formal conceptual model for describing observations, the approach shows inconsistencies and lacks the required precision for semantic interoperability [12]. Furthermore, it relies on an externally defined ontology to describe a domain.

In order to promote semantic interoperability for the OOWM, a meta structure for domain modeling as well as a

 ISBN: 978-1-61208-246-2

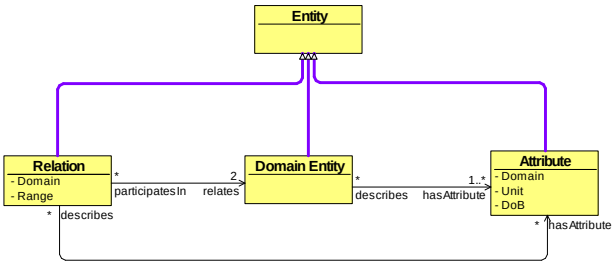

Figure 2. Conceptual view on the OOWM meta model, defining how real-world entities are represented as concepts in background knowledge. The concept Domain Entity models the common features of entities of interest.

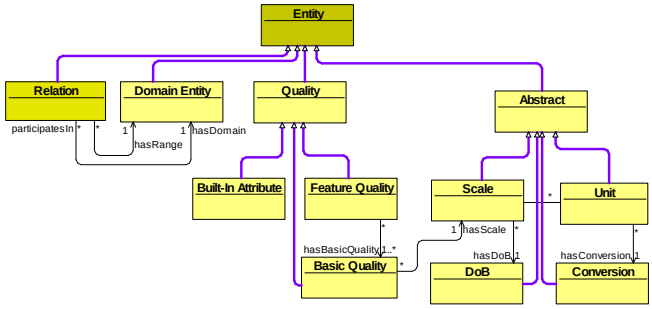

Figure 3. Basic concepts of the OOWM meta model refined as ontology. Attributes are represented by the categories of Quality, constituting attribute domains, and Abstract, defining the features needed to describe attributes.

conceptual model for interface information is needed. This can be achieved by employing an ontology as an integrated approach. To facilitate the use of ontologies as semantic background knowledge for domain modeling as well as to describe interface information objects, we propose to define and employ a meta model for knowledge representation within OOWM. In [13], we took a first step into this direction by presenting an abstract meta model for object-oriented domain modeling, developed with respect to enable extension to existing domain models. In this contribution, we propose a formal representation based on description logic, implementing the model as an OWL DL [14] ontology. This approach allows us to make use of well-supported ontology reasoning technologies for tasks like querying or consistency checking. Furthermore, it allows to share the meta model ontology, e.g. allowing a sensor system not only to provide its observations as an ontology instance, but to perform remote consistency checks prior to transmitting its data. Similar rationales and approaches are followed in [12], [15], where ontologies are used to represent the fundamental terms of OGC observations [11] or pervasive computing context.

Figure 2 displays the conceptual view on the OOWM meta model. In OOWM Background Knowledge, basically an entity-relationship [16] approach is used to model entities occurring in a domain of interest. The most important entities concerned in domain modeling are entities like objects, persons, events or abstractions of these, which are subsumed in the category of Domain Entity. A Domain Entity is characterized by Attributes which describe its qualities, given as the domain of an Attribute, and their quantitative characteristics, given as a probability distribution representing the Degree-of-Belief (DoB) in these values, and, if needed, a unit of measurement. Furthermore, relations can be used to describe the relationships that possible exist between entities in the application domain. A Relation is characterized by a domain and a range of entities on which this relation can be applied. The conceptual view in Figure 2 constitutes an adapted UML specification of the meta model presented in [13]. As a next step, the meta model, and thus the ontology, has to be further refined.

IV. Ontology-based Background Knowledge

In structured approaches to ontology design like [17] an important step is to determine the intended scope of the ontology. This includes the domain, uses and level of abstraction the ontology is intended for. For the OOWM meta model, the scope is to define a semantic meta structure for background knowledge, in which entities from different domains of interest as well as their observations can be described according to the principles of the OOWM approach. This structure is aimed at supporting a semantic access to the observation information stored in the OOWM. It shall support different domains of interest, ranging from large-scale surveillance applications to indoor robotic scenarios. As one ontological commitment, a descriptive approach is chosen, describing real-world entities on a level of abstraction corresponding to human environment perception. Furthermore, a presentism and actualism approach is taken, making the intended knowledge structure time-independent and free of modality, since the concepts of time and probability will have to be represented within the model itself.

For general knowledge to be structured within an ontology, it is recommended to commit to the basic categories of an existing upper level ontology. For the OOWM meta model, the descriptive foundational ontology DOLCE [18] was chosen. In DOLCE, a top-level category named particulars is subdivided into the categories of endurants (entities which are present in their whole at any time and can truly change with time), perdurants (entities existing only in time), qualities (entities that can be observed) and abstracts (entities without spatial or temporal qualities). This high level categorization is adopted to structure the OOWM meta model refinement, as depicted in Figure 3. Besides Relation the concepts of Domain Entity, Quality and Abstract are defined. Domain Entity constitutes the union of all the DOLCE endurants and perdurants which represent the entities being subject to domain modeling. Though not depicted in Figure 3, the categories of Endurant and Perdurant are defined as subcategories of Entity. A Quality describes measurable entities and is further subdivided into a Basic Quality, which constitutes a one-dimensional measurand (like a length, an

 ISBN: 978-1-61208-246-2

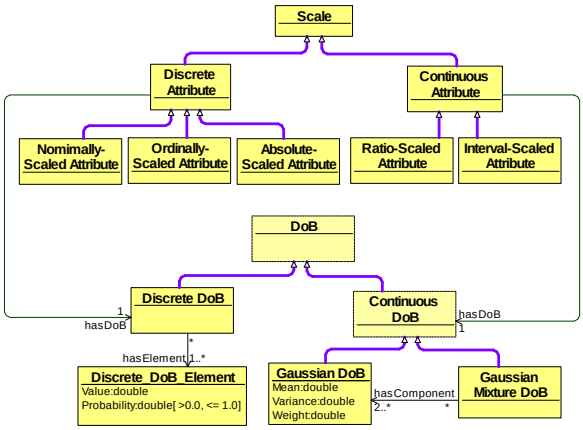

Figure 4. Implementation of attributes in the refined OOWM meta model. Each attribute has a Scale, (e.g., a nominal, ordinal or cardinal scale) and each Scale is associated with a DoB distribution.

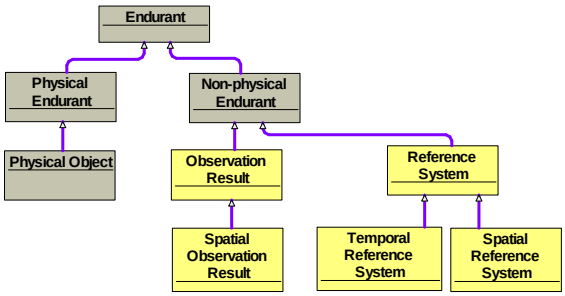

Figure 5. The structure of Endurants as used by the OOWM meta model, with gray boxes representing DOLCE categories. Observations are modeled as the result of an observation process.

angle, etc.), and a Feature Quality, which is build using Basic Qualities (like a position or bounding box). Abstract entities are used to characterize the features of attributes like their Scale, DoB distributions and Unit.

Due to the dedication to DOLCE categories, Attributes in the refined meta model are represented by using the concept of Quality in conjunction with the concept of Abstract. A probabilistic OOWM attribute is thus represented as semantic net in the model. Qualities constitute the possible domains of attributes. Basic Qualities need to specify a Scale. The Scale concept defines subconcepts for the different types of measurement scales, i.e., nominal, ordinal, and cardinal scales. Each Scale is associated with a DoB distribution. As subconcepts of DoB, discrete distributions (specifying a list of value-probability pairs), normal distributions (represented by a mean value and a variance) and sums of normal distributions are modeled. For cardinally scaled attributes, a Unit of measurement has to be specified. The OOWM meta model for example specifies different units of measurement for describing a length, an angle or a velocity. Each Unit of measurement is associated with a Conversion that characterizes how different units can be converted (e.g., by scaling or shifting). For associating Qualities and a respective Unit, SWRL [19] rules can be employed. Figure 4 illustrates the modeling of attributes in the OOWM meta model. Besides using probabilistic attributes, a Built-In Attribute concept needs to be defined for specifying deterministic values, e.g. for the handling of time.

For representing interface information like observation results and structuring background knowledge, the concept of Endurant has to be further refined. This subdivision is illustrated in Figure 5, where categories taken from DOLCE are depicted in gray. Physical Endurant forms the basis for modeling physical entities in the domain of interest. The most important subconcept is Physical Object, which models all entities that exist in space as an entire object. Physical Objects are constituents to the union concept Domain Entity. The other important contribution to this union concept is made by temporal entities (which are subconcepts of Perdurant) like Events or Processes.

As Non-Physical Endurant, the OOWM meta model defines the concepts of Observation Result and Reference System. Observation Result constitutes the most important concept for data input to the OOWM. Contrary to [11], [12], observations are not considered as a process, but as a piece of information representing its results. Thus, the concept of Observation Results is modeled as Endurant. A Spatial Observation Result represents an observation containing a spatial reference. Figure 6 depicts the definition of observation results. For defining spatial and temporal references, the meta model defines the concept of Reference System.

For stochastic information processing as employed in the OOWM, observations as well as entity representations have to be assigned with a tangible time reference. Due to this, the OOWM meta model has to define time entities and a temporal reference system. The handling of time in the OOMW meta model is based on the two notions of time instant and time interval, as used for example in OWL-Time [20] and ISO 19108 [21] (here the notion period is used instead of interval). As time instant, the OOWM meta model defines the concept of Point of Time. Points of time are described by a Temporal Position, i.e., a temporal distance to a reference point of time. As mentioned earlier, Temporal Attributes like Temporal Positions constitute Built-In Attributes which are not modeled to be probabilistic but deterministic. Subconcepts of Temporal Position are thus directly represented by standard data types. The details of time representation within the OOWM meta model are depicted in Figure 7. As standard Temporal Reference System, a Gregorian calendar with a ISO 8601 dateTime [22] as Temporal Position description is employed. If needed, the meta model can be extended (in analogy to [21]) by specifying an additional Temporal Reference System, which has to define a temporal reference point, denoting its beginning, as a Gregorian DateTime. Discrete Relative Time is an example of such a Temporal Reference System.

 ISBN: 978-1-61208-246-2

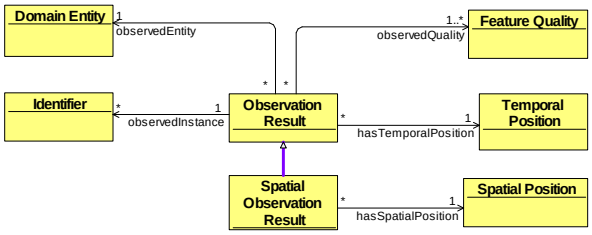

Figure 6. Definition of the concept Observation Result, which models the result of an observation process as information object. It specifies the Domain Entity and Quality observed as well as the observation time.

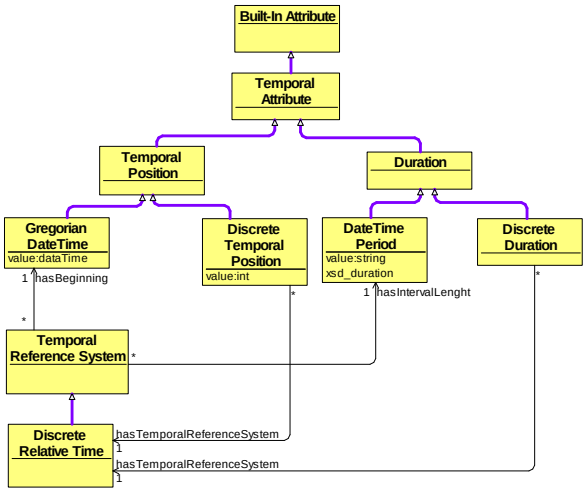

Figure 7. Handling of time in the OOWM meta model. As Temporal Attributes, the concepts Temporal Position and Duration are defined. The concept Temporal Reference System allows extensions to these concepts.

The handling of geospatial information in the meta model concerns qualities like positions, locations and extends. A Spatial Position, being a Quality associated to a Physical Object, is specified using the known World Geodetic System 84 (WGS84) in the meta model. Similar to the handling of time, it is possible to add a Spatial Reference System defining additional Spatial Positions, for example a local Cartesian coordinate system.

V. Web-Based Information Access Interfaces

As described in Section III the OOWM currently does not provide semantic access interfaces for inserting and retrieving OOWM information. To overcome these limitations we propose the use of standardized web-service interfaces and a model-based approach, relying on the proposed ontology, for generating these interfaces. As the OOWM mainly represents geographic information, the proposed interfaces are based upon the well-standardized and widely accepted OGC standards Web Feature Service (*WFS*) [6] and Sensor Observation Service (*SOS*) [7], and the currently discussed OGC standard Sensor Event Service (*SES*) [23].

Figure 8 depicts the current OOWM architecture (see [24]) with the proposed service-oriented extensions. In the

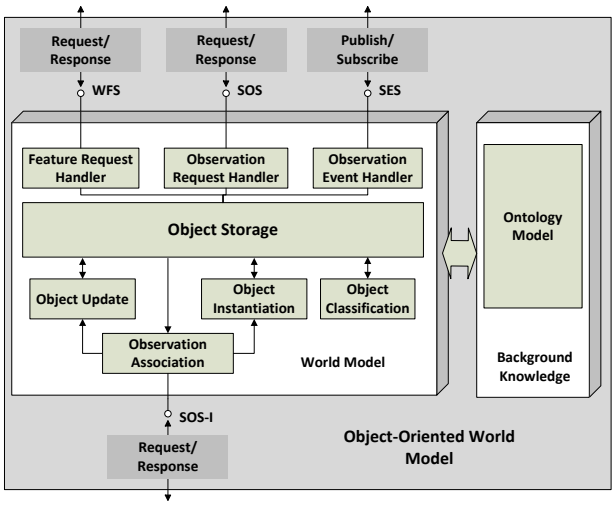

Figure 8. Service-oriented interface definitions. The OGC standard WFS, SOS and SES are employed for accessing OOWM information.

context of the OOWM, the SOS can be used for retrieving information concerning specific entity attributes according to a request/response protocol initiated by a client application like a high level processing module. In case an application wants to get actively informed about new OOWM information, the SES provides an event notification to previously subscribed consumers (push mode). Additionally, the WFS provides a request/response interface for the OOWM that can be used to retrieve aggregated, object-based entity information, which are to be represented as OGC features [25]. As a fourth OGC compliant interface an advanced SOS (SOS-I; I = Insert) [7] interface is available to allow insertion of observations supplied by sensing systems.

Besides the proposed interfaces the extension includes the depicted components Feature Request Handler, Observation Request Handler and Observation Event Handler. These handlers process incoming OGC compliant service requests and respond with adequate OGC compliant service results. The handlers operate on the Object Storage of the World Model and make use of the Ontology Model stored in Background Knowledge. This Ontology Model constitutes a domain-specific extension of the OOWM meta model ontology, thus describing interface objects as well as domain entities. Figure 9 depicts an exemplary domain-specific ontology as extension to the OOWM meta model. The taxonomy of domain entities is to be used in the WFS, SOS and SES for querying object information and in the SOS-I for inserting new observation data to the OOWM.

The SOS-I in conjunction with the Ontology Model can be used to facilitate the semantic integration of additional sensing systems into the OOWM. When using the SOS-I to provide observations to the OOWM, each sensing system will have to describe its observations as an information object which allows to instantiate an Observation Result

 ISBN: 978-1-61208-246-2

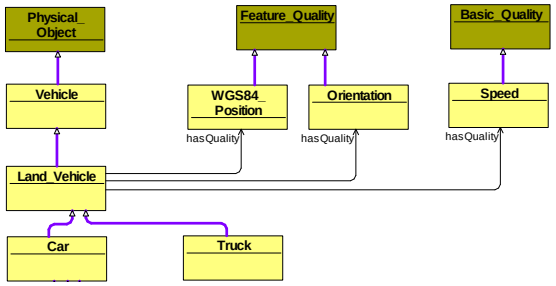

Figure 9. Exemplary domain model based on the OOWM meta model. The taxonomy of concepts is used for queries in the WFS and SOS.

concept in the OOWM. Thus, each SOS-I message must at least specify

- a feature of interest describing either a Domain Entity concept (e.g., Vehicle) or a reference to an known Domain Entity instance (then acting as Identifier),
- an observed property describing the Feature Quality which was observed,
- a measurement value specified as DoB in a unit of measurement corresponding to the observed quality,
- and a time stamp representing the Temporal Position.

Additionally, a Spatial Position can be specified. An example of an XML encoded SOS-I message is given in Listing 1.

```
<sos:InsertObservation service="SOS" version="2.0.0">
 <sos:observation> [...]
  <om:name xlink:href=".../BkOnto.owl#WGS84_Position"/>
  <om:value> <gml:Point gml:id="Spatial_Position">
    <gml:pos srsName=".../EPSG/0/4326">54.9 10.5</gml:pos>
  </gml:Point> </om:value> [...]
  <om:phenomenonTime>
   <gml:TimeInstant gml:id="Temporal_Position">
    <gml:timePosition>2012-09-25T13:01:00.7Z</
        gml:timePosition>
  </gml:TimeInstant></om:phenomenonTime>
  <om:observedProperty xlink:href=".../BkOnto.owl#Speed"/>
  <om:featureOfInterest xlink:href=".../BkOnto.owl#
      Land_Vehicle"/>
   <om:result> [...]
    <swe:elementType name="Speed_GaussianDoB"> [...]
     <swe:field name="GaussianDoB_Mean">
      <swe:Quantity definition=".../BkOnto.owl#Mean">
       <swe:uom code=".../BkOnto.owl#milesperhour"/>
      </swe:Quantity> </swe:field>
     <swe:field name="GaussianDoB_Variance">
      <swe:Quantity definition=".../BkOnto.owl#Variance">
       <swe:uom code=".../BkOnto.owl#milesperhour"/>
      </swe:Quantity> </swe:field> [...]
    </swe:elementType>
    <swe:encoding>
     <swe:TextBlock decimalSeparator="." tokenSeparator=",
         " blockSeparator="@@"/>
    </swe:encoding>
    <swe:values>45,2.5@@</swe:values>
  [...]
</sos:InsertObservation>
```

Listing 1. Excerpt of an XML encoded SOS-I message providing observation information about the velocity of a land vehicle.

For the WFS, the structure of a result message is defined by the queried feature, which in the OOWM corresponds to the queried Domain Entity. When querying for entity information via the WFS, the concept taxonomy will be searched,

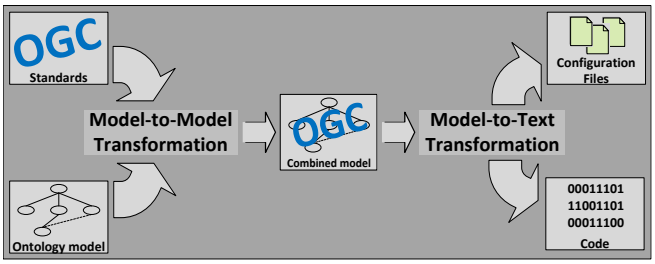

Figure 10. Model transformation process employed in a model-driven approach for generating application code for SOS-I clients in the OOWM.

acquiring and returning all instances of subconcepts for the queried concept, described as instance of the queried concept (according to a cast to a superclass).

To ensure for client applications to comply to OGC standards as well as to the OOWM conceptual domain model, methods of model-driven software development (e.g., [26]) can be applied for generating parts of a client implementation, based upon the presented OGC-based interface standards and the OOWM Ontology Model. An automated model transformation process for this purpose is depicted in Figure 10. It can be based upon existing modeling tools like the Eclipse Modeling Project [27]. As initial parts, relevant OGC standards and the Ontology Model form the input to the transformation process. The first step of the process is a model-to-model transformation weaving OGC interface definitions and ontology to one combined model that includes both source models. The second step is a model-to-text transformation of the combined model, resulting in platform specific code and configuration files.

As advantages of this model-driven approach, client applications can be provided with an integrated data model. This data model can address syntactic and semantic aspects of information exchange with the OOWM by providing common data structures as well as formalizing their conceptual meaning. In addition, remote consistency checks on observation data can be performed prior to transmitting it to the OOWM via SOS-I, for ensuring model-compliant data. An issue to be solved within this approach is to define a way for receiving the ontology model via OGC web-services in a standard-conform manner.

VI. Conclusion

For promoting semantic interoperability in Object-Oriented World Modeling, an ontology-based meta model for structuring domain knowledge and interface information objects has been presented. This meta model facilitates the integration of additional sensing systems into the OOWM and enables information exchange on a semantic level. Furthermore, it can serve as an overarching ontology for various domain models when employing the OOWM in different application domains. When implemented as a formal ontology, reasoning and consistency checks can be performed by available tools, thus allowing sensing systems to perform such

 ISBN: 978-1-61208-246-2

checks prior to transmitting their observations. Furthermore, semantic interface descriptions for a web-service access to OOWM information based on standards like OGC WFS and SOS have been proposed on the basis of the meta model.

Beside promoting interoperability, the proposed meta model ontology can be used as structure for semantically extending an existing background knowledge by concept learning approaches. In addition to formal knowledge sharing as enabled by ontologies, it is even possible to perform a kind of distributed concept learning in this way.

REFERENCES

[1] I. Gheta, M. Heizmann, and J. Beyerer, "Object Oriented Environment Model for Autonomous Systems," in *Proceedings of the second Skövde Workshop on Information Fusion Topics*, H. Boström, R. Johansson, and J. van Laere, Eds. Skövde Studies in Informatics, 2008, pp. 9–12.

[2] A. Belkin, A. Kuwertz, Y. Fischer, and J. Beyerer, "World Modeling for Autonomous Systems," in *Innovative Information Systems Modelling Techniques*, C. Kalloniatis, Ed. InTech, 2012.

[3] T. Emter, I. Gheta, and J. Beyerer, "Object Oriented Environment Model for Video Surveillance Systems," in *Fraunhofer Symposium Future Security. 3rd Security Research Conference*, 2008, pp. 315–320.

[4] A. Kuwertz, Y. Fischer, B. Essendorfer, and E. Peinsipp-Byma, "Using Context Knowledge for Maritime Situation Assessment," in *Proceedings of 3nd International WaterSide Security Conference (to appear)*, 2012.

[5] J. Sander, A. Kuwertz, G. Schneider, and B. Essendorfer, "ISR Analytics: Architectural and Methodic Concepts," in *Proceedings of the 7th Workshop on Sensor Data Fusion: Trends, Solutions, Applications (SDF 2012)*, 2012.

[6] P. A. Vretanos, "OpenGIS® Web Feature Service 2.0 Interface Standard (OGC 09-025r1)," Version 2.0, OpenGIS Implementation Standard, Nov. 2010.

[7] A. Broering, C. Stasch, and J. Echterhoff, "OGC® Sensor Observation Service Interface Standard (OGC 12-006)," Version 2.0, OpenGIS Implementation Standard, Apr. 2012.

[8] D. Musicki and R. Evans, "Joint Integrated Probabilistic Data Association - JIPDA," in *Proceedings of the Fifth International Conference on Information Fusion, 2002*, vol. 2, 2002, pp. 1120 – 1125.

[9] C. Erbas, F. T. Cetin, B. Yilmaz, and E. Akagunduz, "Open and Interoperable Maritime Surveillance Framework Set to Improve Sea-Border Control," in *Proceedings of the 7th Workshop on Sensor Data Fusion: Trends, Solutions, Applications (SDF 2012)*, 2012.

[10] M. Botts, G. Percivall, C. Reed, and J. Davidson, "OGC Sensor Web Enablement: Overview And High Level Architecture." OGC, Tech. Rep., Dec. 2007.

[11] *ISO 19156:2011 – Geographic information - Observations and measurements*, ISO Std., 2011.

[12] F. Probst, "An Ontological Analysis of Observations and Measurements," in *Proceedings of the 4th. International Conference on Geographic Information Science (GIScience 2004)*, 2006, pp. 304–320.

[13] A. Kuwertz, "Towards Adaptive Open-World Modeling," in *Proceedings of the 2011 Joint Workshop of Fraunhofer IOSB and Institute for Anthropomatics, Vision and Fusion Laboratory*, J. Beyerer and A. Pak, Eds. Karlsruhe: KIT Scientific Publishing, 2012, pp. 139 – 161.

[14] M. Dean and G. Schreiber, "OWL," Feb. 2004.

[15] X. H. Wang, D. Q. Zhang, T. Gu, and H. K. Pung, "Ontology Based Context Modeling and Reasoning using OWL," *Pervasive Computing and Communications Workshops, IEEE International Conference on*, 2004.

[16] P. P.-S. Chen, "The entity-relationship model toward a unified view of data," *ACM Transactions on Database Systems (TODS)*, vol. 1, no. 1, pp. 9–36, Mar. 1976.

[17] A. De Nicola, M. Missikoff, and R. Navigli, "A Software Engineering Approach to Ontology Building," *Information Systems*, vol. 34, no. 2, pp. 258 – 275, Apr. 2009.

[18] A. Gangemi, N. Guarino, C. Masolo, A. Oltramari, and L. Schneider, "Sweetening Ontologies with DOLCE," in *Proceedings of the 13th International Conference on Knowledge Engineering and Knowledge Management. Ontologies and the Semantic Web*, ser. EKAW '02. London, UK: Springer-Verlag, 2002, pp. 166–181.

[19] I. Horrocks, P. F. Patel-Schneider, H. Boley, S. Tabet, B. Grosof, and M. Dean, "SWRL: A Semantic Web Rule Language Combining OWL and RuleML," W3C Member Submission, May 2004.

[20] J. R. Hobbs and F. Pan, "Time Ontology in OWL," September 2006. [Online]. Available: http://www.w3.org/TR/owl-time/

[21] *ISO 19108:2002 – Geographic information – Temporal schema*, ISO Std., 2002.

[22] *ISO 8601:2004 – Data elements and interchange formats – Information interchange – Representation of dates and times*, ISO Std., 2004.

[23] J. Echterhoff and T. Everding, "OpenGIS® Sensor Event Service Interface Specification (proposed) (OGC 08-133)," Version 0.3.0, OpenGIS® Discussion Paper, Oct. 2008.

[24] Y. Fischer and A. Bauer, "Object-Oriented Sensor Data Fusion for Wide Maritime Surveillance," in *Proceedings of 2nd NURC International WaterSide Security Conference*, 2010.

[25] *OGC Reference Model – OGC 08-062r7*, Version 2.1, OGC Std., Dec. 2011.

[26] M. Voelter, T. Stahl, J. Bettin, A. Haase, and S. Helsen, *Model-Driven Software Development*. John Wiley & Sons, 2006.

[27] Eclipse Modeling Project, http://www.eclipse.org/modeling/.

 ISBN: 978-1-61208-246-2

RedNoCs: A Runtime Configurable Solution for Cluster-based and Multi-objective System Management in Networks-on-Chip

Philipp Gorski[1], Claas Cornelius[1], Dirk Timmermann[1], Volker Kühn[2]
Institute of Applied Microelectronics and Computer Engineering[1]
Institute of Communication Engineering[2]
University of Rostock
Rostock, Germany
{philipp.gorski2, claas.cornelius, dirk.timmermann, volker.kuehn}@uni-rostock.de

***Abstract*—Runtime-based monitoring and adaptation are indispensable system management tasks for efficient operation of complex heterogeneous Multi-Processor-System-on-Chip (MPSoC) under dynamic workloads. Thereby, runtime-adaptive mechanisms like application mapping, adaptive routing or thermal management will have their own parameter, requirements and information flows. The main contribution of this work is the evaluation of a cluster-based, runtime-configurable and multi-objective system management strategy that combines the needed information flows of different runtime-mechanisms and supports the reuse of collected data for higher system-level services. This will increase the benefit-cost-ratio of needed hardware extensions and further tackles the system management aspect in a holistic way.**

Keywords-Network-on-Chip, MPSoC, Monitoring, System Control, HW/SW-Co-Design.

I. INTRODUCTION

Networks-on-Chip (NoC) emerged as the next generation of communication infrastructures for the growing number of computational on-chip resources in Multi-Processor-System-on-Chip (MPSoC) [1][2][3]. These complex systems will integrate functionality of various application domains at different regions on a single die. Each domain comes along with specific characteristics regarding the supported degree of parallelism (task-level and/or data-level), typical traffic pattern and loads, use cases, workload timing and constraints. Furthermore, some of these characteristics will change during system-lifetime, because underlying algorithms evolve or user scenarios will be adapted. The efficient operation of such heterogeneous systems depends on the integrated mechanisms for runtime management and their adaptability to the specific requirements of the covered application domains. Typical runtime tasks include application mapping and scheduling, debugging and test, power/energy/thermal management, traffic load management (e.g. adaptive routing in NoC) and fault-tolerance [4][5]. Thereby, the availability and needed quality of monitored system state information is a key concern. Furthermore, the transport of system control data to adjust the system behavior has to be right in time. Both, monitoring and control have their own requirements regarding the current workload, traffic loads and number of parameter needed to be observed/adjusted. Furthermore, the runtime control mechanisms have varying underlying algorithmic scopes (e.g. centralized, distributed or hybrid). This variability makes it hard to design a global solution for a system management, which include the monitoring as well as the control features in a holistic way. Most commonly publicized works present results about single runtime management mechanisms with specifically tailored solutions or utilize simulation-based workload information. Thus, they target a mono-objective management flow for a subset of runtime mechanisms (see Figure 1), which will be optimized for specific problem sizes, application domains or algorithms.

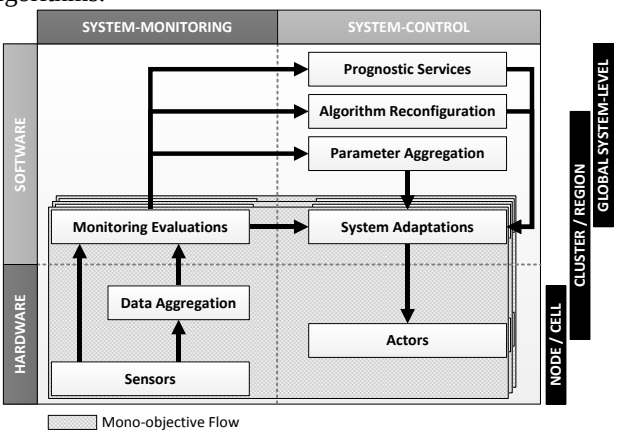

Figure 1. Overview of the multi-objective System Management Flow and its Organization in RedNoCs

The typical mono-objective flow follows the scheme illustrated in Figure 1. At the lowest level on the monitoring side sensors will capture specific parameter data (e.g. traffic or buffer loads for dynamic routing). The data will be further aggregated or fed directly into the unit responsible for monitoring evaluation, which can be implemented in software or hardware with different scopes (locally distributed or centralized). The results of the monitoring evaluation will be used by the system control mechanism to calculate needed adaptations (e.g. changed routing paths or tables) and sends them to its corresponding actors. The main contribution of this work targets the conceptual evaluation of combined information flows from different runtime

 ISBN: 978-1-61208-246-2

mechanisms to support a multi-objective system management flow, and the global reuse of the captured data for higher system-level services. This will increase the benefit-cost-ratio of the additionally implemented functionality. Thereby, the presented solution follows four major design criteria. (1) *Redundant NoCs (RedNoCs):* The general separation of application and system data flows to different redundant infrastructure solutions (Data-NoC and System-NoC). Thereby, the design requirements will be separated too and each NoC can be optimized for its own traffic domain. (2) *Multi-objective Clustering:* The utilization of a software-directed and hardware-assisted clustering methodology, where cluster of different flows exist in parallel and can be reconfigured at runtime (sizing or timing of monitoring) to meet the specific constraints of assigned workload fractions. (3) *Reusability:* The proposed reuse of collected monitoring data for higher system-level services like the reconfiguration of system adaptation algorithms or prognostic services. Furthermore, the implementation of hardware intensive parts will focus their reuse for different domains. (4) *HW/SW-Co-Design:* The functional units of the system management, responsible for evaluation and adaptation, will be realized as software agents. Thus, these agents can migrate between resources and will be exchangeable at runtime. The needed hardware parts cover sensing, acting and extended network interfaces to decouple the cluster communication of different system mechanisms.

The remainder of this work is organized as follows. Section 2 covers the related work of existing approaches. The general concept and analysis of this work will be provided by Section 3. An evaluation of the experimental results for different corner cases will follow in Section 4. Afterwards, Section 5 gives a final conclusion and an outlook for future investigations.

II. RELATED WORK

The majority of published works propose solutions for specific design cases. They can be mainly classified by the infrastructural integration concept, the operational scope/hierarchy and the targeted runtime mechanisms.

The infrastructural integration can be separated into two main directions [5][6] as follows: (1) Shared Infrastructure Solutions (SIS): The application data and the system information use the same NoC as communication infrastructure, which will be designed for the application data requirements. Additionally, to provide less concurrency between the different data domains special time-division-multiplexing (TDM) or the integration of prioritized virtual channels (VC) can be applied and each kind of data has its own reserved bandwidth or time slots. (2) Exclusive Infrastructure Solutions (EIS): The application data and the system information traffic are assigned to different communication infrastructures, which run in parallel. Each infrastructure is designed for the specific requirements of its data domain and there is no concurrency. Thus, a full separation of domain specific concerns at design- and runtime is achieved.

Different publications cover the integration aspect. In [8] Ciordas et. al. present a monitoring-centric evaluation of different EIS and SIS solutions for the *AEthereal* NoC regarding the design flow. Guang et. al. does a similar evaluation with the major focus on runtime monitoring and operational costs in [5][6]. Further, the requirements of different runtime mechanism and results (power, area, latency) for an 8x8 2D-Mesh topology NoC with 8-Bit data width per link direction are presented. These works show that EIS is the most promising way to handle monitoring traffic in NoCs. Similar results are shown by the infrastructure comparison in [9] for the MNoC using 24-Bit data width per link, four flit buffer depth and two virtual channels for the EIS. MNoC is applied for the objective of thermal/latency monitoring to realize a Dynamic Voltage and Frequency Scaling (DVFS). Adaptive routing in NoC represents the most common runtime mechanism for the utilization of mono-objective system management. The solutions differ from distributed to centralized traffic monitoring in combination with routing table/path adaptations. Ebrahimi et. al. presents two different distributed adaptive routing schemes (LEAR and CATRA) with EIS solutions for the aggregation of traffic congestion information. In LEAR [10] the neighboring router nodes share their congestion states via one additional wire per link direction in the range of one hop. A more complex and irregular congestion information aggregation network for the multi-hop regions is used by CATRA in [11], where the number of additional wires per link corresponds to the width/height of the 2D-Mesh topology. A solution between the complexity of LEAR and CATRA is presented by Rantala et. al. [12] using 2 additional wires per link direction for buffer level information sharing with direct-neighbor nodes. Similar regional congestion information aggregation EIS like CATRA can be found in RCA [13] and DBAR [14]. RCA uses 8 up to 16 additional wires per link, while DBAR will need 8 wires per link for the sharing of congestion information. All of these distributed adaptive routing mechanisms will evaluate the shared traffic information locally at each routing node using special hardware. A centralized adaptive routing called ATDOR is presented in [15]. The centralized path management works as additional hardware resource with a fixed coupling to the NoC though an out-of-band traffic monitoring aggregation network (EIS) using 4 additional wires per link. Further, for the distribution of path updates an additional EIS is suggested, but not applied. The global traffic information or the EIS won't be reused. A complete multi-objective distributed system management with combined aspects of connection-oriented traffic monitoring, adaptive routing, and application mapping with clustering is tackled by the publications of Faruque et.al. [16][17].

 ISBN: 978-1-61208-246-2

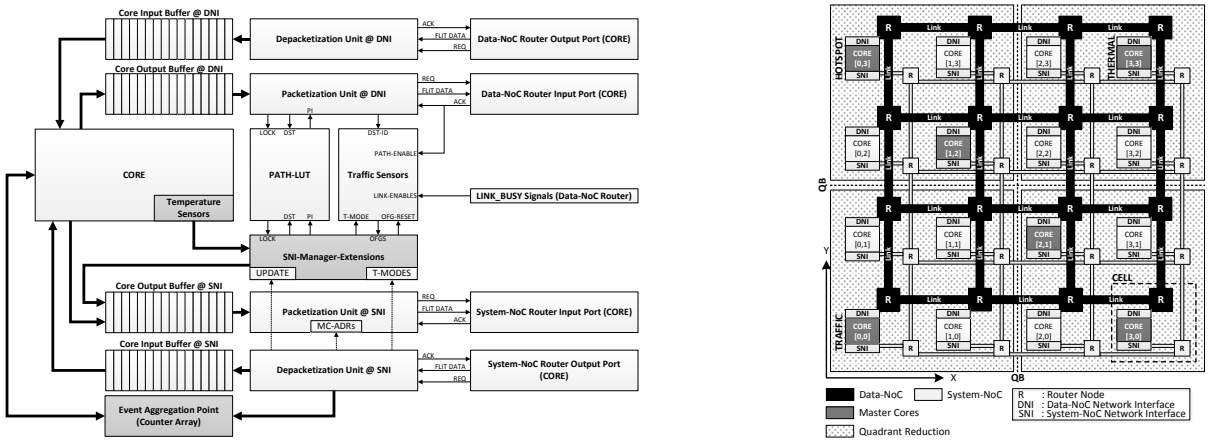

(a) Overview of RedNoCs integration at the CORE (b) 4x4 2D-Mesh NoC/Cluster with RedNoCs

Figure 2. Overview of the RedNoCs integration strategy at different abstraction levels

The supposed AdNoC solution integrates hierarchical software agents (global, cluster) for dynamic application mapping and reconfigurable clustering, distributed NoC traffic and application event monitoring via hardware probes at each resource/router, and distributed deterministic adaptive routing with buffer size reconfiguration. The monitoring traffic uses an SIS with a prioritized VC for this data domain. The complete system management is event-driven and focusses the runtime optimization of bandwidth utilization. An exploration of MPSoC monitoring and management systems is given in [18]. This work further introduces an own hierarchical concept of agent-based MPSoC management. Similar hierarchical approaches are applied by other publications. In [5][6] a hierarchical monitoring consisting of hardware nodes at the IP cores and at the cluster. Further, higher level software-based platform and application agents are proposed. In [19] this concept is applied for hierarchical power monitoring in NoC. Another approach considers the reuse for DVFS scenarios [20]. A event-based SIS monitoring concept including event taxonomy, probe design/programming, and variable hierarchy (distributed or centralized) for the *AEthereal* NoC is presented in [21]. The targeted use case scenarios are system- and application level debugging at runtime. This work is extended in [22] to support different abstraction-levels. Furthermore, the solutions in [23][24] covers the transaction-based debugging and the integration of special monitoring probes at design time.

In summary, most of the published works present good solutions for specific mono-objective flows, but they do not consider the synergistic potential of the flexible reuse of collected information or of the implemented hardware.

III. REDNOCS CONCEPT

RedNoCs is a HW/SW-based system management solution that covers the infrastructural separation of different traffic domains. The targeted NoC topology is a wormhole-switching 2D-Mesh with applied EIS, where two separated NoCs, called System-NoC and Data-NoC, work in parallel (see Figure 2 (b)). The links between neighboring routers are bidirectional point-to-point connections, which transmit a certain portion of a communication packet in parallel (called flit). The first flit of a packet (header) contains the routing information, while following flits carry the payload. Each packet will finalize with a tail flit that transports payload data too. A packet will enter the NoC at the source node flit-by-flit (wormhole-switching), passes the intermediary router nodes (hops) and finally reaches its destination, where the contained payload data will be processed. The Data-NoC covers the transport of application data, while the System-NoC is used for system management. The System-NoC has the same topology as the Data-NoC to provide the same resource-connectivity, but both infrastructures can be individually adapted to the domain-specific requirements. The Data-NoC integrates more complex routing algorithms, link data width (64-Bit or higher) and resource functionality, while the System-NoC works with reduced link data width (5- or 7-Bit), minimal input buffering (one flit) and dimension-ordered XY/YX-Routing. As illustrated in Figure 2 each NoC-Resource (CORE) is connected independently to both NoCs via Data-Network- and System-Network-Interface (DNI and SNI). The smallest management unit of RedNoCs is a CELL and includes the CORE, DNI, SNI and the connected router nodes (R) of both NoCs. These CELLs are further sub-classified into Slaves and Master. A Master-CELL is suited with special hardware resources and software agents to manage a CLUSTER or global system-level operations. Slave-CELLs are dynamically grouped into a CLUSTER by a corresponding Master-CELL. These CLUSTERs are the fundamental components for the system management and can be configured individually. The following sub-sections describe the specific details of the RedNoCs functionality and its organization.

A. Clustering

The implemented clustering is reconfigurable at runtime and context-based. The creation and management of CLUSTERs is realized via software agents at the Master-

CELLs and utilizes a messaging/organization concept as follows:

CLUSTER-REQUEST (CREQ): For the initial creation of a CLUSTER the Master-CELL sends allocation packets to all CELLs that need to be part of the CLUSTER. These packets consist of the destination routing information (CELL-ADR), the NoC-Address of Master-CELL as source information (MC-ADR), the context identifier of the CLUSTER (CTX-ID) and further context data for Slave-CELL configuration (CTX-DATA). The list of CELLs that will be grouped to a CLUSTER and the corresponding Master-CELL will be selected by global domain agents (e.g. application mapping agent).

CREQ = {CELL-ADR | MC-ADR | CTX-ID | CTX-DATA}

CLUSTER-ACKNOWLEDGE (CACK): The Slave-CELLs receive the request/update of the Master and returns a binding packet as acknowledgement. The packet contains the MC-ADR as routing header, the CELL-ADR as source information and the special CTX-ID to classify the packet.

CACK = {MC-ADR | CELL-ADR | CTX-ID}

CLUSTER-UPDATE (CUP): During CLUSTER operation the configuration data (monitoring periods, routing path updates) need to be adapted, the software agent migrates to another Master-CELL or the CLUSTER will be deleted. Thus, the Slave-CELLs are informed via update packets, which have the same format like the CREQ.

CUP = {CELL-ADR | MC-ADR | CTX-ID | CTX-DATA}

The context of a CLUSTER describes the system management domain (e.g. traffic or thermal monitoring/control) it is used for. Each Slave-CELL can be assigned to multiple CLUSTERs of different CTX-IDs at the same time, but not to different CLUSTERs of the same CTX-ID. Thus, if multiple CLUSTERs of the same CTX-ID coexist, they will be spatial separated and do not share any CELLs. Moreover, this separation concerns the exclusive clustering for different workload fractions/applications and avoids interferences. Each clustering context has its own configuration data, parameter and identifier. Domains that are integrated at design time and supported by special hardware resources (e.g SNI-Manager-Extensions at Figure 2 (a)) have a reserved set of CTX-IDs assigned. The rest of freely available CTX-IDs can be used for software-driven and dynamically defined services (e.g. execution monitoring of individual applications). The allocation of CTX-IDs is managed at runtime by a global domain agent. Before a new service is allowed to start a CTX-ID must be requested by its Master-CELL agent. Furthermore, after finalization of the CLUSTER service the global agent must be informed that the reserved CTX-ID is freed. At this state of research, the restriction of the CTX-ID to one byte seems sufficient and allows the integration of 256 clustering domains. While the CLUSTER will be created and managed by the cluster agent, the planning, resource assignment and placement of CLUSTERs will be processed by upper-level global software agents, which are responsible for specific domains. Furthermore, domain-independent global agents will assembly and process global cross-domain parameter. Below, Figure 3 illustrates the global dataflow concept and separation of concerns for the agent/data architecture of RedNoCs. This concept targets a hierarchical problem separation, where the global scope for parameter adjustments, algorithms and adaptation policies will be configured by the global agents and the cluster agents will work on these globally configured data sets to manage the assigned workload fractions and regional configurations.

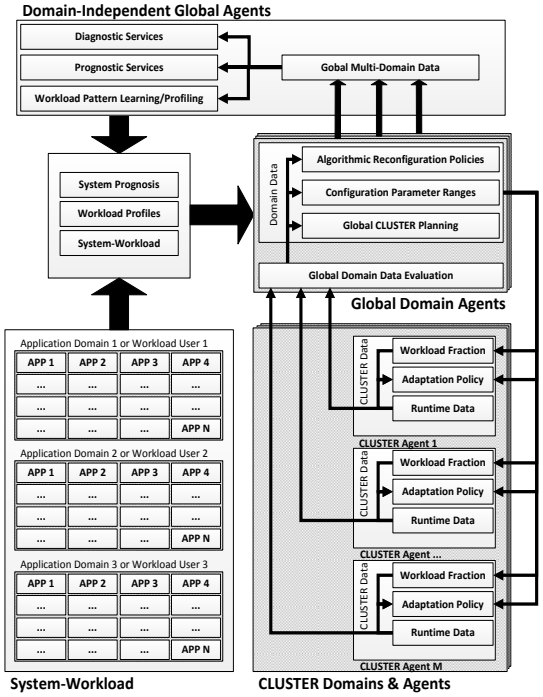

Figure 3. Global software-agent hierarchy in RedNoCs

B. System-NoC Design and Optimization

The System-NoC necessitates the integration of additional hardware resources. The System-NoC topology is fully redundant to the Data-NoC, because the support of multi-objective flows needs a general connectivity that covers the potential resource interactions. This design strategy will increase the benefit-cost-ratio. As entry-point for the dimensioning of the System-NoC the minimal data width for the link is adjusted. Furthermore, this parameter defines the number of parallel transmitted data-bits per flit, the sizing of the router node and the number of wires per link direction. In the utilized XY/YX-Routing the header flit contains the complete position [x, y] of the destination CELL as bit-vector and one additional bit for the path selection (XY | YX). Inside a $N_X \times N_Y$ 2D-Mesh NoC the number of addressable CELLs is given by (1) as well as the number of CELLs in a rectangular CLUSTER *Ci*.

$$N_{CELLS}^{noc} = N_X \cdot N_Y \;;\; N_{CELLS}^{Ci} = N_X^i \cdot N_Y^i \leq N_{CELLS}^{C\max} \quad (1)$$

Thus, the minimal link data width in bit needs to be at least $ldw_{\min}$ as formulated in (2).

$$ldw_{\min} = \log_2\left(N_{CELLS}^{noc}\right) + 1 \quad (2)$$

Additional wiring per link direction will be needed by the hop-based REQ/ACK flow control (2-bit/wires) and the flit identifier (2-bit to mark as header '11', payload '01' or tail '00'). Thus, the final link width per direction as number of bit/wires can be obtained from (3).

$$lw_{\min} = ldw_{\min} + 4 \quad (3)$$

Exemplary, for a 4×4/8×8/16×16 NoC the minimal link data width would be 5/7/9-bit per flit and per link direction 9/11/13 additional wires are needed. The XY/YX-Routing was chosen to support a balanced link utilization over system lifetime and the XY or YX path option will be toggled globally if the System-NoC has no load (e.g. power-on state). The System-NoC packets consist of static and context-based data. The static parts contain the routing information and context identification {DST|SRC|CTX-ID}. The header flit carries the packet destination (DST) and the second flit transports the source node address (SRC) of the packet. These flits will be followed by the context identifier, which needs 8-bit. The additional bits needed for the context data ($n_{CTX\text{-}DATA}$) will complete the packet to its final length (4) (in number of flit). The optimal per-hop-latency of the packet header (without congestions) for the targeted System-NoC design is 3 clock cycles (REQ/ACK-handshaking and routing/arbitration delay).

$$l_{packet} = \left\lceil \frac{2 \cdot ldw_{\min} + n_{CTX-DATA} + 8}{ldw} \right\rceil \; ; \; ldw \geq ldw_{\min} \quad (4)$$

A resource/IP core allows the consumption of one flit in a period of two clock cycles (REQ/ACK) through its network interface. Generally, we can define the reception rate (RR) per IP core as the ratio of received flits to the observed time period in clock cycles and the injection rate (IR) as the ratio of injected flits to the observed time period in clock cycles (see eq. (5)).

$$RR = \frac{sum_{flit}^{in}}{sum_{clock\ cycles}^{period}} \leq 0.5 \; ; \; IR = \frac{sum_{flit}^{out}}{sum_{clock\ cycles}^{period}} \leq 0.5 \quad (5)$$

The typical traffic pattern inside the System-NoC and its CLUSTERs partially varies from those inside the Data-NoC. For centralized managed CLUSTER the traffic flow will be N_S:1 and 1: N_S. The N_S:1 pattern implies that the Master-CELL of a CLUSTER is the hotspot and all Slave-CELLs (N_S) transmit data to it. This pattern is typical for monitoring tasks. On the other hand, the Master-CELL needs to reconfigure the Slave-CELLs or other runtime mechanisms, which comply with the 1: N_S traffic pattern. Another traffic category is the non-centralized/distributed one from Node-to-Node (N2N). This fraction of System-NoC traffic typically correlates with the traffic pattern of the Data-NoC and concerns distributed mechanisms like flow-control or error management. The standard configuration of the System-NoC, implementing the above mentioned requirements, is called FULL. To optimize the System-NoC design regarding area consumption and/or data-throughput three major strategies can be applied as follows:

QUADRANT REDUCTION: The additional wiring of the System-NoC and the router area are mainly defined by the $ldw_{\min}$ parameter. Thus, a smaller $ldw_{\min}$ would reduce the additional hardware costs, but also increases the needed packet length (4). Resizing $ldw_{\min}$ can be realized via address-space reduction. The address-space-reduction targets the minimization of the coordinate data width. Therefore, the NoC will be divided into quadrants (see Figure 2 (b)) and inside a quadrant each CELL will be addressable directly via a single header flit. If the communication range of a packet exceeds a quadrant, the routing information consists of intermediate header flits ('10') and a final header flit ('11'). The intermediate header flits are needed to pass quadrants that does not contain the final packet destination. Thus, the routing path will be segmented and each time the packet crosses a quadrant border (QB in Figure 2 (b)) the corresponding intermediate header flit can be dropped. The link data width can be reduced by 2-bit (see eq. (6)) and the additional delay correlates to the number of intermediate header (≤ 2).

$$ldw_{\min} = \log_2\left(N_{CELLS}^{quadrante}\right) + 1 \; ; \; N_{CELLS}^{quadrante} = \frac{N_{CELLS}^{noc}}{4} \quad (6)$$

The System-NoC configuration with applied quadrant reduction is called REDUCED.

DUAL-PORTED MASTER: The N_S:1 traffic pattern inside a CLUSTER results in a bottleneck at the SNI of the Master-CELL, because the RR of the SNI limits the number of packets that can be injected by the Slave-CELLs. If the number of injected packets exceeds the number of receivable packets the System-NoC becomes congested. Thus, the formulated condition of (7) restricts the maximal monitoring traffic. The maximal reception rate of the Master-CELL can be doubled by the integration of a second port at the router that is connected to the SNI. Incoming packets at the router node will be randomly assigned to the first or the second core-port. The additional hardware is restricted to the number of potential Master-CELLS ($\leq$ 50% of all CELLs).

$$RR_{Master}^{\max} \geq \sum_{i=1}^{N_{CELLS}^{Cl}} IR_{Slave\ i}^{\max} \quad (7)$$

PATTERN SEPARATION: The interferences of concurrent traffic pattern can be reduced by the integration of two virtual channels (VC) [1][2][3]. Thus, the N_S:1 and 1:N_S pattern will share one VC, while the N2N pattern utilizes a different VC. The concurrency of coexisting N_S:1 patterns depends on the placement of the Master-CELLs. If they are nearby to each other the interference of traffic flows will be high. This can be circumvented by symmetric placements as given in the 4x4 CLUSTER example of Figure 2 (b). The traffic monitor (TRAFFIC) is mapped to the Master-CELL [0,0], while the thermal monitor (THERMAL) runs on Master-CELL [3,3]. Regarding the

 ISBN: 978-1-61208-246-2

bidirectional links, both traffic flows from all Slave-CELLs to these two hotspots will be independent. Thus, the resulting minimal interference allows the sharing of a single VC. N2N pattern will be more variable in timing and the distribution of source-destination-pairings. Hence, this traffic load will be assigned to the second VC.

C. Monitoring

The availability of current system state information is indispensable for runtime-based application mapping [25][26][27][28][29], power management [6][9][30] and adaptive routing [11][31][32][33][34] in communication-centric complex MPSoC. Therefore, RedNoCs integrates runtime configurable and cluster-based solutions for thermal and traffic monitoring. The dynamic clustering enforces full application/regional isolation [11][14][32][33]. Thus, the monitored data is associated exclusively to the workload fraction inside the CLUSTER and the sampling periods/timing can be configured at runtime under consideration of the current load.

1) Traffic Monitoring

The traffic monitoring of RedNoCs integrates a periodic and centralized mechanism that is hierarchical organized at three different levels (PATH/LINK, CELL, and CLUSTER).

PATH/LINK-LEVEL: The basic traffic sensor is a simple combination of an external triggered binary counter and a configurable comparator (see Figure 4). The counter increments each clock cycle the ENABLE signal is active. In parallel the comparator checks the current counter value against a reference value that is set by the T-MODE. The supported T-MODEs of the presented RedNoCs traffic monitoring can be obtained from Figure 4. If the counter value reaches the configured T-MODE reference, it sets an overflow flag (OFG) that is captured by the register R and external resettable. This unified solution is used in two different ways: (1) *LINK LOAD:* Each output port of a Data-NoC routing node (e.g. North, East, South, West, and Core at 2D-Mesh topology) is connected to a traffic sensor to measure the current link load (LL). The ENABLE signal is connected to the status signal of the port output arbitration unit. The total number of traffic sensors will be 5 per CELL. (2) *INJECTION RATE:* Selected path table entries (DST-ID) of the DNI at each CELL gets a traffic sensor assigned to cover the injection rates at the path level. The assignment of DST-ID to specific application tasks is performed by the mapping algorithm and will be set during the cluster creation. Furthermore, one traffic sensor captures the overall injected traffic. The ENABLE input is connected to the acknowledgment signal (ACK) of the DNI output. The number of needed traffic sensors depends on the maximum sizing of a CLUSTER the monitoring should work path-accurate for. At the current progress, RedNoCs works with 16 path sensors (e.g. 4x4 or 8x2 CLUSTER).

All traffic sensors of a CELL run at the same T-MODE, which is set at the SNI-Manager-Extension by the Master of the corresponding traffic monitoring CLUSTER (Figure 2 (a)). Furthermore, they are grouped and located at the SNI of the CELL (see Figure 5).

CELL-LEVEL: The OFG registers of all traffic sensors inside a CELL are connected to the SNI-Manager-Extension responsible for the RedNoCs Traffic Monitoring (see Figure 5). This functional unit generates the traffic monitoring packets for the System-NoC and works periodically. Thereby, the period (TIMER) is set by the T-MODE value (same as for traffic sensors) of the CELL. For a Data-NoC running on 1 GHz, the traffic situation for each CELL is sampled in intervals configurable from 64 up to 2048 ns. After the expiration of a period, the finite state machine (FSM) tests if at least one OFG is set (OFG-CHECK) all register will be read out and reset at the traffic sensors. If no OFG is active there is no need to generate a traffic monitoring event packet for the expired period. Otherwise the FSM generates a new packet with a defined static order of the OFG-bits (CTX-DATA). The packet destination is the Master-CELL of the corresponding traffic monitoring CLUSTER. Afterwards, the packet is pushed to the output buffer at the SNI of the CELL.

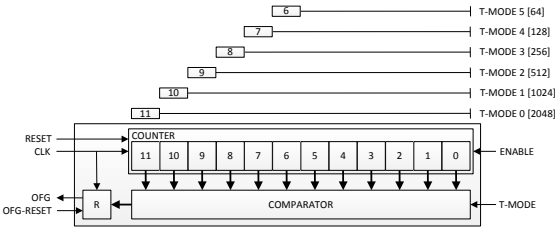

Figure 4. Basic runtime configurable Traffic Sensor of RedNoCs

CLUSTER-LEVEL: At this point, the traffic monitoring packets periodically leaves the CELLs and need to be aggregated by the Master-CELL, after they have passed the System-NoC towards it. Therefore, special Event Aggregation Points (EAPs) are present as exclusive hardware at all Master-CELLs (Figure 6 and Figure 2 (a)). These EAPS are needed to scale the generated OFG data to the final parameter of injection rate (IR) and link load (LL). IR as well as LL will be mapped to scales from 0 up to 100 percent with k_S percentage stepping. Thus, the aggregation for the events of $100/k_S$ traffic monitoring periods is needed. Each period event of a traffic sensor with a reported OFG of '1' represents k_S scale percent of IR or LL. This is done using grouped binary 7-bit counters, where each group is assigned to a monitored CELL of the CLUSTER and each counter inside a group is assigned to the OFG of a specific traffic sensor of this CELL. The counters are triggered by the incoming OFG-DATA and are incremented by one if the corresponding OFG-Bit is '1'. The OFG-DATA is fed as fix-ordered parallel bit-vector into the counter group, where the index of each bit corresponds to the traffic sensor identifier. The groups are addressed by the GROUP ID, which is equal to the CELL-ID. The EAP has a buffer at the input and can process the complete OFG-DATA of a traffic

 ISBN: 978-1-61208-246-2

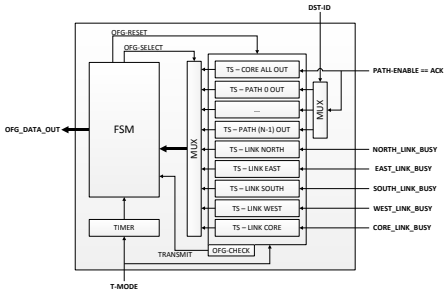

Figure 5. SNI-Manager-Extension for RedNoCs traffic monitoring

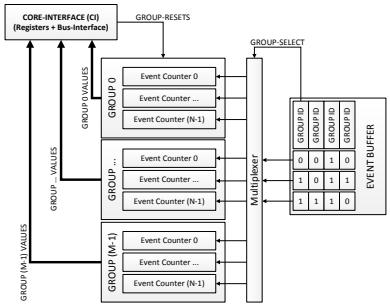

Figure 6. Functional blocks of an Event Aggregation Point

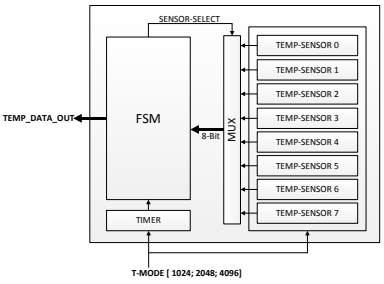

Figure 7. SNI-Manager-Extension for RedNoCs thermal monitoring

monitoring packet in one clock cycle. At the current status of research, a maximal CLUSTER size of 16 CELLS with 21 traffic sensors (5 links/15 paths/1 overall) per CELL was applied. This results in 16 groups with 21 binary 7-Bit counters at each. Moreover, the EAP represents the HW/SW-Interface of the traffic monitoring and the final traffic data can be accessed through the CORE-INTERFACE (CI) that is directly coupled to the internal bus of the Master. The counter values are captured by registers at the CI and the cluster agent will access and store them after a monitoring period has finished or during a current period. The duration of a period can be calculated by eq. (8) and depends on the configured T-MODE period ($r_{T\text{-}MODE}$), the clock frequency of the System-NoC ($f_{System\text{-}NoC}$) and the scale resolution k_S (e.g. k_S =1% or 2%).

$$t_{period}^{Ci} = \frac{r_{T-MODE}}{f_{System-NoC} \cdot k_S} \quad (8)$$

In example, for a T-MODE of 256 clock cycles at 1GHz the complete path accurate traffic situation of the CLUSTER *Ci* can be capture in periods of 25,6 µs (k_S =1%) or 12,8 µs (k_S =2%). Afterwards, the counter needs to be reset for the next period. Furthermore, the variation of the traffic situation can be recorded by intermediate snapshots during a period without reset. The EAP and the CI are key components to achieve a light-weighted software agent, because the agent is operating on final parameter values and does not need to perform further aggregation steps. Regarding the CLUSTER sizing under consideration of a specified T-MODE the formula of (9) can be deduced from (7) and (4). Thereby, the interference factor k_i reduces the allowed cluster sizing depending on the traffic situation in the System-NoC.

$$N_{CELL}^{Ci\,\max} \leq \left\lfloor \frac{RR_{master}^{\max} \cdot l_{packet}}{r_{T-MODE}} \cdot k_i \right\rfloor \quad with \quad 0 < k_i \leq 1 \quad (9)$$

2) Thermal Monitoring

The integrated thermal monitoring of RedNoCs is a modification of the solution presented in [9]. Each CELL is suited with 8 temperature sensors that offer measured temperature as 8-bit data values. Thus, 64-bit CTX-DATA will be reported by each thermal monitoring packet. These sensors are connected to a special SNI-Management-Extension (see Figure 7) and will be read out periodically (configured by T-MODE). The T-MODE controls a TIMER and RedNoCs works will periods of 1024, 2048 and 4096 clock cycles to enable different temperature resolutions. If the current period is finished, the FSM reads out all temperature sensors (cycle by cycle), generates the monitoring packet and sends it through the System-NoC towards the Master-CELL of the CLUSTER. The software agent at the Master-CELL is able to consume the temperature data directly without further aggregation. The software agent collects these data until all temperature sensors reported its values for the current observation cycle. Afterwards, the new observation cycle starts. The maximal CLUSTER sizing can be calculated by (9).

D. System Control

The system control features of the RedNoCs solution targets the utilization of the collected monitoring information at different system-levels (outlined in Figure 3) as well as the reuse of the EAPs. The workload-specific collection of thermal and traffic load data enables the integration of: (1) *Runtime-based selection of dedicated routing algorithms* [35][36] *and/or application mapping strategies* [25] *for different workloads and optimization scenarios* (Algorithm Reconfiguration/Adapdation at Figure 1/3). Moreover, depending on the current and historic workload, the optimization objectives can vary between wear-out minimization, performance/delay or energy consumption (Diagnostic/Prognostic Services at Figure 1/3). Thus, different parameter will be aggregated and combined with dedicated strategy selection policies. (2) *Active Workload/Traffic-Pattern learning at runtime*. This reduces the need of preliminary offline-profiling and data collection as used in [35][36][25]. The attributes of nodes and edges in an application task graphs (like computational costs and traffic injection rates) and their final mappings [4] will be collected/refined during system operation.

Another important system management feature is the observation of task execution [35] to measure application performance or register erroneous interrupts. Therefore, the unused EAPs at the Master-CELLs will be reused. Selected tasks generate events or different types of events, when they process their computation on the IP cores. These events are encoded as special bit-vectors to trigger dedicated counter of an EAP counter group (similar to traffic monitoring). The GROUP-ID and counter assignment is performed by the

 ISBN: 978-1-61208-246-2

TABLE I. SIMULATION RESULTS FOR REDNOCS CORNER-CASES WITH BEST ACHIEVABLE PARAMETER CONFIGURATIONS (APL: # OF CLOCK CYCLES ; MANAGER: # OF CLOCK CYCLES ; CBW: MBIT/S)

		Parameter Configuration				Average Packet Latencies (APL)									
		N2N IR		TSP		TRAFFIC		TEMP		N2N		MANAGER		CBW	
Design	**Pattern**	*4x4*	*8x2*	*4x4*	*8x2*	*4x4*	*8x2*	*4x4*	*8x2*	*4x4*	*8x2*	*4x4*	*8x2*	*4x4*	*8x2*
FULL	hotspot	0.025	0.025	256	512	109.2	117.1	234.1	233.9	122.9	84.9	910	1556	357.4	275.3
	uniform	0.025	0.05	256	512	112.6	113.9	238.3	236.5	85.6	91.3	629	913	357.4	511.2
	bit comp	0.025	0.05	256	512	111.1	114.9	237.2	236.8	79.5	93.9	640	980	357.4	511.2
	transpose	0.025	0.05	256	512	110.1	115.3	237.2	237.2	76.4	95.9	633	935	357.4	511.2
FULL DP	**hotspot**	**0.025**	**0.025**	**256**	**512**	**89.1**	**83.4**	**167.7**	**133.1**	**69.5**	**45.9**	**1000**	**1003**	**357.4**	**275.3**
	uniform	**0.05**	**0.025**	**256**	**256**	**93.8**	**74.7**	**172.2**	**140.4**	**69.4**	**41.8**	**576**	**795**	**593.2**	**357.4**
	bit comp	**0.05**	**0.025**	**256**	**256**	**92.1**	**74.2**	**171.8**	**140.1**	**60.3**	**40.9**	**610**	**767**	**593.2**	**357.4**
	transpose	**0.05**	**0.025**	**256**	**256**	**92.6**	**73.6**	**173.7**	**140.5**	**66.8**	**40.8**	**610**	**779**	**593.2**	**357.4**
FULL 2 VC	hotspot	0.025	0.025	256	512	119.5	127.9	235.1	234.1	**62.9**	**53.4**	668	544	357.4	275.3
	uniform	0.025	0.05	256	512	113.9	120.9	260.7	297.5	**23.7**	**30.1**	658	577	357.4	511.2
	bit comp	0.025	0.05	256	512	114.1	121.5	260.3	296.4	**23.9**	**29.9**	683	589	357.4	511.2
	transpose	0.025	0.05	256	512	115.6	118.9	259.8	297.9	**24.2**	**29.9**	688	578	357.4	511.2
REDUCED DP	hotspot	0.025	0.025	512	512	102.7	94.1	209.3	164.1	66.7	56.7	785	1100	209.1	209.1
	uniform	0.05	0.05	512	512	106.8	89.7	214.2	185.4	57.5	55.6	662	918	373.1	373.1
	bit comp	0.05	0.05	512	512	105.6	89.3	214.3	184.8	57.3	56.6	695	1262	373.1	373.1
	transpose	0.05	0.05	512	512	105.9	90.4	214.9	184.1	58.1	56.3	694	1183	373.1	373.1

software agent responsible for the execution monitoring. After the event generation a packet towards the EAP is send out and the EAP counters will be adjusted according to the event data. The software agent regularly captures the counter values and controls the operation progress of the workload. Thus, if tasks do not generate events a problem might be occurred or the performance is not as expected. Further, measuring the progress in periodic intervals allows the evaluation of application performance and gives additional feedback to the selection strategies of routing and mapping algorithms.

IV. EXPERIMENTAL RESULTS

The evaluation of the RedNoCs solution was realized via system simulations for operational performance and hardware synthesis for the cost approximation. Thereby, the basic System-NoC design parameter configuration can be obtained from TABLE II.

TABLE II. SYSTEM-NOC CONFIGURATION FOR SIMULATION AND SYNTHESIS

Parameter	Value
Clock Rate	1 ns
Topology	2D-Mesh
NoC-Size	8x8
Cluster Size	4x4, 8x2
Input Buffer Depth	1 Flit
# of Master-CELLs	32 (=50%)
Traffic Sensors per CELL	21
7-Bit Counter per EAP	336
N2N Injection Rates	0.025 up to 0.05
N2N Traffic Pattern	random uniform distributed, transpose, hotspot (H=20%) and bit complement

A. System Simulations

The first evaluation step was the corner-case simulations of the maximum CLUSTER size (16 CELLs) at different shapes (4x4 and 8x2) and workloads. Therefore, an own cycle accurate SystemC/TLM-based simulator was used. For different CLUSTER shapes and System-NoC designs the simulated workloads contained a traffic monitoring cluster, thermal monitoring cluster and synthetic traffic patterns for the N2N traffic component. Those three CLUSTERs ran in parallel with full spatial coverage. The placement of the Master-CELL for thermal monitoring was the upper right corner and the Master-CELL of the traffic monitoring was assigned to the lower left corner (see Figure 2 (b)). The configured T-MODE for the thermal monitoring period (TMP) was fixed to 2048 clock cycles. This results in a 30% higher sampling rate than used in the reference of [9].

The T-MODE for the traffic sampling period (TSP) was varied between 256 and 1024 clock cycles. Furthermore, the worst-case of monitoring packet injections per CELL at each sample period was simulated (without the OFG-CHECK). The N2N traffic was simulated under consideration of the random uniform, bit complement, transpose and hotspot pattern [1][2][3]. Thereby, the injection rate (N2N IR) was varied between 0.025 and 0.05 flit/clock cycle per CELL. For the simulated designs these two cases imply that each CELL generates packets with 1 up to 4 byte CTX-DATA in average intervals of 200 and 100 ns. This is more than sufficient for N2N-based transaction- and/or connection management [18][24]. The hotspot pattern furthermore covers the EAP reuse scenario for task observation and performance measurements. The HOTSPOT Master-CELL was placed in the upper left corner of the CLUSTER (see Figure 2 (b)) and receives a 20% fraction of the total injected N2N traffic of all CELLs inside the CLUSTER. Thus, each CELL will generate task events with an average interval of 1 µs or 0.5 µs. This worst-case assumes that all CELLs of the NoC will be active computational nodes running tasks with the periodicity of 0.5-1 µs. For the estimation of the communicational delay if the cluster agent migrates from one Master-CELL to another the cluster agents transmitted *CUP* packets to all Slave-CELL in intervals of 200 µs and the maximum packet latency (in # of clock cycles) over this complete procedure was captured (MANAGER). For the other monitoring (TRAFFIC and TEMP) and N2N traffic loads the average packet delay (in # of clock cycles) was recorded. Thereby, the packet delay is measured as timing

 ISBN: 978-1-61208-246-2

interval from the transmission buffer injection of the header flit at the source CELL to the final consumption of the tail flit at the destination CELL. The simulation results for different System-NoC designs are summarized in TABLE I. The listed parameter configurations represent traffic scenarios, where each CLUSTER achieves its timing constraints (packets arrives Master-CELL inside the adjusted sample period) and the highest achievable TSP was focused, because the information about generated and transmitted data per CELL/path/link has the highest weight as activity indicators for traffic, performance and energy management. The resulting average bandwidth utilization per CELL (CBW) per CELL for the System-NoC traffic is given in Mbit/s. The results cover the average of 100 simulation runs per parameter configuration with a system operation time of 1 second at each run. They show that the dual-ported (DP) optimization strategy for the FULL System-NoC configuration performs best in all simulated traffic cases. The average packet latency improvement of the FULL DP over the FULL design case is 23.2% at the 4x4 and 42.9% at the 8x2 CLUSTER shape, while the additional hardware overhead scales with the number of Master-CELLs. The evaluation of the pattern separation optimization (2 VC) proves the better performance of the N2N traffic, if it has its own VC (average latency improvement ~62.5%). But the latencies of the remaining traffic domains will increase because of the bandwidth reduction introduced with the utilization of VCs and the additional hardware costs depends on the number CELLs. Furthermore, the simulations showed up that the packets of the traffic monitoring domain were the first which ran out of their latency constraints and thus the most vulnerable regarding interferences.

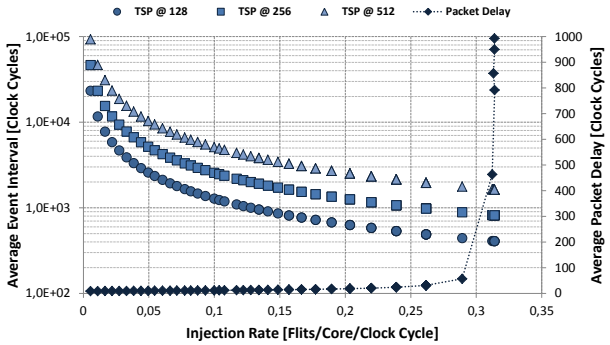

Figure 8. Real traffic monitoring packet injection intervals for varying Data-NoC traffic loads and active OFG-CHECK

To evaluate the traffic reduction caused by the OFG-CHECK a complete 8x8 Data-NoC was simulated under different traffic loads and patterns. The adjusted T-MODEs were 128, 256 and 512 clock cycles. The diagram of Figure 8 shows that the average event interval for the monitoring packet generation by the CELLs is at least three times greater than the adjusted period. In the unsaturated operational region of the Data-NoC (IR < 0.3) the difference is even higher. Thus, the results of TABLE I correlate to the worst-case and demonstrate that real system operation metric will become even better. For the REDUCED design case only the Dual-Ported results are presented in TABLE I. The increased packet lengths, regarding the lower link data width, of the REDUCED designs influence the traffic situation and omit to reach the same performance as observed for the FULL design cases. Thereby, the degradation in achievable sample rates for monitoring will be even higher than the minimization of the System-NoC hardware overhead. The captured overall delay for MANAGER communication of the cluster agents show that reconfiguration or changes of the CLUSTER will take effect after hundreds of clock cycles. In the observed case the needed time would be approximately 0.5 µs up to 1 µs, which is low enough to provide dynamical adaptations for workloads that may change/vary in the order of hundreds of µs up to a few ms.

B. *Hardware Synthesis*

The ASIC design flow was realized with the Synopsys™ DesignCompiler™ using the 45 nm Nangate FreePDK45 Generic Open Cell Library. The presented results in TABLE III show the total cell area (TCA) costs for each of the functional RedNoCs components (SNI-Manager Extensions, Traffic Sensors, EAP) for REDUCED and FULL design.

TABLE III. TOTAL CELL AREA (TCA) HARDWARE COSTS FOR FUNCTIONAL REDNOCS COMPONENTS INSIDE AN 8X8 NOC AT ALL

	TCA [8x8 NoC] [mm²]	
Design Component	*REDUCED*	*FULL*
SNI TEMPERATURE EXT.	0.05311488	0.05452736
SNI TRAFFIC LOAD EXT.	0.06155904	0.09676416
TRAFFIC SENSORS	0.17410176	0.17410176
AGGREGATION POINT	0.71138176	0.71138176
SUM OF ALL UNITS	**1.00015744**	**1.03677504**

TABLE IV contains the hardware costs for the System-NoC routers (TCA) and the complete RedNoCs designs (TCA ALL). The targeted operational frequency was set to 1 GHz and met for all evaluated design cases.

TABLE IV.TOTAL CELL AREA (TCA) HARDWARE COSTS FOR ROUTER UNITS OF AN 8X8 SYSTEM-NOC AND ALL UNITS OF REDNOCS (TCA ALL)

Design	TCA [mm²]	TCA ALL [mm²]	Linkwidth *lw*
FULL	0.17815616	1.2149312	11
FULL DP	**0.19422688**	**1.2310019**	**11**
FULL 2 VC	0.39875328	1.4355283	11
REDUCED DP	0.18442976	1.1845872	9

The main hardware overhead of RedNoCs belongs to the EAPs (>50%) and relativizes the potential savings of the REDUCED design (~3.8% compared to FULL DP). These costs can be reduced if the number of Master-CELLs decreases. Furthermore, the comparison of FULL DP against the FULL design proves the benefits of this optimization strategy. The hardware costs will be only ~1.3% higher, while the operational performance improves by ~23.2% at least. Regarding the hardware costs in the context of the final MPSoC that contain the targeted amount of CELLs on a 45nm silicon die (areas: 280-400 mm² [36][37]) the relative overhead due to RedNoCs will be less than ~2%.

 ISBN: 978-1-61208-246-2

V. CONCLUSION AND FUTURE WORK

The evaluation results show that the presented RedNoCs concept is applicable and supports the integration of multi-objective system management flows at runtime under consideration of affordable costs. Furthermore, the dual-ported optimization strategy was purposed and showed up good performance improvements. The next steps of future investigations target the full integration of adaptive routing and application mapping mechanisms in combination with RedNoCs. Especially, the runtime-based workload pattern learning, prognostic services for long-term reliability improvements, and the scalability analysis of the software agents will be evaluated for scenarios of different application domains.

REFERENCES

[1] E. Salminen, A. Kulmala, and T. D. Hämäläinen, "Survey of Network-on-chip Proposals," *WHITE PAPER, OCP-IP, MARCH*, no. March, pp. 1–12, 2008.

[2] A. Agarwal, C. Iskander, H. T. Multisystems, and R. Shankar, "Survey of Network on Chip (NoC) Architectures and Contributions," *scientificjournals.org*, vol. 3, no. 1, 2009.

[3] T. Bjerregaard and S. Mahadevan, "A survey of research and practices of network-on-chip," *ACM Computing Surveys (CSUR)*, vol. 38, no. 1, p. 1, 2006.

[4] R. Marculescu, U. Y. Ogras, L.-S. Peh, N. E. Jerger, and Y. Hoskote, "Outstanding Research Problems in NoC Design: System, Microarchitecture, and Circuit Perspectives," *IEEE Transactions on Computer-Aided Design of Integrated Circuits and Systems*, vol. 28, no. 1, pp. 3–21, Jan. 2009.

[5] U. Y. Ogras, J. Hu, and R. Marculescu, "Key research problems in NoC design: a holistic perspective," *Proceedings of the 3rd IEEE/ACM/IFIP international conference on Hardware/software codesign and system synthesis*, pp. 69–74, 2005.

[6] L. Guang, E. Nigussie, J. Isoaho, P. Rantala, and H. Tenhunen, "Interconnection alternatives for hierarchical monitoring communication in parallel SoCs," *Microprocessors and Microsystems*, vol. 34, no. 5, pp. 118–128, Aug. 2010.

[7] L. Guang, P. Rantala, E. Nigussie, J. Isoaho, and H. Tenhunen, "Low-latency and Energy-efficient Monitoring Interconnect for Hierarchical-agent-monitored NoCs," *2008 Norchip*, pp. 227–232, Nov. 2008.

[8] C. Ciordas, K. Goossens, A. Radulescu, and T. Basten, "NoC Monitoring: Impact on the Design Flow," in *2006 IEEE International Symposium on Circuits and Systems*, 2006, pp. 1981–1984.

[9] J. Zhao, S. Madduri, R. Vadlamani, W. Burleson, and R. Tessier, "A Dedicated Monitoring Infrastructure for Multicore Processors," *IEEE Transactions on Very Large Scale Integration (VLSI) Systems*, vol. 19, no. 6, pp. 1011–1022, Jun. 2011.

[10] M. Ebrahimi, M. Daneshtalab, P. Liljeberg, J. Plosila, and H. Tenhunen, "LEAR -- A Low-Weight and Highly Adaptive Routing Method for Distributing Congestions in On-chip Networks," in *2012 20th Euromicro International Conference on Parallel, Distributed and Network-based Processing*, 2012, vol. 1, pp. 520–524.

[11] M. Ebrahimi, M. Daneshtalab, P. Liljeberg, and J. Plosila, "CATRA-Congestion Aware Trapezoid-based Routing Algorithm for On-Chip Networks," in *Design, Automation & Test in Europe Conference & Exhibition (DATE'12)*, 2012, pp. 320 – 325.

[12] V. Rantala, T. Lehtonen, P. Liljeberg, and J. Plosila, "Distributed Traffic Monitoring Methods for Adaptive Network-on-Chip," in *2008 NORCHIP*, 2008, pp. 233–236.

[13] P. Gratz, B. Grot, and S. W. Keckler, "Regional congestion awareness for load balance in networks-on-chip," *2008 IEEE 14th International Symposium on High Performance Computer Architecture*, pp. 203–214, Feb. 2008.

[14] S. Ma, N. Enright Jerger, and Z. Wang, "DBAR: An Efficient Routing Algorithm to Support Multiple Concurrent Applications in Networks-on-Chip," in *Proceeding of the 38th annual international symposium on Computer architecture - ISCA '11*, 2011, p. 413.

[15] R. Manevich, I. Cidon, A. Kolodny, I. Walter, and S. Wimer, "A Cost Effective Centralized Adaptive Routing for Networks-on-Chip," *2011 14th Euromicro Conference on Digital System Design*, vol. 9, no. 2, pp. 39–46, Aug. 2011.

[16] M. A. Al Faruque, T. Ebi, and J. Henkel, "ROAdNoC: Runtime observability for an adaptive network on chip architecture," *2008 IEEE/ACM International Conference on Computer-Aided Design*, pp. 543–548, Nov. 2008.

[17] M. A. Al Faruque, T. Ebi, and J. Henkel, "AdNoC: Runtime Adaptive Network-on-Chip Architecture," *IEEE Transactions on Very Large Scale Integration (VLSI) Systems*, vol. 20, no. 2, pp. 257–269, Feb. 2012.

[18] M. Fattah, M. Daneshtalab, P. Liljeberg, and J. Plosila, "Exploration of MPSoC monitoring and management systems," in *6th International Workshop on Reconfigurable Communication-Centric Systems-on-Chip (ReCoSoC)*, 2011, pp. 1–3.

[19] L. Guang, A. W. Yin, P. Rantala, P. Liljeberg, J. Isoaho, and H. Tenhunen, "Hierarchical Power Monitoring for On-chip Networks." Turku, Finland, pp. 2–3, 2009.

[20] A. W. Yin, L. Guang, P. Rantala, P. Liljeberg, J. Isoaho, and H. Tenhunen, "Hierarchical Agent Monitoring NoCs: A Design Methodology with Scalability and Variability," *2008 Norchip*, pp. 202–207, Nov. 2008.

[21] C. Ciordas, T. Basten, A. Radulescu, K. Goossens, and J. Meerbergen, "An event-based network-on-chip monitoring service," in *Proceedings. Ninth IEEE International High-Level Design Validation and Test Workshop (IEEE Cat. No.04EX940)*, 2004, pp. 149–154.

[22] C. Ciordas, K. Goossens, T. Basten, A. Radulescu, and A. Boon, "Transaction Monitoring in Networks on Chip: The On-Chip Run-Time Perspective," in *2006 International Symposium on Industrial Embedded Systems*, 2006, pp. 1–10.

[23] H. Yi, S. Park, and S. Kundu, "A Design-for-Debug (DfD) for NoC-Based SoC Debugging via NoC," *2008 17th Asian Test Symposium*, pp. 289–294, Nov. 2008.

[24] B. Vermeulen and K. Goossens, "A Network-on-Chip monitoring infrastructure for communication-centric debug of embedded multi-processor SoCs," in *2009 International Symposium on VLSI Design, Automation and Test*, 2009, pp. 183–186.

[25] E. Carvalho, C. Marcon, N. Calazans, and F. Moraes, "Evaluation of Static and Dynamic Task Mapping Algorithms in NoC-Based MPSoCs," *inf.pucrs.br*, pp. 4–7, 2009.

[26] E. Carvalho, N. Calazans, and F. Moraes, "Heuristics for Dynamic Task Mapping in NoC-based Heterogeneous MPSoCs," in *18th IEEE/IFIP International Workshop on Rapid System Prototyping (RSP '07)*, 2007, pp. 34–40.

[27] E. Carvalho and F. Moraes, "Congestion-aware task mapping in heterogeneous MPSoCs," *2008 International Symposium on System-on-Chip*, pp. 1–4, Nov. 2008.

[28] C.-L. Chou and R. Marculescu, "Run-Time Task Allocation Considering User Behavior in Embedded Multiprocessor Networks-on-Chip," *IEEE Transactions on Computer-Aided Design of Integrated Circuits and Systems*, vol. 29, no. 1, pp. 78–91, Jan. 2010.

[29] Y. Cui, W. Zhang, and H. Yu, "Decentralized agent based re-clustering for task mapping of tera-scale network-on-chip system," in *2012 IEEE International Symposium on Circuits and Systems*, 2012, pp. 2437–2440.

[30] J. Plosila, K. Latif, and H. Tenhunen, "Hierarchical power monitoring on NoC - a case study for hierarchical agent monitoring design approach," in *NORCHIP 2010*, 2010, pp. 1–6.

[31] E. a. Carara and F. G. Moraes, "Flow oriented routing for NOCS," *23rd IEEE International SOC Conference*, pp. 367–370, Sep. 2010.

[32] M. Palesi, S. Kumar, and V. Catania, "Bandwidth-aware routing algorithms for networks-on-chip platforms," *IET Computers & Digital Techniques*, vol. 3, no. 5, p. 413, 2009.

[33] M. Palesi, R. Holsmark, S. Kumar, and V. Catania, "Application Specific Routing Algorithms for Networks on Chip," *IEEE Transactions on Parallel and Distributed Systems*, vol. 20, no. 3, pp. 316–330, Mar. 2009.

[34] R. Manevich, I. Cidon, A. Kolodny, and I. Walter, "Centralized Adaptive Routing for NoCs," *IEEE Computer Architecture Letters*, vol. 9, no. 2, pp. 57–60, Feb. 2010.

[35] L. Leem, H. Cho, and J. Bau, "ERSA: error resilient system architecture for probabilistic applications," in *Proceedings of the Conference on Design, Automation and Test in Europe (DATE'10)*, 2010, vol. 31, no. 4, pp. 546–558.

[36] P. Salihundam, S. Jain, and T. Jacob, "A 2 Tb/s 6× 4 mesh network for a single-chip cloud computer with DVFS in 45 nm CMOS," *IEEE Journal of Solid-State Circuits*, vol. 46, no. 4, pp. 757–766, 2011.

[37] Y. Hoskote, S. Vangal, A. Singh, N. Borkar, and S. Borkar, "A 5-GHz Mesh Interconnect for a Teraflops Processor," *IEEE Micro*, vol. 27, no. 5, pp. 51–61, Sep. 2007.

 ISBN: 978-1-61208-246-2

Interplay Between Traffic Dynamics and Network Structure

Ziping Hu, Pramode K. Verma
School of Electrical & Computer Engineering
The University of Oklahoma
Tulsa, OK 74135
{ziping.hu, pverma}@ou.edu

Krishnaiyan Thulasiraman
Department of Computer Science
The University of Oklahoma
Norman, OK 73019
thulasi@ou.edu

***Abstract*—This paper studies the interplay between traffic dynamics and network structure in complex communication networks. Complex communication networks of distinct structural features are chosen as the underlying networks. We use node betweenness centrality, network polarization, and average path length to capture the structural characteristics of a network. Network throughput and average packet delay are the main performance measures. We study how internal traffic, throughput, and delay change with increasing incoming traffic through simulation. We further investigate the relationship between network performance and network structure. Our work reveals that the parameters chosen to reflect network structure, including node betweenness centrality, network polarization, and average path length, play important roles in different states of the underlying networks.**

Keywords-Complex networks; traffic; network structure; network performance.

I. INTRODUCTION

Many social, biological, and communication systems are called complex systems. In network science, complex systems are described as networks consisting of vertices and interactions or connections among them. The study of structural and dynamical properties of complex systems has been receiving a lot of interests. One of the ultimate goals of the studies is to understand the influence of topological structures on the behaviors of various complex systems, for instance, how the structure of social networks affects the spread of diseases, information, rumors, or other things [1-3]; how the structure of a food web affects population dynamics [4-5]; how the structure of a communication network affects its robustness, reliability [6-7], and so on.

There is a wealth of literature focusing on different performance aspects of communication networks. By viewing communication networks as weighted graphs, authors in [7-9] have developed a concept called network criticality. They found that network criticality directly relates to network performance metrics such as average network utilization and average network cost. Most network centrality indices have structural significance. In [10], the authors compare different centrality indices for the measuring of nodal contribution to global network robustness. Since the discovery of power-law degree distribution of the Internet topology [11], much effort has been made on the study of scale-free (SF) networks. In [12-17], different routing strategies have been proposed in order to improve the performance of SF networks. To enhance the traffic transport efficiency of SF networks, an optimal resource allocation scheme is presented in [18]. Lattice networks are widely used, for example, in distributed parallel computation [19], distributed control [20], satellite constellations [21], and sensor networks [22]. Authors in [22] study the effect of routing on the queue distribution, and investigate the routing algorithms in lattice networks that achieve the maximum rate per node under different communication models.

In our previous work [23], we compared the latency of SF networks and random networks under different routing strategies. In order to better understand the structural influence on the performance of communication networks, in this paper, we devote ourselves to explore the relationship between network structure and network performance under dynamic input traffic. Four different types of networks are chosen as the underlying networks. They are SF networks, square lattice (SL) networks, random networks, and ring lattice (RL) networks. We use node betweenness centrality, network polarization, and average path length, to capture the structural features of different networks. Since both throughput and delay are especially important for communication networks, they are used here as main performance measures.

In the work, based on observed traffic dynamics in the networks studied, three network states are classified: traffic free flow state, moderate congestion state, and heavy congestion state. Simulation results indicate that during each different state, the structural differences among the underlying networks play important roles in network performance. Through the work, it is possible that a better comprehension of the interplay between traffic dynamics and network structure could help in designing better network structures and better routing protocols.

The paper is organized as follows. Section II presents our network model. Simulation results and analysis are provided in Section III. Section IV concludes the work.

II. NETWORK MODEL

In the paper, four different types of networks are chosen as the underlying networks. They are the SF network, the random network, the SL network, and the RL network. One of their

 ISBN: 978-1-61208-246-2

structural differences lies in their distinct nodal degree distribution. The degree of a node is the total number of links connecting it. The SF network is built based on the Barabasi-Albert (BA) model proposed in [24]. It has a power law degree distribution so that most nodes have very low degrees, but a few nodes (called hubs) could have extremely high degrees. The random network is formed according to the Erdős-Rényi (ER) model proposed in [25]. The random ER network follows Poisson degree distribution when network size is large. In the random ER network, the degrees of most nodes are around the mean degree. In the SL network, all the nodes except those located on the edge of the square have the same degree. The RL network is constructed by connecting each node on a circle to its $2m$ ($m \geq 1$) nearest neighboring nodes. Apparently, all the nodes in the RL network have the same degree.

In the paper, we use node betweenness centrality, network polarization, and average path length to capture the structural characteristics of complex communication networks. The node betweenness B_i for a node i is defined here as the total number of shortest path routes passing through that node. Nodes with high betweenness values participate in a large number of shortest paths. Therefore, initial congestion usually happens at nodes of the highest betweenness value. Node betweenness reflects the role of a node in a communication network. Normally, high betweenness nodes also have high degrees. The node betweenness distribution of a communication network is demonstrated through a measure of the polarization, π, of the network [26]. It is defined as:

$$\pi = \frac{B_{\max} - \langle B \rangle}{\langle B \rangle} \quad (1)$$

Where B_{max} is the maximum betweenness value, $<B>$ is the average betweenness value. We find that π as an indication of node betweenness distribution suits our work better than others (e.g. standard deviation). The large polarization value of a network tells us that at least one node possesses much larger betweenness values than most of the other nodes in the network. Therefore, the larger the value π is, the more heterogeneous the network is. On the other hand, for very homogeneous networks, π is very small. For example, for the RL network, we have $\pi \approx 0$. The average path length $<D>$ of a network is defined as the average of the shortest path lengths among all the source-destination pairs. We will show in the next section that the average path length directly relates to the total amount of internal traffic in the network. It also relates to average packet delay.

The above three parameters capture the structural features of a network from different angles. They are also interrelated. Usually, the more heterogeneous (larger π, or relatively higher B_{max}) the network is, the shorter the average path length $<D>$ is. The reason is that high betweenness (or degree) nodes serve as shortcuts for connecting node pairs. In addition, the following relationship between shortest path length and node betweenness centrality can be easily found,

$$\sum_{i,j} D_{ij} = \sum_{i} B_i \quad (2)$$

Where D_{ij} stands for the shortest path length from node i to node j, B_i stands for the betweenness value of node i.

The networks are treated as packet-switched networks. In these networks, fixed shortest path routing strategy is implemented. The length of the shortest path is the minimum hop count between a source-destination pair. Given network topology, each node calculates the shortest paths to all the other nodes using Dijkstra's algorithm. Then a routing table is constructed at each node. A routing table contains three columns: the destination node, next node to route a packet to the destination, and the hop count to the destination.

In the networks studied, traffic dynamic is governed by the following network model, similar to the one discussed in [27]. In the model, we assume that time is slotted. During each time slot, first, packets are generated at each node i with a rate λ_i, the destination of a packet is randomly chosen among all other nodes. Each node is endowed with a first-in-first-out (FIFO) queue in which packets are stored waiting to be processed. Then, if its queue is not empty, each node i transmits packets at a rate r_i, which represents bandwidth, to one of its neighbors according to its routing table. When a packet reaches its destination, it is absorbed by the destination node. For simplicity, for all the nodes, we assume the packet generation rate is the same or let λ_i equals to λ. We also assume r_i equals to 1, which means during each time slot, each node can process one packet.

We use throughput and average packet delay as two main performance measures. Throughput is defined as the average number of delivered packets per time slot. The average packet delay is defined as the average time that a delivered packet spent in the network. Our task is by observing traffic dynamics in different networks, to find out the relationship between network structure and network performance.

III. SIMULATION RESULTS AND ANALYSIS

In the simulation, a discrete time clock k is used. Simulation starts with $k = 0$, for each passed time slot, k is incremented by 1. The performance of a packet-switched network is measured by its throughput $o(k)$ and average packet delay $\tau(k)$.

TABLE I
NETWORK PARAMETERS

	B_{max}	$<B>$	π	$<D>$
SF network	802	127	5.32	2.59
Random ER	449	141	2.19	2.87
SL network	376	224	0.68	4.67
Ring lattice	416	325	0.28	6.63

Both $o(k)$ and $\tau(k)$ are calculated respectively as the average from the start of simulation ($k = 0$) to time k. We use $n(k)$ to represent the total number of packets within the network at time k. In the simulation, the SF network, the random ER

 ISBN: 978-1-61208-246-2

network, and the RL network are all generated with 50 nodes and 100 links. The SL network is generated with 49 nodes and 84 links because of its structural restriction. Simulation includes two parts. The first part investigates how $n(k)$ change as a function of λ and k. In this part, we observe a network phase transition from traffic free flow to congestion as reported in [27-28]. The second part investigates network performance as a function of λ. Three network states are classified accordingly. At last, we demonstrate that how, in different network states, the structure of a network influences its performance.

Table I lists the related parameters of the underlying networks. It tells us that the RL network has the longest average path length $<D>$; while the average path length of the SF network is the shortest. In addition, the RL network has the lowest polarization value π, which shows its almost homogeneous structure in terms of node betweenness distribution; while the SF network has the highest π, which demonstrates its most heterogeneous structure. The corresponding parameters of the random ER network and the SL network lie somewhere in between. One exception is that the SL network has the lowest B_{max}. In our simulation, each data obtained is averaged over 100 runs.

A. n(k) vs. λ, k

This part investigates the change of $n(k)$ as a function of λ and k in the networks studied. Simulation results are plotted in Fig.1and Fig. 2.

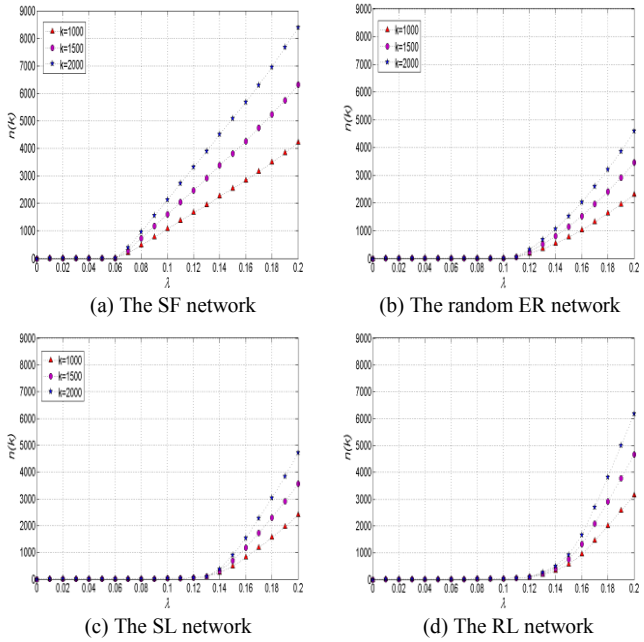

(a) The SF network (b) The random ER network

(c) The SL network (d) The RL network

Fig. 1 $n(k)$ as a function of λ (k = 1000, 1500, 2000)

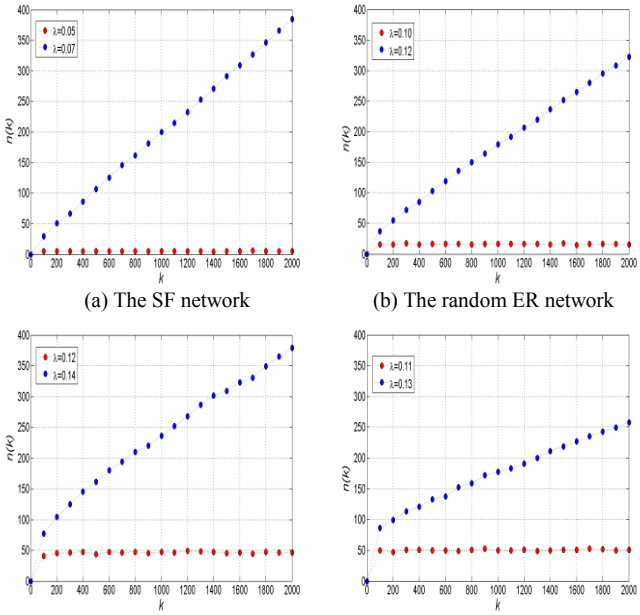

(a) The SF network (b) The random ER network

(c) The SL network (d) The RL network

Fig. 2 $n(k)$ as a function of k for subcritical and supercritical values of λ

Fig. 1 shows that all four networks display similar performance. When the incoming traffic λ increases, a critical point λ_c is observed in all these networks where a network phase transition takes place from traffic free flow to congestion. Fig. 2 presents the change of $n(k)$ as a function of time k for subcritical and supercritical values of λ. In the case of subcritical value of λ, $n(k)$ remains constant; while in the case of supercritical value of λ, we observe continuous accumulation of packets in the networks with the passing of time k.

When $\lambda < \lambda_c$, a network is in steady state or traffic free flow state. In this sate, $n(k)$ remains almost unchanged with the increase in incoming traffic λ, and/or time k. However, for different networks, $n(k)$ is proportional to the average path length of a network (shown in Fig. 2). According to Little's law, for a network of size N, the number of packets created per unit time (given by $N \times \lambda$) must be equal to the number of packets delivered per time slot. Since the number of delivered packets per time slot is $\frac{n(k)}{\tau(k)}$, hence $\frac{n(k)}{\tau(k)} = N\lambda$.

When $\lambda > \lambda_c$, the networks enter into congestion state, where $n(k)$ start increasing quickly with the increase in λ, and /or time k. From Fig. 1, we observe that compared with the other networks, the SF network has the lowest value of λ_c. The reason lies in its highest B_{max} among all the networks studied. According to the definition of node betweenness, the node with maximum betweenness value B_{max} has to handle the heaviest traffic because it participates in the largest number of shortest path routes. With increasing incoming traffic, initial congestion (or quick accumulation of packets) shall take place first at the node with B_{max}. The results conform to the theoretical analysis provided in [17].

 ISBN: 978-1-61208-246-2

B. o(k), τ(k) vs. λ

Performance comparison among the networks is shown in Fig. 3 in terms of throughput $o(k)$ and average packet delay τ(k). Based on network performance, three network states are classified: traffic free flow state, moderate congestion state, and heavy congestion state.

As stated in previous section, when $\lambda < \lambda_c$, a network is said to be in traffic free flow state. From Fig. 3 (a), we observe that in this sate, all the networks perform the same in terms of throughput (throughput increases linearly with λ.), but not so in terms of average packet delay. In traffic free flow state, from $\frac{n(k)}{\tau(k)} = N\lambda$, we obtain $\tau(k) = \frac{n(k)}{N\lambda}$. Since $n(k)$ depends on the average path length of a network, the average packet delay $\tau(k)$ also depends on the average path length $<D>$ of the network. Our simulation results show that the SF network has the lowest $\tau(k)$ because it has the shortest average path length. Therefore, in traffic free flow state, the average path length plays a major role in network performance.

When λ exceeds the critical point λ_c, congestion happens because packets start to accumulate in the network. When $\lambda > \lambda_c$, Fig. 3 (a) shows that with continuous increase in λ, the increase in throughput becomes slower. We say that a network is in moderate congestion state. With further increase in λ, if the throughput starts to decrease, we say that the network has entered into heavy congestion state.

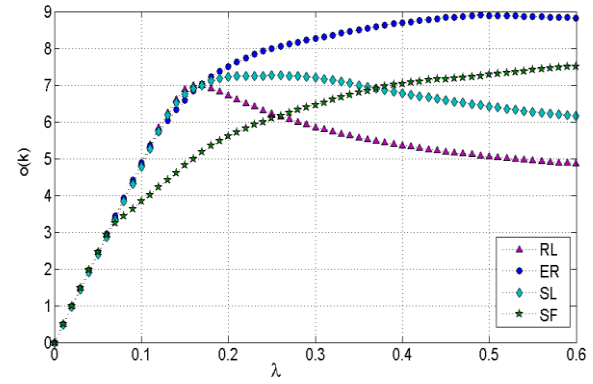

(a) $o(k)$ vs. λ

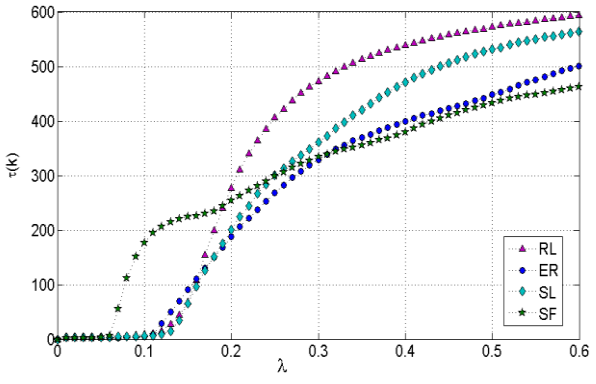

(b) $\tau(k)$ vs. λ

Fig. 3 Performance comparison among the networks (k = 2000)

From Fig. 3, we find that the SF network is the first that enters into moderate congestion state, during which the increase in throughput slows down, and its average packet delay starts to increase very quickly. Compared to the others, the performance of the SF network is the worst. The reason lies in its most heterogeneous structure (largest π). In the SF network, huge amount of packets start to accumulate at one or several nodes of extremely high betweenness values when many other nodes are idle (or do not have enough packets to send). A similar phenomenon is observed in the random ER network in moderate congestion state, but the random ER network performs much better than the scale-free network because of its much smaller polarization value π. According to the same reasoning, we find that both the RL network and the SL network achieve higher throughput and lower delay than the other two because of their much lower polarization value π. However, Fig. 3 shows that with just a little increase in λ, they quickly enter into heavy congestion state. We find that even though in moderate congestion state, congestion happens at only a few nodes, the performance of a network depends heavily on the traffic load distribution. The less the value of network polarization is, the more homogeneous (in terms of node betweenness distribution) a network is, the more balanced the traffic load is distributed; therefore, the better the network performs. For the RL and SL networks, their almost uniform node betweenness distribution results in more balanced traffic load distribution among all the nodes so that many packets are delivered successfully. Therefore, we may say that in moderate congestion state when traffic is not yet very heavy, network performance strongly relates to network polarization.

When λ increases beyond a specific value (this value is different for different networks), the networks enter into heavy congestion state. In this state, network throughput starts to decrease. For the SF network and the random network, because of their heterogeneous structure (large π), most traffic is jammed at more nodes of high betweenness values, only a small amount of traffic bypassing those congested nodes can still be delivered successfully. However, compared to the SF network, the performance of the random network is much better because the random network is relatively less heterogeneous (relatively smaller π). For the RL network and the SL network, their structures are more homogeneous. However, since the incoming traffic becomes very heavy, their very long average path length and high average betweenness value causes huge amount of internal traffic. In addition, since their node betweenness distribution is almost uniform, almost all the nodes are congested (few packets can be delivered successfully). Compared to the RL network, the SL network performs better because of its relatively shorter average path length and lower betweenness values. Therefore, in heavy congestion state, both average path length and node betweenness distribution play important roles in network performance.

The above analysis is verified by our observation on the changes in queue length (total number of packets in a queue) through simulation. In traffic free flow state (we choose λ =

 ISBN: 978-1-61208-246-2

0.05), most queues in all the networks are almost empty. In moderate congestion state (we choose $\lambda = 0.13$), most queues in the RL network contain several packets, a few queues contain several tens of packets, and the length of one queue exceeds one hundred packets. It is similar for the SL network. Most queues in the random network are almost empty, but the queues at a few nodes of high betweenness values contain hundreds of packets. Similar to the random network, most queues in the SF network are almost empty, but two queues at two nodes of extremely high betweenness values contain thousands of packets respectively. In heavy congestion state (a different λ is chosen for each network), for the RL network, the whole network is congested (most queues contain several tens of packets, a few queues contain even hundreds of packets). It is similar to the SL network. While for the random network and the SF network, more than half of the queues are still almost empty, more nodes of high betweenness values are heavily congested. Interestingly, we find that no matter what the structure of the underlying network is, congestion always takes place when a large number of packets start to accumulate at a few nodes.

IV. CONCLUSIONS

We have investigated how internal traffic, throughput, and average packet delay change as a function of incoming traffic in networks of different structures. Three network states have been classified: traffic free flow state, moderate congestion state, and heavy congestion state. Network performance has been measured and compared in terms of throughput and average packet delay. Under fixed shortest path routing, node betweenness, network polarization, and average path length all play important roles in different states of the underlying networks. In traffic free flow state, average path length plays the major role; it directly affects average packet delay. In moderate congestion state and heavy congestion state, both average path length and node betweenness distribution play important roles in network performance. Based on our investigation, an optimal network structure should have short average path length (which results in less total internal traffic), and small network polarization π (which leads to more balanced traffic load distribution).

REFERENCES

[1] Simon Cauchemez, Achuyt Bhattarai, Tiffany L. Marchbanks, Ryan P. Fagan, Stephen Ostroff, Neil M. Ferguson, David Swerdlow, and the Pennsylvania H1N1 working group, "Role of social networks in shaping disease transmission during a community outbreak of 2009 H1N1 pandemic influenza," *Proceedings of the National Academy of Sciences* 108, 2825–2830, 2011

[2] D. Wang, Z. Wen, H. Tong, C.-Y. Lin, C. Song, and A.-L. Barabasi. "Information spreading in context," *The International World Wide Web Conference*, 2011

[3] B. Doerr, M. Fouz, and T. Friedrich, "Social networks spread rumors in sublogarithmic time," *Proceedings of the 43rd ACM Symposium on Theory of* Computing (STOC'11), 21-30, 2011.

[4] Sharon P. Lawler and Peter J. Morin, "Food web architecture and population dynamics in laboratory microcosms of protists," *The American Naturalist*, Vol. 141, No. 5, 675-686, 1993.

[5] Gary A. Polis and Donald R. Strong, "Food web complexity and community dynamics," *The American Naturalist*, Vol. 147, No. 5, 813-846, 1996.

[6] Ziping Hu and Pramode K. Verma, "Improved reliability of free-space optical mesh networks through topology design," *Journal of Optical Communications and Networking*, Vol. 7, Issue 5, 436-448, 2008.

[7] Ali Tizghadam, Alberto Leon-Garcia, "Robust network planning in non uniform traffic scenarios," *Computer Communications*, *Elsevier*, 2011

[8] Ali Tizghadam, Alberto Leon-Garcia, "On traffic-aware betweenness and network criticality," *Proceedings of IEEE INFOCOM*, 2010.

[9] Ali Tizghadam, Alberto Leon-Garcia, "A graph theoretical approach to traffic engineering and network control problem," *IEEE 21st International Teletraffic Congress*, 2009

[10] T. Feyessa and M. Bikdash, "Measuring nodal contribution to global network robusness," *Proceedings of IEEE Southeastcon*, 2011.

[11] M. Faloutsos, P. Faloutsos, and C. Faloutsos, "On the power-law relationships of the Internet topology," *Computer Communication Review,* vol. 29, pp. 41-51, 1999.

[12] Zhi-Hong Guan, Long Chen, Tong-Hui Qian, "Routing in scale-free networks based on expanding betweeness centrality," *Physica A: Statistical mechanics and its applications*, Vol. 390, 1131-1138, 2011.

[13] Xiao-Gai Tang, Eric W. M. Wong, Zhi-Xi Wu, "Integrating network structure and dynamic information for better routing strategy on scale-free networks," *Physica A: Statistical mechanics and its applications*, Vol. 388, 2547-2554, 2009.

[14] Jianwei Wang, Lili Rong, Liang Zhang, "Routing strategies to enhance traffic capacity for scale-free networks," *The IEEE International Conference on Intelligent Computation Technology and Automation*, 451-455, 2008.

[15] Ming Tang, Zonghua Liu, Xiaoming Liang, and P. M. Hui, "Self-adjusting routing schemes for time-varying traffic in scale-free networks," *Physical Review E* 80, 2009.

[16] Ming Tang, Tao Zhou, "Efficient routing strategies in scale-free networks with limited bandwidth," *Physical Review E* 84, 2011.

[17] Sameet Sreenivasan, Reuven Cohen, Eduardo Lopez, Zoltan Toroczkai, and H. Eugene Stanley, "Structural bottlenecks for communication in networks," *Physical Review E* 75, 2007.

[18] Liu Wei-Kai, Guan Zhi-Hong, Liao Rui-Quan, "Optimal capacity allocation on heterogeneous complex transport networks," *Chinese Physics Letters*, Vol. 27, No. 10, 2010.

[19] R. Duncan, "A survey of parallel computer architectures," *IEEE Computer*, vol. 23, no. 2, pp. 5–16, Feb. 1990.

[20] R. D'Andrea and G. E. Dullerud, "Distributed control design for spatially interconnected systems," *IEEE Trans. Autom. Contr.*, vol. 48, no. 9, pp. 1478–1495, Sep. 2003.

[21] J. Sun and E. Modiano, "Routing strategies for maximizing throughput in satellite networks," *IEEE J. Sel. Areas Commun.*, vol. 22, no. 2, pp.273–286, Feb. 2004.

[22] Guillermo Barrenetxea, Baltasar Berefull-Lozano, and Martin Vetterli, "Lattice networks: capacity limits, optimal routing, and queuing behavior," *IEEE/ACM Transactions on Networking*, Vol. 14, No. 3, 492-505, 2006

[23] Ziping Hu and Pramode K. Verma, "Impact of network structure on latency in complex networks," *IEEE 35th Sarnoff Symposium*, 2012.

[24] Albert-László Barabási and Réca Albert, "Emergence of scaling in random networks," *Science*, Vol. 286, No. 5439, pp. 509-512, 1999.

[25] P. Erdős, and A. Rényi, "On random graphs I," *Publicationes Mathematicae* 6: 290–297, 1959.

[26] R. Guimera et al., "Optimal network topologies for local search with congestion," *Physics Review Letters* 89, 248701, 2002.

[27] Daniele De Martino, Luca Dall Asta, Ginestra Bianconi, and matteo Marsili, "Congestion phenomena on complex networks," *Physics Review E*. Vol. 79, Issue 1, 2009.

[28] P. Echenique, J. Gomez-Gardenes, and Y. Moreno, "Dynamics of jamming transitions in complex networks," Europhysics letters 71, 325 (2005).

 ISBN: 978-1-61208-246-2

Centralized Adaptive Source-Routing for Networks-on-Chip as HW/SW-Solution with Cluster-based Workload Isolation

Philipp Gorski[1], Claas Cornelius[1], Dirk Timmermann[1], Volker Kühn[2]
Institute of Applied Microelectronics and Computer Engineering[1]
Institute of Communication Engineering[2]
University of Rostock
Rostock, Germany
{philipp.gorski2, claas.cornelius, dirk.timmermann, volker.kuehn}@uni-rostock.de

Abstract—**The growing number of applications and processing units in modern MPSoCs comes along with dynamic and diverse workload characteristics at runtime. Thus, the communication infrastructure, e.g., Networks-on-Chip (NoC), operation on time dependent dynamic traffic loads makes adaptive congestion and load management indispensable. This paper introduces a centralized adaptive path management for oblivious source routing. Thereby, a cluster-based, runtime-configurable software solution continuously monitors the global traffic situation and calculates the needed routing adaptations for each active source-destination pair of the current workload inside a cluster. Contrary to other published solutions, a HW/SW-Co-Design for configurable clustering, traffic monitoring and path calculation is applied. Furthermore, the isolation of workload fractions by the spatial clustering allows application specific configurations.**

Keywords-Network-on-Chip, MPSoC, Adaptive Routing, Traffic Monitoring, Clustering, HW/SW-Co-Design.

I. INTRODUCTION

Networks-on-Chip (NoC) emerged as the next generation of communication infrastructures for the growing number of computational on-chip resources in Multi-Processor-System-on-Chip (MPSoC) [1][2][3][4][5][6][7]. These complex systems will integrate functionality of various application domains at different regions on a single die. Each domain comes along with specific characteristics regarding the supported degree of parallelism (task-level and/or data-level), typical traffic pattern and loads, use cases, workload timing and constraints. Furthermore, some of these characteristics will change during system-lifetime, because underlying algorithms evolve or user scenarios will be adapted. The efficient operation of such heterogeneous systems depends on the integrated mechanisms for runtime management and their adaptability to the specific requirements of the covered application domains. Typical runtime tasks include application mapping and scheduling, debugging and test, power/energy/thermal management, traffic load management (e.g. adaptive routing in NoC) and fault-tolerance. Thereby, the selected routing policy in NoC is one of the major design aspects, as it defines the degree of parallelism and redundancy of the NoC that will be utilized for the communication of the workload applications. Most commonly oblivious, minimal and dimension ordered (DOR) algorithms, like the XY-Routing, are used. This class of routing algorithms results in low hardware costs, deterministic behavior, and, shows good performance results for static workloads. But concerning unpredictable dynamic workloads including the presence time dependent and domain-specific traffic, they suffer from the absence of path adaptability for load balancing and system stabilization. Thus, adaptive routing strategies became research focus, which adjust the routing paths at runtime based on current traffic information. Thereby, the proposed algorithms mainly differ in the criteria, where the routing path will be adjusted, if the paths are minimal or not, and the scope of traffic information used for the decisions. The majority of existing works about adaptive routing for NoC treat the routing adjustment as encapsulated self-adaptation mechanism at runtime, which is integrated at all router nodes and/or the network interfaces of IP cores. The mechanisms are distributed and each node itself performs adaptations using local or regional traffic/failure information without global coordination. Contrary, centralized solutions will operate on global system information, but may suffer from long latencies for traffic monitoring and routing updates. The research of this work was mainly inspired by the ATDOR solution presented in [8]. To the best knowledge of the authors, ATDOR is the first fully evaluated approach of centralized adaptive source routing for MPSoC. It offers a good solution to avoid high latencies of centralized path adaptations, but has different limitations. The presented solution of this work goes beyond these limitations and offers more flexibility, reuse, and fault tolerance. The main contribution of the presented approach targets the following changes and improvements: (1) *Redundant NoCs:* The ATDOR approach integrates a dedicated traffic aggregation network to provide global load information for the exclusive out-of-band hardware processor that calculates the path updates. This work generalizes approach to an exclusive infrastructure for system management information. Two redundant NoC work in parallel (Data-NoC and System-NoC) and will fully separate application data and system management data transport. Thereby, the design requirements will be separated too and each NoC can be optimized for its own traffic domain. (2) *Runtime-Configurable Clustering and Monitoring:* The centralized traffic monitoring and path adaptation is applied to spatial separated clusters and not as global approach. The dynamic clustering is managed at runtime by software agents and each cluster gets a defined fraction of the runtime workload assigned. Furthermore, the monitoring at the cluster-level is

 ISBN: 978-1-61208-246-2

configurable regarding the data capturing periods. Thus, monitoring as well as path adaptation can be configured for specific workload fractions. (3) *HW/SW-CoDesign:* To minimize the hardware overhead and raise the flexibility/configurability, a modular HW/SW-Co-Design is applied. The hardware only consists of needed mechanisms to realize the source routing and the monitoring of traffic information. The evaluation of monitoring information and calculation of routing paths is realized in software as centralized software agent inside a cluster. The combinations of clustering and migratable software further avoid the integration of a single point of failure. (4) *Full Runtime Integration:* The ATDOR solution is a two-phased approach that calculates the path updates in parallel to normal operations and afterwards distributes the path updates. Thereby, static workloads are assumed and calculation phases of 0.5 up to 1 ms. The proposed solution works continuously and intermediately distributes calculated path updates to provide more dynamic workload conditions.

The remainder of this work is organized as follows. Section 2 covers the related work. The third Section describes the conceptual part of the proposed solution and its global design aspects. A detailed evaluation regarding hardware costs, software timing, and simulated runtime characteristics will be given in Section 4. Afterwards, this work will be finalized with a conclusion and outlook for future investigations in Section 5.

II. RELATED WORK

Adaptive routing mechanisms in Networks-on-Chip mainly differ in the criteria, where the routing path will be adjusted, if the paths are minimal or not, and the scope of traffic information used for the decisions [1][2][3][4][5][6][7]. The majority of works focus a distributed adaptation at the router nodes under consideration of aggregated traffic information, targeting the direct proximity or regional scopes [3]. Thus, the router calculates the direction of the next hop of an incoming packet. The degree of adaptivity further varies between minimal and non-minimal route selection.

Ebrahimi et. al. presents two different distributed adaptive routing schemes (LEAR and CATRA) with exclusive solutions for the aggregation of traffic congestion information. In LEAR [9] the neighboring router nodes share their congestion states via one additional wire per link direction in the range of one hop. The adaptive routing is non-minimal. A more complex and irregular congestion information aggregation network for trapezoidal multi-hop regions is used by CATRA in [10], where the number of additional wires per link corresponds to the width/height of the 2D-Mesh topology. The applied routing is minimal. A solution between the complexity of LEAR and CATRA is presented by Rantala et. al. [11] using 2 additional wires per link direction for buffer level information sharing with direct-neighbor nodes to find non-congested minimal paths. Similar regional congestion information aggregation like CATRA can be found in the minimal adaptive routing strategies of RCA [12] and DBAR [13]. RCA offers different regional scopes and uses 8 up to 16 additional wires per link, while DBAR needs 8 wires per link for the sharing of congestion information. A complete multi-objective distributed system management with combined aspects of connection-oriented traffic monitoring, adaptive routing, and application mapping with clustering, is tackled by the publications of Faruque et.al. in [14]. The supposed AdNoC solution integrates hierarchical software agents (global, cluster) for dynamic application mapping and reconfigurable clustering, distributed NoC traffic and application event monitoring via hardware probes at each resource/router, and distributed deterministic adaptive routing with buffer size reconfiguration. The complete system management is event-driven and focusses the runtime optimization of bandwidth utilization. A centralized adaptive routing called ATDOR is presented in [8]. The centralized path management works as additional hardware resource with a fixed coupling to the NoC through an out-of-band traffic monitoring aggregation network using 4 additional wires per link. Path updates will be calculated as a hole and in parallel to NoC operation under consideration of the global traffic situation and include the end-to-end (E2E) switching between XY and YX routes at the network interfaces of the IP cores. Path updates will be distributed over the normal NoC or an exclusive infrastructure. In [15], Cho et. al. suggests a Path-Based, Randomized, Oblivious, Minimal Routing (PROM) strategy. This solution contains a distributed local path adaptation at every router node with randomized decisions, based on probabilities. Especially, the simple O1TURN [15] technique of randomly toggling between XY and YX paths at the network interface shows optimal load balancing results. Kim et. al. provides a two-staged solution of source-initiated distributed path discovery and maintenance to increase the fault tolerance of NoC-based MPSoCs [16]. In [17], Asad et. al. presents a quite similar predominant routing approach using flooding based path exploration mechanisms. Routes between source-destination-pairings will be discovered and maintained using hop-restricted flooding techniques. Traffic optimization is out of scope and no hardware costs are presented. All of these adaptive routing mechanisms will evaluate the shared traffic information locally at each routing node using special hardware. Furthermore, the integration of virtual channels (VC) is needed to provide deadlock-freedom.

A comparable solution to LEAR, that applies minimal routing without VCs but using proximity traffic information is DyXY, presented in [18]. A similar solution, called DyAD, can be found in [19]. A different approach targets the selection of different routing algorithms for specific application workloads or flows at design time. At runtime the routings tables will be changed globally or regional optimized for the current of workload. In [20], Moreno et. al. proposes a routing scheme called planned source routing (PSR), which is a design time solution for traffic optimization. In [14][15] Palesi et. al. provides the APSRA technique including precompiled runtime adaptation of routing algorithms for workload specific demands.

 ISBN: 978-1-61208-246-2

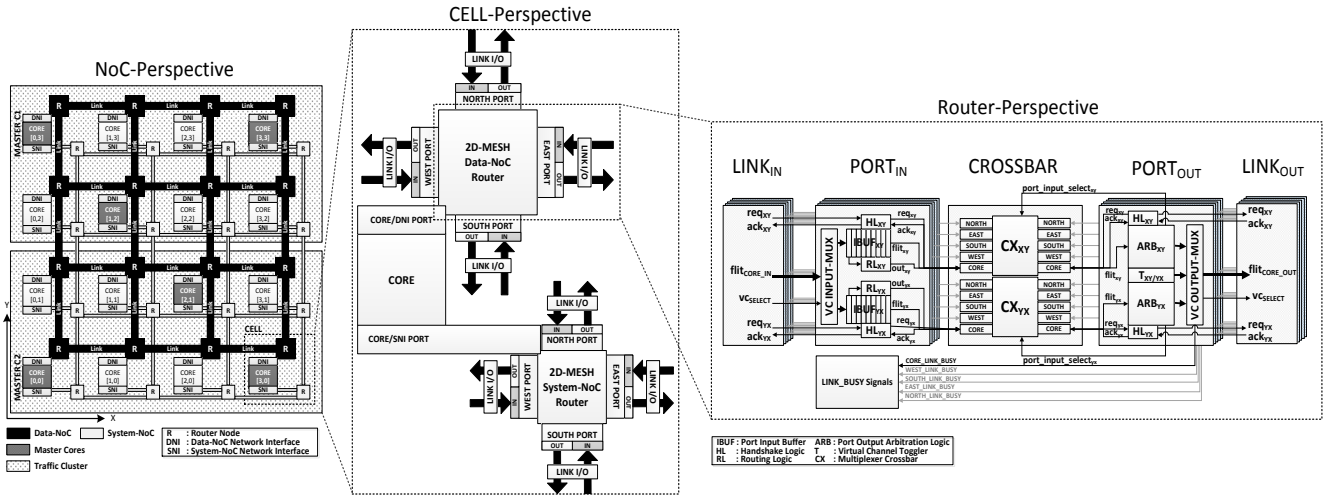

Figure 1. Overview of the targeted Network-on-Chip solution at different implementation levels

III. ADAPTIVE ROUTING CONECPT

The targeted NoC topology is a wormhole-switching 2D-Mesh, where two separated NoCs, called System-NoC and Data-NoC, work in parallel (see Figure 1). The links between neighboring routers are bidirectional point-to-point connections, which transmit a certain portion of a communication packet in parallel (called flit). The first flit of a packet (header) contains the routing information, while following flits carry the payload. Each packet will finalize with a tail flit that transports payload data too. A packet will enter the NoC at the source node flit-by-flit (wormhole-switching), passes the intermediary router nodes (hops) of a path and finally reaches its destination, where the contained payload data will be processed. As flow control a hop-based request/acknowledge-scheme (req/ack) is applied. The Data-NoC covers the transport of application data, while the System-NoC is used for system management. The System-NoC has the same topology as the Data-NoC to provide the same resource-connectivity, but both infrastructures can be individually adapted to the domain-specific requirements. The Data-NoC integrates a XY/YX-Routing that will be adapted at the network interface (PATH-LUT at DNI), higher link data width (64-Bit or higher) and more complex resource functionality, while the System-NoC works with reduced link data width (7-Bit for a 8x8 NoC), minimal input buffering (one flit) and XY-Routing. To provide deadlock-freedom for the path adaptations at the Data-NoC at least two virtual channels (VC_{XY} and VC_{YX}) for both selectable path configurations must be integrated [8]. As illustrated in Figure 1 and Figure 2 each NoC-Resource (CORE) is connected independently to both NoCs via Data-Network- and System-Network-Interface (DNI and SNI). The smallest management unit is a CELL and includes the CORE, DNI, SNI and the connected router nodes (R) of both NoCs. These CELLs are further sub-classified into Slave and Master. A Master-CELL is suited with special hardware resources and software agents to manage a CLUSTER regarding the traffic monitoring and path updates. Slave-CELLs are dynamically grouped into a CLUSTER by a corresponding Master-CELL (see 4x2 C1 and C2 at Figure 1). These CLUSTERs are the fundamental components. Inside a CLUSTER the software agent is able to migrate between the existing Master-CELLs. The number of potential Master-CELLs is defined at design time.

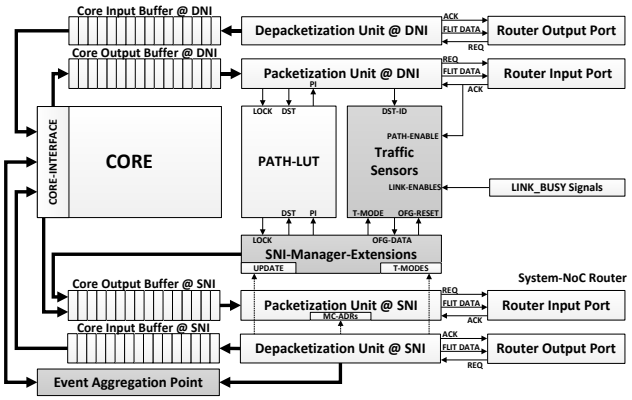

Figure 2. Overview of the Network Interfaces and IP core integration

The communication at the Data-NoC integrates an end-to-end based path adaptation concept, which is coordinated by the software agent of the CLUSTER. If the CORE sends a data through the Data-NoC it pushes a packet to the output buffer of the DNI. The packet header contains the position information of the source (SRC) and the destination (DST) as 2D-Mesh position. The information if the packet should take the XY or the YX path to the DST is stored at the PATH-LUT and needs one bit per destination in the NoC. Thus, for the n×n NoC the PATH-LUT contains (n^2-1) registers. At the packetization unit of the DNI the direction bit will be read out from the PATH-LUT and added to the packet header. Afterwards, the packet will be pushed to the corresponding VC and this won't change until the packet has traversed all router and links on its path to the DST. Thus, the VC assignment is static. At the router-level both

 ISBN: 978-1-61208-246-2

VC have an equal prioritization with a flit-based time-division-multiplexing (TDM). This will be managed by a special TDM unit (see $T_{XY/YX}$ in Figure 1). If two concurring packet of different VC will be routed to the same output port, the TDM unit toggles the selection signal at the output multiplexer every 2 clock cycles, because each flit needs this period to pass the link to the input port of the next router due to the hop-based req/ack flow control. Thus, each VC gets assigned the half of the link bandwidth and the transported packets will not run into a blocking situation. If only one VC will access the output port it will get the full bandwidth assigned by the TDM unit.

The adaptive source-routing works centralized and is applied to the spatial scope of the CLUSTER. Thus, each software agent of a CLUSTER monitors the traffic situation and performs the path updates. The following sub-sections describe the specific details of the adaptive source-routing functionality and its organization.

A. Clustering

The implemented clustering is reconfigurable at runtime and context-based. The creation and management of CLUSTERs is realized via software agents at the Master-CELLs and utilizes a messaging/organization concept via the System-NoC as follows:

CLUSTER-REQUEST (CREQ): For the initial creation of a CLUSTER the Master-CELL sends allocation packets to all CELLs that need to be part of the CLUSTER. These packets consist of the destination routing information (CELL-ADR), the NoC-Address of Master-CELL as source information (MC-ADR), the context identifier of the CLUSTER (CTX-ID) and further context data for Slave-CELL configuration (CTX-DATA).

CREQ = {CELL-ADR | MC-ADR | CTX-ID | CTX-DATA}

CLUSTER-ACKNOWLEDGE (CACK): The Slave-CELLs receive the request/update of the Master and returns a binding packet as acknowledgement. The packet contains the MC-ADR as routing header, the CELL-ADR as source information and the special CTX-ID to classify the packet.

CACK = {MC-ADR | CELL-ADR | CTX-ID}

CLUSTER-UPDATE (CUP): During CLUSTER operation the configuration data (monitoring periods, routing path updates) need to be adapted, the software agent migrates to another Master-CELL or the CLUSTER will be deleted. Thus, the Slave-CELLs are informed via update packets, which have the same format like the CREQ.

CUP = {CELL-ADR | MC-ADR | CTX-ID | CTX-DATA}

The context of a CLUSTER describes the system management domain (e.g. traffic or thermal monitoring/control) it is used for. At this specific case for the adaptive source-routing uses one dedicated CTX-ID. Each Slave-CELL can be assigned to multiple CLUSTERs of different CTX-IDs at the same time, but not to different CLUSTERs of the same CTX-ID. Thus, if multiple CLUSTERs of the same CTX-ID coexist, they will be spatial separated and do not share any CELLs (see C1 and C2 at Figure 1). Moreover, this separation concerns the exclusive clustering for different workload fractions/applications and avoids interferences. Thus, for the traffic monitoring and adaptive source-routing inside the CLUSTER, full spatial workload fraction isolation can be realized. Each clustering context has its own configuration data. While the CLUSTER will be created and managed by the cluster agent, the planning, resource assignment and placement of CLUSTERs will be processed by upper-level global software agents, which are responsible for specific domains. The workload fractions and clustering is precalculated at the global agent that covers the runtime-based application mapping.

B. Traffic Monitoring

The traffic monitoring integrates a periodic and centralized mechanism that is hierarchical organized at three different levels (PATH/LINK, CELL, and CLUSTER).

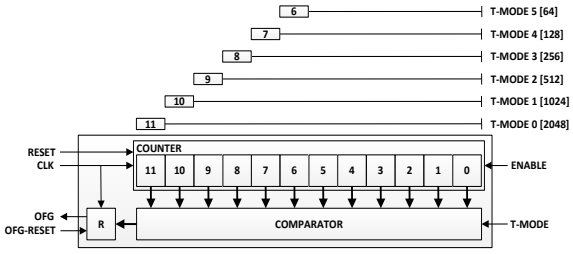

Figure 3. Basic Traffic Sensor concept

PATH/LINK-LEVEL: The basic traffic sensor is a simple combination of an external triggered binary counter and a configurable comparator (see Figure 3). The counter increments each clock cycle the ENABLE signal is active. In parallel, the comparator checks the current counter value against a reference value that is set by the T-MODE. The supported T-MODEs of the traffic monitoring can be obtained from Figure 3. If the counter value reaches the configured T-MODE reference, it sets an overflow flag (OFG) that is captured by the register R and external resettable. This unified sensor solution is used in two different ways: (1) *LINK LOAD*: Each output port of a Data-NoC routing node (NORTH, EAST, SOUTH, WEST, and CORE) is connected to a traffic sensor to measure the current link load (LL). The ENABLE signal is connected to the status signal of the port output multiplexing unit (see LINK_BUSY Signals). The total number of traffic sensors will be 5 per CELL. (2) *INJECTION RATE:* Selected path table entries (DST-ID) of the DNI at each CELL gets a traffic sensor assigned to cover the injection rates (IR) at the path level inside the CLUSTER. Furthermore, one traffic sensor captures the overall injected traffic of the CELL. The ENABLE input is connected to the acknowledgment signal (ACK) of the DNI output (PATH-ENABLE). The number of needed traffic sensors depends on the maximum sizing of a CLUSTER the monitoring should work path-accurate for.

 ISBN: 978-1-61208-246-2

At the current progress, it works with 16 path sensors (e.g., 4x4 or 8x2 CLUSTER).

All traffic sensors of a CELL run at the same T-MODE, which is set at the SNI-Manager-Extension by the Master of the corresponding CLUSTER (Figure 2). Furthermore, they are grouped and located at the SNI of the CELL.

CELL-LEVEL: The OFG registers of all traffic sensors inside a CELL are connected to the SNI-Manager-Extension responsible for the Traffic Monitoring (see Figure 2). This functional unit generates the traffic monitoring packets for the System-NoC and works periodically. Thereby, the period is set by the T-MODE value (same as for traffic sensors) of the CELL. For a Data-NoC running on 1 GHz, the traffic situation for each CELL is sampled in intervals configurable from 64 up to 2048 ns. After the expiration of a period, a finite state machine tests if at least one OFG is set. If true then all register will be read out and reset at the traffic sensors. If no OFG is active there is no need to generate a traffic monitoring event packet for the expired period. Otherwise the FSM generates a new packet with a defined static order of the OFG-bits (CTX-DATA). The packet destination is the Master-CELL of the corresponding traffic monitoring CLUSTER. Afterwards, the packet is pushed to the output buffer at the SNI of the CELL.

CLUSTER-LEVEL: At this point, the traffic monitoring packets periodically leaves the CELLs and need to be aggregated by the Master-CELL, after they have passed the System-NoC towards it. Therefore, special Event Aggregation Points (EAPs) are present as exclusive hardware at all Master-CELLs. These EAPS are needed to scale the generated OFG data to the final parameter of injection rate (IR) and link load (LL). IR as well as LL will be mapped to scales from 0 up to 100 percent with k_S percentage stepping. Thus, the aggregation for the events of $100/k_S$ traffic monitoring periods is needed. Each period event of a traffic sensor with a reported OFG of '1' represents k_S scale percent of IR or LL. This is done using grouped binary 7-bit counters, where each group is assigned to a monitored CELL of the CLUSTER and each counter inside a group is assigned to the OFG of a specific traffic sensor of this CELL. The counters are triggered by the incoming OFG-DATA and are incremented by one if the corresponding OFG-Bit is '1'. The OFG-DATA is fed as fix-ordered parallel bit-vector into the counter group, where the index of each bit corresponds to the traffic sensor identifier. The groups are addressed by the GROUP ID, which is equal to the CELL-ID. The EAP has a buffer at the input and can process the complete OFG-DATA of a traffic monitoring packet in one clock cycle. At the current status of research, a maximal CLUSTER size of 16 CELLS with 21 traffic sensors (5 links/15 paths/1 overall) per CELL was applied. This results in 16 groups with 21 binary 7-Bit counters at each. Moreover, the EAP represents the HW/SW-Interface of the traffic monitoring and the final traffic data can be accessed through the CORE-INTERFACE (CI) that is directly coupled to the internal bus of the Master. The counter values are captured by registers at the CI and the cluster agent will access and store them after a monitoring cycle has finished or during a current cycle. The duration of a cycle can be calculated by eq. (1) and depends on the configured T-MODE period ($r_{T\text{-}MODE}$), the clock frequency of the System-NoC ($f_{System\text{-}NoC}$) and the scale resolution k_S (e.g., k_S =1% or 2%).

$$t_{cycle} = \frac{r_{T-MODE}}{f_{System-NoC} \cdot k_S} \quad (1)$$

In example, for a T-MODE of 256 clock cycles at 1GHz the complete path accurate traffic situation of the CLUSTER can be capture in cycles of 25,6 µs (k_S =1%) or 12,8 µs (k_S =2%). Afterwards, the counter needs to be reset for the next period. Furthermore, the variation of the traffic situation can be recorded by intermediate snapshots during a period without reset. The EAP and the CI are key components to achieve a light-weighted software agent, because the agent is operating on final parameter values and does not need to perform further aggregation steps. At this point the software agent at the Master-CELL has full information about the traffic situation inside the CLUSTER and is able to perform its path update evaluations.

C. Source-Routing

The routing path adaptation exclusively runs in software at the Master-CELL and focuses an incremental improvement for the traffic load of the current assigned workload fraction of the CLUSTER. After a finalized traffic monitoring cycle, the path adaptation starts and runs through all CELLs of the CLUSTER in a fixed order. For each CELL all observed paths will be evaluated in a fixed order and the following optimization procedure will be processed in the given sequence:

1. TEST: Initially the path will be tested for shared position coordinates, because if the path targets CELLs at the same row/column of the 2D-Mesh no minimal path alternatives are available and the path will be removed from the optimization list.

2. PREPARATION: The monitored injection rate (IR) of the current path is used to prepare the monitoring data for the new path evaluation run. The IR will be removed from the link load (LL) values of each link traversed by the path in its current assigned configuration (XY or YX).

3. EVALUATION: At this step the fitness for the XY and the YX configuration of the path will be calculated, which is simply the sum of LL values for all links traversed by a path. Afterwards, the lowest sum will be selected and its corresponding path configuration (XY or YX) will be assigned (minimal path load strategy.

4. UPDATE: After the evaluation of the path, the monitoring data will be updated with the injection rate of the path at the traversed link positions in the resulting configuration (XY or YX). This ensures the operation on the new traffic constellation for subsequent optimization runs of

 ISBN: 978-1-61208-246-2

other paths. Furthermore, if the path has changed an update packet will be sent to the CELL via the System-NoC to register the new path configuration at the lookup-table of the DNI (PATH-LUT). The update will be performed by the SNI and contains the bit flip at the PATH-LUT for the DST for the evaluated path.

Contrary to ATDOR [8], this solution only works continuously and triggers updates of single paths intermediately after processing. Furthermore, the timing depends on the monitoring interval, which can be configured individually for each CLUSTER and thus allows full adaptation for the traffic of the assigned workload fraction. The fixed ordered processing should lead to an incremental optimization of the traffic load balancing in case of static traffic patterns. For dynamic variations the traffic balancing will be slightly improved. The configurability of path updates for specific traffic pattern of the assigned workload fraction may be further improved by more selective ordering during path processing. This will be part of future investigations.

IV. EXPERIMENTAL EVALUATION

The evaluation of the presented solution was realized via software profiling and system simulations for operational performance as well as hardware synthesis for the cost approximation. Thereby, the basic Data-NoC design parameter configuration can be obtained from TABLE I.

TABLE I. DATA-NOC CONFIGURATION FOR SIMULATION AND SYNTHESIS

Parameter	Value
NoC Clock Rate	1 ns
Master-CELL CPU Clock Rate	0.5 ns
NoC Topology	2D-Mesh
Synthesized NoC-Size	8x8
Simulated Cluster Size	16 CELLS at 4x4 spatial shape
Data-NoC Input Buffer Depth	4 Flit
System-NoC Input Buffer Depth	1 Flit
Data-NoC Link data width	64 Bit
System-NoC Link data width	7 Bit
Average Link wire length [23]	0.83 mm
Wire width/spacing [23]	140/140 nm
# of I/O-Links in 8x8 NoC	224
# of Master-CELLs in NoC	32 (=50%)
Traffic Sensors per CELL	21
7-Bit Counter per EAP	336 (=16*21)
Simulated Data-NoC Packet Sizes	2 up to 9 Flit (uniform)
Traffic Pattern	random uniform distributed, transpose, hotspot (H=20%) and bit complement Hotspot Position = CORE [0,0]

A. Software Profiling

The main parameter for the evaluation of the ANSI-C based software agent is the computational latency/delay for the routing path calculation. Hence, the software profiling for the UPDATE/PREPARATION steps and the EVALUATION was carried out. As reference platform, a PowerPC 440 32-bit RISC CPU was used, which is implemented as hardcore on a Xilinx Virtex5 device. It is suited with 32-kB Data and Instruction Cache. The minimalistic Xilkernel from Xilinx served as basic integration environment for the centralized source adaptation software, which is implemented as standalone thread. To provide accurate timing information, the duration of path computations was measured in clock ticks via special timer commands.

TABLE II. SOFTWARE PROFILING RESULTS, GIVEN AS AVERAGE DELAY IN NUMBER OF CPU CLOCK CYCLES, FOR DIFFERENT NOC SIZES, AND MAXIMAL ALLOWED HOPS (MAXHOP) FOR ROUTING PATHS CALCULATIONS

NoC Size	Maxhop	PREPARE/UPDATE	XY/YX
4 x 4	-	36	132
4 x 4	4	34	118
4 x 4	3	32	104
8 x 8	-	46	174
8 x 8	8	42	157
8 x 8	4	34	119
8 x 8	3	32	105

For different 2D-Mesh NoC sizes (4x4 and 8x8), one million source-destination-pairings were generated and the routing path calculation processed. Further, uniform distributions with defined maximal hop distances (Maxhop) between these pairings were profiled. Afterwards, the average calculation delay, as number of passed CPU clock cycles, over all pairings was recorded. The results are included in Table II. The delay values for the full path calculation at different parameter variations (XY/YX) already contain the latencies for the PREPARE/UPDATE procedures. Observing the case of a 2GHz CPU running the thread with a budget of 20 %, the full XY/YX path calculation at the 4x4 CLUSTER without hop constraints is able to provide ~3000 single path updates per millisecond. The obtained profiling results were used for the timing accurate simulation of a complete workload simulation inside a CLUSTER.

B. Hardware Synthesis

The ASIC design flow was realized with the Synopsys™ DesignCompiler™ using the 45 nm Nangate FreePDK45 Generic Open Cell Library. The presented results in TABLE III show the total cell area costs for each of the functional components (SNI-Manager Extension, Traffic Sensors, EAP) and the router nodes of both NoC. Further, the NoC area costs of the complete NoC solution are given

TABLE III. TOTAL CELL AREA (TCA) HARDWARE COSTS FOR SINGLE DESIGN COMPONENTS INSIDE A CELL AND AN 8X8 NOC AT ALL

	Total Cell Area	
Design Component	*CELL [µm²]*	*8x8 NoC [mm²]*
SYSTEM-NOC ROUTER	2783.69	0.178156
SYSTEM-NOC LINK	1510,6*	0.3383744
DATA-NOC ROUTER	40174.51	2.571169
DATA-NOC LINK	14641.2*	3.279628
SNI TRAFFIC LOAD EXT.	1511.94	0.096764
TRAFFIC SENSORS	2720.34	0.174102
AGGREGATION POINT	22230.68	0.711382
SUM OF ALL UNITS	**85572.96**	**7.3495754**

**area of a single I/O NoC-Link*

The targeted operational frequency was set to 1 GHz and met for all evaluated design cases. Regarding the hardware costs in the context of the final MPSoC that contain the

 ISBN: 978-1-61208-246-2

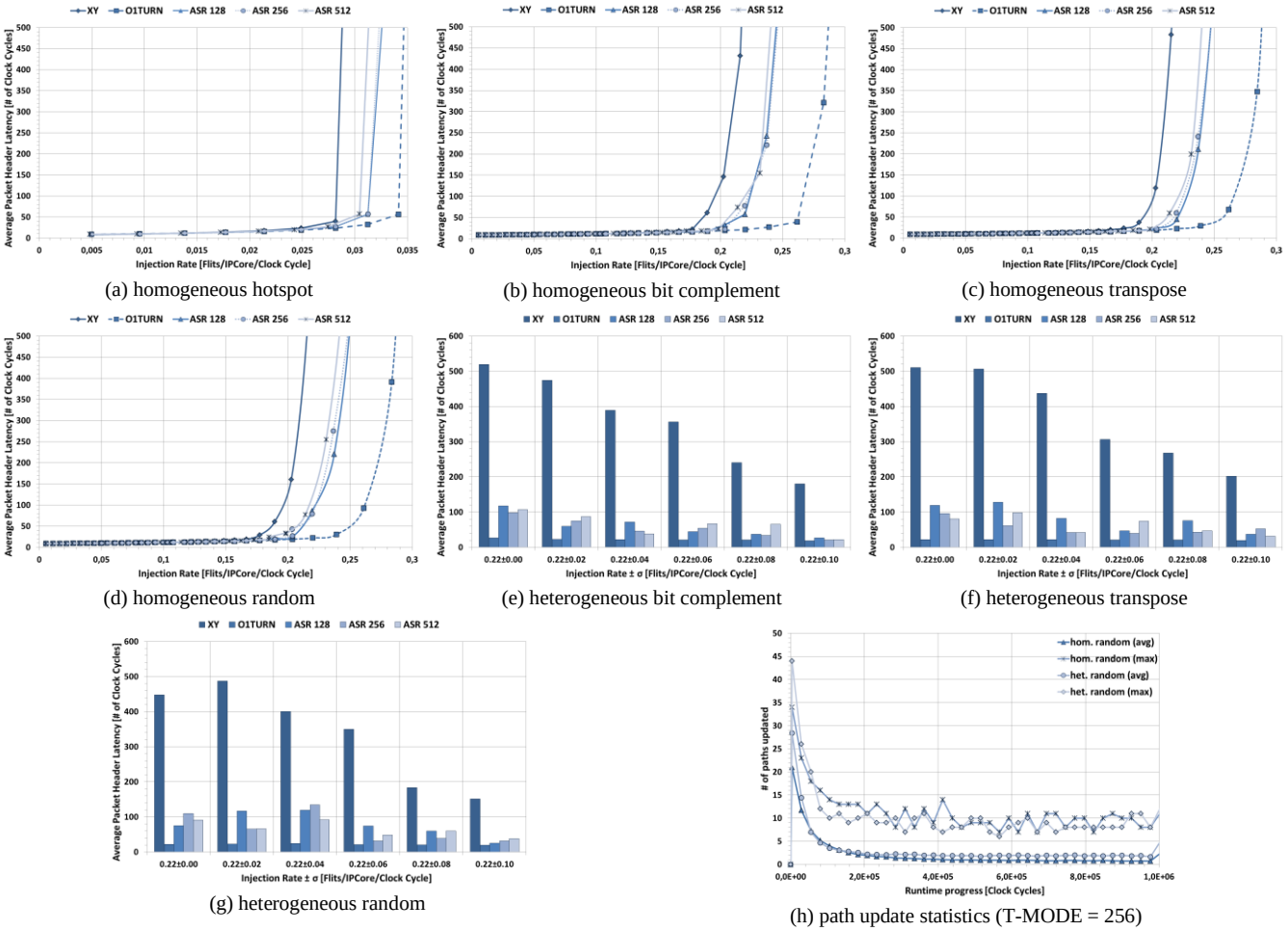

(a) homogeneous hotspot (b) homogeneous bit complement (c) homogeneous transpose

(d) homogeneous random (e) heterogeneous bit complement (f) heterogeneous transpose

(g) heterogeneous random (h) path update statistics (T-MODE = 256)

Figure 4. Summarized results of the 4x4 CLUSTER simulations for homogeneous task loads [(a), (b), (c), (d)], heterogeneous task loads [(e), (f), (g)], and path update statistics (h)

targeted amount of CELLs on a 45nm silicon die (areas: 280-400 mm² [24][25]) the relative overhead due to both complete NoC will be less than circa 2.6% down to 1.8%. Thereby, the total link area costs was estimated using the configuration of [23] as presented in TABLE I.

C. Simulation Results

The full system simulations target the maximum CLUSTER size (16 CELLs) at a spatial 4x4 shape with different workload configurations and monitoring cycles. This allows the fully path-accurate monitoring of the traffic situation inside a CLUSTER. Therefore, an own cycle accurate SystemC/TLM-based simulator was used. The dynamic workload consists of 10 tasks per CORE/CELL with a uniform random scheduling. Each task gets a fixed packet destination assigned depending on the four simulated synthetic traffic pattern as mentioned in TABLE I. For the hotspot pattern, H=20% of the tasks per core are communicating with the assigned CORE [0,0] in the lower left corner. Furthermore, two different traffic load strategies at the task-level were applied. At the homogeneous strategy each tasks has the same traffic injection rate, while the heterogeneous case works with an injection rate (IR) interval [IR±σ] and each task gets assigned a uniform random distributed injection rate out of this defined range. This allows the general evaluation of different traffic situations with more balanced or mixed loads at the path level. The monitoring was configured to work with different T-MODEs of 128, 256 and 512 at a scale resolution k_S=1%. This results in monitoring/path evaluation cycles of 12.8 µs, 25.6 µs and 51.2 µs. As references, the simple dimension-ordered XY-Routing and the probability-based adaptive O1TURN-Routing [15] were simulated. O1TURN toggles the VC (XY or YX) for each injection packet of a task and thus enforces a fully balanced VC utilization. The evaluation in [15] showed, that O1TURN offers the best average case throughput and latency. The newly introduced adaptive source-routing is called ASR <T-MODE>. The summarized results of all simulated parameter variations are depicted in Figure 4. The diagrams (a)-(g) contain the average packet header latency over varying traffic injection rates. The results were calculated as average from 100 simulations runs of workloads at each parameter constellation. Thereby, each simulation runs covers the

 ISBN: 978-1-61208-246-2

system operation time of 1 millisecond. For the homogeneous traffic load strategies in (a)-(d) the proposed ASR clearly outperforms the XY-Routing, but for all simulated traffic pattern it does not reach the performance of O1TURN and the latency improvements over XY-Routing ranges at circa 50% of the O1TURN results. Furthermore, the impact of reduced monitoring/evaluation cycles is smaller than expected. The simulation results for the heterogeneous tasks load strategy (see Figure 4 (e) - (g)) show that the advantage of O1TURN over ASR decreases with the increasing spread of task injection rates at highly intensive overall traffic loads (Traffic Load > 20 %) inside the CLUSTER. The difference between ASR traffic optimization performance of homogeneous and heterogeneous spread task loads relies on the resulting overall distribution of the traffic load inside the CLUSTER. At homogeneous task injection rates the traffic situation inside the CLUSTER will be more balanced and thus the dedicated assignment of specific path configurations is harder, because XY and YX path only slightly differs in the resulting fitness values (sum of link loads for each path). The higher the spread of task injection rates becomes the delta of these values increase, because the overall traffic situation becomes more heterogeneous. The diagram in Figure 4 (h) plots the registered path updates (average and maximum) at the homogeneous and heterogeneous case for the random traffic pattern over the proceeding operation time of the workload. Both cases show a similar convergence behavior at the maximum and the average case. The results for the other simulated traffic pattern are quite similar, but the random pattern is the most interesting, because it generates the most equal balanced overall traffic load inside the CLUSTER. As expected, the number of path updates reaches its peak at the beginning of operations. After the exponential decrease it works continuously at low update rates and the resulting computational demand for the software agent is suitable. The performing CPU at the Master-CELL of the software-agent was configured to operate with a clock frequency of 2 GHz.

V. CONCLUSION AND FUTURE WORK

The presented HW/SW-ASR concept, including clustering and path-accurate traffic monitoring, and its evaluation show that the intended runtime-configurable approach is feasible and superior to dimension-ordered XY-Routing. But the comparison to the O1TURN solution outlines its limitation as standalone solution. The additional hardware overhead is comparable to the solutions of [8][10][12][13], but has a more general focus on system management communication and makes workload specific traffic information available for global reuse. Thus, the presented cluster-based centralized ASR is only one integration aspect of the clustering and the System-NoC approach. The presented results brings the focus of future investigation on ASR to direction targeted by [14][15][26][27][28][29][30]. Specifically, the following aspects will be highly interesting:

Evaluate hybrid solutions that combine ASR and O1TURN. Both routing algorithms work at the end-to-end path level and can be merged without high additional hardware efforts. Thus, a more pattern-specific assignment to different CLUSTERs and inside these CLUSTER workloads may results in an attractive combination. Thereby, ASR will be pushed to support the planning of guaranteed bandwidth connections for specific application tasks or paths. Furthermore, the integration of failure handling for reliable NoC communication is a desired extension.

The globally available traffic information allows a better evaluation of the current system states and makes an interaction of runtime-based application mapping, routing strategy selection and spatial clustering more valuable. Furthermore, the integrated software-agents of ASR will support a better integration of these aspects, which targets runtime optimization at different abstraction levels and operational aspects.

REFERENCES

[1] W. J. Dally and T. B, "Route packets, not wires: on-chip interconnection networks," in *Design Automation Conference, 2001. Proceedings*, 2001, pp. 684–689.

[2] A. Jantsch and H. Tenhunen, *Networks on chip*, 1st ed. Kluwer Academic Publishers, 2003, p. 312.

[3] E. Salminen, A. Kulmala, and T. D. Hämäläinen, "Survey of Network-on-chip Proposals," *WHITE PAPER, OCP-IP, MARCH*, no. March, pp. 1–12, 2008.

[4] E. Salminen, A. Kulmala, and T. D. Hamalainen, "On network-on-chip comparison," *10th Euromicro Conference on Digital System Design Architectures, Methods and Tools (DSD 2007)*, pp. 503–510, Aug. 2007.

[5] T. Bjerregaard and S. Mahadevan, "A survey of research and practices of network-on-chip," *ACM Computing Surveys (CSUR)*, vol. 38, no. 1, p. 1, 2006.

[6] A. Agarwal, C. Iskander, H. T. Multisystems, and R. Shankar, "Survey of Network on Chip (NoC) Architectures and Contributions," *scientificjournals.org*, vol. 3, no. 1, 2009.

[7] B. A. Abderazek, "Basic Network-on-Chip Interconnection for Future Gigascale MCSoCs Applications: Communication and Computation Orthogonalization," *Information Systems*, pp. 1–7, 2006.

[8] R. Manevich, I. Cidon, A. Kolodny, I. Walter, and S. Wimer, "A Cost Effective Centralized Adaptive Routing for Networks-on-Chip," *2011 14th Euromicro Conference on Digital System Design*, vol. 9, no. 2, pp. 39–46, Aug. 2011.

[9] M. Ebrahimi, M. Daneshtalab, P. Liljeberg, J. Plosila, and H. Tenhunen, "LEAR -- A Low-Weight and Highly Adaptive Routing Method for Distributing Congestions in On-chip Networks," in *2012 20th Euromicro International Conference on Parallel, Distributed and Network-based Processing*, 2012, vol. 1, pp. 520–524.

[10] M. Ebrahimi, M. Daneshtalab, P. Liljeberg, and J. Plosila, "CATRA-Congestion Aware Trapezoid-based Routing Algorithm for On-Chip Networks," in *Design, Automation & Test in Europe Conference & Exhibition (DATE'12)*, 2012, pp. 320 – 325.

[11] V. Rantala, T. Lehtonen, P. Liljeberg, and J. Plosila, "Distributed Traffic Monitoring Methods for Adaptive Network-on-Chip," in *2008 NORCHIP*, 2008, pp. 233–236.

 ISBN: 978-1-61208-246-2

[12] P. Gratz, B. Grot, and S. W. Keckler, "Regional congestion awareness for load balance in networks-on-chip," *2008 IEEE 14th International Symposium on High Performance Computer Architecture*, pp. 203–214, Feb. 2008.

[13] S. Ma, N. Enright Jerger, and Z. Wang, "DBAR: An Efficient Routing Algorithm to Support Multiple Concurrent Applications in Networks-on-Chip," in *Proceeding of the 38th annual international symposium on Computer architecture - ISCA '11*, 2011, p. 413.

[14] M. A. Al Faruque, T. Ebi, and J. Henkel, "AdNoC: Runtime Adaptive Network-on-Chip Architecture," *IEEE Transactions on Very Large Scale Integration (VLSI) Systems*, vol. 20, no. 2, pp. 257–269, Feb. 2012.

[15] M. H. Cho, M. Lis, K. S. Shim, M. Kinsy, and S. Devadas, "Path-based, randomized, oblivious, minimal routing," in *Proceedings of the 2nd International Workshop on Network on Chip Architectures - NoCArc '09*, 2009, p. 23.

[16] Y. B. Kim and Y. Kim, "Fault Tolerant Source Routing for Network-on-chip," in *22nd IEEE International Symposium on Defect and Fault-Tolerance in VLSI Systems (DFT 2007)*, 2007, pp. 12–20.

[17] A. Asad, M. Seyrafi, A. E. Zonouz, M. Soryani, and M. Fathy, "A Predominant Routing for on-chip networks," in *2009 4th International Design and Test Workshop (IDT)*, 2009, pp. 1–6.

[18] M. Li, Q. Zeng, and W. Jone, "DyXY - a proximity congestion-aware deadlock-free dynamic routing method for network on chip," *2006 43rd ACM/IEEE Design Automation Conference*, pp. 849–852, 2006.

[19] J. Hu and R. Marculescu, "DyAD: smart routing for networks-on-chip," in *Proceedings of the 41st annual Design Automation Conference*, 2004, vol. 04, p. 263.

[20] E. I. Moreno, C. A. M. Marcon, N. V. Calazans, and F. G. Moraes, "Arbitration and routing impact on NoC design," in *2011 22nd IEEE International Symposium on Rapid System Prototyping*, 2011, vol. 3, pp. 193–198.

[21] M. Palesi, R. Holsmark, S. Kumar, and V. Catania, "Application Specific Routing Algorithms for Networks on Chip," *IEEE Transactions on Parallel and Distributed Systems*, vol. 20, no. 3, pp. 316–330, Mar. 2009.

[22] M. Palesi, S. Kumar, and V. Catania, "Bandwidth-aware routing algorithms for networks-on-chip platforms," *IET Computers & Digital Techniques*, vol. 3, no. 5, p. 413, 2009.

[23] C. Hernandez, F. Silla, and J. Duato, "A methodology for the characterization of process variation in NoC links," in *Design, Automation & Test in Europe Conference & Exhibition (DATE'10)*, 2010, pp. 685–690.

[24] P. Salihundam, S. Jain, and T. Jacob, "A 2 Tb/s 6× 4 mesh network for a single-chip cloud computer with DVFS in 45 nm CMOS," *IEEE Journal of Solid-State Circuits*, vol. 46, no. 4, pp. 757–766, 2011.

[25] Y. Hoskote, S. Vangal, A. Singh, N. Borkar, and S. Borkar, "A 5-GHz Mesh Interconnect for a Teraflops Processor," *IEEE Micro*, vol. 27, no. 5, pp. 51–61, Sep. 2007.

[26] S. Azampanah, A. Khademzadeh, N. Bagherzadeh, M. Janidarmian, and R. Shojaee, "LATEX: New Selection Policy for Adaptive Routing in Application-Specific NoC," *2012 20th Euromicro International Conference on Parallel, Distributed and Network-based Processing*, pp. 515–519, Feb. 2012.

[27] E. a. Carara and F. G. Moraes, "Flow oriented routing for NOCS," *23rd IEEE International SOC Conference*, pp. 367–370, Sep. 2010.

[28] E. Carvalho, N. Calazans, and F. Moraes, "Heuristics for Dynamic Task Mapping in NoC-based Heterogeneous MPSoCs," in *18th IEEE/IFIP International Workshop on Rapid System Prototyping (RSP '07)*, 2007, pp. 34–40.

[29] C.-L. Chou and R. Marculescu, "Run-Time Task Allocation Considering User Behavior in Embedded Multiprocessor Networks-on-Chip," *IEEE Transactions on Computer-Aided Design of Integrated Circuits and Systems*, vol. 29, no. 1, pp. 78–91, Jan. 2010.

[30] A. Kumar, B. Mesman, B. Theelen, H. Corporaal, and Y. Ha, "Analyzing composability of applications on MPSoC platforms," *Journal of Systems Architecture*, vol. 54, no. 3–4, pp. 369–383, Mar. 2008.

 ISBN: 978-1-61208-246-2